USC
UNIVERSIDADE DE SANTIAGO DE COMPOSTELA

INTERNATIONAL DOCTORAL SCHOOL OF THE USC

Anxo Méndez Villar

PhD Thesis

A holistic evaluation of an efficient and environmentally-sound public lighting system to control biological colonisation on architectural heritage

Santiago de Compostela, 2025

Doctoral Programme in Environmental and Natural Resources

INTERNATIONAL DOCTORAL
SCHOOL OF THE USC

PHD THESIS

A HOLISTIC EVALUATION OF AN EFFICIENT AND ENVIRONMENTALLY-SOUND PUBLIC LIGHTING SYSTEM TO CONTROL BIOLOGICAL COLONISATION ON ARCHITECTURAL HERITAGE

Author

Anxo Méndez Villar

Supervisor/s:
Patricia Sanmartín Sánchez

Tutor:
Patricia Sanmartín Sánchez

PHD PROGRAMME IN ENVIRONMENTAL AND NATURAL RESOURCES

SANTIAGO DE COMPOSTELA
2025

DECLARACIÓN DE CONFLICTO DE INTERESES

A HOLISTIC EVALUATION OF AN EFFICIENT AND ENVIRONMENTALLY-SOUND PUBLIC LIGHTING SYSTEM TO CONTROL BIOLOGICAL COLONISATION ON ARCHITECTURAL HERITAGE

El doctorando declara no tener ningún conflicto de interés en relación a la elaboración de esta tesis doctoral.

Santiago de Compostela, 7 de octubre de 2025

Fdo. Anxo Méndez Villar

Agradecimientos

Primero de todo tengo que agradecerle esta tesis a Patricia, mi directora, por guiarme y acompañarme durante estos años, y por enseñarme a cómo ser un mejor investigador. Por supuesto, a Bea, a Javi, a todos mis compañeros del departamento de Edafología y Química Agrícola, tanto a los que siguen aquí como a los que ya se han marchado. A Elsa, Diana, Juanpe, Fabi, Pablo, Miguel, Nico y Martina, por el compañerismo, la ayuda, y por convertir este espacio de trabajo en un lugar tan agradable. A Haizea un abrazo enorme desde Santiago a Valencia.

Esta tesis no podría haberse realizado sin la ayuda de todos los investigadores que han colaborado conmigo, y de los cuales he aprendido tanto. A todos vosotros gracias.

Y a todas las personas de mi vida que me han acompañado este tiempo, a mis amigos y a mi familia, gracias por vuestro cariño. Por último, a mi madre y a mi padre, gracias y os quiero mucho.

Abstract

Ornamental lighting is increasingly used in towns and cities at night to accentuate the aesthetic value of architectural heritage (understood here as monuments, architectural ensembles and sites of historical, archaeological, artistic, scientific, social or technical interest). Lighting plans typically prioritize aesthetics, energy efficiency and compliance with environmental guidelines, while also attempting to mitigate light pollution; however, they generally overlook the impact of the light on phototrophic lithobionts growing on the illuminated surfaces. Granitic (intrusive igneous) rock, the predominant geological substrate in architectural heritage in Galicia (NW Spain), is susceptible to physical, chemical and biological weathering, despite being strong and durable. Phototrophic subaerial biofilms (SABs), which are mainly composed of algae and (to a lesser extent) cyanobacteria, and also heterotrophic bacteria and fungi, are commonly found on architectural heritage in Galicia due to its climate. The climate in Galicia is classified as oceanic or Atlantic, according to the FAO's agro-ecological zoning, and the typically high humidity is caused by high rainfall and mild temperatures throughout the year. Previous studies have shown that growth of phototrophs on architectural heritage may be encouraged by night-time exposure to artificial light that includes wavelengths that stimulate photosynthesis. The enhanced growth increases the potential biodeteriorative role of SABs, even if only aesthetic, on stone materials.

The overall aim of the CromaLux project (2020–2024) was to develop an energetically-efficient, environmentally-sound ornamental lighting system with biostatic capacity, i.e. the ability to halt the growth of phototrophic SABs. This novel ornamental lighting system is therefore proposed as a preventive conservation tool that utilises the existing public lighting infrastructure to illuminate stone-built monuments, enhancing the beauty and artistic value of architectural heritage through ornamental lighting while reducing maintenance costs. The biostatic capacity of the system is achieved by the use of a combination of narrow bandwidth amber (593 nm) and green (528 nm) LED lights, which emit light at wavelengths weakly absorbed by the main photosynthetic pigments, chlorophylls and carotenoids. The absorption spectra of these pigments peak around the blue part of the visible light spectrum, at 372-392 nm for chlorophylls and 448 nm for β-carotene, and around the red part, at 626-642 nm for chlorophylls. The amber+green light is therefore expected to have a low photosynthetic efficiency and reduce SAB growth (and potentially exert stress on the SABs) relative to traditional white light sources. The bimodal spectrum resulting from the combination of amber and green LED lights (hereinafter amber+green) appears white (3000 K) to the human eye, as coloured lighting

is generally strongly discouraged for permanent ornamental illumination in urban spaces for aesthetic reasons. To comply with energy efficiency requirements, the CromaLux lighting system also uses a highly efficient warm white LED light with a very low blue component during the first hours of the night, and prior to use of the novel biostatic amber+green light.

The CromaLux project was carried out in Santiago de Compostela (Galicia, UNESCO World Heritage City since 1985) by the companies Televés S.A.U. and Ferrovial Energía S.A. (previously Ferrovial Servicios S.A.) and the University of Santiago de Compostela (USC). The project formed part of the SMARTiAGO initiative of innovative public procurement, aimed at developing innovative technological solutions within the framework of smart cities, with the objective of addressing specific challenges faced by heritage cities such as Santiago de Compostela. This doctoral thesis (2020-2025), framed within the aforementioned CromaLux project, was carried out within an Industrial Doctorate programme, in a collaboration between Ferrovial Energía S.A. and the USC. The research, which also fulfils the requirements for an International Doctorate distinction, is relevant and timely, in accordance with European policies and frameworks, considering that sustainability regarding preservation of the stone-built heritage involves both stone preservation and also the ecological context, thus enabling the joint conservation of natural and cultural heritage. The study first aimed to validate the biostatic capacity of amber+green lighting in the short- to medium-term (in laboratory-based experiments) and in the long-term (in the field). The research also aimed to validate the environmentally-sound impact of the novel lighting on biodiversity, and to evaluate its energy efficiency and aesthetic and social perception, through a comprehensive, holistic approach. The research was divided in four specific parts:

Part 1 of the research (**Chapter 1**) examined the legislative framework governing ornamental lighting of architectural heritage, with particular attention on Spanish regulations, to evaluate the impact of lighting policies on light pollution and on the environment. ***Part 2*** (**Chapters 2 to 6**) focused on validating the biostatic capacity (ability to halt growth) of the amber+green lighting and elucidating the mechanisms of action of the physiological responses to ornamental lighting of phototrophic SABs present on architectural heritage surfaces. ***Part 3*** (**Chapters 7 and 8**) studied the impact of ornamental lighting on biodiversity, considering the bacterial and fungal microbiota inhabiting the granite-built heritage and also the surrounding nocturnal insect biodiversity. Finally, ***Part 4*** (**Chapters 9 and 10**) assessed the environmental and economic impact of the ornamental lighting, focusing on the CromaLux lighting system and also the public response to the amber+green light, with a view to designing implementation strategies.

Illumination of monuments in urban areas is an emerging contribution to light pollution that has scarcely been considered to date. As described in **Chapter 1**, a literature review on the topic of light pollution and related policies was conducted between 2020 and 2022. The review enabled assessment of the prevailing legislation governing the use of

ornamental lighting in both Spain and Europe and examined the trends in monument illumination and policymaking aimed at environmentally sustainable management. It was concluded that the discrepancies in the definition of light pollution extend to the policies and regulations, which should be updated to enable development of new lighting technologies. Regulation of ornamental illumination should balance energy, environment and the enhancement and conservation of stone monuments, which can be achieved by implementing the findings of recent research in heritage sciences.

The research reported in **Chapter 2** focused on examining the duration of the ornamental illumination with the aim of exerting a biostatic effect on SABs. Laboratory-grown SABs (derived from an algal SAB colonizing a granite-built monument) were subjected to 16 hours of daylight followed by photoperiods of 2, 4, 6 and 8 hours of respectively red, green, blue and warm white ornamental LED lighting (a control without ornamental illumination was included); the 24 h photoperiod was completed with the corresponding number of hours of darkness in each case. Growth of the SABs was assessed after 35 days by quantifying biomass and photosynthetic pigments, cell counting and PAM chlorophyll fluorometry. Exposure to between 4 and 6 hours of red and green light was found to be sufficient to reduce the biomass of SAB (in terms of wet biomass and cell count), while exposure to 8 hours of blue light promoted further growth. Both the red and green LED lights caused a sharp decrease in the biomass of green algae but increased the biomass of cyanobacteria. The findings reported in this chapter were used to determine the duration of illumination with the amber+green lighting required for a biostatic effect, while also following the regulations regarding artificial lighting in Santiago de Compostela.

Outdoor monuments are obviously exposed to daylight, and the research reported in **Chapter 3** aimed to investigate whether the efficacy of amber+green lighting as a biostatic tool for controlling phototrophic colonisation on architectural heritage is influenced by different levels of daylight illuminance. Photoperiods of 13 hours of two levels of daylight illuminance (low, LDI, ~2050 lx and high, HDI, ~10200 lx; based on field measurements) were followed by ornamental lighting produced by cool white (4300 K), warm white (2580 K) and amber+green (3000 K) LED ornamental lighting (also including a control without ornamental illumination) and by 5 hours of darkness. After 37 days of exposure to this lighting regime, the growth of laboratory-produced SABs (mainly composed of *Chlorella vulgaris*, *Klebsormidium flaccidum* and *Synechocystis* sp.) was assessed by biomass and diversity measurements, biochemical profiling (quantification of photosynthetic pigments, EPS and ATP content), confocal microscopic and PAM chlorophyll fluorometry. The biostatic capacity of amber+green light was verified under both LDI and HDI conditions, as the SAB biomass yield was reduced, and production of both exopolysaccharides and extracellular proteins was lower than under cool and warm white lights. The biomass of the SABs growing in the HDI set-up was higher than that produced under LDI. All ornamental lighting conditions failed to alter the biochemical profile (in terms of contents of

chlorophyll, exopolysaccharides and extracellular proteins) under the HDI. The HDI also yielded a decrease in the quantum yield of the SABs under all ornamental lighting conditions. Both the warm white and amber+green lights decreased the relative abundance of *Klebsormidium flaccidum* in the LDI condition. The findings reported in this chapter validated the use of the novel biostatic light in variable solar exposure, which is particularly important in urban environments due to urban morphology and/or climatic factors.

With the aim of elucidating the mechanisms of action underlying the biostatic effect, the laboratory study reported in **Chapter 4** investigated the influence of three types of LED lighting used to illuminate monuments (cool white, warm white and amber+green) on the growth of SABs. Environmental proteomics provided information about the changes in the SAB metabolism under stress inflicted by nocturnal lighting, by quantifying and identifying peptides in proteins expressed by the microorganisms forming the SABs. The analysis accounted for changes in the species assembly and in protein/peptide composition in the SABs. Amber+green lighting was found to have the strongest inhibitory effect on the SAB cultures, detected through a negative impact on photosystems I and II and production of photosystem antenna protein-like. In particular, the amber+green light impaired production of the PsbO subunit of the photosystem II, which catalyses the splitting of water to O_2 and $4H^+$ and is needed to initiate the electron transport chain for the synthesis of ATP and NADPH in photosynthesis. The biostatic light also had a triggering effect on protein metabolism (synthesis, folding and degradation) and induced synthesis of heat shock proteins related to stress. Likewise, exposure to the warm white light caused an increase in the number of peptides related to cyanobacterial structures and pigment related (phycobilisomes and phycocyanin).

The biostatic effect, initially studied using membrane-grown biofilms (**Chapters 2 to 4**), was also assessed using sample blocks of different substrates (**Chapter 5**). Granite (the main building material used in architectural heritage in Galicia and other regions of the world) and cement mortar (widely used in construction, especially in modern and contemporary architecture) were used as test substrates. SABs (mainly composed of the green algae *Bracteacoccus minor* and *Stichococcus bacillaris*) were grown on the granite and cement blocks in a custom-built flow cascade. The samples were then exposed, during a period of 3 months, to a lighting set-up comprising 13 hours of daylight, 6 hours of ornamental LED illumination (cool white, warm white and amber+green) and 5 hours of darkness. Controls without ornamental illumination and uncolonized blank specimens were also included. The SAB-mineral interface exposed to amber+green light behaved similarly to the control without ornamental illumination, minimizing the effects of ornamental lighting relative to both white lights tested in terms of roughness deviations, Leeb hardness values, static contact angle, water absorption time and colour differences. Colour measurements also indicated that the amber+green light reduced growth of the SABs relative to that observed under the white lights, particularly in terms of the CIELAB

yellow-blue coordinate (b*). Petrographic analysis also revealed mineral-dependent SAB coverage of the granite. The results reported in this chapter extended the validation of the biostatic effect of the amber+green light to mineral substrates, thus reinforcing use of the lighting set-up as a preventive conservation technology beyond membrane-growth SABs in the laboratory.

In conclusion to ***Part 2*** of the research, the study presented in **Chapter 6** consisted of the long-term validation of the biostatic effect of the amber+green lighting: monitoring conducted in the inner courtyard of the *Pazo de Raxoi* (a granite-built neoclassical monument currently city council buildings of Santiago de Compostela) over a period of 3.4 years. The effect of amber+green light on algal SABs (mainly composed by *Myrmecia irregularis*, with some cyanobacteria and diatoms) growing on granite ashlars was compared with the effects of a metal halide lamp (4668 K) (used until now to illuminate monuments in Santiago de Compostela) and of an unilluminated control. Non-destructive techniques (PAM chlorophyll fluorometry and colour spectrophotometry) were applied, and the data were analysed using advanced non-parametric statistical tests. The trends in all chlorophyll fluorescence and colour parameters were found to be consistent. The minimum chlorophyll fluorescence (F_0) measured by PAM fluorometry was used as a proxy for SAB growth. The findings showed that, although the SAB initially grew under the amber+green light, it stabilized at the same level as the unilluminated control, while the SAB under metal halide light continued to grow further, which validated the biostatic effect of amber+green light on the walls of an outdoor granite building (real case). The quantum yield of the SABs was unaffected by the ornamental lighting conditions but fluctuated according to the environmental conditions throughout the year.

The research presented in **Chapter 7**, also carried out in the inner courtyard of the *Pazo de Raxoi*, focused on the shifts caused by the ornamental lighting (same lighting set-up as described in **Chapter 6**) on the bacterial and fungal communities. Sequencing of culturable fractions of microbiome and whole-genome sequencing (metabarcoding) were conducted using Oxford Nanopore Sequencing (MinION). The possible biodeteriorative profiles of the isolated strains were determined relative to calcium carbonate precipitation/solubilisation and iron oxidation/reduction by plate assays. Alpha and beta diversity indexes were also determined. As the masonry walls were treated in 2018 with a glyphosate-based biocide, the abundance of biocide and antibiotic resistance genes was also determined. Culture-dependent microbiological analysis did not reveal any changes in community composition. However, some of the isolates yielded positive biodeteriorative profiles for precipitation and solubilisation of calcium carbonate. The bacterial isolate identified as *Pantoea* sp. tested positive for iron oxidation. The MinION analysis identified shifts in the granite microbiome elicited by ornamental lighting, and the bacterial and fungal communities corresponding to the amber+green light and the unilluminated control were more similar than that produced under the metal halide lamp. Bacteria predominated

in the samples illuminated by the metal halide lamp, and the presence of fungi was negligible.

The objective of the study reported in **Chapter 8** was to assess whether the use of amber+green light reduces the attraction of insects towards ornamental lighting as it avoids the emission of high energy wavelengths (mainly 400 – 500 nm blue wavelengths), typically known to disrupt nocturnal insect communities. The study was again conducted in the inner courtyard of the *Pazo de Raxoi* and with the same lighting set-up as described in Chapter 6. Grey sticky board traps were positioned under the amber+green lamp, and the number and diversity of insects trapped under this lamp, under the metal halide lamp and in an unilluminated area were compared. Insects were captured between June and October 2021, coinciding with the main period of activity. The sticky traps were removed and replaced after 5–16 days, depending on the number of insects trapped on the board and the environmental conditions. The amber+green light greatly reduced attraction to the light, to levels similar to the unilluminated area. This effect has been demonstrated for almost all orders of the insects trapped, especially Diptera, Lepidoptera, Coleoptera, Hemiptera and Hymenoptera. By contrast, members of the order Psocoptera were attracted in a similar way to the amber+green light and to the metal halide lamp. The metal halide lamp attracted a greater number and diversity of insects than the other two types of light. Thus, the amber+green light was validated as an environmentally-sound technology for nocturnal biodiversity by fine-tuning the spectral emission.

Given the impact of nocturnal ornamental lighting on the lithobionts (as demonstrated in the previous chapters), the presence of which leads to biofouling, the study reported in **Chapter 9** evaluated the carbon footprint and economic cost of the lighting and associated biofouling control. A case study was conducted in the *Casa do Cabildo*, a granite-built baroque style historic house facing the *Praza de Praterías* in Santiago de Compostela. The UNE-EN ISO 14067 standard for carbon footprint quantification and cost analysis tools were used to measure the expected improved environmental and economic performance of the CromaLux lighting system (a warm white light used for a short period of time followed by the amber+green light) in comparison the traditional metal halide and white LED systems. Five cleaning methods (laser, water vapour, Biotin T®, Biotin R® and reinforced ethanol) were simulated under the three lighting systems for comparison of the carbon footprint and associated cost. The CromaLux lighting system outperformed the metal halide and white LED systems (reducing carbon footprint by 80% and 20%, respectively). Laser cleaning had the lowest carbon footprint of all methods, and the reinforced ethanol method had the lowest carbon footprint among the chemical cleaning methods. However, this cleaning method was costly as a greater volume of liquid was required to achieve the same level of cleaning efficacy as Biotin T® and Biotin R®. Based on the estimations reported in this chapter, SAB cleaning could be delayed between 1.5 to 6 years by using the CromaLux lighting system. Although the reduction in carbon footprint and cost achieved with the CromaLux lighting system is

low for the example of *Casa do Cabildo*, substantial savings could possibly be made by implementing the system at city level. The findings thus confirm the advantages of CromaLux lighting system for improving the environmental and economic sustainability of illuminating and cleaning architectural heritage.

Finally, as described in **Chapter 10**, environmental psychology methods were used to assess the public perception and acceptance of the amber+green light and to obtain information that could be applied in the design of strategies aimed at overcoming reluctance to acceptance of this technology. Photographic material of the *Casa do Cabildo* with ornamental illumination was utilised. The images were digitally modified to illustrate three light qualities (cool white, warm white and amber+green light) projected on a clean main facade and one affected by simulated biofouling. The research was conducted in two phases. A first qualitative study based on discussion sessions with experts and representatives from neighbourhood associations highlighted key points regarding the perception of problems with building deterioration and attitudes towards the amber+green light. Participants in the first, qualitative study expressed interest in heritage conservation and agreed that information, trust in science and habituation could lead to acceptance of the amber+green light. However, participants preferred the warm white light to the amber+green light, with this preference appearing to be explained by traditional views regarding ornamental lighting. Experts tended to be more cautious than the representatives of neighbourhood associations and expressed concerns about the efficacy and suitability of the white lighting from the perspective of the urban image. A second study was then conducted to quantify the preference regarding the three types of lighting and general attitudes towards the amber+green light. This quantitative study also included how different types of message - transmitted using the images of the clean facade and of the facade affected by biofouling - affected acceptance of the amber+green light. The study participants showed neutral attitudes towards the amber+green light, despite its lower visual appeal. In addition, the messages transmitted (images) did not alter the lighting preference. The study also revealed that participants with strong attachment to the area were more likely to choose the amber+green light in preference to either of the white lights. Moreover, strong social identification with the community increased the attitudes that people had about the amber+green light. Thus, raising awareness of the conservation benefits, fostering community and place identity were identified as strategies for enhancing acceptance of the amber+green light, which is switched on for longer than the another warm white light used before in the CromaLux system and is the most important (owing to its biostatic effect).

Resumen

La iluminación ornamental se utiliza cada vez más en pueblos y ciudades durante la noche para resaltar el valor estético del patrimonio arquitectónico (entendido aquí como monumentos, conjuntos arquitectónicos y sitios de interés histórico, arqueológico, artístico, científico, social o técnico). Los planes de iluminación suelen priorizar la estética, la eficiencia energética y el cumplimiento de las directrices ambientales, intentando también mitigar la contaminación lumínica; sin embargo, generalmente pasan por alto el impacto de la luz sobre los litobiontes fototróficos que crecen en las superficies iluminadas. La roca granítica (ígnea e intrusiva), el sustrato geológico predominante en el patrimonio arquitectónico de Galicia (NO de España), es susceptible a la meteorización física, química y biológica, a pesar de su resistencia y durabilidad. Las biopelículas (o *biofilms* en inglés) subaéreas fototróficas (SABs por sus siglas en inglés), compuestas principalmente por algas y, en menor medida, por cianobacterias, además de bacterias y hongos heterótrofos, son comunes en el patrimonio arquitectónico gallego por su clima. El clima en Galicia se clasifica como oceánico o atlántico, según la zonificación agroecológica de la FAO, y la alta humedad típica está causada por abundantes precipitaciones y temperaturas suaves durante todo el año. Estudios previos han demostrado que el crecimiento de fotótrofos en el patrimonio arquitectónico puede verse favorecido por la exposición nocturna a luz artificial que incluya longitudes de onda que estimulen la fotosíntesis. Este crecimiento incrementado aumenta el potencial papel biodeteriorante de los SABs, aunque sea sólo estético, sobre los materiales pétreos.

El objetivo general del proyecto CromaLux (2020–2024) fue desarrollar un sistema de iluminación ornamental energéticamente eficiente y ambientalmente sostenible con capacidad biostática, es decir, con la funcionalidad de detener el crecimiento de SABs fototróficos. Este novedoso sistema de iluminación ornamental se propone, por tanto, como una herramienta de conservación preventiva que aprovecha la infraestructura de la iluminación pública existente para iluminar monumentos construidos en piedra, consiguiendo realzar la belleza y el valor artístico del patrimonio arquitectónico mediante iluminación ornamental mientras reduce los costes de mantenimiento. La capacidad biostática del sistema se logra mediante el uso de una combinación de luces LED ámbar (593 nm) y verde (528 nm) de banda estrecha, que emiten luz en longitudes de onda débilmente absorbidas por los principales pigmentos fotosintéticos: clorofilas y carotenoides. Los espectros de absorción de estos pigmentos presentan picos en la parte azul del espectro visible, en 372-392 nm para las clorofilas y 448 nm para el β-caroteno, y en la parte roja, en 626-642 nm para las clorofilas. Por tanto, se espera que la luz

ámbar+verde tenga una baja eficiencia fotosintética y reduzca el crecimiento de los SABs (y potencialmente ejerza estrés sobre ellos) en comparación con las fuentes de luz blanca tradicionales. El espectro bimodal resultante de la combinación de luces LED ámbar y verde (en adelante ámbar+verde) presenta una apariencia blanca (3000 K) para el ojo humano, ya que la iluminación coloreada está generalmente muy desaconsejada para la iluminación ornamental permanente en espacios urbanos por razones estéticas. Para cumplir los requisitos de eficiencia energética, el sistema CromaLux utiliza también una luz LED blanca cálida altamente eficiente con un componente azul muy bajo durante las primeras horas de la noche, y antes del uso de la novedosa luz biostática ámbar+verde.

El proyecto CromaLux se llevó a cabo en Santiago de Compostela (Galicia, Ciudad Patrimonio de la Humanidad por la UNESCO desde 1985) por las empresas Televés S.A.U. y Ferrovial Energía S.A. (anteriormente Ferrovial Servicios S.A.) y la Universidad de Santiago de Compostela (USC). El proyecto formó parte de la iniciativa SMARTiAGO de compra pública innovadora, orientada a desarrollar soluciones tecnológicas innovadoras en el marco de las ciudades inteligentes, con el objetivo de abordar retos específicos de ciudades patrimoniales como Santiago de Compostela. Esta tesis doctoral (2020-2025), enmarcada en el mencionado proyecto CromaLux, se llevó a cabo dentro de un programa de Doctorado Industrial, en colaboración entre Ferrovial Energía S.A. y la USC. La investigación, que también cumple los requisitos para la mención internacional, es relevante y oportuna, en consonancia con las políticas y marcos europeos, considerando que la sostenibilidad en la preservación del patrimonio construido en piedra implica tanto la conservación de la piedra como el respeto al contexto ecológico, permitiendo así la conservación conjunta del patrimonio natural y cultural. El estudio tuvo como primer objetivo validar la capacidad biostática de la iluminación ámbar+verde a corto y medio plazo (en experimentos de laboratorio) y a largo plazo (en campo). La investigación también buscó validar el impacto ambientalmente sostenible de la novedosa iluminación sobre la biodiversidad, así como evaluar su eficiencia energética y su percepción estética y social, mediante un enfoque integral y holístico. La investigación se dividió en cuatro partes específicas:

En la ***Parte 1*** (**Capítulo 1**) se examinó el marco legislativo que regula la iluminación ornamental del patrimonio arquitectónico, con especial atención a la normativa española, para evaluar el impacto de las políticas de iluminación sobre la contaminación lumínica y el medio ambiente. La ***Parte 2*** (**Capítulos 2 a 6**) se centró en validar la capacidad biostática (funcionalidad para detener el crecimiento) de la iluminación ámbar+verde y en dilucidar los mecanismos de acción de las respuestas fisiológicas a la iluminación ornamental de los SABs fototróficos presentes en las superficies del patrimonio arquitectónico. En la ***Parte 3*** (**Capítulos 7 y 8**) se estudió el impacto de la iluminación ornamental sobre la biodiversidad, considerando la microbiota bacteriana y fúngica que habita en el patrimonio construido en granito y también la biodiversidad circundante de insectos nocturnos. Finalmente, en la ***Parte 4*** (**Capítulos 9 y 10**) se evaluó el impacto

ambiental y económico de la iluminación ornamental, centrándose en el sistema de iluminación CromaLux y también en la respuesta pública a la luz ámbar+verde, con vistas a diseñar estrategias de implementación.

La iluminación de monumentos en áreas urbanas es una contribución emergente a la contaminación lumínica que apenas se ha considerado hasta la fecha. Tal como se describe en el **Capítulo 1**, se realizó una revisión bibliográfica sobre el tema de la contaminación lumínica y las políticas relacionadas entre 2020 y 2022. La revisión permitió evaluar la legislación vigente que regula el uso de iluminación ornamental tanto en España como en Europa y examinó las tendencias en la iluminación de monumentos y la formulación de políticas orientadas a una gestión ambientalmente sostenible. Se concluyó que las discrepancias en la definición de contaminación lumínica se extienden a las políticas y regulaciones, las cuales deberían actualizarse para permitir el desarrollo de nuevas tecnologías de iluminación. La regulación de la iluminación ornamental debe equilibrar energía, medio ambiente y la mejora y conservación de los monumentos pétreos, lo que puede lograrse implementando los hallazgos de investigaciones recientes en ciencias del patrimonio.

La investigación descrita en el **Capítulo 2** se centró en examinar la duración de la iluminación ornamental con el objetivo de ejercer un efecto biostático sobre los SABs. SABs cultivados en laboratorio (derivados de un SAB algal que colonizaba un monumento construido en granito) fueron sometidos a 16 horas de luz diurna seguidas por fotoperíodos respectivamente de 2, 4, 6 y 8 horas de iluminación ornamental LED roja, verde, azul y blanca cálida (incluyendo un control sin iluminación ornamental); el fotoperíodo de 24 h se completó con el número correspondiente de horas de oscuridad en cada caso. El crecimiento de los SABs se evaluó tras 35 días mediante cuantificación de biomasa y pigmentos fotosintéticos, conteo celular y fluorometría de clorofila PAM. Se encontró que la exposición entre 4 y 6 horas a luz roja o luz verde fue suficiente para reducir la biomasa del SAB (en términos de biomasa húmeda y conteo celular), mientras que la exposición a 8 horas de luz azul promovió un mayor crecimiento. Tanto las luces LED roja como verde causaron una marcada disminución en la biomasa de algas verdes, pero aumentaron la biomasa de cianobacterias. Los hallazgos descritos en este capítulo se utilizaron para determinar la duración de iluminación con luz ámbar+verde necesaria para lograr un efecto biostático, siguiendo también las regulaciones sobre iluminación artificial en Santiago de Compostela.

Los monumentos exteriores están obviamente expuestos a la luz diurna, y la investigación descrita en el **Capítulo 3** tuvo como objetivo investigar si la eficacia de la iluminación ámbar+verde como herramienta biostática para controlar la colonización fototrófica en el patrimonio arquitectónico está influenciada por diferentes niveles de iluminancia diurna. Fotoperíodos de 13 horas con dos niveles de iluminancia diurna (baja, LDI, ~2050 lx y alta, HDI, ~10200 lx; basados en mediciones de campo) fueron seguidos por iluminación ornamental LED blanca fría (4300 K), blanca cálida (2580 K) y

ámbar+verde (3000 K) (incluyendo también un control sin iluminación ornamental) y por 5 horas de oscuridad. Tras 37 días de exposición a este régimen lumínico, el crecimiento de SABs producidos en laboratorio (compuestos principalmente por *Chlorella vulgaris*, *Klebsormidium flaccidum* y *Synechocystis* sp.) se evaluó mediante mediciones de biomasa y diversidad, perfil bioquímico (cuantificación de pigmentos fotosintéticos, EPS y contenido de ATP), microscopía confocal y fluorometría de clorofila PAM. La capacidad biostática de la luz ámbar+verde se verificó bajo condiciones LDI y HDI, ya que el rendimiento de biomasa del SAB se redujo y la producción tanto de exopolisacáridos como de proteínas extracelulares fue menor que bajo luces blanca fría y cálida. La biomasa de los SABs que crecían en el montaje HDI fue mayor que la producida bajo LDI. Ninguna de las condiciones de iluminación ornamental logró alterar el perfil bioquímico (en términos de contenido de clorofila, exopolisacáridos y proteínas extracelulares) bajo HDI. La iluminancia HDI también produjo una disminución en el rendimiento cuántico de los SABs bajo todas las condiciones de iluminación ornamental. Tanto la luz blanca cálida como la ámbar+verde disminuyeron la abundancia relativa de *Klebsormidium flaccidum* en la condición LDI. Los hallazgos descritos en este capítulo validaron el uso de la nueva luz biostática en exposición solar variable, lo cual es particularmente importante en entornos urbanos debido a la morfología urbana y/o factores climáticos.

Con el objetivo de dilucidar los mecanismos de acción subyacentes al efecto biostático, el estudio de laboratorio descrito en el **Capítulo 4** investigó la influencia de tres tipos de iluminación LED utilizados para iluminar monumentos (blanca fría, blanca cálida y ámbar+verde) sobre el crecimiento de los SABs. La proteómica ambiental proporcionó información sobre los cambios en el metabolismo del SAB bajo el estrés infligido por la iluminación nocturna, mediante la cuantificación e identificación de péptidos en proteínas expresadas por los microorganismos que forman los SABs. El análisis consideró los cambios en la composición de especies y en la composición proteína/péptido en los SABs. Se encontró que la iluminación ámbar+verde tuvo el efecto inhibidor más fuerte sobre los cultivos de SAB, detectado a través de un impacto negativo en los fotosistemas I y II y en la producción de proteínas tipo antena del fotosistema. En particular, la luz ámbar+verde afectó la producción de la subunidad PsbO del fotosistema II, que cataliza la división del agua en O_2 y $4H^+$ y es necesaria para iniciar la cadena de transporte de electrones para la síntesis de ATP y NADPH en la fotosíntesis. La luz biostática también tuvo un efecto desencadenante sobre el metabolismo proteico (síntesis, plegamiento y degradación) e indujo la síntesis de proteínas de choque térmico relacionadas con el estrés. Asimismo, la exposición a la luz blanca cálida causó un aumento en el número de péptidos relacionados con las estructuras y pigmento (ficobilisomas y ficocianina) de las cianobacterias. El efecto biostático, inicialmente estudiado utilizando biopelículas cultivadas sobre membranas (**Capítulos 2 a 4**), también se evaluó utilizando bloques de muestra de diferentes sustratos (**Capítulo 5**). El granito (el principal material de construcción utilizado en el patrimonio arquitectónico de Galicia y otras regiones del mundo) y el mortero de cemento (ampliamente utilizado en construcción, especialmente en arquitectura moderna y

contemporánea) se emplearon como sustratos de ensayo. Los SABs (compuestos principalmente por las algas verdes *Bracteacoccus minor* y *Stichococcus bacillaris*) se desarrollaron sobre los bloques de granito y cemento en una cascada de flujo diseñada a medida. Las muestras se expusieron, durante un período de 3 meses, a un montaje de iluminación compuesto por 13 horas de luz diurna, 6 horas de iluminación ornamental LED (blanca fría, blanca cálida y ámbar+verde, respectivamente) y 5 horas de oscuridad. También se incluyeron controles sin iluminación ornamental y sin colonización (bloques de granito y cemento sin SAB). La interfaz SAB-mineral expuesta a luz ámbar+verde se comportó de manera similar al control sin iluminación ornamental, minimizando los efectos de la iluminación ornamental en comparación con ambas luces blancas probadas en términos de desviaciones de rugosidad, valores de dureza Leeb, ángulo de contacto estático, tiempo de absorción de agua y diferencias de color. Las mediciones de color también indicaron que la luz ámbar+verde redujo el crecimiento de los SABs en comparación con el observado bajo las luces blancas, particularmente en términos de la coordenada amarillenta-azulada (b*) del espacio CIELAB. El análisis petrográfico también reveló una cobertura algal dependiente del mineral en el granito. Los resultados descritos en este capítulo ampliaron la validación del efecto biostático de la luz ámbar+verde a sustratos minerales, reforzando así el uso del montaje lumínico como tecnología de conservación preventiva más allá de los SABs cultivados sobre membranas en laboratorio.

Para concluir la ***Parte 2*** de la investigación, el estudio presentado en el **Capítulo 6** consistió en la validación a largo plazo del efecto biostático de la iluminación ámbar+verde: una monitorización realizada en el patio interior del *Pazo de Raxoi* (un monumento neoclásico construido en granito que actualmente alberga las dependencias del Ayuntamiento de Santiago de Compostela) durante un período de 3,4 años. El efecto de la luz ámbar+verde sobre los SABs algales (compuestos principalmente por *Myrmecia irregularis*, con algunas cianobacterias y diatomeas) que crecían sobre sillares de granito se comparó con los efectos de una lámpara de halogenuros metálicos (4668 K) (utilizada hasta ahora para iluminar monumentos en Santiago de Compostela) y con un control sin iluminación. Se aplicaron técnicas no destructivas (fluorometría de clorofila PAM y espectrofotometría de color), y los datos se analizaron mediante pruebas estadísticas avanzadas no paramétricas. Se encontró que las tendencias en todos los parámetros de fluorescencia de clorofila y color fueron consistentes. La fluorescencia mínima de clorofila (F_0) medida mediante fluorometría PAM se utilizó como variable *proxy* del crecimiento del SAB. Los resultados mostraron que, aunque el SAB creció inicialmente bajo la luz ámbar+verde, se estabilizó al mismo nivel que el control sin iluminación, mientras que el SAB bajo luz de halogenuros metálicos continuó creciendo, lo que validó el efecto biostático de la luz ámbar+verde en las paredes de un edificio de granito en exteriores (caso real). El rendimiento cuántico de los SABs no se vio afectado por las condiciones de iluminación ornamental, pero fluctuó según las condiciones ambientales a lo largo del año.

La investigación presentada en el **Capítulo 7**, también realizada en el patio interior del *Pazo de Raxoi*, se centró en los cambios causados por la iluminación ornamental (el mismo montaje lumínico descrito en el **Capítulo 6**) en las comunidades bacterianas y fúngicas. Se llevó a cabo la secuenciación de fracciones cultivables del microbioma y la secuenciación de genoma completo (*metabarcoding*) utilizando *Oxford Nanopore Sequencing* (MinION). Los posibles perfiles biodeteriorantes de las cepas aisladas se determinaron en relación con la precipitación/solubilización de carbonato cálcico y la oxidación/reducción de hierro mediante ensayos en placa. También se determinaron índices de diversidad alfa y beta. Como las paredes de mampostería fueron tratadas en 2018 con un biocida conteniendo el herbicida glifosato, también se determinó la abundancia de genes de resistencia a biocidas y antibióticos. El análisis microbiológico dependiente de cultivo no reveló cambios en la composición de la comunidad. Sin embargo, algunos aislados presentaron perfiles biodeteriorantes positivos para la precipitación y solubilización de carbonato cálcico. El aislado bacteriano identificado como *Pantoea* sp. dio positivo para la oxidación de hierro. El análisis MinION identificó cambios en el microbioma del granito inducidos por la iluminación ornamental, y las comunidades bacterianas y fúngicas correspondientes a la luz ámbar+verde y al control sin iluminación fueron más similares entre sí que las producidas bajo la lámpara de halogenuros metálicos. Las bacterias predominaron en las muestras iluminadas por la lámpara de halogenuros metálicos mientras la presencia de hongos fue prácticamente nula.

El objetivo del estudio presentado en el **Capítulo 8** fue evaluar si el uso de luz ámbar+verde reduce la atracción de insectos hacia la iluminación ornamental, ya que evita la emisión de longitudes de onda de alta energía (principalmente entre 400 y 500 nm, correspondientes a la luz azul), típicamente conocidas por alterar las comunidades de insectos nocturnos. El estudio se realizó nuevamente en el patio interior del *Pazo de Raxoi* y con el mismo montaje lumínico descrito en el **Capítulo 6**. Se colocaron trampas adhesivas grises bajo la lámpara ámbar+verde, y se comparó el número y la diversidad de insectos atrapados bajo esta lámpara, bajo la lámpara de halogenuros metálicos y en una zona sin iluminación. Los insectos se capturaron entre junio y octubre de 2021, coincidiendo con el principal período de actividad. Las trampas adhesivas se retiraron y reemplazaron cada 5–16 días, dependiendo del número de insectos atrapados y de las condiciones ambientales. La luz ámbar+verde redujo considerablemente la atracción hacia la luz, a niveles similares a la zona sin iluminación. Este efecto se demostró en casi todos los órdenes de insectos atrapados, especialmente Diptera, Lepidoptera, Coleoptera, Hemiptera y Hymenoptera. Por el contrario, los miembros del orden Psocoptera mostraron una atracción similar hacia la luz ámbar+verde y hacia la lámpara de halogenuros metálicos. La lámpara de halogenuros metálicos atrajo un mayor número y diversidad de insectos que los otros dos tipos de luz (ámbar+verde y sin iluminación). Así, la luz ámbar+verde se validó como una tecnología ambientalmente sostenible para la biodiversidad nocturna mediante el ajuste fino de la emisión espectral.

Dado el impacto de la iluminación ornamental nocturna sobre los litobiontes (como se ha demostrado en los capítulos anteriores), cuya presencia conduce a la formación de *biofouling*, el estudio presentado en el **Capítulo 9** evaluó la huella de carbono y el coste económico de la iluminación y del control asociado del *biofouling*. Se realizó un estudio de caso en la *Casa do Cabildo*, una casa histórica de estilo barroco construida en granito frente a la *Praza de Praterías* en Santiago de Compostela. Se empleó la norma UNE-EN ISO 14067 para la cuantificación de la huella de carbono y herramientas de análisis de costes para medir el rendimiento ambiental y económico esperado del sistema de iluminación CromaLux (una luz blanca cálida utilizada durante un corto período seguida de la luz ámbar+verde) en comparación con los sistemas tradicionales de halogenuros metálicos y LED blanco. Se simularon cinco métodos de limpieza (láser, vapor de agua, Biotin T®, Biotin R® y etanol reforzado) bajo los tres sistemas de iluminación para comparar la huella de carbono y el coste asociado. El sistema de iluminación CromaLux superó a los sistemas de halogenuros metálicos y LED blanco (reduciendo la huella de carbono en un 80% y un 20%, respectivamente). La limpieza láser tuvo la menor huella de carbono de todos los métodos de limpieza, y el método con etanol reforzado tuvo la menor huella entre los métodos de limpieza químicos. Sin embargo, este método resultó costoso, ya que se requirió un mayor volumen de líquido para lograr el mismo nivel de eficacia que Biotin T® y Biotin R®. Según las estimaciones presentadas en este capítulo, la limpieza de SABs podría retrasarse entre 1,5 y 6 años mediante el uso del sistema CromaLux. Aunque la reducción de huella de carbono y coste lograda con el sistema CromaLux es baja para el ejemplo de la *Casa do Cabildo*, los posibles ahorros si se implementa a nivel ciudad podrían ser sustanciales para el municipio. Los hallazgos confirman así las ventajas del sistema CromaLux para mejorar la sostenibilidad ambiental y económica de la iluminación y limpieza del patrimonio arquitectónico.

Finalmente, tal como se describe en el **Capítulo 10**, se emplearon métodos de psicología ambiental para evaluar la percepción y aceptación pública de la luz ámbar+verde y obtener información que pudiera aplicarse en el diseño de estrategias destinadas a superar la reticencia a aceptar esta tecnología. Se utilizó material fotográfico de la *Casa do Cabildo* con iluminación ornamental. Las imágenes se modificaron digitalmente para ilustrar tres calidades de luz (blanca fría, blanca cálida y luz ámbar+verde) proyectadas sobre una fachada principal limpia y otra afectada por *biofouling* simulado. La investigación se realizó en dos fases. Un primer estudio cualitativo, basado en sesiones de discusión con expertos y representantes de asociaciones vecinales, destacó puntos clave sobre la percepción de problemas de deterioro de edificios y actitudes hacia la luz ámbar+verde. Los participantes en el estudio cualitativo expresaron interés en la conservación del patrimonio y coincidieron en que la información, la confianza en la ciencia y la habituación podrían conducir a la aceptación de la luz ámbar+verde. Sin embargo, los participantes prefirieron la luz blanca cálida frente a la luz ámbar+verde, una preferencia que parece explicarse por visiones tradicionales sobre la iluminación ornamental. Los expertos tendieron a ser más cautelosos que los

representantes de asociaciones vecinales y expresaron preocupaciones sobre la eficacia y la idoneidad de la luz desde la perspectiva de la imagen urbana. Posteriormente, se realizó un segundo estudio para cuantificar la preferencia respecto a los tres tipos de iluminación y las actitudes generales hacia la luz ámbar+verde. Este estudio cuantitativo también incluyó cómo diferentes tipos de mensajes, transmitidos mediante imágenes de la fachada limpia y de la fachada afectada por *biofouling*, afectaron la aceptación de la luz ámbar+verde. Los participantes mostraron actitudes neutras hacia la luz ámbar+verde, a pesar de su menor atractivo visual. Además, los mensajes transmitidos (imágenes) no alteraron la preferencia de iluminación. El estudio también reveló que los participantes con fuerte apego al lugar tenían más probabilidades de elegir la luz ámbar+verde frente a cualquiera de las luces blancas. Asimismo, una alta identificación social con la comunidad aumentó las actitudes positivas hacia la luz ámbar+verde. Por tanto, aumentar la concienciación sobre los beneficios de la conservación y fomentar la identidad comunitaria y del lugar fueron identificadas como estrategias para mejorar la aceptación de la luz ámbar+verde, que permanece encendida durante más tiempo que la otra luz blanca cálida utilizada anteriormente en el sistema CromaLux y es la más importante (debido a su efecto biostático).

Resumo

A iluminación ornamental utilízase cada vez máis en vilas e cidades durante a noite para resaltar o valor estético do patrimonio arquitectónico (entendido aquí como monumentos, conxuntos arquitectónicos e sitios de interese histórico, arqueolóxico, artístico, científico, social ou técnico). Os plans de iluminación adoitan priorizar a estética, a eficiencia enerxética e o cumprimento das directrices ambientais, intentando tamén mitigar a contaminación lumínica; porén, xeralmente pasan por alto o impacto da luz sobre os litobiontes fototróficos que medran nas superficies iluminadas. A rocha granítica (ígnea e intrusiva), o substrato xeolóxico predominante no patrimonio arquitectónico de Galicia (NO de España), é susceptible á meteorización física, química e biolóxica, a pesar da súa resistencia e durabilidade. As biopelículas (ou *biofilms* en inglés) subaéreas fototróficas (SABs polas súas siglas en inglés), compostas principalmente por algas e, en menor medida, por cianobacterias, ademais de bacterias e fungos heterótrofos, son comúns no patrimonio arquitectónico galego polo seu clima. O clima en Galicia clasifícase como oceánico ou atlántico, segundo a zonificación agroecolóxica da FAO, e a alta humidade típica está causada por abundantes precipitacións e temperaturas suaves durante todo o ano. Estudos previos demostraron que o crecemento de fotótrofos no patrimonio arquitectónico pode verse favorecido pola exposición nocturna a luz artificial que inclúa lonxitudes de onda que estimulen a fotosíntese. Este crecemento incrementado aumenta o potencial papel biodeteriorante dos SABs, aínda que sexa só estético, sobre os materiais pétreos.

O obxectivo xeral do proxecto CromaLux (2020–2024) foi desenvolver un sistema de iluminación ornamental enerxeticamente eficiente e ambientalmente sostible con capacidade biostática, é dicir, a funcionalidade de deter o crecemento dos SABs fototróficos. Este innovador sistema de iluminación ornamental proponse, por tanto, como unha ferramenta de conservación preventiva que aproveita a infraestrutura de iluminación pública existente para iluminar monumentos construídos en pedra, realzando a beleza e o valor artístico do patrimonio arquitectónico mediante iluminación ornamental mentres reduce os custos de mantemento. A capacidade biostática do sistema lógrase mediante o uso dunha combinación de luces LED ámbar (593 nm) e verde (528 nm) de banda estreita, que emiten luz en lonxitudes de onda débilmente absorbidas polos principais pigmentos fotosintéticos: clorofilas e carotenoides. Os espectros de absorción destes pigmentos presentan picos na parte azul do espectro visible, en 372-392 nm para as clorofilas e 448 nm para o β-caroteno, e na parte vermella, en 626-642 nm para as clorofilas. Por tanto, espérase que a luz ámbar+verde teña unha baixa eficiencia fotosintética e reduza o crecemento dos SABs (e potencialmente exerza estrés sobre eles) en comparación coas fontes de luz branca

tradicionais. O espectro bimodal resultante da combinación de luces LED ámbar e verde (en diante ámbar+verde) presenta unha aparencia branca (3000 K) para o ollo humano, xa que a iluminación coloreada está xeralmente moi desaconsellada para a iluminación ornamental permanente en espazos urbanos por razóns estéticas. Para cumprir os requisitos de eficiencia enerxética, o sistema CromaLux utiliza tamén unha luz LED branca cálida altamente eficiente cun compoñente azul moi baixo durante as primeiras horas da noite, e antes do uso da nova luz biostática ámbar+verde.

O proxecto CromaLux levouse a cabo en Santiago de Compostela (Galicia, Cidade Patrimonio da Humanidade pola UNESCO desde 1985) polas empresas Televés S.A.U. e Ferrovial Energía S.A. (anteriormente Ferrovial Servicios S.A.) e a Universidade de Santiago de Compostela (USC). O proxecto formou parte da iniciativa SMARTiAGO de compra pública innovadora, orientada a desenvolver solucións tecnolóxicas innovadoras no marco das cidades intelixentes, co obxectivo de abordar retos específicos de cidades patrimoniais como Santiago de Compostela. Esta tese doutoral (2020-2025), enmarcada no mencionado proxecto CromaLux, levouse a cabo dentro dun programa de Doutoramento Industrial, en colaboración entre Ferrovial Energía S.A. e a USC. A investigación, que tamén cumpre os requisitos para a mención internacional, é relevante e oportuna, en consonancia coas políticas e marcos europeos, considerando que a sustentabilidade na preservación do patrimonio construído en pedra implica tanto a conservación da pedra como o respecto ao contexto ecolóxico, permitindo así a conservación conxunta do patrimonio natural e cultural. O estudo tivo como primeiro obxectivo validar a capacidade biostática da iluminación ámbar+verde a curto e medio prazo (en experimentos de laboratorio) e a longo prazo (en campo). A investigación tamén buscou validar o impacto ambientalmente sostible da nova iluminación sobre a biodiversidade, así como avaliar a súa eficiencia enerxética e a súa percepción estética e social, mediante un enfoque integral e holístico. A investigación dividiuse en catro partes específicas:

Na ***Parte 1*** (**Capítulo 1**) examinouse o marco lexislativo que regula a iluminación ornamental do patrimonio arquitectónico, con especial atención á normativa española, para avaliar o impacto das políticas de iluminación sobre a contaminación lumínica e o medio ambiente. A ***Parte 2*** (**Capítulos 2 a 6**) centrouse en validar a capacidade biostática (funcionalidade para deter o crecemento) da iluminación ámbar+verde e en dilucidar os mecanismos de acción das respostas fisiolóxicas á iluminación ornamental dos SABs fototróficos presentes nas superficies do patrimonio arquitectónico. Na ***Parte 3*** (**Capítulos 7 e 8**) estudouse o impacto da iluminación ornamental sobre a biodiversidade, considerando a microbiota bacteriana e fúngica que habita no patrimonio construído en granito e tamén a biodiversidade circundante de insectos nocturnos. Finalmente, na ***Parte 4*** (**Capítulos 9 e 10**) avaliouse o impacto ambiental e económico da iluminación ornamental, centrándose no sistema de iluminación CromaLux e tamén na resposta pública á luz ámbar+verde, con vistas a deseñar estratexias de implementación.

A iluminación de monumentos en áreas urbanas é un contribuínte emerxente á contaminación lumínica que apenas se tivo en conta ata a data. Así, o **Capítulo 1** presenta unha revisión bibliográfica (entre 2020 e 2022) sobre o tema da contaminación lumínica e as políticas relacionadas, e analiza a lexislación vixente que regula o uso da iluminación ornamental en Europa e España, considerando as tendencias na iluminación de monumentos e a formulación de políticas cara a unha xestión ambientalmente sostible. Este capítulo de revisión atopou que as discrepancias na definición de contaminación lumínica se estenden ás políticas e regulacións, as cales deberían actualizarse conforme ao desenvolvemento de novas tecnoloxías de iluminación. A regulación da iluminación ornamental debe equilibrar enerxía, medio ambiente e a mellora e conservación dos monumentos pétreos, o que pode lograrse seguindo a investigación actual en ciencias do patrimonio.

O **Capítulo 2** centrouse en examinar a duración da iluminación ornamental para acadar un efecto biostático sobre os SABs. SABs cultivados en laboratorio (derivados dunha biopelícula algal naturalmente desenvolvida nun monumento construído en granito) foron sometidos a 16 horas de luz diurna seguidas por fotoperíodos respectivos de 2, 4, 6 e 8 horas de luz ornamental LED vermella, verde, azul e branca cálida (incluíndo un control sen iluminación ornamental), completando as 24 horas diarias con escuridade segundo o fotoperíodo de luz ornamental. O desenvolvemento dos SABs tras 35 días de crecemento avaliouse mediante cuantificación de biomasa e pigmentos fotosintéticos, reconto celular e fluorometría de clorofila PAM. Os resultados mostraron que 4 a 6 horas de luz vermella ou verde foron suficientes para reducir o rendemento de biomasa nos SABs (en termos de biomasa húmida e reconto celular), mentres que 8 horas de luz azul promoveron un maior crecemento. Tanto as luces LED vermella como verde causaron unha marcada diminución na abundancia de células de algas verdes, pero aumentaron as cianobacterias. Os resultados deste capítulo permitiron determinar o tempo de iluminación axeitado para acadar o efecto biostático coa luz ámbar+verde, seguindo tamén a normativa sobre iluminación artificial en Santiago de Compostela.

Dado que a luz diurna é unha fonte inevitable nos monumentos exteriores, o Capítulo 3 tivo como obxectivo investigar se a efectividade da iluminación ámbar+verde como ferramenta biostática para controlar a colonización fototrófica no patrimonio arquitectónico está influenciada por diferentes niveis de iluminancia diurna. Fotoperíodos de 13 horas con dous niveis de iluminancia diurna (baixa, LDI, ~2050 lx e alta, HDI, ~10200 lx; baseados en medicións de campo) foron seguidos polo uso de iluminación ornamental LED branca fría (4300 K), branca cálida (2580 K) e ámbar+verde (3000 K) (incluíndo un control sen iluminación ornamental) e 5 horas de escuridade. Tras 37 días de crecemento, o desenvolvemento de SABs cultivados en laboratorio (compostos principalmente por *Chlorella vulgaris*, *Klebsormidium flaccidum* e *Synechocystis* sp.) avaliouse mediante medicións de biomasa e diversidade, perfil bioquímico (cuantificación de pigmentos fotosintéticos, EPS e contido de ATP), microscopía confocal e fluorometría de clorofila PAM. A capacidade biostática da luz ámbar+verde verificouse en condicións LDI e HDI,

reducindo o rendemento de biomasa en ambas e diminuíndo a produción de EPS (tanto exopolisacáridos como proteínas extracelulares) en comparación coas luces branca fría e cálida. Os SABs no montaxe HDI produciron máis biomasa que baixo LDI. Ningunha das condicións de iluminación ornamental logrou alterar o perfil bioquímico (en termos de contido de clorofila, exopolisacáridos e proteínas extracelulares) en HDI. A iluminancia HDI tamén produciu unha diminución no rendemento cuántico dos SABs baixo todas as condicións de iluminación ornamental. Tanto a luz branca cálida como a ámbar+verde diminuíron a abundancia relativa de *Klebsormidium flaccidum* na condición LDI. Os resultados deste capítulo validaron o uso da nova luz biostática en exposición solar variable, o cal é particularmente relevante en contornos urbanos debido á morfoloxía urbana e/ou factores climáticos.

Para dilucidar os mecanismos de acción detrás do efecto biostático, o **Capítulo 4** estudou as influencias de tres tipos de iluminación LED utilizada en monumentos (branca fría, branca cálida e ámbar+verde) sobre os SABs en condicións de laboratorio mediante análise proteómica. A proteómica ambiental proporcionou información sobre os cambios no metabolismo dos SABs baixo o estrés inflixido pola iluminación nocturna, a través da cuantificación e identificación de péptidos de proteínas expresadas pola comunidade do SAB. A análise considerou os cambios na composición de especies e na composición proteína/péptido dos SABs. Concluíuse que a iluminación ámbar+verde tivo o efecto máis inhibidor sobre os cultivos de SAB, detectado especialmente polo seu impacto negativo nos fotosistemas I e II e na produción de proteínas tipo antena do fotosistema. En particular, a luz ámbar+verde afectou a produción da subunidade PsbO do fotosistema II, que cataliza a división da auga en O_2 e $4H^+$ e é necesaria para iniciar a cadea de transporte de electróns para a síntese de ATP e NADPH na fotosíntese. A luz biostática tamén tivo un efecto desencadeante sobre o metabolismo proteico (síntese, pregamento e degradación) e inducíu a síntese de proteínas de choque térmico relacionadas co estrés. Así mesmo, a luz branca cálida aumentou o número de péptidos relacionados coas estruturas e pigmento (ficobilisomas e ficocianina) das cianobacterias. O efecto biostático previamente estudado en biopelículas desenvolvidas sobre membranas (**Capítulos 2 a 4**) avaliouse no **Capítulo 5** sobre probetas minerais. O granito (material principal no patrimonio arquitectónico de Galicia e outras rexións do mundo) e o morteiro de cemento (amplamente utilizado en construción, especialmente en arquitectura moderna e contemporánea) empregáronse como substratos de ensaio. Os SABs (compostos principalmente polas algas verdes *Bracteacoccus minor* e *Stichococcus bacillaris*) desenvolvéronse sobre as probetas de granito e morteiro de cemento utilizando unha cascada de fluxo deseñada a medida. Logo foron sometidos durante 3 meses a un montaxe de iluminación composto por 13 horas de luz diurna, 6 horas de iluminación ornamental LED (branca fría, branca cálida e ámbar+verde, respectivamente) e 5 horas de escuridade. Tamén se incluíron controis sen iluminación ornamental e sen colonización (probetas de granito e cemento sen SAB). O estudo atopou que a interface SAB-mineral exposta á luz ámbar+verde comportouse de maneira similar ao control sen iluminación ornamental, minimizando os efectos da iluminación ornamental en comparación con ambas

luces brancas probadas en termos de desviacións de rugosidade, valores de dureza Leeb, ángulo de contacto estático, tempo de absorción de auga e diferenzas de cor. A medición da cor tamén indica que a luz ámbar+verde reduciu o desenvolvemento dos SABs en comparación coas luces brancas, especialmente na coordenada amarelenta-azulada (b*) do espazo CIELAB. A análise petrográfica tamén mostrou unha cobertura algal dependente do mineral no granito. Os resultados deste capítulo ampliaron a validación do efecto biostático da luz ámbar+verde para funcionar tamén sobre probetas minerais, reforzando o seu uso como tecnoloxía de conservación preventiva máis alá dos SABs desenvolvidos sobre membranas en laboratorio.

Para concluír a ***Parte 2*** da investigación, o estudo presentado no **Capítulo 6** consistiu na validación a longo prazo do efecto biostático da iluminación ámbar+verde: unha monitorización realizada no patio interior do Pazo de Raxoi (un monumento neoclásico construído en granito que actualmente alberga as dependencias do Concello de Santiago de Compostela) durante un período de 3,4 anos. O efecto da luz ámbar+verde sobre os SABs algais (compostos principalmente por *Myrmecia irregularis*, con algunhas cianobacterias e diatomeas) que medraban sobre sillares de granito comparouse cos efectos dunha lámpada de haluros metálicos (4668 K) (utilizada ata agora para iluminar monumentos en Santiago de Compostela) e cun control sen iluminación. Aplicáronse técnicas non destrutivas (fluorometría de clorofila PAM e espectrofotometría de cor), e os datos analizáronse mediante probas estatísticas avanzadas non paramétricas. Atopouse que as tendencias en todos os parámetros de fluorescencia de clorofila e cor foron consistentes. A fluorescencia mínima de clorofila (F_0) medida mediante fluorometría PAM utilizouse como variable *proxy* do crecemento do SAB. Os resultados mostraron que, aínda que o SAB medrou inicialmente baixo a luz ámbar+verde, estabilizouse ao mesmo nivel que o control sen iluminación, mentres que o SAB baixo luz de haluros metálicos continuou medrando, o que validou o efecto biostático da luz ámbar+verde nas paredes dun edificio de granito en exteriores (caso real). O rendemento cuántico dos SABs non se viu afectado polas condicións de iluminación ornamental, pero fluctuou segundo as condicións ambientais ao longo do ano.

A investigación presentada no **Capítulo 7**, tamén realizada no patio interior do Pazo de Raxoi, centrouse nos cambios causados pola iluminación ornamental (o mesmo montaxe lumínico descrito no **Capítulo 6**) nas comunidades bacterianas e fúngicas. Levouse a cabo a secuenciación de fraccións cultivables do microbioma e a secuenciación de xenoma completo (*metabarcoding*) utilizando *Oxford Nanopore Sequencing* (MinION). Os posibles perfís biodeteriorantes das cepas illadas determináronse en relación coa precipitación/solubilización de carbonato cálcico e a oxidación/redución de ferro mediante ensaios en placa. Tamén se determinaron índices de diversidade alfa e beta. Como as paredes de cachotería foron tratadas en 2018 cun biocida contendo o herbicida glifosato, tamén se determinou a abundancia de xenes de resistencia a biocidas e antibióticos. A análise microbiolóxica dependente de cultivo non revelou cambios na composición da comunidade. Porén, algúns illados presentaron perfís biodeteriorantes positivos para a precipitación e

solubilización de carbonato cálcico. O illado bacteriano identificado como *Pantoea* sp. deu positivo para a oxidación de ferro. A análise MinION identificou cambios no microbioma do granito inducidos pola iluminación ornamental, e as comunidades bacterianas e fúngicas correspondentes á luz ámbar+verde e ao control sen iluminación foron máis similares entre si que as producidas baixo a lámpada de haluros metálicos. As bacterias predominaron nas mostras iluminadas pola lámpada de haluros metálicos mentras a presenza de fungos foi practicamente nula.

O obxectivo do estudo presentado no **Capítulo 8** foi avaliar se o uso de luz ámbar+verde reduce a atracción de insectos cara á iluminación ornamental, xa que evita a emisión de lonxitudes de onda de alta enerxía (principalmente entre 400 e 500 nm, correspondentes á luz azul), típicamente coñecidas por alterar as comunidades de insectos nocturnos. O estudo realizouse novamente no patio interior do Pazo de Raxoi e co mesmo montaxe lumínico descrito no **Capítulo 6**. Colocáronse trampas adhesivas grises baixo a lámpada ámbar+verde, e comparouse o número e a diversidade de insectos atrapados baixo esta lámpada, baixo a lámpada de haluros metálicos e nunha zona sen iluminación. Os insectos capturáronse entre xuño e outubro de 2021, coincidindo co principal período de actividade. As trampas adhesivas retiráronse e substituíronse cada 5–16 días, dependendo do número de insectos atrapados e das condicións ambientais. A luz ámbar+verde reduciu considerablemente a atracción cara á luz, a niveis similares á zona sen iluminación. Este efecto demostrouse en case todas as ordes de insectos atrapados, especialmente Diptera, Lepidoptera, Coleoptera, Hemiptera e Hymenoptera. Polo contrario, os membros da orde Psocoptera mostraron unha atracción similar cara á luz ámbar+verde e cara á lámpada de haluros metálicos. A lámpada de haluros metálicos atraeu un maior número e diversidade de insectos que os outros dous tipos de luz (ámbar+verde e sen iluminación). Así, a luz ámbar+verde validouse como unha tecnoloxía ambientalmente sostible para a biodiversidade nocturna mediante o axuste fino da emisión espectral.

Dado o impacto da iluminación ornamental nocturna sobre os litobiontes (como se demostrou nos capítulos anteriores), cuxa presenza conduce á formación de *biofouling*, o estudo presentado no **Capítulo 9** avaliou a pegada de carbono e o custo económico da iluminación e do control asociado do *biofouling*. Realizouse un estudo de caso na Casa do Cabildo, unha casa histórica de estilo barroco construída en granito fronte á Praza das Praterías en Santiago de Compostela. Empregouse a norma UNE-EN ISO 14067 para a cuantificación da pegada de carbono e ferramentas de análise de custos para medir o rendemento ambiental e económico esperado do sistema de iluminación CromaLux (unha luz branca cálida utilizada durante un curto período seguida da luz ámbar+verde) en comparación cos sistemas tradicionais de haluros metálicos e LED branco. Aplicáronse cinco métodos de limpeza (láser, vapor de auga, Biotin T®, Biotin R® e etanol reforzado) baixo os tres sistemas de iluminación para comparar a pegada de carbono e o custo asociado. O sistema de iluminación CromaLux superou aos sistemas de haluros metálicos e LED branco (reducindo a pegada de carbono nun 80% e nun 20%, respectivamente). A limpeza láser tivo

a menor pegada de carbono de todos os métodos, e o método con etanol reforzado tivo a menor pegada entre os métodos químicos. Porén, este método resultou custoso, xa que se requiriu un maior volume de líquido para acadar o mesmo nivel de eficacia que Biotin T® e Biotin R®. Segundo as estimacións presentadas neste capítulo, a limpeza dos SABs podería atrasarse entre 1,5 e 6 anos mediante o uso do sistema CromaLux. Aínda que a redución de pegada de carbono e custo lograda co sistema CromaLux é baixa para o exemplo da Casa do Cabildo, os posibles aforros se se implementa a nivel cidade poderían ser substanciais para o municipio. Os achados confirman así as vantaxes do sistema CromaLux para mellorar a sustentabilidade ambiental e económica da iluminación e limpeza do patrimonio arquitectónico.

Finalmente, tal como se describe no **Capítulo 10**, empregáronse métodos de psicoloxía ambiental para avaliar a percepción e aceptación pública da luz ámbar+verde e obter información que puidese aplicarse no deseño de estratexias destinadas a superar a reticencia a aceptar esta tecnoloxía. Utilizouse material fotográfico da Casa do Cabildo con iluminación ornamental. As imaxes modificáronse dixitalmente para ilustrar tres calidades de luz (branca fría, branca cálida e luz ámbar+verde) proxectadas sobre unha fachada principal limpa e outra afectada por *biofouling* simulado. A investigación realizouse en dúas fases. Un primeiro estudo cualitativo, baseado en sesións de discusión con expertos e representantes de asociacións veciñais, destacou puntos clave sobre a percepción de problemas de deterioro de edificios e actitudes cara á luz ámbar+verde. Os participantes no estudo cualitativo expresaron interese na conservación do patrimonio e coincidiron en que a información, a confianza na ciencia e a habituación poderían conducir á aceptación da luz ámbar+verde. Porén, os participantes preferiron a luz branca cálida fronte á luz ámbar+verde, unha preferencia que parece explicarse por visións tradicionais sobre a iluminación ornamental. Os expertos tenderon a ser máis cautelosos que os representantes de asociacións veciñais e expresaron preocupacións sobre a eficacia e a idoneidade da luz desde a perspectiva da imaxe urbana. Posteriormente, realizouse un segundo estudo para cuantificar a preferencia respecto aos tres tipos de iluminación e as actitudes xerais cara á luz ámbar+verde. Este estudo cuantitativo tamén incluíu como diferentes tipos de mensaxes, transmitidas mediante imaxes da fachada limpa e da fachada afectada por *biofouling*, afectaron a aceptación da luz ámbar+verde. Os participantes mostraron actitudes neutras cara á luz ámbar+verde, a pesar do seu menor atractivo visual. Ademais, as mensaxes transmitidas (imaxes) non alteraron a preferencia de iluminación. O estudo tamén revelou que os participantes con forte apego ao lugar tiñan máis probabilidades de elixir a luz ámbar+verde fronte a calquera das luces brancas. Así mesmo, unha alta identificación social coa comunidade aumentou as actitudes positivas cara á luz ámbar+verde. Porén, incrementar a sensibilización sobre os beneficios da conservación e fomentar a identidade comunitaria e do lugar foron identificadas como estratexias para mellorar a aceptación da luz ámbar+verde, que permanece acesa durante máis tempo ca outra luz branca cálida utilizada anteriormente no sistema CromaLux e é a máis importante (debido ao seu efecto biostático).

INDEX

1 INTRODUCTION

The Cathedral of Burgos was first illuminated by ornamental lighting on the night of 25 November 1935, thus becoming the first monument in Spain with a facade permanently illuminated at night (Calvo, 2024). The National Palace of Montjuïc in Barcelona had previously been illuminated for ornamental purposes, but only temporarily, during the Barcelona Exhibition in 1929 (Rodriguez Lorite, 2016). The project at the Cathedral of Burgos, carried out by the Burgos-born industrial valid engineer Carlos Aparicio, consisted of 50 incandescent luminaires of 1,000 W, providing an intensity between 8,200 and 9,080 lumens of light flux, which highlighted the cathedral's gothic features each night through contrasts of light and shadow (**Fig. 1a**) (Galve, 1935).

Figure 1. a) Image of the Cathedral of Burgos illuminated in 1935 (Galve, 1935), b) announcement of the inauguration of the permanent lighting of the Cathedral of Burgos (Redacción del periódico Diario de Burgos, 1935).

The concept of permanent illumination was promoted by the then Mayor of Burgos, Perfecto Ruíz Dorronsoro, and was implemented thanks to funding from the Ministry of Public Instruction and Fine Arts, as well as several local entities such as the local Tourism Society, after overcoming initial financial difficulties due to the scale of the project. One year before the inauguration, the editorial team of the newspaper El Castellano (Redacción del periódico El Castellano, 1934) published the following text, which connects with current considerations regarding the exterior lighting of monuments, such as its role in

increasing night-time tourism and enhancing architectural details: *"[...] no one can doubt the importance this holds for our artistic jewel, which can be admired in all its beauty with a perfect installation that fills all the admirable reliefs in its stones with rays of light."* The event was attended by the then President of the Republic, Niceto Alcalá-Zamora (**Fig. 1b**), and a connection was established with Joseph Deleuil's experiments in photoelectric lighting for aesthetic purposes at the Place de la Concorde in Paris in 1844 (Rodriguez Lorite, 2016), aiming to create "architecture of the night", as reported in contemporary news (Galve, 1935), through the illumination of architectural heritage.

The conservation of architectural heritage is a priority objective recognised by international organisations such as the International Council on Monuments and Sites (ICOMOS), which defined architectural heritage in its 1985 Granada Convention as *"all groups of monuments, architectural ensembles and sites of significance for their historical, archaeological, artistic, scientific, social or technical interest, including installations or decorative elements that form an integral part of such works"* (Council of Europe, 1985). In line with this, the United Nations (UN) includes in the eleventh of its Sustainable Development Goals (SDG 11) the promotion of resilient and sustainable cities, highlighting in target 11.4 the need to *"strengthen efforts to protect and safeguard the world's cultural and natural heritage"* (United Nations, 2023). Both ICOMOS (2003) and UNESCO (2023) also emphasise the importance of including technical infrastructures associated with heritage in management and conservation plans. Consequently, the exterior lighting of monuments and historic buildings is considered by several authors a matter relevant to the conservation of architectural heritage (Espejo Gutierrez and González Gasca, 2008). Indeed, Zielinska-Dabkowska and Xavia (2018) argue that the definition of *urban cultural heritage* should incorporate nightscapes, in line with the principles of the 1972 Charter of Restoration (MIBACT, 1972), thus considering ornamental lighting, its aesthetic character and physical elements, and including aspects such as luminaire infrastructure, the quantity (intensity) and quality (colour) of light, and the style of lighting used. Nevertheless, current management, conservation and urban planning strategies prioritise aesthetic, energy and sustainability aspects, while ignoring the effect of ornamental exterior lighting on biological colonisation and its potential to cause biodeterioration.

1.1 OUTDOOR PUBLIC LIGHTING IN SPAIN

1.1.1 Historical overview

Electric lighting has constituted the main source of energy consumption in Spain since the beginning of statistical records in 1901, representing approximately 65% of total national electricity demand (Bartolomé Rodriguez, 2007). The significant demographic growth at the turn of the twentieth century drove the spread of public electric lighting,

which was facilitated by the creation of the first electricity companies in Spain from the 1880s onwards. These companies promoted the installation of urban lighting systems for streets (Maluquer de Motes, 1992; Bartolomé Rodriguez, 2007). Gas lighting, which had previously predominated, was gradually relegated to the domestic sphere, a situation that persisted until the expiry of concessions granted to gas companies for exterior public lighting, which occurred at the beginning of the twentieth century (Huguet, 2013). The first electric lighting systems used arc lamps based on carbon electrodes, but these were quickly replaced by more efficient incandescent lamps. In the first decade of the 1900s, 99.3% of luminaires in Spain were incandescent lamps (Fernández Paradas, 2008). Installation of incandescent lamps remained in Spain over the following decades until the introduction of discharge technologies (such as fluorescent, mercury vapour, sodium and metal halide lamps), which began to be marketed from 1930 and accounted for around 25% of global electricity consumption until the introduction of LED technology (Lister et al., 2004). The acronym LED stands for Light Emitting Diode, a diode (allowing the flow of electric current in one direction and restricting it in the other) made of a semiconductor material that releases energy in the form of photons (electroluminescence) when traversed by an electric current (for more information, see Wood, 2009; Nanishi, 2014). LEDs have displaced other technologies, as they are comparatively more efficient - both energetically and economically. The advantages of LEDs have led to an exponential increase in night-time lighting, with associated environmental impacts resulting from increased light pollution.

1.1.2 Technical considerations

The development of new LED lighting technologies aimed to achieve greater efficiency and energy savings at lower cost and also to produce white light with high colour rendering, understood as the *"degree of change in the appearance of colours perceived under artificial light compared to those perceived under natural or standardised light"* (Nickerson, 1960). LED lighting also enabled modification of the emitted white light spectrum by adjusting the Correlated Colour Temperature (CCT), which refers to the *"temperature of a Planckian radiator whose perceived colour most closely resembles that of a light source with the same brightness under the same viewing conditions"* (Schanda, 2007). The CCT is measured in kelvin (K) and, in lighting, refers to the hue of the white light emitted by a light source.

Until recently, the light spectrum and CCT were determined by the technology used. For example, natural sunlight varies throughout the day from between approximately 3,000 K and 25,000 K or more (see Hernández-Andrés et al., 1999), while sodium vapour lamps (high or low pressure) traditionally emit warm orange light at around 2,000 K, and metal halide lamps range from approximately 3,000 K to 6,500 K (see Lister et al., 2004). The development of white LED lighting became possible thanks to the invention of the high-intensity blue LED around 1994 (through the joint work of Shuji Nakamura, Isamu

Akasaki and Hiroshi Amano, who were awarded the Nobel Prize in Physics in 2014, see Nanishi, 2014), which could then be combined with previously developed red and green LEDs. Since then, LED diode development has enabled light emission across a wide range of the electromagnetic spectrum, with increasingly narrow spectral bandwidths (ranges of emitted wavelengths), applicable in diverse fields, such as the agriculture and livestock industries (e.g. Singh et al., 2015; Mahmoud, 2021; Shirobokova et al., 2022).

In the 1930s, the International Commission on Illumination (CIE, for its French acronym) established wavelength ranges within the electromagnetic spectrum (measured in nm) based on their effects in photobiology (Sliney, 2016): ultraviolet (UV) light, classified in three bands (UV-C: 100–280 nm; UV-B: 280–315 nm; and UV-A: 315–≈400 nm), visible light (≈360–380 to 780 nm) and near-infrared (IR-A) (between 780 and 1,000 nm). Photon energy is inversely proportional to wavelength (λ), so that shorter wavelengths correspond to higher photon energy. Within the visible spectrum, the distribution of wavelengths determines the CCT and thus the visual appearance of artificial light. A higher proportion of short, high-energy wavelengths increases the CCT, while longer, low-energy wavelengths reduce the CCT. For example, a white LED luminaire with a CCT of 6,000 K will have a greater contribution of wavelengths in the blue-green range and a cooler appearance, whereas one with a CCT of 2,500 K will emit more in the amber-red range and appear warmer.

Photon flux density (PFD) measures the number of photons reaching a surface per unit area and time and is generally expressed as μmol photons s^{-1} m^{-2} (see e.g. Walter and Schöbel, 2023). The term Photosynthetically Active Radiation (PAR) is also used in relation to photosynthetic organisms. It is calculated by integrating all wavelengths by the product of the PFD function and the photosynthetic sensitivity curve, based on the absorption spectrum of photosynthetic pigments) and resulting in the photosynthetic photon flux density (PPFD).

Use of an artificial light source, whether in a natural environment or an urban setting, alters the natural photoperiod received by organisms (i.e. the amount of light and darkness they experience in a daily cycle). The intensity and spectrum of artificial light also differ from that of daylight, potentially disrupting the circadian rhythms of organisms (i.e. the self-sustained biological cycles or rhythms of an organism over a 24-hour period, which persist even when external time cues are altered (Vitaterna et al., 2001). Flora, fauna and ecosystems in general are affected within the broader context of light pollution.

1.1.3 Current legislation

In Spain, exterior lighting is regulated by Royal Decree 1890/2008 of 14 November, which approves the Regulation on Energy Efficiency in Outdoor Lighting Installations and its Complementary Technical Instructions EA-01 to EA-07 (MINCOTUR, 2008). This regulation establishes the technical conditions for the design, execution and maintenance of

exterior lighting, in line with the Energy Saving and Efficiency Strategy in Spain 2004–2012, aimed at improving the Spanish electricity system (IDAE, 2003). The permitted duration of artificial night-time lighting in Spain falls under the direct competence of local councils, which must manage and regulate the conditions of their public lighting in accordance with both national and EU legislation. For example, in the city of Santiago de Compostela, the switch-on time varies according to sunset, while switch-off is set at 03:00.

In Spain, ornamental lighting is covered by one of the Complementary Technical Instructions (known as ITC-EA), specifically ITC-EA-02 on lighting levels, which establishes the recommended illuminance levels for different spaces, including ornamental lighting, defined as *"the lighting of facades of buildings and monuments, as well as statues, walls, fountains, etc."* (MINCOTUR, 2008). Table 11 of the ITC-EA-02 (**Fig. 2**) lists the minimum illuminance levels (i.e. total luminous flux incident on a surface per unit area) in lux (lm m^{-2}), with the lumen (lm) being the SI unit for measuring luminous flux (i.e. the amount of light emitted by a source in all directions). The table specifies that three factors determine the correct ornamental lighting of a surface: i) the nature of the illuminated material; ii) the average illuminance levels of the surroundings; and iii) correction factors related to the type of lamp used and the condition of the illuminated surface.

Instruction ITC-EA-02 defines illuminance ranges according to the type of construction material, for example, light stone, light marble, dark brown brick or pink granite (**Fig. 2**). Depending on the physical characteristics of the material, it will have a higher or lower reflection index (ρ). A higher ρ indicates that more light is reflected, and less luminous intensity is therefore required to achieve the necessary illuminance. In Galicia, for instance, traditional granite constructions (ρ = 0.1–0.3) require higher electricity consumption for illumination than contemporary constructions made of cement (ρ = 0.3–0.4). Furthermore, ITC-EA-02 establishes the need to apply a correction factor depending on the conservation state of the illuminated surface, as the accumulation of dirt reduces the ρ of the material, requiring increased lighting power to maintain the specified illuminance levels. However, the regulation only distinguishes between "dirty" and "very dirty" surfaces, without precisely or quantifiably defining the criteria for each category, which introduces a high degree of subjectivity in its application.

NATURALEZA DE LOS MATERIALES DE LA SUPERFICIE ILUMINADA	NIVELES DE ILUMINANCIA MEDIA (Lux) (1)			COEFICIENTES MULTIPLICADORES DE CORRECCIÓN (2)			
	Iluminación de los alrededores			Corrección para el tipo de lámpara		Corrección para el estado de la superficie iluminada	
	Baja	Media	Elevada	H.M. LED	S.A.P. S.B.P.	Sucia	Muy Sucia
Piedra clara, mármol claro	20	30	60	1,0	0,9	3,0	5,0
Piedra media, cemento, mármol coloreado claro	40	60	120	1,1	1,0	2,5	5,0
Piedra oscura, granito gris, mármol oscuro	100	150	300	1,0	1,1	2,0	3,0
Ladrillo amarillo claro	35	50	100	1,2	0,9	2,5	5,0
Ladrillo marrón claro	40	60	120	1,2	0,9	2,0	4,0
Ladrillo marrón oscuro, granito rosa	55	80	160	1,3	1,0	2,0	4,0
Ladrillo rojo	100	150	300	1,3	1,0	2,0	3,0
Ladrillo oscuro	120	180	360	1,3	1,2	1,5	2,0
Hormigón arquitectónico	60	100	200	1,3	1,2	1,5	2,0
REVESTIMIENTO DE ALUMINIO:							
- Terminación natural	200	300	600	1,2	1,1	1,5	2,0
- termolacado muy coloreado (10%) rojo, marrón, amarillo	120	180	360	1,3	1,0	1,5	2,0
- termolacado muy coloreado (10%) azul – verdoso	120	180	360	1,0	1,3	1,5	2,0
- termolacado colores medios (30 – 40%) rojo, marrón, amarillo	40	60	120	1,2	1,0	2,0	4,0
- termolacado colores medios (30 – 40%) azul – verdoso	40	60	120	1,0	1,2	2,0	4,0
- termolacado colores pastel (60 – 70%) rojo, marrón, amarillo	20	30	60	1,1	1,0	3,0	5,0
- termolacado colores pastel (60 – 70%) azul - verdoso	20	30	60	1,0	1,1	3,0	5,0

(1) Valores de referencia mínimos de iluminancia media en servicio con mantenimiento de la instalación sobre la superficie limpia iluminada con lámparas de incandescencia.

(2) Coeficientes multiplicadores de corrección para lámparas de halogenuros metálicos (H.M.), LED's, de vapor de sodio a alta presión (S.A.P.) y a baja presión (S.B.P.), así como para el estado de limpieza de la superficie iluminada

Figure 2. Average illuminance levels in service for ornamental lighting. Extracted from MINCOTUR (2008). For the English version, see Chapter 1.

1.2 COLONISATION OF GRANITE ARCHITECTURAL HERITAGE IN GALICIA BY PHOTOTROPHS

1.2.1 Granitic rocks in Galicia

The lithology in Galicia is predominantly composed of metamorphic rocks, with representations of various metamorphic grades ranging from slates to gneisses, mainly formed during the Cambrian period (540–360 Ma), as well as igneous rocks, particularly granitic plutonic types. Other igneous rocks such as gabbros and peridotites are also present, although in smaller proportions (Silva, 2024). In the field of construction, the abundance of these two rock types has positioned Galicia as the leading European region and global leader in the exploitation of slates (a metamorphic rock used as a roofing material owing to its pronounced planar orientation, shown in light green in **Figure 3**), and

granites *sensu lato* (an igneous rock predominantly used in Galician architecture, shown in red and orange in **Figure 3**) (IGME, 2008).

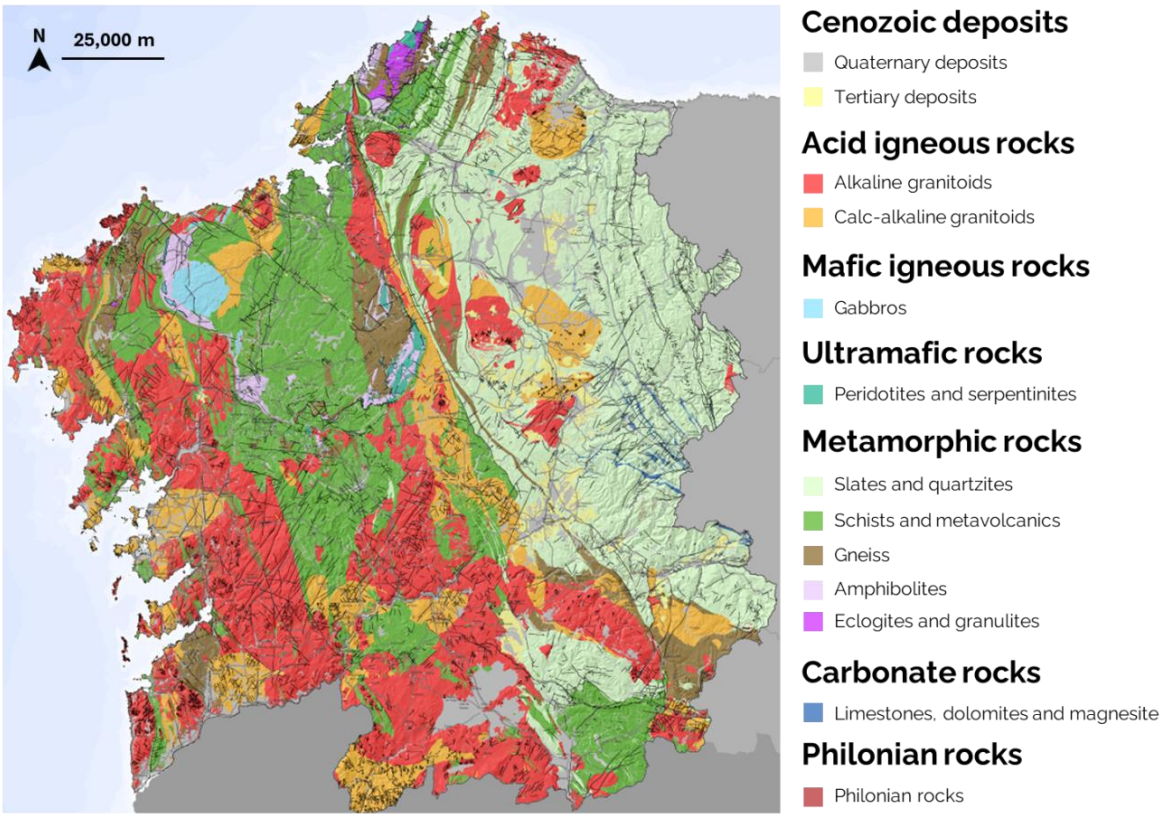

Figure 3. Geological map of the autonomous community of Galicia (NW Spain). Reference system: ETRS89. Image by A. Méndez, modified from Instituto de Estudos do Territorio (2025).

Granitoid rocks, which mainly include granites *sensu stricto* and granodiorites but are generally referred to as "granite", are the most abundant in Galicia, covering more than one third of its surface within the Galicia–Tras-Os-Montes geological domain. This abundance has favoured the extensive use of these rocks as traditional construction material in the region (Hernández et al., 2023). Granitoid rocks in Galicia can be classified into two major series based on their chemical and mineralogical characteristics, (i) the series of two-mica alkaline granitoids, and (ii) the series of calc-alkaline granitoids with dominant biotite. Granitoid rocks originated in Galicia during the Hercynian Orogeny, between the Late Devonian (380 Ma) and the Middle Permian (280 Ma), associated with the subduction of Gondwana and Laurasia during the formation of Pangaea. This subduction generated magmatic bodies that reached the surface and were later exposed through erosion during the Mesozoic (250–65 Ma), following the accumulation of materials from the collision of the two ancient continents (Romaní, 2023). Granite is the most widely used plutonic rock globally in construction, as it accounts for approximately 87% of the upper continental crust (Hans Wedepohl, 1995). Its widespread use is due to its

varied colour and mineral composition, low porosity and high resistance to alteration and weathering compared to other rocks (Siegesmund and Török, 2011).

The general composition of granitoid rocks includes quartz (SiO_2), alkali feldspars (mixtures of sodium and potassium aluminosilicates), plagioclases (calcium-sodium aluminosilicates) and micas (muscovite and biotite, which is mainly altered to chlorite or vermiculite), along with other minerals such as allanite, apatite, rutile and zircon, which may appear in low proportions or as trace elements. Biotite-type micas are aluminosilicates containing iron or magnesium: $(Mg,Fe)_3AlSi_3O_{10}(OH,F)_2$, whereas muscovite-type micas are potassium aluminosilicates: $KAl_2(AlSi_3O_{10})(OH)_2$.

In the Streckeisen diagram (Streckeisen, 1976), granitoid rocks are located near the centre of the triangle formed by quartz (Q), alkali feldspars (A) and plagioclases (P) (**Fig. 4a**). These rocks include a minimum of 20% quartz in their mineral composition, and depending on whether alkali feldspars or plagioclases predominate, they belong to the granite or granodiorite group. Their composition influences both mechanical and aesthetic properties. Granites with 20% – 40% quartz typically have an achromatic appearance, being greyish or slightly pink. Their appearance is affected by alteration processes or inclusions of other minerals. Iron oxidation in biotite-type micas gives a brownish-yellow hue; plagioclases may have greenish tones; and rutile inclusions in quartz can produce a bluish tint (Siegesmund and Török, 2011). This colour variability is highly valued regarding the use of granite as building and ornamental stone. Additionally, Galician granite exhibits a wide range of textures, both porphyritic (i.e. with varied grain sizes) and non-porphyritic, and it is always phaneritic i.e. crystals visible to the naked eye) (Ferrero et al., 1992; Silva, 2024).

From a mechanical perspective, granites are low-porosity rocks (i.e. low volume ratio occupied by pores or microcracks, mostly of fissure type). Commercially available ornamental granites typically have an open porosity between 0.1% and 2.0%, often around 1.0% (Silva et al., 2019). The study by Calleja et al. (2020) shows that the Albero (3.9%) and Traspielas (3.6%) varieties are slightly porous rocks (2.5%–5.0% porosity), while the Gris Alba (0.9%) and Rosa Porriño (0.9%) varieties are compact rocks (< 1% porosity), according to the classification by von Moos and de Quervain (1948).

Granite's low porosity compared to other construction materials such as limestones and sandstones (porosity around 1%–25%) and mortars (porosity 20%–30%) affects the water dynamics, resulting in lower water absorption values (both liquid water and ambient water vapour) (Siegesmund and Dürrast, 2011). According to Rojo et al. (2003), the amount of water that granite can retain depends on its porosity, but also on pore interconnectivity. These authors note that ornamental granite varieties in Spain generally exhibit similar sorption kinetics, with an initial rapid water absorption phase followed by a gradual decrease until equilibrium is reached. After desorption (water loss), a small amount of water remains trapped inside.

Regarding the hardness, Siegesmund and Dürrast (2011) state that granite is generally considered a robust, hard material. Quartz and feldspars have Mohs hardness values of 7 and 6, respectively (the Mohs scale measures a material's resistance to scratching, with diamond rated highest at 10). However, less abundant minerals such as micas have hardness values of 2 to 3, and the hardness of granite is thus very variable at the microscopic level. As a construction material, plutonic rocks exhibit compressive strengths (i.e. ability to withstand loads that reduce volume) ranging from 60 MPa to 292 MPa, with an average around 160 MPa, exceeding many other rocks such as sandstones or limestones. Nevertheless, the strength of granite varies depending on the direction of the applied force (a property known as anisotropy), which is, in turn, determined by the orientation of macroscopic elements (Siegesmund and Dürrast, 2011); these factors influence the deterioration processes.

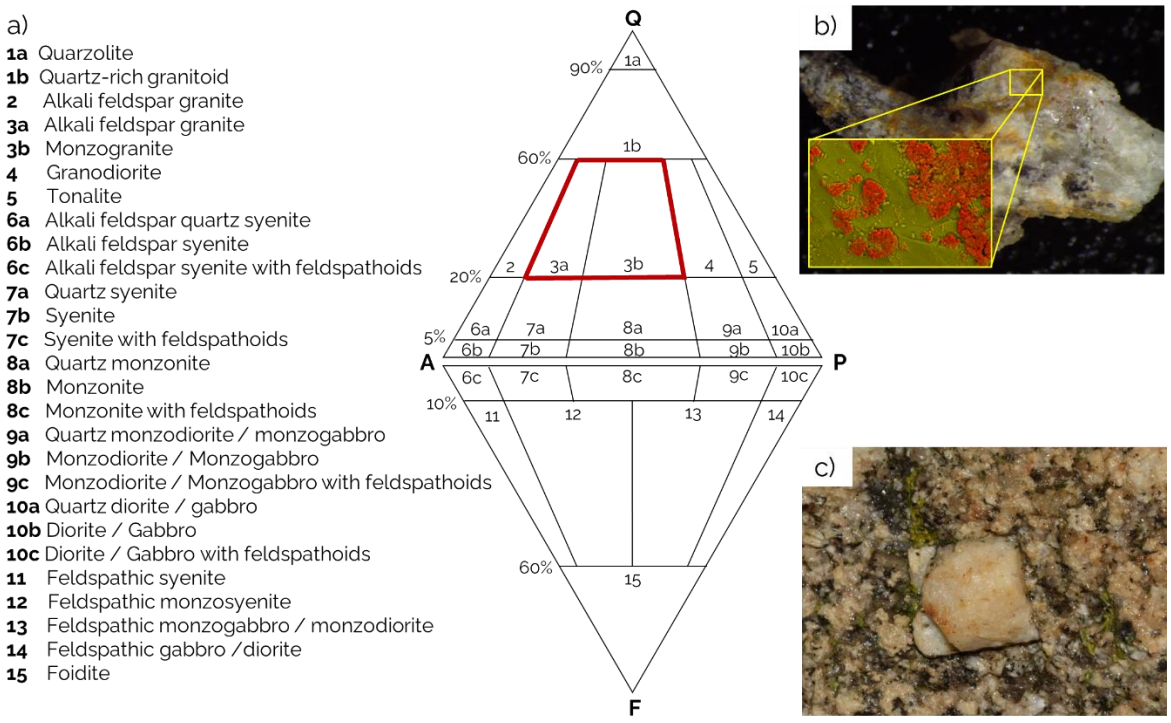

Figure 4. a) Simplified Streckeisen diagram for the most common plutonic rocks. Image by A. Méndez, modified from Siegesmund and Török (2011), b) Detail of a granite fragment with signs of Fe oxidation, with detail SEM-EDS image showing elemental Fe (orange-reddish) over the Si (yellow-greenish) from the quartz. Image by A. Méndez, modified from Méndez, Maisto et al. (2024), c) Optical microscopy image from a granite ashlar showing early signs of colonisation by phototrophic SABs. Image by P. Sanmartín.

1.2.2 Granite deterioration and alteration processes

The alteration, deterioration and weathering of granitoid rocks are natural processes that begin once the rocks are exposed at the surface. Interaction with the atmosphere, hydrosphere and biosphere triggers a series of physical and chemical reactions that inevitably modify the rock's original properties (Silva, 2024). These processes also affect

monuments and buildings, together with architectural, social, economic, historical and usage-related factors (Freire-Lista, 2016).

Temperature fluctuations cause mechanical damage in dimension stones (i.e. natural rock extracted for blocks or slabs) due to volumetric changes from expansion and contraction. Each mineral has its own thermal expansion coefficient (K^{-1}), so that rocks with phaneritic textures, such as some granitoids, undergo differential expansion and contraction cycles for each mineral - a process known as thermoclastism. Granitoid minerals have varying expansion coefficients. For instance, quartz and micas exhibit K^{-1} values of approximately 7.7–17.8 μm per unit of temperature (K), depending on the crystal axis (Steiger et al., 2011), while the corresponding value for plagioclases may reach up to 45.6 μm (Tribaudino et al., 2010). These temperature-induced stresses can lead to irreversible microcracking (Steiger et al., 2011).

Volumetric changes due to temperature are often associated with variations in moisture content (hydric dilation) and cycles of wetting and drying, which structurally weaken the rock and damage its internal microstructure (Chen et al., 2018). If water within the rock freezes (i.e. temperatures below 0°C), the volume increase during ice formation generates even greater stress, causing more inter- and intra-crystalline cracking, especially in granites with large crystals and in feldspars (Freire-Lista et al., 2015).

The dissolution and/or alteration of minerals in granitoid rocks leads to chemical weathering, which may also result in physical weathering. Water induces hydrolysis reactions by replacing metallic cations with H^+ ions. Environmental pollutants (e.g. SO_2 or nitrogen oxides) are another significant source of H^+, greatly increasing the rate of mineral dissolution through cation substitution (Steiger, 2016). For example, hydrolysis of feldspars (alkali and plagioclase) and micas and their transformation into kaolinite (i.e. a clay mineral formed by alteration of feldspars and micas) causes disintegration of granitoid rock. The disintegration, or granular disaggregation, may also be caused by salt crystallisation within the porous network of the rock, which increases internal pressure and leads to cracking (Silva, 2024). The most common salts affecting construction stones are chlorides, nitrates, sulphates and carbonates, typically of sodium, potassium, magnesium and calcium. Their solubility, whether dissolved or crystallised, varies depending on environmental conditions, chemical composition, and whether they occur individually or in complex mixtures. Dissolved salts can penetrate and migrate through the rock via pores and microcracks by capillary action. Upon water evaporation and concentration of the saline solution, salts may precipitate as crystals - either as surface efflorescence or exerting pressure within the rock's porous structure (Steiger et al., 2011). Biotite is also susceptible to water-induced deterioration, as iron in biotite oxidises from Fe^{2+} to Fe^{3+} at the mineral–water interface (**Fig. 4b**).

Granite's susceptibility to deterioration is also influenced by the orientation of ashlar blocks in construction, due to its anisotropic behaviour. When a granite block is extracted from a quarry, the plane known as *andar* or *levante* is horizontal relative to the outcrop and

coincides with exfoliation and dip planes, facilitating cutting due to lower resistance. The grain, plumb or *trinque* plane corresponds to the vertical orientation, while the north or face is perpendicular to both *andar* and grain planes and exhibits greater mechanical resistance. When the *andar* plane is exposed as the visible face of an ashlar, it becomes more vulnerable to deterioration processes such as scaling, where material detaches parallel to exfoliation planes (Taboada et al., 2005; Freire-Lista and Fort, 2016).

1.2.3 Subaerial biofilms (SABs): Phototrophic colonisation on granite

A biofilm (also referred to as *biopelícula* in Spanish, although the term is not widely standardised) is a highly structured, self-sustaining community of microorganisms adhered to a surface, either actively growing or capable of growth, and bound together by a matrix of self-produced extracellular polymeric substances (EPS) (O'Toole, 2003; Bremer et al., 2015; Myckatyn et al., 2016).

When a biofilm develops at the air–rock interface (or on other materials exposed to the atmosphere), it is referred to as a subaerial biofilm (SAB). Although monospecific biofilms exist, multispecies biofilms are more common in natural environments (Zhao et al., 2023). SABs include microalgae, cyanobacteria, heterotrophic bacteria and fungi (Caneva et al., 2008). Within this system, cells interact with each other and with their environment, forming a heterogeneous structure shaped by the physiological and phenotypic differences among the populations comprising the biofilm (de Beer et al., 1994; Pavissich et al., 2021). Biofilm formation occurs in four stages: initial adhesion of microorganisms to the surface, colony formation and development, biofilm maturation (with EPS production) and finally dispersion of cells in the environment (Negi and Sarethy, 2019).

In architectural heritage, the presence of SABs leads to biodeterioration of the substrate (ICOMOS-ISCS, 2008), although the changes may only be aesthetic. On stone surfaces (**Fig. 4c**), SABs typically appear in damp areas, cracks and/or zones sheltered from direct sunlight, particularly in locations with high water availability due to leaks, poor drainage or frequent exposure to rainwater (Saiz-Jimenez, 1995) (**Fig 5a**). High porosity and surface roughness further promote organism adhesion and penetration, increasing potential damage (Saiz-Jimenez, 1995; Negi and Sarethy, 2019). Algal biomass predominates in SABs found on European heritage sites (Gaylarde and Gaylarde, 2005), forming greenish films where light is the primary energy source, influencing their structure, growth and composition (Zippel and Neu, 2005). The EPS matrix embedding the microorganisms provides surface adhesion and protection, enabling sessile organisms to withstand adverse conditions such as high irradiance, UV radiation, desiccation and environmental pollutants (Rossi et al., 2012; Pinna, 2017). The matrix is a colloid composed of water, polysaccharides, proteins and extracellular DNA. In algal SABs, the matrix also serves as a refuge for heterotrophic microorganisms such as fungi and bacteria, which can cause greater damage to heritage surfaces than phototrophs (Pinna, 2021). Environmental factors such as water availability and ambient humidity influence EPS formation (Villa and Cappitelli, 2019;

Fuentes and Prieto, 2021), as does light, which regulates matrix production. Changes in light intensity, spectrum and photoperiod modulate the synthesis of extracellular polysaccharides and proteins (Ge et al., 2014; Kumar et al., 2017; Dahech et al., 2021; Pinna, 2021).

The microalgae and cyanobacteria colonising architectural heritage are typically subaerial, freshwater or lithobiontic species (Rifón-Lastra and Noguerol-Seoane, 2001). Microalgae are unicellular eukaryotes, while cyanobacteria are prokaryotes. Both may occur as isolated cells or colonies and are predominantly obligate photoautotrophs. However, some species can grow chemoautotrophically in the absence of light or mixotrophically under low light conditions and in combination with other substrates Caneva et al., 2008. Microalgae and cyanobacteria may develop epilithically (i.e. on the surface of lithic materials) or endolithically (i.e. within the material, in cavities or cracks) (Gaylarde et al., 2012).

Chlorophyceae is one of the most common classes of microalgae colonising lithic materials in architectural heritage (Ortega-Calvo et al., 1995). In north-western Spain, green microalgae species in this class, including *Stichococcus bacillaris*, *Stichococcus jenerensis*, *Trentepohlia umbrina*, *Desmococcus olivaceus*, *Chlorella vulgaris*, *Apatococcus lobatus*, *Coccomyxa subellipsoidea*, *Gloeocystis polydermatica*, *Trebouxia* sp., and *Geminella* sp., have been found on granite monuments (Rifón-Lastra and Noguerol-Seoane, 2001; Vázquez-Nion et al., 2016; Fuentes et al., 2021). The filamentous alga *Klebsormidium flaccidum*, belonging to the class Streptophyta (formerly Charophyta), is also frequently found on granite (Rifón-Lastra and Noguerol-Seoane, 2001). Diatoms (class Bacillariophyta) are commonly found in areas with high water availability. These microalgae possess a rigid silica (SiO_2) wall composed of two interlocking valves (Caneva et al., 2008). For example, diatoms in the genera *Navicula* and *Cyclotella* have been identified on the Church of Gonçalo de Amarante (Portugal), built using two-mica granites and associated with salt-induced deterioration (Begonha, 2009).

Cyanobacteria (class Cyanobacteriota) are photoautotrophic bacteria that have historically been referred to as blue-green algae due to pigments such as phycocyanin (bluish), although they may also contain phycoerythrins (reddish) or other pigments like scytonemins (brown-black) (Pinna, 2021; Villa et al., 2022). They are ubiquitous in terrestrial and aquatic environments and commonly co-occur with microalgae in SABs on built heritage. Cyanobacteria are more abundant than microalgae in constructions located in tropical climates such as Latin America and Southeast Asia (Gaylarde and Gaylarde, 2005; Hauer et al., 2015; Pinna, 2021). Filamentous cyanobacteria have a vegetative filamentous structure, called a thallus, that can penetrate the substrate and potentially damage the rock (Chen et al., 2021). The species commonly found on granite monuments in north-western Spain include *Phormidium autumnale*, *Tychonema bourrellyi*, *Nostoc* sp., *Phormidium* sp., *Plectonema* sp., *Chroococcopsis* sp., *Synechocystis* sp., and *Synechococcus* sp. (Rifón-Lastra and Noguerol-Seoane, 2001; Leite Magalhães and Sequeira Braga, 2000; Fuentes et al., 2021).

1.2.4 Photosynthesis and photosynthetic pigments

The electron transport chain of photosynthesis occurs in the thylakoid membrane of chloroplasts, following the Z-scheme described by Hill and Bendall (1960). This model outlines the light-dependent reactions in the electron transport pathway, beginning with water photolysis and culminating in the formation of the reducing molecule NADPH, the release of oxygen, and the increase in hydrogen ion concentration within the thylakoid lumen, necessary for ATP synthesis. ATP production is subsequently used for CO_2 fixation and glucose synthesis via the Calvin cycle in the light-independent reactions of photosynthesis (Govindjee, 2004). Electrons are transferred through Photosystems (PS) I and II, pigment–protein complexes containing chlorophyll-a and accessory pigments such as chlorophyll-b and carotenoids. These pigments absorb light energy at different wavelengths and transfer it to the reaction centre. In PSII, a special pair of chlorophyll-a molecules (P680) reduces pheophytin by transferring the electron obtained from water photolysis. In PSI (P700), the pair facilitates electron transfer from plastocyanin to primary acceptors, leading to the reduction of $NADP^+$ to NADPH (Govindjee, 2004; Nelson and Yocum, 2006). PS contain light-harvesting complexes (LHCs), protein complexes bound to chlorophylls (a and b) and carotenoids, which enhance light capture (by acting like an antenna) and transfer energy to the PS I and II reaction centres, initiating electron flow (Nicol and Croce, 2018). When a photosynthetic organism experiences stress due to excess light (either in intensity or photoperiod duration), photoadaptation or photoprotection mechanisms are activated (i.e. biochemical changes in LHC composition) to prevent photoinhibition (i.e. a reduction in photosynthetic efficiency in the electron transport chain of the photosystems, which helps to prevent photooxidative damage (Han et al., 2000).

Chlorophylls are composed of a hydrophilic ring called porphyrin, which has a central Mg atom and a long lipophilic hydrocarbon alcohol chain known as phytol (**Fig. 5b**). The porphyrin ring is responsible for light absorption, resulting in two absorption peaks: 642 nm and 372 nm for chlorophyll-a, and 626 nm and 392 nm for chlorophyll-b (Villa et al., 2022). The difference between the two chlorophylls lies in the presence of a methyl group in chlorophyll-a (**Fig. 5b**) and an aldehyde group in chlorophyll-b (**Fig. 5c**). Under stress conditions, chlorophyll may degrade, reducing its efficiency (loss of phytol forming chlorophyllide) or losing its function entirely (loss of Mg forming pheophytin).

Carotenoids are organic lipophilic pigments that are yellow–orange in colour, with β-carotene being the most abundant, showing maximum absorption at 448 nm (Gantt and Cunningham Jr., 2001; Villa et al., 2022). Their primary role is as accessory pigments, but they are also involved in photoprotection and possess antioxidant properties due to their eleven conjugated double bonds (**Figure 5d**), which neutralise reactive oxygen species (Villa et al., 2022). The xanthophyll cycle (i.e. oxygenated derivatives of carotenoids) regulates the dissipation of excess light energy. In microalgae, this cycle is modulated by specific LHCs known as LHC Stress-Related (LHSR) complexes (Peers et al., 2009; Lacour et al., 2020).

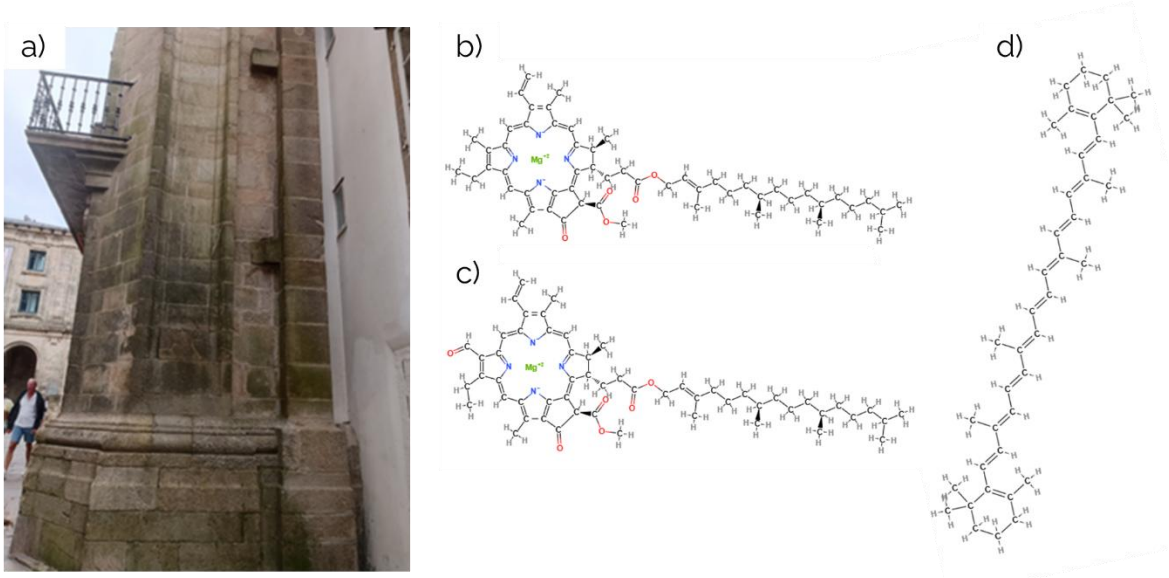

Figure 5. a) Lateral facade of *Casa do Cabildo* in *Praza de Praterías* (Santiago de Compostela). Image by A. Méndez. Chemical structure of b) chlorophyll-a, c) chlorophyll-b, and d) ß-carotene. Extracted from MolView v2.4 (open to use).

1.2.5 Biodeterioration: Types and open questions. Bioprotection

Biodeterioration was defined by Hueck (1968) as *"any undesirable change in the properties of a material caused by the vital activities of organisms"*. Biological agents pose significant risks to the conservation of architectural heritage, which conservators and scientists aim to halt, mitigate and prevent, whether the damage is caused by bacteria, (micro)algae, fungi, lichens, plants or animals (Pinna, 2021). Biodeterioration occurs via a range of processes, which rarely act in isolation (Nowicka-Krawczyk et al., 2022) and can be grouped into three types: physical/mechanical or biogeophysical, chemical or biogeochemical and aesthetic.

According to Gaylarde and Baptista-Neto (2021), it is difficult to distinguish between physical deterioration of stone by abiotic agents and that associated with microorganisms (biogeophysical). Biogeophysical deterioration processes cause deformation and fracture of lithic material due to the movement, growth, development and contraction–expansion of microorganisms, although not through the use of the substrate as a nutrient source (Allsopp et al., 2004; Nowicka-Krawczyk et al., 2022). Fracturing of mineral grains increases the reactive surface area, making the rock more vulnerable to biogeochemical deterioration (Cutler and Viles, 2010).

The presence of a SAB on lithic surfaces can alter water vapour diffusion between the material and the atmosphere, thereby changing the normal hydric dynamics of the rock by blocking pores, reducing permeability and retaining subsurface moisture (Gaylarde et al., 2003; Cutler et al., 2013). The EPS matrix can also mechanically deteriorate dimension stones (Papida et al., 2000) through expansion and contraction cycles associated with

wetting–drying and caused by volume changes in the hydrophilic EPS components and increased water infiltration at the surface (Cutler and Viles, 2010). Additionally, when ambient temperatures drop below zero, freeze–thaw cycles increase mechanical damage due to the volume expansion of water at the rock surface (Young and Wainwright, 1995). The presence of EPS also promotes biogeochemical deterioration by chelating metal cations and solubilising and precipitating calcium from the rock minerals (Ortega-Morales et al., 2000; Kala and Pandey, 2023).

Biogeochemical deterioration results from the dissolution and/or alteration of the mineral components of the substrate rock, induced by the metabolic activity of microorganisms. Nowicka-Krawczyk et al. (2022) further indicate that these processes may be assimilatory or dissimilatory. Assimilatory processes involve microorganisms absorbing elements from the substrate as sources of energy or nutrients, providing them with essential trace metals, phosphates, sulphates and other metabolites (Dakal and Cameotra, 2012). Dissimilatory processes occur through the excretion of metabolites into the substrate, thus weakening the crystalline structure of the rock minerals. The emission of inorganic and organic acids by bacteria and fungi leads to biocorrosion, endangering material integrity. For example, nitrifying bacteria produce nitric acid, which solubilises calcium from rocks and degrades carbonates, aluminates and silicates. All fungal species produce organic acids (such as oxalic, citric, gluconic, glyoxylic and oxaloacetic acid) that can solubilise aluminium, potassium, calcium and iron from silicates, feldspars and micas in granite (Gaylarde et al., 2003). Anions excreted with these acids may also react with rock cations to form salts, potentially resulting in salt efflorescence (Yadav and Purchase, 2025). Green microalgae species are also capable of excreting organic acids (such as oxalic, citric, gluconic, fumaric, malic, or formic acid) as secondary metabolites (Borderie et al., 2015), which may contribute to deterioration (Nowicka-Krawczyk et al., 2022).

Aesthetic biodeterioration is mainly caused by changes in the colour and appearance of surfaces due to the presence of organisms, their secretions and related alterations (Wakefield and Jones, 1998; Nowicka-Krawczyk et al., 2022). In the case of SABs, colour changes are produced by the presence of mainly photosynthetic pigments, which give a green-like colour to the surface (**Fig. 5a**), and by atmospheric particles being trapped in the EPS matrix, which leads to blackening the surface (Allsopp et al., 2004; Prieto and Sanmartín, 2016). However, aesthetic biodeterioration has been less well studied than the other two types of biodeterioration. In the author's opinion, there is a lack of a clear, precise definition that would enable objective distinction between what is and is not aesthetic biodeterioration, avoiding subjective criteria linked to current aesthetics. Evidence of this is the absence (to the author's knowledge) of scientific publications including the term "aesthetic biodeterioration" in their title, and the ones that deal with aesthetic biodeterioration only measure changes in the colour of a surface. Applying tools from social psychology to understand the perception and attitudes of such biodeterioration could help establish its definition based on objective criteria. In this regard, Favero-Longo and Viles (2020) have recently advocated for greater attention to be given to aesthetic

biodeterioration, especially in the context of the growing interest in bioprotection of heritage.

Bioprotection can be understood as the physical protection of a surface provided by organisms covering that surface (referred to as the umbrella effect by Mottershead and Lucas, 2000) or by the biomineralisation of salts (i.e. bioprecipitation of minerals on the surface), which can impart bioconsolidating properties to stone (Favero-Longo and Viles, 2020; Liu et al., 2022; Berti et al., 2024). Bioprotection may serve as a sustainable strategy for preventive conservation, understood as the implementation of measures to minimise or prevent the deterioration of cultural heritage (Wirilander, 2012). For example, the study by Cao et al. (2023) shows that the presence of natural biocrusts formed by cyanobacteria, lichens and mosses reduces erosion and improves the stability of the walls of the Great Wall of China by creating a cohesive layer between the organisms, their EPS and environmental particles, which protects the underlying material. Regarding biomineralisation, Liu et al. (2018) proposed that colonisation by the fungus *Colletotrichum acutatum*, which is capable of promoting $CaCO_3$ formation through the secretion of citric acid (as well as formic and propionic acids), could be a viable method for conserving stone relics, provided that the environmental conditions under which the fungus develops are controlled to ensure proper acid production. As several authors have noted (Favero-Longo and Viles, 2020; Liu et al., 2022; Berti et al., 2024), further research is needed to evaluate the balance between the biodeteriorative and bioprotective processes of lithobionts and their net impact on stone monuments.

1.3 BIOSTATIC CAPACITY REGARDING PHOTOTROPHS AND ENVIRONMENTAL FOOTPRINT OF A NEW LIGHTING SYSTEM FOR ARCHITECTURAL HERITAGE IN GALICIA

1.3.1 Assessment of biostatic capacity

There is a growing trend for cities to install exterior lighting systems on buildings and monuments, driven by technological advances in LED lighting. However, any type of nocturnal lighting, including LED, alters the microenvironmental conditions of the area where it is applied. On masonry facades, it can increase surface temperature, reduce relative humidity and disrupt the natural light–dark cycle, provoking physiological responses in colonising phototrophic organisms that may favour their further development (Sanmartín, 2021). Current legislation aims to keep up with the current increase in artificial lighting at night (ALAN), by regulating the different aspects such as energy consumption or light pollution but resulting in disperse laws that do not address the impact on biological colonisation (**Chapter 1**).

The negative effect of ALAN has previously been described in subterranean heritage sites (catacombs, caves, necropolises, etc.), where the term “lampenflora” was coined to refer to the massive biological growth induced by artificial lighting for tourism purposes (Mulec, 2019). The phenomenon was mitigated by implementing solutions based on modifying artificial lighting (Albertano et al., 2003; Albertano and Bruno, 2017; Muñoz-Fernández et al., 2021).

Historic city centres, in addition to their cultural value, are key tourism assets for the local economy. Within the framework of smart city strategies, the use of technologies that optimise urban management and improve sustainability is promoted (Toli and Murtagh, 2020). In this context, the innovative public procurement project CromaLux (2020–2024, http://cromalux.santiagodecompostela.gal/es), within which this doctoral thesis is framed, was developed to design a commercial ornamental lighting solution that is both energy-efficient and environmentally responsible, focusing on the preventive conservation of architectural heritage against biological colonisation by phototrophs.

The CromaLux lighting system uses two successive lighting phases: a highly efficient warm white LED light (CCT: 2,580 K, with a main spectral peak at 613 nm and a secondary peak at 451 nm), from sunset until 23:00, followed by a combination of amber and green LED lights (CCT: 3,000 K, with a main spectral peak at 593 nm and a secondary peak at 528 nm), from 23:00 to 03:00. It is the combination of amber and green LED lights (hereinafter referred to amber+green light) that potentially has a biostatic capacity (understood here as the ability to inhibit the development of phototrophic microorganisms colonising architectural heritage). The amber+green light, which can be considered analogous to the ‘active ingredient’ in pharmacological treatments, is the effective part of the CromaLux lighting system. The warm white LED light was originally included in the CromaLux lighting system in order to optimize the energy efficiency of the lighting and complete the stipulated illumination time of monuments in the urban fabric. The CromaLux lighting system (warm white LED, used for around two hours, depending on the time of year, and the amber+green LED, used for four hours) is examined in **Chapter 9**, which considers the carbon footprint and economic cost, including the associated biofouling control, of the CromaLux lighting system in comparison with other ornamental lighting systems. The performance of the amber+green light is analysed in the remaining chapters. The spectra of both lights are shown in **Figure 6a**. The visual appearance of the amber+green light is very warm and almost white (**Fig. 6b**), making it suitable for urban environments, where the use of coloured lights is strongly discouraged (Méndez, Prieto et al., 2024).

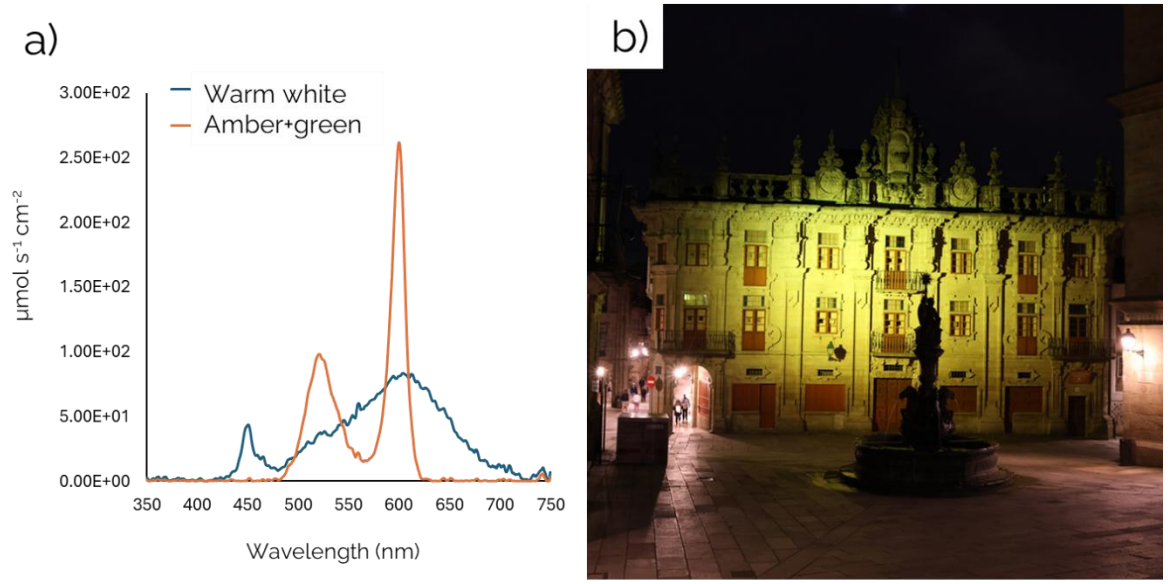

Figure 6. a) Emission spectra of the CromaLux ornamental lighting system, adjusted to an illuminance of 20 lx; b) *Casa do Cabildo* in *Praza de Praterías* (Santiago de Compostela) illuminated by the amber+green light of the CromaLux system. Image by A. Méndez.

1.3.2 Impact on biodiversity

Light pollution has many definitions but can basically be defined as the *"alteration of the natural darkness of the night sky caused by artificial lighting sources"* (Pelegrina et al., 2024). Population growth, together with reduced lighting costs, has led to a sustained increase in ALAN in recent decades, with estimated annual growth rates between 2% and 10%, depending on the country. This has resulted in two thirds of the world's population living under skies polluted by artificial light (Katz and Levin, 2016; Azman et al., 2019). To align it with other types of pollution, Bará et al. (2022) proposed quantifying light pollution in terms of the volumetric concentration of anthropogenic photons in the atmosphere (expressed as photons m^{-3}), moving away from non-standard measures such as lux (lx), used in Spanish legislation (MINCOTUR, 2008).

Light pollution can be understood from several perspectives. Traditionally, it refers to the degradation of night sky visibility for humans, known as "astronomical light pollution" (Longcore and Rich, 2004), which has cultural implications (Hamacher et al., 2020) as well as a direct impact on astronomical research (Varela Perez, 2023). Longcore and Rich (2004) introduced the concept of ecological light pollution, or photopollution, to refer to the *"harmful effects of artificial light on living organisms"*, including direct glare, sudden fluctuations in ambient light, or a chronic increase in illumination during hours when darkness should prevail. Exposure to ALAN can influence biomass, species composition and alter the distribution of photosynthetic microorganisms in the environment (Falcón et al., 2020), as these organisms are affected by the characteristics of the light used (**Chapters 7 and 8**). The introduction of white LEDs has led to "whitening" of the light spectra (i.e. the emission of light in all the wavelengths of the visible light spectrum)

relative to the narrower spectrum emitted from discharge technologies (Evans, 2023). In particular, there is an increase in the blue-light part of the spectrum that produces more skyglow (Jechow et al., 2018), which has a greater impact on the circadian rhythm of animals than other wavelengths and promotes microalgal growth (Falcón et al., 2020).

When designing more sustainable ornamental lighting and reducing its contribution to light pollution, researchers such as Mohar et al. (2014) and Rodriguez Lorite (2016) have suggested moderating illuminance and controlling lighting hours, with CCT not exceeding 3,000 K, and avoiding upward facing lighting (towards the sky). Additionally, projects such as that of Kyba et al. (2018) propose adjusting the light beam to the contours of monuments to prevent light spill beyond the boundaries.

1.3.3 Socio-economic and environmental impact

Night-time tourism has experienced significant growth in Europe and North America, with examples such as New York, where urban lighting is itself a tourist attraction (Eldridge and Smith, 2019). Urban lighting, beyond street lighting, was previously more restricted to specific events, but with the increase in tourism and the use of urban spaces at night, perceptions of urban lighting have changed, and lighting projects have proliferated (Giordano, 2018) (**Chapter 10**). According to Chevrier (2019), contemporary nightlife is concentrated in urban capitals and revolves around festive and leisure activities, in which lighting plays a central role. In Santiago de Compostela, tourism has increased by 420% over the past two decades (Sequeiro, 2024).

The direct relationship between tourism and CO_2 emissions, in the context of climate change, remains a subject of debate (Sun et al., 2022). However, it is clear that tourism models, especially those related to night-time tourism, must be reconsidered. According to public lighting data for Spain, urban lighting accounts for electricity consumption amounting to 2,900 GWh $year^{-1}$ (1.8% of national electricity consumption), corresponding to emissions of 1,740,000 tonnes CO_2 $year^{-1}$. In Santiago de Compostela, the cost of maintaining and supplying power for urban lighting is approximately €3.5 million a year (including €24,500 for ornamental lighting), which is equivalent to 9% of the annual municipal budget (Innovation Procurement Compass, 2024) (**Chapter 9**). The recurring costs associated with maintaining the architectural heritage, which amounted to €923,000 in 2023 (Consorcio de Santiago, 2022), must also be added to this cost.

2 JUSTIFICATION AND OBJECTIVES

The SMARTiAGO initiative (https://smartiago.santiagodecompostela.gal/es/portada), launched by the Santiago de Compostela City Council in 2018, promoted a series of strategic lines aimed at developing innovative technological solutions within the framework of smart cities, with the objective of addressing specific challenges faced by Heritage Cities such as Santiago de Compostela. The three proposed lines focused on sustainable waste management, mobility within the historic centre, and the development of an innovative ornamental lighting system oriented towards heritage conservation. This third line led to the creation of the CromaLux project (https://cromalux.santiagodecompostela.gal/es/), designed for implementation in the city of Santiago de Compostela, designated a UNESCO World Heritage Site in 1985, where the high influx of tourists, particularly pilgrims, adds significant value to ornamental lighting.

The CromaLux project (2020–2024), developed jointly by the companies Televés S.A.U. and Ferrovial Servicios S.A. (currently Ferrovial Energía S.A.) and the University of Santiago de Compostela (USC), was considered the most successful of the three strategic lines of SMARTiAGO. This doctoral thesis was carried out within the framework of the project, under the Industrial Doctorate modality (04_IN606D_2021_2598528), in collaboration between Ferrovial Energía S.A. and the USC. The doctoral work, which also holds an international distinction, was selected in July 2025 for the dissemination campaign of the Industrial Doctorates programme by the Galician Innovation Agency (Gain-Xunta de Galicia). It is also referenced in the guidelines of the international project competition for ornamental and artistic lighting of the monumental surroundings of the Cathedral of Santiago de Compostela (https://compostelanocturna.santiagodecompostela.gal), where it is considered to be acknowledged, respected and supported.

Ornamental lighting plans are governed by aesthetic considerations, energy efficiency, and recommendations regarding their environmental impact; however, they do not account for their potential effect on the biological colonisation present on architectural heritage. Artificial light can promote the development of phototrophic colonisation (in the form of SABs composed of algae and cyanobacteria) if emitted at wavelengths that stimulate photosynthesis. The implementation of innovative lighting solutions must comply with the strict regulatory framework within the urban fabric, resembling white light due to the impossibility of using monochromatic lighting on a permanent basis. It has been hypothesised that the combination of narrow-band amber and green LED light (with a

primary peak at 593 nm and a secondary peak at 528 nm) will have a biostatic effect by illuminating between the main absorption peaks of photosynthetic pigments (chlorophylls and carotenoids) while maintaining and adequate white-like appearance. Nevertheless, its biostatic capacity over phototrophic colonisation must be validated against the effects of other ornamental lighting sources. The study of amber and green light has been approached holistically, also considering its environmental, economic and social impact. This general objective has been divided into four specific objectives, corresponding to the four parts into which the research of this thesis has been structured:

Part 1: To examine the legislative framework governing ornamental lighting of architectural heritage, with particular attention to Spanish regulations, and to understand the impact of lighting policies on light pollution and their environmental implications.

Part 2: To gain deeper insights into the physiological responses to ornamental lighting of phototrophic SABs present on heritage surfaces, with the aim of validating the biostatic capacity of the amber+green light used in the CromaLux lighting system and its mechanisms of action in comparison with other lighting sources.

Part 3: To study the effects of the amber+green LED light from the CromaLux lighting system on biodiversity, considering not only the microbial biodiversity colonising architectural heritage but also the surrounding insect biodiversity. ***Part 4:*** Assess the environmental and economic impact of implementing the CromaLux lighting system compared to other lighting sources, as well as the public response towards designing strategies for its acceptance.

3 METHODOLOGY

3.1 STRUCTURE OF THE THESIS

The thesis is divided into four parts, each with a different objective, and a total of ten chapters, as summarised in **Table 1.** ***Part 1***, comprising **Chapter 1**, deals with the legislative framework governing outdoor ornamental lighting, with particular focus on the illumination of monuments in Spain. ***Part 2*** focuses on validation of the biostatic capacity of the amber+green light from the CromaLux lighting system, in **Chapters 2 to 6**, while ***Part 3*** examines the impact of this system on biodiversity in **Chapters 7 and 8**. Finally, ***Part 4*** assesses the environmental and economic impact of the CromaLux lighting system, in **Chapter 9**, and its social acceptance, in **Chapter 10**. In all chapters, the amber+green light formed part of a lighting set-up, which included other ornamental lights as controls, for purpose of comparison.

The experimental and lighting set-up referred to in **Chapters 2 to 10** of the thesis are summarised in **Table 2**. **Chapter 1** is not included as it is a literature review. The table includes information about the sites where the experiments were performed, the organisms or systems targeted and technical data on the daylight and ornamental lighting set-ups used throughout the research. In all chapters, all lighting set-ups were compared with a negative control with no ornamental illumination.

The duration of the ornamental lighting was based on the results reported in **Chapter 2**, in which was concluded that illumination for between 4 to 6 hours with green light was the most effective way of inducing a biostatic effect. From the studies reported in **Chapter 3** onwards, the green light was combined with amber light to produce a white-like effect (amber+green light at 3000 K) suitable for the urban fabric, as the use of coloured light is strongly discouraged for permanent ornamental illumination. The biostatic capacity of the amber+green light was then assessed for different times, of between 4 and 6 hours, in the subsequent research: for 6 hours in the studies reported in **Chapters 3 to 5** and for 5 hours in those reported in **Chapter 6**. In the research reported in **Chapter 9,** the CromaLux lighting system used 4 hours of amber+green light, after two hours of a warm white light used for energy efficiency purposes.

Laboratory studies provided a controlled environment for validation of the biostatic capacity (i.e. halting growth), by employing custom-built cabinets for the installation of the lighting set-up. All laboratory-cultured SABs (**Chapters 2 to 5**) were derived from natural phototrophic SABs (mainly composed by green algae and to a lesser extent of

cyanobacteria) growing on architectural heritage built from granite in the historical centre of Santiago de Compostela. SABs were developed on polycarbonate membrane discs (**Chapters 2 to 4)**, taking as a reference the study of Anderl et al. (2000), implemented for phototrophs by Sanmartín et al. (2011). The polycarbonate membranes enable permeation of water and solutes to the organisms, while enabling manipulation of the SAB. Aliquots of 250 µL (**Chapter 2**) or 50 µL (**Chapter 3 and 4**) of liquid culture of phototrophic cells in exponential growth were inoculated on the sterile membranes placed on agar plates (**Fig. 7a**). The agar plates were changed every 3 to 4 days under sterile conditions to ensure full nutrient and water availability to the SABs. The plates were held under the experimental conditions of the lighting set-up for 35-37 days until the SABs reached maturity. The culture medium originally used was BG11 (Rippka et al., 1979) which is composed of the green algae *Bracteacoccus minor*, *Chlorella* sp. and *Stichococcus bacillaris*, and the cyanobacteria *Isocystis* sp. and *Aphanocapsa* sp. (**Chapter 2**). The BG11 medium, which is designed for culturing cyanobacteria, was subsequently replaced with Bold Basam Medium (BBM), which is optimised for culturing microalgae Bischoff and Bold, (1963) (**Chapters 3 and 4**). The culture used in the studies reported in **Chapters 3 and 4** was mainly composed by the green algae *Chlorella vulgaris* and *Klebsormidium flaccidum*, and the cyanobacterium *Synechocystis* sp.

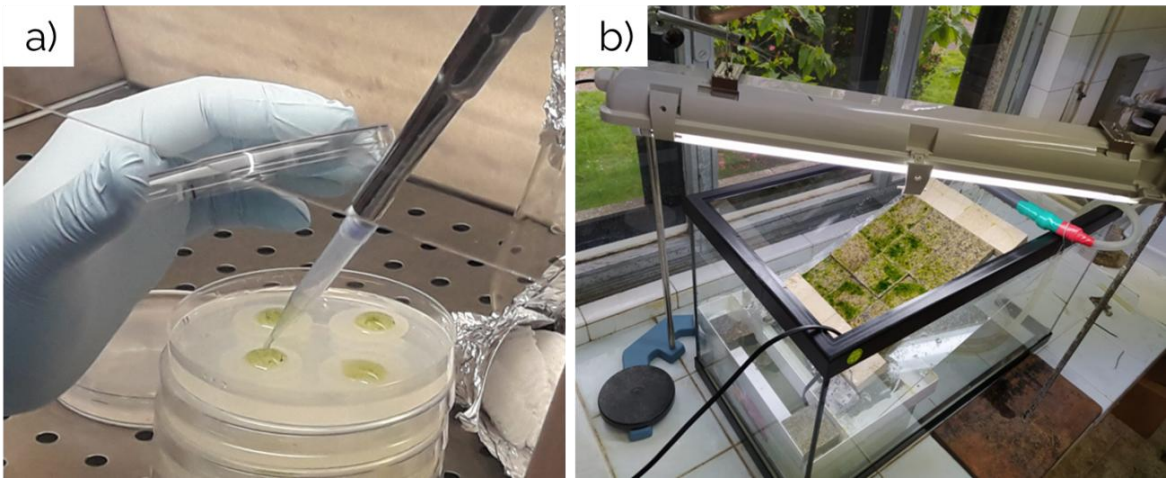

Figure 7. a) Inoculation of polycarbonate membranes with liquid algal culture over agar plates, b) custom-built flow cascade with colonised granite probes. Images by P. Sanmartín.

In later research (**Chapter 5**), small granite or cement sample blocks (instead of membranes) were inoculated with a phototrophic culture in a custom-built flow cascade (**Fig. 7b**, see e.g. Guillitte and Dreesen, 1995; Goeres et al., 2009). The stone samples were placed in the cascade system with an angle of ≈25º under the intermittent flow (4 flows of 15 minutes per day) of a heavily diluted algal BBM culture (5-10%) for 2 months until a SAB formed on the surface. The samples colonised in the laboratory were placed on plastic trays with full water availability and under the corresponding lighting set-up for 3 months.

The inoculation culture mainly contained green algae *Bracteacoccus minor*, *Stichococcus bacillaris* and *Chlorella vulgaris*, and the cyanobacterium *Synechocystis* sp.

The research reported in **Chapters 6 to 8** was conducted in one of the buildings used in the CromaLux pilot project, the *Pazo de Raxoi* (city council buildings). The *Pazo de Raxoi* is a neoclassical palace completed in 1766 and located in the historical centre of Santiago de Compostela, opposite the cathedral of Santiago de Compostela (see Méndez, Maisto et al., 2024). The inner courtyard was selected for the study to minimise any influence from pedestrians on the experimental set-up. Its location out of public view allowed the installation of a positive control (metal halide lamp) for comparison with the amber+green light, as installation of more than one type of luminaire on visible facades is not feasible. Both the metal halide and the amber+green luminaires were shielded to direct their light beams towards the corresponding ashlar and avoid interference between lighting conditions.

The facades of the inner courtyard have heterogeneous masonry. In the research reported in **Chapters 6 and 7**, ashlars of the same type of granite rock (coarse-medium grained with some ochre spots surrounding biotite and reddish-brown colouration on feldspars) were selected for illumination by the corresponding lighting system. The ashlars were covered by a visible SAB, mainly composed of *Myrmecia irregularis*, *Geminella minor* and *Calothrix* sp., as well as species of bacillariophytas (diatoms) and cyanobacteria. At the beginning of the study (June 2021), the selected ashlars were mechanically cleaned by brushing with distilled water, to ensure a standardized starting condition.

Microbiological samples were collected from certain points of the wall exposed to the lighting system on small areas (10 cm^2) by swabbing the surface with sterile cotton swabs, which were then resuspended in Phosphate-Buffered Saline (PBS). The sampling described in **Chapter 6** was performed 4 times (before cleaning in April 2020 and after cleaning in May 2021, February 2022 and February 2024) to monitor any changes in the phototrophic community under the lighting set-up. The sampling described in **Chapter 7** was performed once (May 2022), to assess the shifts in the microbiome (mainly bacteria and fungi) under the influence of the lighting system. In **Chapter 7,** the PBS samples were frozen at -20ºC until analysis.

Insect sampling (**Chapter 7)** was carried out using sticky traps installed directly under the lighting system (**Fig. 8a**). The sticky traps under the metal halide lamp were removed and replaced after 5–16 days, depending on the number of insects trapped on the board (assisting identification by avoiding having large numbers of insects) and also on the probability of rain (potentially damaging the boards). Sampling was carried out between 1 June and 20 October 2021 to cover the main period of activity of insects.

The studies reported in **Chapters 9 and 10** were carried out in the other building used in the CromaLux pilot project, the *Casa do Cabildo*, which was built between 1755

and 1758 as a private residence and with a workshop on the ground floor, and which now houses a museum Taín Guzmán, 2012. The CromaLux lighting system was installed in November 2021 to illuminate the main facade of the building.

In the study reported in **Chapter 9**, the *Casa do Cabildo* was used to determine the environmental and economic performance of the CromaLux lighting system (**Fig. 8b**), in comparison with the traditional metal halide lamps used in Santiago de Compostela for ornamental illumination and with widely used white LED lighting. The environmental and economic performance of commonly used techniques for cleaning SABs (laser cleaning, water vapour and three chemical biocides) was also evaluated. In addition, the interaction between the lighting and cleaning functions of the architectural heritage was also considered, taking into account the results obtained in the research reported in **Chapters 2 to 6** on the effect of ornamental lighting on SAB development.

Finally, **Chapter 10** deals with the public acceptance of the amber+green light, towards designing strategies towards its implementation based on the citizens' responses obtained by qualitative (discussion sessions) and quantitative (field surveys) methods.

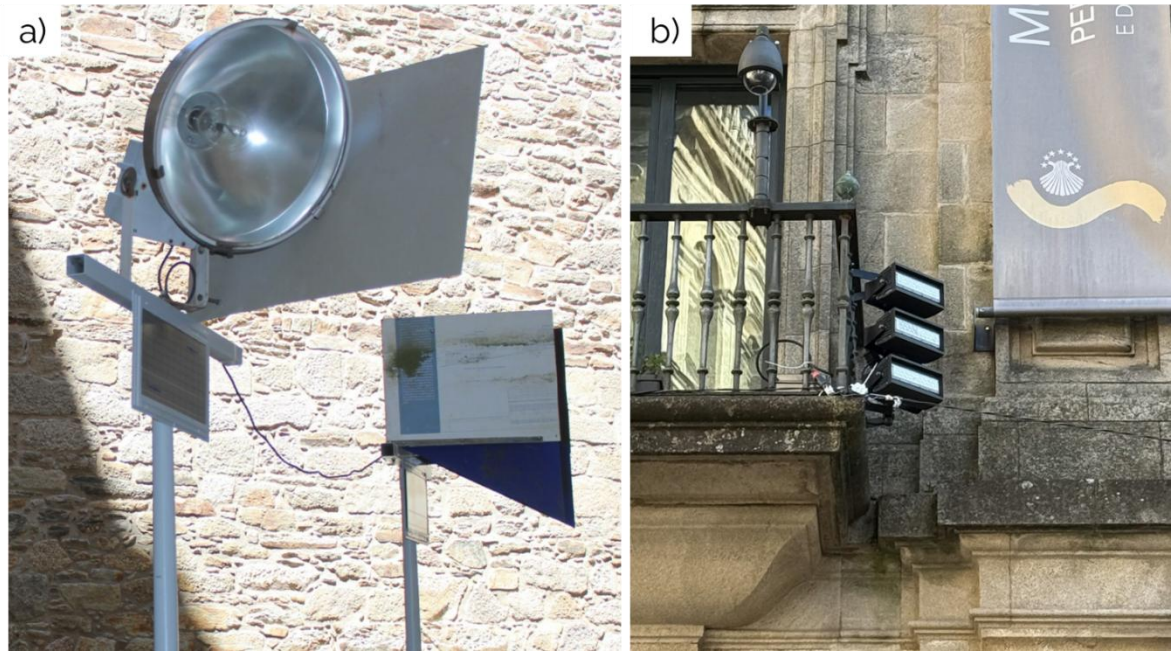

Figure 8. a) Metal halide (left) and amber+green (right) luminaires with sticky boards located underneath (Image by P. Sanmartín), b) CromaLux lighting system installed in *Praza de Praterías* for the illumination of *Casa do Cabildo* (Image by A. Méndez).

Table 1. Overview of the thesis structure, which consists of four parts and ten chapters, including the aims and research methods used.

Part	Chapter	Title	Aim	Approach and methodology
1. Legislative framework	1	Better, not more, lighting: Policies in urban areas towards environmentally-sound illumination of historical stone buildings that also halts biological colonization	To provide an up-to-date view on policies and legislation on outdoor illumination regarding historical stone buildings and light pollution, as well as the associated environmental impact	Literature review on light pollution and policies; Review of the prevailing legislative framework in Europe and how monumental lighting is regulated in Spain
2. Assessment of biostatic capacity	2	Duration of illumination of architectural heritage: A key methodological consideration to control phototrophic colonisation	To determine whether exposure to green, red and blue light at night (2, 4, 6 or 8 hours) decreases or increases the development of phototrophic SABs	Biofilm wet weight; Cell counting; Photosynthetic pigments; PAM fluorometry; Morphological taxonomic identification of phototrophs
	3	Novel ornamental lighting used to halt phototrophic colonisation on architectural heritage is effective under low and high daylight illuminance conditions	To confirm the biostatic (halting growth) effect of the CromaLux amber+green light under low and high daylight illumination conditions	Biofilm wet weight; Cell counting; Photosynthetic pigments; EPS matrix; Confocal microscopy; PAM fluorometry; Morphological taxonomic determination of phototrophs
	4	Environmental proteomics elucidates phototrophic biofilm responses to ornamental lighting on stone-built heritage	To elucidate light-triggered mechanisms that cause the biostatic effect of the CromaLux amber+green light	Environmental proteomics; Morphological taxonomic identification of phototrophs
	5	Biogeophysical impact of algal biofilms developed on granite and mortar substrates under night-time ornamental lighting	To determine the impact of the CromaLux amber+green light on SAB-mineral interface and colonisation patterns on granite and cement mortar samples	Surface roughness and hardness; Contact angle and water absorption time; Colour spectrophotometry; Petrographic microscopy
	6	Long-term validation of the biostatic effect of ornamental lighting on phototrophs: Towards the sustainable conservation of architectural heritage	To confirm the biostatic effect of the CromaLux amber+green light on an outdoor monument over a long period of 3.4 years	Literature review on long term research in cultural heritage; Review of the environmental data for the study period; PAM fluorometry; Colour spectrophotometry; Morphological taxonomic determination of phototrophs

Part	Chapter	Title	Aim	Approach and methodology
3. Biodiversity impact	7	Microbiome shifts elicited by ornamental lighting of granite facades identified by MinION sequencing	To study the biodeteriorative profiles of the microbiome by using culture-dependent and culture-independent approaches in an outdoor monument under the CromaLux amber+green light	Culture dependent methods, Metagenomics; XRD and SEM
	8	Attraction of insects to ornamental lighting used on cultural heritage buildings: a case study in an urban area	To assess the number and diversity of insects attracted to the CromaLux amber+green light on an outdoor monument	Review of the environmental data for the study period; Morphological taxonomic determination of insects
4. Socio-economic impact	9	Carbon footprint of biostatic, targeted ornamental lighting and related cleaning service for sustainable conservation of architectural heritage	To quantify the environmental and economic performance of the illumination and cleaning of architectural heritage of the CromaLux lighting system	Carbon footprint (following standard UNE-EN ISO 14067) and economic performance analysis based on De Bruyn et al. 2023
	10	Social acceptance of ornamental lighting for the conservation of architectural heritage: Use of the CromaLux technology in the heritage city of Santiago de Compostela	To assess the public perception of the CromaLux amber+green light towards designing strategies for its acceptance	Qualitative analysis based on discussion groups and quantitative analysis based on field surveys

EPS: extracellular polymeric substances; PAM fluorometry: pulse amplitude modulated fluorometry; SAB: subaerial biofilm; SEM: Scanning electron microscopy; XRD: x-ray diffraction.

Table 2. Experimental set-up and lighting conditions used in the different studies reported in each chapter.

Chapter	Site	Target	Daylight				Ornamental lighting				
			Technology	Time (h)	CCT (K)	Intensity	Technology	Time (h)	CCT (K)	Spectra (Main peaks, nm)	Intensity
2	Laboratory	SAB (on membrane)	Fluorescent lighting	16	6400	≈19.95 µmol s^{-1} m^{-2}	Green LED	2, 4, 6 and 8	2700-3200	530	5.71 ± 2.41 µmol s^{-1} m^{-2}
							Red LED	2, 4, 6 and 8	2700-3200	631	6.39 ± 2.77 µmol s^{-1} m^{-2}
							Blue LED	2, 4, 6 and 8	2700-3200	450	6.75 ± 2.35 µmol s^{-1} m^{-2}
							White LED (control)	2, 4, 6 and 8	2700-3200	448.5 and 611	6.26 ± 0.47 µmol s^{-1} m^{-2}
3	Laboratory	SAB (on membrane)	Daylight LED	13	5500	50.07 µmol s^{-1} m^{-2} (2,050 lx) and 252.59 µmol s^{-1} m^{-2} (10,200 lx)	Cool white LED (control)	6	4300	457 and 560	1.84 µmol s^{-1} m^{-2} (20 lx)
							Warm white LED (control)	6	2580	604 and 451	1.13 µmol s^{-1} m^{-2} (20 lx)
							Amber+green LED	6	3000	593 and 528	0.89 µmol s^{-1} m^{-2} (20 lx)
4	Laboratory	SAB (on membrane)	Daylight LED	13	5500	252.59 µmol s^{-1} m^{-2} (10,200 lx)	Same as Chapter 3				
5	Laboratory	SAB (on granite and mortar samples)	Daylight LED	13	5500	122.12 µmol s^{-1} m^{-2} (5000 lx)	Cool white LED (control)	Same as Chapter 3			9.20 µmol s^{-1} m^{-2} (100 lx)
							Warm white LED (control)	Same as Chapter 3			5.65 µmol s^{-1} m^{-2} (100 lx)
							Amber+green LED	Same as Chapter 3			4.45 µmol s^{-1} m^{-2} (100 lx)
6	*Pazo de Raxoi*	SAB (on granite facade)	Sunlight	Variable throughout the day and the year			Metal halide (control)	5	4668	435, 508, 546, 578 and 589	32.00 lx
							Amber+green LED	5	Same as Chapter 3		18.45 lx

Chapter	Site	Target	Daylight				Ornamental lighting				
			Technology	Time (h)	CCT (K)	Intensity	Technology	Time (h)	CCT (K)	Spectra (Main peaks, nm)	Intensity
7	*Pazo de Raxoi*	Microbiome (on granite facade)	Sunlight	Variable throughout the day and the year			Same as Chapter 6				
8	*Pazo de Raxoi*	Insects	Sunlight	Variable throughout the day and the year			Same as Chapter 6				
9	*Casa do Cabildo*	Carbon footprint and economic performance	Sunlight	Variable troughout the day and the year			Metal halide (control)	6	4668	N.A.	20 lx
							White LED (control)	6	4000	N.A.	20 lx
							CromaLux lighting system	6	3000	N.A.	20 lx
10	*Casa do Cabildo*	Citizens' response	N.A.				Cool white LED (control)	N.A.	≈ 4000	N.A.	20 lx
							Warm white LED (control)	N.A.	≈ 3000	N.A.	20 lx
							Amber+green LED	N.A.	≈ 3000	N.A.	20 lx

N.A. Not Applicable.

3.2 General description of the methodologies and data sources used in this thesis

3.2.1 Part 1: Review of the policies and legislation on outdoor illumination

A literature review was conducted considering the articles published between 1 January 2020 and 31 October 2022 on the ISI Web of Science (WOS) website, accessed through the Spanish Foundation for Science and Technology (FECYT, for its title in Spanish) (https://www.recursoscientificos.fecyt.es/) and is reported in **Chapter 1.** The search included the term "light pollution" and was refined using the terms "policies", "cultural heritage", "monument", "ornamental" and "facade".

A comprehensive review of legislation concerning light pollution and artificial lighting was conducted at the European, national (Spanish) and regional levels, with particular emphasis on the regulatory frameworks governing ornamental lighting of cultural heritage sites.

A second literature review was conducted considering the articles published between 1 January 1995 and 1 September 2025 on the WOS website, as reported in **Chapter 6**. The search included the terms "long term monitoring" and "cultural heritage". A co-occurrence network analysis was then performed with the keywords from results found in the search with a minimum of 5 co-occurrences, using WOSviewer (version 1.6.20).

3.2.2 Part 2: Non-destructive techniques for assessment of biostatic capacity

3.2.2.1 Chlorophyll PAM fluorometry

Chlorophyll-a (Chl-a) fluorescence has been used in the last two decades as a way of studying photosynthetic performance and interpreting phototrophic microorganisms and plant leaf physiology (see e.g. Govindjee, 2004; Papageorgiou et al., 2007). Warburg (1920) found that Chl-a fluorescence increased quickly after light exposure and then decreased slowly, coinciding with the increase in CO_2 assimilation. Kautsky and Hirsch (1931) described what is today known as the *Kaustsky transient* or *effect*, correlating the fluctuations in Chl-a fluorescence with the changes in photosynthetic activity and providing information on the efficiency of primary energy conversion. Most of the Chl-a fluorescence is derived from the Photosystem II (PSII) (<90%), which transiently reduces its first electron acceptor, phaeophytin; the reduction is reflected by a transient increase in the fluorescence yield Tyystjärvi et al., (1999). When dealing with Chl-a fluorescence, the intensity of the fluorescence does not carry information, but rather the yield of the fluorescence is correlated with the organism's physiology in a dark-adapted state (Tyystjärvi et al., 1999).

In dark-adapted organisms (i.e. held in darkness for at least 20 minutes), all of the reaction centres in PSII are open (i.e. all the primary plastoquinone acceptors Q_a and Q_b are in their oxidised form). When subjected to actinic light (i.e. light with enough energy to cause photochemical reactions), the absorbed energy of photons is transferred, and the electron transport starts on PSII from P680 to phaeophytin and to the plastoquinone acceptors, which closes the reaction centres (i.e. partial reduction of the primary plastoquinone acceptors occurs). The rate of energy conversion at PSII is limited by the primary plastoquinone acceptor Q_a. Thus, an increase in the fluorescence signal will occur from the minimum fluorescence (F_0, which can be measured with a non-actinic light, measured in a.u.). If the intensity of the actinic light used is high enough (a saturation pulse), all of the Q_a acceptors will close (i.e. all the primary plastoquinone acceptors Q_a and Q_b will be in their reduced form) and a maximum fluorescence (F_m, measured in a.u.) will be recorded, with the increment between both states (F_m - F_0) known as F_v (measured in a.u.). The fluorescence at F_0 comes exclusively from the Light Harvesting Complexes (LHC) in PSII, whereas the reaction centre is also involved in the increase of F_m (Lichtenthaler et al., 2005).

Development of Pulse Amplitude Modulated (PAM) fluorometry in 1986 (Schreiber, 2004) enabled study of all of the rapid changes in fluorescence yield upon dark-light and light-dark transitions by using a measuring light consisting of very short pulses applied repetitively at different frequencies. This technique results in a characteristic *Kautsky curve* that reflects the transient between the pulses. Determination of the F_0 and F_m parameters enables estimation of the quantum yield of energy conversion in the PSII ($QY_{max} = F_v/F_m$, ranging from 0 to 1). However, in normal light conditions the energy conversion is lowered as there is partial closure of the reaction centres (decreased photochemical quenching) and by heat dissipation (increased non-photochemical quenching). Thus, the effective quantum yield can be calculated from the maximum fluorescence recorded from a saturating pulse on a non-dark-adapted organism. In green algae, the values of QY_{max} normally range from 0.6 to 0.7, whereas in cyanobacteria they range from 0.4 to 0.6 (Schuurmans et al., 2015; Macário et al., 2023), and changes in the QY_{max} value will thus signal stress that directly affect the PSII system (e.g. light-related stress) or that forces the organism to increase its photosynthetic activity to counteract the stress. Non-photochemical quenching (NPQ) reflects dissipation of energy by antenna pigments in the LHC. Typically, electron transport from P680 to phaeophytin accounts for approximately 97% of the photons absorbed by the LHC, and the fluorescence signal accounts for only 0.5% (Ke, 2001). Around 2.5% of the photons are dissipated in the form of heat, and an increase in the NPQ will thus account for a decrease in photochemical quenching (qP).

Two PAM fluorometry devices were used in the research presented in this thesis. First, in the studies reported in **Chapter 2** a portable Phyto-PAM model EDF version (Walz, Effeltrich, Germany) equipped with a fiber optic emitter-detector unit (PHYTO-EDF) was used to excite Chl-a fluorescence at four different wavelengths from a LED

source: 470, 520, 645 and 665 nm. The parameters obtained were F_0 (through the use of non-actinic light) and F_m, with a saturating light pulse of 8,000 µmol photons m^{-2} s^{-1} for 0.8 s, retrieving the quantum yield (QY_{max}). In the studies reported in **Chapters 3 and 6**, a Handy FluorCam FC 1000-H (Photon Systems Instruments, Czech Republic) was used (**Fig. 9**). This is an imaging-PAM that enables capture of the fluorescence signal over a 4x3 cm^2 surface with a digital camera filtered at 695 nm to record the fluorescence of the PSII. This device uses a non-actinic LED light at 640 nm to capture the F_0, and 4 white light LED panels for determination of the other parameters: Fm, QY_{max}, QY, NPQ, qP and fluorescence decline ratio (R_{fd}, calculated according to Lichtenthaler et al., 2005). The Handy FluorCam FC 1000-H also uses a far-red light at 740 nm for determination of F_0 in the light-adapted state via the selective excitation of the PSI to forcibly oxidise Q_a Schreiber, 2004a. For recording the PAM parameters, the SABs were subjected to alternating pulses of actinic white light at 206.00 µmol s^{-1} m^{-2} and 1046.00 µmol s^{-1} m^{-2} for the saturating pulse. In the studies reported in **Chapter 3,** the far-red light was also used at an intensity of 10.50 µmol s^{-1} m^{-2}. In the research reported in **Chapter 6,** it was not possible to cover the walls selected for the experiment, and estimation of dark adaptation was therefore not possible. Nonetheless, the Handy FluorCam FC 1000-H enables measurement of samples in a light-adapted state. Thus, the F_0, F_m and quantum yield values reported in this chapter do not include the maximum or minimum values (for which the dark-adaptation is necessary) and correspond to the light-adapted state.

Figure 9. Use of the imaging PAM fluorometer over a granite ashlar in the inner courtyard of *Pazo de Raxoi*. Image by P. Sanmartín.

3.2.2.2 Colour spectrophotometry

Colour spectrophotometry measurements were carried out in the studies reported in **Chapters 5 and 6** following the European Standard, 2010, which is based on the CIELAB colour space (established, 1967). The CIE L*a*b* (CIELAB) standard colour space European Standard, 2010 is the colourimetric model developed by the *Commission Internationale d'Eclairage* (International Commission on Illumination) used to reproduce and analyse the colour of samples. This colour space aims to be perceptively linear, meaning that it attempts to equate changes in magnitude with changes in the visual appearance (Schanda, 2007). The CIELAB colour space can be represented in a colourimetric sphere, with three scalar coordinates that represent the measured parameters: L*, a* and b*. Each colour can be defined by these three dimensions: L* defines the lightness, with values ranging from 0 (absolute black) to 100 (absolute white) CIELAB units, a* represents the red-green component (red > 0 > green), and b* represents the yellow-blue component (yellow > 0 > blue). Although the limit of the range is sometimes established at 60 and 120 CIELAB units, both a* and b* have unlimited range. The system is based on the Ewald Hering's opposing process theory, which states that colour information is processed through three systems with opposing colour pairs, so that a colour cannot be red and green, blue and yellow, or light and dark at the same time (Hering, 1964).

CIELAB colour measurements were conducted with a CM-600D VIS-light (**Chapter 5**) or a CM-700 VIS-light (**Chapter 6**) spectrophotometer (Konica Minolta, Japan), equipped with an 8 mm aperture and a standard D65 illuminant with light reflected at 8°. A flash of white light is emitted (from a xenon lamp) and the optical system collect the reflected light. The device can then include the specular reflectance (SCI) or compute the diffuse reflectance (SCE). In materials of heterogeneous texture, inclusion of the specular reflectance is recommended, and thus only the SCI data was utilized in the corresponding studies (**Chapters 5 and 6**). In these studies, the parameters L*, a* and b* were recorded, and the differences between colour samples (ΔE^*_{ab}) were calculated using the formula:

$$(\Delta E^*_{ab} = \sqrt{(\Delta L^*)^2 + (\Delta a^*)^2 + (\Delta b^*)^2})$$

Threshold colourimetric values were used to determine whether the colour changes were perceptible by the human eye, as proposed by Mokrzycki and Maciej (2011). The colour differences perceived by a standard observer are indicated values between 0 and 5, as follows: between 0 and 1 the observer does not note any difference ($0 < \Delta E^*_{ab} < 1$), from 1 to 2 only experienced observers can note a difference ($1 < \Delta E^*_{ab} < 2$), from 2 to 3.5 an unexperienced observer can also note the difference ($2 < \Delta E^*_{ab} < 3.5$), from 3.5 to 5 there is a clear difference in colour ($3.5 < \Delta E^*_{ab} < 5$) and beyond 5 the observer clearly sees two different colours ($5 < \Delta E^*_{ab}$). In the studies reported in **Chapter 5,** the spectral reflectance of the samples (in %) was in the spectral range 400 - 700 nm.

3.2.3 Part 2: Destructive techniques for assessment of biostatic capacity

3.2.3.1 Wet weight of biomass, cell counting and photosynthetic pigments quantification

The biofilm biomass was measured directly by wet weighing (precision laboratory balance, Denver Instruments: readability, 0.001 mg; uncertainty, i.e. repeatability, 0.002 g), before and after the biofilm was removed from the membrane. The SAB biomass was removed with a sterile loop and resuspended in a buffer for posterior analysis: PBS for cell counting, pigment content, ATP quantification and for taxonomic identification; and ethylenediaminetetraacetic acid (EDTA) for EPS characterization and environmental proteomics.

For cell counting, an Utermöhl sedimentation chamber (Utermohl, 1958) was used to determine the concentration of cells in the SABs (cells mL^{-1}). At least 1000 cells were counted across 100 fields of view at 40× magnification.

The pigment content was determined in the research presented in **Chapters 2 and 3** by extraction with dimethylsulfoxide (DMSO, Sigma Aldrich, Italy) following the methodology of Bell and Sommerfeld (1987). The pigment extracts were then analysed spectrophotometrically, and the absorbance was measured at 480 nm, 647 nm, 664 nm and 750 nm to determine the chlorophyll-a and -b (**Chapters 2 and 3**) and total carotenoids (**Chapter 2**) using the equations proposed by Wellburn (1994).

3.2.3.2 Characterisation of extracellular polymeric substance (EPS) matrix composition

The exopolysaccharides and extracellular proteins from the EPS matrix were extracted using the methodology proposed by Villa et al. (2015), with the modifications described by Sanmartín et al. (2020). The phenol-sulphuric acid method was used to determine the exopolysaccharides (DuBois et al., 1956) and the Bradford assay for the extracellular proteins (Bradford, 1976). The exopolysaccharide and protein content was quantified spectrophotometrically (Multiskan SkyHigh spectrophometer, Thermo Sicentific) in microplates at 490 nm for the determination of exopolysaccharides and at 562 nm for extracellular proteins.

3.2.3.3 Confocal laser scanning microscopy (CLSM)

The chlorophyll, polysaccharides and proteins contained in the was also quantified (**Chapter 3**) by Confocal Laser Scanning Microscopy (CLSM) at the Research Infrastructures Area of University of Santiago de Compostela (Microscopy Unit) using a laser scanning spectral confocal microscope (LEICA TSC SP5 X, Leica Microsystems Heidelberg GmbH, Germany) equipped with white laser and a hybrid detector (HyD).

Complete SABs on the membranes were carefully stained to prevent damaging the internal structure of the biofilm, following the protocol described by Wang et al. (2018), with concanavalin A, tetramethylrhodamine conjugate (lectin ConA-TMR: excitation, 552 nm; emission, 578 nm) for determination of the polysaccharides and fluorescein isothiocyanate isomer I (FITC: excitation, 495 nm; emission, 525 nm) (Invitrogen) for the proteins. Chlorophyll was detected by autofluorescence (excitation, 664 nm; emission, 725 nm).

3.2.4 Part 2: Advanced non-parametric statistical tests for long-term assessment of biostatic capacity

The long-term monitoring (3.4 years) reported in **Chapter 6** was conducted with the aim of confirming the biostatic capacity of the amber+green light in the lighting set-up. PAM fluorometry and colour spectroscopy measurements were performed from June 2021 to November 2024 on the granite ashlars from the inner courtyard of *Pazo de Raxoi*. The parameters recorded were F_0 and QY (PAM fluorometry) and L*, a* and b*, including the calculation of ΔE^*_{ab} (colour spectrophotometry).

The statistical analysis focused on characterizing behaviour of the parameters over time, using nonparametric regression tools, where Y is the outcome parameter and t is the time when measurements were taken. The goal is to model the relation between Y and t, without imposing a parametric model as follows:

$$Y=m(t)+\varepsilon \quad (1)$$

where ε is a zero-mean error term and $m(t)$ is the regression function, which intends to capture the expected value of Y given a time moment t by using (Y_i, t_i) with $i = 1, \ldots, n$ the sample of observed date. Flexible models (Wand and Jones, 1994) do not impose a parametric form on the regression function and estimate the regression function at a certain time t_0 by a weighted average of responses whose corresponding observation time is close to t_0. Specifically,

$$\hat{m}(t_0)=\sum_{i=1}^{n} w_h(t_i-t_0)Y_i \quad (2)$$

is the estimator of the regression function at time t_0, where $w_h(\cdot - t_0)$ is a weight function that places more weight on the values of Y_i with t_i close to t_0. These functions are usually rescaled kernels, being the most widely used the Gaussian kernel, based on the real-valued Gaussian density. Specifically, for the Gaussian kernel, the weight function is expressed as follows:

$$w_h(t)=\frac{1}{\sqrt{2\pi}h} e^{-\frac{t^2}{2h^2}} \quad (3)$$

which corresponds to a Gaussian density with mean zero and standard deviation h. In equation (2), the weight function acts on the difference $(t_i - t_0)$. Hence, for a fixed point t_0, the greatest weights correspond to values of t close to t_0.

These methods depend on a so-called smoothing parameter or bandwidth, namely *h*, which indicates the temporal range which is used to compute the weighted average in equation (2). The bandwidth parameter can be identified with a standard deviation in a normal density in equation (3) for the Gaussian kernel. In practice, selection of *h* is a crucial problem in nonparametric smoothing methods. In general, large values of *h* lead to oversmoothed estimators, with low variance but high bias. On the contrary, small values of the bandwidth parameter result in undersmoothed estimators, with low bias but high variance. For selection of this tunning parameter, a trade-off between bias and variance must be found (see Fan and Gijbels, 2018). An effective way to obtain a bandwidth value from an observed sample is by cross-validation, i.e. minimizing *h* in the following function:

$$CV(h)=\sum_{i=1}^{n}\left(Y_i-\widehat{m_{-i,h}}(t_i)\right)^2 \quad (4)$$

which is the sum of the squares of the prediction errors when, for each datum, the estimator is computed without it. For instance, for the first datum in the sample, Y_1 will be compared with the prediction obtained for t_1 using all the data points in the sample except the first.

The use of model (1) enables the following two research questions to be addressed: (i) if the change in response *Y* is affected by time, and (ii) if *Y* is influenced by time, if it can be determined whether the effect is linear.

Bowman and Azzalini (1997) proposed the use of non-effect and linearity tests, based on the estimator in equation (2). For the non-effect test, the null hypothesis H_0 is that *t* has no effect on *Y*, whereas the alternative hypothesis is that there is a nonparametric relation. The nonparametric (smooth) fit in (2) is then compared with the fit that would be considered under the non-effect hypothesis, i.e. a horizontal line (on the average of the values of *Y*). If there is a large difference between the flat/horizontal line and the nonparametric fit, then the non-effect hypothesis will be rejected. The comparison is carried out using an F-type test to compare the residual sums of squares for each fit. Specifically, the test statistic for testing non-effect is given by

$$T=\frac{RSS_0-RSS_1}{RSS_1} \quad (5)$$

where *RSS* is "residual sum of squares". Under the null hypothesis of non-effect:

$$RSS_0=\sum_{i=1}^{n}(Y_i-\mu)^2 \quad (6)$$

where μis a constant value (corresponding with the mean of the observed values of the response). If there is no effect of time on the response, then the best fit will be a horizontal line. For the alternative hypothesis, the responses can be compared with a nonparametric fit:

$$RSS_1 = \sum_{i=1}^{n} \left(Y_i - \hat{m}(t_i)\right)^2 (7)$$

The test statistic *T* can be expressed as a ratio of quadratic forms of the response (see Bowman and Azzalini, 1997) and its asymptotic distribution can be determined by estimation methods. From this distribution, a p-value is obtained, and the test can be performed in practice.

A similar procedure is used for the test of linearity. First, the null hypothesis in this case can be expressed as H_0: *t* has a linear effect *Y*, whereas the alternative hypothesis is the same as before (nonparametric relation). The test statistic compares the estimation of the fit under H_0, i.e. a least-squares linear fit, with the smooth estimator in equation (2). The test statistic has the same expression as before (an F-type statistic), comparing the residual sums of squares under the null and the alternative hypothesis. For the linearity test, the RSS_1 is the same as before. However, the residual sum of squares under the null (linear model) is expressed as follows:

$$RSS_0 = \sum_{i=1}^{n} \left(Y_i - \hat{\alpha} - \hat{\beta} t_i\right)^2 (8)$$

where $\hat{\alpha}$ and $\hat{\beta}$ are the estimators of the intercept and the slope in a linear model, which aims to collect the linear effect of the time over the response. As for the non-effect test, the test statistic can be written as a ratio of quadratic forms, and the p-value can be estimated (see Bowman and Azzalini, 1997).

Categorical variables can also play a role in characterizing the relationship between *Y* and *t*. These are the so-called ANCOVA models. In this case, the categorical variable is determined by the type of lighting, with three different ornamental lighting conditions. When a categorical variable is included in a regression model, two questions arise: (i) if it can be assessed whether the variation pattern of *Y* along *t* is the same for the different groups, and (ii) if it is not the same, if is it possible to assess whether the variation patterns are parallel. If parallelism is not rejected, then the difference can be explained by an offset (a "gap" between both curves). For simplicity in interpreting the results, two curves can be compared (equality and parallelism) using a nonparametric ANCOVA approach. Formally, the equality test is stated as follows: H_0 (the regression functions are the same in all the groups) vs. H_a (each group has its own regression function).

In this setting, some new notation must be introduced: Y_{ij} the *i*-th observation in the *j*-th group (with *j*=1,2,…, *J* in general for the number of groups, and *J*=3 in our example). Under the null hypothesis H_0, all of the data are pooled together, and a single smooth estimator is computed, using equation (1), denoted by $\hat{m}(t_{ij})$.

Under the alternative hypothesis, H_a, a different regression function (using the estimator in equation (2)) is used for each group, i.e. $\hat{m_j}(t_{ij})$. In this case, a quadratic distance between the estimators under the null and the alternative hypothesis is computed, and a p-value is obtained from this test statistic:

$$T=\frac{\sum_{j=1}^{J}\sum_{i=1}^{n_j}\left(\hat{m}(t_{ij})-\widehat{m_j}(t_{ij})\right)^2}{\widehat{\sigma^2}} \quad (9)$$

which compares the estimator with the whole dataset (under H_0, ignoring the groups) with the estimator by groups. This comparison is standardized by dividing the squared distance by the estimator of the error variance, which is obtained from the sum of squares of the residuals under the null hypothesis. This test statistic can also be expressed as a ratio of quadratic forms, but in practice in this case the distribution can be estimated by simulations. Finally, for the parallelism test, the null hypothesis is stated as follows: H_0 (the regression functions are parallel for the different groups) vs. H_a (each group has its own regression function). The estimator under the alternative (the one obtained with equation (1) for each group *j*) is compared with an estimator under the alternative, which considers that the curves are parallel. In this case, a global estimator for the whole dataset is computed, and it is shifted in each group by a parameter $\widehat{\alpha_j}$, as follows:

$$T=\frac{\sum_{j=1}^{J}\sum_{i=1}^{n_j}\left(\widehat{\alpha_j}+\hat{m}(t_{ij})-\widehat{m_j}(t_{ij})\right)^2}{\widehat{\sigma^2}} \quad (10)$$

For further details regarding the estimation procedure, see Bowman and Azzalini (1997).

Regarding interpretation of the p-values, the output indicates the probability of obtaining a more extreme value of the test statistic than that corresponding to the observed sample. Hence, small p-values < 5% lead to rejection of the null hypothesis. It can be argued that the tools presented in Bowman and Azzalini, (2021) are designed for independent observations, and in this case, the observations were made over time, so they are expected to be correlated. With the formulation of model (1), the time is the explanatory remaining remains unexplained (the temporal correlation is capture by $m(t)$). Under this premise, the error term ε is assumed to be independent across observations. This hypothesis is assessed in practice: after fitting the model, the residuals (differences between observed and fitted values) are obtained. These residuals are the sample counterpart of the errors, and a correlation test is applied on the residual samples. In all cases, a Durbin-Watson test for correlation was applied, and the null hypothesis of no correlation between residuals was not rejected. In addition, a normality test was also applied to the residuals, and normality was never rejected. Uncorrelated and normal residuals imply independent residuals. The use of nonparametric methods is therefore justified in this case.

The statistical analysis was performed in R (v. 4.4.2, R Core Team, 2024), using the sm package (Bowman and Azzalini, 2021). This package contains all the functions required to run the nonparametric fits, as well as the non-effect, linearity, equality and parallelism tests.

3.2.5 Parts 2 and 3: Analysis of biological communities for assessment of biostatic capacity and biodiversity impact

3.2.5.1 Morphological taxonomic determination of phototrophs and insects

(Morpho)species determination by examining morphological characteristics and using taxonomic keys is an inexpensive method used to identify organisms. In the studies reported in **Chapters 2, 3, 4 and 6** this method was used to identify phototrophic microorganisms (green algae, diatoms and cyanobacteria), and in the study reported in **Chapter 7** it was used to identify insects.

Green microalgae, diatoms and cyanobacteria were identified by examination under a Nikon Eclipse E600 stereomicroscope equipped with an E-Plan 40x objective (N.A. 0.65) and differential interference contrast optics (Nikon, Japan). Optical micrographs were captured with a Zeiss AxioCam ICc5 digital camera. The following taxonomic keys were used: Ettl and Gärtner (1995); Rifón-Lastra and Noguerol-Seoane (2001); Khaybullina et al. 2010; Fuíková et al. (2012); Komárek (2013) and Škaloud et al. (2018).

Insects captured on the sticky traps were examined under a stereomicroscope (Olympus SZX7, Olympus, Hamburg, Germany), photographed with an Olympus C180 digital camera (Olympus, Hamburg, Germany) and identified by an entomologist (Luis Martín). The taxonomic keys used were Barrientos, (2005) for the general study of Iberian arthropods, Malicky, (2004) for Trichoptera, Oosterbroek, (2015) for Diptera, and Leraut, (2007) for other taxa.

3.2.5.2 Biodiversity indexes

The biodiversity was quantified using different indexes to assess how the project affected the surrounding environment. Alpha diversity measures species diversity within a single community or sample, and beta diversity is a measure of dissimilarity between sites Ter Braak, (1983). Alpha-diversity indexes, namely observed species richness, Chao1 and Shannon–Wiener, were used in the studies reported in **Chapters 7 and 8.**

The alpha-diversity of bacterial and fungal communities was evaluated using observed species richness, which refers to the actual number of different species found in a particular area or community. The Chao1 estimator, which estimates total species richness in a particular area or community based on the observed number of species and their frequencies, giving more weight to species present at low abundance. It uses the concept of singletons (F_1 or number of species recorded only once) and doubletons (F_2 or number of species recorded only twice) and the number of observed species (S):

$$S_{chao} = S + F_1(F_1-1)/2(F_2+1)$$

The Shannon diversity index quantifies species diversity by considering both the number of species (richness) and their relative abundance (evenness) in a particular area or community of each species (p_i or proportion of individuals of each species):

$$(H' = -\sum_{i=1}^{S} p_i \ln p_i)$$

3.2.5.3 Culture-dependent analysis

Culture-dependent microbiological analysis involves techniques that require cultivation of isolated microorganisms on a specific medium. Typically, around 99% of viable microorganisms in the soil and in the environment cannot be cultivated (Rappé and Giovannoni, 2003; Dakal and Arora, 2012). However, incomplete information about microbial communities can be supported by culture-independent methods. The proportion of non-culturable microorganisms may be much higher in samples from stone monuments, as the culturable fraction in the microbial biomass (less diverse than in soil, for example) will probably represent a higher proportion of the total microbiota. Additionally, cleaning procedures introduce bias in the microbial composition, as metabolically active microorganisms that remain on the stone surface after the application of biocides will probably be responsible for ongoing biodeterioration (see e.g. Urzì et al., 2016). Culture-independent methods are usually more appropriate for studying the whole community. However, culture-independent techniques do not discriminate between living and dead biomass, and they cannot discriminate the microbiota from the monument and that introduced by dust.

The use of both approaches is recommended as cultivating microorganisms is the most reliable way of validating data obtained by culture-independent techniques like metagenomics (Gutleben et al., 2018). Thus, in the study reported in **Chapter 8**, both culture-dependent and culture-independent approaches were used. For determination of the culturable fraction, the samples from the granite ashlars in the inner courtyard of *Pazo de Raxoi* were plated on Tryptone Soy Agar (TSA) to isolate heterotrophic bacterial species and on Potato Dextrose Agar (PDA) to isolate the fungal species. The species were then further isolated through successive cultivation of morphologically distinct colonies and described by their size, colour, texture and particular characteristics. The bacterial and fungal DNA extracts from the isolates were amplified by PCR (Polymerase Chain Reaction), sequenced by Sanger sequencing and directly compared with sequences in GenBank for the identification. For the bacterial isolates the 16S rRNA gene was amplified using the primers 27F (5'–AGA GTT TGA TCC TGG CTC AG-3′) and 685R (5′-TCT ACG CAT TTC ACC GCT AC–3') (Lane, 1991), whereas for the fungal identification the ITS fragment was amplified using the primers ITS1 (5'–TCC GTA GGT GAA CCT GCG G–3') and ITS4 (5'–TCC TCC GCT TAT TGA TAT GC–3') (White et al., 1990).

Microbial metabolism can be studied at the biochemical level in the bacterial cultures on agar plates. Detection of metabolites that directly affect the stone weathering

(e.g. precipitated soluble salts) can help elucidate the risks of biological colonisation and prevent further risks. The culturable fraction was subjected to specific plate assays using B4 media (for $CaCO_3$ precipitation) and $CaCO_3$ glucose media ($CaCO_3$ solubilisation) **(Chapter 8**). Moreover, iron reducing bacteria (IRB) and iron oxidizing bacteria (IOB) were also detected. The oxidation of iron often results in visible chemical weathering effects, such as stains and surface coatings (Hernandez et al., 2024), and which can be caused by the active role of microorganisms (Sanjurjo-Sánchez et al., 2024).

3.2.5.4 Omics techniques for culture-independent analysis

Omics techniques are culture-independent methods that provide insights into the genetic structure and the metabolic potential and activity of the whole microbial community (Gutleben et al., 2018). The aim of these high-throughput techniques is to detect biomolecules of a specific biological system: genomics for the analysis of genomes, transcriptomics for mRNA, proteomics for proteins, and metabolomics for metabolites (see e.g. Marvasi et al., 2019). In the context of this thesis, environmental proteomics (**Chapter 4**) and metagenomics (**Chapter 8**) techniques were used.

3.2.5.4.1 Environmental proteomics

The aim of environmental proteomics is to study the proteome of samples obtained from the environment (Schneider and Riedel, 2010). A proteome refers to the functional (protein) molecular specifications of a genome (Anderson and Anderson, 1998), i.e. the entire complement of proteins that is (or can be) expressed as cell, tissue or organism. This thesis focuses on the community proteomics of a laboratory-grown SAB, to gain insight into the changes that ornamental illumination triggers over the SAB proteome to study changes in the community by assigning the proteins to specific phylotypes.

Protein expression can be quantified by labelling proteins with stable isotopes to increase the accuracy of quantification. However, this process greatly increases costs and the sample processing time and leads to poor detection of peptides present in low abundance (Zhang et al., 2013). Label-free methods can be used to avoid those drawbacks. In the study reported in **Chapter 4**, proteins were quantified by a label-free method through spectral counting, which uses the frequency of peptide identification of a particular protein as a measure of relative abundance. Thus, a *bottom-up* or *shotgun* approach was used, as the analysis was carried out by examining the peptides released by proteolysis rather than intact proteins (*top-down*) (Zhang et al., 2013). The analysis was conducted using high performance liquid chromatograph (HPLC) coupled to mass spectrometry (MS). Peptides were identified by matching tandem mass spectra obtained from peptide fragmentation with theoretical spectra generated through silico digestion of a protein database, thereby assigning peptide sequences to their corresponding proteins. Proteomic taxonomic results were restricted to the genus level, and proteins identified with <2 unique peptides were excluded. Prior identification of the specific composition of the SABs was

conducted, by morphological taxonomic characterisation, to select the most appropriate database for the protein identification. Thus, the NCBI protein database (https://www.ncbi.nlm.nih.gov/protein/) was used for the phyla Streptophyta, Chlorophyta and Cyanobacteriota. Proteomic taxonomic results were restricted to the genus level, and changes in abundance were considered to have occurred when the relative contribution was > 1%. The proteins detected were classified into families according to InterPro active site classification (https://www.ebi.ac.uk/interpro/). They were also categorized to wider biological processes by the Gene Ontology classification of cellular compartments (https://www.informatics.jax.org/vocab/gene_ontology/).

3.2.5.4.2 Metagenomics

Metagenomics refers to the study of the genome derived from samples of complex communities, identifying the composition and activities of whole community including the non-culturable species (National Research Council, 2007). Next-generation sequencing (NGS) techniques enable multiple DNA sequences to be processed in parallel (NIH, 2025), greatly decreasing the time required to deal with complex samples. In the study reported in **Chapter 8**, Oxford Nanopore Technology (ONT) sequencing was used, which enabled long sequencing reading. In particular, the Oxford Nanopore's third-generation MinION was used for characterisation of the microbiomes. Despite its low accuracy relative to other NGS technologies, the method is relatively inexpensive and is portable. This technology is based on a nanopore structure that allows the flow of single DNA molecules per pore by an ionic current that passes through the flow cell, distinguishing nucleotide bases by the changes in current as they pass through the nanopores without the need for PCR amplification (Laver et al., 2015; Petersen et al., 2020). Moreover, the long reads obtained by MinION sequencing can identify the presence or absence of resistance genes (Petersen et al., 2020), which in the context of biodeterioration and weathering on architectural heritage is of great concern as the presence of resistance genes can render the use of antimicrobials (e.g. biocides, antibiotics or metals) ineffective (see e.g. He et al., 2022). The metagenomic reads were subjected to antibiotic resistance gene (ARG) annotation by comparison against the comprehensive antibiotic resistance database (CARD; https://card.mcmaster.ca/download) and a biocide resistance gene (BRG) annotation against the biocide BacMet2 database (http://bacmet.biomedicine.gu.se/download/BacMet2_EXP_database.fasta) (**Chapter 8**). For microbiome profiling, the metagenomic data was compared against the Kraken2 database (http://ccb.jhu.edu/software/kraken2/index.shtml?t=downloads) for virus, Archea, Eukaryota and Prokaryota, although the focus was made over the bacterial and fungal communities.

3.2.6 Parts 2 and 3: Environmental conditions and architectural stone heritage

3.2.6.1 Weather data

In the studies reported in **Chapter 6 and 8,** weather data were extracted from the web-based repository of the Galician meteorological service (https://www.meteogalicia.gal/web/) to support interpretation of the results. Daily data and average air temperature (ºC), relative humidity (%), rain (L m^{-2}) and sunshine hours (h) were retrieved for the study reported in **Chapter 6**, while monthly data on average air temperature (ºC), relative humidity (%), global irradiation (kJ m^{-2} day^{-1}) and sunshine hours (h) were retrieved for the research reported in **Chapter 8**. The "Estación Santiago-EOAS" weather station (42.87596; -8.559434; WGS84, EPSG:4326) was selected for its proximity to the study sites.

In the study reported in **Chapter 8**, the temperature around the sticky traps positioned below the lighting set-up was monitored with data-loggers HOBO MX2202 (Onset, Bourne, OR, USA) to detect any possible differences in temperature that could influence the attraction of insects. The relative humidity of the inner courtyard of *Pazo de Raxoi* was also monitored using data-loggers HOBO MX2302A data (Onset, Bourne, OR, USA). The relative humidity in the inner courtyard was consistent with the web-based repository.

3.2.6.2 X-Ray diffraction (XRD) and scanning electron microscopy (SEM)

X-Ray diffraction (XRD) was used to verify the visual identification of the lithic material in the selected granite ashlars (**Chapter 7)**. The mineralogical composition of the ashlars was determined by XRD analysis, and the granitic rock was correctly identified from the proportions of quartz alkali feldspars and plagioclases by use of a Streckeisen diagram (Streckeisen, 1976).

Small fragments of the target granite ashlars from the inner courtyard of *Pazo de Raxoi* were analysed by X-Ray diffraction (XRD), in a PW1710 Philips diffractometer equipped with a PW 1820/00 goniometer and an Enraf Nonius FR590 generator operated at 40 kV and 30 mA. The minerals were identified by comparison with the Inorganic Crystal Structure Database (ICSD) and Crystallography Open Database (COD).

Scanning electronic Microscopy (SEM) was used to verify the presence of iron oxides in the quartz minerals, to complement the iron reducing and oxidizing plate assays (**Chapter 7**). The analysis was conducted using an EVO-LS15 scanning electronic microscope (ZEISS, Germany) with variable pressure mode (10–400 Pa) and coupled with an energy-dispersive X-ray spectroscopy (EDS) micro-probe, with an X-Ray detector (Oxford Inca X-act, of resolution 129 eV).

3.2.6.3 Petrographic microscopy

Petrographic microscopes are designed to identify minerals from their optical properties (colour, texture, cleavage by passing polarized light (both parallel and crossed), which distinctively changes their interference colour and appearance. Moreover, petrographic analysis enables assessment of the microstructure of a building material, in order to detect signs of biodeterioration (e.g. cracks) and observe the interaction between the mineral surface and the colonizing organisms (see e.g. Herrera et al., 2008). In the study reported in **Chapter 5**, thin sections were prepared from selected specimens of granite and cement mortar and observed under a polarization microscope Leica DM4500 P, equipped with a digital FireWire Camera Leica DFC 290 HD (Lieca, Wetzlar, Germany). The petrographic observations enabled detailed characterisation of the granite and mineral samples. They also allowed measurement of the thickness of the SAB over the sample surface, as well as observation of the physical interactions between the SAB and the surface.

3.2.6.4 Surface roughness and hardness

Roughness is a textural property of a surface, characterized by the presence of peaks and valleys with various heights, depths and distances. The specific area increases with surface roughness, and larger areas of the surface will thus be exposed and interact with the environment, leading to greater biological colonisation and concomitant biodeterioration (albeit only subjectively aesthetic). The roughness parameter R_a, which reflects the average distance (in µm) of the absolute deviations of the surface profile over a line was determined using a 3D digital microscope (VHX-6000, Keyence Corp., Japan) (**Chapter 5**). Although R_a is one of the most commonly used roughness parameters, it is not very sensitive to individual peaks and valleys in the profile (Rosentritt et al., 2024), and its use is not recommended for very abrupt surfaces.

Surface hardness can be quantified as the resistance of surface to an impacting device, which measures the impact and rebound velocity of a hard spherical body propelled by spring force against the surface. During impact, the kinetic energy of the sphere becomes elastic strain energy stored in the impact body, plastic energy that deforms the surface and heat. As some deformation of the plastic is expected, measurements of surface hardness must be carefully applied when dealing with heritage objects. The measurements were made using an Equotip 550 device (Proceq, Switzerland) equipped with a C specimen (3 Nmm impact energy) (**Chapter 5**), as this minimises surface deformation in stone (Desarnaud et al. 2019).

3.2.6.5 Contact angle and water absorption time

The water absorption time (WAT, in s) and the contact angle (CA, in º) of the SAB-mineral interface of colonised granite and cement mortar test blocks exposed to the

lighting set-up were measured using A Krüss DSA100 - Drop Shape Analyzer (KRÜSS, Germany) (**Chapter 5**). The device deposits and records how a drop of 5 µL of distilled water interacts and is absorbed by the material.

The WAT was measured from the moment the droplet was released from the needle until complete absorption.

CA was measured following the Standard BS EN 15802:2009 "Conservation of cultural property - Test methods – Determination of static contact angle" (European Standard, 2009). It is defined as the "*angle between a tangential to the liquid surface (drop) at the line of meeting of three phases (air – liquid - solid) and the plane of the solid surface"* (Drelich, 2013). However, the standard states that for correct definition, the CA must be measured on a surface composed of a single material and that is completely dry and smooth (for which the standard recommends polishing). According to Volpe and Siboni (2017), incorrect application of these fundamental theoretical considerations has led to careless use of the term. Thus, as the granite and mortar specimens are composed of multiple substances, and polishing and drying was not possible (as it would destroy the SABs), the contact angle was defined as the first angle immediately after drop stabilization over the surface **(Chapter 5)**.

3.2.7 Part 4: Carbon footprint and economic performance of outdoor illumination

Sustainable Development Goal (SDG) number 13 states the need to take urgent action to combat climate change and its impacts through the reduction of greenhouse gases (GHG) (United Nations, 2025). In Spain, the family of standards UNE-EN ISO 14060 supports the quantification, monitoring, communication and validation of the emissions and removal of GHG to support sustainable development. Particularly, the UNE-EN ISO 14067 details the principles for the quantification of carbon footprints of goods and services according to their emissions and emotions during its life cycle (ISO, 2019). The life cycle perspective considers all the stages in a product or service, including the acquisition of raw material, production, transportation, use and end of life. The standard ISO (2019) defines carbon footprint (CF) as "*the sum of all the GHG emissions and emotions, expressed as CO_2 equivalent and based on a life-cycle evaluation utilizing the climate change impact category*". A simplified workflow for the calculation of the CF follows four steps: definition of the objectives and scope, recompilation of the life cycle inventory, evaluation of the impact and interpretation. In the research reported in **Chapter 9**, the CF of the lighting set-up of *Casa do Cabildo* was quantified along with the CF of the several methods to clean biological colonisation (laser cleaning, water vapour and three chemical biocides) and the interactions between the two.

When defining the CF scope, is essential to correctly define the functional unit (FU) of the product or service. The standard defines FU as the "*quantity of a product or service*

on the basis of the performance delivered in the end-use application", which enables valid comparisons. It is also possible to establish cut-off criteria that exclude matter and energy flows because they are insignificant, the data are impossible to acquire, the flows are equal between FUs (thus they can be excluded when comparing CFs) or because they are beyond the defined scope. In all cases, exclusion of any flows must be clearly notified. The inventory collects and quantifies the inputs and outputs of matter and energy for a product or service throughout its life cycle, which will be used to evaluate the impact. Assumptions and simplifications can be made during the construction of the inventory, if they are coherent and correctly noted. In the study reported in **Chapter 9**, the environmental impact evaluated in terms of Global Warming Potential for 100 years (GWP100) according to the UNE-EN ISO 14067:2019 standard (ISO, 2019) in kg of $CO_{2\text{-eq}}$.

There is no standard method for calculating the economic performance of a product or service, although tools have been developed to calculate the costs associated with the life cycles. In the research reported in **Chapter 9**, the economic performance (in €) of the CromaLux lighting system (a warm white light followed by the amber+green light) was evaluated in terms of capital expenditure (cost of acquiring, building or installing physical assets) and operational expenditure (cost of running and maintaining said physical assets) using the same FU and inventory used for the CF. The analysis also included the environmental economic cost, which reflects the cost of mitigating or preventing the environmental damage caused by the emissions of GHG of a product or service, expressed as €/$kg_{CO2\text{-eq}}$ (see e.g. De Bruyn et al., 2023).

3.2.8 Part 4: Psychosocial perception analysis of outdoor illumination

Environmental psychology is a subfield of psychology that studies the interplay between individuals and the built and natural environment (Steg and de Groot, 2018). Applying tools from environmental psychology can provide insights into the underlying attitudes and feelings and thus understand the possible reluctance of the public towards accepting the introduction of new technologies. An attitude can be defined as "*a psychological tendency that is expressed by evaluating a particular entity with some degree of favor or disfavor*" (Eagly and Chaiken, 1993), which translates to environmental attitudes as "*the collection of beliefs, affect, and behavioral intentions a person holds regarding environmentally related activities or issues*" (Schultz et al., 2004). Moreover, when the introduction of new technologies directly affects the image of the city (as ornamental illumination changes the appearance of the urban fabric at night), the emotional bonds that tie the public to a city and their neighbors should be considered. Williams and Vaske (2003) considered that the attachment of people to a place is composed of two dimensions: place dependence and place identity. According to Proshansky et al. (1983), place identity defines people as their relationships with and connections to the physical environment, whereas place dependency is the degree to which a place can support needs. Identification with the people in the surroundings also plays a role in people's behaviours

and attitudes. Social identity can be understood as an individual's awareness of belonging to certain social groups, together with the emotional significance and value that this belonging has for them (Tajfel, 1981). This includes all of the social norms, opinions and values that define a community (such as traditional views on the aesthetics of ornamental illumination; see e.g. Zielinska-Dabkowska and Xavia, 2018). These aspects play a role in if and how a community will accept or reject any changes derived from the introduction of a new technology (see e.g. Gómez-Román et al., 2024).

To understand public perceptions of the amber+green light from the CromaLux lighting system and to inform strategies for overcoming potential resistance, stemming from concerns about visual appeal, doubts regarding effectiveness or negative attitudes, the research reported in **Chapter 10** addresses social acceptance of the lighting system as a preventive conservation strategy for architectural heritage. Two approaches are reported in this chapter.

First, a qualitative approach was used to analyse the responses of several discussion groups to topics such as their perception of building deterioration and their solutions, the institutions that manage the conservation of the architectural heritage in Santiago de Compostela and their attitudes towards the amber+green light and its biostatic effect on biofouling caused by phototrophic SABs. Five experts in ornamental lighting, with professional backgrounds in urban planning, heritage architecture, lighting engineering and ecological research participated in the first discussion session. Four representative members of neighborhood associations in Santiago de Compostela participated in the other sessions. The qualitative study focuses on individuals' real-world experiences, using these descriptions to generate a comprehensive portrait and to identify broader principles and theories (Seamon and Gill, 2015). Discussion sessions were recorded and transcribed (following the procedures established by the University of Santiago de Compostela regarding bioethics and data protection).

The information obtained using this approach was used in applying the second, quantitative, approach in a form of a survey. Surveys can quantify and describe the behaviours and people's perceptions, opinions attitudes, and beliefs about an issue, and to establish relationships between two or more variables (Steg and de Groot, 2018). A framework was also applied during the survey, modifying descriptions to an identical issue to alter people's decisions and perceptions (Steg and de Groot, 2018).

Both approaches used the same graphical material, derived from a high-resolution image of the main facade of the ornamentally illuminated *Casa do Cabildo*, taken with a Canon EOS R7 (Canon, Japan) in July 2024. The image was digitally modified to produce 6 different images in which the light quality and conservation state of the building differed (for use in the second approach). Three types of light with different correlated colour temperatures (CCTs, measured in K) and qualities were first applied to the building: (i) a cool white light (~4000K), (ii) a warm white (~3000K), and (iii) the amber+green light from the CromaLux lighting system (3000K). Each of the three types of light were then

presented through two building deterioration conditions: (a) clean building and (b) affected building. The definition of the clean and affected conditions as such was determined from an environmental psychology perspective. These simple terms convey the idea of the presence (affected) or absence (clean) of biofouling caused by a SAB, without introducing technical or complex terminology, which could have affected the participants' understanding of the matter.

4 RESULTS

4.1 PART 1: LEGISLATIVE FRAMEWORK

4.1.1 CHAPTER 1

BETTER, NOT MORE, LIGHTING: POLICIES IN URBAN AREAS TOWARDS ENVIRONMENTALLY-SOUND ILLUMINATION OF HISTORICAL STONE BUILDINGS THAT ALSO HALTS BIOLOGICAL COLONIZATION

Anxo Méndez, Beatriz Prieto, Josep M. Aguirre i Font, Patricia Sanmartín

Science of the Total Environment 906, 167560 (2024). doi: 10.1016/j.scitotenv.2023.167560

JCR index (IF) 2024 = 8.0 (39/374, 89.7 percentile in Environmental Sciences)

Open access. Citations (to September 2025): 14

Science of the Total Environment 906 (2024) 167560

Contents lists available at ScienceDirect

Science of the Total Environment

journal homepage: www.elsevier.com/locate/scitotenv

Better, not more, lighting: Policies in urban areas towards environmentally-sound illumination of historical stone buildings that also halts biological colonization

Anxo Méndez [a,b], Beatriz Prieto [a,b], Josep M. Aguirre i Font [c], Patricia Sanmartín [a,d,*]

[a] GEMAP (GI-1243), Departamento de Edafoloxía e Química Agrícola, Facultade de Farmacia, Universidade de Santiago de Compostela, 15782 Santiago de Compostela, Spain
[b] CISPAC, Cidade da Cultura, Santiago de Compostela, Spain
[c] Departament de Dret Públic, Universitat de Girona, 17003 Girona, Spain
[d] CRETUS, Universidade de Santiago de Compostela, Santiago de Compostela, Spain

HIGHLIGHTS

- Light pollution policies in European countries are ill-defined and generally scarce.
- Illumination of monuments is an emerging contribution to ALAN pollution.
- ALAN pollution caused by illumination of monuments is defined.
- Illumination policies could help to reduce biodeterioration and protect biodiversity.

GRAPHICAL ABSTRACT

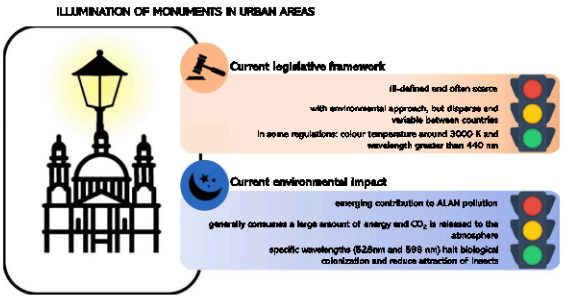

ARTICLE INFO

Guest Editor: Xiaobo Liu

Keywords:
ALAN pollution
Biodeterioration
Environmental policy for sustainability
Monumental illumination
Smart cities
Stone monuments

ABSTRACT

Anthropogenic or Artificial light at night (ALAN) pollution, or more simply light pollution, is an issue of increasing concern to the general public, as well as to scientists and politicians. However, although advances have been made in terms of scientific knowledge, these advances have not been fully transferred to or considered by politicians. In addition, illumination of stone monuments in urban areas is an emerging contribution to ALAN pollution that has scarcely been considered to date. This paper presents a literature review of the topic of light pollution and related policies, including a bibliometric analysis of studies published between 2020 and 2022. The prevailing legislation in Europe regarding the regulation of outdoor lighting, which emphasises the complexity of controlling light pollution, is summarised and the regulation of monumental lighting in Spain is discussed. Findings concerning the impact of ALAN on biodiversity in urban areas, and the promising biostatic effect of ornamental lighting (halting biological colonization on stone monuments, mainly caused by algae and

* Corresponding author at: GEMAP (GI-1243), Departamento de Edafoloxía e Química Agrícola, Facultade de Farmacia, Universidade de Santiago de Compostela, 15782 Santiago de Compostela, Spain.
E-mail address: patricia.sanmartin@usc.es (P. Sanmartín).

https://doi.org/10.1016/j.scitotenv.2023.167560
Received 4 August 2023; Received in revised form 28 September 2023; Accepted 1 October 2023
Available online 4 October 2023

cyanobacteria) are described. Finally, trends in monument illumination and policymaking towards environmentally sustainable management are considered.

1. Introduction

Until the introduction of public lighting in the 17th century, outdoor illumination of building façades, with flame lanterns in many European cities, was the responsibility of private citizens (Schivelbusch, 1995). The illumination served both to enhance the beauty of buildings at night and to ensure visibility and safety in the street, functions that remain relevant today (Žák and Vodráčková, 2016). Since their introduction, light infrastructures have been managed by public authorities, with control increasing with the popularity of ornamental illumination during the 18th and 19th centuries (Seitinger, 2014). Public lighting has gradually evolved from the original gas lamps to electric lamps (Schivelbusch, 1995).

Illumination of outdoor monuments should aim to highlight natural colours and shapes, and it thus often bathes monuments in upward and lateral directions, thereby contributing to the phenomenon of artificial light at night (ALAN) pollution or light pollution (the main negative effect). The terms light pollution and ALAN pollution are almost synonymous; however, the former can also include poorly implemented daytime lighting, and the latter is less commonly used and more closely linked to biological effects. Light pollution is rather ill-defined, varies between different fields and is subject to debate, as will be explained in more detail below. For our purpose and considering built monuments, and also taking into account the suggestions of various authors (ILP, 2011; Aubé, 2015; Żagan and Skarżyński, 2017; Stone, 2019), ALAN pollution derived from monument illumination can be defined as "the ornamental lighting on monuments that is not being efficiently or completely utilized and exceeds the limits of the object and scatters to the atmosphere (often because is pointed outwards or upwards), causing artificial ambient brightness that has an overall negative effect on the environment". According to a study of about ten years ago (Mohar et al., 2014), 60 %–80 % of the ornamental lighting on monuments is emitted to the sky and the surroundings, not reaching the monument façade, and at that time it was estimated that it would give rise to the 5 %–20 % of total ALAN pollution in developed countries.

Light pollution (whether ornamental or for other uses) can affect all ecosystems, both terrestrial and aquatic, on the planet. In Europe, light pollution is increasing at a rate of 2 % to 10 % each year, reflecting the lack of sustainability of the outdoor lighting model used in various countries (Hölker et al., 2010; Kyba et al., 2014, 2017). The wide variety of definitions of light pollution, derived from the different unwanted side-effects of ALAN and considered in various research fields, has been pointed out (Schulte-Römer et al., 2019). This variety also leads to a diversity of views and findings that are difficult for policymakers to combine in cohesive legislation. Astronomers consider ALAN detrimental regarding observation of the night sky (Smith, 2009), and biologists consider ALAN harmful to nocturnal species and ecosystems (Gaston et al., 2015). Nocturnal animals in urban and other artificially lit areas can be attracted towards ALAN and become disorientated, affecting foraging, reproduction and other behaviours, resulting in disruption of interspecific relationships, with serious implications for community ecology (Longcore and Rich, 2004). Humans are also affected, as disruption of the natural circadian rhythm is linked to various health problems such as cancer, Alzheimer's disease, depressive disorder, atherosclerosis and cardiovascular diseases (Menéndez-Velázquez et al., 2022). Around 55 % of the world's population already lives in urban areas and this figure is expected to increase to 68 % by 2050 (Katabaro et al., 2022). Individuals exposed to high levels of ALAN are more likely to have poorer health, with disrupted sleeping patterns and increased levels of stress and anxiety leading to hormonal and metabolic changes (Widmer et al., 2022). Plants and other photosynthetic organisms are also impacted by ALAN, with negative effects on natural primary production and photosynthetic performance and signs of metabolic stress observed (Singhal et al., 2019).

In stone-built heritage, the impact of ornamental ALAN not only affects the surrounding environment, but also the building façades themselves. Artificial light can directly influence the biological colonization of these sites, in particular driving biofouling by phototrophic organisms (Sanmartín et al., 2017, 2021; Zafra-Castro, 2020; Sanmartín, 2021). However, the issues concerning heritage conservation in that sense are overlooked by current legislation on outdoor lighting and light pollution, probably due to the lack of knowledge about the concrete impact of ornamental lighting at night on the potential biodeterioration risks.

Illumination of monuments should focus on the yellow part of the spectrum (between 565 nm and 625 nm wavelengths, in a broad sense) and use as little blue light (between 400 nm and 500 nm wavelengths, in a broad sense) as possible. In other words, the lighting should not emit wavelengths less than 500 nm and have low emission above 650 nm, to minimize the impact on animals, humans and plants. Bluish light causes more light pollution than yellowish or reddish light because, according to Rayleigh's law, shorter wavelengths (like blue light) scatter exponentially more than longer wavelengths (like yellow and red light). A serious shortcoming of the regulations regarding the lights used to illuminate cultural monuments is that they do not focus on restricting use to the yellow part of the spectrum (i.e. less than 3300 K–2700 K and main peak wavelength around 580 nm) or limiting to less than 10 %–15 % the share of blue light (with a main peak around 440–450 nm). Note that colour temperature in degrees kelvin (K) increases with the proportion of the blue part of the spectrum the emitted light contains; e.g. a white light with a high percentage of blue colour can reach a colour temperature of 6500 K.

The aim of this review is to provide an up-to-date view on policies and legislation of outdoor illumination regarding historical stone buildings and light pollution, as well as the associated environmental impact. Thus, following on from this introductory Section 1, the paper is structured as follows. Section 2 presents a literature review of the topic on light pollution and policies, including a bibliometric analysis of studies published in the past three years (2020–2022). Section 3 outlines the prevailing legislative framework in Europe in regard to the regulation of outdoor lighting, emphasising the complexity of regulating light pollution and discussing how monumental lighting is regulated in Spain. Spain is a pioneer in this regard, with the first legislation appearing in 1988, and it also has the challenge of protecting its cultural heritage, one of the most extensive in the world. Spain is therefore used as an example for studying the regulation of lighting historical stone building. Section 4 deals with the impact of ALAN on biodiversity in urban areas, and the promising biostatic effect (halting biological colonization, mainly by algae and cyanobacteria) of ornamental lighting for the conservation of stone monuments. Finally, Section 5 concludes with an analysis of trends in monument illumination and policymaking towards environmentally sustainable management of the lighting.

2. Previous research reviews on ALAN pollution

In a recent review on literature regarding light pollution (Rodrigo-Comino et al., 2021), most of the 621 papers (published between 2003 and 2019) considered involve light pollution in general, the impact of light pollution on ecosystems and human health, and the economic implications. However, policies regulating light pollution were not considered, probably because very few of the 621 papers address this topic. Thus, it seems that there is little or no connection between

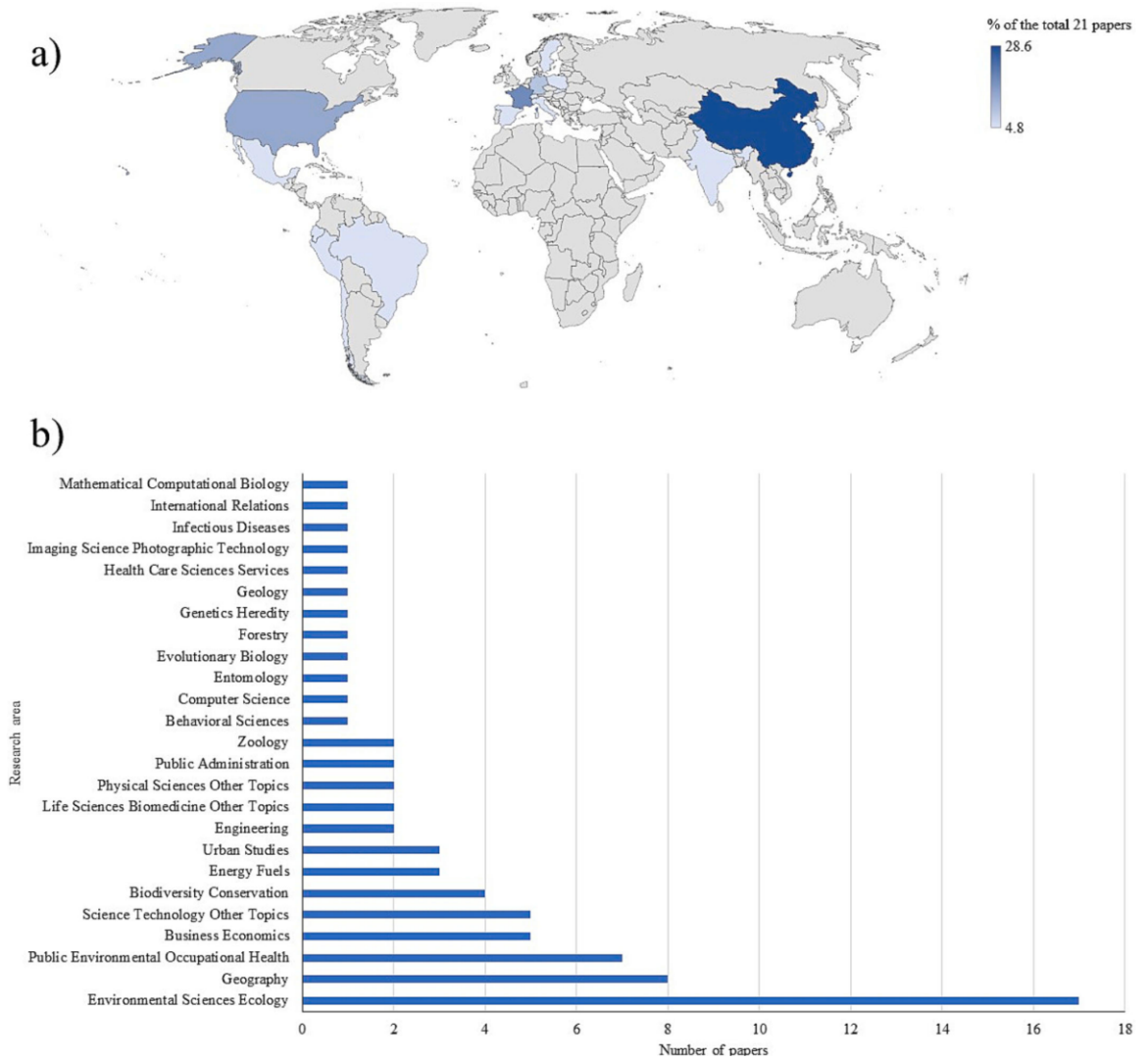

Fig. 1. a) Distribution of the 21 papers by research area, and b) contribution (in %) of the 21 papers by country. In both cases they show the results found between 1 January 2020 and the 31 October 2022.

research and policies or that the knowledge produced by research does not lead to the development of sustainable management plans.

In the present study, a new review was conducted considering literature published between 1 January 2020 and 31 October 2022, by using the ISI Web of Science. Use of the search term "light pollution" yielded a total of 821 publications. Refining the search with the term "policies" produced only 21 papers. Fig. 1a shows the distribution of the 21 papers by research area. Although most are included in the Environmental Science category, those included in the Urban studies (3), Public administration (2) and Business economy (4) categories were those that focused most on policies involving outdoor ornamental illumination for historical stone buildings. In Fig. 1b the distribution of those 21 papers is shown by country. Most of the studies reported in the papers were conducted in China (28.6 %), followed by France (19.0 %) and the USA (14.3 %). For each of the other countries, only one paper was published in the study period, except Germany with 2 papers.

A search within the abovementioned 821 papers was conducted using different terms to select those papers focused on monumental illumination. Four papers appear under the topic of "cultural heritage", but none of these were included in the papers concerning policies. Three of those four papers deal with the dark night as part of the intangible cultural heritage and one concerns tangible built heritage. In the latter, Kobav et al. (2021) proposed a sustainable exterior lighting design for cultural heritage buildings, according to the prevailing legislation concerning light pollution in Slovenia, which is based on general recommendations for the sustainable illumination of cultural heritage objects; however, these recommendations are not reported in the paper. Replacement of the term "cultural heritage" with "monument" produced only one paper. This paper concerns the impact on bats of the illumination of a historic building inside a Natura 2000 national park in Poland (Zielinska-Dabkowska et al., 2021), focusing on the biodiversity conservation policies in the national park but not on policies regarding

illumination. Use of the term "ornamental" yielded only two papers, both about ornamental vegetation and not built construction. Use of the term "façade" produced six papers, which deal with the contribution of the illumination of façades to light pollution, but do not include the term "policies".

Among the abovementioned 21 reviewed papers concerning light pollution policies, the paper by Galindo et al. (2022) is the only one that addresses current policies regarding public lighting services. Most of these policies are related to energy efficiency but they also include environmental policies used as guidelines to establish the technical specifications for luminaries in order to reduce light pollution. All of the other articles suggest the need to generate policies to reduce outdoor light pollution because of its deleterious effects (e.g. Argentiero et al., 2021; Vaz et al., 2021; Yu et al., 2022), and they emphasize the importance of establishing plans such as those existing in relation to air, noise, water and soil (Gonzalez-Madrigal et al., 2020). In this respect, Jagerbrand (2020) suggests that exterior lighting should contribute to, and not counteract, the sustainable development of the planet, pointing out that the interactions between sustainable development and energy performance can be used to produce more efficient policies for decision-making processes regarding exterior lighting. Policies mitigating light pollution have been applied in Japan and the USA since the 1990s, and their success has resulted in the sustainable development of ecology and environment in and around urban domains (Mu et al., 2021).

Some authors suggest measures to resolve the impacts of light pollution. Thus, Kaushik et al. (2022) pointed out some adaptive measures: i) increasing awareness in both individuals and communities, ii) minimizing excess light through technical improvements, iii) making changes in the policies, as the luminance limits established by the International Commission on Illumination (CIE) are not effective for regulating light trespass, iv) minimizing the ecological impact by reducing light trespass. Hu et al. (2021) and Sordello et al. (2022) proposed implementing (in the context of green and blue infrastructure policies) a dark infrastructure to prevent landscape fragmentation due to the impact of artificial light on biodiversity, and Lapostolle and Challeat (2021) point out the convenience, in terms of both preserving biodiversity and fostering the energy transition of planning policies, of taking advantage of darkness as a resource for sustainable development.

Although reducing light intensity and using modern lighting technologies are effective measures for reducing light pollution, air pollution (mainly derived from aerosols) should also be considered as this also increases the brightness of the night sky (Kocifaj and Barentine, 2021).

Kim and Kim (2021) highlight the importance of predicting light pollution in the early stages of building design in order to control light pollution. The "light pollution Prevention Act" in Korea classifies areas where light management is envisaged in categories ranging from E1 (Green areas for conservation, darkest areas) to E4 (semi-industrial and commercial areas, brightest areas) and indicating the permissible luminance values for lighting spaces, advertisements and decorative lighting, thus enabling prediction methodologies to be developed.

One point underlying all the articles is that future lighting policies should be developed within a collaborative framework involving a transdisciplinary process; e.g. Pérez Vega et al. (2021) suggest including environmental experts, lighting professionals and experts from other fields.

3. Legislative framework in Europe: the Spanish example

3.1. Current legislation for ALAN from monumental illumination

As already indicated, light pollution has significant impacts on safety, human health and the environment and in recent years there has been some debate among scientists regarding its definition and measurement (Schulte-Römer et al., 2019; Jägerbrand et al., 2022). This open debate is reflected in the regulations implemented in various European countries, which have adopted different strategies and legal means of addressing the problem of light pollution (Morgan-Taylor, 2015). In Croatia, Germany, France, Spain and Malta, light pollution is directly act upon, from the perspective of energy saving for environmental and economic reasons. Regarding the illumination of public buildings, Italy and Spain have implemented some policies aimed at lowering ornamental ALAN, such as aiming the lights downwards when illuminating building façades and other monuments, reducing the time during which monuments are illuminated, using the minimum intensity of light, reducing the colour temperature of light and shielding the luminaire to restrict the lighting to the shape of the object (Kyba et al., 2018; Falchi et al., 2019). Also in Italy, illumination of buildings in an upward direction is forbidden (Zitelli et al., 2001), to prevent direct light pollution, and Bavarian state law prohibits lighting building façades (churches, castles and administrative buildings) between 23:00 and sunrise (Schroer et al., 2020). However, Finland, Hungary and Slovakia do not have any designated legislative act that addresses light pollution, although provisions from other legislative acts or even non-binding guidelines or instructions from the Belgian and Polish governments are applied (Ministry of the Environment of the Czech Republic, 2022).

Another good example of the disperse actions can be found in the EU. Thus, although the EU promotes the study of light pollution in its EU Action Plan "Zero pollution for air, water and soil" (European Commission (EC), 2021), it has been unable to approve a global regulation on the matter, which was only addressed peripherally in the eco-design requirements for the marketing of lamps in the repealed Commission Regulation (EC) No 245/2009 of 18 March 2009 (European Commission (EC), 2009) and in the current EU green public procurement criteria for road lighting and traffic signs (Donatello et al., 2019). In the case of Spain, as an example of a European country, the fight against light pollution, which has its origins in the pioneering Law 31/1988, of 31 October, on the Protection of the Astronomical Quality of the Observatories of the Instituto de Astrofísica de Canarias (Heading of the Spanish State, 1988), is addressed through different jurisdictional titles: those linked to environmental protection (article 149.1.23 EC) and those linked to the regulation of economic or energy activity (articles 149.1.13 EC and 149.1.25 EC). This has enabled a double-headed approach; on the one hand, environmental regulation with state regulations that have established the basic conditions in this area and autonomous regional regulations that have developed additional rules for the protection of light pollution; and on the other hand, economic or energy-related regulation by the state.

From an environmental perspective, the fight against light pollution has given rise to diverse regulations, depending on the autonomous community, but which share common bases established in the State Law 34/2007, of 15 November, on air quality and protection of the atmosphere (Heading of the Spanish State, 2007), which defines "light pollution" as any artificial glow that "alters the natural conditions of night-time hours and hinders astronomical observations" and establishes common objectives for all public administrations in the fight against light pollution in its fourth additional provision:

"a) To promote efficient use of outdoor lighting, without detriment to the safety it should provide for pedestrians, vehicles and property.

b) To preserve as much as possible the natural conditions of night-time hours for the benefit of fauna, flora and ecosystems in general.

c) To prevent, minimize and correct the effects of light pollution in the night sky, and in particular in the vicinity of astronomical observatories working in the visible spectrum.

d) To reduce light intrusion in areas other than those intended to be illuminated, mainly in natural environments and inside buildings".

Also from an environmental perspective, the following autonomous regions have legislation on light pollution: the Canary Islands (through a state law), Catalonia, the Balearic Islands, Navarre, Cantabria, Andalusia, Castile and Leon and Extremadura (Ríos, 2008; García Gil et al., 2012). As in the regulations in other states, diverse approaches to the problem are also taken, ranging from individual laws to regulations that fall within the framework of environmental assessment legislation.

Table 1
Average illuminance levels for ornamental lighting as a function of the type of material in the illuminated construction and the level of illumination of the surroundings. The correction factors to be applied according to the type of lamp and the degree of fouling. Extracted and modified from ITC-EA-02 (Ministry of Industry, Trade and Tourism, 2008) are also shown.

Type of material in the illuminated construction	Average illuminance levels (Lux)			Multiplying coefficients for correction			
	Lighting in surroundings			Correction for lamp type		Correction for fouling degree	
	Low	Medium	High	LED and MH	HPS and LPS	Dirty	Very dirty
Light-coloured stone, light marble	20	30	60	1.0	0.9	3.0	5.0
Medium-coloured stone, cement, coloured light marble	40	60	120	1.1	1.0	2.5	5.0
Dark-coloured stone, grey granite, dark marble	100	150	300	1.0	1.1	2.0	3.0
Light yellow brick	35	50	100	1.2	0.9	2.5	5.0
Light brown brick	40	60	120	1.2	0.9	2.0	4.0
Dark brown brick, pink granite	55	80	160	1.3	1.0	2.0	4.0
Red brick	100	150	300	1.3	1.0	2.0	3.0
Dark brick	120	180	360	1.3	1.2	1.5	2.0
Architectural concrete	60	100	200	1.3	1.2	1.5	2.0

However, in Spanish regulations the most specific measures designed to combat light pollution are not found in any environmental regulations, but rather in the Regulation on energy efficiency in outdoor lighting installations and its complementary technical instructions EA-01 to EA-07 (approved by Royal Decree 1890/2008 of 14 November), which establishes the technical criteria for outdoor luminaires, determining factors for preventing or accelerating light pollution. These regulations have dated rapidly with the proliferation of LED technology, which has replaced traditional light bulbs and has made it possible to augment lighting at less cost, but also increasing light pollution (García Gil et al., 2022). In fact, as the authors point out, "the most efficient LED lamps, the 4000 K white ones, are also those with the highest radiation below 500 nm. Therefore, they are potentially the most polluting". As explained in the Section 1, a higher proportion of the blue component will increase the colour temperature of the lamp, making it more energy efficient but also more polluting. The current trend in Spanish and European regulations is to use lamps of around 3000 K and below 4000 K, avoiding spectra with radiances below 440 nm (blue light).

The existing regulation was intended to be reformulated with the "Regulation on energy saving and efficiency and reduction of light pollution in outdoor lighting installations and its complementary technical instructions" (Ministry of Industry, Trade and Tourism and the Ministry for Ecological Transition and the Demographic Challenge, 2021), which began to be processed in 2022 and remains paralysed at the time of writing this paper. The initially high expectations of the draft regulation have led to frustration regarding its content, which not only fails to establish limits and objective values for the control of light pollution, but also directly favours an increase in outdoor lighting by establishing lighting obligations that have not existed until now, e.g. the compulsory lighting of all roundabouts and an area of 200 m along their exits (Malón et al., 2022). In this regard, administrative paralysis of the new regulation has made it necessary to advance some of the provisions in the recently published Royal Decree-Law 18/2022 of 18 October, issued in the context of the crisis caused by Russia's invasion of Ukraine and its consequences on international energy markets. The new regulation incorporates new lighting technologies that were not contemplated in 2008, increases the energy efficiency requirements for outdoor lighting installations and makes the energy label more visible to citizens.

Focusing on the regulation of ornamental lighting concerning this review article, at state level it is specified in the non-binding technical guide for the practical application of the provisions of the Regulation and its Supplementary Technical Instructions provided for in the single additional provision of Royal Decree 1890/2008, of 14 November. This guide, in its different versions (Ministry of Industry, Trade and Tourism, 2008), regulates in its Complementary Technical Instruction (abbreviated to ITC in Spanish) EA-02 on lighting levels for ornamental lighting that includes façades of buildings and monuments, as well as statues, walls and fountains; it also includes landscaping of rivers and riverbanks and incorporates a practical chart analysed in the following subsection.

Finally, at the regional level, the ornamental lighting regulations developed through the regulations of some autonomous communities, such as Catalonia (Decree 190/2015), Navarre (Decree 199/2007), Cantabria (Decree 48/2010), Andalusia (Decree 357/2010), and the Balearics (draft regulation currently being processed). These regulations control aspects related to the type of lamps, their installation, maximum lighting levels, switching off at night, and the municipal competence regarding determination of the illuminated assets or their administrative authorisation.

Table 2
Reflection factor for some materials. Extracted and modified from ITC-EA-02 (Ministry of Industry, Trade and Tourism, 2008).

Material[a]	Reflection factor (ρ)
Grey granite	0.10–0.15
Red brick	0.15
Dark marble	0.15
Dark-coloured stone	0.15
Brown brick	0.3
Pink granite	0.3
Clear-coloured marble	0.3
Medium stone	0.3
Cement	0.3–0.4
Light yellow brick	0.35
Light-coloured tone	0.5
Light marble	0.50–0.60

[a] All materials considered clean.

3.2. Practical chart regarding the illumination of stone monuments in urban areas

The Complementary Technical Instruction ITC-EA-02, in the aforementioned Spanish Royal Decree 1890/2008 of 14 November, includes a chart or summary with practical guidelines (Table 1) defining the minimum mean illuminance values (in Lux) according to the colour (light, dark, pink, red, brown, yellow or grey) and type of construction material (marble, cement, granite, brick, also stone in general) being illuminated and the level of illumination (low, medium and high) of the surroundings, along with the correction factors to be applied according to the type of lamp (light emitting diode, LED; metal halide, MH; high-pressure sodium vapour, HPS; and low-pressure sodium vapour, LPS) and the degree of fouling due to exposure to environmental conditions (dirty and very dirty).

However, despite its apparent usefulness, Table 1 lacks some relevant information, since it does not indicate the thresholds for considering the surrounding illumination as low, moderate or high. Nor does it specify what should be considered dirty or very dirty in relation to the illuminated surface. In addition, the chart covers the use of all types of lamp technology, ranging from LED to LPS. This is influenced by the fact that the instruction is now fifteen years old and has not yet been

updated. Today the global trend is towards the exclusive use of LEDs. LPS and HPS lamps are the oldest styles and contain metals such as mercury (Rodrigues et al., 2011) and have a low efficiency and lifespan relative to MH and LED lamps (Stone et al., 2015; Sadeghian, 2018). Their replacement by MH lamps has led to lower maintenance costs and higher energy efficiency. However, use of MH lamps still requires the consumption of large amounts of energy and leads to the release of large amounts of CO_2 to fulfil the requirements of most streetlight illumination. The use of LEDs reduces the amount of energy required by up to between one third and one half (Aoyama and Yachi, 2008), with a low maintenance cost and a compact volume (Vu et al., 2017), suitable for illuminating monuments (Zafra-Castro, 2020).

One aspect that can be extracted from Table 1 is that the amount of illumination required depends on how dark the surface is (owing to the reflection factor, Table 2). For instance, illumination proposed for dark brick is six times greater than that for light marble and twice as much as that proposed for concrete. In addition, ornamental illumination in a moderately illuminated environment must be 1.5 times higher and in strongly illuminated surroundings it must be 3 times higher than in weakly illuminated surrounding environment. Likewise, illumination of buildings in areas with high surrounding illumination should be twice than in moderately illuminated surroundings. In addition, the correction factors for the type of lamp are always higher (with a difference of between 0.1 and 0.3, with the highest corresponding to chromatics in brown, red, yellow-coloured illuminated materials) for LED and MH than for HPS and LPS, except in the case of dark-coloured stone, grey granite and dark marble. In this respect, LED and MH lamps have a lower colour temperature, with a lower blue component and a higher yellow component, than HPS and LPS, which leads to loss of intensity when illuminating surfaces with a reddish-yellow component (such as pink granite and red brick) but to strong illumination of grey-blackish surfaces (such as grey granite and dark marble). Finally, the presence of fouling decreases the reflection factor (Table 2), darkening the illuminated surface, so that illumination of between 1.5 and 3 times higher is required for dirty surfaces and of between 2 and 5 higher for very dirty surfaces. Fouling has less impact on dark brick and architectural concrete and a greater impact on light-coloured stone and light marble.

4. Biological impacts

4.1. Biodiversity and ALAN

The International Union for Conservation of Nature (IUCN) has warned that the extinction of animal and plant species has never occurred as rapidly as at present, and the rate is increasing annually. ALAN pollution is exacerbating the rate of extinction, being listed among ten main factors endangering nocturnal animal biodiversity. Many animal species are dormant during the daytime and become more active at night, especially in urban areas (Hölker et al., 2010). Some nocturnal animals are attracted by light (positive phototaxis), and some are repelled by it (negative phototaxis). This effect is species-specific, and e.g. some bat species have started to go towards light to feed while many other bat species tend to avoid lamps (see e.g. Salinas-Ramos et al., 2020). Animals caught in light can be killed by direct collision with the lit structures, predated by other organisms or become exhausted and run out of time for feeding, reproduction and migration due to the disorientation (Méndez et al., 2022), while those avoiding light are losing their natural habitats. ALAN pollution also interferes with the moonlight and starlight used by many animals for navigation (Barta et al., 2014). Moonlight is highly polarized, and insects like beetles have receptors that detect that polarization for orientation at night (Dacke, 2014). Likewise, moonlight serves as a major environmental cue for aquatic organisms, for example entraining diel vertical migration of zooplankton at depths down to 50 m (Last et al., 2016).

Scotobiology or the biology of darkness has been defined as the study of the biological need for periods of darkness (Dick, 2014). Scotobiological studies allow to determine the ecological limits for ALAN according biological and behavioural drivers, a task complicated by the wide range of tolerance of different nocturnal life forms, with five critical lighting attributes identified: the amount of illumination, the extent of the illuminated area, the glare, the spectrum of the emitted light, and the duration of the illumination (Dick, 2021).

Hölker et al. (2021) have identified eleven main research questions regarding how light pollution affects biodiversity, ranging from genes to ecosystems. According to these authors, the impact of ALAN on the multiple levels of biodiversity (genes and cells, individuals, populations, communities, ecosystems and landscapes) is largely unknown, making it difficult to design effective mitigation measures at present. In addition, photobiological responses to ALAN have not been adequately described for most species. For example, although the insects are probably the group of organisms that have been most widely studied in this respect, and half of the one million species of insects that have been described are nocturnal, information about the spectral sensitivity of insect photoreceptors is only available for 221 species (less than 0.03 %) (Hölker et al., 2021). Moreover, the lack of knowledge affects the species directly impacted by ALAN but also those indirectly affected throughout interactions with the former in ecological communities. In addition, such heterogeneous responses to ALAN among and within species groups can alter distribution patterns and create novel communities (Voigt et al., 2021), with potential concomitant effects on ecosystem functions such as mineralization, pollination and seed dispersal. Furthermore, responses to light colour and intensity are not uniform across taxonomic groups (Burt et al., 2023). In relation to outdoor lighting policies, species and landscapes with special protection status, e.g. migrating birds and Natura 2000 sites, are generally only considered in existing regulations regarding ALAN (Schroer et al., 2020).

ALAN pollution, especially that caused by blue light, can directly disrupt melatonin (sleep hormone) synthesis, even at low illumination levels; it can also have other negative impacts on the circadian (day-night) rhythm, which balances body temperature and blood pressure, and other physiological processes, in both people and animals (e.g. Cajochen et al., 2005). Melatonin is present in almost all life forms and has functioned as a cellular protectant against free radicals and oxidation for ~3.6 billion years, and is secretion at night is essential (Tan et al., 1993). Melatonin may promote regeneration of cells or tissues and prevent carcinogenic alterations (Li et al., 2017).

Insects constitute a high proportion of nocturnal species (Baz et al., 2022) and are essential organisms in the ecosystem because they have many important ecological roles. However, insect numbers have declined significantly, especially in urban areas, because of ALAN (Owens and Lewis, 2018). The insect orders Diptera, Hymenoptera, Lepidoptera and Coleoptera have been found to be the most strongly impacted by ALAN in urban areas of Chongqing (southwest China), i.e. urban parks (Liu, 2019), and Santiago de Compostela (northwest Spain), i.e. the historical centre (Méndez et al., 2022). Selection of specific wavelengths (528 nm and 593 nm in the green and amber part of the spectrum) by ALAN has been observed to reduce both the abundance and diversity of insects attracted to the light source, with similar numbers captured as in the unilluminated area (Méndez et al., 2022).

The spread of ALAN within ecosystems varies according to the medium and is not the same in air as in water. In this respect, more studies have been conducted in aerial environments than in aquatic environments. Indeed, according to Hölker et al. (2021) most research regarding the effects of ALAN on biodiversity has focused on a very limited range of ecosystems: natural terrestrial systems in temperate and developed regions. An interesting case study in the rivers and riverbanks integrated in the urban fabric, where it would be of high interest to capture the impact of ALAN, is that of the *El Muelle de la Compañía Río Tinto* (The Rio Tinto Company Pier) in Huelva, southwest Spain. The pier is an example of 19th century industrial heritage located near a biosphere reservoir (UNESCO Odiel Marshlands Biosphere Reserve), and it is illuminated by an impressive lighting display (completed in 2020). However, doubts

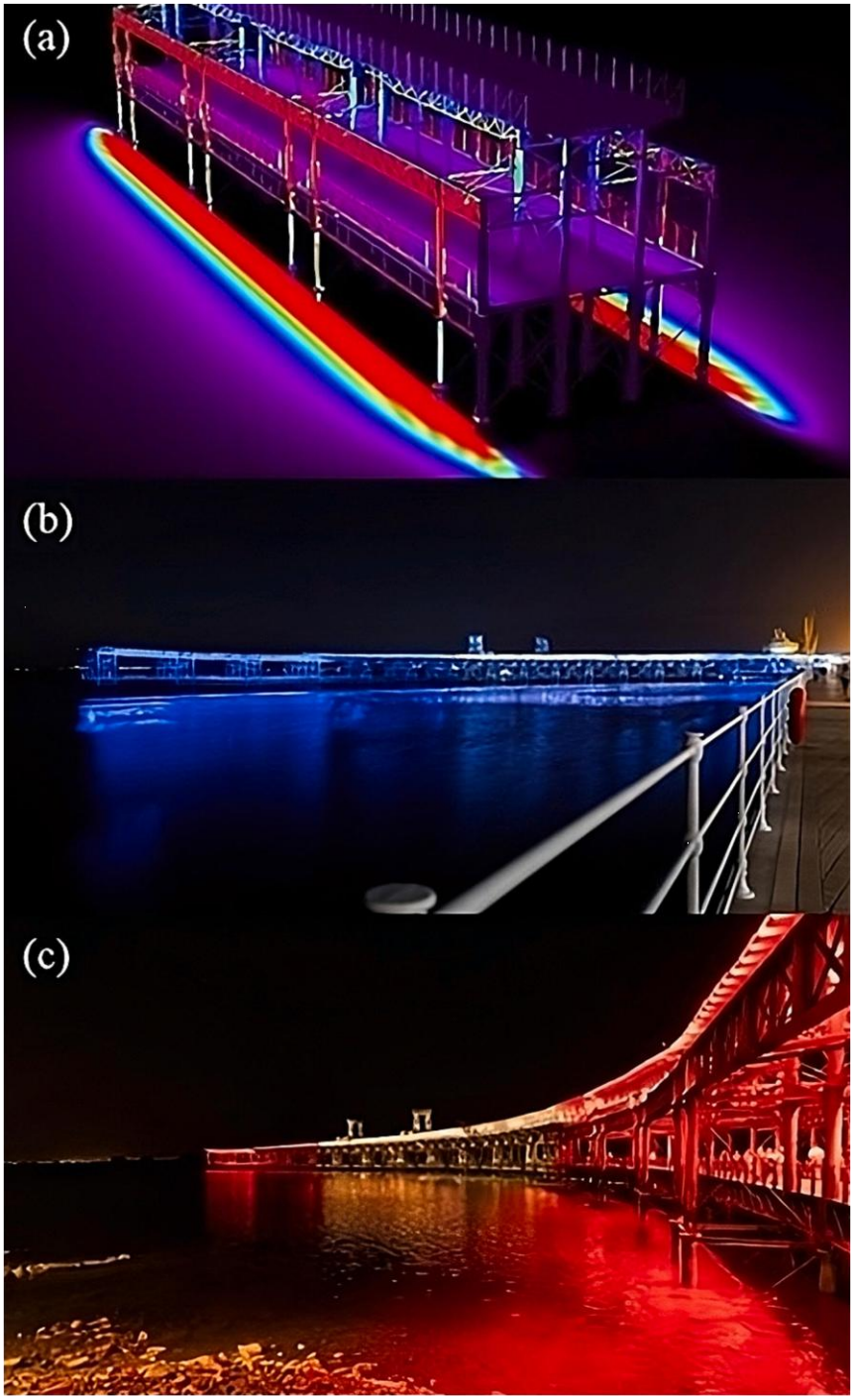

Fig. 2. (a) Rendered image of a section of *El Muelle de la Compañía Rio Tinto* (Rio Tinto Company Pier) in the Odiel estuary (Huelva, Spain), (b) photograph of the pier illuminated in blue and (c) photograph of the pier illuminated in red. All images are extracted from https://www.huelvainformacion.es/.

have emerged that have not yet been resolved about the impact of the lighting on the biodiversity in the surroundings. The illumination system comprises 700 LED spotlights with a wide range of colours, ranging from warm and cold white, to red, green and blue coloured light (Carrasco, 2019). Fig. 2 shows a rendered (synthesised) image of the lighting system, as well as photographs of the lighting in red and blue, the latter being the most frequently used to illuminate the pier. As it can be seen in the images, a large fraction of the light misses the structure and directly affects the surrounding water. Moreover, its impact on birds must be monitored as the marshes and estuaries in this region of Spain are a stopping point for migratory birds and protected species emigrating from North Africa (Báez et al., 2007).

4.2. Novel light that halts biological colonization

Public outdoor lighting systems that illuminate important stone-built buildings in urban areas during evening hours may have biostatic effects (new and poorly known) that potentially halt biological colonization, mainly by algae and cyanobacteria. Research work in this direction has only been carried out in the past five years or so, and albeit with significant differences, is based on those carried out in hypogeal spaces such as caves and catacombs. For example, lighting systems emitting blue light in the Roman Catacombs of St. Callistus and Domitilla in Rome (Italy) have reduced by ten years the extent of cyanobacterial and chemoorganotrophic bacterial biofilms (Bruno et al., 2014; Urzì et al., 2014), and green lighting in the Nerja Cave in Malaga (Spain) has reduced growth of biofilms formed by *Chroococcidiopsis* sp., other cyanobacteria taxa, red alga, *Cyanidium* sp., and green algae (Del Rosal, 2015).

The situation in outdoor lighting is very different from that of subterranean environments, for three main reasons: (1) during the daytime solar illumination of the façade of buildings and monuments affects the development of biological colonization by phototrophs (Sanmartín et al., 2017), (2) the lighting that can be projected continuously in the urban fabric is conditioned by aesthetic aspects, as it is visible to passers-by (in caves the light is usually applied while these are closed to the public) so that it must be deemed acceptable. Blue, green and red light are not acceptable for the long-term illumination of a monument or building, and therefore the biostatic capacity must be sought in amber-white light (The CromaLux project. Available online: http://cromalux.santiagodecompostela.gal/en). Finally (3), the surrounding nocturnal biodiversity (considering the insect community as the reference group), which is specific to the open space, must be taken into account and the luminaires installed must not have any negative impact on these communities (Méndez et al., 2022). These three aspects, together with several others (e.g. the greater variability for the same area of biological colonization outside vs. inside), make achieving correct outdoor illumination with biostatic capacity against phototrophs a difficult task. Work in progress continuing research conducted within the framework of the doctoral thesis of the first author of this paper has already yielded the first good results with a prototype lamp comprising a combination of green and amber LEDs, with two peaks, one at 528 nm, and a main peak at 593 nm. However, no similar studies on lichens or bryophytes have been published. A few studies, not involving the field of cultural heritage, concerning vascular plants have been conducted, considering for example how specific wavelengths of LED lights affects the horticultural plants growth (Ma et al., 2021).

5. Final remarks, conclusions and prospects

The discrepancies as regards the definition of light pollution are reflected in existing policies and regulations, which should be up-dated to include new technologies and also reviewed and reanalysed from the point of view of sustainability. Legislators appear to find defining light pollution challenging. However, permitted concentrations of other environmental pollutants, such as particulate matter and sulphur dioxide (SO_2), have been established in regulations, facilitating control of emissions. Bará et al. (2022) suggest that light pollution levels could be expressed in terms of volume concentration of anthropogenic photons (as photons m^{-3}) in the atmosphere, so that light pollution would be considered the result of the propagation of these photons through the atmosphere. These authors also note that the establishment of artificial light levels during night in photons would help to specify exposure limits in terms of allowed atmospheric concentrations of anthropogenic light particles, unifying these with existing regulations for other atmospheric pollutants. In the case of ornamental illumination, this approach would be helpful for regulating the contribution of monument lighting to urban light pollution, which could be defined as the volume concentration of photons that outline the object shape and affect the surrounding area.

Spain has fairly detailed legislation regarding monumental illumination dispersed throughout energetic efficiency legislation and more regional environmental policies that include light pollution, in one way or another, and therefore this country can be used as an example to analyse the sustainability of the current model of ornamental illumination. Nevertheless, in most European countries the current scientific debate on light pollution is not reflected in the prevailing regulations or the as yet unavailable European light pollution common framework (Widmer et al., 2022). Light pollution is mentioned in environmental directives on different subjects such as the Biodiversity Strategy, Birds and Habitats Directives and Pollinators Initiative (European Commission (EC), 2018). However, the spotlight is only placed directly on light pollution in non-binding recommendations such as the EU Green Public Procurement (Donatello et al., 2019), which promotes ways of reducing light pollution and its negative impacts on biodiversity. From a research perspective, only a small fraction of all research on light pollution carried out between 2020 and 2022 focuses on policies developed for light pollution, and most of the body of research involves the environmental impacts of light pollution without considering the impact of its regulation. This reflects the need for a transdisciplinary approach to light pollution research in the development of regulations and policies, including lighting professionals and policymakers (Pérez Vega et al., 2021), as well as professionals involved in architecture conservation, in both science and art. With proper regulation, it would be possible to maintain an appropriate aesthetic standard, emphasising the historical and aesthetic importance of monuments, while ensuring a sustainable lighting model. This model could be achieved with technologies such as LED lighting, which has low energy consumption (Phannil et al., 2018), thus reducing emissions of CO_2 to the atmosphere (Hong and Rahmat, 2022).

In conclusion, a good balance must be struck between energy, the environment and the enhancement and conservation of stone monuments. Legislation establishes lower thresholds than health and environmental studies. However, improvements in LED technology should shift the trend towards ornamental lamps with a colour temperature between 2500 K and 3000 K and including only bands in the 500 nm to 650 nm range of the light spectrum.

CRediT authorship contribution statement

Conceptualization, P.S.; investigation, A.M., B.P., J.M.A.F., and P.S.; writing—original draft preparation, A.M., B.P., J.M.A.F., and P.S.; writing—review and editing, A.M., B.P., J.M.A.F., and P.S.; supervision, P.S.; project administration, P.S. All authors have read and agreed to the published version of the manuscript.

Declaration of competing interest

The authors declare that they have no known competing financial interests or personal relationships that could have appeared to influence the work reported in this paper.

Data availability

No data was used for the research described in the article.

Acknowledgements

This review study was developed in the framework of the CROMA-LUX project: Third SMARTIAGO Challenge – Smart lighting system for Heritage Conservation. A. Méndez acknowledges receipt of a grant in the Programa de Doutoramento Industrial (04_IN606D_2021_2598528) financed by the Xunta de Galicia. P. Sanmartín acknowledges receipt of the Ramón y Cajal contract (RYC2020-029987-I) financed by the Spanish State Research Agency (AEI) of the Ministry of Science and Innovation (MCIN). The authors are also grateful to the Xunta de Galicia for concession of the FONTES project (ED431F 2022/14) and the Competitive Reference Group (GRC) grant ED431C 2022/09.

Data accessibility

This work has no electronic supplementary material data.

References

Aoyama, Y., Yachi, T., 2008. An LED module array system designed for streetlight use. In: IEEE Energy 2030 Conference. EEUU, Atlanta (November 17–18, 2008).

Argentiero, A., Cerqueti, R., Maggi, M., 2021. Outdoor light pollution and COVID-19: the Italian case. Environ. Impact Assess. Rev. 90, 106602. https://doi.org/10.1016/j.eiar.2021.106602.

Aubé, M., 2015. Physical behaviour of anthropogenic light propagation into the nocturnal environment. Phil. Trans. R. Soc. B. 370 (1667), 20140117. https://doi.org/10.1098/rstb.2014.0117.

Báez, J., Camiñas, J., Torreblanca, D., 2007. Analysis of spatial distribution for the marine bird and mammal in the Gulf of Cadiz (South-west of the Iberian Peninsula) during spring period. Bol. R. Soc. Esp. Hist. Nat. Sec. Biol. 102, 93–97.

Bará, S., Bao-Varela, C., Falchi, F., 2022. Light pollution and the concentration of anthropogenic photons in the terrestrial atmosphere. Atmos. Pollut. Res. 13 (9), 101541. https://doi.org/10.1016/j.apr.2022.101541.

Barta, A., Farkas, A., Száz, D., Egri, Á., Barta, P., Kovács, J., Csák, B., Jankovics, I., Szabó, G., Horváth, G., 2014. Polarization transition between sunlit and moonlit skies with possible implications for animal orientation and Viking navigation: anomalous celestial twilight polarization at partial moon. Appl. Optics 53 (23), 5193–5204. https://doi.org/10.1364/AO.53.005193.

Baz, E., Hussein, A., Vreeker, E., Soliman, M., Tadros, M., El-Shenawy, N., 2022. Consequences of artificial light at night on behavior, reproduction, and development of Lymnaea stagnalis. Environ. Pollut. 307, 119507. https://doi.org/10.1016/j.envpol.2022.119507.

Bruno, L., Belleza, S., Urzì, C., De Leo, F., 2014. A study for monitoring and conservation in the Roman Catacombs of St. Callistus and Domitilla, Rome (Italy). In: Saiz-Jimenez, C. (Ed.), The Conservation of Subterranean Cultural Heritage. CRC Press, London, pp. 37–44.

Burt, C., Kelly, J., Trankina, G., Silva, C., Khalighifar, A., Jenkins-Smith, H., Foz, A., Fristrup, K., Horton, K., 2023. The effects of light pollution on migratory animal behavior. Trends Ecol. Evol. 38 (4), 355–368. https://doi.org/10.1016/j.tree.2022.12.006.

Cajochen, C., Münch, M., Kobialka, S., Kräuchi, K., Steiner, R., Oelhafen, P., Orgül, S., Wirz-Justice, A., 2005. High sensitivity of human melatonin, alertness, thermoregulation, and heart rate to short wavelength light. J. Clin. Endocrinol. Metab. 90 (3), 1311–1316. https://doi.org/10.1210/jc.2004-0957.

Carrasco, A., 2019. El Muelle de la Río Tinto Company estrenará iluminación ornamental en Colombinas. https://www.huelvainformacion.es/huelva/Muelle-Rio-Tinto-Company-Colombinas_0_1349265457.html. (Accessed 27 July 2023).

Dacke, M., 2014. Polarized light orientation in ball-rolling dung beetles. In: Hováth, G. (Ed.), Polarized Light and Polarization Vision in Animal Sciences. Springer, Berlin, pp. 27–39.

Del Rosal, Y., 2015. Análisis, impacto y evolución de los biofilms fotosintéticos en espeleotemas. El caso de la Cueva de Nerja. https://riuma.uma.es/xmlui/handle/10630/14129. (Accessed 27 July 2023).

Dick, R., 2014. Applied scotobiology in luminaire design. Light. Res. Technol. 46, 50–66. https://doi.org/10.1177/1477153513505750.

Dick, R., 2021. Canadian Guidelines for Outdoor Lighting (Low-Impact Lighting) for Dark-Sky Protection Programs. https://www.rasc.ca/sites/default/files/RASC-CGOL_2020.PDF. (Accessed 27 July 2023).

Donatello, S., Rodríguez Quintero, R., Gama Caldas, M., Wolf, O., Van Tichelen, P., Van Hoof, V., Geerken, T., 2019. Revision of the EU Green Public Procurement Criteria for Street Lighting and Traffic Signals: Technical Report and Criteria Proposal, first ed. Publications Office of the European Union, Luxembourg.

European Commission (EC), 2009. Commission Regulation (EC) No 245/2009 of 18 March 2009 implementing Directive 2005/32/EC of the European Parliament and of the Council with regard to ecodesign requirements for fluorescent lamps without integrated ballast, for high intensity discharge lamps, and for ballasts and luminaires able to operate such lamps, and repealing Directive 2000/55/EC of the European Parliament and of the Council. https://eur-lex.europa.eu/legal-content/EN/TXT/?uri=celex%3A32009R0245. (Accessed 27 July 2023).

European Commission (EC), 2018. Communication from the Commission to the European Parliament, the European Council, the Council, the European Economic and Social Committee and the Committee of the Regions. EU Pollinators Initiative. https://eur-lex.europa.eu/legal-content/EN/TXT/?uri=CELEX%3A52018DC0395. (Accessed 15 March 2023).

European Commission (EC), 2021. Communication from the Commission to the European Parliament, the Council, the European Economic and Social Committee and the Committee of the Regions, Pathway to a Healthy Planet for All EU Action Plan: 'Towards Zero Pollution for Air, Water and Soil'. https://eur-lex.europa.eu/legal-content/EN/ALL/?uri=COM%3A2021%3A400%3AFIN. (Accessed 27 July 2023).

Falchi, F., Furgoni, R., Gallaway, T., Rybnikova, N., Portnov, B., Baugh, K., Cinzano, P., Elvidge, C., 2019. Light pollution in USA and Europe: the good, the bad and the ugly. J. Environ. Manage. 248, 109227. https://doi.org/10.1016/j.jenvman.2019.06.128.

Galindo, S.P., Borge-Diez, D., Icaza, D., 2022. Novel control system applied in the modernization of public lighting systems in heritage cities: case study of the City of Cuenca. Energy Rep. 8, 10478–10491. https://doi.org/10.1016/j.egyr.2022.08.191.

García Gil, M., Francia Payàs, P., San Martí Páramo, R., Solano Lamphar, H., 2012. Contaminación lumínica: una visión desde el foco contaminante: el alumbrado artificial, first ed. Universitat Politècnica de Catalunya. Iniciativa Digital Politècnica, Barcelona.

García Gil, M., Paricio Ferreró, S., Masana Fresno, E., 2022. Limitaciones en la normativa y oportunidades para la reducción de la contaminación lumínica. Luces CEI 75, 10–18.

Gaston, K., Visser, M., Hölker, F., 2015. The biological impacts of artificial light at night: the research challenge. Philos. Trans. R. Soc. Lond. B Biol. Sci. 370 (1667), 20140133. https://doi.org/10.1098/rstb.2014.0133.

Gonzalez-Madrigal, J., Solano-Lamphar, H., Ramirez, M., 2020. Light pollution as an approach to urban planning in Mexican cities. Eure 46 (138), 155–174.

Heading of the Spanish state, 1988. Ley 31/1988, de 31 de octubre, sobre Protección de la Calidad Astronómica de los Observatorios del Instituto de Astrofísica de Canarias. https://www.boe.es/buscar/doc.php?id=BOE-A-1988-25332. (Accessed 27 July 2023).

Heading of the Spanish State, 2007. Ley 34/2007, de 15 de noviembre, de Calidad del Aire y Proteccion de la Atmosfera. https://www.boe.es/buscar/act.php?id=BOE-A-2007-19744. (Accessed 27 July 2023).

Hölker, F., Moss, T., Griefahn, B., Kloas, W., Voigt, C.C., Henckel, D., Hänel, A., Kappeler, P., Völker, S., Schwope, A., Franke, S., Uhrlandt, D., Fischer, J., Klenle, R., Wolter, C., Tockner, K., 2010. The dark side of light: a transdisciplinary research agenda for light pollution policy. Ecol. Soc. 15 (4). https://www.jstor.org/stable/26268230.

Hölker, F., Bolliger, J., Davies, T., Giavi, S., Jechow, A., Kalinkat, G., Longcore, T., Spoelstra, K., Tidau, S., Visser, M., Knop, E., 2021. 11 pressing research questions on how light pollution affects biodiversity. Front. Ecol. Evol. 9, 767177. https://doi.org/10.3389/fevo.2021.767177.

Hong, W., Rahmat, B., 2022. Energy consumption, CO2 emissions and electricity costs of lighting for commercial buildings in Southeast Asia. Sci. Rep. 12 (1), 1–11. https://doi.org/10.1038/s41598-022-18003-3.

Hu, J., Liu, Y., Fang, J., 2021. Ecological corridor construction based on least-cost modeling using visible infrared imaging radiometer suite (VIIRS) nighttime light data and normalized difference vegetation index. Land 10 (8), 782. https://doi.org/10.3390/land10080782.

Institution of Lighting Professionals (ILP), 2011. Guidance Notes for the Reduction of Obtrusive Light. Institution of Lighting Professionals, Rugby, UK. https://www.theilp.org.uk/documents/. (Accessed 27 July 2023).

Jagerbrand, A., 2020. Synergies and trade-offs between sustainable development and energy performance of exterior lighting. Energies. 13 (9), 2245. https://doi.org/10.3390/en13092245.

Jägerbrand, A., Gasparovsky, D., Bouroussis, C., Schlangen, L., Lau, S., Donners, M., 2022. Correspondence: obtrusive light, light pollution and sky glow: areas for research, development and standardisation. Light. Res. Technol. 54 (2), 191–194. https://doi.org/10.1177/14771535211040409.

Katabaro, J., Yan, Y., Hu, T., Yu, Q., Cheng, X., 2022. A review of the effects of artificial light at night in urban areas on the ecosystem level and the remedial measures. Front. Public Health 10, 969945. https://doi.org/10.3389/fpubh.2022.969945.

Kaushik, K., Nair, S., Ahamad, A., 2022. Studying light pollution as an emerging environmental concern in India. J. Urban Manag. 11 (3), 392–405. https://doi.org/10.1016/j.jum.2022.05.012.

Kim, K., Kim, G., 2021. Using simulation-based modeling to evaluate light trespass in the design stage of sports facilities. Sustainability. 13 (9), 4725. https://doi.org/10.3390/su13094725.

Kobav, M.B., Eržen, M., Bizjak, G., 2021. Sustainable exterior lighting for cultural heritage buildings and monuments. Sustainability. 13 (18), 10159. https://doi.org/10.3390/su131810159.

Kocifaj, M., Barentine, J., 2021. Air pollution mitigation can reduce the brightness of the night sky in and near cities. Sci. Rep. 11 (1) https://doi.org/10.1038/s41598-021-94241-1.

Kyba, C., Hänel, A., Hölker, F., 2014. Redefining efficiency for outdoor lighting. Energy Environ. Sci. 7 (6), 1806–1809. https://doi.org/10.1039/C4EE00566J.

Kyba, C., Kuester, T., Sánchez de Miguel, A., Baugh, K., Jechow, A., Hölker, F., Bennie, J., Elvidge, C.D., Gaston, K.J., Guanter, L., 2017. Artificially lit surface of earth at night

increasing in radiance and extent. Sci. Adv. 3, e1701528. https://www.science.org/doi/10.1126/sciadv.1701528.
Kyba, C., Mohar, A., Pintar, G., Stare, J., 2018. Reducing the environmental footprint of church lighting: matching facade shape and lowering luminance with the EcoSky LED. Int. J. Sustain. Light 20 (1), 1–10. https://doi.org/10.26607/ijsl.v19i2.80.
Lapostolle, D., Challeat, S., 2021. Making darkness a place-based resource: how the fight against light pollution reconfigures rural areas in France. Ann. Am. Assoc. Geogr. 111 (1), 196–215. https://doi.org/10.1080/24694452.2020.1747972.
Last, K.S., Hobbs, L., Berge, J., Brierley, A.S., Cottier, F., 2016. Moonlight drives ocean-scale mass vertical migration of zooplankton during the Arctic winter. Curr. Biol. 26 (2), 244–251.
Li, Y., Li, S., Zhou, Y., Meng, X., Zhang, J., Xu, Li, H., 2017. Melatonin for the prevention and treatment of cancer. Oncotarget 8 (24), 39896–39921. https://doi.org/10.18632/oncotarget.16379.
Liu, Y., 2019. Study on the Influence of Landscape Illumination on the Phototactic Behavior of Common Nocturnal Insects in Chongqing (Master's degree thesis). Chongqing University, Chongqing.
Longcore, T., Rich, C., 2004. Ecological light pollution. Front. Ecol. Environ. 2 (4), 191–198. https://doi.org/10.1890/1540-9295(2004)002[0191:ELP]2.0.CO;2.
Ma, Y.C., Xu, A., Cheng, Z.M., 2021. Effects of light emitting diode lights on plant growth, development and traits a meta-analysis. Hortic. Plant J. 76, 552–564.
Malón, S., de Miguel, A., Dorremochea, C., 2022. La luz de la razón: la normativa de alumbrado y el futuro de la contaminación lumínica es España. Astronomía 273, 32–37.
Méndez, A., Martín, L., Arines, J., Carballeira, R., Sanmartín, P., 2022. Attraction of insects to ornamental lighting used on cultural heritage buildings: a case study in an urban area. Insects 13 (12), 1153. https://doi.org/10.3390/insects13121153.
Menéndez-Velázquez, A., Morales, D., García-Delgado, A., 2022. Light pollution and circadian misalignment: a healthy, blue-free, white light-emitting diode to avoid chronodisruption. Int. J. Environ. Res. Public Health 19 (3), 1849. https://doi.org/10.3390/ijerph19031849.
Ministry of Industry, Trade and Tourism, 2008. Reglamento de Eficiencia Energética en Instalaciones de Alumbrado Exterior y sus Instrucciones Técnicas Complementarias EA-01 a EA-07. https://www.boe.es/buscar/doc.php?id=BOE-A-2008-18634. (Accessed 27 July 2023).
Ministry of Industry, Trade and Tourism and the Ministry for Ecological Transition and the Demographic Challenge, 2021. Proyecto de Real Decreto por el que se aprueba el reglamento de eficiencia energética en instalaciones de alumbrado exterior y sus instrucciones técnicas complementarias EA-01 a EA-08. https://industria.gob.es/_layouts/15/HttpHandlerParticipacionPublicaAnexos.ashx?k=3057. (Accessed 27 July 2023).
Ministry of the Environment of the Czech Republic, 2022. Light Pollution Reduction Measures in Europe. Working paper for the international workshop Light Pollution 2022. https://www.mzp.cz/C1257458002F0DC7/cz/news_20221027/$FILE/Light_pollution_reduction_measures.pdf. (Accessed 27 July 2023).
Mohar, A., Zagmajster, M., Verovnik, R., Skaberne, B., 2014. Nature-friendlier lighting of objects of cultural Heritage (churches). https://www.anl.bayern.de/publikationen/anliegen/additional_data/an37200notizen_2015_kulturdenkmaeler_life_bericht_engl.pdf. (Accessed 27 July 2023).
Morgan-Taylor, M., 2015. Regulating light pollution in Europe: legal challenges and ways forward. In: Meier, et al. (Eds.), Urban Lighting, Light Pollution and Society. Routledge, New York and London, pp. 125–140.
Mu, H., Li, X., Du, X., Huang, J., Su, W., Hu, T., Wen, Y., Yin, P., Han, Y., Xue, F., 2021. Evaluation of light pollution in global protected areas from 1992 to 2018. Remote Sens. (Basel) 13 (9), 1849. https://doi.org/10.3390/rs13091849.
Owens, A., Lewis, S., 2018. The impact of artificial light at night on nocturnal insects: a review and synthesis. Ecol. Evol. 8, 11337–11358. https://doi.org/10.1002/ece3.4557.
Pérez Vega, C., Zielinska-Dabkowska, K.M., Hölker, F., 2021. Urban lighting research transdisciplinary framework—a collaborative process with lighting professionals. Int. J. Environ. Res. Public Health 18 (2), 624. https://doi.org/10.3390/ijerph18020624.
Phannil, N., Jettanasen, C., Ngaopitakkul, A., 2018. Harmonics and reduction of energy consumption in lighting systems by using LED lamps. Energies 11 (11), 3169. https://doi.org/10.3390/en11113169.
Ríos, I., 2008. La contaminación lumínica: implicaciones urbanísticas, demaniales y de eficiencia energética. Rev. Estudios Admin. Local Autonómica 307, 27–65.
Rodrigo-Comino, J., Seeling, S., Seeger, M., Ries, J., 2021. Light pollution: a review of the scientific literature. Anthr. Rev. 0 (0) https://doi.org/10.1177/205301962110512.
Rodrigues, C., Almeida, P., Soares, G., Jorge, J., Pinto, D., Braga, H., 2011. Experimental characterization regarding two types of phosphor-converted white high-brightness LEDs: low power and high-power devices. In: IEEE XI Brazilian Power Electronics Conference (Natal, Brazil. September 11–15, 2011).
Sadeghian, E., 2018. Modeling and checking the power quality of high pressure sodium vapor lamp. Int. J. Adv. Res. Electron. Commun. Eng. 7 (3), 232–237.
Salinas-Ramos, V., Ancillotto, L., Bosso, L., Sánchez-Cordero, V., Russo, D., 2020. Interspecific competition in bats: state of knowledge and research challenges. Mamm. Rev. 50, 68–81. https://doi.org/10.1111/mam.12180.
Sanmartín, P., 2021. New Perspectives Against Biodeterioration Through Public Lighting (Chapter 7). In: Joseph, E. (Ed.), Microorganisms in the Deterioration and Preservation of Cultural Heritage. Springer International Publishing, Springer, Cham, pp. 155–171. https://doi.org/10.1007/978-3-030-69411-1_7.
Sanmartín, P., Vázquez-Nion, D., Arines, J., Cabo-Domínguez, L., Prieto, B., 2017. Controlling growth and colour of phototrophs by using simple and inexpensive coloured lighting: a preliminary study in the Light4Heritage project towards future strategies for outdoor illumination. Int. Biodeter. Biodegr. 122, 107–115. https://doi.org/10.1016/j.ibiod.2017.05.003.
Sanmartín, P., Méndez, A., Carballeira, R., López, E., 2021. New insights into the growth and diversity of subaerial biofilms colonizing granite-built heritage exposed to UV-A or UV-B radiation plus red LED light. Int. Biodeterior. Biodegrad. 161, 105225 https://doi.org/10.1016/j.ibiod.2021.105225.
Schivelbusch, W., 1995. Disenchanted Night: The Industrialization of Light in the Nineteenth Century, first ed. The University of California Press, Berkley.
Schroer, S., Huggins, B.J., Azam, C., Hölker, F., 2020. Working with inadequate tools: legislative shortcomings in protection against ecological effects of artificial light at night. Sustainability 12 (6), 2551. https://doi.org/10.3390/su12062551.
Schulte-Römer, N., Meier, J., Dannemann, E., Söding, M., 2019. Lighting professionals versus light pollution experts? Investigating views on an emerging environmental concern. Sustainability 11 (6), 1696. https://doi.org/10.3390/su11061696.
Seitinger, S., 2014. Vienna. In: Isenstald, S., et al. (Eds.), Cities of Light: Two Centuries of Urban Illumination. Routledge, New York and London, pp. 130–136.
Singhal, R.K., Kumar, M., Bose, B., 2019. Eco-physiological responses of artificial night light pollution in plants. Russ. J. Plant Physiol. 66 (2), 190–202. https://doi.org/10.1134/S1021443719020134.
Smith, M., 2009. Time to turn off the lights. Nature 457 (7225), 27. https://doi.org/10.1038/457027a.
Sordello, R., Busson, S., Cornuau, J.H., Deverchere, P., Faure, B., Guette, A., Hoelker, F., Kerbiriou, C., Lengagne, T., Le Viol, I., Longcore, T., Moeschler, P., Ranzoni, J., Ray, N., Reyjol, Y., Roulet, Y., Schroer, S., Secondi, J., Valet, N., Vanpeene, S., Vauclair, S., 2022. A plea for a worldwide development of dark infrastructure for biodiversity - practical examples and ways to go forward. Landsc. Urban Plan. 219, 104332. https://doi.org/10.1016/j.landurbplan.2021.104332.
Stone, T., 2019. Designing for darkness: urban nighttime lighting and environmental values. In: Simon Stevin Series in the Ethics and Technology. 4TU.Centre for Ethics and Technology. https://doi.org/10.4233/uuid:eeb2da3c-83e4-4837-87fd-3e446d401736.
Stone, E., Wakefield, A., Harris, S., Jones, G., 2015. The impacts of new street light technologies: experimentally testing the effects on bats of changing from low-pressure sodium to white metal halide. Philos. Trans. R. Soc. Lond. B Biol. Sci. 370 (1667) https://doi.org/10.1098/rstb.2014.0127.
Tan, D., Chen, L., Poeggeler, B., Manchester, L., Reiter, R., 1993. Melatonin: a potent, endogenous hydroxyl radical scavenger. Endocr. J. 1, 57–60.
Urzì, C., De Leo, F., Bruno, L., Pangallo, D., Krakova, L., 2014. New species description, biomineralization processes and biocleaning applications of Roman Catacombs-living bacteria. In: Saiz-Jumenez, C. (Ed.), The Conservation of Subterranean Cultural Heritage. CRC Press, Bakelma, pp. 65–72.
Vaz, S., Manes, S., Gama-Maia, D., Silveira, L., Mattos, G., Paiva, P., Figueiredo, M., Lorini, M., 2021. Light pollution is the fastest growing potential threat to firefly conservation in the Atlantic Forest hotspot. Insect Conserv. Divers. 14 (2), 211–224. https://doi.org/10.1111/icad.12481.
Voigt, C., Dekker, J., Fritze, M., Gazaryan, S., Hölker, F., Jones, G., Lewanzik, D., Limpens, H., Mathews, F., Rydell, J., Spoelstra, K., Zagmajster, M., 2021. The impact of light pollution on bats varies according to foraging guild and habitat context. BioScience 71, 1103–1109. https://doi.org/10.1093/biosci/biab087.
Vu, N., Pham, T., Shin, S., 2017. LED uniform illumination using double linear fresnel lenses for energy saving. Energies 10 (12), 2091. https://doi.org/10.3390/en10122091.
Widmer, K., Beloconi, A., Marnane, I., Vounatsou, P., 2022. Review and Assessment of Available Information on Light Pollution in Europe (Eionet Report–ETC HE 2022/8). https://www.eionet.europa.eu/etcs/etc-he/products/etc-he-products/etc-he-report-2022-8-review-and-assessment-of-available-information-on-light-pollution-in-europe. (Accessed 28 July 2023).
Yu, Z., Hu, N., Du, Y., Wang, H., Pu, L., Zhang, X., Pan, D., He, X., Li, J., 2022. Association of outdoor artificial light at night with mental health among China adults: a prospective ecology study. Environ. Sci. Pollut. Res. 29 (54), 82286–82296. https://doi.org/10.1007/s11356-022-21587-y.
Zafra-Castro, D., 2020. Criterios para la planificación de la iluminación patrimonial desde la Conservación. https://diposit.ub.edu/dspace/bitstream/2445/177972/1/ZafraCastro_Memoria_363385_1920.pdf. (Accessed 28 July 2023).
Żagan, W., Skarżyński, K., 2017. Analysis of light pollution from floodlighting: is there a different approach to floodlighting? Light. Eng. 25 (1), 75–82.
Žák, P., Vodráčková, S., 2016. Conception of public lighting. In: IEEE Lighting Conference of the Visegrad Countries (Karpacz, Poland. September 13.16, 2016).
Zielinska-Dabkowska, K., Szlachetko, K., Bobkowska, K., 2021. An impact analysis of artificial light at night (ALAN) on bats. A case study of the historic monument and Natura 2000 Wisłoujście ortress in Gdansk, Poland. Int. J. Environ. Res. Public Health 18 (21), 11327. https://doi.org/10.3390/ijerph182111327.
Zitelli, V., Sora, M., Ferrini, F., 2001. Local and national regulations on light pollution in Italy. Symp. - Int. Astron. Union 196, 111–116. https://doi.org/10.1017/S0074180900163910.

4.2 PART 2: ASSESSMENT OF BIOSTATIC CAPACITY

4.2.1 CHAPTER 2

DURATION OF ILLUMINATION OF ARCHITECTURAL HERITAGE: A KEY METHODOLOGICAL CONSIDERATION TO CONTROL THE PHOTOTROPHIC COLONISATION

Anxo Méndez, Rafael Carballeira, Stefano Bertuzzi, Patricia Sanmartín

Submission to the journal at the end of 2025 - beginning 2026

Duration of illumination of architectural heritage: A key methodological consideration to control the phototrophic colonisation

Anxo Méndez[1], Rafael Carballeira[2], Stefano Bertuzzi[3], Patricia Sanmartín[1]

1. CRETUS, Departamento de Edafoloxía e Química Agrícola, Universidade de Santiago de Compostela, Santiago de Compostela, 15782, Spain
2. Departamento de Ciencias Farmacéuticas y de la Salud, Facultad de Farmacia, Universidad San Pablo-CEU, CEU Universities, Urbanización de Montepríncipe, 28668 Boadilla del Monte, Spain
3. Independent Researcher, Cantalupa, Torino, Italy

Abstract

At present, there is an increasing trend for illuminating night-time urban landscape, especially in historic and heritage cities, which is known to affect the growth and diversity of phototrophic biological colonisation forming biofilms (SABs) in the architectural heritage. Although previous studies have demonstrated that phototrophic (mainly algal) SABs thrived well under blue LEDs, whereas red and especially green LEDs had a biostatic effect, the optimal durations of illumination to achieve both effects are overlooked aspects that have not yet been investigated. In this study, 2, 4, 6 and 8 hours of duration of ornamental LED illumination in red, green, blue and warm white (positive control), along with no LED (i.e. darkness, negative control) were compared over phototrophic SABs, with 16 hours of daylight, recreated in the laboratory for 35 days. At the end of the experiment, SABs were analysed by PAM fluorometry and characterised their diversity by morphology characters, biofilm biomass was measured by wet weighing and cell counting and phototrophic pigment content quantified. A duration between 4 and 6 hours of green LED light, and at lesser extent red LED light, reduced SAB development, while a period of 8 hours of blue LED light was optimal for further growth. Both red and green LED light increased the proportion of cyanobacterial cells. Light colour and not duration alter relative diversity in the SABs.

Keywords: Cultural heritage lighting; environmental technologies; growth control; LED illumination; optimized exterior lighting; subaerial biofilms (SABs).

Highlights:

- Duration of artificial illumination impacts on development of phototrophic SABs
- Green light (4 to 6 h) and blue light (8 h) reduced and promoted SAB development
- There was a positive correlation between minimum fluorescence and pigments and wet SAB biomass
- Both red and green LED light increased the proportion of cyanobacterial cells
- Light colour and not duration alter relative diversity in the SABs

1. Introduction

Artificial light at night (ALAN) has become a key consideration in urban planning (Hopkins et al., 2018), enabling safe use of public spaces after dark and enhancing the aesthetic value of the built environment through ornamental illumination (Oliva et al., 2020). The introduction of Light Emitting Diode (LED) technology has reduced the energy demand and cost of ALAN, allowing municipalities to increase the number of luminaires. This has led to a rebound effect, further intensifying the ecological impact of ALAN over the flora and fauna (see Falcón et al., 2020; Martinsons et al., 2025). As light is a critical factor regulating the physiological processes of phototrophic organisms, ALAN can stimulate photosynthesis during periods when it would not naturally occur (Aubé et al., 2013). Friulla and Varone (2025) reported that nighttime exposure to ALAN reduces intracellular CO_2 concentrations, suggesting CO_2 mobilization for photosynthetic activity that may impair diurnal photosynthetic efficiency. Microalgae is also affected by ALAN, leading to alterations in community assemblage, alter the biomass yield or affect its photosynthetic efficiency (see e.g. Poulin et al., 2014; Hölker et al., 2015; Maggi et al., 2019). This includes phototrophic colonisation in the form of subaerial biofilms (SABs) that inhabit stone built heritage surfaces. SABs form a heterogeneous layer over the mineral substrate of microorganisms embedded in a matrix of extracellular polymeric substances (EPS) (Gorbushina, 2007). In European countries, green microalgae represent the dominant photosynthetic microorganisms within SABs (Gaylarde and Gaylarde, 2005), although they host other microorganisms like bacteria (both heterotrophic and phototrophic) and fungi (see Villa et al., 2015). Strategies focused on modifying the artificial illumination have been used in underground heritage to help mitigate the biodeterioration caused by the growth of SABs due to artificial lighting (see e.g. Albertano and Bruno, 2017). Among these strategies, the use of coloured LED light is presented as an economical and simple way to counteract the development of photosynthetic microorganisms, mainly focused on the use of primary light-colours (blue, red and green).

Blue LED light is known promote development of green microalgae biofilms as their chlorophyll content absorption peak at the light spectra of 420–480 nm, thus driving photosynthesis effectively (see Yuan, Zhang, et al., 2020; Yuan, Wang, et al., 2020). In the study from Hsieh et al., (2013) blue LED light promoted cyanobacterial photosystem activity in biofilms derived from several roman hypogea. However, other authors have proposed the use of blue LED light as a measure to avoid the development of cyanobacterial SABs in caves, hypogea and other underground heritage (see e.g. Muñoz-Fernández et al., 2021) In the Ocean's Cubiculum from Roman Catacombs of St. Callistus the illumination with blue LED light (peaking around 435 nm) drastically reduced the phototrophic colonisation after 10 years (Bruno et al., 2014). The Cubiculum had initially a high degree of coverage by SABs, composed by *Leptolyngbya* sp., *Synphynemopsis* sp., and *Diadesmis gallica* (among other species). The SABs grew over the limestone walls and frescoes, supported by the fluorescent lamp used for illumination and the high humidity of

the environment, although the bacterial colonisation persisted despite the new blue illumination (Bruno et al., 2014; Urzì et al., 2014).

As blue light seems ineffective for the inhibition of some cyanobacteria, other authors have proposed the use of red or green LED lights to effectively control SAB development and their potential biodeterioration (see e.g. Hsieh et al., 2013). Bao et al. (2023) reported that red (peaking at 640 nm) and green (peaking at 530 nm) LED light significantly reduce the production of organic acids (like lactic, citric and tartaric acids) that are known to have a degradative effect on stone monuments (see Nowicka-Krawczyk et al., 2022). Red LED light (peaking at 625 nm) also caused cellular damage to biofilms composed of *Leptolyngbya* sp. collected from the Catacombs of Domitilla (Italy) at an intensity of 12.5 μmol photons m^{-2} s^{-1} that simulated illumination inside the catacombs (Hsieh et al., 2013b). However, Bruno and Valle (2017) found that biofilms composed by *Oculatella subterranea*, *Leptolyngbya* sp. and *Fischerella* sp. (also derived from the Catacombs of St. Callistus) successfully grew under red LED lighting, obtaining a higher biomass yield than blue or green LED lighting (with an intensity up to 2.4 μmol m^{-2} s^{-1}) and displaying the highest rates of electron transport rate.

Research performed in outdoor monuments (where the effects of sunlight are unavoidable) showed that SABs, mainly formed by green algae, thrived well under blue LEDs, whereas green and red LEDs had biostatic effects (i.e. halting their development) (Sanmartín et al., 2017). Although the effects of light quality on SABs have been studied, illumination time of outdoor lighting to control said colonisation with ALAN remains an unexamined aspect. Thus, the aim of this study is to determine the optimal duration of illumination required to manage the development SABs using nocturnal coloured LED light in a laboratory setting, as a first approach to understand how time exposure in nocturnal illumination affects growth and diversity on phototrophic biofilms. This would allow not only to better control the phototrophic colonisation over architectural heritage using public ornamental lighting, but also to promote microalgae growth when needed. This is the case of green microalgae facades or other Nature Based Solutions with microalgae integrated urban structures for carbon sequestration and biomass production, air quality improvement or potentially thermal regulation (see e.g. Elrayies, 2018; Oncel and Şenyay Öncel, 2020; Kisser et al., 2020; Mata et al., 2021). For this purpose, periods of 2, 4, 6 and 8 hours of illumination during dark period with red, green, blue, and white LED light and no LED illumination (control) were used over phototrophic biofilms. After 35 days, the extent of the effects generated in biomass, pigment production, photosynthetic efficiency and biofilm composition was measured. A multi-species culture from a natural biofilm growing on a granite monument was used, mainly composed of the algae *Bracteacoccus minor*, *Chlorella* sp. and *Stichococcus bacilaris* and the cyanobacteria *Isocystis* sp. and *Aphanocapsa* sp.

2. Materials and methods

2.1.Microorganisms and biofilm culture

The inoculum, growing on BG11 medium (Rippka et al., 1979) and derived from a phototrophic biofilm collected from the granite walls of the Monastery of San Martiño Pinario (Santiago de Compostela, Galicia, Spain), presented a ratio of green algae and cyanobacteria 3:1, with the following algal composition: *Bracteacoccus* minor (Schmidle ex Chodat) Petrová (57.3 %) and *Stichococcus bacillari*s Nägeli (6.1 %), *Chlorella* sp. (14.1 %) (green algae); *Isocystis* sp. (17.1 %) and *Aphanocapsa* sp. (5.3 %) (cyanobacteria).

Following the implemented procedure for phototrophs by Sanmartín et al. (2011) and first described by Anderl et al. (2000), subaerial biofilms (SABs) were prepared using a suspension of exponentially growing cells previously homogenate from the inoculum. Polycarbonate membrane discs (0.22 µm pore, 25 mm diameter, Millipore) previously sterilised by exposure to 1 hour of UV-C light in both sides (Philips TUV F17T), were inoculated with 250 µl aliquots of the suspension (corresponding to a DO_{750nm} of 0.28 ± 0.02 a.u. corresponding to 0.76 ± 0.11 mg of biomass) and were placed in Petri plates. Eighteen Petri plates (16 for the different treatments and 2 controls) were prepared, each containing four membranes. The plates were placed inside a controlled cabinet divided in 4 separated quadrants for each of the nocturnal LED lights considered (red, green, blue and white) with 4 plates on each quadrant (**Fig. 10a**). The SABs were grown over a period of 35 days, transferring the membranes to fresh plates every 3 days using a sterile forceps to ensure full nutrient availability.

2.2.Lighting set-up

The SABs were cultured under simulated daylight in a controlled cabinet environment, using a fluorescent light (Mazda Fluor Lumiere du Jour C9 TF 65, 85 W, United Kingdom) to provide a 16-hour daylight period, followed by an 8-hour darkness period. Because the goal of the experiment was to study the effects of different time lapses in coloured LED light application during the night, the 8-hour dark period was interrupted with different times of illumination. For each colour (monochromatic red, green and blue LED and white LED), the four plates in each quadrant were exposed to 2, 4, 6 and 8 hours of LED light, covering the plates with a black cardboard cover to establish each exposure time. The controls were fully covered during night-time, resulting in an 8-hour darkness period after the daylight. To ensure equally exposure to Photosynthetically Active Radiation (PAR) (ranged between 9.2 to 30.7 µmol s^{-1} cm^{-2} of fluorescent daylight and 2.7 to 12.1 µmol s^{-1} cm^{-2} of nocturnal LED light) and temperature (ranged between 22 to 25 ºC) due to variations inside the cabinet, the plates were periodically rotated each day through the entire experiment, both the position within the quadrant and the position within the cabinet (along with a change of position of the coloured LED lights). The experimental setup can be seen in **Figure 10a**.

The nocturnal LED light was achieved using adjustable light colour LED spots (Mi.Light GU10 RGBW series, 4W, MiLight, Spain). The mean PAR intensity (measured in µmol s^{-1} cm^{-2}) set for each light throughout the entire experiment was 5.71 ± 2.41 for green LED light, 6.39 ± 2.77 for red LED light, 6.75 ± 2.35 for blue LED light and 6.26 ± 0.47 for white LED light. The intensity of both the fluorescent daylight and the LED lights was measured using a spectrometer StellarNet Blue-Wave (StellarNet, USA). Emission spectra for the fluorescent daylight and the ornamental LEDs can be found in **Figure 10b**.

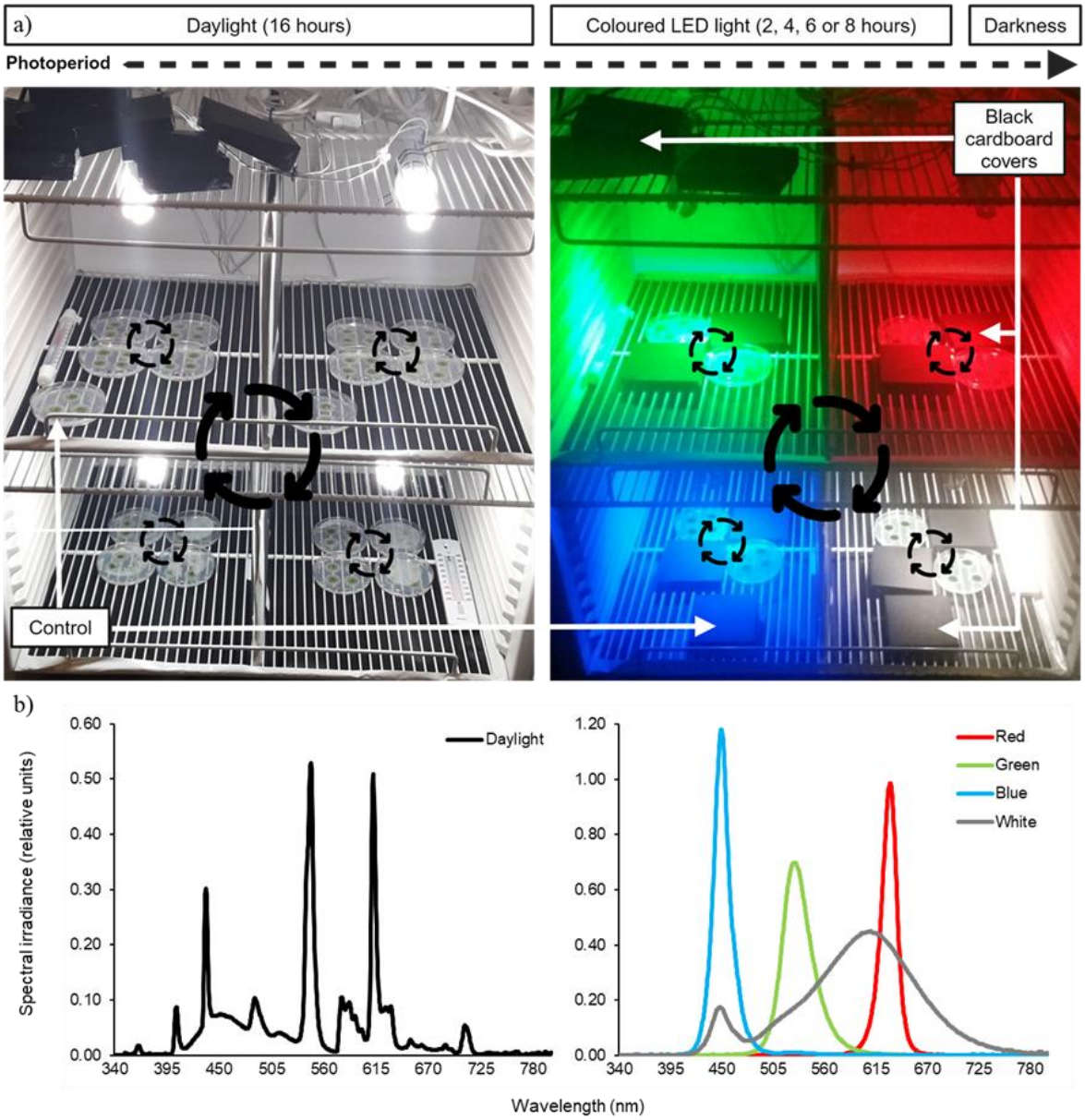

Figure 10. a) Experimental setup in the controlled cabinet. Petri dishes were covered with black cardboard covers to give the desired time of exposure of the coloured LED light. Circle arrows represent the daily rotations of the position of the plates throughout the experiment, both within the quadrant (small circles) or within the whole cabinet (big circles). b) Emission spectra of the lights used.

2.3.Determination of SAB biomass and pigments

After the 35 days, the biofilms were collected to directly measure its wet weight through gravimetry. The pigment content in the biofilm was analysed by resuspending the biofilm biomass in 2 mL of dimethylsulfoxide (DMSO, Sigma Aldrich, Italy) and heated to 65ºC for 1 hour (Bell and Sommerfeld, 1987), following a centrifugation for 10 min at 7000g. The supernatant was analysed spectrophotometrically (Varian Cary 100), followed by the calculations of pigment content via the equations proposed by Wellburn (1994) for chlorophyll-a, chlorophyll-b and total carotenoids.

2.4. Pulse Amplitude Modulated (PAM) fluorometry

Chlorophyll-a fluorometry (Chl_aF) measurements were carried out after 35 days of exposure to the different light treatments on the membrane discs using a multi-wavelength Phyto-PAM fluorometer (Heinz Walz GmbH, Effeltrich, Germany) equipped with a fibre optic emitter-detector unit (PHYTO-EDF) for studying the physiological state of the organisms of the SAB. The measurements were repeated in 5 randomly selected points in each membrane. The fluorescence signal of dark adapted samples (30 minutes of dark adaptation) was recorded before and after light pulses generated by an array of light-emitting diodes (LED) featuring 4 different wavelengths: 470, 520, 645 and 665 nm: the not actinic light was turned on to obtain minimal Chl_aF level (F_0), then a saturating light pulse of ca. 8,000 µmol photons m^{-2} s^{-1} for 0.8 s was emitted to obtain the transient maximum Chl_aF level (F_m) and thus to calculate the variable Chl_aF level (F_v) and the maximum quantum efficiency of PSII photochemistry (F_v/F_m) (Genty et al., 1989).

2.5. Cell counting and SAB diversity

The diversity analysis was conducted in conjunction with the cell counting. The algal and cyanobacterial species were distinguished under light microscopy using a Nikon Eclipse E600 microscope with an E-Plan 40× objective (N.A. 0.65) and differential interference contrast (Nomarski) optics. The proportions of different taxa were determined relative to the total cells counted (minimum of 1000 cells across 100 fields of view at 40× magnification) and expressed as percentages. Species present in proportions less than 0.1% in the counts were not considered. Taxonomic determinations were based on the morphometry and reproduction of the species in the cultures. The primary taxonomic references employed for the identification of green algae were Ettl and Gäertner (1995), Khaybullina et al. (2010), Fuíková et al. (2012). For cyanobacteria, Komárek (2013) was the principal source of information.

2.6.Statistical analysis

Data were tested for significant differences between light treatments by using a Kruskal-Wallis test and a post-hoc Conover's test with Benjamini-Yekutieli adjustment ($p \leq 0.05$). A t-test to test the Pearson correlation between biomass (wet weight) and pigments (chlorophyll-a, chlorophyll-b and total carotenoids) and minimum fluorescence (F_0) of the

four channels of the Phyto-PAM was performed to determine the level of significance between the variables. All statistical analyses were conducted using R software (version 4.4.2), R Studio (version 2024.12.1 +563). software SPSS (SPSS v.25.0 for Windows).

3. Results

3.1.SAB biomass and pigments

The growth in wet biomass between the different exposure times of the four nocturnal coloured LED lights was compared to the control in **Figure 11**. Statistically significant differences in biomass were observed in comparison to the control (3.07 ± 0.30 $x10^{-2}$ g) under four hours of nocturnal green LED light with a decrease to 2.83 ± 0.11 $x10^{-2}$ g, and under eight hours of blue LED light in which wet biomass increased to 3.71 ± 0.24 $x10^{-2}$ g.

The pigment composition of the SABs also underwent a change under the nocturnal coloured LED lights, as illustrated in **Figure 12a**. Nocturnal green LED light reduced the concentration on chlorophyll-a in the SAB in all exposure times, with 6 hours yielding the lowest result with 5.52 ± 0.17 mg Chl-a L^{-1}. Red and white LED light also reduce the concentration of chlorophyll-a to a lesser extent, but only under two, four and six hours. No changes were detected under nocturnal blue LED light, except for an increase to 8.75 ± 1.18 mg Chl-a L^{-1} with a two-hour exposure. Chlorophyll-b decreased significantly under all light colours and exposure times, with the lowest value found again under 6 hours of green light (5.52 ± 0.17 mg Chl-b L^{-1}). However, under two and eight hours of blue LED light the chlorophyll-b concentration did not change. The only significant differences found regarding total carotenoids were found in the six-hour exposure of white and green nocturnal LED light, with the latter yielding the lowest carotenoid concentration with 2.12 ± 0.11 mg Car L^{-1}. **Figure 12b** shows a positive correlation between all three pigments (chlorophyll-a, chlorophyll-b and total carotenoids) to wet biomass, with a positive correlation ($p < 0.01$) according to the Pearson correlation t-test.

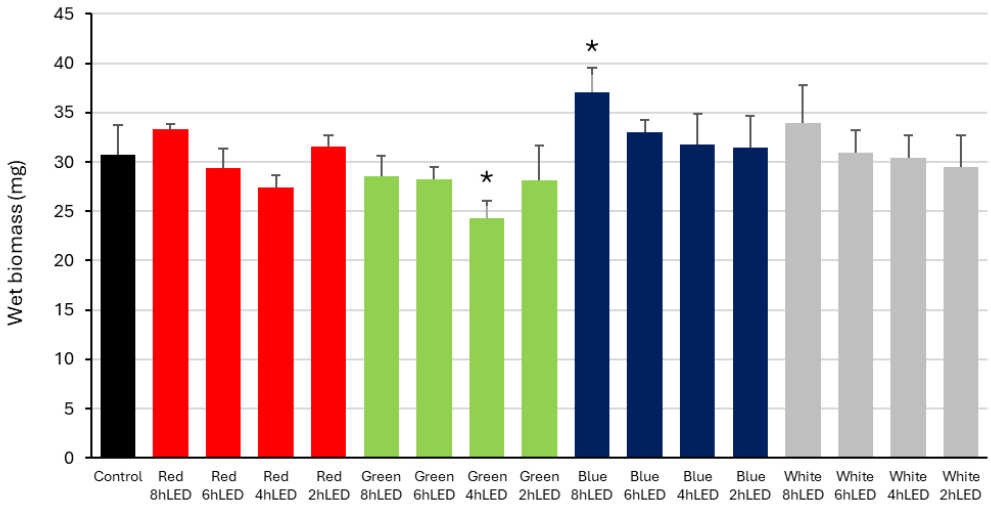

Figure 11. Biomass content as wet weight (x10^2 g / membrane) SABs under the four nocturnal LED lights (red, green, blue and white) with the different time of LED application. The histogram represents mean values of four replicates, while vertical bars represent the SD). Different letters indicate differences ($p < 0.05$) among the different treatments.

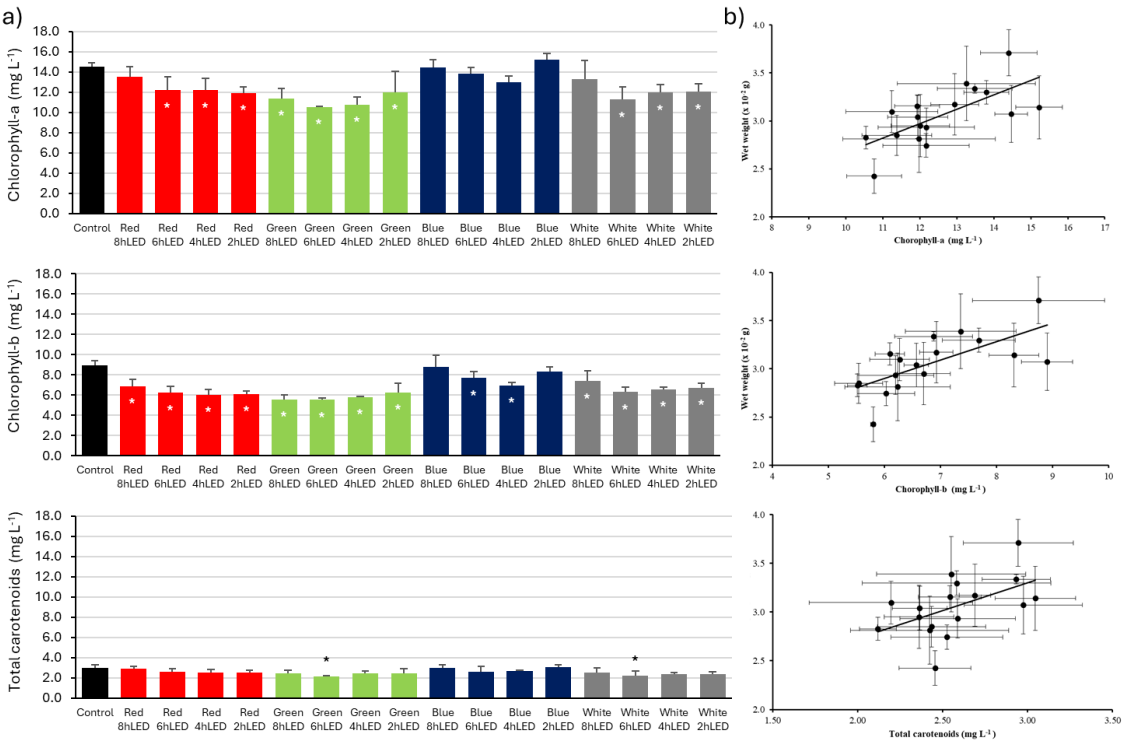

Figure 12. a) Chlorophyll-a, Chlorophyll-b and total carotenoids content (mg L^{-1}) on SABs under the four nocturnal LED lights (red, green, blue and white) with the different time of LED application. The histogram represents mean values of four replicates, while vertical bars represent the SD). Statistically significant differences with respect to control are represented with (*) when $p < 0.05$. b) Relationship between chlorophyll-a, chlorophyll-b and total carotenoids (mg L^{-1}) and values and wet weight (x10-2 g) after the exposure to the four light monochromatic colours (red, green, blue, and white) with the different time (2, 4, 6, 8 hours) of LED application. Chl-a: y=0.1502x+1.1686, R^2=0.4771; Chl-b: y=0.1915x+1.7521, R^2=0.4746; Total Car: y=0.5707x+1.5879, R^2=0.2709.

3.2.PAM fluorometry

The effects of the treatments on the photosynthetic efficiency (F_v/F_m) are not particularly pronounced, although some discernible differences can be observed due to the varying light exposures (**Fig. 13**). In general, F_v/F_m is more adversely affected by the blue and white exposures compared to the control. In contrast, the green light (2, 4, 6, 8 hours) and red light (6 hours) result in a significant increase in F_v/F_m, as measured after the pulse of 520 nm. It is noteworthy that the more pronounced declines in F_v/F_m are observed in the treatments with 2 and 8 hours of red light (both with 470 and 520 nm saturation pulse), yet not in those with 4 and 6 hours. This could be attributed to an increase in F_0 for these samples, as evidenced in the Supplementary Material (SM1**)**. The results demonstrated that there was no significant reduction in photosynthetic efficiency following the saturation pulse at 645 and 665 nm. However, there was an increase in efficiency under four hours of red and green LED light (645 nm) and six and four hours of red LED light and four hours of green LED light (665 nm). The data presented in **Figure 14** shows a significant correlation between the minimum fluorescence (F_0) (see Supplementary Material SM1) and the wet biomass of the SABs in the four channels (470, 520, 645 and 665 nm). A positive correlation ($p < 0.01$) according to the Pearson correlation t-test between wet biomass and F_0 in the four channels, however, no significant differences were observed between the four channels.

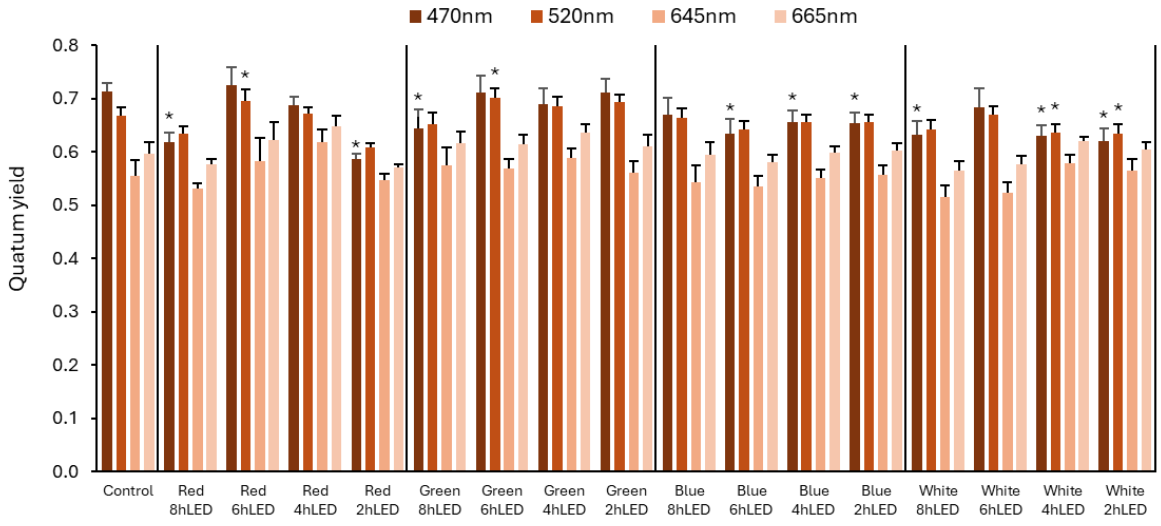

Figure 13. F_v/F_m values (Maximum photosynthetic yield) measured at 470 nm, 520 nm 645 nm and 665 nm on resuspended samples of biofilm after the exposure to the four nocturnal LED lights (red, green, blue, and white) with the different time (2, 4, 6, 8 hours) of LED application. The histogram and the bars represent the I, II and III quartiles of five randomly selected points for four replicates. Statistically significant differences with respect to control are represented with (*) when p < 0.05.

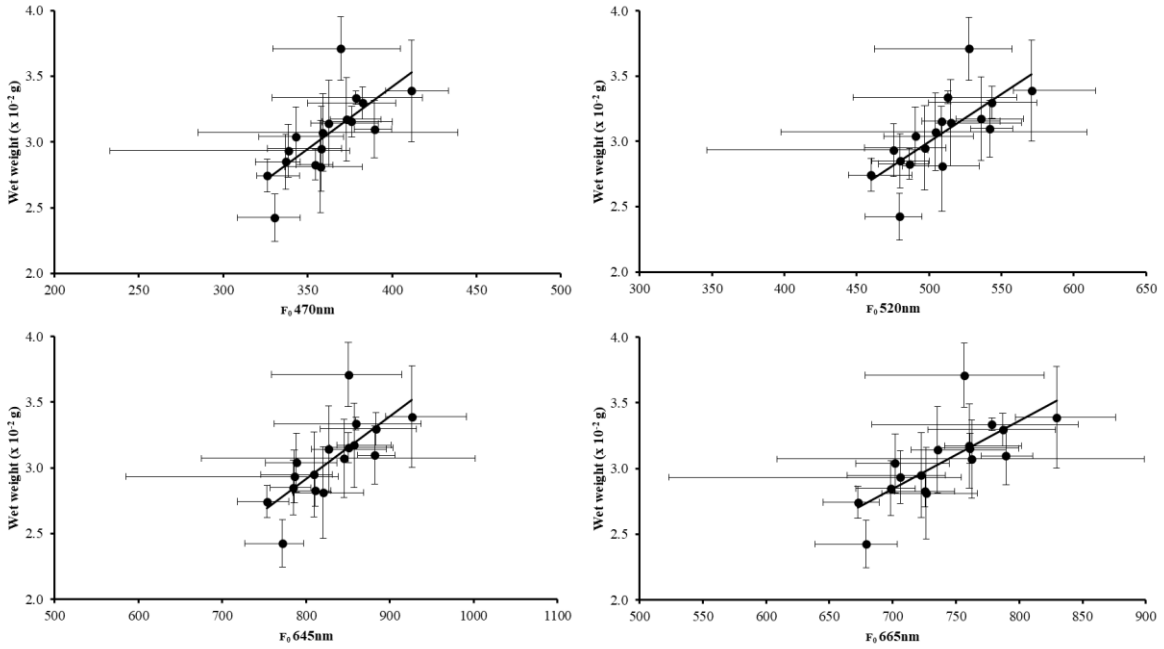

Figure 14. Relationship between minimum fluorescence (F_0) values and wet weight (x10^{-2} g) measured at 470, 520, 645 and 665 nm on resuspended samples of biofilm after the exposure to the four nocturnal LED lights (red, green, blue, and white) with the different time (2, 4, 6, 8 hours) of LED application. 470 nm: y=0.009x-0.363, R^2=0.529; 520 nm: y=0.007x-0.633, R^2=0.513; 645 nm: y=0.004x-0.896, R^2=0.546; 665 nm: y=0.005x-0.780, R^2=0.563.

3.3. Cell counting and SAB diversity

The number of cells in the SABs, shown in **Figure 6**, follows a similar trend to biomass (**Fig. 11**) and chlorophylls (Chl-a, Chl-b) (**Fig. 12a and 12b**). The cell density is significantly lower under the exposure with red and green LED light (lowest at both six and four hours with 5.06 ± 0.30 x10^9 and 5.05 ± 0.58 x10^9 cell L^{-1} respectively) compared to the control (7.94 ± 0.57 x10^9 cell L^{-1}), but the algal density was not different from the control under blue and white LED light (**Fig. 15**). Exposure times (2h, 4h, 6h and 8h) do not have a significant effect on the algal density under any LED light, except for 4 hours of blue LED light that yielded a similar result than the green light (5.06 ± 0.34 x10^9 cell L^{-1}). Despite the observed differences in total cell numbers in the SAB, those related to algal species exhibited a reduction under all LED lights and time exposures, with the exception of 2 hours of blue light. The most notable decline was observed under green LED light, particularly under four and six hours, resulting in 2.72 x10^9 cell L^{-1} and 2.69 x10^9 cell L^{-1} cells, respectively. This was followed by red LED light. Notwithstanding the observed reduction in algal cells under the two LED lighting conditions, cyanobacterial cells exhibited an inverse trend, with green LED light being the most influential in promoting their growth.

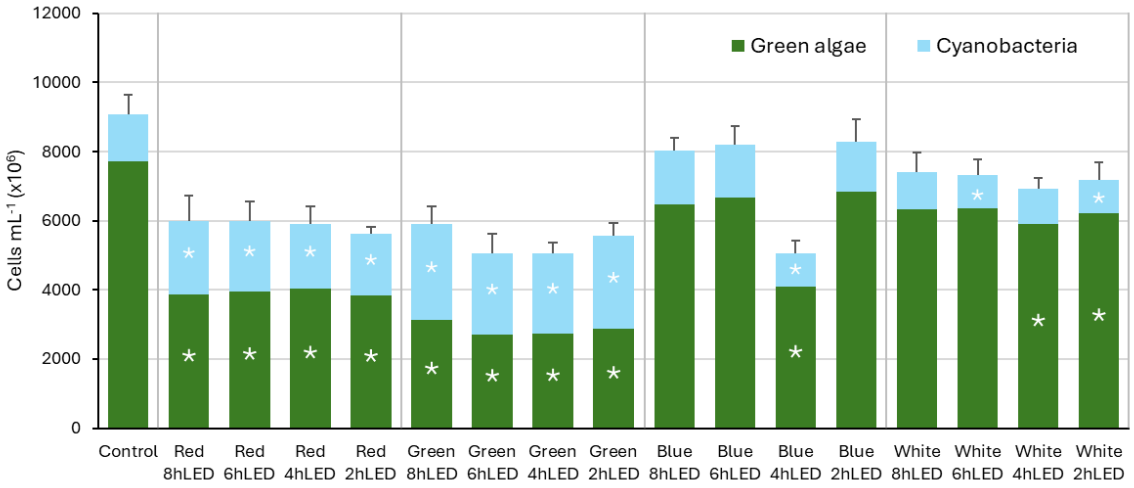

Figure 15. Total cell count (cell L^{-1}) and cell count (cell L^{-1}) of green algae (green) and cyanobacteria (blue) on SABs under the four nocturnal LED lights (red, green, blue, and white) with the different time of LED application. The histogram represents mean values of four replicates, while vertical bars represent the SD). Statistically significant differences with respect to control are represented with (*) when p < 0.05.

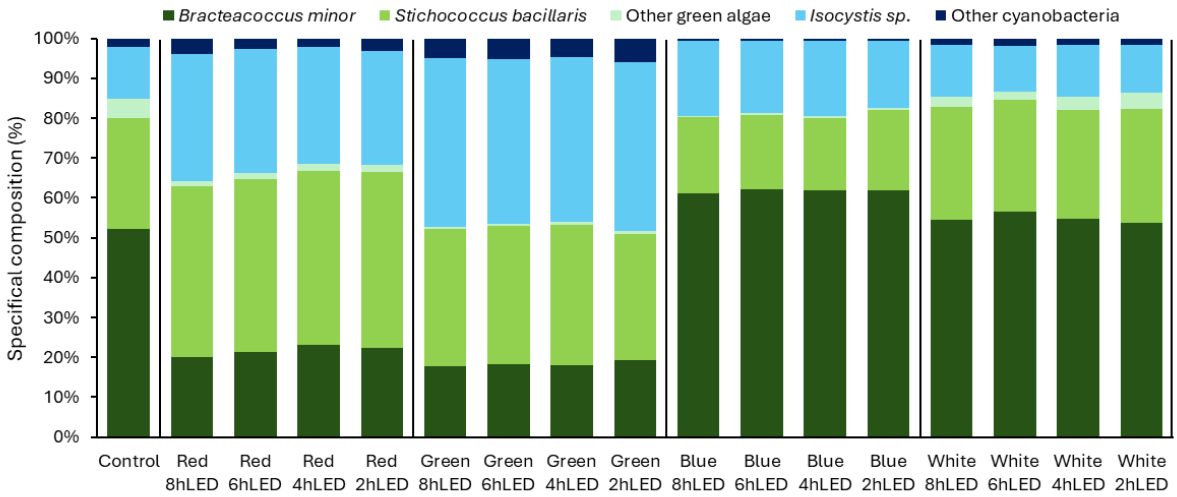

Figure 16. Relative abundance of the different species found in the SABs under the four nocturnal LED lights (red, green, blue, and white) with the different time of LED application.

Following the 35-day experiment, the control SAB was predominantly composed of algal species, with *Bracteacoccus minor* (52.27%) and *Stichococcus bacillaris* (27.77%) collectively accounting for up to 80% of the SAB community, while *Isocystis* sp. (13.15%) and other cyanobacterial species were present in smaller quantities. A graphical representation of the changes in relative abundance is shown in **Figure 16** (a detailed table about the changes in relative abundance is also included in Supplementary Material SM2).

The exposure times of the nocturnal LED lights did not result in any significant changes in the abundance of the SAB species, which were only observed between the

different colours used. The red LED light resulted in a reduction in the presence of *Bracteacococcus minor* to 20% of the SAB and other green algae species. The space was occupied by *Stichococcus bacillaris*, which exhibited the greatest increase in relative abundance, reaching a maximum of 43.48%. This was the largest increase observed among the tested lights. *Isocystis* sp. also exhibited an increase in relative abundance, while other cyanobacteria species were not affected by the red LED light. A similar pattern is observed in the green LED light, with *Bracteacococcus minor* exhibiting the most significant decline, reaching 17.86%, while the other green algae species demonstrated a reduction to 0.54%. Similarly, the presence of *Stichococcus bacillaris* increased, although to a lesser extent than under red light. The green light exposure resulted in the greatest increase in cyanobacterial presence in this experiment, with both *Isocystis* sp. and other cyanobacteria species exhibiting an increase of up to 42.40% and 6.02%, respectively. In contrast to the previously mentioned light conditions, green algae underwent an inverse change in abundance under blue LED light, with *Bracteacococcus minor* increasing to 62.18% and *Stichococcus bacillaris* decreasing to 18.27%. The abundance of all the other algal species was also reduced. In contrast to the other cyanobacterial species, which exhibited a decrease in abundance, *Isocystis* sp. did not undergo any changes under the blue LED light at night. No change was observed under the white LED nocturnal light.

4. Discussion

Nocturnal illumination is now regarded as a major environmental challenge affecting animal and plant physiology and human health (see e.g. Bashiri, 2014; Kyba, 2018). This research provides clear information about the effects of different time regimens for ornamental lighting on the development of SABs, which have direct implications for the conservation of built cultural heritage. The specific composition of the algal inoculum used to create the SABs is typical of granite-stone monuments in the north-west of Spain, specifically of the city of Santiago de Compostela (see Rifón-Lastra and Noguerol-Seoane, 2001), as well as the proportion between green algae and cyanobacteria. It is notable that the first is more prevalent in European regions with an Atlantic climate (Gaylarde and Gaylarde, 2005).

Two lighting regimes were identified as effective for the management of biofilm development in terms of biomass production. Continuous eight-hour blue LED lighting was found to favour algal growth. Indeed, blue light has been demonstrated to increase biomass concentration, productivity and growth rate in continuous light in both *Chlorella* sp. and *Nannochloris oculata* in photobioreactors (Yuan, Zhang, et al., 2020). Furthermore, it has been shown to have a similar effect when applied as nocturnal illumination in the case of *Scenedesmus obliquus* (Abomohra et al., 2019).

This finding can have important implications in the context of microalgal bioreactive facades in green cities, both for the mitigation of harsh environments and energy productions (Ahmad et al., 2022). While terrestrial plants in cities provide environmental benefits, the photosynthetic efficiency and purification capacity of airborne pollutants

(such as particulate matter, SO_2, N_2O, etc.) of microalgae are much higher (Kisser et al., 2020). Projects using microalgae within the urban fabric like the Culture Urbaine project (performed in Geneva, Switzerland in 2014, see https://urbannext.net/culture-urbaine/) which installed microalgae bioreactor besides highways could use ornamental illumination to increase the yield of microalgal biomass intended to dimmish the CO_2 concentration from fuel-based transit. This would not only would improve its environmental benefits but could also be used to create aesthetics artworks during the night.

Alternatively, the use of monochromatic light in wavelengths poorly utilised by microbial photosynthesis may also serve to diminish biofilm formation (Albertano et al., 2003). Nocturnal green LED light was found to decrease SAB biomass with a four-hour exposure time, although no changes were found under the other periods. This result goes in accordance with the aforementioned work from Abomohra et al., 2019, in which 8 hours of nocturnal green light did not alter biomass production of *S. obliquus* in comparison to a normal dark 3period and in contrast with the other coloured light they tested. Some species of freshwater green algae, nonetheless, have been observed to increase in abundance and biomass under nocturnal green or red light, as evidenced by the case of *Tetraselmis suecica* (Diamantopoulou et al., 2021). This suggests that different species may exhibit varying sensitivities and adaptation strategies towards ALAN. The results of this study demonstrate that *Stichococcus bacillaris* can resist exposure to red and green light, which is detrimental to *Bracteacoccus minor*. This allows *S. bacillaris* to exploit the gap left by *B. minor*, which consistent with the results of Sanmartín et al. (2021), who observed that nocturnal red LED light (either alone or in combination with UV-A radiation) promoted the growth of *S. bacillaris* and inhibited the proliferation of *B. minor* within a SAB community.

Nocturnal red and blue light was found to increase chlorophyll content and dry weight in *Scenedesmus obliquu*s cultivation (a specie also found in stone colonizing SABs) compared to green light (Abomohra et al., 2019), The supplementation of white light with blue light or red light also caused a higher chlorophyll concentration and dry weight in *Stichococcus* sp. (Mutaf et al., 2019; Psachoulia and Chatzidoukas, 2021).

The positive correlation between wet biomass and pigments indicates that pigment concentration can be used as a proxy indicator for algal biomass (Mineeva, 2011). Considering this relation, more differences between the coloured lights tested and their application times can be observed. The lowest concentration of chlorophyll (a and b) is observed under four and six hours of green light at night. Furthermore, the results indicate the lowest biomass values (outlined above under a four-hour exposure) and total carotenoids (under a six-hour exposure), thus demonstrating that a nocturnal illumination of between four and six hours of green LED light during the night is the optimal methodology for reducing biological colonisation of illuminated built heritage sites. The comparison of these results with the available literature is complicated by the fact that, as mentioned in the introduction, the majority of studies of the effect of photoperiod and/or light quality on biomass and pigment production in green microalgae are focused on industrial production in bioreactors. The results of these studies vary considerably,

depending on the conditions set and the strains used. For example, the microalgae *Chlorella vulgaris* and *Gloeothece membranacea* show a differential production of chlorophyll-a through time when growth in a photobioreactor under red light, one increasing and the other decreasing over time, but both being always lower than the production obtained in the photobioreactor subjected to green light (Mohsenpour and Willoughby, 2013). These results are in contradiction with the ones presented in this study, where a higher concentration of chlorophyll was obtained under the exposure of red LED light than green LED light. The correlation between F_0 and the biomass (expressed as wet weight) allows us to use the ChlaF to estimate the amounts of organisms and therefore their growth on the surface. However, the R^2 values are similar for all the wavelengths used. From one side this confirm that F_0 could be a good indicator for the biomass for green algae and cyanobacteria (e.g. Serôdio et al., 2001; Honeywill et al., 2002); by contrast this result (and the no correlation found with pigments) make the use of F_0 from the different channels quite difficult to identify with accuracy the groups of organisms in biofilms.

The low effects of the treatments on F_v/F_m indicate that the vitality is not significantly affected by the treatments. This is likely due to the diverse range of algae present, which enables the algae to counteract the varying effects of the different light sources on specific groups of organisms; moreover this parameter is often less sensitive than other ChlaF ones such as NPQ, qP and others to some stress (Narayan et al., 2012). Here, the different composition of the species can compensate for the decrease of vitality in one or more of them; many authors (e.g. Masojídek et al., 2000; Lichtenthaler et al., 2007; Singh et al., 2016) report that the pigments can influence different ChlaF parameters. Therefore, the reaction of the SABs, in terms of F_v/F_m variation, to the different excitation lights can depend by groups of organisms having different pigments contents (Santabarbara et al., 2019). In cyanobacteria the determination of the F_0 and F_m depends by the phycobilisomes that bring to higher basal fluorescence than in green algae and plants (Grigoryeva and Grigoryeva, 2020). In the present study a different growth of green algae and cyanobacteria after the different light treatment was detected (**Fig. 16**), however the relation between these two groups of organisms remained too balanced to determine a strong difference in terms of ChlaF variation. Curiously at 520 nm F_v/F_m is higher after the exposure to the blue and white light and this looks in contrast with the species composition data. The presence of cyanobacteria is higher after red and green light exposure since the 520 nm light should help to detect a mix of carotenoids and phycoerythrin (see, for example, the absorption spectrum of the phycoerythrin in Glazer and Hixson, 1977). However, the cyanobacteria should in general lower the level of F_v/F_m (Misumi et al., 2016; Acuña et al., 2015), in particular with the PAM illuminations with specific wavelength, which could explain the differences with both saturation lights (470 and 520 nm) between the Green/Red LED light and Blue/White LED lighting conditions.

5. Conclusions

The results of this research provide clear evidence that the growth and physiology of biofilms can be controlled in terms of their specific composition, cell density, biomass, and pigments by applying coloured light at night with different exposure times. It was concluded that the optimal time to induce a biostatic effect (i.e. halting their development) over phototrophic SAB is with 4 to 6 hours of green LED light, while 8 hours of blue light increase the development of the SAB. However, blue light does not cause differences in total pigment concentration. The ornamental lighting regimes barely affected the photosynthetic efficiency of the SABs, which is counteracted by changes in the pigment composition and the specifical composition. Light colour affected the diversity of the species comprising the SAB, with red and green LED light reducing the total cell count but increasing the proportion of cyanobacteria. However, light duration failed to alter the relative diversity. These findings are of interest to policymakers when contemplating the potential effects of the hours of illumination of monuments on their vulnerability to biodeterioration.

Authors' contribution

Conceptualization, P.S.; investigation, A.M., R.C., S.B. and P.S.; formal analysis, A.M., R.C., S.B. and P.S.; writing—original draft preparation, A.M., R.C., S.B. and P.S.; writing—review and editing, A.M., R.C., S.B. and P.S.; supervision, P.S.; resources and funding, P.S.

4.2 PART 2: ASSESSMENT OF BIOSTATIC CAPACITY

4.2.2 CHAPTER 3

NOVEL ORNAMENTAL LIGHTING USED TO HALT PHOTOTROPHIC COLONISATION ON ARCHITECTURAL HERITAGE IS EFFECTIVE UNDER LOW AND HIGH DAYLIGHT ILLUMINANCE CONDITIONS

Anxo Méndez, Rafael Carballeira, Sabela Balboa, Patricia Sanmartín

Journal of Building Engineering 112, 113798 (2025). doi: 10.1016/j.jobe.2025.113798

JCR index (IF) 2024 = 7.4 (10/183, 94.8 percentile in Engineering, Civil)

Open access

The work from this chapter was also presented in an international conference:

Méndez, A.; Balboa, S.; Carballeira, R; Sanmartín, P. Effect of sunlight on the efficacy of a novel ornamental light that halts phototrophic colonisation on architectural heritage: a laboratory approach. Oral communication. European Conference on Biodeterioration of Stone Monuments (ECBSM2024). 7-8 November 2024, Milan, Italy.

Journal of Building Engineering 112 (2025) 113798

Contents lists available at ScienceDirect

Journal of Building Engineering

journal homepage: www.elsevier.com/locate/jobe

Novel ornamental lighting used to halt phototrophic colonization on architectural heritage is effective under low and high daylight illuminance conditions

Anxo Méndez [a,*], Rafael Carballeira [b], Sabela Balboa [c], Patricia Sanmartín [a]

[a] CRETUS, Gemap (GI-1243), Departamento de Edafoloxía e Química Agrícola, Facultade de Farmacia, Universidade de Santiago de Compostela, Santiago de Compostela, 15782, Spain
[b] Cavanilles Institute for Biodiversity and Evolutionary Biology, University of Valencia, 46980, Paterna, Valencia, Spain
[c] CRETUS, Departamento de Microbiología y Parasitología, CIBUS-Facultad de Biología, Universidade de Santiago de Compostela, Santiago de Compostela, 15782, Spain

ARTICLE INFO

Keywords:
Biofilm
Environmental technologies
LED luminaires
Lighting treatment
Treatment validity

ABSTRACT

Nocturnal ornamental lighting may serve as a biostatic tool to control phototrophic colonization on architectural heritage, though the influence of daylight illuminance on this effect remains unclear. This study is the first to consider the effect of the amount of daylight on responses to nocturnal lighting, by combining two levels of daylight illuminance (low, LDI, ~2050 lx and high, HDI, ~10200 lx), selected on the basis of field measurements, and three ornamental LED lighting conditions: cool white, warm white and amber + green (which has a biostatic effect on phototrophic growth) and a control (i.e. darkness). Subaerial biofilms (SABs) were generated using green algae (mainly *Chlorella vulgaris* and *Klebsormidium flaccidum*) and cyanobacteria (mainly *Synechocystis* sp.) isolated from biofilms growing on granite monuments. Changes triggered by the combination of daylight and artificial light at night were evaluated by biomass and diversity measurements, biochemical profiling, confocal microscopic examination and PAM fluorometry of mature biofilms. Cool white light enhanced biomass growth relative to the other conditions, while amber + green light halted biomass growth in both daylight scenarios. Amber + green light also decreasing the relative abundance of *Klebsormidium flaccidum* in LDI. Biofilm matrix production was reduced when illuminated with amber + green light in the LDI set-up. In the HDI set-up, all ornamental lighting conditions failed to alter the biochemical profile. However, amber + green light did reduce the R_{df} vitality index compared to other conditions. Amber + green light effectively halted biofouling under both daylight conditions, potentially mitigating its impacts and enhancing the sustainability of urban heritage management through better lighting practices.

1. Introduction

Urban structures shape urban ecosystems. Buildings block direct daylight and thus create shadows and gradients of solar irradiation on the facades and the surrounding streets (see e.g. Refs. [1–3]), with variable effects throughout the day depending on the position of the sun in the sky. Solar irradiation influences the growth of phototrophic organisms that form subaerial biofilms at the solid-air

* Corresponding author.
E-mail address: anxo.mendez.villar@usc.es (A. Méndez).

https://doi.org/10.1016/j.jobe.2025.113798
Received 24 March 2025; Received in revised form 30 July 2025; Accepted 18 August 2025
Available online 23 August 2025

interface (SABs). It thus has a direct effect on the photosynthetic capacity of the organisms [4], and it also has indirect effects by altering the temperature and moisture of the substrate on which the SABS are formed [5]. These effects determine which phototrophic organisms grow (i.e. algae or cyanobacteria) and how they are distributed on urban facades (see e.g., Ref. [6]). The aforementioned variations in solar irradiation force phototrophic organisms to manage light harvesting for photosynthesis. The organisms must achieve a balance between photochemical reactions and photoprotection from excess light to prevent oxidative damage [7], which affects their overall development (see e.g. Ref. [8]). In natural environments, organisms perform this balancing act in response to changes in correlated colour temperature (CCT, i.e. the measure of the quality, colour or wavelength of a white light) and intensity of light (see e.g. Refs. [9,10]). However, in urbanised environments, the introduction of artificial light at night (ALAN) extends the time during which phototrophic organisms must manage light exposure (see e.g. Refs. [11,12]). This particularly applies to the different CCT derived from the lighting technologies used in urban lighting (see e.g. Refs. [12,13]). For example, white LEDs and metal halide lamps emit light in the short wavelength region (i.e. around the blue region of the visible light spectra), resulting in a higher CCT, and thus have a higher relative quantum yield than high- and low-pressure sodium lamps, which have a lower CCT [12]. The artificial lighting used to illuminate heritage buildings and monuments is usually more intense than other lighting in the surrounding environment, to highlight or enhance the aesthetic value of the architecture. Longer photoperiods can promote the growth and productivity of green algae in bioreactors, in species such as *Chlorella vulgaris* [14], *Scenedesmus obliquus* (currently known as *Tetradesmus obliquus* [15]) and *Botryococcus braunii* [16]. Nevertheless, the effects of the longer photoperiods may differ in aeroterrestial biofilms, which exhibit higher tolerance to variations in light intensity and the presence of ultraviolet radiation than algal cultures (see e.g. Refs. [17, 18]).

The growth of phototrophic SABs on architectural heritage (i.e. monuments and groups of buildings with historic and artistic interest, see Ref. [19]) results in the formation of greenish coatings that stain and soil their facades. The coatings have a negative aesthetic impact and under certain circumstances may cause biodeterioration of the substrate. The generation of a coherent layer of extracellular polymeric substance (EPS) (which mainly consists of polysaccharides, proteins and eDNA) during biofilm formation provides protection to the sessile (micro)organisms within biofilms, enabling them to resist adverse conditions (e.g. high light, UV radiation, desiccation and pollutants) (see e.g. Refs. [20,21]). The extracellular matrix also serves as a refuge for other heterotrophic microorganisms such as fungi and bacteria, which can cause greater damage to heritage surfaces than phototrophs (see e.g. Refs. [22, 23]).

Algae and cyanobacteria obtain some minimal nutrients from the substrate on which they are attached to form a biofilm and/or the surrounding environment in the form of dust and soil particles ([5,24]). However, the primary source of sustenance is the light used for photosynthesis, whether daylight or artificial light. The main pigments used by phototrophs to harness light are chlorophyll *a* and *b*. The maximum absorption peaks of these pigments are usually centred in the blue and red parts of the visible light spectrum, around 428 nm and 660 nm for chlorophyll *a* [25] and 460 nm and 650 nm for chlorophyll *b* [26]. Cyanobacteria have chlorophyll *a* as the main pigment in the antenna complex, although they also have phycobilins as characteristic accessory pigments, with the blue phycocyanins absorbing in the 620–640 nm range of the spectrum with a maximum peak at 620–625 nm, and the red phycoerythrins absorbing in the 495–570 nm range of the spectrum, with a maximum peak at 540 nm (see e.g. Refs. [27,28]).

The use of artificial light to manage phototrophic colonization of heritage surfaces has already been the subject of study and implemented in underground heritage, using visible light (see e.g. Refs. [29,30]) and even UV radiation (see e.g. Ref. [31]). With the absence of natural sunlight in underground heritage sites [30], demonstrated that the photosynthetic activity was higher in cyanobacterial biofilms located closer to artificial light sources. These authors also reported a reduction in the emission spectra of the biofilm caused by the absorption of light due to the intrinsic characteristics of the phototrophic community. This observation suggests that the photosynthetic apparatus of these biofilms acclimates in response to light quality and intensity, as determined by the spectral composition and proximity to the artificial light source (fluorescent lamps with emission peaks at 540 nm and 575–632 nm).

As it is not possible to modify the exposure of outdoor building/monument facades to daylight, ornamental lighting can be used in an alternative approach to managing or even reducing phototrophic colonization on architectural heritage. The advent of LED technology has caused a notable shift in the range of light spectra available for nocturnal illumination, enabling more precise control of the wavelengths emitted [32]. This presents an opportunity to illuminate facades at the ranges within which the absorption of photosynthetic pigments is low, such as the amber and green region of the visible light (PAR: Photosynthetically Active Radiation) spectrum [33]. This could potentially control the development of phototrophic organisms and their subsequent impact by using existing lighting infrastructure. Thus, ornamental illumination could ultimately be used in a multifunctional approach to maintaining the ornamental illumination of architectural heritage while enhancing protection against SABs. It was within this context that the CromaLux project (http://cromalux.santiagodecompostela.gal/en) arose. The project focuses on how to reduce SABs growth on architectural heritage by using suitable white-like light and has led to the development of a novel LED lighting system with a biostatic effect (halting biological colonization, mainly caused by algae and cyanobacteria) based on the combination of amber and green LED lights. However, it is not clear whether application of this novel LED lighting at night is affected by different sunlight scenarios during the daytime, i.e. low and high daylight illuminance (i.e. total luminous flux incident on a surface, per unit area). It is also not yet known whether the intensity of daylight affects the SABs formed under exposure to ornamental light. The present study investigated the effects of high daylight illuminance (hereinafter, HDI) and low daylight illuminance (hereinafter, LDI) in combination with four night-time ornamental light regimes, i.e. cool white LED (CCT, 4300K), warm white light LED (CCT, 2580K) and amber + green LED (CCT, 3000K, potentially with a biostatic effect) and a control without light (i.e. darkness) on laboratory-grown phototrophic multi-species SABs. The HDI and LDI levels were based on field measurements made in facades with different orientations in the urban fabric. Growth and diversity, biochemical profiling (pigment production, exopolysaccharides and levels of ATP), confocal microscopy and pulse-amplitude modulated (PAM) fluorometry of the target SABs were used to evaluate the efficiency and effects of the new

ornamental lighting (amber + green) relative to other ornamental lighting and in relation to high and low levels of daylight. If the biostatic capacity is confirmed under varying daylight irradiance conditions, ornamental nocturnal lighting could serve as an effective tool for mitigating phototrophic colonization across a broader range of urban heritage structures. Thus, the end-goal is to reduce the frequency of cleaning interventions with more efficient ornamental illumination practices and thereby enhancing the sustainability of urban architectural heritage management.

2. Material and methods

2.1. Experimental lighting set-up

The lighting set-up consisted of a custom-built cabinet, divided into four compartments. An artificial photoperiod was established in each compartment (Fig. 1a), consisting of 13 h of LED simulating daylight (SUN@HOME, Spot PAR16 40 GU10 TW, Ledvance, Germany) with a colour temperature of 5500K, followed by 6 h of three different nocturnal ornamental LED lights (cool white, warm white and amber + green, the latter with potentially biostatic effect) and a control with no nocturnal light (i.e. darkness). The photoperiod ended with 5 h of darkness for all different light regimes. The ornamental lighting consisted of illuminance of 20 lux, supplied by a radiometer (DHD 2302.0, HERTER). This is the minimum level recommended for highlighting facades and is in keeping with the principles of energy conservation and reduction of light pollution (see e.g. Ref. [34]). Lux, lx (lumen per m^2) was chosen as the unit of luminous illuminance because it is the unit used in the regulations for Spanish ornamental and urban lighting (see Ref. [35]), regardless of light spectrum emitted by the light source used. Three ornamental lights were tested: cool white (4300K, 1.84 μmol s^{-1} m^{-2}, A5 GU10 9W, Aigostar, Spain), warm white (2580K, 1.13 μmol s^{-1} m^{-2}, cod. 671992, Televés, Spain) and a combination of monochromatic amber plus green LED lights (3000K, 0.89 μmol s^{-1} m^{-2}, cod. 671990-1, Televés, Spain). Both white lights emit the full range of the visible light spectrum (≈380 nm–700 nm), with the cool white generating a bluish tone due to the main peak being at 457 nm. The cool white LED was shaded with a slightly yellowish, heat-resistant paper film to dim the light to an illuminance of 20 lx, resulting in a change in the correlated colour temperature (CCT) from 6400K (as specified by the manufacturer) to 4300K, which is more similar to outdoor cool white light sources such as metal halide lamps (see Ref. [36]). The warm white LEDs are characterised by a reduction in the blue region (with a secondary, less intense peak at 450 nm), resulting in a yellowish tone with the main peak around 600 nm. The amber + green LED emits a bimodal spectrum with two peaks, one at 528 nm (green) and a main peak at 593 nm (amber), with no emission at wavelengths in the blue and red parts of the spectrum. The complete photoperiod is depicted in Fig. 1a, and the light spectra of daylight and ornamental LED lights are shown in Fig. 1b.

The experiment was conducted twice under identical experimental conditions, except for the daylight illuminance. Two daylight

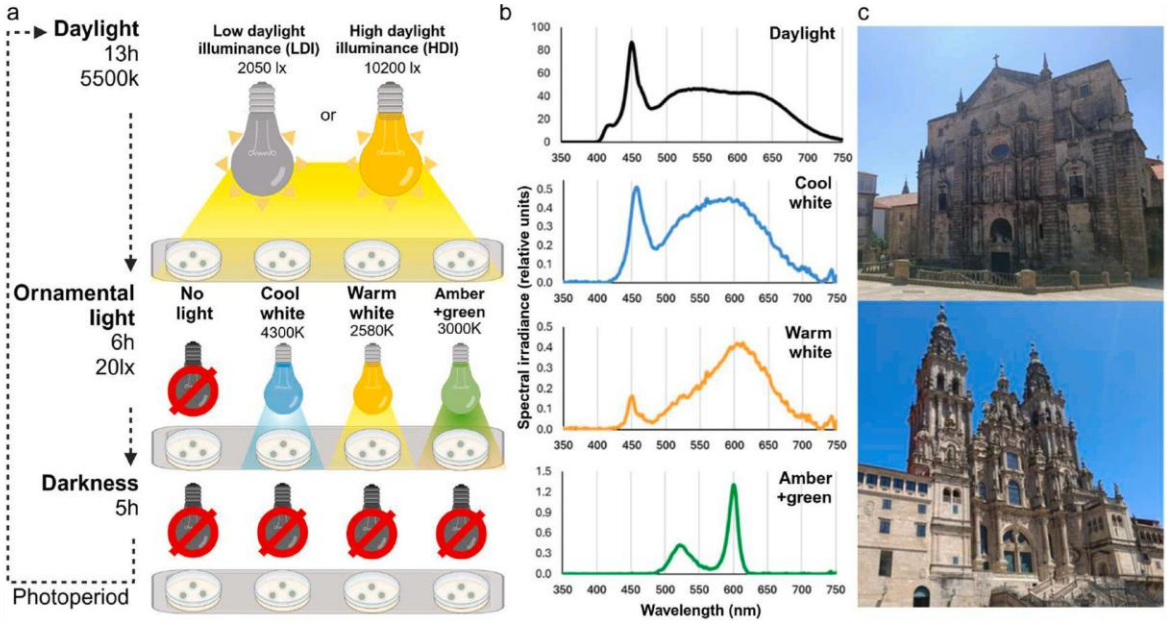

Fig. 1. a) Diagram illustrating the experimental design, including the characteristics of the photoperiod used to culture subaerial biofilms (SABs); b) Emission spectra of the lights used. The daylight irradiance level corresponds to high daylight illuminance (HDI). c) Examples of some of the surveyed facades in the historical centre of Santiago de Compostela, which are exposed during daytime to low levels of solar illuminance (upper image, Church of the Convent of San Martiño Pinario, east-(slightly north)facing) and high levels of solar illuminance (lower image, Cathedral of Santiago de Compostela main entrance, west-(slightly south)facing) (images provided by Anxo Méndez).

regimes were selected: one of low solar illuminance (LDI) and the other of high solar illuminance (HDI). Two surveys (one on a cloudy day and one in a sunny day) were conducted in the spring of 2022, at midday, on various facades of the architectural heritage of the historical centre of Santiago de Compostela (Fig. 1c). Eight granite heritage buildings were selected according to their orientation, position and surrounding architecture: three being subjected to direct insolation and five subjected to indirect insolation throughout the day. Examples of two the surveyed facades are shown in Fig. 1c. The direct insolation ranged at midday between around 2000 to 2500 lux in the cloudy day and 40,000 to 60,000 lux in the sunny day, while the indirect insolation ranged between around 1000 to 3,00 lux in the cloudy day and 2000 and 6000 lux in the sunny day. The seasonal average daily insolation in the city, as reported by the Galician meteorological service (https://www.meteogalicia.gal/), was used to assess whether the cumulative solar illuminance applied during the 13-h daylight period was consistent with the daily insolation in spring. Considering the aforementioned factors, an illuminance level of approximately 2050 lux (50.07 μmol s^{-1} m^{-2}) was determined for the LDI (simulating an indirect facade or a cloudy day) and 10200 lux (252.59 μmol s^{-1} m^{-2}) for the HDI (simulating a direct facade on a sunny day).

2.2. Biofilm culture and SAB formation

Subaerial biofilms (SABs) were prepared following a previously described procedure [37]. The SABs were generated using Bold's Basal Medium (BBM) liquid cultures derived from natural phototrophic biofilms growing on architectural heritage built in granite of the historical centre of Santiago de Compostela (UNESCO World Heritage City since 1985, north-western Spain), mainly composed of green algae but also including cyanobacteria. The species grown in the broth culture were examined under light microscopy, with a Nikon Eclipse E600 equipped with an E-Plan 40 × objective (N.A. 0.65) and differential interference contrast (Nomarski) optics. Taxonomic determinations were based on the morphometry and reproduction of the species isolated from the culture. The main taxonomic references used for the identification of green algae were [38–41] for cyanobacteria.

Aliquots of a suspension of exponentially growing cells (50 μL, equivalent to depositing a dry weight biomass of 6.85 x10^{-2} μg for the experiment under the LDI conditions and 7.60 x10^{-2} μg for the experiment under the HDI conditions) were used to inoculate the shiny side of each sterile polycarbonate membrane disc (Nuclepore™ track-etch membrane filtration products, diameter 2.5 cm, area 4.9 cm^2, pore diameter 0.2 μm, Whatman™). The membrane discs were sterilized by exposure to UV-C light (Philips TUV F17T) for 1 h on each of the two sides (shiny and matt). Three membranes were placed in each of four BBM agar plates. One plate was then placed in each compartment in the cabinet, for exposure to the ornamental light regimes tested (cool white, warm white, amber + green, and no light), under LDI and then HDI conditions (Fig. 1). The membranes were transferred, with the aid of plastic forceps, to fresh agar plates twice a week, to ensure full nutrient availability. The subaerial biofilms (SABs) were cultured for 37 days until they reached maturity. Twelve membranes (three per ornamental light regime) were then selected at random for analysis by confocal microscopy. The remaining membranes were subjected to PAM fluorometry tests and biomass determination. Of these, three groups of three membranes per ornamental light regime were randomly selected for pigment quantification (chlorophylls *a* and *b*), extracellular polymeric substance (EPS) matrix analysis and diversity study.

2.3. Biomass and diversity

The mature biofilms (37 days old) on membrane discs were weighed on a precision laboratory balance (Denver Instruments). Whole colonies were then removed from the membrane discs by gentle scraping with a sterile loop and transferred to a tube containing 1.5 mL of Phosphate-Buffered Saline (PBS). Colonies used for EPS analysis were suspended in 2 mL of 2 % ethylenediaminetetraacetic acid (EDTA). Homogeneous suspensions were used for subsequent determination of pigment content, EPS matrix and analysis of species diversity. The biofilm was removed from the membrane discs, which were then re-weighed on the same balance. The wet weight biomass of the biofilm was determined as the difference between the weight of the discs before and after the biofilm was removed.

Membranes intended for species diversity analysis were used to quantify the cell concentration (n° cell mg^{-1} SAB) in an Utermöhl sedimentation chamber [42], with at least 1000 cells counted across 100 fields at 40 × magnification. Changes in specific diversity were examined and determined by the same taxonomic techniques and equipment already described (see Section 2.2).

2.4. Biochemical profile

Homogeneous suspensions of biofilm in PBS were resuspended in 2 mL of dimethylsulfoxide (DMSO, Sigma Aldrich, Italy), heated to 65 °C for 1 h [43] and centrifuged for 10 min at 7000g. The supernatant was then collected from each sample and used to determine the chlorophyll (a and b) contents by spectrophotometric measurements (UV/VIS Spectrometer T8DCS, Persee, Germany). The values were calculated using the equations proposed by Ref. [44].

The main extracellular polymeric substances (EPS) (i.e. exopolysaccharides and extracellular proteins) were extracted using a modified version of the method described by Ref. [45] with the modifications described by Ref. [46]. The extracellular matrix was separated from the cells by placing the biofilm samples in 2 % EDTA and sonicating them at 40Hz in a water bath for 10 min. The samples were then incubated for 3 h at 4 °C and centrifuged at 300 rpm for 20 min. The supernatant was centrifuged again, at 5000 rpm for 20 min at 4 °C, and then filtered through 0.22 μm filter paper. The filtrate was placed in ethanol and left overnight at −20 °C to precipitate. The pellet obtained after centrifugation of the precipitate at 13000 rpm for 30 min was then resuspended in M9 minimal medium. The exopolysaccharide fraction of the supernatant was quantified spectrophotometrically in microplates at 490 nm in a Multiskan SkyHigh spectrophometer (Thermo Sicentific) and analysed with Skanlt Software, by the phenol-sulphuric acid method [47]

with D (+)-glucose (Panreac) as standard. The protein content was measured using the Bradford assay [48].

The ATP content was determined in aliquots (0.5 mL) of the biofilm samples in PBS and ATP, by using a luminometry-based cell viability kit (Cell Viability Kit AB, BioTherma, Sweden) and following the luciferase-based protocol for tube luminometers (Junior LB 9509, Berthold Technologies, Germany). Luminescence units (RLU) were converted to ATP concentration (pmol) according to the manufacturer's protocol.

All assays were conducted in triplicate.

2.5. Confocal microscopy

Microscopic observation of the mature biofilms (37 days old) on membrane discs was performed in a laser scanning spectral confocal microscope (LEICA TSC SP5 X, Leica Microsystems Heidelberg GmbH, Germany) equipped with white laser, in the Research Infrastructures Area of University of Santiago de Compostela (Microscopy Unit). Samples were observed with an HCX PL APO CS 40.0 x1.25 OIL UV objective. Data were captured with Leica LAS AF software, in spatial scanning mode (XYZ) with a scan format resolution of 1024 x 1024 pixels. SABs were stained following the method described by Ref. [49] with concanavalin A, tetramethylrhodamine conjugate (lectin ConA-TMR) and fluorescein isothiocyanate isomer I (FITC) (Invitrogen). One image was captured on a random area around the centre of each biofilm. A hybrid detector (HyD) was used to obtain the emission signal from the biofilm sample: polysaccharides were recorded in the blue channel (ConA-TMR: excitation, 552 nm; emission, 578 nm), extracellular proteins were recorded in the red channel (FITC: excitation, 495 nm; emission, 525 nm) and chlorophyll autofluorescence was recorded in the green channel (excitation, 664 nm; emission, 725 nm). The signal of chlorophyll autofluorescence within the cells was used to obtain the cell count and average cell size. The images covered each an area of 30,303.84 μm^2 and were analysed using ImageJ 1.54 software.

2.6. PAM fluorometry

Chlorophyll *a* fluorescence images of the mature biofilms (37 days old) on membrane discs were captured using a Handy FluorCam FC 1000-H PAM (Pulse Amplitude Modulated) imaging fluorometer (Photon Systems Instruments, Czech Republic). The mean values of the whole biofilm surface were thus recorded for the parameters under study. The device uses a non-actinic light at 640 nm to record the minimum fluorescence (F_0), followed by a pulse of saturating actinic white light at 1046.00 µmol s^{-1} m^{-2} to record the maximum fluorescence (F_{max}). The samples were subjected to alternating pulses of actinic white light at 206.00 µmol s^{-1} and far-red light (740 nm) at 10.50 µmol s^{-1} to record other relevant parameters derived from the resulting Kautsky curve. The following parameters were determined, in addition to the F_0 and F_{max}: maximum quantum yield (QY_{max}) and light-adapted quantum yield (QY), non-photochemical quenching (NPQ), coefficient of photochemical quenching (qP) and fluorescence decline ratio (R_{df}). All fluorescence parameters were measured in relative units, with the exception of QY and QY_{max}, which ranged from 0 to 1.

2.7. Statistical analysis

The Kolmogorov-Smirnov test was used to test the normality of the data. As the wet biomass, the biochemical profile and the QY and qP parameters from the PAM fluorometry analysis were not normally distributed ($p \leq 0.05$), a non-parametric approach was adopted. Data regarding the daylight set-up (LDI and HDI) were compared using Wilcoxon test ($p \leq 0.05$). Data regarding the

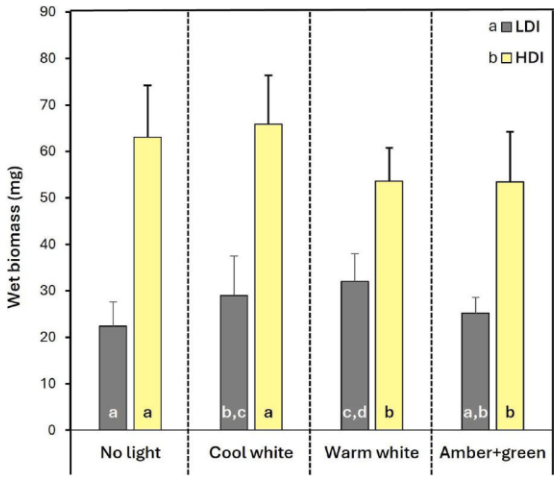

Fig. 2. Growth of subaerial biofilms (SABs) expressed as wet biomass (mg), under different ornamental lighting conditions. Bars indicate mean values and lines represent SDs. Different letters indicate significant differences in relation to ornamental illumination and the daylight scenario (LDI: low daylight illuminance; HDI: high daylight illuminance).

ornamental lighting conditions were compared using a Kruskal-Wallis test and a *post-hoc* Conover's test with Benjamini-Yekutieli adjustment ($p \leq 0.05$).

A Pearsons correlation matrix was constructed ($p \leq 0.05$) and principal Component Analysis (PCA) was performed to examine the relationship between wet biomass (WB) and the PAM fluorometry parameters.

All statistical analyses were conducted using R software (version 4.4.2) and R Studio (version 2024.12.1 + 563).

3. Results

3.1. Biofilm growth

Growth of the SABs under the ornamental light regimes in both daylight scenarios is summarised in Fig. 2. Regardless of the type of ornamental lighting, the wet biomass yield was significantly greater under HDI (58.96 ± 11.15 mg) than under LDI (27.18 ± 6.84 mg). In the LDI set-up, biomass production was significantly higher under both ornamental white lights (29.02 ± 8.48 mg under cool white and 32.01 ± 5.95 mg under warm white) than under no light at night (22.41 ± 5.18 mg). There was no difference in biomass production under the amber + green light (25.26 ± 3.30 mg) and the no light and the cool white light conditions. In the HDI set-up, no light and exposure to cool white light yielded significantly more wet biomass (63.09 ± 11.16 mg and 65,90 ± 10.46 mg, respectively) than exposure to warm white and amber + green lights (53.58 ± 7.18 mg and 53.42 ± 10.77 mg, respectively).

3.2. Species diversity

The taxonomic identification by examination of morphological characters of the inoculum of phototrophs mainly revealed the presence of green algae, such as *Chlorella vulgaris* Beijerinck (44.14 %), *Klebsormidium flaccidum* (Kützing) P.C. Silva, Mattox & W.H. Blackwell (19.99 %) and some *Chlamydomonas* spp. (2.63 %), *Coelastrella terrestris* (Reisigl) Hegewald & N. Hanagata (2.02 %), *Ettlia* sp. (2.71 %), *Monoraphidium obtusum* (Korshikov) Komárková-Legnerová (1.81 %), *Scenedesmus* sp. (4.56 %) and *Tetradesmus obliquus* (Turpin) M.J. Wynne (2.63 %). There was also a notable presence of cyanobacteria belonging to *Synechocystis* spp. 17.66 %) and some *Pseudoanabaena* spp. (1.84 %). Light-triggered changes in the relative abundance of the species in the SABs formed under the combination of daylight and artificial light at night are shown in Table 1. The three ornamental LED lighting conditions yielded minimal changes in the relative abundance of the species in the SABs relative to no light (control). Significant differences were only observed in the LDI set-up, with warm white and amber + green lights affecting green algae and by cool white light affecting cyanobacteria. *Chlorella vulgaris*, the most abundant species in the SABs comprising around 50 % of the specifical abundance, was not affected by the ornamental lights, but was two times more abundant in the HDI set-up (23.68 %) than in the LDI set-up (10.88 %). Under LDI and compared with no light, the proportion of *Klebsormidium flaccidum* significantly decreased from 14.61 % to 6.09 % under warm white light and to 8.82 % under amber + green light Moreover, generally decreased from LDI to HDI between 3.27 % and 13.58 % depending on the ornamental light applied. The relative abundance of *Ettlia* sp. also differed significantly, between the no light condition (1.31 %) and the (amber + green light condition (3.26 %). The relative abundance of *Monoraphidium obtusum* and of *Coelastrella terrestris* increased significantly from respectively 0.72 % and 0.51 % (no light) to 2.15 % and 2.34 % (warm white light). The relative

Table 1
Relative abundance (in %) of the different species detected in the subaerial biofilms (SABs) under combined low and high daylight illuminance (LDI and HDI) and ornamental LED lighting conditions (no light, cool white, warm white and amber + green lights). Statistically significant differences (at $p < 0.05$) relative to the control (no light) are indicated by (*).

Species	Daylight	No light		Cool white		Warm white		Amber + green	
		Mean	SD	Mean	SD	Mean	SD	Mean	SD
Chlorella vulgaris	LDI	52.40	12.33	55.91	7.47	47.05	8.11	43.60	5.40
	HDI	63.80	9.47	66.78	6.67	63.53	7.48	67.28	0.82
Klebsormidium flaccidum	LDI	14.61	1.58	16.08	0.17	6.09*	1.54	8.82*	5.69
	HDI	2.60	1.65	2.50	0.70	3.49	0.67	5.55	2.60
Scenedesmus spp.	LDI	1.80	0.75	3.49	1.91	2.88	1.24	3.05	1.00
	HDI	1.95	0.80	2.00	0.01	1.82	1.56	2.22	1.10
Ettlia spp.	LDI	1.31	2.27	0.76	0.39	1.74	0.42	3.26*	0.29
	HDI	1.54	0.33	0.69	0.70	1.23	0.37	1.39	0.04
Tetradesmus obliquus	LDI	0.79	0.43	2.82	2.34	2.36	0.82	2.63	1.63
	HDI	0.98	0.92	1.17	0.21	1.37	0.87	1.33	0.63
Monoraphidium obtusum	LDI	0.72	0.06	1.08	0.70	2.15*	0.70	1.81	0.58
	HDI	1.07	0.54	1.03	0.03	1.94	0.42	1.05	0.30
Coelastrella terrestris	LDI	0.51	0.88	1.01	0.66	2.34*	1.22	1.69	0.66
	HDI	1.46	0.71	0.66	0.59	1.87	0.43	1.65	0.84
Chlamydomonas spp.	LDI	0.49	0.32	0.79	0.15	0.71	0.40	0.77	0.79
	HDI	0.73	0.37	0.77	0.52	1.26	0.71	0.77	0.18
Synechocystis spp.	LDI	27.39	6.74	16.51*	2.41	33.53	5.91	33.89	1.51
	HDI	25.77	11.85	24.37	9.01	23.43	5.62	18.69	1.45
Pseudoanabaena sp.	LDI	<0.01	0.00	1.56*	1.13	1.16	0.13	0.47	0.50
	HDI	0.11	0.11	0.03	0.05	0.07	0.07	0.08	0.04

abundance of *Synechocystis* spp. differed significantly between the no light (27.39 %) and cool white light (16.51 %) conditions. The presence of *Pseudoanabaena* sp. was almost negligible in the unlit control, but the relative abundance was significantly higher under cool white light (1.56 %).

3.3. Biochemical profile and confocal microscopy

Fig. 3 presents the effects of different night-time ornamental light regimes on the contents of chlorophyll *a* (Fig. 3a) and chlorophyll *b* (Fig. 3b), exopolysaccharides (Fig. 3c) and ATP (Fig. 3d).

LDI favoured an increase in chlorophyll *a* (1.51 ± 0.38 mg g^{-1} SAB) while HDI favoured an increase in chlorophyll *b* (1.03 ± 0.27 mg g^{-1} SAB). In the LDI set-up, the warm white light caused a significant reduction in chlorophyll *a* (1.12 ± 0.11 mg g^{-1} SAB) relative to the no light control (1.84 ± 0.50 mg g^{-1} SAB). There were no significant differences in chlorophyll *a* concentration in the HDI scenario, despite the increase observed under the warm white and amber + green lights. Similarly, there were no significant differences in chlorophyll *b* concentrations between the ornamental lights in either of the two daylight conditions.

The protein content in the EPS was below 5 μg mL^{-1} in all of the samples analysed. Thus, reliable quantification was not possible with the technique used due to the low protein content of the matrix. Thus, the analysis focused exclusively on the exopolysaccharide fraction of the EPS.

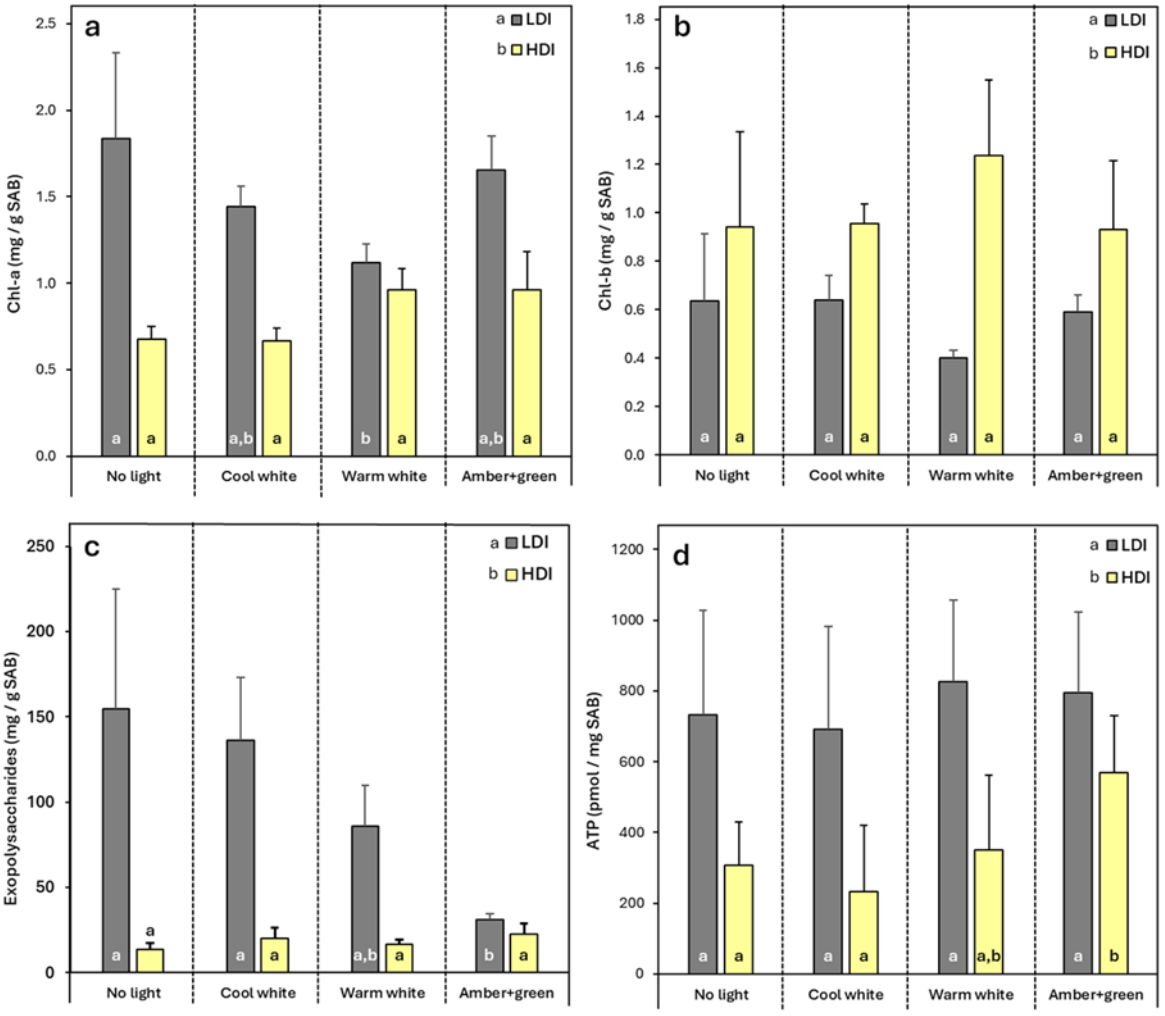

Fig. 3. Biochemical profile of subaerial biofilms (SABs) under the different ornamental lighting conditions: a) Chlorophyll *a* content (mg g^{-1} SAB), b) Chlorophyll *b* content (mg g^{-1} SAB), c) exopolysaccharide content (mg g^{-1} SAB) and d) ATP content (pmol μg^{-1} SAB). Bars indicate mean values and lines represent SD. Different letters indicate significant differences in relation to ornamental illumination and the daylight scenario (LDI: Low Daylight Illuminance; HDI: High Daylight Illuminance).

The exopolysaccharide content was significantly lower in the HDI set-up (18.35 ± 5.52 mg mg^{-1} SAB) than in the LDI set-up (101.89 ± 59.73 mg mg^{-1} SAB). In LDI a reduction in exopolysaccharides was detected under warm white (85.71 ± 24.08 mg EPS mg^{-1} SAB) and amber + green (31.34 ± 3.17 mg mg^{-1} SAB) lights, with the latter being significantly lower than in the no light control (154.46 ± 70.83 mg mg^{-1} SAB). In the HDI set-up, there were no significant differences between the light conditions tested.

Finally, the ATP content was significantly higher under HDI (467.24 ± 216.56 pmol ATP mg^{-1} SAB) than under LDI (270.90 ± 155.25 pmol ATP mg^{-1} SAB), in which no significant differences were detected. Under HDI, the amber + green light (569.23 ± 161.53 pmol ATP mg^{-1} SAB) increased the ATP concentration significantly, relative to the no light control (307.45 ± 122.77 pmol ATP mg^{-1} SAB).

The average contents of polysaccharides, extracellular proteins and chlorophyll in the confocal microscopy images, as well as the cell count per μm^2 and the average cell size, are shown in Fig. 4. Ornamental lighting conditions caused significant differences in all parameters examined by confocal microscopy in the LDI scenario but not in the HDI scenario.

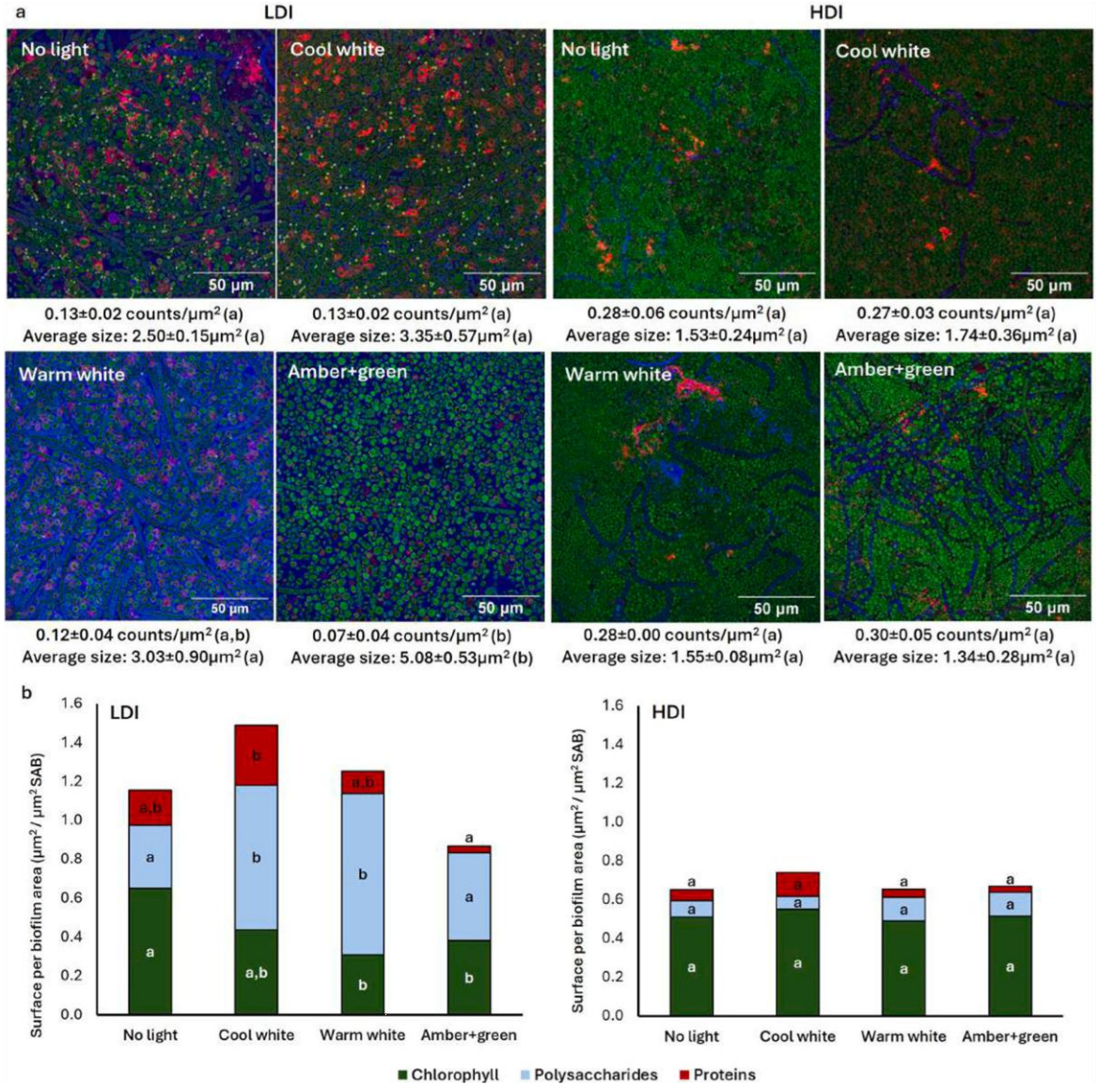

Fig. 4. a) Confocal microscope images of subaerial biofilms (SABs) under the different ornamental lighting conditions (green indicates chlorophylls; blue indicates polysaccharides; and red. indicates proteins). b) Surface area occupied by each component in the images of the SAB captured by confocal microscopy. Different letters indicate significant differences relative to ornamental illumination for the same daylight illuminance (LDI: low daylight illuminance; HDI: high daylight illuminance).

In the LDI set-up, the algal cells were more separated, with a lower cell density per μm^2 (0.07–0.13 counts μm^{-2}) than in the HDI set-up (0.27–0.30 counts μm^{-2}). Considering the differences between the ornamental lighting conditions in LDI, there was a significant reduction in cell counts per surface area under the amber + green light (0.07 ± 0.04 counts μm^{-2}) than in the no light control (0.13 ± 0.02 counts μm^{-2}). In terms of mean average cell size in the LDI scenario, amber + green light produced a significantly greater increase in average cell size (5.08 ± 0.53 μm^2) than both white lights (3.35 ± 0.57 μm^2, cool white and 3.03 ± 0.90 μm^2, warm white) and the no light control (2.50 ± 0.15 μm^2). The relative abundance of filamentous algal cells was higher in the LDI set-up than in the HDI set-up (Fig. 4a). According to the taxonomic data, *Klebsormidium flaccidum* was the only filamentous alga present in the SABs. Remains of membranes and walls (indicating polysaccharides) without chlorophyll were observed in the HDI set-up, following the reduction in the relative abundance of this species in the SAB observed in the taxonomic analysis (Table 1).

The polysaccharide content was lower in the HDI set-up (0.10 ± 0.02 μm^2 μm^{-2} SAB) than in the LDI scenario (0.59 ± 0.24 μm^2 μm^{-2} SAB). In the LDI set-up, the surface area occupied by polysaccharides was higher in the cool white light (0.74 ± 0.30 μm^2 μm^{-2} SAB) and the warm white light (0.83 ± 0.10 μm^2 μm^{-2} SAB) conditions than in the amber + green (0.45 ± 0.25 μm^2 μm^{-2} SAB) light and the no light control (0.32 ± 0.30 μm^2 μm^{-2} SAB) conditions. The ornamental lighting conditions yielded a significant reduction in the quantity of chlorophyll per biofilm surface area in the LDI set-up, relative to the no light control (0.65 ± 0.33 μm^2 μm^{-2} SAB) under the warm white light (0.31 ± 0.14 μm^2 μm^{-2} SAB) and the amber + green light (0.38 ± 0.15 μm^2 μm^{-2} SAB) conditions. Proteins were

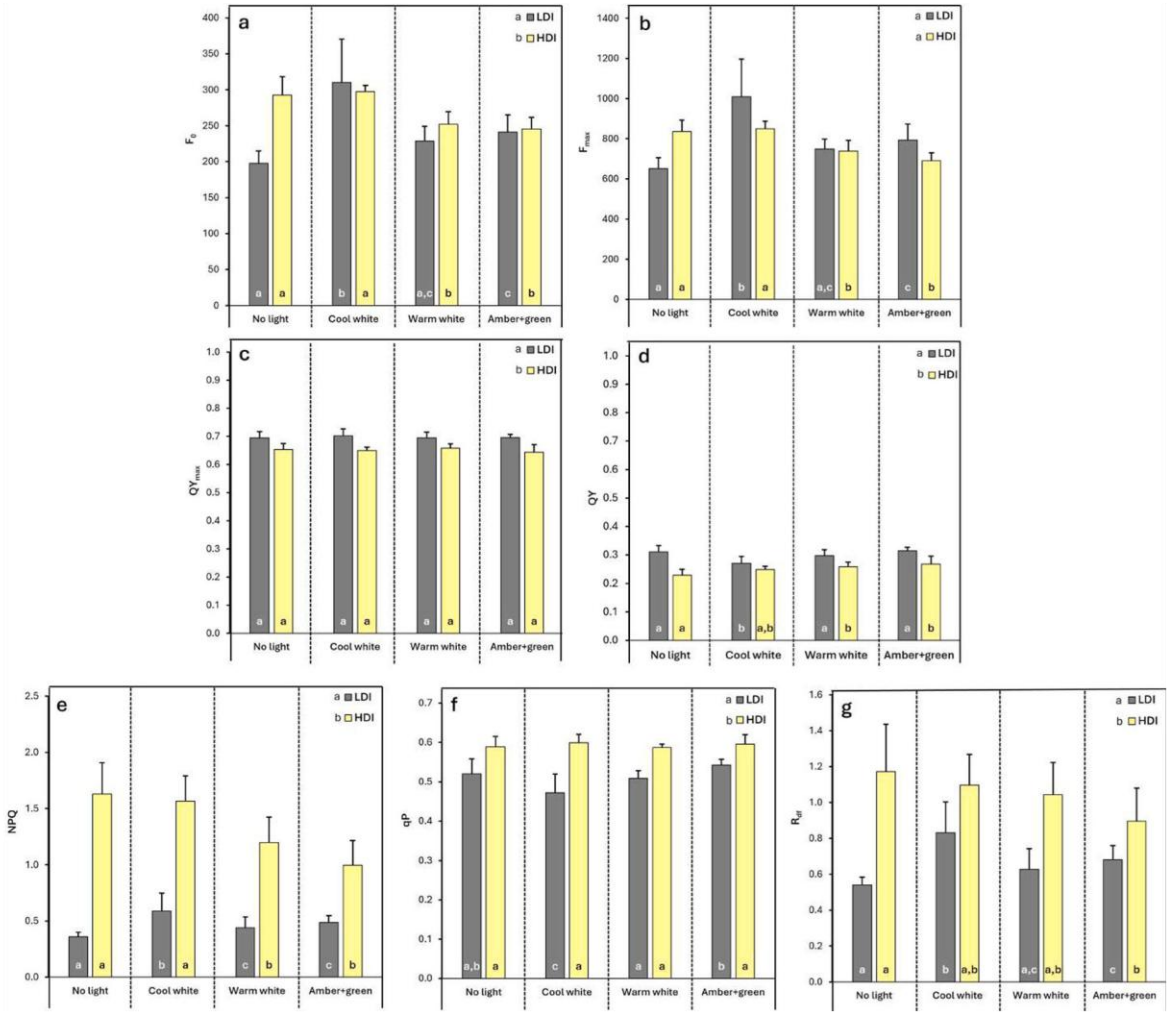

Fig. 5. PAM fluorometry results for analysis of subaerial biofilms (SABs) under the different ornamental lighting conditions: a) minimum fluorescence (F_0), b) maximum fluorescence (F_{max}), c) maximum quantum yield (QY_{max}), d) light-adapted quantum yield (QY), e) non-photochemical quenching (NPQ), f) photochemical quenching (qP), and g) fluorescence decline ratio (R_{df}). Bars indicate mean values and lines represent SD. Different letters indicate significant differences in relation to ornamental illumination and the daylight scenario (LDI: low daylight illuminance; HDI: high daylight illuminance).

significantly more affected by cool white light (0.31 ± 0.26 $\mu m^2\ \mu m^{-2}$ SAB) than by the no light condition (0.18 ± 0.06 $\mu m^2\ \mu m^{-2}$ SAB) in the LDI set-up (Fig. 4b).

3.4. PAM fluometry

The minimum and maximum fluorescence (F_0 and F_{max}) values exhibited a similar pattern to that observed for biomass in both the LDI and HDI conditions (Fig. 5a and b).

In the LDI set-up, all ornamental LED light conditions caused an increase in F_0 and F_{max}, but only the cool white light (310.25 ± 60.40 for F_0 and 1010.44 ± 186.58 for F_m) and the amber + green light (241.25 ± 23.89 for F_0 and 792.93 ± 81.37 for F_m) yielded significant differences relative to the no light control (197.70 ± 17.14 for F_0 and 651.70 ± 53.91 for F_m). No significant differences in QY_{max} were observed for the illumination conditions in either the LDI or HDI set-up (Fig. 5c). However, the average QY_{max} values were significantly higher in the LDI set-up (0.70 ± 0.02) than in the HDI set-up (0.65 ± 0.01). The light-adapted quantum yield (QY) was significantly lower under the cool white light (0.27 ± 0.03) than in the no light control (0.31 ± 0.02) in the LDI set-up. In the HDI set-up, the QY was higher in both the warm white (0.26 ± 0.02) and the amber + green light (0.27 ± 0.03) conditions than under the no light condition (0.23 ± 0.02).

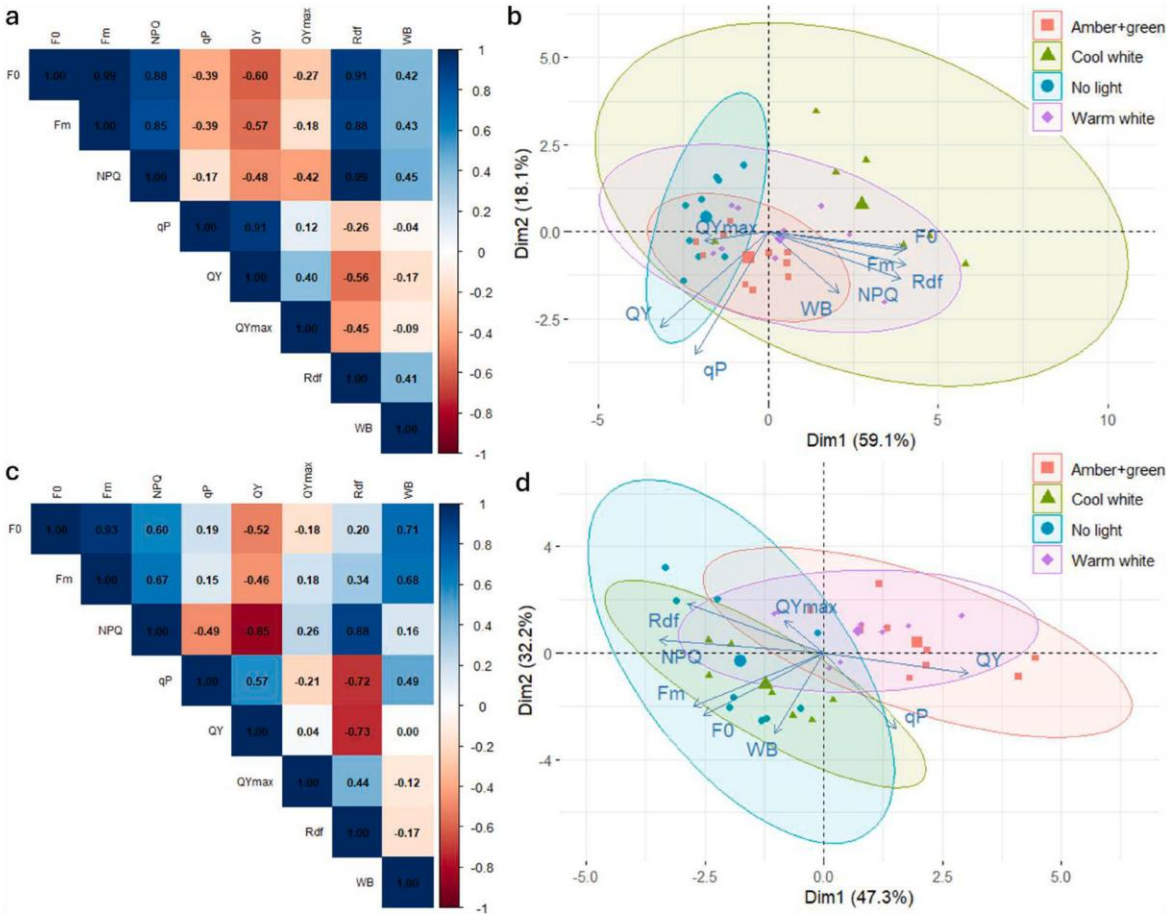

Fig. 6. a) Correlation matrix according to Pearson's test for the PAM fluorometry variables and the wet biomass (WB) of subaerial biofilms (SABs) under the different ornamental lighting conditions in the low daylight illuminance (LDI) set-up, b) Principal Component Analysis (PCA) plot for the PAM fluorometry variables and the wet biomass (WB) of subaerial biofilms (SABs) under the different ornamental lighting conditions in the low daylight illuminance (LDI) set-up, c) Correlation matrix according to Pearson's test for the PAM fluorometry variables and the wet biomass (WB) of subaerial biofilms (SABs) under the different ornamental lighting conditions in the high daylight illuminance (HDI) set-up and d) Principal Component Analysis (PCA) plot for the PAM fluorometry variables and the wet biomass (WB) of subaerial biofilms (SABs) under the different ornamental lighting conditions in the high daylight illuminance (HDI) set-up. The symbols indicate the position of each sample within the plot (large symbols indicate each centroids). Coloured ellipses are based on the centroids for each ornamental lighting condition. The arrows indicate the variables used for the PCA.

The non-photochemical quenching (NPQ) (Fig. 5d) was significantly higher in the LDI set-up with the cool white light (0.59 ± 0.16) and the amber + green light (0.49 ± 0.06) than in the no light control condition (0.36 ± 0.04). In the HDI set-up, the NPQ was significantly lower in the warm white light condition (1.20 ± 0.23) and the amber + green light (1.00 ± 0.22) condition than in the control condition. NQP was significantly higher in the HDI set-up (1.33 ± 0.35) than in the LDI set-up (0.47 ± 0.13).

The photochemical quenching coefficient (qP) was also higher in the HDI set-up (0.59 ± 0.02), in which no differences were found between conditions, than in the LDI set-up (0.51 ± 0.04) in which only the cool white light (0.47 ± 0.05) caused a significant reduction (Fig. 5e). Finally, the fluorescence decline ratio (R_{df}) (Fig. 5f) was significantly higher in the HDI set-up (1.05 ± 0.22) than in the LDI set-up (0.67 ± 0.15). In the LDI set-up, the R_{df} was higher in the cool white light (0.83 ± 0.04) and the amber + green light (0.68 ± 0.12) conditions than in the control condition. In the HDI set-up, only the amber + green light (0.90 ± 0.18) reduced the R_{df} relative to the no light control (1.17 ± 0.26).

A Pearson correlation matrix was constructed (Fig. 6a and c) and principal Component Analysis (PCA) (Fig. 6b and d) was conducted to examine the relationships between the wet biomass (WB) and the PAM fluorometry parameters.

The correlation matrix shows that wet biomass was positively correlated with F_0 (r = 0.42 in LDI and r = 0.71 in HDI) and F_m (r = 0.43 in LDI and r = 0.68 in HDI) in both daylight set-ups, although that correlation was stronger for HDI than for LDI. There was also a positive correlation between wet biomass and NPQ (r = 0.45) and R_{df} (r = 0.41) in the LDI set-up, but the correlation was weaker in the HDI set-up for NPQ (r = 0.16) and was negative for R_{df} (r = −0.17). qP and QY were negatively correlated with NPQ and R_{df} in both the LDI and HDI set-ups. qP was also negatively correlated with F_0 and F_m in LDI (r = −0.39), but the correlation was positive in HDI (r = 0.19 for F_0 and r = 0.15 for F_m). This was also observed with the correlation between QY_{max} and NPQ and R_{df}, which was negative in LDI (r = −0.42 for NPQ and r = −0.45 for R_{df}) and changed to positive in the HDI set-up (r = 0.26 for NPQ and r = 0.44 for R_{df}). Finally, Rfd was strongly and positively correlated with NPQ in both LDI (r = 0.99) and HDI (r = 0.88), and the relationship with WB was positive in LDI (r = 0.41) but negative in HDI (r = −0.17).

The first two dimensions of the PCA (Dim1 and Dim2) explained 77.2 % of the variance in the data in the LDI set-up (Dim1 = 59.1 % and Dim2 = 18.1 %) (Figs. 6b) and 79.5 % of the variance in the HDI set-up (Dim1 = 47.3 % and Dim2 = 32.2 %) (Fig. 6d). In the LDI set-up, the Dim2 mainly explained the no light control, whereas the Dim1 displacing the SABs subjected to ornamental lightning away from the control SABs, with F_0, F_m, NPQ, R_{fd} and WB being the main parameters causing the displacement. The PCA shows that in the LDI set-up the SABs subjected to amber + green ornamental lighting were more similar to the no light control, followed by the warm white light and the cool white light. However, in the HDI set-up, the PCA showed that the SABs under amber + green light were the most displaced from the no light control and the SABs under cool white light the most similar. For both warm white and amber + green lights, the Dim1 mainly explained the variance, with the QY parameter being the most important causing the displacement from the control. The SABs under amber + green light appear on opposing axes in the PCAs to the F_0, F_m, NPQ, R_{fd} and WB parameters in both the LDI and HDI conditions.

4. Discussion

4.1. Biofilm growth

Ornamental illumination of architectural heritage artificially increases the time that phototrophic colonisers are exposed to light and carry out photosynthesis. However, most of the literature regarding changes derived from different lighting regimes has focused on algal bioreactors.

In the present study, the use of both cool and warm white lights increased the wet biomass in the LDI set-up (Fig. 2a). A study by Ref. [50] investigating the effects of photoperiod duration under low light conditions (50 μmol s^{-1} m^{-2}, comparable to the LDI condition), revealed a gradual increase in the density of *Nannochloropsis* spp. cells as the photoperiod was increased from a 12:12 h light-dark cycle to an 18:6 h cycle, with a maximum observed under continuous illumination (24:0 h cycle). However, under higher light intensity (200 μmol s^{-1} m^{-2}, similar to the HDI condition), although the cell density was generally higher than at low light intensity (below 50 μmol s^{-1} m^{-2}), there were no significant differences between the 12:12 h and 18:6 h cycles, and continuous illumination caused a reduction in cell density. Similar findings to those observed in planktonic cultures (in bioreactors) have also been reported for biofilms [51]. found that the biomass of algal biofilms of *Chlorella vulgaris* was slightly but significantly higher under continuous illumination than under a 12:12 h cycle.

Nevertheless, it is not known whether variations in daylight illuminance interfere with the capacity of night-time lighting systems to generate the light-related stress that affects the growth and development of organisms. The use of amber + green light did not enhance wet biomass production of the SABs in the LDI, unlike the cool and warm white lights tested. Moreover, in the HDI set-up the amber + green light resulted in a reduction in both wet biomass of the SABs (Fig. 2), suggesting a potential biostatic effect at both levels of sunlight intensity. Light in the 500–600 nm range (green to yellow/amber) is conventionally regarded as less efficient for photosynthesis, as it results in lower CO_2 assimilation per mole of photons than wavelengths in the 450–500 nm (blue) and 600–750 nm (orange to red) ranges. This is consistent with the peak absorption spectra of chlorophyll, in which blue and red light are most effectively used for photosynthetic activity (see e.g.[52]). Cultures of *Chlorella vulgaris* grown in a column bioreactor under continuous monochromatic illumination (500–2000 lx) exhibited lower specific growth rates and cell concentrations when exposed to green light (510–540 nm) than when exposed to red (650–680 nm) or blue (440–470 nm) light [53] Similar findings were reported by [54], in a study in which the dry mass density of *Chlorella vulgaris* cultures subjected to continuous monochromatic light (150 μmol s^{-1} m^{-2}) was lower after exposure to yellow (590 nm) and green (525 nm) light than after exposure to blue (467 nm), red (625 nm) and white light.

Although warm light produced similar positive results to amber + green light in the HDI in terms of biomass, warm white light

yielded the greatest amount of wet biomass in the LDI (Fig. 2a). These inconsistencies between the two types of daylight illuminance may hinder the potential use of warm white light to reduce the development of SABs [55] demonstrated that higher cell density was reached in *Chlorella vulgaris* cultures grown under warm white light with an 18:8 h photoperiod than in those exposed to cooler white light, regardless of the light intensity (50, 80, or 110 μmol s^{-1} m^{-2}). However [56], reported no significant difference in dry density of *Chlorella vulgaris* cultures grown under cool white (6500K) and warm white (3200K) light at an intensity of 50 μmol s^{-1} m^{-2}. The findings suggest that the effects of white light spectra on microalgal growth are influenced by other culture conditions beyond light quality alone.

The phototrophic community within the SABs underwent changes in response to both sunlight intensity and the spectral characteristics of the ornamental lighting applied in the experiment. Biofouling tends to be more prevalent on north- and west-facing facades, which in the Atlantic region are typically more shaded and humid [57] Additionally, the diversity of colonising species is generally higher on surfaces that receive less direct sunlight, whether due to orientation or external shading [58]. In the present study, humidity was not a limiting factor, as culture on the agar plates ensured continuous water availability. Consequently, higher solar irradiation resulted in increased biomass production (Fig. 2a), contrary to expectations for facades exposed to strong insolation. This also applies to species diversity, given that the system is closed, and the species composition remained unchanged, with only the relative abundance varying under different light regimes.

4.2. Species diversity

The most abundant species in the SABs generated were *Chlorella vulgaris* (Chlorophyta), *Klebsormidium flaccidum* (Charophyta) and *Synechocystis* sp. (Cyanobacteriota) (Table 1). *Chlorella vulgaris*, a coccoid unicellular green alga, is one of the most important initial pioneering species [60] and it is found in Galicia (NW Spain) in heritage constructions built in granite ([61,62]), in limestone buildings in France [63], in marble fountains in Bratislava [64] and even on architectural concrete ([65,66]). The filamentous green alga *Klebsormidium flaccidum* is commonly associated with mineral substrates on building facades [59]. This cosmopolitan species is found across various lithotypes [67] and it has specifically been reported on granite buildings in Galicia (NW Spain) [68] and as endolithic growth in the granite masonry of the Ordem de São Francisco Church in Porto (Portugal) ([69,70]. In Europe, members of the phylum Cyanobacteriota are generally less abundant than green algae in phototrophic biofilms [71]. However, the genus *Synechocystis* has been detected on various lithic substrates, including travertine in Italy [72], calcareous substrates such as mortar or limestone [73] and in granite in Portugal [69].

Chlorella vulgaris was much less abundant in the LDI set-up (50.07 μmol s^{-1} m^{-2}) than in the HDI set-up (252.59 μmol s^{-1} m^{-2}), with the biomass increasing by between 10.88 % and 23.68 % depending on the ornamental lighting condition (Table 1). In a closed bioreactor, *Chlorella vulgaris* increased its growth rate consistently between 130 and 520 μmol s^{-1} m^{-2} [74], revealing the capacity of this species to thrive under higher insolation. By contrast, the presence of *Klebsormidium flaccidum* was found to be lower in the HDI than in the LDI set-up [75]. showed that the growth rate of the related species *Klebsormidium dissectum* was maximum at 30 μmol s^{-1} m^{-2} and then declined when the light intensity was increased to 120 μmol s^{-1} m^{-2}. Although *K. flaccidum* seems to prefer lower light intensity similar to that in shaded areas of facades, the presence of ornamental warm white and amber + green ornamental lighting caused a decrease in abundance of the species in the LDI set-up (Table 1). As a member of the streptophyte clade (a monophyletic group encompassing terrestrial plants and charophyte algae) the response of *Klebsormidium* spp. to variations in light spectra is expected to differ from that of the other microalgae and may exhibit similarities to higher plants. Members of the *Klebsormidium* genus possess blue-sensitive phototropins (photoreceptor proteins involved in phototropic responses) that are more closely related to those found in higher plants than to those found in other green algae [76]. Algal phototropins appear to regulate fewer key physiological functions than their plant counterparts [77]. This distinction may be particularly important when considering the different contribution of blue wavelengths under the various ornamental lighting conditions tested.

The reduction in *Klebsormidium flaccidum* by warm white and amber + green light in the LDI scenario is particularly interesting from a conservation standpoint, considering the capacity of the filaments for endolithic growth ([69,78]) filling cracks in the substrate which could become source mechanical stress resulting in the loss of cohesion, rupture or disintegration by mechanical pressure ([50, 79]).

Nonetheless, some green algal species can utilize the amber + green light more effectively than others for growth. Although not one of the predominant species in the SABs, the relative abundance of *Ettlia* sp. increased by 1.96 % under amber + green light conditions, relative the no light control in the LDI scenario [80]. showed that members of the genus *Ettlia* can grow effectively under continuous monochromatic green LED light, yielding the same biomass as when grown under monochromatic blue or red lights and outcompeting *Chlorella vulgaris* when present in mixed cultures. While species of the genus *Ettlia* are primarily associated with soil environments, they have also been detected on monuments and stone walls, albeit in low abundance (see e.g. Refs. [34,62,81]).

The abundance of cyanobacteria in the SABs was not affected by exposure to the amber + green light, although previous studies showed higher DNA counts [47] and peptides of cyanobacterial origin in phototrophic biofilms exposed to amber + green light than in films exposure to other white lights [34]. [82] suggested that nocturnal green lighting used to illuminate the stone walls of a millennial mausoleum in Shaanxi (China) affected the biodeterioration caused by metabolic activity of cyanobacteria, by reducing the production of lactic and citric acids. Cyanobacteriota have accessory pigments such as phycocyanins and phycoerythrins that absorb light at 610–625 nm and 490–570 nm [27]. Cyanobacteria possessing these pigments are more likely to be found on the surfaces of caves illuminated by warm light (which usually peaks around 600 nm due to the low blue component) [83]. However, in the present study no significant changes in cyanobacterial abundance were observed in areas exposed to warm light. Instead, a reduction in the abundance of *Synechocystis* sp. was noted under cool white light. This finding is consistent with previous research demonstrating that blue light

can have an inhibitory effect on *Synechocystis* sp. PCC 6803 [84], which is particularly relevant given that the cool white light used in this study peaked at 457 nm.

4.3. Biochemical profile and confocal microscopy

The biochemical profile of the SABs was influenced by ornamental lighting in the LDI set-up. However, no significant alterations were observed in the HDI set-up (Fig. 3), suggesting that the increased solar intensity during the day had a greater effect than any biochemical changes induced by nocturnal ornamental lighting. The chlorophyll *a* content of the SABs was reduced by ornamental lighting in the LDI set-up, whereas chlorophyll *b* remained unchanged. However, the reduction in chlorophyll *a* in the LDI set-up was only statistically significant for the warm white light condition. In a study involving *Nannochloropsis* sp. cultures, the chlorophyll *a* content decreased when the proportion of red wavelengths to blue wavelengths was increased [85]. The increase in the proportion of red light would cause a decrease in the CCT, thus resulting in a warmer white light.

In the previously mentioned study [56] cultures of *Chlorella vulgaris* produced more chlorophyll *a* than chlorophyll *b*, regardless of light quality or light intensity. The present findings show that under higher solar irradiance (HDI set-up), the concentration of chlorophyll *a* is reduced (Fig. 3a) but the concentration of chlorophyll *b* increases (Fig. 3b), regardless of the impact of ornamental lighting.

EPS production tends to be higher on sunny surfaces that on shaded surfaces, to protect cells from adverse conditions (see e.g. Refs. [24,86]) [87]. reported that the cyanobacteria *Microcoleus vaginatus* produced more EPS (in the form of polysaccharides) in a culture when the light intensity was increased from 4 to 80 μmol s^{-1} m-2. However, in a culture of the green alga *Dictyosphaerium chlorelloides* EPS production increased with light intensity at between 11.9 and 50.3 μmol s^{-1} m^{-2} (at the same light intensity as the LDI set-up) and then decreased at 68.6 μmol s^{-1} m^{-2} [88]. In the present study, the SABs produced a lower amount of exopolysaccharides (both in the direct determination and the confocal images, Figs. 3c and 5b) in the HDI set-up than in the LDI set-up. These findings suggest that higher light intensity may impede exopolysaccharide production, at least under laboratory conditions. The methods used to quantify exopolysaccharides yielded different results in response to ornamental lighting in the LDI scenario. Direct quantification indicated that the highest concentration of polysaccharide occurred in the control group without night-time lighting, with values undistinguishable from those observed under cool and warm white lights (Fig. 3c). Conversely, confocal microscopy analysis revealed that the exopolysaccharide concentration was higher under these two lighting conditions, than in the control, in which exopolysaccharide levels were lowest (Fig. 5b). This discrepancy may be attributed to variations in the spatial distribution of exopolysaccharides within the biofilm matrix, which exhibits some heterogeneity across three dimensions [89], as confocal microscopy measures polysaccharides in a specific area and depth whereas the direct determination quantifies the total amount in the SAB. The amber + green ornamental lighting condition produced a consistent response across both quantification methods, with exopolysaccharide production remaining low, both in direct determination (compared to the no-light control and the two white light conditions, Fig. 3c) and in confocal microscopy (relative to the two white lights and similar to the no-light control, Fig. 4b).

Confocal imaging analysis also revealed that extracellular protein levels were lowest under amber + green lighting. Light wavelength is known to modulate extracellular protein production, as demonstrated in previous studies in which exposure to red (630–675 nm) and in particular to blue (460–475 nm) light led to greater accumulation of both intracellular and extracellular proteins than exposure to white light in multi-species algal-bacterial consortia [90]. Similarly, in the present study, the higher proportion of blue wavelengths in the ornamental cool white light was associated with an increased proportion of extracellular proteins under the test conditions. The low levels of extracellular protein produced under the amber + green ornamental lights may be an important factor in controlling the colonization of the architectural heritage. Indeed [91], reported that the protein secreted by the green alga *Botryococcus braunii* accounted for strong adhesion of the cells to glass fibre, and the same protein has been reported to increase hydrophobicity in algal biofilms by cation bonding ([92,93]).

Although the biochemical profile was not affected by the ornamental lights tested in the HDI set-up, the amber + green light increased the ATP content of the SABs relative to the other ornamental lighting conditions (Fig. 3d). This can be tentatively attributed to the fact that light-induced stress at amber + green wavelengths is unable to efficiently drive photosynthesis at night-time. ATP is necessary to maintain proteostasis, fuelling protein synthesis and repair [94], and the increase in ATP content could therefore indicate an increase in protein metabolism. Indeed, previous studies investigated the effect of ornamental lighting in the proteome of SABs and found that exposure to amber + green light increased protein metabolism and even increased heat shock proteins HSP70 and HSP90, which is a sign of oxidative stress [34].

4.4. PAM fluorometry

PAM fluorometry was conducted in this study to examine changes in light use by SABs under nocturnal lighting. The correlation matrix (Fig. 6a and c) revealed a positive correlation between the wet biomass (Fig. 2) of SABs and both minimum (F_0) (Fig. 5a) and maximum (F_m) (Fig. 5b) fluorescence, with the relationship becoming strengthened in the HDI relative to the LDI condition. This suggests that under LDI, ornamental lighting exerts a greater influence on the direct correlation between biomass and fluorescence. This may have a stronger impact on biofilm physiology, consistent with the observed biochemical profile changes (Figs. 3 and 4). Measuring F_0 (as well as F_m) is sometimes considered a suitable in situ proxy method of estimating algal biomass (see e.g Ref. [95]., although the reliability of the method can be affected by external factors [96] such as, in this case, ornamental lighting.

The PCA plots (Fig. 6b and) revealed that the use amber + green light for ornamental illumination shifted the SABs in LDI opposing the F_0, F_m, NPQ and R_{df} parameters, driving the SABs under cool and warm white light to deviate from the control SABs. In the LDI set-

up, the F_0 was higher under amber + green than under warm white light, despite the lower amount of biomass produced (Fig. 2). It has been shown that F_0 increases at sub-optimal conditions [97], which supports the potential of amber + green as a biostatic light. In the PCA of the HDI set-up, the F_0, F_m, NPQ and R_{df} parameters were on opposing axes to the SABs under amber + green light but were more scattered along the y-axis (Dim2). Thus, the effect of the ornamental lighting at night loses strength against the higher solar irradiance during the day.

The quantum yield of the SABs was lower in the HDI set-up than in the LDI set-up, indicating the efficiency with which absorbed light is capable of driving photochemistry in both the maximum and light adapted photosystem II (PSII). Similarly [95], reported that maximum quantum yield in microphytobenthos was negatively correlated with ambient irradiance ranging from 200 to 1000 μmol s^{-1} m^{-2}. However, the ornamental lighting conditions did not modify the QY_{max} (Fig. 5c) following the conclusions of [98] who deemed that QY_{max} was not a wavelength-dependent parameter (between 440 and 625 nm) in a natural phytoplankton community. However, under the amber + green light, the light adapted quantum yield (QY) was higher in both daylight scenarios than in the no light control. Cultivation of *Dunaliella bardawil* under monochromatic red and blue light affected the QY_{max} and QY of cultures relative to cultivation under white light, indicating that changes in from a white light spectra can cause an increase in quantum yield. Moreover [99], found that green light can penetrate deeper into higher plant leaves that blue or red light in strong white light, thus increasing leaf photosynthesis to a greater extent. SABs consist of a structured community of cells that can reach a considerable thickness, particularly when grown in the laboratory. For example [100], produced biofilms of *Chlorella sorokiniana* of thickness up to 847 μm. Thus, mechanisms such as that occurring in leaves (see Ref. [101]) may explain the higher QY after exposure to daylight observed under amber + green light (Fig. 5d) despite the lower biomass yield.

In the non-photochemical quenching (NPQ) mechanism, the excessive excitation energy that cannot be used for photosynthesis is dissipated as heat [102]. The NPQ was higher in the HDI set-up than in the LDI set-up for all the ornamental light conditions tested (Fig. 5e). Indeed, increases in non-photochemical quenching has been observed on increasing the irradiance from 0 to 400 μmol s^{-1} m^{-2} [103] and from 50 to 2000 μmol s^{-1} m^{-2} [104] in several green macroalga species. Contrary to NPQ, photochemical quenching (qP) is proportional to the photon energy captured by open PSII reaction centres and dissipated via photosynthetic electron transport [105]. The qP tends to decrease when photosynthesis is saturated, as shown by Ref. [106] in cultures of the microalga *Koliella antarctica* from 0 to 1000 μmol s^{-1} m^{-2}. However, in the present study, the qP was higher in the SABs formed in the HDI set-up than in the LDI set-up (Fig. 5f), possibly indicating that the photosynthetic machinery of the SABs was not saturated at the levels of daylight irradiance tested.

Finally, parameter R_{df}, also termed the "vitality index", is considered a good measure of stress effects on the PSII [107]. The R_{df} was higher in the SABs formed in the HDI scenario than in those formed in the LDI set-up, further indicating that the HDI irradiance did not lead to saturation or photoinhibition. In the LDI set-up, the use of ornamental lighting increased the R_{df}, particularly under cool white light. However, the use of amber + green light caused a significant reduction in R_{df} relative to the no light control and the other ornamental lighting conditions tested (Fig. 5g). To the best of our knowledge, light intensity and light quality have not been shown to affect the vitality of green algae. [108] showed that the cyanobacteria *Anabaena* CPB4337 and the green alga *P. subcapitata* (grown at an irradiance of 65 μmol s^{-1} m^{-2}) suffered a decrease in R_{df}, indicating signs of stress, when subjected to high concentrations of CeO_2 nanoparticles. Similarly to the present study, the decrease in R_{df} was followed by a decrease in NPQ, and both parameters were positively correlated.

5. Conclusions

The use of nocturnal ornamental illumination has been proposed as a potential biostatic strategy to manage phototrophic colonization on architectural heritage. However, the extent to which variations in daylight illuminance modulate the efficacy of nocturnal lighting in inducing light-related stress responses that influence the growth and development of phototrophic organisms remains unknown.

In the LDI set-up, exposure to both types of white light increased biomass production in the SABs, whereas exposure to amber + green light did not cause any difference in biomass production relative to the no light control. In the HDI set-up, the biomass of the SABs was lower in both the warm white light and the amber + green light conditions than in the cool white light and the no light conditions. The distribution of the species within the SAB were different in the LDI and HDI conditions, but the ornamental lighting barely altered the species composition. The relative abundance of *Chlorella vulgaris* increased under all ornamental lighting conditions in the HDI set-up. The relative abundance of *K. flaccidum* was lower in the HDI than in the LDI set-up; in the LDI set-up, the relative abundance was lower after exposure to warm white and the amber + green lights than after exposure to the other ornamental lighting conditions.

Nocturnal ornamental illumination did not alter the biochemical profile (in terms of contents of chlorophyll, exopolysaccharides and extracellular proteins) in the HDI set-up. However, in the LDI set-up, exposure to amber + green light reduced the exopolysaccharide content in the extracellular matrix, detected by both direct quantification and confocal microscopy. Confocal microscopy analysis also revealed that exposure to the amber + green ornamental light reduced the extracellular proteins compared to the white lights tested.

Analysis of the samples by PAM fluorometry showed that the effect of the ornamental lighting conditions was weaker under the higher solar irradiance in the HDI than in the LDI set-up. The HDI also yielded a decrease in the quantum yield of the SABs under all ornamental lighting conditions. Finally, the vitality of the SABs was reduced after exposure to amber + green light in the HDI set-up.

The biostatic capacity of amber + green light was validated in both LDI and HDI scenarios, which is particularly relevant in urban environments with variable solar exposure due to urban morphology or climatic factors. This research could serve to better guide

designers and/or policymakers to adapt ornamental illumination practices towards the preventive conservation of architectural heritage.

Future research should focus on proving the efficacy of the combination of amber and green LED light in terms of the effect on biodeterioration (both physical and chemical) of the substrate. Further studying the specific responses of some species like *Klebsormidium flaccidum* or whether the same principles apply to other organisms causing biodeterioration on architectural heritage, such as lichens and fungi, would also be of interest.

CRediT authorship contribution statement

Anxo Méndez: Writing – review & editing, Writing – original draft, Methodology, Investigation, Formal analysis, Conceptualization. **Rafael Carballeira:** Methodology, Investigation, Formal analysis. **Sabela Balboa:** Supervision, Methodology, Investigation, Formal analysis. **Patricia Sanmartín:** Writing – review & editing, Supervision, Project administration, Methodology, Investigation, Funding acquisition, Formal analysis.

Data accessibility

Data will be made available on request.

Declaration of competing interest

The authors declare the following financial interests/personal relationships which may be considered as potential competing interests:Anxo Mendez reports financial support was provided by Government of Galicia. Patricia Sanmartin reports financial support was provided by Government of Galicia. Sabela Balboa reports financial support was provided by Government of Galicia. Patricia Sanmartin reports financial support was provided by Spain Ministry of Science and Innovation. If there are other authors, they declare that they have no known competing financial interests or personal relationships that could have appeared to influence the work reported in this paper.

Acknowledgements

This study was conducted in the framework of the CROMALUX project: Third SMARTIAGO Challenge – Smart lighting system for Heritage Conservation. A. Méndez acknowledges the Industrial Doctorate grant (04_IN606D_2021_2598528) financed by the Xunta de Galicia. P. Sanmartín acknowledges a Ramón y Cajal contract (RYC2020-029987-I) financed by AEI/MCIU. The authors are also grateful to the Xunta de Galicia for concession of the FONTES project (ED431F 2022/14) and the Competitive Reference Group (GRC) grants ED431C 2022/09 (Gemap: A. Méndez & P. Sanmartín) and ED431C-2021/37 (Biogroup: S. Balboa).

Data availability

Data will be made available on request.

References

[1] D. Robinson, Urban morphology and indicators of radiation availability, Sol. Energy 80 (2006) 1643–1648, https://doi.org/10.1016/j.solener.2006.01.007.
[2] P. Redweik, C. Catita, M. Brito, Solar energy potential on roofs and facades in an urban landscape, Sol. Energy 97 (2013) 332–341, https://doi.org/10.1016/j.solener.2013.08.036.
[3] A. Martínez-Rubio, F. Sanz-Adan, J. Santamaría-Peña, A. Martínez, Evaluating solar irradiance over facades in high building cities, based on LiDAR technology, Appl. Energy 183 (2016) 133–147, https://doi.org/10.1016/j.apenergy.2016.08.163.
[4] R.U. Tanvir, J. Zhang, T. Canter, D. Chen, J. Lu, Z. Hu, Harnessing solar energy using phototrophic microorganisms: a sustainable pathway to bioenergy, biomaterials, and environmental solutions, Renew. Sustain. Energy Rev. 146 (2021) 111181, https://doi.org/10.1016/j.rser.2021.111181.
[5] A.A. Gorbushina, Life on the rocks, Environ. Microbiol. 9 (2007) 1613–1631, https://doi.org/10.1111/j.1462-2920.2007.01301.x.
[6] W.K. Hofbauer, G. Gärtner, Microbial Life on Façades, Springer Berlin Heidelberg, Berlin, Heidelberg, 2021, ISBN 978-3-662-54831-8.
[7] A.W. Larkum, Photosynthesis and light harvesting in algae, in: The Physiology of Microalgae, Springer International Publishing, Cham, 2016, pp. 67–87.
[8] E. Erickson, S. Wakao, K.K. Niyogi, Light stress and photoprotection in *Chlamydomonas reinhardtii*, Plant J. 82 (2015) 449–465, https://doi.org/10.1111/tpj.12825.
[9] M. DeNicola, K.D. Hoagland, Effects of solar spectral irradiance (visible to UV) on a prairie stream epilithic community, J. North Am. Benthol. Soc. 15 (1996) 155–169, https://doi.org/10.2307/1467945.
[10] A.V. Ruban, Nonphotochemical chlorophyll fluorescence quenching: mechanism and effectiveness in protecting plants from photodamage, Plant Physiol 170 (2016) 1903–1916, https://doi.org/10.1104/pp.15.01935.
[11] J.A. Raven, C.S. Cockell, Influence on photosynthesis of starlight, moonlight, planetlight, and light pollution (reflections on photosynthetically active radiation in the universe), Astrobiology 6 (2006) 668–675, https://doi.org/10.1089/ast.2006.6.668.
[12] J. Bennie, T.W. Davies, D. Cruse, K.J. Gaston, Ecological effects of artificial light at night on wild plants, J. Ecol. 104 (2016) 611–620, https://doi.org/10.1111/1365-2745.12551.
[13] C. Gardner, The use and misuse of coloured light in the urban environment, Opt Laser Technol 38 (2006) 366–376, https://doi.org/10.1016/j.optlastec.2005.06.022.
[14] Z. Amini Khoeyi, J. Seyfabadi, Z. Ramezanpour, Effect of light intensity and photoperiod on biomass and fatty acid composition of the microalgae, Chlorella vulgaris, Aquac. Int. 20 (2012) 41–49, https://doi.org/10.1007/s10499-011-9440-1.
[15] M.J. Wynne, J.K. Hallan, Reinstatement of *Tetradesmus* G. M. Smith (sphaeropleales, chlorophyta), Feddes Repert. 126 (2015) 83–86, https://doi.org/10.1002/fedr.201500021.

[16] I. Krzemińska, B. Pawlik-Skowrońska, M. Trzcińska, J. Tys, Influence of photoperiods on the growth rate and biomass productivity of green microalgae, Bioproc. Biosyst. Eng. 37 (2014) 735–741, https://doi.org/10.1007/s00449-013-1044-x.

[17] U. Karsten, S. Lembcke, R. Schumann, The effects of ultraviolet radiation on photosynthetic performance, growth and sunscreen compounds in aeroterrestrial biofilm algae isolated from building facades, Planta 225 (2007) 991–1000, https://doi.org/10.1007/s00425-006-0406-x.

[18] L. Katarzyna, G. Sai, O.A. Singh, Non-enclosure methods for non-suspended microalgae cultivation: literature review and research needs, Renew. Sustain. Energy Rev. 42 (2015) 1418–1427, https://doi.org/10.1016/j.rser.2014.11.029.

[19] Council of Europe Convention for the Protection of the Architectural Heritage of Europe 1985, 1-8.

[20] F. Rossi, E. Micheletti, L. Bruno, S.P. Adhikary, P. Albertano, R. De Philippis, Characteristics and role of the exocellular polysaccharides produced by five cyanobacteria isolated from phototrophic biofilms growing on stone monuments, Biofouling 28 (2012) 215–224, https://doi.org/10.1080/08927014.2012.663751.

[21] D. Pinna, Coping with Biological Growth on Stone Heritage Objects, Apple Academic Press: Toronto ; [Waretown, New Jersey] : Apple Academic Press, 2017. |, 2017. ISBN 9781315365510.

[22] N. Cutler, H. Viles, Eukaryotic microorganisms and stone biodeterioration, Geomicrobiol. J. 27 (2010) 630–646, https://doi.org/10.1080/01490451003702933.

[23] E. Gallego-Cartagena, H. Morillas, M. Maguregui, K. Patiño-Camelo, I. Marcaida, W. Morgado-Gamero, L.F.O. Silva, J.M. Madariaga, A comprehensive study of biofilms growing on the built heritage of a caribbean industrial city in correlation with construction materials, Int. Biodeterior. Biodegrad. 147 (2020) 104874, https://doi.org/10.1016/j.ibiod.2019.104874.

[24] D. Pinna, Microbial growth and its effects on inorganic heritage materials, in: Microorganisms in the Deterioration and Preservation of Cultural Heritage, Springer International Publishing, Cham, 2021, pp. 3–35.

[25] L.O. Björn, G.C. Papageorgiou, R.E. Blankenship, Govindjee A viewpoint: why chlorophyll a? Photosynth. Res. 99 (2009) 85–98, https://doi.org/10.1007/s11120-008-9395-x.

[26] A. Kume, T. Akitsu, K.N. Nasahara, Why is chlorophyll b only used in light-harvesting systems? J. Plant Res. 131 (2018) 961–972, https://doi.org/10.1007/s10265-018-1052-7.

[27] D.K. Saini, S. Pabbi, P. Shukla, Cyanobacterial pigments: perspectives and biotechnological approaches, Food Chem. Toxicol. 120 (2018) 616–624, https://doi.org/10.1016/j.fct.2018.08.002.

[28] M.K. Mandal, NgK. Chanu, N. Chaurasia, Cyanobacterial pigments and their fluorescence characteristics: applications in research and industry, in: Advances in Cyanobacterial Biology, Elsevier, 2020, pp. 55–72.

[29] P. Albertano, L. Bruno, S. Bellezza, New strategies for the monitoring and control of cyanobacterial films on valuable lithic faces, Plant Biosystems - An International Journal Dealing with all Aspects of Plant Biology 139 (2005) 311–322, https://doi.org/10.1080/11263500500342256.

[30] P. Albertano, L. Bruno, The importance of light in the conservation of hypogean monuments, in: Molecular Biology and Cultural Heritage, Routledge, 2017, pp. 171–178.

[31] F. Borderie, B. Alaoui-Sossé, L. Aleya, Heritage materials and biofouling mitigation through UV-C irradiation in show caves: state-of-the-art practices and future challenges, Environ. Sci. Pollut. Control Ser. 22 (2015) 4144–4172, https://doi.org/10.1007/s11356-014-4001-6.

[32] J.D. Stamford, J. Stevens, P.M. Mullineaux, T. Lawson, LED lighting: a grower's guide to light spectra, Hortscience 58 (2023) 180–196, https://doi.org/10.21273/HORTSCI16823-22.

[33] A. Kume, Importance of the green color, absorption gradient, and spectral absorption of chloroplasts for the radiative energy balance of leaves, J. Plant Res. 130 (2017) 501–514, https://doi.org/10.1007/s10265-017-0910-z.

[34] D. Zafra-Castro, Criterios Para La Planificación de La Iluminación Patrimonial Desde La Conservación: Propuesta de Alumbrado Ornamental y Vial Ambiental Del Castillo de Cardona, Universitat de Barcelona, 2020.

[35] MINCOTUR Real Decreto 1890/2008, de 14 de Noviembre, Por El Que Se Aprueba El Reglamento de Eficiencia Energética En Instalaciones de Alumbrado Exterior y Sus Instrucciones Técnicas Complementarias EA-01 a EA-07.

[36] A. Méndez, B. Prieto, J.M. Aguirre i Font, P. Sanmartín, Better, not more, lighting: policies in urban areas towards environmentally-sound illumination of historical stone buildings that also halts biological colonization, Sci. Total Environ. 906 (2024) 167560, https://doi.org/10.1016/j.scitotenv.2023.167560.

[37] A. Méndez, P. Sanmartín, S. Balboa, A. Trueba-Santiso, Environmental proteomics elucidates phototrophic biofilm responses to ornamental lighting on stone-built heritage, Microb. Ecol. 87 (2024) 147, https://doi.org/10.1007/s00248-024-02465-1.

[38] H. Ettl, G. Gärtner, Syllabus Der Boden-, Luft- Und Flechtenalgen, Springer Berlin Heidelberg, Berlin, Heidelberg, 1995. ISBN 978-3-642-39461-4.

[39] L.S. Khaybullina, L.A. Gaysina, J.R. Johansen, M. Krautová, Examination of the terrestrial algae of the great smoky mountains national park, USA, Fottea 10 (2010) 201–215, https://doi.org/10.5507/fot.2010.011.

[40] K. Fuňková, V.R. Flechtner, L.A. Lewis, Revision of the genus bracteacoccus tereg (chlorophyceae, chlorophyta) based on a phylogenetic approach, Nova Hedwigia 96 (2012) 15–59, https://doi.org/10.1127/0029-5035/2012/0067.

[41] J. Komárek, Süßwasserflora von Mitteleuropa, Bd. 19/3: Cyanoprokaryota, first ed., 2013. Heidelberg.

[42] H. Utermohl, Zur ver vollkommung der quantitativen phytoplankton-methodik, Mitteilung Internationale Vereinigung Fuer Theoretische unde Amgewandte Limnologie 9 (1958) 39.

[43] R.A. Bell, M.R. Sommerfeld, Algal biomass and primary production within a temperate zone sandstone, Am. J. Bot. 74 (1987) 294–297, https://doi.org/10.1002/j.1537-2197.1987.tb08608.x.

[44] A.R. Wellburn, The spectral determination of chlorophylls a and b, as well as total carotenoids, using various solvents with spectrophotometers of different resolution, J. Plant Physiol. 144 (1994) 307–313, https://doi.org/10.1016/S0176-1617(11)81192-2.

[45] F. Villa, B. Pitts, E. Lauchnor, F. Cappitelli, P.S. Stewart, Development of a laboratory model of a phototroph-heterotroph mixed-species biofilm at the stone/air interface, Front. Microbiol. 6 (2015), https://doi.org/10.3389/fmicb.2015.01251.

[46] P. Sanmartín, F. Villa, F. Cappitelli, S. Balboa, R. Carballeira, Characterization of a Biofilm and the Pattern Outlined by Its Growth on a Granite-Built Cloister in the Monastery of San Martiño Pinario (Santiago de Compostela , NW Spain), Int. Biodeterior. Biodegrad. 147 (2020) 104871, https://doi.org/10.1016/j.ibiod.2019.104871.

[47] Michel DuBois, K.A. Gilles, J.K. Hamilton, P.A. Rebers, Fred Smith, Colorimetric method for determination of sugars and related substances, Anal. Chem. 28 (1956) 350–356, https://doi.org/10.1021/ac60111a017.

[48] M.M. Bradford, A rapid and sensitive method for the quantitation of microgram quantities of protein utilizing the principle of protein-dye binding, Anal. Biochem. 72 (1976) 248–254, https://doi.org/10.1016/0003-2697(76)90527-3.

[49] P. Wang, G. You, J. Hou, C. Wang, Y. Xu, L. Miao, T. Feng, F. Zhang, Responses of wastewater biofilms to chronic CeO2 nanoparticles exposure: structural, physicochemical and microbial properties and potential mechanism, Water Res. 133 (2018) 208–217, https://doi.org/10.1016/j.watres.2018.01.031.

[50] S. Wahidin, A. Idris, S.R.M. Shaleh, The influence of light intensity and photoperiod on the growth and lipid content of microalgae Nannochloropsis sp, Bioresour. Technol. 129 (2013) 7–11, https://doi.org/10.1016/j.biortech.2012.11.032.

[51] X. Zhang, H. Yuan, L. Guan, X. Wang, Y. Wang, Z. Jiang, L. Cao, X. Zhang, Influence of photoperiods on microalgae biofilm: photosynthetic performance, biomass yield, and cellular composition, Energies 12 (2019) 3724, https://doi.org/10.3390/en12193724.

[52] M. Mutschlechner, H. Schöbel, Illuminating life sciences: a biophysical guide to the use of chromatic and white light sources in photobiology, Photonics 11 (2024) 487, https://doi.org/10.3390/photonics11060487.

[53] C. Shu, C. Tsai, W. Liao, K. Chen, H. Huang, Effects of light quality on the accumulation of oil in a mixed culture of *Chlorella* sp. and *Saccharomyces cerevisiae*, Journal of Chemical Technology & Biotechnology 87 (2012) 601–607, https://doi.org/10.1002/jctb.2750.

[54] J. Park, J. Seo, E.E. Kwon, Microalgae production using wastewater: effect of light-emitting diode wavelength on microalgal growth, Environ. Eng. Sci. 29 (2012) 995–1001, https://doi.org/10.1089/ees.2012.0082.

[55] A. Khalili, G.D. Najafpour, G. Amini, F. Samkhaniyani, Influence of nutrients and LED light intensities on biomass production of microalgae Chlorella vulgaris, Biotechnol. Bioproc. Eng. 20 (2015) 284–290, https://doi.org/10.1007/s12257-013-0845-8.

[56] P. Kondzior, D. Tyniecki, A. Butarewicz, Influence of Color Temperature of White LED Diodes and Illumination Intensity on the Content of Photosynthetic Pigments in Chlorella Vulgaris Algae Cells. In Proceedings of the Innovations-Sustainability-Modernity-Openness Conference (ISMO'19); MDPI: Basel Switzerland, July 18 2019, 46.

[57] H. Barberousse, R.J. Lombardo, G. Tell, A. Couté, Factors involved in the colonisation of building façades by algae and cyanobacteria in France, Biofouling 22 (2006) 69–77, https://doi.org/10.1080/08927010600564712.

[58] M. Ramírez, M. Hernández-Mariné, E. Novelo, M. Roldán, Cyanobacteria-containing biofilms from a mayan monument in palenque, Mexico, Biofouling 26 (2010) 399–409, https://doi.org/10.1080/08927011003660404.

[59] O. Guillitte, R. Dreesen, Laboratory chamber studies and petrographical analysis as bioreceptivity assessment tools of building materials, Sci. Total Environ. 167 (1995) 365–374, https://doi.org/10.1016/0048-9697(95)04596-S.

[60] A. Rifón-Lastra, Á. Noguerol-Seoane, Green algae associated with the granite walls of monuments in Galicia (NW Spain), Cryptogam. Algol. 22 (2001) 305–326, https://doi.org/10.1016/S0181-1568(01)01069-8.

[61] E. Fuentes, R. Carballeira, B. Prieto, Role of exposure on the microbial consortiums on historical rural granite buildings, Applied Sciences 11 (2021) 3786, https://doi.org/10.3390/app11093786.

[62] S. Eyssautier-Chuine, N. Vaillant-Gaveau, M. Gommeaux, C. Thomachot-Schneider, J. Pleck, G. Fronteau, Efficacy of different chemical mixtures against green algal growth on limestone: a case study with Chlorella vulgaris, Int. Biodeterior. Biodegrad. 103 (2015) 59–68, https://doi.org/10.1016/j.ibiod.2015.02.021.

[63] A. Hindáková, F. Hindák, Green algae of five city fountains in Bratislava, Biologia-Bratislava 53 (1998) 481–494.

[64] W. De Muynck, A.M. Ramirez, N. De Belie, W. Verstraete, Evaluation of strategies to prevent algal fouling on white architectural and cellular concrete, Int. Biodeterior. Biodegrad. 63 (2009) 679–689, https://doi.org/10.1016/j.ibiod.2009.04.007.

[65] S. Manso, W. De Muynck, I. Segura, A. Aguado, K. Steppe, N. Boon, N. De Belie, Bioreceptivity evaluation of cementitious materials designed to stimulate biological growth, Sci. Total Environ. 481 (2014) 232–241, https://doi.org/10.1016/j.scitotenv.2014.02.059.

[66] L. Tomaselli, G. Lamenti, M. Bosco, P. Tiano, Biodiversity of photosynthetic micro-organisms dwelling on stone monuments, Int. Biodeterior. Biodegrad. 46 (2000) 251–258, https://doi.org/10.1016/S0964-8305(00)00078-0.

[67] D. Vázquez-Nion, J. Rodríguez-Castro, M.C. López-Rodríguez, I. Fernández-Silva, B. Prieto, Subaerial biofilms on granitic historic buildings: microbial diversity and development of phototrophic multi-species cultures, Biofouling 32 (2016) 657–669, https://doi.org/10.1080/08927014.2016.1183121.

[68] B. Pereira de Oliveira, A. Miller, M.A. Sequeira Braga, M.F. Macedo, A. Dionisio, T. Silveira, Characterization of Dark Films in Granites. The Case Study of Igreja Da Ordem de Sao Francisco in Oporto (Portugal), in: C. Urzì (Ed.), Proceedings of the Proceedings of the 14th Interational Biodeterioration and Biodegradation Symposium, International Biodeterioration and Biodegradation Society, 2008, p. 72. Messina.

[69] M.F. Macedo, A.Z. Miller, A. Dionísio, C. Saiz-Jimenez, Biodiversity of cyanobacteria and green algae on monuments in the mediterranean basin: an overview, Microbiology (N. Y.) 155 (2009) 3476–3490, https://doi.org/10.1099/mic.0.032508-0.

[70] C.C. Gaylarde, P.M. Gaylarde, A comparative study of the major microbial biomass of biofilms on exteriors of buildings in europe and Latin America, Int. Biodeterior. Biodegrad. 55 (2005) 131–139, https://doi.org/10.1016/j.ibiod.2004.10.001.

[71] A.M. Bellinzoni, G. Caneva, S. Ricci, Ecological trends in travertine colonisation by pioneer algae and plant communities, Int. Biodeterior. Biodegrad. 51 (2003) 203–210, https://doi.org/10.1016/S0964-8305(02)00172-5.

[72] C.A. Crispim, P.M. Gaylarde, C.C. Gaylarde, Algal and cyanobacterial biofilms on calcareous historic buildings, Curr. Microbiol. 46 (2003) 79–82, https://doi.org/10.1007/s00284-002-3815-5.

[73] M.N. Metsoviti, G. Papapolymerou, I.T. Karapanagiotidis, N. Katsoulas, Effect of light intensity and quality on growth rate and composition of Chlorella vulgaris, Plants 9 (2019) 31, https://doi.org/10.3390/plants9010031.

[74] U. Karsten, A. Holzinger, Green algae in alpine biological soil crust communities: acclimation strategies against ultraviolet radiation and dehydration, Biodivers. Conserv. 23 (2014) 1845–1858, https://doi.org/10.1007/s10531-014-0653-2.

[75] S. Sharma, A.K. Gautam, R. Singh, S. Gourinath, S. Kateriya, Unusual photodynamic characteristics of the light-oxygen-voltage domain of phototropin linked to terrestrial adaptation of *Klebsormidium nitens*, FEBS J. (2024), https://doi.org/10.1111/febs.17284.

[76] F.-W. Li, C.J. Rothfels, M. Melkonian, J.C. Villarreal, D.W. Stevenson, S.W. Graham, G.K.-S. Wong, S. Mathews, K.M. Pryer, The origin and evolution of phototropins, Front. Plant Sci. 6 (2015), https://doi.org/10.3389/fpls.2015.00637.

[77] M. Komar, P. Nowicka-Krawczyk, T. Ruman, J. Nizioł, M. Dudek, B. Gutarowska, Biodeterioration potential of algae on building materials - model study, Int. Biodeterior. Biodegrad. 180 (2023) 105593, https://doi.org/10.1016/j.ibiod.2023.105593.

[78] A. Negi, I.P. Sarethy, Microbial biodeterioration of cultural heritage: events, colonization, and analyses, Microb. Ecol. 78 (2019) 1014–1029, https://doi.org/10.1007/s00248-019-01366-y.

[79] J.-Y. Lee, S.-H. Seo, C.-Y. Ahn, C.S. Lee, K.-G. An, A. Srivastava, H.-M. Oh, Green light as supplementary light for enhancing biomass production of Ettlia sp. and preventing population invasion from other microalgae, J. Appl. Phycol. 31 (2019) 2207–2215, https://doi.org/10.1007/s10811-019-1737-x.

[80] K. Chekanov, Diversity and distribution of carotenogenic algae in europe: a review, Mar. Drugs 21 (2023) 108, https://doi.org/10.3390/md21020108.

[81] A. Méndez, F. Maisto, J. Pavlović, M. Rusková, D. Pangallo, P. Sanmartín, Microbiome shifts elicited by ornamental lighting of granite facades identified by MinION sequencing, J. Photochem. Photobiol., B 261 (2024) 113065, https://doi.org/10.1016/j.jphotobiol.2024.113065.

[82] Y. Bao, Y. Ma, W. Liu, X. Li, Y. Li, P. Zhou, Y. Feng, M. Delgado-Baquerizo, Innovative strategy for the conservation of a millennial mausoleum from biodeterioration through artificial light management, NPJ Biofilms Microbiomes 9 (2023) 69, https://doi.org/10.1038/s41522-023-00438-9.

[83] S. Popović, M. Pećić, G. Subakov Simić, Exploring Lampenflora of Resavska Cave, Serbia. In Proceedings of the the 2nd International Electronic Conference on Diversity (IECD 2022)—New Insights into the Biodiversity of Plants, Animals and Microbes; MDPI: Basel Switzerland, March 15 2022, 33.

[84] V.M. Luimstra, J.M. Schuurmans, K.J. Hellingwerf, H.C.P. Matthijs, J. Huisman, Blue light induces major changes in the gene expression profile of the cyanobacterium <scp> *Synechocystis* </Scp> sp. PCC 6803, Physiol Plant 170 (2020) 10–26, https://doi.org/10.1111/ppl.13086.

[85] H. Matsui, K. Anraku, T. Kotani, Spectrophotometry can monitor changes in algal metabolism triggered by nutrient deficiency in Nannochloropsis oculata cultured under various light-emitting diode light regimes, Fisheries Science 85 (2019) 167–176, https://doi.org/10.1007/s12562-018-1261-y.

[86] P. Dahech, M. Schlömann, C. Ortiz, Light intensity stimulates the production of extracellular polymeric substances (EPS) in a culture of the desert cyanobacterium trichormus sp, J. Appl. Phycol. 33 (2021) 2795–2804, https://doi.org/10.1007/s10811-021-02516-x.

[87] H. Ge, J. Zhang, X. Zhou, L. Xia, C. Hu, Effects of light intensity on components and topographical structures of extracellular polymeric substances from *Microcoleus vaginatus* (cyanophyceae), Phycologia 53 (2014) 167–173, https://doi.org/10.2216/13-163.1.

[88] D. Kumar, J. Kvíderová, P. Kaštánek, J. Lukavský, The green alga *Dictyosphaerium chlorelloides* biomass and polysaccharides production determined using cultivation in crossed gradients of temperature and light, Eng. Life Sci. 17 (2017) 1030–1038, https://doi.org/10.1002/elsc.201700014.

[89] J.P. Pavissich, M. Li, R. Nerenberg, Spatial distribution of mechanical properties in *Pseudomonas aeruginosa* biofilms, and their potential impacts on biofilm deformation, Biotechnol. Bioeng. 118 (2021) 1545–1556, https://doi.org/10.1002/bit.27671.

[90] W. Liu, Y. Ji, Y. Long, W. Huang, C. Zhang, H. Wang, Y. Xu, Z. Lei, W. Huang, D. Liu, The role of light wavelengths in regulating algal-bacterial granules formation, protein and lipid accumulation, and microbial functions, J Environ Manage 337 (2023) 117750, https://doi.org/10.1016/J.JENVMAN.2023.117750.

[91] Y. Shen, H. Zhang, X. Xu, X. Lin, Biofilm Formation and lipid accumulation of attached culture of Botryococcus braunii, Bioproc. Biosyst. Eng. 38 (2015) 481–488, https://doi.org/10.1007/s00449-014-1287-1.

[92] V. Urbain, J.C. Block, J. Manem, Bioflocculation in activated sludge: an analytic approach, Water Res. 27 (1993) 829–838, https://doi.org/10.1016/0043-1354(93)90147-A.

[93] Y.T. Cheah, D.J.C. Chan, Physiology of microalgal biofilm: a review on prediction of adhesion on substrates, Bioengineered 12 (2021) 7577–7599, https://doi.org/10.1080/21655979.2021.1980671.

[94] H.T. Schroeder, C.H. De Lemos Muller, T.G. Heck, M. Krause, P.I. Homem de Bittencourt, The dance of proteostasis and metabolism: unveiling the caloristatic controlling switch, Cell Stress Chaperones 29 (2024) 175–200, https://doi.org/10.1016/j.cstres.2024.02.002.
[95] C. Honeywill, D. Paterson, S. Hagerthey, Determination of microphytobenthic biomass using pulse-amplitude modulated minimum fluorescence, Eur. J. Phycol. 37 (2002) 485–492, https://doi.org/10.1017/S0967026202003888.
[96] W. Stock, L. Blommaert, I. Daveloose, W. Vyverman, K. Sabbe, Assessing the suitability of imaging-PAM fluorometry for monitoring growth of benthic diatoms, J. Exp. Mar. Biol. Ecol. 513 (2019) 35–41, https://doi.org/10.1016/J.JEMBE.2019.02.003.
[97] A. Eggert, N. Häubner, S. Klausch, U. Karsten, R. Schumann, Quantification of algal biofilms colonising building materials: chlorophyll α measured by PAM-fluorometry as a biomass parameter, Biofouling 22 (2006) 79–90, https://doi.org/10.1080/08927010600579090.
[98] M. Michel-Rodriguez, S. Lefebvre, M. Crouvoisier, X. Mériaux, F. Lizon, Underwater light climate and wavelength dependence of microalgae photosynthetic parameters in a temperate sea, PeerJ 9 (2021) e12101, https://doi.org/10.7717/peerj.12101.
[99] I. Terashima, T. Fujita, T. Inoue, W.S. Chow, R. Oguchi, Green light drives leaf photosynthesis more efficiently than red light in strong white light: revisiting the enigmatic question of why leaves are green, Plant Cell Physiol. 50 (2009) 684–697, https://doi.org/10.1093/pcp/pcp034.
[100] W. Blanken, M. Cuaresma, R.H. Wijffels, M. Janssen, Cultivation of microalgae on artificial light comes at a cost, Algal Res. 2 (2013) 333–340, https://doi.org/10.1016/j.algal.2013.09.004.
[101] I. Terashima, T. Fujita, T. Inoue, W.S. Chow, R. Oguchi, Green light drives leaf photosynthesis more efficiently than red light in strong white light: revisiting the enigmatic question of why leaves are green, Plant Cell Physiol. 50 (2009) 684–697, https://doi.org/10.1093/PCP/PCP034.
[102] J. Chauhan, M.D. Prathibha, P. Singh, P. Choyal, U.N. Mishra, D. Saha, R. Kumar, H. Anuragi, S. Pandey, B. Bose, et al., Plant photosynthesis under abiotic stresses: damages, adaptive, and signaling mechanisms, Plant Stress 10 (2023) 100296, https://doi.org/10.1016/J.STRESS.2023.100296.
[103] Y. Wang, T. Qu, X. Zhao, X. Tang, H. Xiao, X. Tang, A comparative study of the photosynthetic capacity in two green tide macroalgae using chlorophyll fluorescence, SpringerPlus 5 (2016) 775, https://doi.org/10.1186/s40064-016-2488-7.
[104] F.L. Figueroa, R. Conde-Álvarez, I. Gómez, Relations between electron transport rates determined by pulse amplitude modulated chlorophyll fluorescence and oxygen evolution in macroalgae under different light conditions, Photosynth. Res. 75 (2003) 259–275, https://doi.org/10.1023/A:1023936313544.
[105] P. Juneau, B.R. Green, P.J. Harrison, Simulation of pulse-amplitude-modulated (PAM) fluorescence: limitations of some PAM-parameters in studying environmental stress effects, Photosynthetica 43 (2005) 75–83, https://doi.org/10.1007/S11099-005-5083-7/METRICS.
[106] A. Meneghesso, Investigation of mechanisms modulating photosynthetic efficiency in Nannochloropsis gaditana. Università degli Studi di Padova: Padova, 2016.
[107] K. Roháček, Chlorophyll fluorescence parameters: the definitions, photosynthetic meaning, and mutual relationships, Photosynthetica 40 (2002) 13–29, https://doi.org/10.1023/A:1020125719386/METRICS.
[108] I. Rodea-Palomares, S. Gonzalo, J. Santiago-Morales, F. Leganés, E. García-Calvo, R. Rosal, F. Fernández-Piñas, An insight into the mechanisms of nanoceria toxicity in aquatic photosynthetic organisms, Aquat. Toxicol. 122–123 (2012) 133–143, https://doi.org/10.1016/j.aquatox.2012.06.005.

4.2 PART 2: ASSESSMENT OF BIOSTATIC CAPACITY

4.2.3 CHAPTER 4

ENVIRONMENTAL PROTEOMICS ELUCIDATES PHOTOTROPHIC BIOFILM RESPONSES TO ORNAMENTAL LIGHTING ON STONE-BUILT HERITAGE

Anxo Méndez, Patricia Sanmartín, Sabela Balboa, Alba Trueba-Santiso

Microbial Ecology 87, 147 (2024). doi: 10.1007/s00248-024-02465-1

JCR index (IF) 2024 = 4.0 (8/119, 93.7 percentile in Marine and Freshwater Biology)

Open access. Citations (to September 2025): 3

The work from this chapter was also presented in an international conference:

Méndez, A.; Trueba-Santiso, A.; Balboa, S.; Sanmartín, P. Preventive conservation of stone-built heritage through ornamental lighting: a proteomics approach towards understanding the physiological response of phototrophic biofilms. Oral communication. 19th International Biodeterioration and Biodegradation Symposium (IBBS19). 9-12 September 2024, Berlin, Germany.

Microbial Ecology (2024) 87:147
https://doi.org/10.1007/s00248-024-02465-1

RESEARCH

Environmental Proteomics Elucidates Phototrophic Biofilm Responses to Ornamental Lighting on Stone-built Heritage

Anxo Méndez[1] · Patricia Sanmartín[1] · Sabela Balboa[2] · Alba Trueba-Santiso[3]

Received: 28 June 2024 / Accepted: 15 November 2024

Abstract
Recent studies are showing that some lights suitable for illuminating the urban fabric (i.e. that do not include the red, green and blue sets of primary colours) may halt biological colonisation on monuments, mainly that caused by phototrophic subaerial biofilms (SABs), which may exacerbate the biodeterioration of substrates. However, the light-triggered mechanisms that cause changes in the growth of the phototrophs remain unknown. Environmental proteomics could be used to provide information about the changes in the SAB metabolism under stress inflicted by nocturnal lighting. Here, laboratory-produced SABs, composed of Chlorophyta, Streptophyta and Cyanobacteriota, were subjected to three types of lighting used for monuments: cool white, warm white and amber + green (potentially with a biostatic effect). A control without light (i.e. darkness) was also included for comparison. The nocturnal lighting impaired the capacity of the SABs to decompose superoxide radicals and thus protect themselves from oxidative stress. Cool white and warm white light both strongly affected the proteomes of the SABs and reduced the total peptide content, with the extent of the reduction depending on the genera of the organisms involved. Analysis of the photo-damaging effect of amber + green light on the biofilm metabolism revealed a negative impact on photosystems I and II and production of photosystem antenna protein-like, as well as a triggering effect on protein metabolism (synthesis, folding and degradation). This research provides, for the first-time, a description of the proteomic changes induced by lighting on SABs colonising illuminated monuments in urban areas.

Keywords Lighting Treatment · Triggered Processes · Environmental Proteomics · Green Algae · Cultural Heritage · Biofilms

Introduction

Lighting of the urban fabric at night is a controversial issue. It is debated if increasing the number of points that are illuminated in cities makes transit safer and more secure for pedestrians [1]. Illumination can also make cities appear more modern and aesthetically pleasing (in the eyes of some). Lighting cultural and architectural assets of cities to enhance and valorize the cultural heritage has grown in popularity since the 1990s, especially since around 2010 [2]. Lighting should highlight specific features and the geometric shapes of monuments or generate visual contrasts while remaining respectful of the original aesthetics of the buildings [3]. Night-time tourism is now more common in cities than it was in the early 1990s, and the change has been attributed to increased illumination [4]. However, illumination of monuments is an emerging contribution to artificial light at night (ALAN) pollution—or more simply, light pollution—[5], which increased by 9.6% between 2011 and 2022 [6]. ALAN affects the survival, existence and well-being of people, microorganisms and plants and eventually disrupts the entire ecosystem [7]. However, appropriate ornamental lighting could help to reduce biodeterioration of monuments and protect biodiversity [5].

✉ Anxo Méndez
anxo.mendez.villar@usc.es

1 CRETUS, Gemap (GI-1243), Departamento de Edafoloxía E Química Agrícola, Facultade de Farmacia, Universidade de Santiago de Compostela, 15782 Santiago de Compostela, Spain

2 CRETUS, Departamento de Microbiología y Parasitología, CIBUS-Facultad de Biología, Universidade de Santiago de Compostela, 15782 Santiago de Compostela, Spain

3 CRETUS, Department of Chemical Engineering, University of Santiago de Compostela, Campus Vida, Galicia, 15782 Santiago de Compostela, Spain

Published online: 22 November 2024

Light emitting diodes (LEDs) are increasingly used to illuminate monuments [8] because they use less energy, yield more light, last longer than other types of light technologies and are also mercury-free. However, illumination can cause biodeterioration of heritage monuments by promoting colonisation by phototrophic organisms [9], which use light as the main source of energy for metabolism (i.e. photosynthesis). Testing has been carried out to evaluate the use of different artificial monochromatic lights (blue, green and red) to shape the ecophysiological features of the algae and cyanobacteria to exert a biostatic (halting growth) effect on the organisms. Studies conducted in subterranean heritage such as caves, catacombs and mausoleums [9–11] and on outdoor monuments [12] have demonstrated inhibition of colonisation by phototrophs, especially of cyanobacteria rich in phycocyanin exposed to blue light and of algae exposed to green light. In the first study, carried out in the early 2000s in the Roman Catacombs of St. Callistus and Domitilla, Rome (Italy), the photosynthetic activity of the cyanobacterial and chemoorganotrophic bacterial biofilms was inhibited after 5 months under blue lighting [10], and the area occupied by phototrophic communities was reduced after 10 years [11]. Green lighting tested in on-site studies has been found to inhibit the growth of phototrophic biofilms, such as those predominated by the alga *Chlorella sorokiniana* in the Bats' Cave, Zuheros, Spain [13], by the cyanobacterium *Chroococcidiopsis* sp. and red microalga *Cyanidium* sp. in the Nerja Cave, Malaga, Spain [14] and by cyanobacteria and heterotrophic species belonging to proteobacteria in two Mausoleums of the Southern Tang Dynasty, Nanjing, China [9]. Compared to a non-illuminated or white light control, illumination with red light inhibited growth of biofilms mainly predominated by the green alga *Bracteacoccus minor* (in this case in combination with a period of daylight) [15] and the green alga *Chlamydomonas reinhardtii* CC-1690 [16].

The aim of these lighting-based strategies is to prevent further biodeterioration on outdoor stone monuments (sometimes only aesthetic) by using narrow-band LEDs avoiding certain photosynthetic active radiation (PAR) spectral bands, between 350–400 nm and 700–750 nm [17, 18]. These strategies are much more difficult to apply to naturally lit outdoor monuments, where the use of monochromatic colours for lighting is not acceptable in urban planning for aesthetic reasons, and negative effects on humans and animals must be avoided [5]. However, exposure of monuments to the light generated by combining amber and green LEDs (CromaLux light, currently under trial), which generates warm tones, has shown an impact similar to an unlit area; with little to no impact on the insects of the surrounding area [19] and a slightly enhancing impact on bacterial and fungal microbiota of monument facades [20], and also a long-term biostatic effect on phototrophs, especially algae (unpublished data). The use of this light is proposed as a preventive conservation tool, using the existing ornamental lighting infrastructure, in order to achieve also reduce the cleaning campaigns of facades and structures. It is not a biocidal light so its role is not to replace the use of chemicals to remove biocolonisation already present at the field site.

Different spectral bands affect the various taxonomic groups that comprise SABs differently, and the specific changes exerted by the lighting in the underlying metabolic machinery remain unknown. Considering the heterogeneity of the SABs and the long times required to remove them from heritage surfaces (10 years in the study by Bruno et al. [11]), research should involve different taxonomic groups and different types of illumination. The data obtained could then be used as the basis for selecting lights to eliminate existing SABs or to prevent the appearance of SABs on particular monuments. Thanks to great technical advances achieved in recent years, environmental proteomics provides information on both the taxonomies and the functionalities from complex mixed microbial communities. We hypothesize that this approach could be useful to cover the gap in information on the molecular damage induced by the different types of lights, as it has been previously shown to elucidate the links between proteome alteration, metabolism and phenotype changes under environmental stresses [21].

In the present study, SABs [22, 23] were generated in the laboratory to further understand the molecular mechanism of phototrophic SABSs under nocturnal ornamental lighting using a culture obtained from natural phototrophic biofilms of granite monuments in Santiago de Compostela (UNESCO World Heritage City since 1985, NW Spain). The SABs were subsequently grown under a photoperiod comprised of 13 h of LED daylight simulating the solar illuminance in spring in the historical centre of Santiago de Compostela (see the "SAB formation and lighting set-up" section), followed by 6 h of different types of ornamental lighting and 5 h of darkness, to simulate outdoor conditions. The following types of ornamental lighting, considered suitable for the urban fabric, were tested: the amber + green light combination currently under trial, a warm white light (yellow tone), a cool white light (blue tone) and no light. Environmental proteomics analysis was used to study the effect of ornamental lighting on the physiology of the different species forming the mature SABs, with a particular focus on the photosynthetic machineries. To our knowledge, this is the first proteomics study of SABs colonizing illuminated monuments in urban areas.

Materials and Methods

SAB Formation and Lighting Set-up

Multi-species SABs, mainly composed of eukaryotic microalgae (hereinafter green algae) but also including prokaryotic

microalgae (hereinafter cyanobacteria), were grown according to the membrane-supported biofilm protocol first described by Anderl et al. [24] and later implemented for phototrophs by Sanmartín et al. [25]. The species comprising the SABs were examined under light microscopy, with a Nikon Eclipse E600 equipped with an E-Plan 40× objective (N.A. 0.65) and differential interference contrast (Nomarski) optics. Taxonomic determinations were based on the morphometry and reproduction of the species in the cultures. The main taxonomic references used for the identification of green algae were [26–28] and for cyanobacteria [29]. The results were used to select an adequate database to perform the proteomic data analyses. The biomass of each SAB was also measured gravimetrically by weighing the membrane before and after removal of the biofilm (by gentle scraping with a sterile loop) with a precision laboratory balance (Denver Instruments, USA, readability, 0.001 mg; uncertainty, i.e. repeatability, 0.002 g).

Aliquots of exponentially growing cells from a homogeneous suspension (50 µL, corresponding to 1.52 mg L^{-1} of dry mass) were used to inoculate sterile (by exposure to UV-C light) polycarbonate membrane discs (Nuclepore™ Track-Etch Membrane Filtration products, diameter 2.5 cm, area 4.9 cm^2, pore diameter 0.2 µm, Whatman™). Twelve inoculated membrane discs were placed on Bold's Basal Medium (BBM) [30]. The membranes were transferred, with the aid of sterile plastic forceps, to fresh agar plates, every 3 days. The SABs were cultured until they reached maturity (after 37 days) in controlled ad hoc customised cabinets (Fig. 1), with one compartment for each of the four LED light photoperiods. Each compartment held a plate with three membrane discs. After the growing period, the SABs were scraped from the membranes, to enable quantification of the biomass of each (values ranged from 65.90 ± 10.46 mg to 53.42 ± 10.77 mg) and were stored at − 80 °C before further processing.

In all four compartments, the photoperiod comprised 13 h of LED daylight (SUN@HOME, Spot PAR16 40 GU10 TW, Ledvance, Germany) represented by high illuminance (10,000 lx, corresponding to 252.59 µmol s^{-1} m^{-2}) and colour temperature of 5500 K, followed by 6 h of different test ornamental illuminations and 5 h of darkness. The diurnal illuminance was based on light measurements taken in spring 2022 on the facades of six granite-built heritage buildings in the historical centre of Santiago de Compostela (the Cathedral, the Monastery of San Martiño Pinario, the Palace of Xelmírez, the School of Medicine, the Cabildo House and the old town hall). The light was measured with a radiometer (DHD 2302.0, HERTER) on each (differently oriented) facade. In addition, the seasonal average daily insolation in the city, reported on the website of the Galician meteorological service (https://www.meteogalicia.gal/), was used to assess whether the cumulative solar intensity applied during the 13 h daylight period was consistent with the daily insolation in spring. The three (test) ornamental lighting set-ups were adjusted with a radiometer (DHD 2302.0, HERTER) to yield an illuminance (quantity) of 20 lx and different light quality (spectral composition) with an associated correlated colour temperature (CCT), both measured with a StellarNet Blue-Wave spectrometer (StellarNet, USA) (Fig. 2). The ornamental illuminance (20 lx) was based on urban planning directives of the city of Santiago de Compostela for the illumination of historical building facades, which included a reduction in nocturnal lighting to the minimum possible while being higher than the average illuminance on the street (10–15 lx) to make the facade more prominent. The unit of measurement for illuminance was selected as Lx (lumens m^{-2}), as it is the preferred unit used by urban planners to mark the intensity of artificial light at night, regardless of the type of light used.

Furthermore, it is used by Spanish legislation to indicate acceptable thresholds for night-time lighting [31].

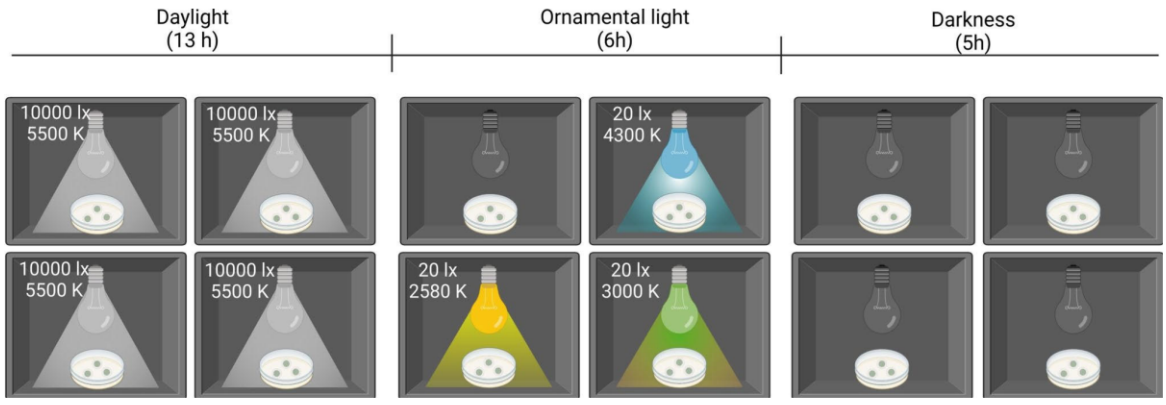

Fig. 1 Schematic diagram of the experimental set-up of the cabinets for the four LED light photoperiods

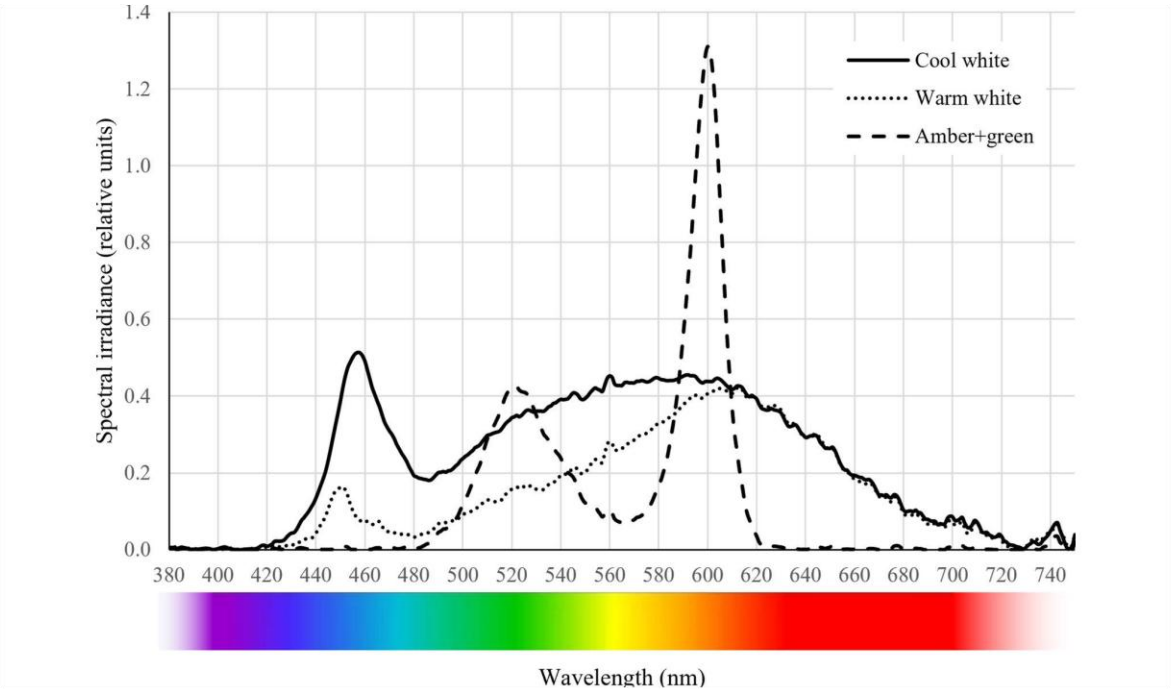

Fig. 2 Light quality (spectra) in the PAR region yielded by the three ornamental lightings. The cool white spectrum was measured after dimming the light bulb with a slightly yellowish, heat-resistant paper film

Both types of white light (cool and warm) comprise the full range of visible light spectrum (around 380–700 nm). Cool white light (blueish tone, A5 GU10 9W, Aigostar, Spain) contains more blue light than warm white light (yellowish tone, cod. 671992, Televés, Spain). The spectrum of cool white light thus has a peak centred at 457 nm, while that of warm white lights has a less intense peak centred at 450 nm. For both types of white light, a wide band between 480 and 700 nm was observed in the spectra, with a main peak around 600 nm (amber). The cool white luminaire was shielded with a slightly yellowish, heat-resistant paper film to dim the light to an illuminance of 20 lx. The shading led to a change in the correlated colour temperature (CCT) from 6400 K (as stated by the manufacturer) to 4300 K yielding a photon flux density of 1.84 µmol s^{-1} m^{-2}. The CCT of the warm white light is 2580 K and produces a photon flux density of 1.13 µmol s^{-1} m^{-2}. The amber + green light (combination under trial, cod. 671990–1, Televés, Spain) yields a bimodal spectrum with two peaks, one at 528 nm (green) and a main peak at 593 nm (amber), producing a CCT of 3000 K with no emission of wavelengths in the blue and red parts of the spectrum (Fig. 2), resulting in an emission of 0.89 µmol s^{-1} m^{-2} of photon flux density. The photon flux density of the ornamental lights was obtained from the spectra measured over the samples, according to the photon energy equation.

Protein Extraction

A total of 12 SAB samples (three per ornamental lighting condition) were resuspended in 0.5 mL of EDTA (0.1 M) and centrifuged at 8000 rpm for 15 min at 4 °C to separate the extracellular matrix from the cellular material. The pellets were resuspended in extraction buffer (50 mM Tris Buffer, 1% SDS, pH = 7.5) and incubated at 90 °C for 20 min. The cells were then lysed by shaking with glass beads in a cell disruptor (Vortex Genie, Scientific Industries, USA), with three cycles of shaking, each lasting 4 min, alternated with incubation on ice for 1 min. The samples were then centrifuged for 20 min at 3300 rpm and 4 °C. The proteins were precipitated from the samples by two additions of cold acetone (at − 20 °C) to remove organic contaminants, salts and buffer residues. The acetone was carefully removed, and the protein pellets were dried at room temperature. The proteins thus obtained were resuspended in triethylammonium bicarbonate buffer (TEAB buffer, Merck, Germany) and quantified with the BCA Protein Assay Kit (Thermo Fisher Scientific, USA) and a Nanodrop spectrophotometer (Thermo

Fisher Scientific, USA), with bovine serum albumin as the calibration curve standard.

SDS-PAGE Electrophoresis

To assess the quality and integrity of the protein samples, protein electrophoresis was performed in denaturing conditions [32]. Samples were denatured at 70 °C for 10 min and mixed with NuPAGE LDS Sample Buffer and NuPAGE Reducing Agent (Thermo Fisher Scientific), following the manufacturer instructions, and loading 20 µg of protein per gel lane. For the electrophoresis, NuPAGE Bis–Tris 4–12% gels (Thermo Fisher Scientific, USA) were used with 1X Running Buffer (Thermo Fisher Scientific, 20X Running Buffer containing 50 mM MES, 50 mM Tris Base, 0.1% SDS and 1 mM EDTA, pH = 7.3). Three microlitres of prestained protein markers (PageRuler™ Plus Prestained Ladder from 10 to 250 kDa, Thermo Fisher Scientific, USA) were loaded on each side of the gel. The electrophoresis was run at 200 V for 30 min, and the gel was stained with a standard Coomassie Blue staining protocol.

Shotgun Proteomic Analysis by Mass Spectrometry

A label-free approach was used to quantify the proteins in each sample [33]. The samples were first trypsin-digested, reduced-alkylated and finally desalted with ZipTip-µC18 (Merck, Germany). The peptide samples thus obtained were analysed by in-solution shotgun proteomics [33]. Peptide samples (0.3 µg of protein) were injected in a timsTOF Pro mass spectrometer (Bruker, Germany) equipped with a nanoelectrospray source (CaptiveSpray) and a tims-QTOF analyser. The chromatographic analysis was performed using a nanoELUTE chromatograph (Bruker, Germany) with an Aurora analytical column (C18, 250 × 0.075 mm, 1.6 µm, 120 Å, IonOpticks). The nHPLC was configured with binary mobile phases that included solvent A (0.1% formic acid in miliQ H_2O) and solvent B (0.1% formic acid in acetonitrile). The analysis time was 105 min, during which the B/A solvent ratio was gradually increased. Blanks were injected between samples, to check for carry-over, and the analysis time was 60 min. For mass spectrometry (MS) acquisition, a collision-induced dissociation (CID) fragmentation and a nanoESI positive ionization mode were used. PASEF-MS/MS scan mode was established for an acquisition range of 100–1700 m/z [34]. Matches were filtered for 1% false discovery rate (FDR) at the peptide level. MS analyses were performed at the Mass Spectrometry and Proteomics Unit (Area of Infrastructures) of the University of Santiago de Compostela.

MS/MS spectra were processed with PEAKS Studio software (Bioinformatics Solutions, Canada) for protein identification and quantification based on the spectral counting method and the Spec value. The data were compared with a database containing all amino acid sequences available in the NCBI protein database for the phyla Streptophyta (previously Charophyta), Chlorophyta and Cyanobacteriota, in September 2023, selected according to prior taxonomic identification by morphology (see the "SAB formation and lighting set-up" section). The Label-Free module from PEAKS was used for protein quantification in Group Mode.

Proteomic Data Analyses

Proteomic taxonomic results were restricted to the genus level, and proteins identified with < 2 unique peptides were excluded from the study. Only the first identification from each protein group was considered. After applying these quality criteria, the relative contribution of peptides from each genus to the total in each sample was calculated. Those genera contributing < 1% to the total in the samples from all ornamental light tested were eliminated from the study. The relative contribution of each genus in each ornamental light condition tested against their contribution when no light was applied was calculated to evaluate the impact of each ornamental light. A genus was considered to have decreased or increased in abundance when the change in its relative contribution was > 1%. For functional analyses, Unipept 2.0 (https://unipept.ugent.be/) and DAVID (https://david.ncifcrf.gov/) were used. Data were processed with Sigma Plot, and all graphs were generated with GraphPad Prism 10. Data are available via ProteomeXchange with identifier PXD050424.

Results

Identification of SAB Species by Morphological Characters

The taxonomic identification of the sample SABs by morphological characters revealed the presence of 3 different groups: two groups of eukaryotes (Chlorophyta and Streptophyta) and one group of prokaryotes (Cyanobacteriota). The most diverse and abundant group was Chlorophyta with the following composition: *Chlamydomonas* sp., *Chlorella vulgaris* Beijerinck, *Coelastrella terrestris* (Reisigl) Hegewald & N. Hanagata, *Ettlia* sp., *Monoraphidium obtusum* (Korshikov) Komárková-Legnerová, *Scenedesmus* sp., and *Tetradesmus obliquus* (Turpin) M.J. Wynne. The following species of Chlorophyta were also present, although less common: *Raphidocelis* sp., *Asterarcys* sp., *Polytomella* sp., *Tetraselmis* sp., *Astrephomene* sp., *Pleodorina* sp. and *Tetrabaena* sp. Only one species of the Streptophyta group was detected: *Klebsormidium flaccidum* (Kützing) P.C. Silva, Mattox & W.H. Blackwell. Finally, two genera of

Cyanobacteriota were detected: *Pseudoanabaena* sp. and *Synechocystis* sp.

Effect of Different Types of Ornamental Lighting on the Taxonomic Composition of the SABs

Proteomics analysis of SABs under the four different ornamental lighting conditions yielded lists of the proteins expressed by the different coexisting genera (Tables S1–S4 of Supplementary Material). The numbers of identifications obtained for each sample are summarized in Fig. 3a. Relative to the control SABs (not exposed to light), the most significant decrease in the total number of peptides/identifications corresponded to the cool white light followed by the warm white light, while the amber + green light did not decrease the number.

The proteome of all SABs was strongly dominated by green algae (phylum Chlorophyta) (87.2–96.17%) (Fig. 3b). Cyanobacteria (phylum Cyanobacteriota) were detected in very low abundance and represented by two genera. Specifically, *Synechocystis* was present in 1.57–2.67% of all samples, while *Leptolyngbya* was detected in 0.46–1.53% of the samples. Finally, only one genus (*Klebsormidium*) in the phylum Streptophyta (previously Charophyta) was detected and was found to be present in all samples. The relative abundance of the genus was < 2% in the control (no light) and cool white treatments, but it increased to 8.4% in the warm white and 8.8% in amber + green light treatments. The total number of genera was 53 in the control (no light), 36 in the cool white, 42 in the warm white, and 68 in the amber + green light treatments (Table S1).

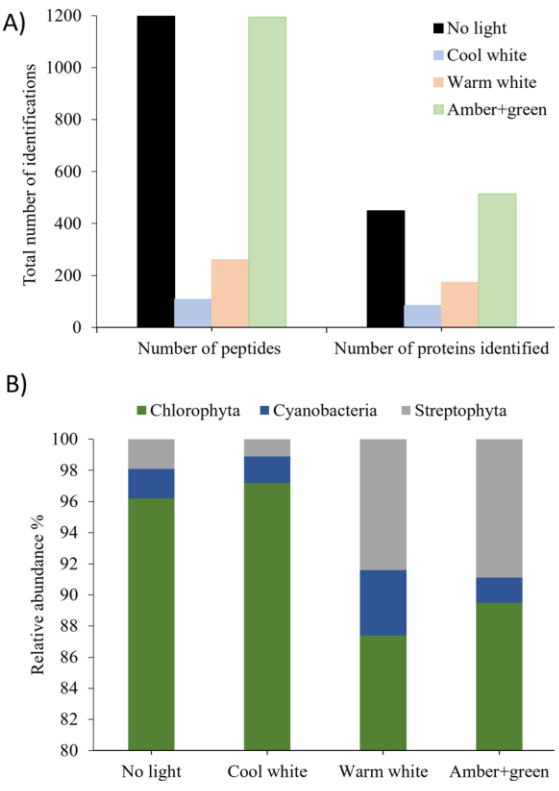

Fig. 3 **a** Total number of identified peptides and proteins under the different light conditions studied. **b** Relative peptide abundances of the 3 phyla under the different ornamental lights

The relative peptide contributions of each genus to the total in each sample are shown in Fig. 4, with the complete data available in Tables S1 to S5 of Supplementary Material. The most abundant genera in the control (no light) treatment were three Chlorophyta genera (*Scenedesmus, Tetradesmus* and *Chlorella*) and the sum of these three constitutes 51.1% of the total peptides detected. Nevertheless, the impact of the lights on peptide abundance varies over the different genera detected (Fig. 4). Most of the genera were negatively affected (decreased > 1%) by the cool white light, except *Scenedesmus*, in which there was no significant difference, and in *Chlamydomonas, Monoraphidium, Raphidocelis* and *Auxenochlorella*, which increased in abundance.

All genera were negatively affected by the warm white light, except *Chlamydomonas, Monoraphidium, Klebsomidium, Synechosysti* and *Tetraselmis*, which increased in abundance. *Raphidocellis, Auxenochlorella, Astrephomene, Pleodorina* and *Tetrabaena* were not affected.

Regarding the amber + green light, *Tetradesmus* was not affected, while *Scenedesumus* decreased slightly and *Chlorella* and *Ettlia* decreased substantially in abundance. By contrast, this type of light positively affected *Monoraphidum, Klebsomidium, Tetraselmis* and *Chlamydomonas* (increased in abundance by > 1%).

The ornamental lighting treatments had different impacts on the relative contributions to the proteomes of the predominant genera: *Scenedesmus, Tetradesmus* and *Chlorella* (Fig. 5). *Scenedesmus* was strongly affected (< 12.1%) by the warm white light and slightly affected by the amber + green (< 1.9%) and cool white lights (< 0.7%), while *Tetradesmus* was strongly affected by the cool white light (< 16.4%), slightly affected by the warm white light (< 2.6%) and not affected by the amber + green light. By contrast, *Chlorella* was affected to a similar extent by all three types of light (6.4–7.8%). All three of these genera belong to the same phylum (Chlorophyta), and *Tetradesmus* and *Scenedesmus* both belong to the family Scenedesmaceae, while *Chlorella* belongs to the family Chlorellaceae. Although *Klebsormidium* (Streptophyta) had a relatively low abundance of peptides, it was strongly and negatively affected by the cool white light, whereas the warm white and the amber + green lights increased the number of peptides.

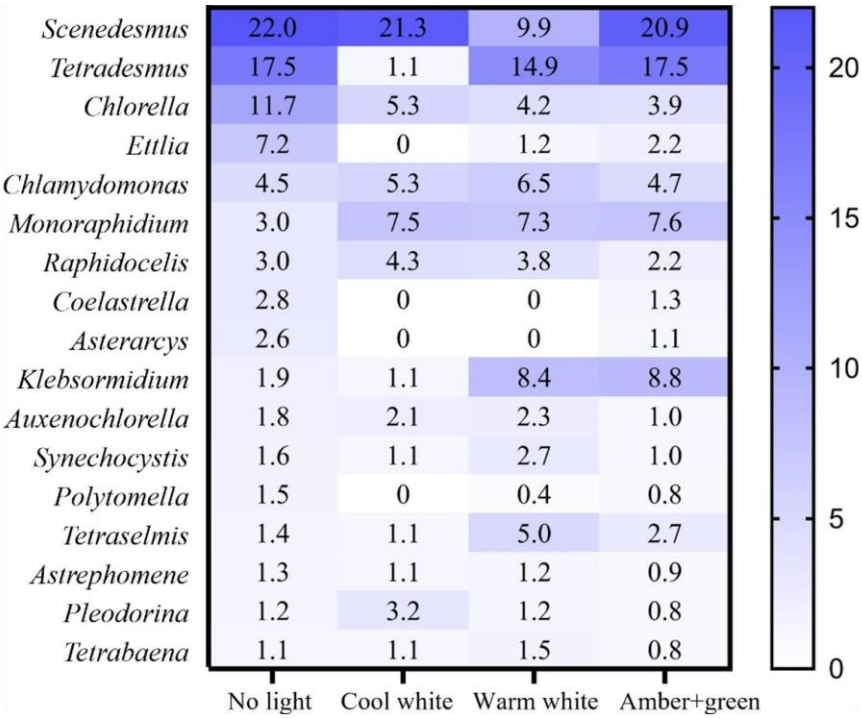

Fig. 4 Relative contribution of each genus to the total number of peptides detected in each sample. Only those taxa with > 1% of relative contribution on the non-light control were evaluated. The effect of the light was considered significant when the relative abundance changed by > 1% in one condition relative to the control (no light) treatment

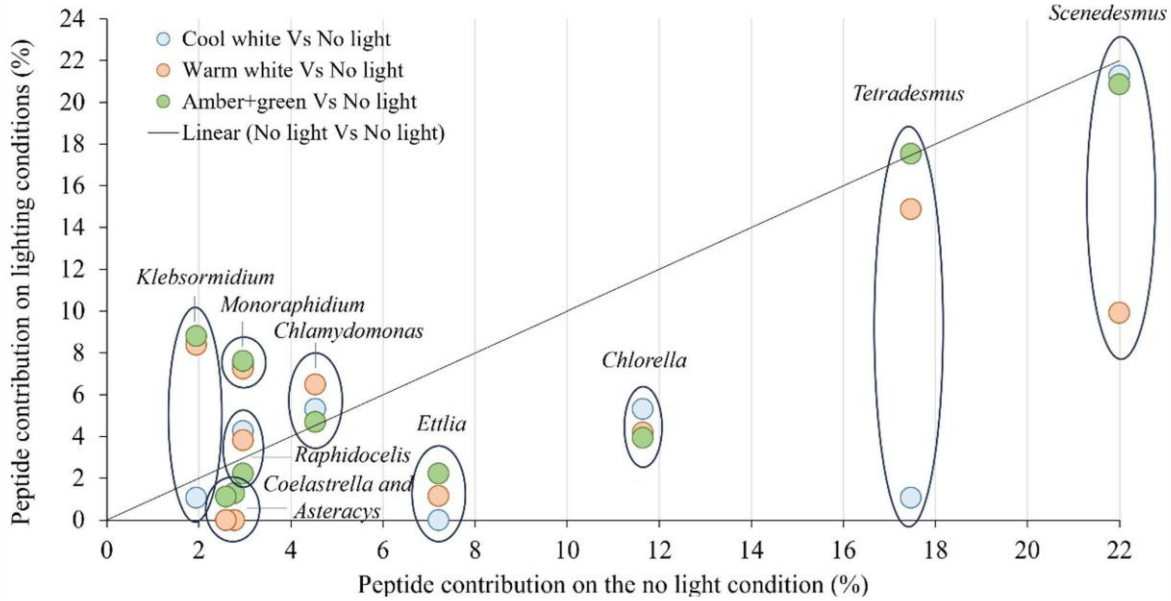

Fig. 5 Effect of the different ornamental lighting conditions on the relative contribution peptides from the 10 most abundant genera present in the SABs

Effect of Different Types of Illumination on the SAB Protein Expression

We categorized the proteins identified from the photosynthesis on each SAB by the Gene Ontology classification of cellular compartments (https://www.informatics.jax.org/vocab/gene_ontology/) focusing on the photosystems I and II in an initial attempt to understand the protein expression regarding the effect of the different ornamental lightings on the light-dependant reactions (Fig. 6). In all categories, no light yielded the highest peptides, followed by amber + green, warm white and cool white in the Photosystem I (GO:0009522) and Photosystem II (GO:0009523) categories. However, this pattern is broken in the subcategories of peptides found in the SAB. First, in the Photosystem I Reaction centre (GO:0009538), containing the primary electron donor of the PSI, the combination of amber + green light yielded 3 peptides in comparison with the 4, 5 and 7 of the warm white, cool white and no light, respectively. Under amber + green also was detected the lowest number of peptides for the Photosystem II Oxygen evolving complex (GO:0009654), and a general reduction in peptides was found under all three ornamental lightings for the Photosystem II Reaction centre (GO:0009539), with only 1 peptide under amber + green against the 4 of the no light condition.

Protein Expression that Decreased Due to the Ornamental Lighting

The proteins detected were classified according to InterPro active site classification to evaluate the impact of ornamental light on more specific SAB protein expression. The lack of a normal photoperiod (i.e. subjected to nocturnal illumination) generally reduced the number of peptides detected in most categories, relative to the no light treatment, and the effect was greater in the cool white light treatment than in the warm white light treatment (Table S6). The effect of amber + green light depended on the category, although the total number of peptides detected in this case was equal to the no light scenario.

The results showed a reduction in the expression of specific proteins involved in the energy metabolism attributed to the disruption of a normal photoperiod. Among the proteins most affected by the nocturnal illumination, some of those involved in carbon metabolism (including the Calvin cycle) are noteworthy. Glyceraldehyde dehydrogenase (IPR020831) and fructose-bisphosphate aldolase (IPR000741) protein families were only absent in the amber + green light treatment. Enolase (IPR000941) and glycosyl transferase (IPR001296), which are involved in the glycolytic and gluconeogenesis pathways, respectively, were only expressed in the SABs in the control (no light) treatment. The same applies to P-Type ATPases (IPR008250) and FAD/NAD(P)-binding domain superfamilies (IPR036188), indicating a decrease in the transportation flux of protons and other cations across the cellular membrane mediated by ATP hydrolysis [35].

In some cases, the negative effect depended on the light type. The NAD(P)-binding domain superfamily (IPR036291) was most strongly impacted by the cool white light, followed by the warm white light and the amber + green light. Expression of the chlorophyll A-B binding protein (IPR022796) was greatly reduced in the cool white and the amber + green light treatments, while

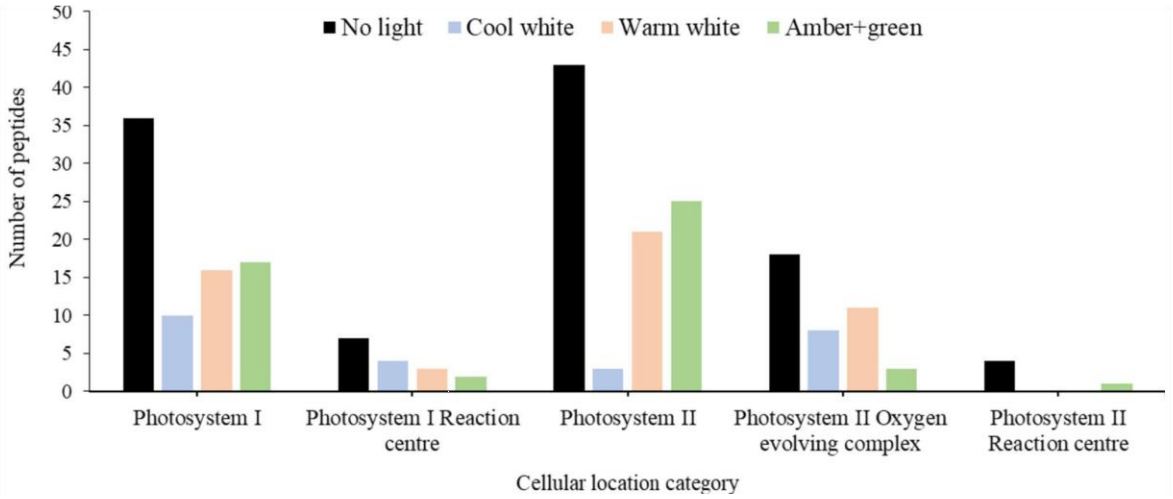

Fig. 6 Number of peptides detected in different cellular compartments found for the two photosystems (according to Gene Ontology categorization) under the different ornamental lights

the decrease in the warm white light treatment was not as evident.

The nocturnal illumination caused impaired defence against oxidative stress, as indicated by the significant decrease in peptides associated with manganese/iron superoxide dismutase (IPR001189) across all three ornamental lighting conditions, reflecting a profound impairment in the capacity of the SABs to decompose superoxide radicals.

Protein Expression that Increased Due to the Ornamental Lighting

Some protein increased their expression under ornamental lighting at night, except in the case of the cool white light, which always yielded a lower abundance of peptides as shown in Table S6 of Supplementary Material. This was the case of the ATP formation through phosphoglycerate kinase superfamily (IPR036043) and the oxygen transport, indicated by the increase in globin-like superfamily (IPR009050). The warm white light treatment increased the abundance of phycocyanin beta subunit (IPR006247) and phycobilisomes (IPR038719).

In particular, the amber + green light triggered the expression of specific proteins in the photosynthetic machinery. This effect deserves some attention, as amber + green light potentially has a biostatic effect on biological colonisation. For example, the photosystem antenna protein-like (IPR036001) binds chlorophyll and β-carotene pigments to the two photosystems, assisting in harnessing energy from wavelengths that PSI and PSII are unable to capture [36]. In addition, peptides related to both photosystems (D1/D2 superfamily of the PSII (IPR036854) and the PsA/PsB proteins of the PSI (IPR001280)) and the photosynthetic reaction centre L/M (IPR000484) in photosynthetic bacteria were found to increase under amber + green light. Surprisingly, photosystem II extrinsic protein O (PsbO) (IPR002628), which catalyses the splitting of water to O_2 and $4H^+$, was not detected in the SABs in the amber + green light treatment (Table S6).

Protein metabolism, including synthesis, assembly and degradation, was also enhanced by the amber + green treatment. Thus, expression of the translation elongation factor EFTu-like, domain 2 (IPR004161) and translation elongation factor EFTu/EF1A, C-terminal (IPR004160), which are involved in protein synthesis, was increased. This was also true for the chaperonin Cpn60/GroEL/TCP-1 family (IPR002423), required for the correct folding of many proteins and for the ClpA/B family (IPR001270), involved in proteolysis. Additionally, Clp ATPase, ClpA/B and ClpB were absent in the SABs in the control (no light) treatment, but 12 peptides were detected in the SABs in the amber + green light treatment for all aforementioned Clp proteins (Table S6).

Histones H2A/H2B/H3 (IPR007125), which provide structural support for chromosomes and are involved in regulating gene expression, were also more abundant in the amber + green light treatment than in the other treatments. The same was observed for the helicase superfamily 1/2 (IPR014001), which catalyses the separation of double-stranded nucleic acids, and nucleotide excision repair and DNA damage recognition occurred during protein synthesis induced by the action of UVR domain proteins (IPR001943).

The P-loop NTPase (IPR027417) catalyses the hydrolysis of bound nucleoside triphosphate (NTP). Adenosine triphosphate AAA-Type ATPases (IPR003593), which catalyses the degradation of ATP in a variety of cellular processes, was the most abundant of that family. The F1/V1/A1 complex of the ATPase (IPR036121), which includes the catalytic core that synthesizes and hydrolyses ATP [37], was over expressed under the amber + green light.

Finally, tubulin, tryptophan synthase and the heat shock proteins Hsp70 (IPR013126) and Hsp90 (IPR001404) families also increased after exposure to nocturnal amber + green light (Table S6). These families are fundamental to proper protein folding and also play an important role in the management of thermal and oxidative stress.

Effect of Different Types of Illumination on the Protein Expression of Different Genera of Algae

As shown in Fig. 5 and discussed in the "Identification of SAB Species by Morphological Characters" section, each lighting condition altered the taxonomic composition of the biofilm. The use of gene ontology (GO) categories, included in Table S8 of Supplementary Material, enabled observation of the different metabolic responses of the most abundant and relevant genera.

The main proteins expressed in *Scenedesmus* under the control (no light) treatment are related to glycolytic processes and other carbohydrate metabolisms, proton export across the plasma membrane and PSII assembly (all with 2 peptides). Some of these proteins were promoted by warm white light (1 peptide detected for glycolytic process and 1 for PSII assembly) and cool white light (only 1 peptide for glycolytic process). However, the amber + green light treatment did not promote these protein expressions, which stimulated protein metabolism expression (biosynthesis of amino acids, translation, and protein refolding, all with 1 peptide).

For *Tetradesmus*, translation was the process for which more peptides were detected under no light (5 peptides), followed by glutamine biosynthesis and photosynthesis (2 peptides each). A similar response was yielded by the cool white treatment, with the only 1 peptide detected falling in the same categories. Warm white stimulated glycolysis and

PSII (1 peptide each), while amber + green light enhanced protein metabolism (as in *Scenedesmus*) and glutamine biosynthesis (2 peptides). The last of the three main Chlorophyta species, *Chlorella*, was most negatively affected by warm white light, as no peptides were detected for any major category. No light and cool white light promoted the production of peptides related to photosynthesis (5 and 1 peptides, respectively), whereas amber + green light promoted carbohydrate metabolism (2 peptides).

The increase in peptide detection under warm white light and amber + green light that *Klebsormidium* suffered relative to the no light treatment is worth noting. Warm white light promoted the production pf peptides related to photosynthesis, photosynthetic electron transport and response to light stimulus (all with 2 peptides each) and amber + green triggered ATP synthesis (3 peptides), photosynthetic electron transport (1 peptide), photorespiration (1 peptide) and the Calvin cycle (1 peptide).

Discussion

In the SAB samples, the predominant taxa identified by morphological taxonomy were Chlorophyta (green algae), accounting for 81% of all taxa, and Cyanobacteriota and Streptophyta, accounting for about 12% and 6%, respectively, of the total. Although the SABs were grown in the laboratory, the planktonic stock culture of the inoculum was generated from phototrophic biofilms growing naturally on granitic facades of historic buildings in Santiago de Compostela (NW Spain), where algae were already relatively much more abundant than cyanobacteria. The predominance of algal biofilms is typical of Atlantic European regions with high rainfall and mild temperatures [38], while occasional rainfall and high temperatures, typical of e.g. Latin America, favour the dominance of cyanobacteria [39].

The most common algal genera identified by proteomics analysis were *Scenedesmus, Tetradesmus* and to a lesser extent *Chlorella,* which is consistent with the initial morphological identification. *Scenedesmus* is one of the most common freshwater algae genera but also commonly occurs as an epilithic alga on rocky substrates and building facades and monuments [40, 41]. According to the review by Macedo et al. [41], species of *Scenedesmus* have been found colonising stone monuments, like *Scenedesmus ecornis* on marble and limestone substratum. In addition, Ortega-Calvo et al. [42] isolated *Scenedesmus quadricauda* from the walls made from calcarenite (from the Puerto de Santa Maria quarry, Spain) in the Cathedral of Seville (SW Spain). *Tetradesmus* was previously considered a subgenus of *Scenedesmus* [43], and several species of *Tetradesmus* were previously classified as *Scenedesmus* species [44], which may explain the lack of specific scientific literature on the presence of *Tetradesmus* as a colonising taxa of cultural heritage structures and the complexity of the discussion regarding the presence of those genera. For example, Rifón-Lastra and Noguerol-Seoane [45] found *Scenedesmus acutus,* which is now regarded as a synonym of *Tetradesmus obliquus* [46], on the granite walls of two monuments in Lugo (Galicia, NW Spain): the Torre del Homenaje in Monforte de Lemos and the Church of Santa María in Meira. The genus *Chlorella* is, along with *Apatococcus*, *Klebsormidium* and *Trentepohlia*, the most frequent algal coloniser in the terrestrial environment [47] and is commonly found on monuments located in Europe, America, and Asia [41, 48]. However, no correlation has been established between these three algal genera and any particular substratum or climate.

When assessing the effects of the lights on the populations of the different phyla, the greatest changes in terms of relative contributions were detected after the warm white and amber + green light treatments. The spectra and colour temperatures of these types of light are furthest from the spectrum of normal sunlight, while cool white light is the most similar. The SAB communities analysed in the present study underwent an increase in cyanobacterial presence under the warm white light treatment (which has a higher proportion of red long wavelengths relative to blue short wavelengths). These findings are consistent with those obtained in benthic mesocosm experiments, in which algal communities shifted to dominance of cyanobacteria with an extended light period including long (red) wavelengths [49]. In addition, in a study of cave lampenflora, cyanobacteria were found to be more abundant in areas illuminated by warm light than by cold light, in contrast to chlorophytes, which were more abundant in areas lit by cool white light [50]. In fact, cyanobacterium absorbs blue light much less efficiently than green algae [51], thus increasing its presence with the reduction of the blue part of the spectrum of the warm white light. A relative increase in *Klebsormidium* occurred in response to illumination by warm white and amber + green lights, but to the best of our knowledge, the relative increase in the *Klebsormidium* genus under warm white and amber + green light has not been explained. The only reference found in relation to this genus and sensitivity to light spectra is the detection of a specific channel-rhodopsine photoreceptor in *Klebsormidium nitens*, which displays a maximum spectrum of action at 450 nm [52]; however, the relationship between this photoreceptor and its impact in photo-stress to changes in abundance due to nocturnal light remains unknown.

The absence of a normal photoperiod due to ornamental illumination produced substantial changes in the biofilm proteome composition depending on the light quality received. The number of peptides and proteins detected in both white light treatments was significantly lower than in the no light and the amber + green light treatments, limiting comparisons

with other treatments. The wet weight of SABs used in the study (53.42 ± 10.77 to 65.90 ± 10.46 mg) and the protein concentration determined in the samples after the extraction (1.78–2.07 µg protein. μL^{-1}) were similar and thus, the low count can possibly be attributed to protein degradation due to the damaging effects of the blue wavelengths of the white lights over the proteins. We tentatively attribute this decrease to a damaging effect of specific wavelengths (blue) on the protein structures. In a similar manner as UV light deteriorates protein structures [53], this may have been the case with the lights being tested. This damaging effect is mainly expected to occur in cells located on the surface of the SABs, with those in underlying layers being protected by the EPS and therefore being less damaged. The predicted alteration of protein structures may have prevented tryptic digestion or correct ionization of the peptides in the MS device. Such changes could explain the overall growth of the biofilms even when exposed to the lights and, at the same time, the lower number of peptides detected in the cool white total proteome sample and, to a lesser extent, in the warm white sample. Blue light exposure has been shown to increase target protein degradation due to activation of a photosensitive degradation-inducing sequence (degron) [54], which undergoes conformational changes making the degron moiety accessible for proteasomal recognition followed by degradation [55], and which is found in algae [56]. More blue light is emitted by the cool white light than by the warm white light and is absent from amber + green light, and this distribution is inversely proportional to the number of peptides detected in the algal species conforming the SABs, which could be part of the reason of the differences between the tested lights.

Nevertheless, both types of white light were compared with the amber + green light to assess the underlying mechanisms that could explain its biostatic effect. The results indicate that night-time lighting affects the proteome of organisms by altering the structure of the proteins; however, no specific signal was detected that might indicate that organisms were undergoing a stress process (considering the possible masking due to detection of small numbers of peptides). By contrast, although amber + green light produced a similar number of proteins to the control (no light) treatment, the data reflect a greater change in the distribution of proteins, with overexpression of proteins related to the photosynthetic machinery and stress management, as well as a reduction of certain proteins also found under the other lights studied.

InterPRO uses predictive models based on different databases of protein signatures to provide functional analysis of proteins by categorising them into families. This approach enables examination of proteins that are over- or under-expressed due to nocturnal illumination, starting with the identification of light stress indicators/signs. Superoxide dismutase (SOD), which catalyses the disproportionation of $O_2\bullet$- to O_2 and H_2O_2 under ROS stress, is known to vary significantly under different light regimes, exhibiting circadian oscillations with wavelength, intensity and photoperiod [57]. Asano [58] showed that manganese-SOD isolated from the microalga *Gonyaulax polyedra* (currently known as *Lingulaulax polyedra* [59]) follows a circadian rhythm, being more active during the day. However, the results of the present study are not consistent with this statement or with those of the studies carried out by Chen et al. [60] with four *Chlorella* species, in which SOD activity was higher in the longer light period. Here, we observed a reduction in Mn/Fe-SOD in response to all three illumination treatments, relative to the control (no light). From the data obtained, it is not possible to distinguish whether the reduction was due to a fluctuation in SOD during different photoperiods or whether light stress due to night illumination affected the capacity of the organisms to overcome oxidative stress.

A stress response, however, was detected via overexpression of Clp and UV responsive (UVR) proteins, particularly under amber + green light, with the ClpA/B family and UVR being significantly overexpressed relative to the levels in the other treatments. On the one hand, UVR proteins are involved in excision repair and DNA damage recognition [61]. On the other hand, ClpA (among other types of Clps) forms associations with ClpP, resulting in a Clp proteolytic complex that specifically targets damaged or misfolded proteins for translocation and degradation [62]. Nevertheless, ClpP was not overexpressed under any nocturnal light conditions tested, which was essential for chloroplast function, as its deletion prevents phototrophic growth [63]. Regardless of whether their expression is stress response-dependent or not, ATPases associated with diverse cell activities (AAA+), of which Clp A/B form a part, are related to the maintenance of proteostasis in algae and cyanobacteria, playing a role in cellular proteolytic systems [64]. To manage the oxidative stress, organisms also produce heat shock proteins (HSPs), which play important roles in cell repair and exert protective mechanisms. The results of this study indicate that the sublethal oxidative stress produced by amber + green light is sufficient to induce expression of Hsps. Moreover, the greater increase in globin-like proteins in the three ornamental lighting treatments (especially warm white and amber + green light) may also indicate some degree of oxidative stress, as globins in green algae (and a cyanoglobin in cyanobacteria) have been linked to regulation of photosynthesis and/or mitigation of oxidative damage [65].

In organisms subjected to nocturnal illumination, stress emerges in the form of photo-oxidative damage due to an imbalance between the light energy received and that which can be utilized in photosynthesis at a time when darkness is needed. The presence of antenna pigments in light-harvesting complexes (LHCs) superfamily generally

has the dual function of capturing and transferring energy for photosynthesis and dissipating the excess light that cannot be used [66] via non-photochemical quenching (NPQ). This process prevents oxidative stress, which in the case of amber + green light is due to low absorption by algal pigments (chlorophylls and carotenoids). Expression of LHC superfamily proteins and photosystem antenna protein-like is altered by ornamental illumination, indicating regulation of the night-time light to which the organisms are subjected. Chlorophyll a-b binding protein was downregulated and its abundance decreased under all of the ornamental lights tested, which could signal stress in the SABs due to the interruption of the normal photoperiod. Under changing light conditions, this protein balances the excitation energy between the two photosystems [67], which regulates light harvesting and is also involved in various types of abiotic stress. This has been demonstrated in studies of *Triticum aestivum*, in which expression of the gene coding for the light-harvesting chlorophyll a/b binding protein (TaLhc2) is downregulated by multiple types of stress [68], and of the microalgae *Tisochrysis lutea*, in which the gene lhcx2 that encodes for a protein that binds chlorophyll a and c was only expressed at night [69].

Cellular component analysis suggested changes in the PSII and PSI dependent on the type of nocturnal light that SAB organisms are exposed to. The decrease in the peptides of the PSII protein complex under amber + green light, and specifically the absence of the PsbO subunit, are particularly noteworthy. Ohnishi et al. [70] suggested that blue and green light can inactivate the water-oxidizing complex to a lesser extent than UV light, followed by red light-driven inactivation of the PSII reaction centre. The combination of amber + green LED light decreased the water-evolving complex by under-expressing proteins of the PsbO and PsbQ subunits of the PSII, but the data do not show any signs of inactivation of the PSII reaction centre, as the analyses performed only determine the number of peptides detected.

The D1 protein of the PSII is generally the primary target of photodamaging stress [71], in the form of ROS that the NPQ alternative electron pathways must manage to prevent excess damage [72, 73] and a consequent reduction in photosynthetic efficiency. The findings reported by Yokthongwattana et al. [74] strongly correlate the amount of photodamaged D1 and the HSP70B protein pool size in the alga *Dunaliella salina*, confirming the involvement of HSP70B in the PSII repair process. In the present study, the biofilm response to amber + green illumination is consistent with the response of *D. salina*, indicating the potential of the amber + green light to cause damage in phototrophic colonisation of monuments due to the increment in Hsp70 protein family. The increment in peptides D1/D2 proteins found under the exposure to warm white light and amber + green light could be attributed to the "D1 repair cycle", as this subunit is constantly replaced when exposed to light stress. This replacement requires the assistance of several auxiliary proteins, e.g. translation factors, for accurate translation during protein synthesis, or of chaperonins for correct folding of the newly formed D1 protein. In the present study, those two scenarios were clearly affected by amber + green light, as this type of light promotes the synthesis of these proteins as a repair response to the photodamage caused by the light. Light-inducible expression of the translation factor EF-Tu is a possible mechanism regulating the repair of PSII in plants and other photosynthetic organisms [75]. In fact, overexpression of EF-Tu in the cyanobacteria *Synechocystis* sp. has been shown to enhance protein synthesis and PSII repair under strong light exposure [76].

Phycocyanin beta subunit and phycobilisomes increased in abundance in the warm white light treatment, consistent with the increase in the proportion of cyanobacteria. The abundance of this photosystem antenna protein-like also increased under amber + green light, although the proportion of cyanobacterial species did not increase accordingly. This could be attributed to a mechanism of photo-oxidative stress avoidance similar to the increase in antenna pigments of green algae, as bulk accumulation of secondary carotenoids in microalgae are mostly induced by oxidative stress of cells [77]. In fact, the cyanobacterium *Spirulina* was found to produce more phycocyanin when cultivated under yellow and red light than under white, blue or green light [78].

The signs of photo-oxidative stress and the consequent alteration in the photosynthetic proteome indicate the survival strategies of the organisms, and there are no clear signs that the energy is used to obtain energy. The protein enolase (2-phospho-D-glycerate dehydroxylase), which catalyses the conversion of 2-phosphoglycerate (2-PG) to phosphoenolpyruvate (PEP) in glycolysis, decreased under all light conditions relative to the control (no light). Other stressors, e.g. hyperosmotic salt stress, have been found to decrease enolase production, while heat-shock treatment induces the production of the enzyme in the green alga *Dunaliella salina* [79]. In another study, the production of enzymes related to glycolysis in *Haematococcus pluvialis* (currently known as *Haematococcus lacustris* [80]) under oxidative stress was either upregulated or downregulated depending on the enzyme [81]. In the present study, the phosphoglycerate kinase (PGK) superfamily, which catalyses the formation of ATP to ADP and vice versa and is involved in glycolysis, was particularly strongly induced under warm white and amber + green light, unlike enolase. Liao et al. [82] showed that exposing the red alga *Pyropia haitanensis* to high light stress resulted in upregulation of one of the two isoforms of the PGK gene, which further strengthens the hypothesis that night-time illumination stresses the organisms that form SABs. This different response seems to indicate that expression of glycolysis proteins is species- and stress-dependent

and that nocturnal light stress seems to specifically downregulate enolase production in algal SABs.

Considering the GO categories by genus and the wider biological processes involving these peptides, the ornamental lights affected each genus differently. Protein metabolism was promoted under amber + green light in the case of the two most abundant genera (*Scenedesmus* and *Tetradesmus*), whereas under the other types of light, the most important categories involved photosynthesis and the glycolytic process. In an experiment with *Scenedesmus obliquus* (currently known as *Tetradesmus obliquus* [83]), light stress due to both high and low light intensities resulted in less protein and carotenoid than optimal illumination [84]. Moreover, other forms of stress are found to modify the proteome profile of *Tetradesmus*. For example, thermal stress due to growth at 34 °C caused downregulation of photosynthesis light-harvesting and an increase in the biosynthesis of polyamine (derived from aminoacid metabolism), accompanied by HSP production [85], or stress due to lack of nitrogen in media that caused downregulation of proteins related to photosynthesis and the photosynthetic machinery in *Scenedesmus acuminatus* [86] (currently known as *Tetradesmus lagerheimii* [87]).

The findings for the GO categories and *Chlorella* presented here also support the reduction in the importance of the photosynthetic protein category relative to no light and cold white light, which are consistent with the findings reported by Cecchin et al. [88]. *Chlorella* downregulated the photosynthetic apparatus (both the PSI and PSII) after acclimatation to high light stress, but no changes in carbon fixation were observed. Interestingly, the peptides for *Chlorella* identified under amber + green light fall in the GO categories for glucose and carbohydrate metabolic processes.

Conclusions

For the first time and to the best of our knowledge, proteomic changes triggered on the SABs that colonize illuminated monuments in urban areas have been reported. The taxonomic composition of the SABs examined in this study is representative of the biofilms that affect granitic monuments in NW Spain, and the proteomics analysis clearly showed that nocturnal illumination affected the proteomes of those organisms.

Impairment of the response to oxidative stress, increased production of photosystem antenna protein-like and increased protein metabolism were generally detected and indicative of an overall stress on the cells transferring their energies to different metabolic processes required to survive luminic stress. These responses were much more pronounced for amber + green light than for the other two types of ornamental lighting (cool white and warm white). Despite the lower number of protein identifications in these two treatments, we could identify a stress response derived from deregulation of the energy metabolism, PGK and Glbs. In addition, warm white light promoted the growth of cyanobacteria.

Exposure of SABs to amber + green lighting at night induces oxidative stress due to the low energy use efficiency, leading to a stress response (via HSPs and Clps, among others) and an increase in LHC superfamily to dissipate excess energy via NPQ. In turn, overexpression of LHC superfamily proteins forces organisms to maintain proteostasis through constant protein synthesis, repair and degradation, in a classic response to photooxidative stress. Energy was not effectively used for photosynthesis due to the lack of stimulation of the Calvin cycle (despite the clear stimulation of the LHCs superfamily), the lack of detection of the PsbO subunit (oxygen-evolving complex) of the PSII and the lack of overexpression of ClpP.

The study findings are of interest for designing ornamental lighting in stone heritage affected by biological colonisation and further reinforce the biostatic effect of the combinatory use of amber and green monochromatic light within preventative conservation strategies, thus reducing cleaning operations, while providing an in-depth explanation of the underlying biochemical mechanisms. Further studies with pure cultures (of *Scenedesmus, Tetradesmus* and *Klebsormidium,* most affected in the present study, and cyanobacteria) and mutant strains would be interesting because evaluation of strains and communities with different taxonomic compositions is necessary in order to establish patterns, as the response to the different types of lights differed among the taxa comprising the SABs. It should also be noted that this was a laboratory approach, so the conclusions drawn should be correlated with future experiments on architectural heritage illuminated with amber + green light.

Supplementary Information The online version contains supplementary material available at https://doi.org/10.1007/s00248-024-02465-1.

Acknowledgements This study was developed within the framework of the CROMALUX project: Third SMARTIAGO Challenge – Smart lighting system for Heritage Conservation. The authors thank Rafael Carballeira for help with morphological identification of the taxa comprising the biofilms. A. Méndez acknowledges receipt of a grant in the Programa de Doutoramento Industrial (04_IN606D_2021_2598528) financed by the Xunta de Galicia. P. Sanmartín acknowledges receipt of a Ramón y Cajal contract (RYC2020-029987-I) financed by the Spanish State Research Agency (AEI) of the Ministry of Science and Innovation (MICIN). The authors are also grateful to the Xunta de Galicia for concession of the FONTES project (ED431F 2022/14) and the Competitive Reference Group (GRC) grants ED431C 2022/09 (Gemap) and ED431C-2021/37 (Biogroup).

Author Contribution Conceptualization, A.M., P.S., S.B., A.T.-S. Data curation, A.M., S.B., A.T.-S. Formal analysis, A.M., A.T.-S. Investigation, A.M., A.T.-S. Writing—original draft, A.M., P.S., A.T.-S. Writing—review and editing, A.M., P.S., S.B., A.T.-S. Funding acquisition,

P.S. Project administration, P.S. Supervision. P.S., A.T.S. All authors have read and approved the final manuscript.

Data Availability Data are available via ProteomeXchange with identifier PXD050424. During the revision process, the data can be accessed using the following username: reviewer_pxd050424@ebi.ac.uk and password: XSSxVmrD.

Declarations

Competing Interests The authors declare no competing interests.

References

1. Marchant P, Hale JD, Sadler JP (2020) Does changing to brighter road lighting improve road safety? Multilevel longitudinal analysis of road traffic collision frequency during the relighting of a UK city. J Epidemiol Community Health 74(5):467–472. https://doi.org/10.1136/jech-2019-212208
2. Tural M, Yener C (2006) Lighting monuments: reflections on outdoor lighting and environmental appraisal. Build Environ 41:775–782. https://doi.org/10.1016/j.buildenv.2005.03.014
3. Deme L (2013) Budapest illuminated. Hung Rev 4(2):112–127
4. Carleo D, Gargiulo M, Scorpio M, Ciampi G, Corniello L, Spanodimitriou Y, Sibilio S, Chìas P, (2021) Lighting solutions to improve the valorisation and fruition of the Parque del Retiro in Madrid. IOP Conf Ser: Mater Sci Eng 1203:022083. https://iopscience.iop.org/article/10.1088/1757-899X/1203/2/022083 Accessed 23 Oct 2024
5. Méndez A, Prieto B, Aguirre i Font JM, Sanmartín P (2024) Better, not more, lighting: policies in urban areas towards environmentally-sound illumination of historical stone buildings that also halts biological colonisation. Sci Total Environ 906:167560. https://doi.org/10.1016/j.scitotenv.2023.167560
6. Kyba CCM, Altıntaş YO, Walker CE, Newhouse M (2023) Citizen scientists report global rapid reductions in the visibility of stars from 2011 to 2022. Science 379:265–268. https://www.science.org/doi/10.1126/science.abq7781 Accessed 23 Oct 2024
7. Hölker F, Bolliger J, Davies T, Giavi S, Jechow A, Kalinkat G, Longcore T, Spoelstra K, Tidau S, Visser M, Knop E (2021) 11 pressing research questions on how light pollution affects biodiversity. Front Ecol Evol 9:767177. https://doi.org/10.3389/fevo.2021.767177
8. Salata F, Golasi I, Falanga G, Allegri M, de Lieto VE, Nardecchia F, Pagliaro F, Gugliermetti F, de Lieto VA (2015) Maintenance and energy optimization of lighting systems for the improvement of historic buildings: a case study. Sustainability 7(8):10770–10788. https://doi.org/10.3390/su70810770
9. Bao Y, Ma Y, Liu W, Li X, Li Y, Zhou P, Feng Y, Delgado-Baquerizo M (2023) Innovative strategy for the conservation of a millennial mausoleum from biodeterioration through artificial light management. NPJ Biofilms Microbiomes 9:69. https://doi.org/10.1038/s41522-023-00438-9
10. Albertano P, Bisconti F, Gallon JR, Giuliani R, Graziottin F, Groth I, Mattila-Sandholm T, Moscone D, Palleschi G, Hermosín Campos G, Hernández-Mariné M, Saarela M, Saiz-Jimenez C, Sánchez-Moral S, Shroeckh V, Urzì C (2003) Cyanobacteria attack rocks (CATS): control and preventive strategies to avoid damage caused by cyanobacteria and associated microorganisms in Roman hypogean monuments. In: Saiz-Jimenez C (ed) Molecular biology and cultural heritage, Swets & Zeitlinger BV, Lisse, pp 151–162
11. Bruno L, Belleza S, Urzì C, De Leo F (2014) A study for monitoring and conservation in the Roman Catacombs of St. Callistus and Domitilla, Rome (Italy). In: Saiz-Jimenez C (ed) The conservation of subterranean cultural heritage, CRC Press/Bakelma/Taylor & Francis Group, Leiden, pp 37–44
12. Sanmartín P (2021) New perspectives against biodeterioration through public lighting. In: Joseph E (ed) Microorganisms in the deterioration and preservation of cultural heritage. Springer International Publishing, New York, pp 155–171
13. Roldán M, Oliva F, Gónzales del Valle MA, Saiz-Jimenez C, Hernández-Mariné M (2006) Does green light influence the fluorescence properties and structure of phototrophic biofilms? Appl Environ Microbiol 72:3026–3303. https://doi.org/10.1128/AEM.72.4.3026-3031.2006
14. Del Rosal Y, Muñoz-Fernández J, Celis-Plá PSM, Hernández-Mariné M, Álvarez-Gómez F, Merino S, Figueroa FL (2022) Monitoring photosynthetic activity using in vivo chlorophylla fluorescence in microalgae and cyanobacteria biofilms in the Nerja Cave (Malaga, Spain). Int J Speleol 51(1):29–42. https://doi.org/10.5038/1827-806X.51.1.2404
15. Sanmartín P, Méndez A, Carballeira R, López E (2021) New insights into the growth and diversity of subaerial biofilms colonizing granite-built heritage exposed to UV-A or UV-B radiation plus red LED light. Int Biodeterior Biodegradation 161:105225. https://doi.org/10.1016/j.ibiod.2021.105225
16. de Mooij T, de Vries G, Latsos C, Wijffels RH, Janssen M (2016) Impact of light colour on photobioreactor productivity. Algal Res 15:32–42. https://doi.org/10.1016/j.algal.2016.01.015
17. Liu XB, Koestler RJ, Warscheid T, Katayama Y, Gu JD (2020) Microbial deterioration and sustainable conservation of stone monuments and buildings. Nat Sustain 3:991–1004. https://doi.org/10.1038/s41893-020-00602-5
18. Muñoz-Fernández J, Del Rosal Y, Álvarez-Gómez F, Hernández-Mariné M, Guzmán-Sepúlveda R, Korbee N, Figueroa FL (2021) Selection of LED lighting systems for the reduction of the biodeterioration of speleothems induced by photosynthetic biofilms in the Nerja Cave (Malaga, Spain). J Photochem Photobiol B 217:112155. https://doi.org/10.1016/j.jphotobiol.2021.112155
19. Méndez A, Martín L, Arines J, Carballeira R, Sanmartín P (2022) Attraction of insects to ornamental lighting used on cultural heritage buildings: a case study in an urban area. Insects 13(12):1153. https://doi.org/10.3390/insects13121153
20. Méndez A, Maisto F, Pavlović J, Rusková M, Pangallo D, Sanmartín P (2024) Microbiome shifts elicited by ornamental lighting of granite facades identified by MinION sequencing. J Photochem Photobiol B Biol 261:113065. https://doi.org/10.1016/j.jphotobiol.2024.113065

21. Guo H, Wang L, Deng Y, Ye J (2021) Novel perspectives of environmental proteomics. Sci Total Environ 788:147588. https://doi.org/10.1016/j.scitotenv.2021.147588
22. Gorbushina AA (2007) Life on the rocks. Environ Microbiol 9:1613–1631. https://doi.org/10.1111/j.1462-2920.2007.01301.x
23. Villa F, Ludwig N, Mazzini S, Scaglioni L, Fuchs AL, Tripet B, Copié V, Stewart PS, Cappitelli F (2023) A desiccated dual-species subaerial biofilm reprograms its metabolism and affects water dynamics in limestone. Sci Total Environ 868:161666. https://doi.org/10.1016/j.scitotenv.2023.161666
24. Anderl JN, Franklin MJ, Stewart PS (2000) Role of antibiotic penetration limitation in Klebsiella pneumoniae biofilm resistance to ampicillin and ciprofloxacin. Antimicrob Agents Chemother 44:1818–1824. https://doi.org/10.1128/aac.44.7.1818-1824.2000
25. Sanmartín P, Villa F, Silva B, Cappitelli F, Prieto B (2011) Colour measurements as a reliable method for estimating chlorophyll degradation to phaeopigments. Biodegradation 22:763–771. https://doi.org/10.1007/s10532-010-9402-8
26. Ettl H, Gärtner G (1995) Syllabus der Boden-, Luft-und Flechtenalgen. Urban and Fischer, New York
27. Khaybullina LS, Gaysina LA, Johansen JR, Krautov AM (2010) Examination of the terrestrial algae of the Great Smoky Mountains National Park, USA. Fottea 10:201–215. https://doi.org/10.5507/fot.2010.011
28. Fučíková K, Flechtner VR, Lewis LA (2012) Revision of the genus *Bracteacoccus tereg* (Chlorophyceae, Chlorophyta) based on a phylogenetic approach. Nova Hedwigia 96:15–59. https://doi.org/10.1127/0029-5035/2012/0067
29. Komárek J (2013) Süsswasserflora von Mitteleuropa. Cyanoprokaryota: 3rd part: Heterocystous genera. Heidelberg, Springer Spektrum, Germany
30. Bischoff HW, Bold HC (1963) Phycological studies IV. Some soil algae from enchanted rock and related algal species. Univ Texas Publ 6318:195
31. Ministry of Industry, Trade and Tourism and the Ministry for Ecological Transition and the Demographic Challenge (2021) Proyecto de Real Decreto por el que se aprueba el reglamento de eficiencia energética en instalaciones de alumbrado exterior y sus instrucciones técnicas complementarias EA-01 a EA-08. Agencia Estatal Boletín Oficial del Estado. https://www.boe.es/buscar/doc.php?id=BOE-A-2008-18634. Accessed 25 June 2024
32. Guzmán-Fierro V, Dieguez-Seoane A, Roeckel M, Lema JM, Trueba-Santiso T (2024) Environmental proteomics as a useful methodology for early-stage detection of stress in anammox engineered systems. Sci Total Environ 912:169349. https://doi.org/10.1016/j.scitotenv.2023.169349
33. Zhang Y, Fonslow BR, Shan B, Baek MC, Yates JR (2013) Protein analysis by shotgun/bottom-up proteomics. Chem Rev 113:2343–2394. https://doi.org/10.1021/CR3003533
34. Quiton-Tapia S, Trueba-Santiso A, Garrido JM, Suárez S, Omil F (2023) Metalloenzymes play major roles to achieve high-rate nitrogen removal in N-damo communities: lessons from metaproteomics. Bioresour Technol 129476:0960–8524. https://doi.org/10.1016/j.biortech.2023.129476
35. Axelsen K, Palmgren M (1998) Evolution of substrate specificitiest in the P-type ATPase superfamily. J Mol Evol 46:84–101. https://doi.org/10.1007/PL00006286
36. Barber J (2002) Photosystem II: a multisubunit membrane protein that oxidises water. Curr Opin Struct Biol 12(4):523–530. https://doi.org/10.1016/S0959-440X(02)00357-3
37. Wilkens S, Zhang Z, Zheng Y (2005) A structural model of the vacuolar ATPase from transmission electron microscopy. Micron 36(2):109–126. https://doi.org/10.1016/j.micron.2004.10.002
38. Barberousse H, Tell G, Yéprémian C, Couté A (2006) Diversity of algae and cyanobacteria growing on buildings facades in France. Algol Stud 120:81–105. https://doi.org/10.1127/1864-1318/2006/0120-0081
39. Gaylarde CC, Gaylarde PM (2005) A comparative study of the major microbial biomass of biofilms on exteriors of buildings in Europe and Latin America. Int Biodeterior Biodegrad 55:31–139. https://doi.org/10.1016/j.ibiod.2004.10.001
40. Samad L, Adhikary S (2008) Diversity of micro-algae and cyanobacteria on building facades and monuments in India. Algae 23(2):91–114. https://doi.org/10.4490/ALGAE.2008.23.2.091
41. Macedo MF, Miller AZ, Dionísio A, Saiz-Jimenez C (2009) Biodiversity of cyanobacteria and green algae on monuments in the Mediterranean Basin: an overview. Microbiology 155:3476–3490. https://doi.org/10.1099/mic.0.032508-0
42. Ortega-Calvo JJ, Hernandez-Marine M, Saiz-Jimenez C (1991) Biodeterioration of building materials by cyanobacteria and algae. Int Biodeterior Biodegradation 28(1–4):165–185. https://doi.org/10.1016/0265-3036(91)90041-O
43. Cho HS, Lee J (2024) Taxonomic reinvestigation of the genus *Tetradesmus* (Scenedesmaceae; Sphaeropleales) based on morphological characteristics and chloroplast genomes. Front Plant Sci 15:1303175. https://doi.org/10.3389/fpls.2024.1303175
44. Turiel S, Garrido-Cardenas JA, Gómez-Serrano C, Acién FG, Carretero-Paulet L, Blanco S (2021) A polyphasic characterisation of *Tetradesmus almeriensis* sp. nov. (Chlorophyta: Scenedesmaceae). Processes 9:2006. https://doi.org/10.3390/pr9112006
45. Rifón-Lastra A, Noguerol-Seoane A (2001) Green algae associated with granite walls of monuments in Galicia (NW Spain). Cryptogam Algol 22:305–326. https://doi.org/10.1016/S0181-1568(01)01069-8
46. Guiry MD, Guiry, GM (2024). AlgaeBase. World-wide electronic publication, National University of Ireland, Galway - *Scenedesmus acutus* Meyen 1829. https://www.algaebase.org/search/species/detail/?species_id=27860. Accessed 23 Oct 2024
47. Nowicka-Krawczyk P, Komar M, Gutarowska B (2022) Towards understanding the link between the deterioration of building materials and the nature of aerophytic green algae. Sci Total Environ 802:149856. https://doi.org/10.1016/j.scitotenv.2021.149856
48. Ortega-Calvo JJ, Ariño X, Hernandez-Marine M, Saiz-Jimenez C (1995) Factors affecting the weathering and colonisation of monuments by phototrophic microorganisms. Sci Total Environ 167:329–341. https://doi.org/10.1016/0048-9697(95)04593-P
49. Stockenreiter M, Isanta Navarro J, Buchberger F, Stibor H (2021) Community shifts from eukaryote to cyanobacteria dominated phytoplankton: the role of mixing depth and light quality. Freshw Biol 66(11):2145–2157. https://doi.org/10.1111/fwb.13822
50. Popović S, Pećić M, Subakov Simić G (2022) Exploring lampenflora of Resavska cave. Serbia Biol Life Sci Forum 15(1):33. https://doi.org/10.3390/IECD2022-12425
51. Zittelli GC, Mugnai G, Milia M, Cicchi B, Benavides AS, Angioni A, Adis P, Torzillo G (2022) Effects of blue, orange and white lights on growth, chlorophyll fluorescence, and phycocyanin production of *Arthrospira platensis* cultures. Algal Res 61:102583. https://doi.org/10.1016/j.algal.2021.102583
52. Tashiro R, Sushmita K, Hososhima S, Sharma S, Kateriya S, Kandori H, Tsunoda SP (2021) Specific residues in the cytoplasmic domain modulate photocurrent kinetics of channel rhodopsin from *Klebsormidium nitens*. Commun Biol 4(1):235. https://doi.org/10.1038/s42003-021-01755-5
53. Neves-Petersen MT, Gajula GP, Petersen BS (2012) UV light effects on proteins: from photochemistry to nanomedicine. In: Saha S (ed) Molecular photochemistry – various aspects. IntechOpen, London, pp 125–158
54. Lutz AP, Renicke C, Taxis C (2016) Controlling protein activity and degradation using blue light. In: Kianianmomeni A (ed)

Optogenetics: methods and protocols. Humana Press, New Jeresy, pp 67–78
55. Wu P, Mann D (2020) Optochemical control of protein degradation. ChemBioChem 21(16):2250–2252. https://doi.org/10.1002/cbic.202000113
56. Losi A, Gärtner W (2008) Shedding (blue) light on algal gene expression. Proc Natl Acad Sci USA 105(1):7–8. https://doi.org/10.1073/pnas.0710523105
57. Barros MP, Pinto E, Sigaud-Kutner TC, Cardozo KH, Colepicolo P (2005) Rhythmicity and oxidative/nitrosative stress in algae. Biol Rhythm Res 36(1–2):67–82. https://doi.org/10.1080/09291010400028666
58. Asano CS (1998) Mecanismos controladores do ritmo endógeno diário da atividade da superóxido dismutase na alga unicelular marinha *Gonyaulax polyedra* stein (Tese Doutorado). Universidade de São Paulo, São Paulo
59. Guiry MD, Guiry, GM (2024) AlgaeBase. World-wide electronic publication, National University of Ireland, Galway - *Gonyaulax polyedra* F.Stein 1883. https://www.algaebase.org/search/species/detail/?species_id=43853. Accessed 23 Oct 2024
60. Chen W, Liu J, Chu G, Wang Q, Zhang Y, Gao C, Gao M (2023) Comparative evaluation of four *Chlorella* species treating mariculture wastewater under different photoperiods: nitrogen removal performance, enzyme activity, and antioxidant response. Bioresour Technol 386:129511. https://doi.org/10.1016/j.biortech.2023.129511
61. Van Houten B, Snowden A (1993) Mechanism of action of the *Escherichia coli* UvrABC nuclease: clues to the damage recognition problem. BioEssays 15(1):51–59. https://doi.org/10.1002/bies.950150108
62. Capestany CA, Tribble GD, Maeda K, Demuth DR, Lamont RJ (2008) Role of the Clp system in stress tolerance, biofilm formation, and intracellular invasion in Porphyromonas gingivalis. J Bacteriol 190(4):1436–1446. https://doi.org/10.1128/jb.01632-07
63. Porankiewicz J, Wang J, Clarke AK (1999) New insights into the ATP-dependent Clp protease: Escherichia coli and beyond. Mol Microbiol 32(3):449–458. https://doi.org/10.1046/j.1365-2958.1999.01357.x
64. Bouchnak I, van Wijk KJ (2021) Structure, function, and substrates of Clp AAA+ protease systems in cyanobacteria, plastids, and apicoplasts: a comparative analysis. J Biol Chem 296:100338. https://doi.org/10.1016/j.jbc.2021.100338
65. Becana M, Yruela I, Sarath G, Catalan P, Hargrove MS (2020) Plant hemoglobins: a journey from unicellular green algae to vascular plants. New Phytol 227(6):1618–1635. https://doi.org/10.1111/nph.16444
66. Schiphorst C, Bassi R (2020) Chlorophyll-xanthophyll antenna complexes: in between light harvesting and energy dissipation. In: Larkum AWD, Grossman AR, Raven JA (eds) Photosynthesis in algae: biochemical and physiological mechanisms. Springer, Berlin, pp 27–55
67. Liu XD, Shen YG (2004) NaCl-induced phosphorylation of light harvesting chlorophyll a/b proteins in thylakoid membranes from the halotolerant green alga. Dunaliella salina FEBS letters 569(1–3):337–340. https://doi.org/10.1016/j.febslet.2004.05.065
68. Han X, Han S, Li Y, Li K, Yang L, Ma D, Fang Z, Yin J, Zhu Y, Gong S (2023) Double roles of light-harvesting chlorophyll a/b binding protein TaLhc2 in wheat stress tolerance and photosynthesis. Int J Biol Macromol 253:127215. https://doi.org/10.1016/j.ijbiomac.2023.127215
69. Pajot A, Lavaud J, Carrier G, Garnier M, Saint-Jean B, Marchal L, Nicolau E (2022) The fucoxanthin chlorophyll a/c-binding protein in *Tisochrysis lutea*: influence of nitrogen and light on fucoxanthin and chlorophyll a/c-binding protein gene expression and fucoxanthin synthesis. Front Plant Sci 13:830069. https://doi.org/10.3389/fpls.2022.830069
70. Ohnishi N, Allakhverdiev SI, Takahashi S, Higashi S, Watanabe M, Nishiyama Y, Murata N (2005) Two-step mechanism of photodamage to photosystem II: step 1 occurs at the oxygen-evolving complex and step 2 occurs at the photochemical reaction center. Biochem 44(23):8494–8499. https://doi.org/10.1021/bi047518q
71. Mulo P, Sakurai I (1817) Aro EM (2012) Strategies for psbA gene expression in cyanobacteria, green algae and higher plants: from transcription to PSII repair. Biochim Biophys Acta Rev Bioenerg 1:247–257. https://doi.org/10.1016/j.bbabio.2011.04.011
72. Roach T (2020) LHCSR3-Type NPQ Prevents photoinhibition and slowed growth under fluctuating light in *Chlamydomonas reinhardtii*. Plants 9(11):1604. https://doi.org/10.3390/plants9111604
73. Saccon F, Wilson S, Morey-Burrows FS, Ruban AV (2022) Quantifying the long-term interplay between photoprotection and repair mechanisms sustaining photosystem II activity. Biochem J 479(5):701–717. https://doi.org/10.1042/BCJ20220031
74. Yokthongwattana K, Chrost B, Behrman S, Casper-Lindley C, Melis A (2001) Photosystem II damage and repair cycle in the green alga *Dunaliella salina*: involvement of a chloroplast-localized HSP70. Plant Cell Physiol 42(12):1389–1397. https://doi.org/10.1093/pcp/pce179
75. Jimbo H, Yutthanasirikul R, Nagano T, Hisabori T, Hihara Y, Nishiyama Y (2018) Oxidation of translation factor EF-Tu inhibits the repair of photosystem II. Plant Physiol 176(4):2691–2699. https://doi.org/10.1104/pp.18.00037
76. Jimbo H, Izuhara T, Hihara Y, Hisabori T, Nishiyama Y (2019) Light-inducible expression of translation factor EF-Tu during acclimation to strong light enhances the repair of photosystem II. Proc Natl Acad Sci USA 116(42):21268–21273. https://doi.org/10.1073/pnas.1909520116
77. Bouzidi NE, Grama SB, Khelef AE, Yang D, Li J (2022) Inhibition of antioxidant enzyme activities enhances carotenogenesis in microalga *Dactylococcus dissociatus* MT1. Front Bioeng Biotechnol 10:1014604. https://doi.org/10.3389/fbioe.2022.1014604
78. Bachchhav MB, Kulkarni MV, Ingale AG (2017) Enhanced phycocyanin production from *Spirulina platensis* using light emitting diode. J Inst Eng (India) E 98:41–45.
79. Ruan K, Duan J, Bai F, Lemaire M, Ma X, Bai L (2009) Function of *Dunaliella salina* (Dunaliellaceae) enolase and its expression during stress. Eur J Phycol 44(2):207–214. https://doi.org/10.1080/09670260802573105
80. Guiry MD, Guiry, GM (2024). AlgaeBase. World-wide electronic publication, National University of Ireland, Galway - *Haematococcus pluvialis* Flotow 1844. https://www.algaebase.org/search/species/detail/?species_id=27370. Accessed 23 Oct 2024
81. Wang SB, Chen F, Sommerfeld M, Hu Q (2004) Proteomic analysis of molecular response to oxidative stress by the green alga *Haematococcus pluvialis* (Chlorophyceae). Planta 220:17–29. https://doi.org/10.1007/s00425-004-1323-5
82. Liao Y, Ji D, Xu Y, Xu K, Chen C, Wang W, Xie C (2023) Cloning and functional analysis of a phosphoglycerate kinase (PhPGK) from *Pyropia haitanensis*. J Appl Phycol 35(4):1933–1943. https://doi.org/10.1007/s10811-023-03013-z
83. Guiry MD, Guiry, GM (2024). AlgaeBase. World-wide electronic publication, National University of Ireland, Galway - *Scenedesmus obliquus* (Turpin) Kützing 1833. https://www.algaebase.org/search/species/detail/?species_id=27885. Accessed 23 Oct 2024
84. Zapata LM, Jimenez Veuthey M, Zampedri PA, Flores A, Zampedri CA, Chabrillón, G (2020) Effect of light stress and concentrations of nitrogen and carbon in the production of phytonutrients in the microalga *Scenedesmus obliquus* (Chlorophyceae, Chlorococcales). J Algal Biomass Util 11(1):9–22
85. Hidehiko K (2022) Effect of temperature on growth and gene expression of *Tetradesmus* sp. for application in wastewater treatment (Master's thesis). Nord Universitet, Bodø

86. Zhang Y, Wu H, Sun M, Peng Q, Li A (2018) Photosynthetic physiological performance and proteomic profiling of the oleaginous algae *Scenedesmus acuminatus* reveal the mechanism of lipid accumulation under low and high nitrogen supplies. Photosynth Res 138:73–102. https://doi.org/10.1007/s11120-018-0549-1
87. Guiry MD, Guiry, GM (2024) AlgaeBase. World-wide electronic publication, National University of Ireland, Galway - *Scenedesmus acuminatus* (Lagerheim) Chodat 1902. https://www.algaebase.org/search/species/detail/?species_id=27857. Accessed 23 Oct 2024
88. Cecchin M, Simicevic J, Chaput L, Hernandez Gil M, Girolomoni L, Cazzaniga S, Remacle C, Hoeng J, Ivanov NI, Titz B, Ballottari M (2023) Acclimation strategies of the green alga *Chlorella vulgaris* to different light regimes revealed by physiologic and comparative proteomic analyses. J Exp Bot 74(15):4540–4558. https://doi.org/10.1093/jxb/erad170

4.2 PART 2: ASSESSMENT OF BIOSTATIC CAPACITY

4.2.4 CHAPTER 5

BIOGEOPHYSICAL IMPACT OF ALGAL BIOFILMS DEVELOPED ON GRANITE AND MORTAR SUBSTRATES UNDER NIGHT-TIME ORNAMENTAL LIGHTING

Anxo Méndez, Davide Gulotta, David M. Freire-Lista, Patricia Sanmartín

Submitted to Journal of Cultural Heritage (accepted with revisions)

JCR index (IF) 2024 = 3.3 (8/44, 83.0 percentile in Spectroscopy)

The work from this chapter, result of the scientific visit of A. Méndez in the Getty Conservation Institute (GCI), Science Department, Los Angeles (US), under supervision D. Gulotta, from August to October 2023, was also presented in an international conference and a national conference:

Méndez, A.; Gulotta, D.; Sanmartín, P. Shedding light on the impact of night-time ornamental illumination on subaerial biofilms (SABs) interaction with granite and concrete substrates. Oral communication. 5th International Congress (TechnoHeritage2024) and the 1st Biannual Meeting of the GEQP-RSEQ. 25-27 September 2024, Santiago de Compostela, Spain.

Méndez, A.; Freire-Lista, D.M.; Gulotta, D.; Sanmartín, P. Pattern and impact of algal biofilm grown under ornamental lighting on granite and cement mortar mineral components: petrographic and minero-chemical implications in the spotlight. Oral communication. XL Biennial Meeting of the Royal Spanish Society of Chemistry. 30 June-3 July 3, 2025, Bilbao, Spain. [A. Méndez was awarded with a registration fee waivers support].

Biogeophysical impact of algal biofilms developed on granite and mortar substrates under night-time ornamental lighting

Anxo Méndez[1], Davide Gulotta[2], David M. Freire-Lista[3,4,5], Patricia Sanmartín[1]

1. CRETUS, Departamento de Edafoloxía e Química Agrícola, Universidade de Santiago de Compostela, 15782 Santiago de Compostela, Spain
2. Getty Conservation Institute, Science Department, 1200 Getty Centre Drive, Los Angeles, CA, 90049, USA
3. National Center Spanish Geological Survey (CN IGME-CSIC). c/ Ríos Rosas 23, Madrid, 28003, Spain
4. Universidade de Trás-os-Montes e Alto Douro. Quinta de Prados. 5001-801 Vila Real, Portugal
5. Centro de Geociências da Universidade de Coimbra. Rua Silvino Lima. Universidade de Coimbra - Polo II. 3030-790 Coimbra, Portugal

Abstract

Ornamental LED lighting is commonly used to illuminate architectural heritage at night. Since phototrophs rely on light as an energy source through photosynthesis, the artificial extension of the natural photoperiod can impact microalgae and cyanobacteria dwelling over stone surfaces. These organisms form subaerial biofilms (SABs) which lead to biofouling of building materials and pose challenges for heritage conservation. For the first time, the present study looked in depth at what happens at the SAB-substrate interface when biofilm formation occurs under daylight followed by ornamental lighting. Granite (the main material in historical buildings and structures in NW Spain and many other regions of the world) and cement (the most widely used material for construction, especially in modern and contemporary architecture) have been used as test substrates, inhabited by algal biofilms mainly composed by the green algae *Bracteacoccus minor* and *Stichococcus bacillaris.* Tests were conducted after a 3-month exposure to different ornamental LED light conditions. The tested conditions comprised a photoperiod of 13 hours of daylight, followed by 6 hours of exposure to different ornamental LED illumination, and 5 hours of darkness (imitating the photoperiod of ornamentally illuminated monuments). The ornamental LED lighting conditions tested were an innovative amber+green light (at 3000K, with biostatic effect and under trial), two lights suitable for illuminating the urban fabric: warm white light (at 2580 K, with a yellower hue) and cool white light (at 4600 K, with bluer hue), and a reference scenario without ornamental lighting (i.e., darkness). Blank specimens without colonisation were also included. Surface roughness and hardness, VIS-light spectrophotometry, static contact angle and water absorption, as well as petrographic and 3D microscopy, were used to evaluate the lighting impact on the SABs interactions with the building material substrates. The presence of SAB increased the surface hardness, water absorption time and static contact angle while reducing the surface hardness of both the granite and mortar specimens. The SAB-substrate interface exposed to amber+green light behaved similarly to the biofouled specimens without ornamental illumination, minimizing its effects in comparison to both white lights tested which further affected those parameters. The colour differences of the surface, changed by the ornamental lighting conditions, were also minimized under the amber+green light. The results seem to indicate a lower level of SAB development under the innovative amber+green light. The petrographic microscopy performed over thin sections reveals differential SAB covering depending on the minerals in the granite surface, with the biotite minerals appearing unbiofouled. In the mortar specimens, the SAB was thinner and appeared filling the macropores. The results could be used to better ornamental lighting in cities, minimizing the development of colonizing SABs through the use of the amber+green light.

Keywords: Anthropogenic or artificial light at night (ALAN); biofouling; Subaerial biofilms; granite; cement-based mortars; outdoor built heritage; petrography.

Highlights:

- Ornamental lighting impacts the SAB-mineral interface in granite and mortar
- R_a and contact angle increase with presence of SAB
- Colour measurement indicates further development of SAB under white lights
- Mortar microstructure and granite textural heterogeneity influence SAB coverage

1. Introduction

The transition to more efficient and manageable LED technologies has increased the number of monuments illuminated at night, and the discussion on how to make outdoor monument lighting more sustainable has become more prominent (Tural and Yener, 2006; Kobav et al., 2021). Night-time ornamental lighting of historic buildings and structures is often an overlooked component in conservation management, only contemplated from an aesthetic and energy-consumption point. Hence, its effect on heritage conservation strategies, in particular in relation to the impact on biological colonisation due to phototrophs, is still uncertain (Méndez, Prieto, et al., 2024). To this date, research on ornamental lighting has been focused on improving energetic performance and decreasing CO_2 emissions (see e.g. Valdez et al., 2017), reducing the contribution of monument lighting to light pollution (see e.g. Bista et al., 2021) and to improving the aesthetic integration of light on buildings of artistic or historical importance in city centers (see e.g. Salata et al., 2015; Skandali and Whitlock Blundell, 2022). Lighting of monuments is often managed by a different set of rules than streetlight, based on aesthetic considerations and the optimization of light intensity against the reflectivity of the facade materials to be illuminated. In the case of Spanish legislation, for example, the normative also incorporates the state of conservation of the facade, considered as the degree of fouling (either biotic or abiotic) on the facade, in the decision-making about the light intensity. A higher degree of (bio)fouling results in multiplying (and thus increasing the energy consumption) the amount of light necessary for proper illuminance to account for the loss of reflectivity (Méndez, Prieto, et al., 2024). Nevertheless, it fails to address the impact that light would have when fouling is caused by living organisms, especially phototrophs, thus considering illumination as a conservation key-point. The effects of artificial lighting on the proliferation of microorganisms are a recent challenge for heritage conservation. For example, the results obtained by Bellia et al., (2025) demonstrated that coloured artificial light (460 nm, 518 nm, 594 nm, and 638 nm) used in museum exhibitions can directly affect the fungal colonisation of heritage objects (particularly animal exhibits), increasing its growth rate despite being heterotrophic organisms and thus increasing the degradation of the pieces. In underground heritage (such as show caves, mausoleums or hypogea) it is well known the role that ornamental illumination has in the proliferation of phototrophic colonisation. The growth of both phototrophic and heterotrophic organisms endangers the preservation of their cultural value through the aesthetic, chemical or physical alteration of the rocks, murals or other surfaces that are artificially illuminated (see e.g. Albertano and Bruno, 2017; Estévez et al., 2019).

Phototrophic subaerial biofilms (SABs) are mainly formed by algae and cyanobacteria and grow forming greenish stains over surfaces of heritage buildings and monuments. Being primary producers, these organisms depend on light as an energy source through photosynthesis and are affected by the use of ornamental light at night (Bao et al., 2023; Méndez, Sanmartín, et al., 2024). They form a layer over the substrate material that directly alters the petrophysical properties like surface roughness, pore structure and

water movement from the stone surface (see e.g. Miller et al., 2012). Thus, SABs could trigger a biogeophysical alteration, i.e. change of the substrate's physical properties due to the presence of the (micro)organisms over the substratum, but not necessarily because the substratum is used as the source of nutrition Nowicka-Krawczyk et al., (2022). The movement and development of organisms can weather the substratum (e.g. by penetration of the filamentous cells in pores or fissures, see Borderie et al., 2015), also through volumetric changes of the extracellular polymeric substance (EPS) matrix caused by drying-wetting cycles (Cutler and Viles, 2010). The presence of the biofilm also changes the natural moisture circulation of the stone. For example, it was found that a cyanobacterial biofilm reduced the water absorption of limestone compared to the bare surface (Schröer et al., 2022), whereas a multi-specifical algal biofilm increased the water absorption of a limestone fountain due to the excretion of gelatinous substances (Peraza Zurita et al., 2005).

In stone-built heritage, biofouling is one of the most important forms of alteration of granite substrates (ICOMOS-ISCS, 2008). Granite is the most common stone in architectural heritage in the NW of the Iberian Peninsula (see e.g Pozo-Antonio et al., 2016a; Hernandez et al., 2024), but also in other parts of Spain and in other countries like Finland, Russia, Norway, United States and South Africa, representing 15.5% of the lithologies in the Global Heritage Stone Resource (see e.g. Hannibal et al., 2020; Santi and Pereira, 2023). Additionally, cement-based mortars and concrete have been increasingly used since the 19th Century for the construction of modern and contemporary architecture and monuments (see e.g. Boichou et al., 2015; Courard et al., 2021). Due to the porosity of cement-based mortars (see e.g. Miller et al., 2012; Boichou et al., 2015) and their composition, they can be exploited as a source of nutrients by various microorganisms, thus making mortars very susceptible to microbial fouling (see e.g. Ferrari et al., 2015).

There is current debate on whether the presence of SABs can deal significant physical and/or chemical damage, besides the aesthetic impact, and even if it can provide a bioprotective role (see e.g. Favero-Longo and Viles, 2020; Berti et al., 2024). It is known that the type of substrate is fundamental in relation to the role to be adopted by the SAB. In rocks with clastic texture and high porosity (such as some sandstones and conglomerates), SAB presence has been reported to serve as a protective physical layer against weathering agents such as wind and heavy rainfall (see e.g. Favero-Longo and Viles, 2020). Pore filling in the stone surface caused by biofilms and their EPS were also observed to act as an anti-infiltration layer blocking external deteriorative agents in the Great Wall of China (Cao et al., 2023). There are also records of cementation in sandstone with iron, manganese and calcium as constituents in relation to cyanobacteria (Viles and Goudie, 2004) and biomineralization of iron by the EPS of lichens (Guglielmin et al., 2011).

The potential biodegradative, neutral or bioprotective role of algal species (main SAB-forming organisms of interest for the present study) cannot be determined *a priori*, since it strongly depends on each specific case and the complex interplay between

substrate properties, biofilm composition and the environmental microclimatic factors. Nonetheless, it is clear that some degree of biogeophysical changes occur at the substrate-SABs interface as a result of biofouling. The combination of amber (593 nm) and green (528 nm) LED light has been proposed as a tool to manage and control phototrophic colonisation of architectural heritage (Méndez, Prieto, et al., 2024), as part of the research undertaken in the CromaLux project (http://cromalux.santiagodecompostela.gal/en). Ongoing research is already demonstrating the impact of ornamental lighting on physiology and diversity of colonizing phototrophic (Méndez, Sanmartín, et al., 2024) and heterotrophic (Méndez, Maisto, et al., 2024) biofilms, but without considering how these changes affect the biofilm and its substrate as a joint system. The development of multi-specifical SABs, measured as wet biomass yield, was found to be reduced in laboratory settings after exposure to amber+green LED light in comparison to cool (4300 K) and warm (2580 K) white lights (Méndez et al., 2025). The reduction in development affected all the species comprising the SAB, maintaining their relative proportions against a control without ornamental illumination. However, it was found that the relative contribution of some species was specifically altered under amber+green light (see e.g. Méndez, Sanmartín, et al., 2024; Méndez et al., 2025), like the filamentous green algae *Klebsormidium flaccidum* or the coccoid *Ettlia sp.*

Recent focus has been put on understanding how biofilms modify the physical surface properties of natural stone (see Schröer et al., 2022), but an in-depth investigation of granite and other artificial stone-like materials, i.e., cement mortar, is still lacking. Moreover, even if the biostatic potential of the use of amber+green light has been studied, how those changes are going to affect the biofouled substrate are still unknown. Is ornamental lighting directly changing the biogeophysical properties of biofouled granite and mortar? Can ornamental lighting be used to mitigate the biodeteriorative effects of SABs, or even to reinforce the bioprotective nature of SABs over said substrates?

To answer these questions, this research aims to study the SAB-mineral substrate interface under different ornamental lighting regimens, using granite and mortar as test substrates. Several biogeophysical features like surface colour, roughness and hardness, together with contact angle and water absorption time were analyzed over colonized granite and mortar test tubes with a SAB mainly composed of the green algae *Bracteacoccus minor* and *Stichococcus bacillaris* (typically found in stone buildings of the NW of Spain). Complementary, thin sections of the specimens were studied under petrographic microscopy to image the interaction between biofilm and substrate surface.

2. Materials and methods

2.1. Natural stone and cement mortar substrates

A granite from the variety Silvestre and a cement mortar were selected as test substrates. Petrographic images can be seen in **Figure 17**.

The granite used in the current study is commercialized as Silvestre Ingemar (from Siverio Obradoiro da Pedra S.L., Spain, hereinafter referred as granite). It is fine-grained and presents an open porosity around 0.9%. The specimens were freshly quarried and showed no surface weather. Very few microcracks were observed, especially intercrystalline. On the surface the fracture network is denser due to the cut. Petrographically, it is a two-mica granodiorite with fine equigranular crystals (between 1 and 2 mm) and a dark colour. Mineralogically, it is composed of plagioclases, slightly altered to sericite and microcline, quartz, biotite, muscovite, and accessories (apatite, zircon, rutile, and opaques). Quartz (about 25%), potassium feldspar (about 27%), plagioclase (about 31%), biotite (about 9%), accessories (about 1.5%). The minerals are mostly allotriomorphic. Microcline and plagioclase have twins. Plagioclase can be perthitic and with myrmektitic growths with quartz. Muscovite and biotite are tabular. The biotite has metamorphic halos due to the decomposition of zircon.

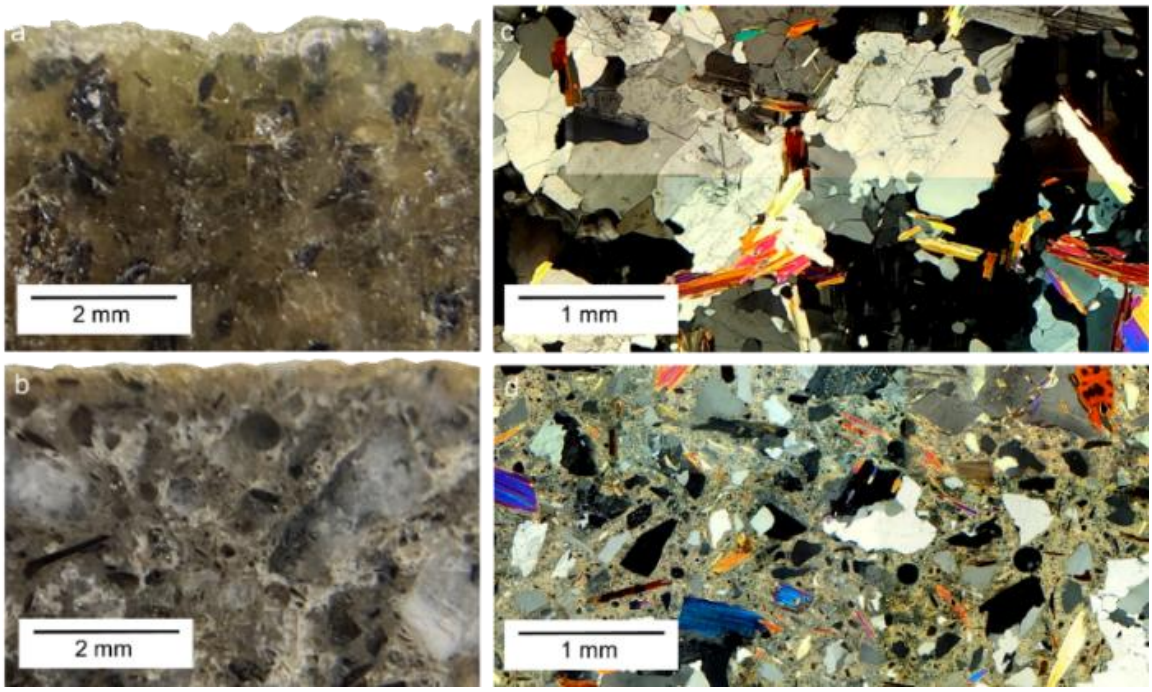

Figure 17. Macroscopic image of a) granite and b) mortar and microscopic images of c) granite and d) mortar of specimens prepared for petrographic study.

The Portland cement mortar used in this study (hereinafter referred as mortar) was prepared in accordance with the EN 197-1:2011 (European Standard, 2012). It presents an open porosity around 20%. It has a heterogeneous matrix. The binding phase (hydrated cement paste): Portlandite ($Ca(OH)_2$): Tabular or lamellar crystals formed during the hydration of tricalcium silicate (C_3S) and dicalcium silicate (C_2S). Portlandite appears with well-defined lamellae and high birefringence. Hydrated calcium silicate gel (C-S-H) appears as a dense amorphous mass in the matrix. Ettringite ($Ca_6Al_2(SO_4)_3(OH)_{12}$-$26H_2O$)

presents as acicular crystals formed during the hydration of tricalcium aluminate (C_3A) in the presence of sulphate. Ettringite is an important indicator in the analysis of possible deterioration mechanisms due to its expansive behavior or sulphate attack. The aggregates are composed of grains up to about 2 mm in size, consisting mainly of quartz sand, characterized by angular grains (about 40%), feldspar fragments (about 20%) and prismatic micas; mainly biotite, which shows halos after microscopy investigation of thin sections due to the decomposition of zircon and muscovite. The mortar has isolated spherical pores about 0.25 mm in diameter. Areas of microcracking or voids resulting from the setting or shrinkage process are observed. The texture is typically microcrystalline in the cementitious phase, with a dense and relatively compact matrix. The aggregates usually show good adhesion with the cementitious matrix.

2.2. Preparation of tests, phototrophs and experimental set-up

For this experiment, a total of 16 granite specimens and 16 mortar specimens (with a dimension of 4 cm × 4 cm × 2 cm) were prepared, on which a SAB was artificially formed by using a custom-made intermittent flow cascade, in which the specimens were maintained until the SAB formed the desired appearance. Inside the cascade, with an inclination of approximately 25º, the test specimens were subjected to 4 flows of 15 minutes each day of algal culture approximately 2 months until a mature biofilm adhered to the surface. Daylight was supplemented using a fluorescent light (Mazda Fluor Lumiere du Jour C9 TF 65, 85 W, United Kingdom) to provide a 10-hour daylight period with an intensity around 3000 lx. The specimens were periodically redistributed within the cascade to ensure that the amount of light and water was even. The cascade system was built following recommendations by Guillitte and Dreesen, (1995) and Goeres et al., (2009). Images of the flow cascade can be found in Supplementary Material (SM3). The algal culture used was based on Bold Basal Medium (BBM) (Bischoff and Bold, 1963) and the SAB was derived from natural phototrophic biofilms growing on architectural heritage built in granite of the historical centre of Santiago de Compostela (UNESCO World Heritage City since 1985, Northwest of Spain). The species comprising the culture were mainly *Bracteacoccus minor* (Schmidle ex Chodat) Petrová, *Stichococcus bacillaris* Nägeli, *Chlorella vulgaris* Beijerinck*, Scenedesmus* sp. and *Ettlia* sp. (Chlorophyta), *Klebsormidium* sp. (Charophyta), *Synechocystis* sp. and *Pseudoanabaena* sp. (Cyanobacteriota). The culture was heavily diluted in water (5-10%) before introducing it on the cascade to avoid overgrowth, being recirculated from a deposit to the cascade with a pump. Once the biofilm was formed, the specimens were distributed in 4 plastic trays (one for each condition studied) and partially immersed in deionized water up to around half their height (constant water supply in the trays ensured adequate moisture conditions for SABs viability throughout the experiment), resulting in 4 test specimens of each material in each tray. Then, the trays ware placed under artificial sunlight (SUN@HOME, Spot PAR16 40 GU10 TW 4.9 W, LEDVANCE, Germany) with an intensity of 5000 lx and a colour temperature of 5500 K, lasting for 13 hours, and followed by 6 hours of different ornamental LED lighting conditions (all set to an

intensity of 100 lx, (see MINCOTUR, 2008) and 5 hours of darkness. The ornamental lighting conditions used were: no ornamental lighting (i.e. darkness, code: L-NO) as a reference for a normal photoperiod, a cold white light (with a bluer hue, 6400 K, A5 GU10 9W, Aigostar, Spain; code: L-CW), a warm white light (with a yellower hue, 2580 K, cod. 671992, Televés S.A.U., Spain; code: L-WW) and the combination of amber+ green light (proposed to have a biostatic capacity over phototrophic colonisation, 3000 K, cod. 671990-1, Televés S.A.U., Spain; code: L-AG). An overview of the experimental set-up and the light spectra of the lights used can be found **in Figure 18**. To facilitate identification in the text, results regarding test specimens will be marked prior to the lighting code with "g" for granite and "m" for mortar. **Table 3** shows a summary of the lighting conditions and substrates used and their codification.

Table 3. Summary of the lighting conditions and codes used for the test specimens.

Substrate	Ornamental light condition	Code	Daylight			Ornamental light		
			CCT (in K)	Power (in W)	Illuminance (in Lx)	CCT (in K)	Power (in W)	Illuminance (in Lx)
Granite	Blank (No biofouling)	Blank	N.A.			N.A.		
	Reference (No ornamental light)	gL-NO	5,500	4.9	5,000	N.A.		
	Cool White	gL-CW	5,500	4.9	5,000	4300	9	100
	Warm White	gL-WW	5,500	4.9	5,000	2580	N.A.*	100
	Amber+green	gL-AG	5,500	4.9	5,000	3000	N.A.*	100
Mortar	Blank (No biofouling)	Blank	N.A.			N.A.		
	Reference (No ornamental light)	mL-NO	5,500	4.9	5,000	N.A.		
	Cool White	mL-CW	5,500	4.9	5,000	4300	9	100
	Warm White	mL-WW	5,500	4.9	5,000	2580	N.A.*	100
	Amber+green	mL-AG	5,500	4.9	5,000	3000	N.A.*	100

N.A.: Not Applicable.

*Technical specifications of the lights manufactured by Televés S.A.U. are confidential.

After a period of 3 months, the tests presented in the following subsections were performed, maintaining the specimens in the set-up for the duration of the experimentation. Prior to testing, specimens were removed from the water for two days allowing the mineral substrates (i.e., granite and mortar) to partially dry on the upper surface while maintaining SAB's humidity conditions close to natural ones, thus still adequate for SABs viability. Specimens were compared to unbiofouled blanks (code: Blank), that were conditioned according to the same protocol as the biofouled specimens. All measurements were performed in areas with comparable colonisation conditions, excluding those with irregularities in coverage.

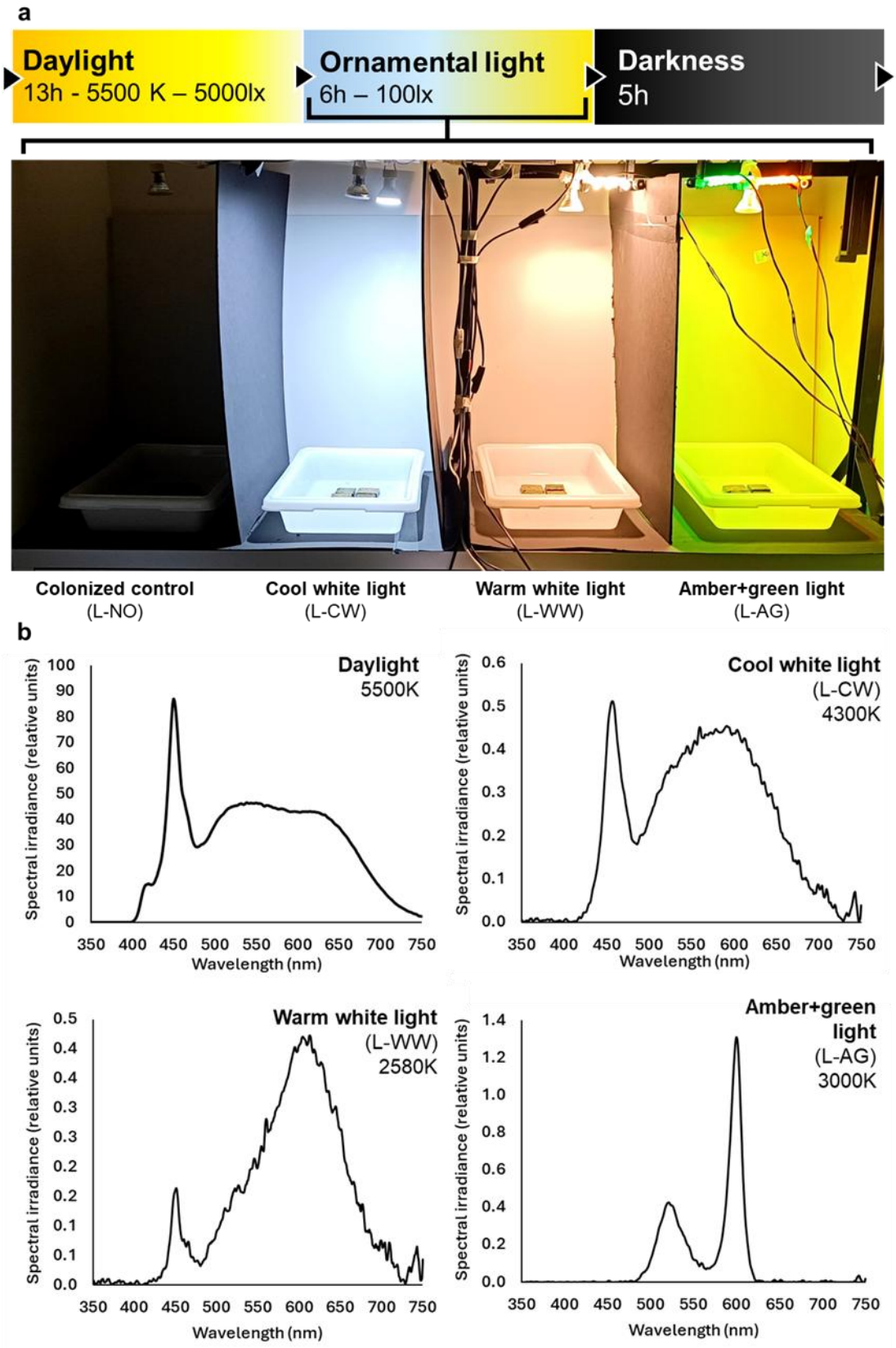

Figure 18. a) Overview of the experimental set-up, indicating the photoperiod and the codification for the ornamental lighting conditions used. b) Light spectra of the lights used.

2.3. Surface roughness and surface hardness

The surface roughness and 3D images on each specimen was measured via 3D microscopy, using a VHX-6000 digital microscope (Keyence Corp., Japan) in visible reflected light mode. 3D surfaces were reconstructed via fine depth-composition of z-stacked images in three areas for each specimen (≈1.29 cm^2) using a 100x objective. 3D images were processed for planarity correction, and the average roughness of each specimen (R_a) was then calculated from 10 linear profiles (5 vertical and 5 horizontal) per area.

Surface hardness was measured using the dynamic rebound testing method, according to Leeb. Measurements were conducted using an Equotip 550 device (Proceq, Switzerland) equipped with a C specimen (3 Nmm impact energy) following the recommendations of Desarnaud et al., (2019) for its use on heritage materials. Values are indicated as Leeb Hardness – specimen C (HLC) following the nomenclature proposed by Wilhelm, Viles, and Burke, (2016), performing 50 measurements per replicate.

2.4. Contact angle and water absorption time

The sessile drop method was applied to determine the static contact angle and water absorption time of the specimens, using a Krüss DSA100 - Drop Shape Analyzer (KRÜSS, Germany). Contact angle measurements were performed adapting the Standard BS EN 15802:2009 (European Standard, 2009) to the specific characteristics of the substrates under investigation. The contact angle is defined for the context of this paper as the first angle immediately after drop stabilization over the surface. To preserve the structure and viability of the SABs, surface polishing and drying were omitted. To ensure comparable moisture conditions for all substrates, granite and concrete specimens were removed 48 hours prior to the test from water and let to equilibrate in laboratory conditions. Water absorption time (WAT) was also measured, as the time interval between droplet release from the needle until complete absorption. To ascertain the contact angle and WAT, 20 replicates were made for each specimen using 5 µL drops of distilled water at room temperature (≈21ºC). The contact angle was analyzed with the ADVANCE software (ver. 1.16, Kruss, Germany), using the ellipse fitting method for angle determination.

2.5. Colour measurements

Colourimetric measurements were performed on the specimens (both biofouled and unbiofouled) using a CM-600D VIS-light spectrophotometer (Konica Minolta, Japan) in the 400-700 nm spectral range, equipped with an 8 mm aperture and a standard D65 illuminant at 8°. Both SCI/SCE conditions (Specular Component Included/Excluded) were recorded, but only SCI was used for the statistical analysis. The complete spectral information was acquired, and the data were elaborated according to the CIELAB or CIEL*a*b* standard colour space (European Standard, 2010). Specimens were completely wet for the colour measurements, and 16 measurements were performed in each specimen. Colour differences (ΔE^*_{ab}) were calculated according to the formula for Euclidean distance between two points in the CIELAB

space, between the biofouled specimens and the blanks and between the reference specimens and the ones under ornamental lighting. Computed pseudo-colours were calculated by transforming the CIELAB units into hex colour codes (#) by an online Colourimetric software by Nix Sensor Ltd (Hamilton, Canada) (https://www.nixsensor.com/free-Color converter/?srsltid=AfmBOorfSaC4clwfm0CNEIfDU0rQjW_nz0KGcgha71CdZq0Dw-beC2pH).

2.6. Imaging and petrographic microscopy

Images of the specimens were taken prior to experimental testing with a digital camera, using a Sony Alpha 7 II digital camera (Sony, Japan), equipped with a 35 mm full frame CMOS sensor and a FE 50mm F2.8 Macro lens. Each specimen was photographed in frontal light and raking light at an angle of approximately 35°. Colour correction was performed using Adobe Camera Raw based on a Calibrite ColorChecker Passport Photo 2 (X-Rite). Lighting conditions during all the documentation phases were kept constant using LED light illuminants.

One representative specimen from each lighting condition and substratum (granite and mortar) was selected and was embedded in bi-component epoxy resin, and thin section cuts were made from each selected specimen with a low-speed saw. The blocks were cut perpendicular to the biofouled surface. Their size was large enough to be representative of the petrographic characteristics of the rock to be studied and of the biological colonisation. The blocks were polished with sandpaper and progressively smaller diameter size of diamond spray (from 6 µm, 3 µm to 1 µm of grain diameter) to get polished thin sections. The dimensions of the thin sections were 33 ± 2 mm × 20 ± 2 mm × 0.030 ± 0.005 mm. The thin sections were observed under a polarization microscope Leica DM4500 P, equipped with a digital FireWire Camera Leica DFC 290 HD that worked with the Leica application suite software LAS 4. The standard UNE-EN 12407:2020 has been followed (European Standard, 2020).

To better understand the biological colonisation pattern by biofilms on the surface of granite and mortar, two micromosaics (parallel and cross Nicols) of each specimen of granite and mortar were analysed. These micromosaics were made with 12 microscopic images each, covering an approximate area of 0.5 cm^2. Based on petrographic observation of thin sections and the different optical properties of the minerals, with parallel and crossed Nicols, the mineralogical and textural identification of the granite and mortar was obtained. The colonisation of the biofilm in relation to the different minerals was then examined. Abbreviations for mineral names are written according to Whitney and Evans, (2010).

2.7. Statistical analysis

All variables studied exhibited a non-normal distribution according to a Kolmogorov-Smirnov test ($p \leq 0.05$). Thus, a non-parametric approach was adopted for the

statistical analysis. A Kruskal-Wallis test coupled with a post-hoc Conover's test with a Benjamini-Yekutieli adjustment ($p \leq 0.05$) was used to test differences between ornamental lighting conditions. All statistical analyses were conducted using the software R (version 4.4.2) and R Studio (version 2024.12.1+563). Boxplot graphs delimit the first and third quartiles, with the internal bar marking the median and whiskers indicating the minimum and maximum range. The values between brackets in the text reflect average and standard deviation of the same data. Boxplots were elaborated using the RWizard Software (Guisande et al., 2014).

3. Results and discussion

3.1. Surface roughness and surface hardness

Phototrophic biofouling over architectural heritage is often subjected to extended photoperiod due to ornamental illumination, being used to emphasize specific architectural and decorative features at night. It is known that extension of normal photoperiods with artificial light can enhance the biomass production of algal species, something exploited in bioreactors to increase algal biomass (see Hu et al., 2024; Amini Khoeyi et al., 2012 ; Krzemińska et al., 2014). The correlated colour temperature (CCT, i.e. measure of the light spectrum or quality of a white light, in K) also affects photosynthetic organisms as their photoreceptors react differently to the light spectra used in artificial illumination (see Bennie et al., 2016). Thus, the selection of the light spectra used in ornamental illumination can change the development of SABs, consequently affecting the SAB-mineral interface and their biogeophysical properties.

Figure 19a shows the surface roughness (R_a in µm) of the test specimens analyzed by 3D microscopy. The blank granite specimens had a higher roughness (103.75 ± 39.42 µm) than the mortar ones (47.90 ± 13.26 µm), which can be observed by illuminating the specimens in raking light conditions (**Fig. 19b**) and in more detail in the 3D microscopy images (**Fig. 19c**). In both materials, the presence of SAB has increased the measured R_a of the combined substrate-SAB system and revealed a similar pattern of response to ornamental lighting conditions. In both materials, the larger increment of surface roughness was found after exposure to cold white light (147.34 ± 43.46 µm for gL-CW and 78.93 ± 20.80 µm for mL-CW), followed by warm white light (142.01 ± 41.04 µm for gL-WW and 76.33 ± 21.01 µm for mL-WW), the reference specimens without ornamental lighting (134.82 ± 41.25 µm for gL-NO and 72.23 ± 24.97 µm for mL-WW) and finally the amber+green light (122.40 ± 34.91 µm for gL-AG and 61.02 ± 24.07 µm for mL-AG), which was lower than the reference specimens.

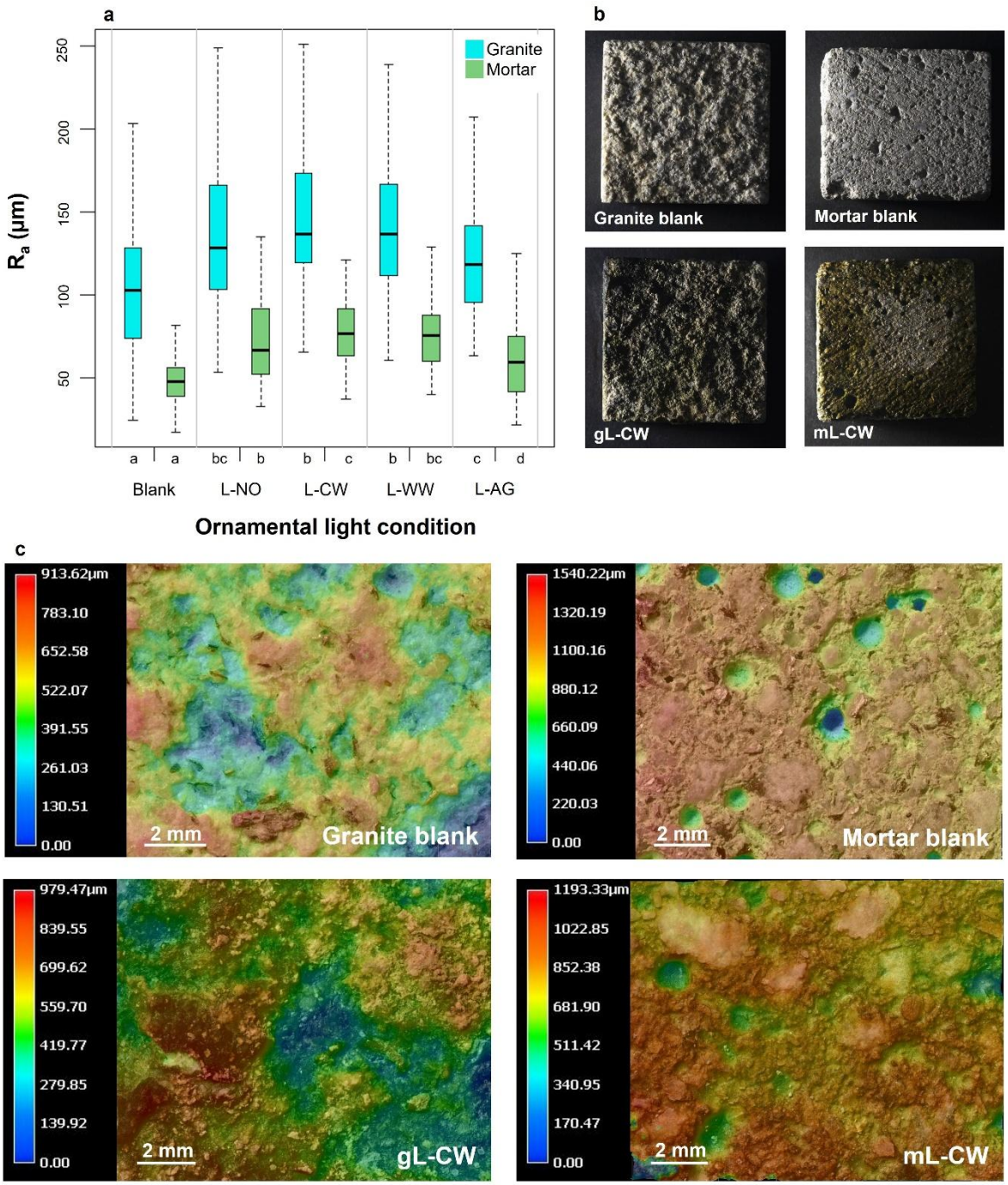

Figure 19. a) Boxplots of the R_a (in µm) for the test specimens subjected to ornamental lighting conditions. Box delimits the first and third quartile, with the internal bar marking the median. Whiskers indicate the minimun and maximum range. Different letters indicate statistical differences between ornamental light conditions in both substrates ($p<0.05$). b) Images with lateral illumination for some of the tested specimens. c) 3D Microscopy images for some of the tested specimens. The heatmap indicates variation in the R_a parameter (in µm).

Surface roughness is especially important for conservation of mineral substrates as a higher roughness can increase microbial, organic material and particle deposition (Korkanç and Savran, 2015), leading to a higher risk of physical and chemical biodeterioration (see Zanardini et al., 2000; Yan and Wang, 2024). The increase in surface roughness due to the presence of the SAB can be linked to a higher development of algal biomass caused by the ornamental lighting. For example, Kidron, (2007) shows that biocrusts in the dunes of the Negev Desert had a higher surface roughness with the increase of biocrust biomass, which in that case was mainly composed of cyanobacterial species. The surface roughness values recorded of the SAB-mineral interface after exposure to amber+green light were statistically equal, both in the granite and mortar, to those of the biofouled control specimens without ornamental illumination. The work of Yuan, Zhang, et al., (2020) stated that green light between 500–550 nm (similar to the range of the green light used for L-AG) was not suitable for cultivation of *Chlorella* sp. biofilms as green light has very limited effect in activating photosynthesis and thus potentially reducing biofilm growth compared to white light.

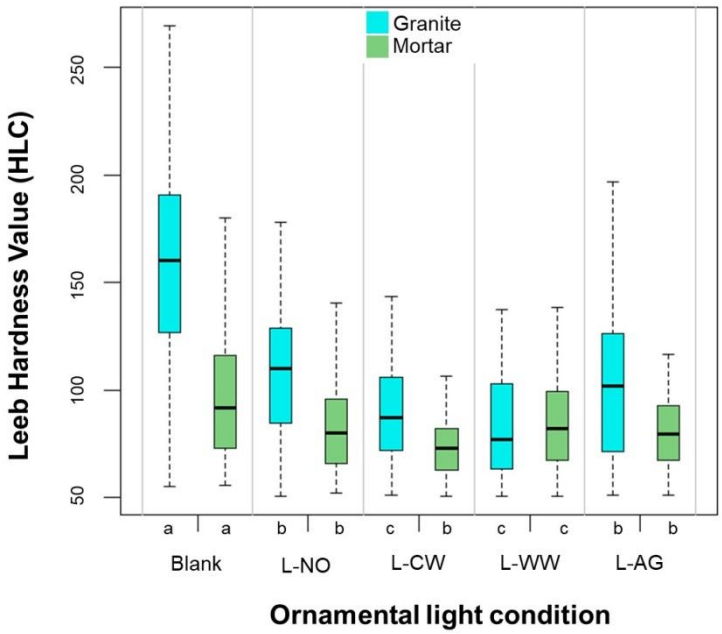

Figure 20. Boxplots of the Leeb Hardness Value (HLC) for the test specimens subjected to ornamental lighting conditions. Box delimits the first and third quartile, with the internal bar marking the median. Whiskers indicate the minimun and maximum range. Different letters indicate statistical differences between ornamental light conditions in both substrates ($p<0.05$).

Regarding surface hardness, the granite used for this study is characterized by initially higher hardness values than Portland mortar (420.65 ± 99.12 HLC for blank granite against 296.72 ± 66.36 HLC for blank mortar), as seen **in Figure 20**. In the granite specimens, gL-AG (307.79 ± 72.04 HLC) displayed the same HLC as the gL-NO reference (314.64 ± 57.42 HLC), with both the gL-CW (279.32 ± 44.80 HLC) and gL-WW (266.41 ± 45.91 HLC) lighting conditions associated with significantly reduce surface hardness

values. For the mortar specimens, both mL-WW (270.20 ± 41.09 HLC) and mL-AG (262.72 ± 35.06 HLC) had the same HLC as mL-NO (266.42 ± 41.57 HLC) and were only significantly reduced under mL-CW (245.75 ± 27.29 HLC).

The change in surface hardness was especially noticeable in the granite specimens. Similarly to the surface roughness, it can be considered that the further decrease in HLC could be linked to a higher development of the biofilm under the white lights compared to gL-NO and gL-AG. A loss in surface hardness was also found in dental cements and materials when colonized by bacterial species (Hyun et al., 2015; Barbosa et al., 2012).

To assess whether the decrease in surface hardness may indicate biodeterioration, the research conducted by Cutler et al., (2013) did not find any compelling evidence that algal fouling was linked to weathering in their study over sandstone-built churches. They found that algal fouling was associated with less weathered surfaces, potentially displaying a bioprotective effect, and that green areas had less variability in surface hardness. On the contrary, limestone headstones in a cemetery in Isle of Portland, United Kingdom displayed a lower surface hardness (measured as HLD as opposed to the present HLC) the older they were and thus indicating a higher degree of weathering (Wilhelm et al., 2016). However, those exhibiting a lichen cover not only show a lower HLD despite being as old as non-colonized ones, and they also showed a slower rate of surface hardness change that might be attributed to bioprotection.

3.2. Contact angle and water absorption time

The initial behavior of the blank substrates is remarkably different between the two blank substrates, reflecting inherent mineralogical, textural and physical differences, e.g., surface compositional heterogeneity of the granite, surface roughness or porosity of the mortar. While in granite the average angle was 1.07 ± 0.96 º, the Portland mortar absorbed the droplet so quickly that it was not possible to determine a contact angle, as seen in **Figure 21c**. The presence of SAB generally increased the contact angle of the microdroplets deposited on the surface of the test specimens (results expressed in º), as shown in **Figure 21a** and **Figure 21c**. In the biofouled granite specimens, the contact angle values obtained were similar across all lighting conditions. The same pattern was found in the biofouled mortar, although mL-WW (125.90 ± 6.31 º) condition caused a significant increase of the contact angle compared to mL-NO (115.96 ± 14.14 º).

Figure 21b shows the results obtained from the water absorption time (WAT) test (results expressed in seconds). The granite blank specimens exhibited a significantly lower WAT (16.79 ± 7.14 s) than the biofouled specimens, except the ones under gL-AG (17.39 ± 16.26 s) in which water was absorbed at the same time as the unbiofouled specimens. The highest WAT was found under gL-WW (51.02 ± 41.78 s). For the mortar specimens, the presence of the biofilm increased the WAT in relation to the blanks, in which the absorption happened almost immediately in all cases (values below 1 second). The only

lighting condition that increased significantly the WAT against the mL-NO (115.96 ± 14.14 s) was mL-WW (125.91 ± 6.31 s).

SABs produce an EPS matrix composed mainly by exopolysaccharides, proteins and nucleic acids (Pinna, 2017), among other biomolecules, that changes the hydrophillity or hydrophobycity of the substrate, which ultimately affects their wetting behaviour compared to the bare stone. The presence of SAB increased the contact angle of both test substrates, without being affected by the use of ornamental lighting (except for the concrete under warm white light that displayed a higher contact angle than the other light conditions). These results is aligned to Schröer et al., (2022), in which the presence of a cyanobacterial biofilm of *Phormidium autumnale* increased the contact angle and WAT of several sedimentary building stones compared to the bare surface. The increase in the contact angle means that the surface behaves more hydrophobic, thus reducing its wettability, of which high values are often linked to biological growth and chemical deterioration (see Magdy, 2024). The presence of SAB also caused an increase in WAT in both test substrates compared to the unbiofouled counterparts. The only exception is the amber+green light, which showed WAT results comparable to the blank granite control. Current research has found that the combinatory use of amber (593 nm) and green (528 nm) LED light (at 3000K and 20 lx) is able to significantly reduce the production of exopolysaccharides from multi-specifical algal SABs, when exposed to daylight irradiances of 2,050 lx. This reduction was caused in comparison to exposure to cool (4300 K) and warm (2580 K) white ornamental LED lighting, but also against the control without ornamental illumination, which displayed the higher amount of exopolysaccharides in the EPS matrix (Méndez et al., 2025). The EPS of biofilms enhances water retention (Seviour et al., 2019; Flemming et al., 2007), thus increasing the water absorption time, in part also due to the partial clogging of the pore structure in the surface of the substrate (see Colica et al., 2014; Fischer et al., 2010). This partial clogging, however, does not completely seal the surface and allows for water vapour permeability (Villa et al., 2023). Considering that the changes in water intake are not as drastic, the presence of biological films can be seen as positive as it reduces possible fluctuations of the substrates' moisture conditions, thus limiting the potential correlated damage mechanisms (see Berti et al., 2024).

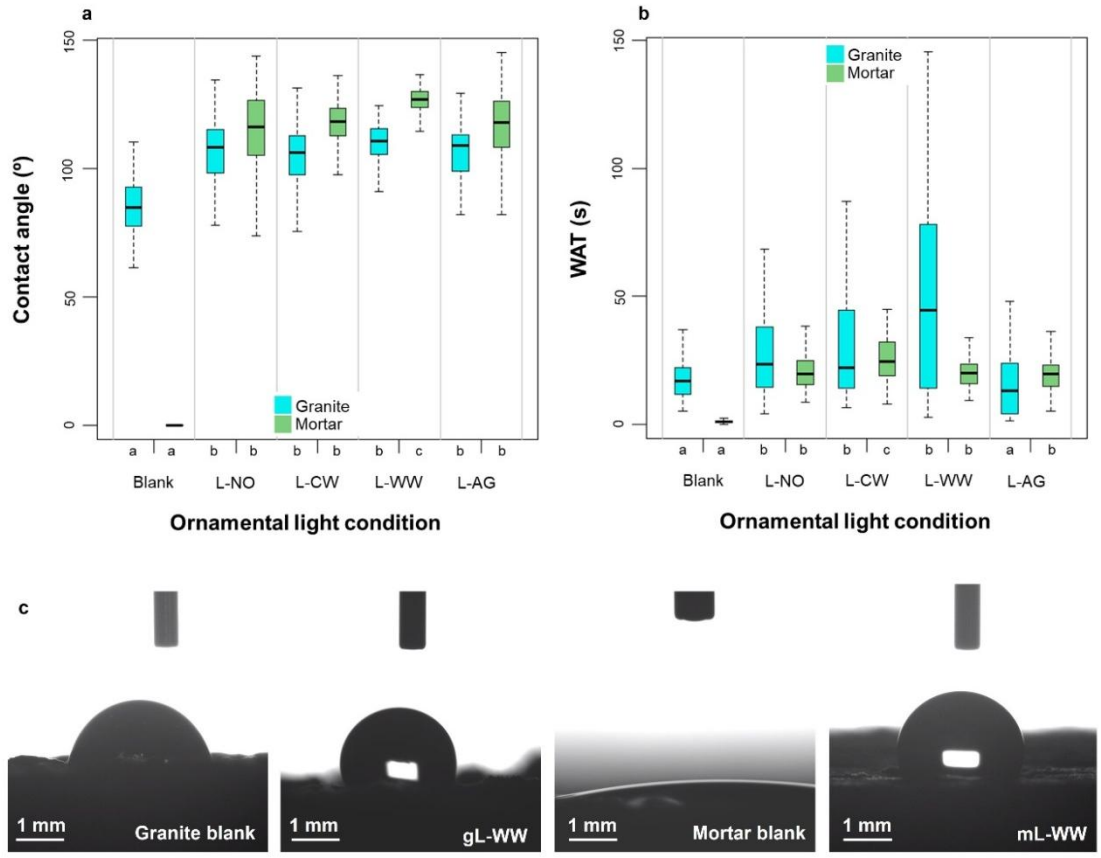

Figure 21. Boxplots of a) the contact angle in (°) and b) the water absorption time (WAT) in seconds (s) of the test specimens subjected to ornamental lighting conditions. Box delimits the first and third quartile, with the internal bar marking the median. Whiskers indicate the minimun and maximum range. Different letters indicate statistical differences between ornamental light conditions in both substrates ($p<0.05$). c) Images of the droplets at the moment of recording of the contact angle for some of the tested specimens.

3.3. Colour measurements

All lighting conditions caused significant differences in at least one of the three CIELAB parameters (L*, a*, b*) in the granite and the mortar specimens (**Table 4**). The presence of the SABs caused a reduction in L* parameter with the lowest value found in gL-WW (L*: 32.46 ± 2.53 CIELAB units) and mL-CW (L*: 34.23 ± 1.85 CIELAB units). An increase in the a* parameter is noticeable for the biofouled mortar specimens, especially in the mL-CW (a*: 6.10 ± 0.89 CIELAB units) and mL-WW (a*: 7.02 ± 0.51 CIELAB units). The changes in the colour parameters resulted in dramatic colour differences (ΔE^*_{ab}) for all conditions, all surpassing the perceptible thresholds in which the observer notices two different colours (i.e. $\Delta E^*_{ab} < 5.0$ CIELAB units, established by Mokrzycki and Maciej, (2011)), both against the blanks and the no light reference (L-NO). The only exception was found between mL-AG and mL-NO where the colour difference is not as clear ($\Delta E^*_{ab} < 3.5$ CIELAB units, established by Mokrzycki and Maciej, (2011)). The difference can be perceived with the help of the computed pseudo-colours in **Table 4** and in the reflectance graph (**Fig. 22a**), in which a reduction in reflectance for all the

wavelengths was caused by the presence of the SAB, resulting in a darker surface (**Fig. 22b**). The use of amber+green light (L-AG) resulted in a curve closer to the no light reference (L-NO) than with the use of the cool (L-CW) and warm (L-CW) white lights.

Table 4. Colour measurements (according to the CIELAB colour system) for the test specimens subjected to ornamental lighting conditions. L* refers to the lightness, a* to the variation in the red-green axis, b* to the variation in the yellow-blue axis and ΔE^*_{ab} to the colour variations.

Ornamental light condition	Substrate	L*	a*	b*	ΔE^*_{ab} (Blank)	ΔE^*_{ab} (L-NO)	Computed pseudo colour
Blank	Granite	51.69 ± 1.47 (a)	1.67 ± 0.22 (a)	11.56 ± 0.81 (a)	-	-	
	Mortar	52.33 ± 1.06 (a)	0.82 ± 0.11 (a)	7.67 ± 0.52 (a)	-	-	
L-NO	Granite	45.53 ± 3.94 (b)	1.64 ± 1.45 (a)	16.09 ± 2.58 (b)	7.65	-	
	Mortar	41.76 ± 5.48 (b)	2.98 ± 1.11 (b)	14.95 ± 2.21 (b)	15.77	-	
L-CW	Granite	34.13 ± 3.11 (c)	-0.31 ± 0.77 (b)	11.94 ± 2.15 (a)	17.68	12.29	
	Mortar	34.23 ± 1.85 (c)	6.10 ± 0.89 (c)	17.69 ± 1.15 (c)	21.35	8.60	
L-WW	Granite	32.46 ± 2.53 (d)	-1.10 ± 0.82 (c)	11.64 ± 1.86 (a)	19.43	14.08	
	Mortar	35.78 ± 1.64 (bc)	7.02 ± 0.51 (d)	19.98 ± 0.97 (d)	21.54	8.80	
L-AG	Granite	37.90 ± 3.00 (e)	0.60 ± 1.28 (d)	11.54 ± 2.43 (a)	13.83	8.94	
	Mortar	38.62 ± 4.14 (bc)	4.31 ± 1.21 (e)	14.98 ± 1.73 (b)	15.92	3.41	

L-NO: Reference; L-CW: Cool White; L-WW: Warm White; L-AG: Amber+green.

Images in **Figure 22a and 22b** show the darkening that the presence of the SAB caused to the surface compared to the blanks in both substrates. SABs in the granite had a greener appearance than the corresponding condition for the mortar. The reddish colour is indicated by a higher value of the a* parameter, being also noticeable in the displacement of a local peak that covers the 500 nm to 675 nm range (**Fig. 22a**). This peak is centred around 565 nm in the granite and around 585 nm in the mortar, in which is also wider.

The presence of algal biofouling is known to cause the darkening of materials. For example, the presence of *Chlorella vulgaris* darkened the surface of white architectural concrete and shift the colour of the concrete surface towards yellow (increase in b* parameter) (De Muynck et al., 2009). Both granite and mortar suffered a decrease in L* and an increase in b* parameters. Positive changes in b* parameter were correlated to the presence of algal biofouling in granite facades, both in terms of chlorophyll-a and dry biomass in the study of Sanmartín et al., (2012) and were used for the early detection of colonisation in architectural heritage. Thus, the increase in b* parameter can be indicative of further development of the SAB under the white lights in concrete, correlating these results with the higher R_a and lower HLC found under the white lights previously discussed. Both substrates, however, differ in the a* parameter as the biofouled granite shifted towards green under the ornamental illumination, with L-AG causing the least

greening. In contrast, the mortar shifted to a reddish colour. A decrease of a* following further colonisation was detected in cotton fabric colonized by *Chlorella vulgaris* that showed a reduction in both lightness (L*) and redness (a*) the more colonized they were (Moreno Osorio et al., 2020).

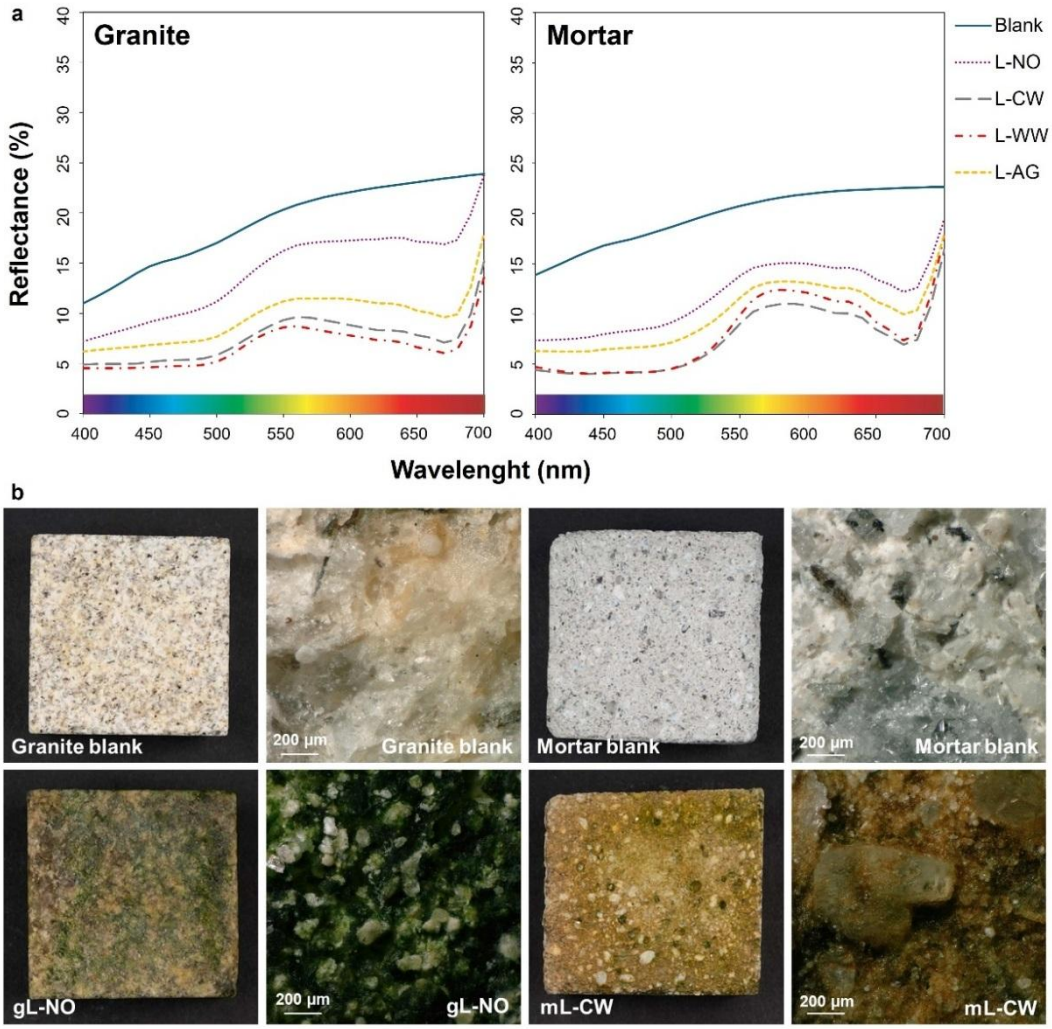

Figure 22. a) Spectral reflectance (in %) for the test specimens subjected to ornamental lighting conditions. b) Images with frontal illumination and 3D Microscopy images for some of the tested specimens.

3.4. Imaging and petrographic microscopy

Petrographic imaging of the thin sections allowed a more detailed analysis of the interactions between the SABs and the mineral surface. The full images of the thin sections can be found in Supplementary Material (SM4 and SM5).

First, thin sections allowed measurements of biofilm thickness under the different ornamental lighting conditions, which are displayed in **Figure 23**. For granite, only gL-WW (0.15 ± 0.08 mm) increased significantly the biofilm thickness in the thin sections

analysed. No differences were found in the mortar specimens. As only one thin section per specimen was prepared, the information extracted regarding biofilm thickness is limited. However, the results are coherent with the observed in previous sections. For example, gL-WW displayed the lowest surfaces hardness (HLC), the second highest R_a and the highest WAT (s) of the granite specimens, also appearing with the highest b* value in both substrates. Altogether these results seem to indicate a further development of the SABs under warm white light. The average thickness of the SABs (and thus the amount of algal biomass) was higher in the granite specimens than in the mortar, which can be explained by the higher surface roughness (R_a) of the granite used in this research. In the experiment of Murdock and Dodds, (2007) and Bergey, (2006) algal biomass increased linearly with increasing surface roughness from several materials like glass, tiles and up to stone retaining the higher algal biomass when exposed to benthic algae in a river stream. Cell adhesion is also higher on rougher surfaces (Sekar et al., 2004). The consideration of the initial surface roughness of the substrates is especially relevant to compare to said studies in river streams as the SABs in this study were developed in a flow-cabinet that deposited the cells with an intermittent flow of algal culture.

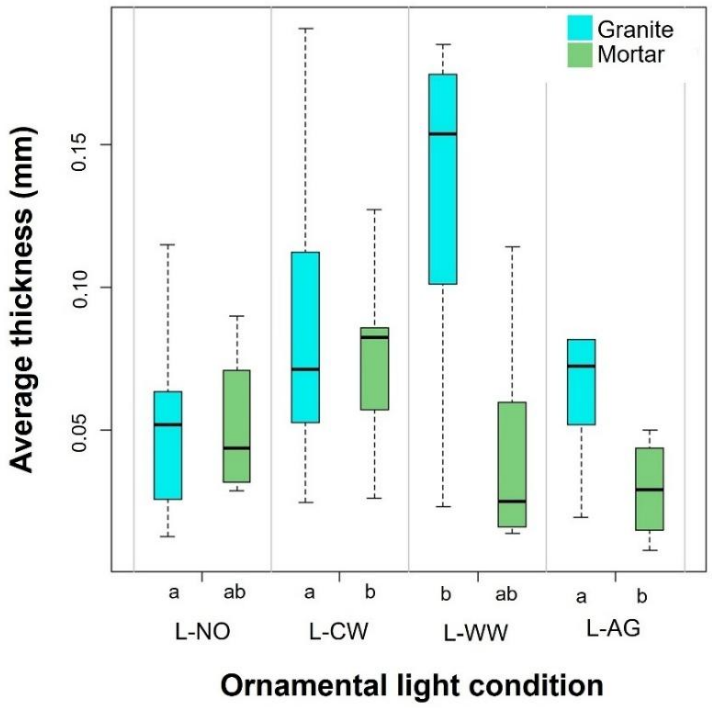

Figure 23. Boxplots of the average thickness (in mm) of the biofilm for the test specimens subjected to ornamental lighting conditions. Box delimits the first and third quartile, with the internal bar marking the median. Whiskers indicate the minimun and maximum range. Different letters indicate statistical differences between ornamental light conditions in both substrates ($p<0.05$).

Figure 24 show a selection of images of petrographic microscopy. More examples can be found in Supplementary Material (SM6 - SM10). The observations of the images of

the thin sections allowed a more detailed understanding of the interaction between the SAB and the minerals present in the substrates.

In several instances it was observed that when minerals of the biotite group were located on the surface of the thin section the SAB did not appear to cover them despite being present onto the surrounding minerals like quartz or plagioclases, according to the microscopy images taken (**Fig. 24a** and SM4). However, muscovite minerals appear to be covered with the SAB when exposed at the surface (**Fig. 24b** and SM7). In the granite specimens, the SAB appears covering all the rest of the minerals present on the surface, like quartzs, potassium feldspars and plagioclases (SM8) and the cementitious phase and aggregates of the mortar (SM5). In those minerals, the SAB appears to be filling some of the more superficial fissures (SM86b, c and e).

Superficial macropores in the mortar have a higher concentration of SAB biomass than other parts of the mortar's surface (**Fig. 24c** and SM9). Surface macropores also appear to be filled with biomass from a cyanobacterial biocrust in the sandy dunal area of the Negev Desert, which ultimately affects the water infiltration as they block approximately 40% of the surface macropores (Verrecchia et al., 1995). The presence of biofouling should greatly affect pore clogging (Kidron et al., 2020), not only by the organisms themselves, but also for the presence of EPS that drastically changes its volume with water retention. As L-AG developed the SAB less in comparison to the white lights (even having the same WAT as the unbiofouled blanks in the case of granite), a lower pore clogging may be expected and thus a lower impact on the water dynamics.

Upon further research, some secondary crystallization in the form of rhombohedral crystals growing within the SAB appeared in the specimens (**Fig. 24d** and SM10), predominantly in the mortar specimens. According to the petrographic analysis, they can be tentatively attributed to gypsum based on their habit and interference colours.

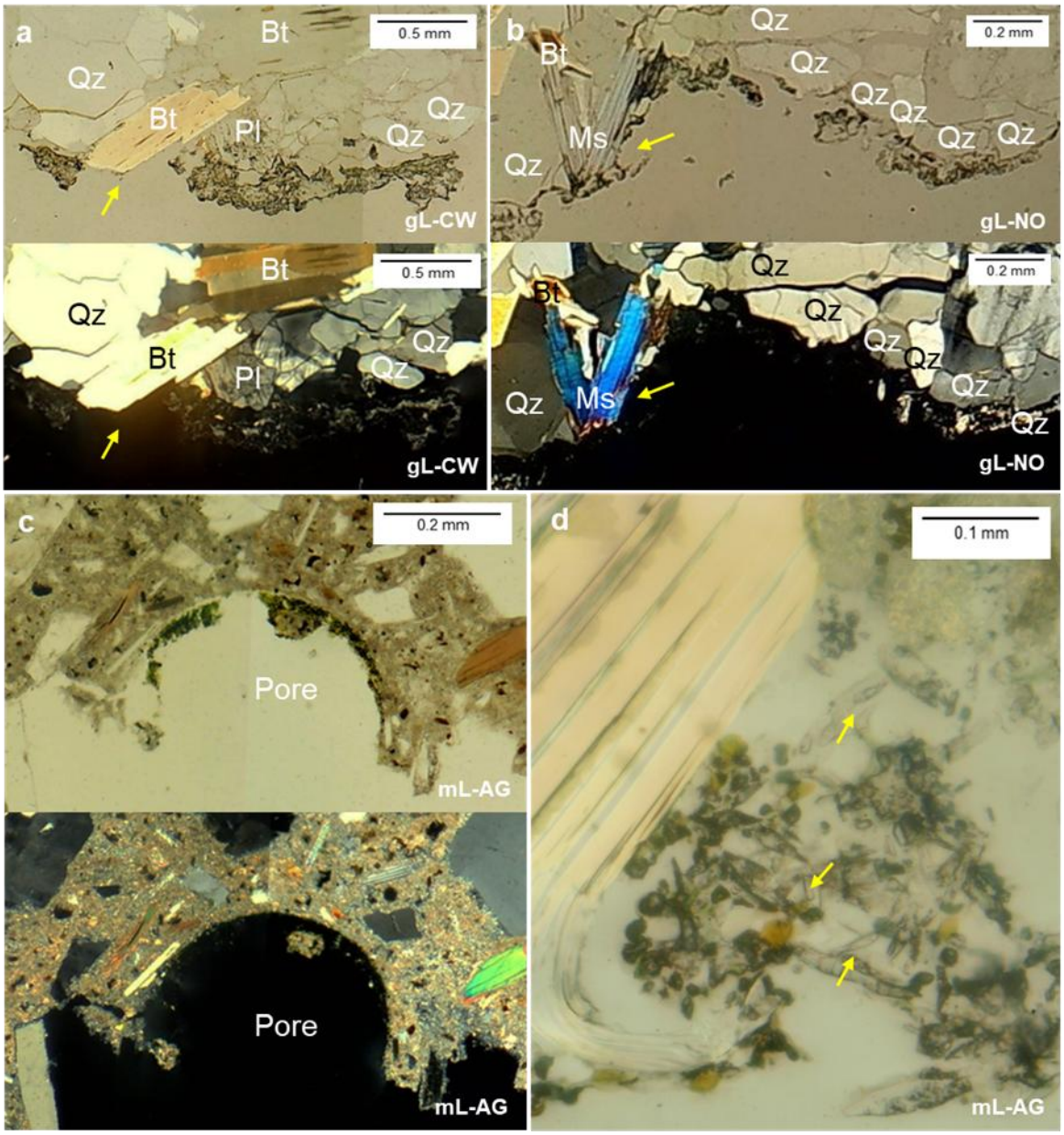

Figure 24. Details of the petrographic images. Top images are made with paralel nicols and bottom images are made woth cross nicols. Abreviations indicate the minerals. a) SAB growing over a section of a granite specimen with minerals from the biotite group, b) SAB growing over a section of a granite specimen with minerals from the moscovite group, c) Superficial pore filled with algal biomass and d) rhombohedral crystals growing into the SAB in a granite specimen. Yellow arrows indicate details in the SAB growth.

4. Conclusions

The use of ornamental lighting changes the biogeophysical properties of the biofouled specimens. The presence of SABs increased the surface roughness (R_a) and decreased the surface hardness (HLD) of the mineral substrate-SAB system, more so under the cool and warm white lights tested. The static contact angle and the water absorption time (WAT) also increased with the presence of SAB, but the use of amber+green light

caused the SAB-mineral interface to behave as the unbiofouled blanks in terms of WAT. Colour measurement also indicates that the amber+green light reduced the development of the SABs in comparison to the white lights, especially in terms of the CIELab coordinate b*. Petrographic microscopy analysis allowed a more detailed view of the interaction between the SAB with the minerals. SAB appears to cover most of the minerals in the granite and mortar, except for the minerals in the biotite group, which remain uncovered. Some secondary crystallizations were also detected growing within the SAB.

Overall, the use of amber+green light seems to minimize the development of the SAB and the subsequent changes caused by its presence over the biogeophysical properties of granite and mortar, reducing the impact caused by white light and potentially the biodeteriorative effects of algal biofouling.

Authors' contribution

Conceptualization, A.M., DG and PS.; methodology, A.M., DG, DF and P.S.; formal analysis, A.M., DG and DF.; investigation, A.M., DG, DF and P.S.; writing—original draft preparation, A.M.; writing—review and editing, DG, DF and PS.; supervision, DG and PS; project administration, P.S.; funding acquisition, DG and P.S.

4.2 PART 2: ASSESSMENT OF BIOSTATIC CAPACITY

4.2.5 CHAPTER 6

LONG-TERM VALIDATION OF THE BIOSTATIC EFFECT OF ORNAMENTAL LIGHTING ON PHOTOTROPHS: TOWARDS THE SUSTAINABLE CONSERVATION OF ARCHITECTURAL HERITAGE

Anxo Méndez, Rosa M. Crujeiras, Justo Arines, Patricia Sanmartín

Submission to the journal at the end of 2025 – beginning 2026

Long-term validation of the biostatic effect of ornamental lighting on phototrophs: Towards the sustainable conservation of architectural heritage

Anxo Méndez[1], Rosa M. Crujeiras[2], Justo Arines[3], Patricia Sanmartín[1]

1. CRETUS, Departamento de Edafoloxía e Química Agrícola, Universidade de Santiago de Compostela, 15782, Santiago de Compostela, Spain
2. CITMAga, Universidade de Santiago de Compostela, 15782, Santiago de Compostela, Spain
3. iMATUS (Instituto de Materiais), Departamento de Física Aplicada, Facultade de Óptica e Optometría, Universidade de Santiago de Compostela, 15782 Santiago de Compostela, Spain

Abstract

The bottleneck of a growth-inhibiting treatment, with biostatic (halting growth) or biocide (inactivating or killing growth) capacity, is its long-term validity. Previous research has proven the efficacy of amber+green light ornamental lighting for the halting of phototrophic colonisation of architectural heritage but is long-term efficacy on an outdoor environment is yet to be validated. This research presents the results of a 3.4-year monitorization over a growing phototrophic biofilm over a granite facade of a heritage building in Santiago de Compostela. Non-destructive techniques (PAM fluorometry and CIELAB colourimetry) were used to monitor the development of a biofilm mainly composed by the green microalga *Myrmecia irregularis* under nocturnal ornamental amber+green LED light, against a metal halide lamp (used traditionally in Santiago de Compostela) and an unilluminated control. The results show that minimum fluorescence (used as proxy for algal biomass) of the biofilms of the unilluminated control remain constant throughout the monitoring whereas increased under the ornamental lights. However, after 404 days the F_0 under amber+green light stabilized to levels like the control while the metal halide continued to increase. The ornamental illumination did not affect the quantum yield of the SABs, which followed fluctuations according with the changes in the environmental conditions through the year. Under the metal halide lamp, the surface became greener (lower a*) indicating algal development, while a* increased under the amber+green light. The abundance of *Myrmecia irregularis* increased with the metal halide lamp, being constant under the amber+green light and the control. These results seem to validate the biostatic capacity in a real outdoor monument over a long-term monitoring.

Keywords: biological colonisation; environmental monitoring; heritage conservation; LED light; Santiago de Compostela; nonparametric trend analysis; *Myrmecia irregularis*

Highlights:

- The long-term validation of the biostatic capacity was assessed in an outdoor heritage building
- Amber+green maintained the SAB development like it was not under ornamental lighting (unilluminated)
- Illumination with metal halide lamps enhance the growth of SABs
- Ornamental illumination did not affect the quantum yield of the SABs

1. Introduction

Long-term monitoring, defined as studies extending beyond three years (Bartoli et al., 2023), is essential in heritage conservation to ensure that biofouling control treatments remain sustainable over time and do not produce unintended side effects, which may not be detectable in short- or medium-term studies. For example, a 16-year monitoring of the Crypt of the Original Sin (Basilicata, Italy) show that the conservation measurements undertaken in 2001 (consisting of application of benzalkonium chloride followed by preventive conservation measures) were successful in reducing the presence and biodiversity of green and black patinas that were covering the mural paintings inside the crypt (Caneva et al., 2019).

Using the terms “long term monitoring” and “cultural heritage” in the WOS database for a bibliometric analysis, a total of 365 published peer-reviewed papers appear since 1995. It is noticeable that the annual number of scientific papers increased significantly since 2010 (**Fig. 25a**). The main research areas for long-term monitoring research in cultural heritage are Environmental Sciences (28.40%), Engineering (26.92%), Science and Technology (18.93%) and Arts and Humanities (18.04%), with Italy (23.01%), the United States (9.86%) and Spain (8.49%) leading the research.

The co-occurrence network analysis of the WOS search (Fig. 25b) identified as one of the most relevant clusters (red cluster) keywords related to biological colonisation as “biodegradation”, “biodeterioration”, “fungi” or “bacteria”, connected to terms like “long term monitoring” or “environmental monitoring”. However, terms related to phototrophic colonisation like “algae”, “cyanobacteria” or “biofilm” do not appear in the co-occurrence analysis, revealing the lack of long-term studies regarding phototrophic colonisation.

When working with heritage materials and buildings, the use of irreversible destructive sampling is limited and restricts the application of numerous analytical techniques, especially during long-term monitoring requiring continuous analysis. Thus, the use of non-destructive techniques is preferable. For example, laser-based tools can be applied for the detection of biocolonisation (Caneve et al., 2019), especially at instances when is not detectable by the naked eye or photographic and microscopy-based tools. In cases of phototrophic colonisation by microalgae and cyanobacteria forming subaerial biofilms (SABs) on building materials, the pigmentation (primarily chlorophylls and carotenoids in green algae, and also phycobiliproteins or scytonemins in cyanobacteria Caneva et al., 2008) can be used to assess the efficacy of treatments via non-destructive techniques. Colourimetric tools have also been proven effective for detecting phototrophic colonisation and estimating cyanobacterial biomass on stone surfaces (Prieto et al., 2004).

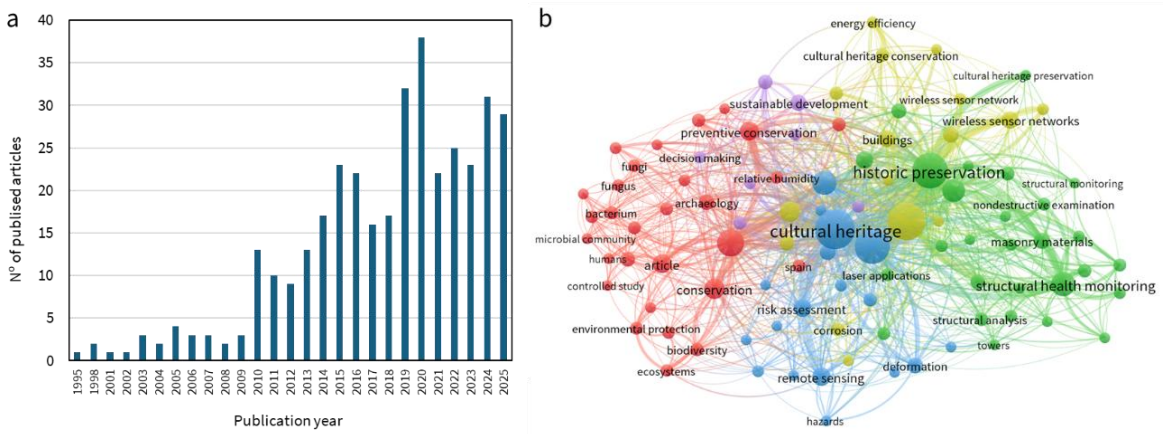

Figure 25. a) Evolution of the number of published papers from 1995 to 2025 (Source: WOS, accessed 29th July 2025); b) Co-occurrence keyword map compiled from the WOS database for the terms "long term monitoring" and "cultural heritage" from 1995 to 2025. The unit of analysis comprises all identified keywords, with a minimum of 5 co-occurrences. Node size reflects the frequency of co-occurrence with other keywords. Node colour denotes cluster membership, with each colour representing a group of keywords that tend to co-occur (Source: WOSviewer, accessed 29th July 2025).

The chlorophyll content in green algae growing on building materials can be also studied through fluorescence techniques. It was Eggert et al. (2006) who first correlated chlorophyll-a (chl-a) measured by Pulse-amplitude modulated (PAM) fluorometry as a biomass parameter for algal colonisation on anthropogenic surfaces (at chl-a concentrations between 3.5 and 20 mg m^{-2}). PAM fluorometry is a specific technique of chlorophyl fluorescence in which very short light pulses (µs range) are used to stimulate the photosystems (Schreiber, 2004), quantitatively assessing photosynthetic performance of the organism through the Kausky effect (also known as chlorophyll fluorescence induction). Since then, PAM fluorometry has been used, for example, to assess the effectiveness of several biocides on the cleaning of endolithic lichens *Acrocordia conoidea* and *Bagliettoa marmorea* on calcareous rocks (Tretiach et al., 2010), to be latter explored as a technique for cultural heritage by Osticioli et al. (2013) to study phototrophic colonisation over stone artifacts in the monumental British Cemetery of Florence (Italy). It should be noted that PAM fluorometry does not fully correlate with algal growth, as it only measures chlorophyll associated with photosystem II (PSII) (Schreiber, 2004). Nonetheless, experiments like the one performed over granite blocks colonized by a multi-specifical biofilm by Ramil et al. (2020) indeed show that the PAM parameter F_0 (minimum fluorescence) increase with the concentration of microorganisms on the granite surface, with a high linear correlation between 1.87 to 5.69 µg chl-a cm^{-2}.

This study was developed within the framework of the CROMALUX project: Third SMARTIAGO Challenge – Smart lighting system for Heritage Conservation (https://cromalux.santiagodecompostela.gal/en/), with the objective of developing a sustainable ornamental lighting system with biostatic capacity over phototrophic colonisation for the preventive conservation of architectural heritage (see (Méndez et al., 2024b). Previous research has proven the efficacy of the use of amber+green LED as a

biostatic light (i.e. halting the development of phototrophic colonisation) (see Méndez, Sanmartín, et al., 2024 Méndez et al., 2025), but its long-term efficacy in an outdoor environment is yet to be validated. Thus, the goal of this research is to test the biostatic capacity of amber+green LED light over a 3.4-year monitoring on an inner courtyard of the *Pazo de Raxoi*, a neoclassical granite palace in Santiago de Compostela (UNESCO World Heritage city since 1985 in NW Spain). To achieve this, two non-destructive techniques (colourimetric measurements and PAM fluorometry) were used to study the development of phototrophic SABs growing over granite ashlars under amber+green LED ornamental lighting, against a metal halide lamp (traditionally used for ornamental illumination in Santiago de Compostela) and unilluminated control. Nonparametric regression models were fitted in order to characterize the pattern of different parameters along time. Specifically, based on nonparametric (smooth) fits, non-effect and linearity test were performed. In addition, this nonparametric approach enables a formal comparison in order to detect statistically significant differences between the parameters of interest (F_0, QY for PAM fluorometry and L*, a*, b* and ΔE^*_{ab}) for different ornamental lighting conditions.

2. Materials and Methods

2.1.Study location and ashlar selection

The study was conducted in the historic centre of Santiago de Compostela (Galicia, NW Spain), an UNESCO World Heritage city since 1985, specifically around the Obradoiro square (*Praza do Obradoiro* in Galician) in which four of the most representative buildings of the city are located: the cathedral of Santiago de Compostela, the Hostel of the Catholic Kings (*Hostal dos Reis Católicos* in Galician), the San Xerome college (*Colexio de San Xerome* in Galician) and the Raxoi's palace (*Pazo de Raxoi* in Galician) (**Fig. 26a**). The research site was located in an inner courtyard situated between the Raxoi's palace, a neoclassical palace completed in 1766 that currently houses the city council, and the local police station. This location was chosen to minimize pedestrian interference with the study, as is closed to the public (Coordinates: UTM 537047 X,4747615 Y, Datum ETRS89; elevation, 250 m a.s.l.). The granite facades within the courtyard display heterogeneous masonry; thus, three ashlars were selected as test subjects based on their homogeneous characteristics and their north-east orientation. The lithic material corresponds to a two-mica granite sensu stricto, according to the Streckeisen ternary diagram (Streckeisen, 1976), with a coarse to medium-grained texture and ochre spots resulting from biotite oxidation. Further details regarding the ashlars can be found inMéndez, Maisto, et al. (2024). Prior to the start of the monitoring, the ashlars were mechanically cleaned using a brush and water to establish a standardized initial condition.

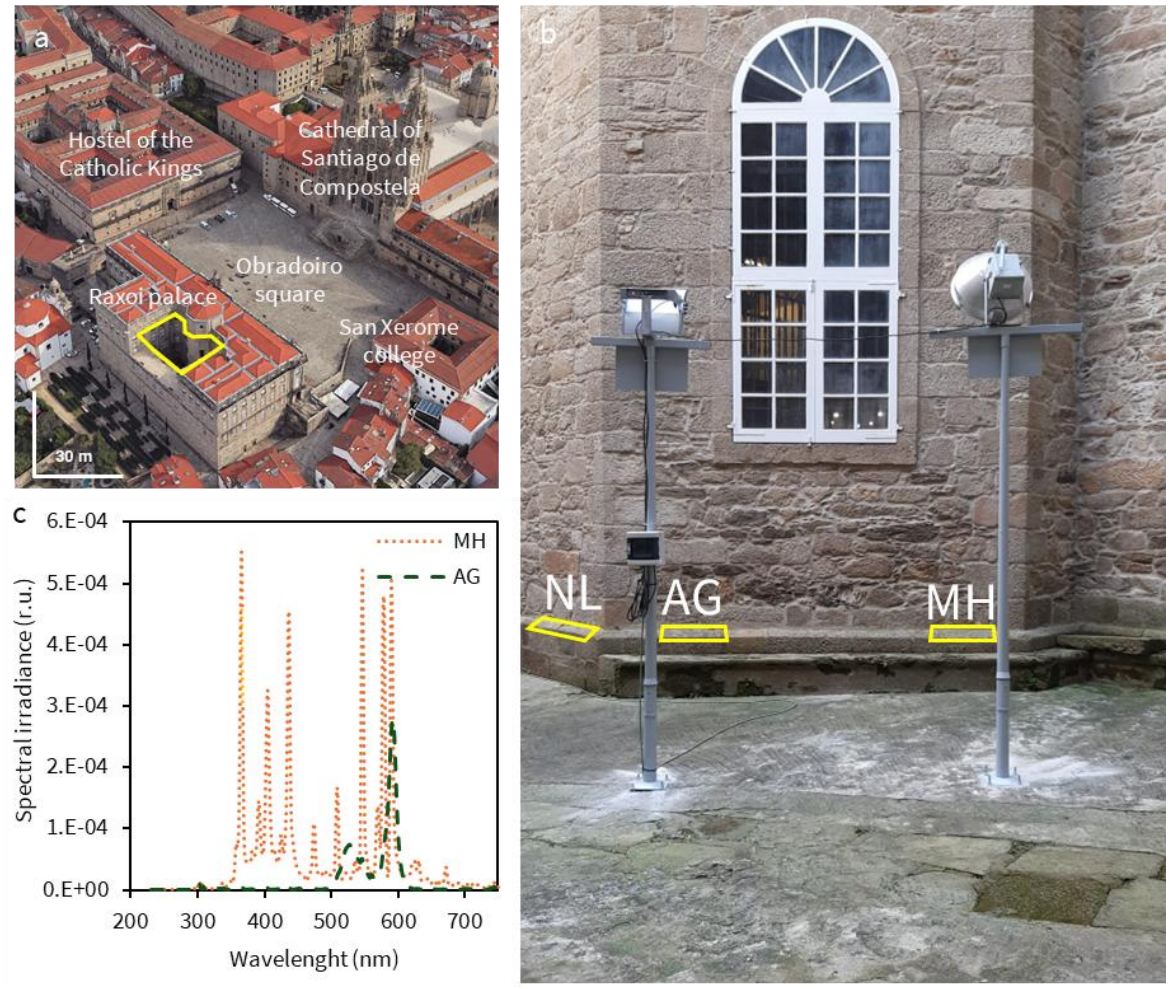

Figure 26. a) 3D aerial view of the Obradoiro square. The yellow line indicates the location of the inner courtyard of *Pazo de Raxoi* (Image modified from Google Earth); b) lighting set-up installed and location of the tested ashlars with the 3 lighting conditions: no light (NL), amber+green LED (AG) and metal halide (MH) (Image by P. Sanmartín) The yellow line indicates the ashlars used in the study; c) Light spectrum of the amber+green LED light (AG) and metal halide light (MH) over the ashlars.

2.2.Lighting set-up

The ornamental lighting set-up comprised two luminaires illuminating two of the ashlars, while a third ashlar remained unilluminated serving as a negative control (**Fig. 26b**). The luminaires were a metal halide lamp, emitting white light (4668 K, 32.00 lx, code: MH) and a novel LED emitting a combination of amber and green LED light (with a narrow spectral bandwidth) with a hypothesized biostatic effect under trial (3000 K, 18.45 lx, code: AG). The light spectrum from both light sources is shown in **Figure 26c**. The unilluminated ashlar was exposed to a nighttime ambient illuminance of 9 lx (code: NL). To prevent spectral overlap between ashlars, the luminaires were shielded. Both lighting systems were programmed to operate for five hours nightly, from 22:00 to 03:00 h. Further information of the ornamental lighting set-up can be found in (Méndez et al., 2022).

2.3.Environmental conditions

Environmental data was retrieved from the web-based repository of the Galician meteorological service www.meteogalicia.gal for the monitoring period (from June 2021 to October 2024). Data reflect monthly average values of mean air temperature (ºC, measured at 1.5 meters from the ground), relative humidity (%, measured at 1.5 meters from the ground), global monthly solar irradiation (kJ m^{-2} $day^{-1}$and sunshine hours (h). The meteorological station from which the data was obtained is located in Santiago de Compostela at the coordinates 42.87596; -8.559434 (WGS84, EPSG:4326) at an altitude of 255 meters from sea level.

2.4.Monitoring planning

The monitoring was conducted in two stages. During the first year (4th June 2021 to 13th July 2022, accounting for 404 days), biweekly measurements were performed using colourimetry and PAM fluorometry. Subsequently, the monitoring continued with measurements approximately every three months (13th July 2022 to 6th Novembre 2024, accounting for 847 days) to validate the predictions and determine whether the observed patterns persisted. A total of 31 measurements were recorded throughout the study in a period of 1251 days (approximately 3.4 years). The effect of ornamental lighting over the SABs was assess via PAM fluorometry and colour measurements. Measurements were always performed approximately between 11:00 am to 13:00 pm. In addition, the environmental conditions around the ashlars were assessed. The specifical composition in the SAB was assessed prior to the start of the experiment in May 2021, and then in February 2022 and last in February 2024.

2.4.1. PAM fluorometry

Chlorophyll a fluorescence was measured using a Handy FluorCam FC 1000-H PAM (Pulse Amplitude Modulated) imaging fluorometer (Photon Systems Instruments, Czech Republic). The monitoring was performed over the same 3 areas (around 10 x10 cm^2 each) per ashlar through the duration of the experiment. Ashlars were wetted before measurements with distilled water. A flash of non-actinic light at 640 nm was used to record minimum fluorescence (F_0), followed by a flash of saturating actinic white light at 1560 µmol s^{-1} m^{-2} to record the maximum fluorescence (F_m) used to calculate the quantum yield (QY: $(F_m-F_0)/F_m$). Chlorophyll a fluorescence in the SABs was captured without dark adaptation of the organisms, so instead of the maximum possible values it records a light-adapted F_0 (i.e. most first plastoquinone electron acceptors in the photosystems II [PSII] are oxidized), a light-adapted F_m (i.e. most electron acceptors are reduced) and consequently a light-adapted QY (i.e. percentage of PSII centres that are capable of photochemistry) (see Baker and Oxborough, 2004). The device was covered with a black cloth during measurements to avoid changes in solar illuminance that could alter the results. Only F_0 (measured in relative units) and QY (accounting for a percentage ranging from 0 to 1) were used for the statistical analysis.

2.4.2. Colour measurements

Colourimetric measurements were performed using a CM-600D VIS-light spectrophotometer (Konica Minolta, Japan) in the 400-700 nm spectral range, equipped with an 8 mm aperture and a standard D65 illuminant at 8°. Both SCI/SCE conditions (Specular Component Included/Excluded) were recorded, but only SCI was used for the statistical analysis. The data were elaborated according to the CIELAB standard colour space through the coordinates L* (lightness), a* (red-green axis) and b* (yellow-blue axis) European Standard, 2010. 60 measurements were taken during each monitoring measurement over the whole wetted surface of each ashlar, following methodological considerations from Prieto, Sanmartín, Silva, et al., (2010) and Prieto, Sanmartín, Aira, et al., (2010). The colour differences (ΔE^*_{ab}) were calculated using the formula $\Delta E^*_{ab} = \sqrt{(\Delta L^*)^2+(\Delta a^*)^2+(\Delta b^*)^2}$, were the differences ($\Delta$) in L*, a* and b* in each measurement are compared to their respective values the beginning of the monitoring at day 0 for each lighting condition.

2.4.3. Taxonomic identification

The SABs found growing over the granite walls in the inner courtyard of Raxoi's palace was mainly composed by green algae and by cyanobacteria to a lesser extent. The specific composition of the SABs from the three ashlar stones was determined at three times during the monitoring (April 2020, May 2021, February 2022 and February 2024) by collecting samples with sterile swabs in PBS buffer over areas of 10 cm² in locations of the ashlars under the different ornamental lighting conditions but without disturbing the measuring areas. The SAB samples were analysed using optical microscopy with a Nikon Eclipse E600 microscope, equipped with an E-Plan 40x objective (N.A. 0.65) and Nomarski differential interference contrast. Species identification and nomenclature primarily followed Rifón-Lastra and Noguerol-Seoane (2001), and Škaloud et al. (2018) for green algae (Chlorophyta), and Komárek (2013) for cyanobacteria (Cyanophyta/Cyanoprokaryota).

2.5.Statistical analysis

The statistical analysis carried out in this work has been focused using nonparametric regression tools for characterizing the behaviour of non-destructive techniques along time. The variables selected were F_0 and QY measured through PAM fluorometry, and L*, a*, b* and ΔE^*_{ab} through VIS-light spectrophotometry. The statistical analysis has been performed in R (v. 4.4.2, R Core Team, 2024), using package sm (Bowman and Azzalini, 2021). This package contains all the functions to run the nonparametric fits, as well as the non-effect, linearity, equality and parallelism tests.

3. Results and discussion

3.1. Environmental conditions

The environmental conditions during the monitoring period are shown in **Table 5**. Average air temperatures range from 8.53 to 21.45ºC. Lower temperatures occur in the late autumn and winter, with the lowest average monthly temperature recorded in December 2022, while the hottest month was June 2022. The relative humidity on the air ranged from 69% in January 2023 to 91% in October 2023, with the autumn months (September, October and November) recording the highest relative humidity on each year. Both the global monthly irradiation and sunshine hours increase in summer, reaching the maximum annual values around June and July and with the maximum irradiation (24560 kJ m^{-2} day^{-1}) and sunshine hours (279.52 h) recorded in June 2022. Similarly to the average temperature, the global monthly irradiation and sunshine hours record their minimum values around the end of autumn (October and November) and the beginning of winter (December).

Table 5. Average monthly values for the environmental variables retrieved from www.meteogalicia.gal. Colour gradients reflect values between the minimum (less saturated) and the maximum (more saturated). Dashed line (---) indicates the change from between the first (June 2021 – July 2022) and second stage (July 2022 – November 2024) of the monitoring.

Date	Average air temperature (ºC)	Relative humidity (%)	Global monthly irradiation (kJ m^{-2} day^{-1})	Sunshine hours (h)
JUN 2021	17.59	81	18410	169.64
JUL 2021	18.64	79	19570	218.70
AUG 2021	17.46	82	14000	168.49
SEP 2021	14.82	84	10490	159.79
OCT 2021	9.84	84	7940	155.04
NOV 2021	10.98	86	4470	96.60
DEC 2021	8.64	78	7390	161.36
JAN 2022	9.53	80	9100	136.50
FEB 2022	10.39	77	11430	138.15
MAR 2022	11.23	77	17410	182.84
APR 2022	16.09	75	19320	196.86
MAY 2022	16.58	83	17240	150.47
JUN 2022	21.45	70	24560	279.52
JUL 2022	20.58	75	21070	243.72
AUG 2022	17.53	81	14110	163.92
SEP 2022	16.18	87	8740	118.20
OCT 2022	12.06	87	5600	86.41
NOV 2022	10.95	88	4050	77.56
DEC 2022	8.53	85	5390	99.28
JAN 2023	8.72	69	11200	181.73
FEB 2023	11.39	81	11290	137.10
MAR 2023	13.84	75	16710	175.14
APR 2023	15.55	74	21570	223.98
MAY 203	18.83	79	21060	216.23
JUN 2023	18.53	80	21650	213.45
JUL 2023	19.86	78	19010	200.18
AUG 2023	18.37	84	14170	164.49
SEP 2023	16.55	84	8890	126.60
OCT 2023	12.3	91	4760	69.06
NOV 2023	9.31	89	4380	84.96
DEC 2023	10.08	86	5020	90.23
JAN 2024	10.97	86	7830	113.98
FEB 2024	9.94	85	10110	117.60
MAR 2024	13.17	72	18380	194.75
APR 2024	13.63	80	17490	158.49
MAY 2024	16.84	80	19640	182.99
JUN 2024	19.2	79	21830	225.17
JUL 2024	20.19	78	19930	216.72
AUG 2024	16.27	80	12920	139.24
SEP 2024	15.77	89	7810	104.16
OCT 2024	14.21	82	6410	115.72

3.2.PAM fluorometry

The monitoring intended to validate the biostatic capacity of the amber+green LED light (AG) against a traditional lighting technology with a white light spectrum like a metal halide lamp (MH). A control with no ornamental lighting was included to observe the development of the SAB after the mechanical cleaning without the influence of ornamental illumination (NL). The metal halide lamp was selected as is the current technology used for ornamental illumination of monuments in Santiago de Compostela (see Méndez et al., 2022).

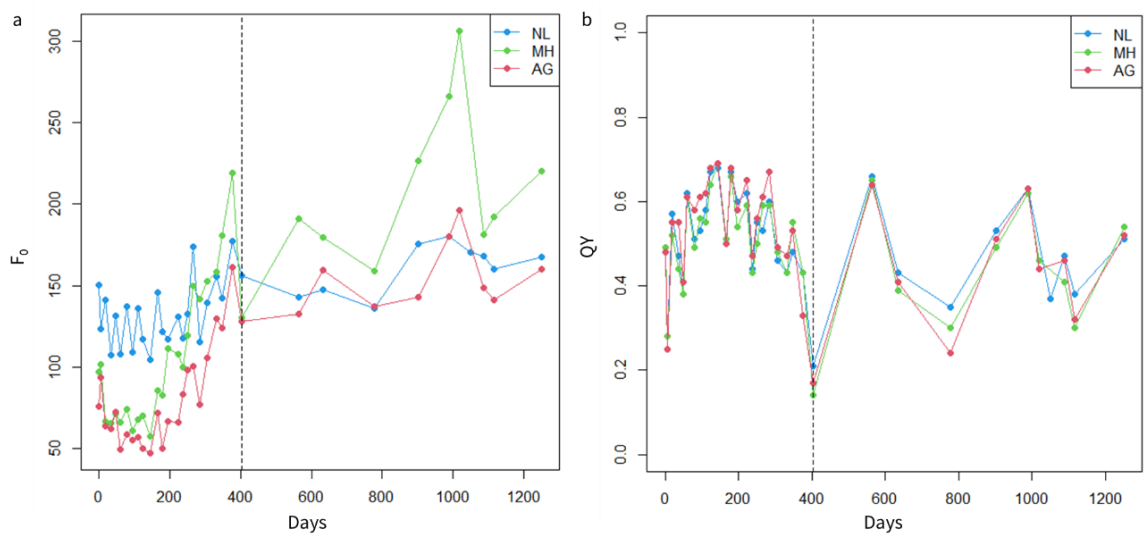

Figure 27. Representation of the a) minimum fluorescence (F_0) and b) quantum yield (QY) in the three ashlars under the studied ornamental lighting conditions during the monitoring. Dashed lines (---) mark the division between the first and second part of the monitoring at 404 days.

Figure 27 shows the variation in minimum fluorescence (F_0, **Fig. 27a**) and the quantum yield (QY, **Fig. 27b**), used as a proxy for SAB development during a long-term monitoring of 1251 days (≈ 3.4 years). Following the initial cleaning of the ashlars, the NL control exhibited higher F_0 values (F_0 = 150.27 ± 32.40) compared to both MH (F_0 = 96.95 ± 10.82) and AG (F_0 = 76.23 ± 1.95) lighting conditions.

Over the entire monitoring, F_0 increased under all lighting conditions as the no-effect hypothesis test was rejected (F_0 non-effect test *p*-value = 0.01 for NL; <0.01 for MH and <0.01 for AG). Nonetheless, the F_0 of the SAB under NL condition was constant for both stages of the monitoring (days 0 – 404. F_0 non-effect test *p*-value = 0.11; days 405 – 1251. F_0 non-effect test *p*-value = 0.12). The F_0 of the SABs under MH and AG increased non-linearly during the first stage of the monitoring (days 0 – 404. F_0 linearity test *p*-values = 0.01 for MH and 0.01 for AG), behaving linearly and increasing by 0.07 and 0.03 per day (**Fig. 27a**) and eventually reaching levels of F_0 (MH: F_0 = 130.26 ± 7.69; AG: F_0 = 127.90 ± 14.98) comparable to the NL control (155.99 ± 18.40). During the second stage of the monitoring, the F_0 continued to increase linearly (days 405 – 1251 F_0 linearity test *p*-values =

0.24 for MH and 0.21 for AG) by 0.12 per day under MH and 0.04 per day under AG (**Fig. 27a**). At the end of the monitoring period, (F_0 = 167.57 ± 24.44) and AG (F_0 = 160.28 ± 31.25) exhibited similar F_0 values, whereas MH had a higher F_0 (F_0 = 220.21 ± 22.24).

Regarding the QY (**Fig. 27b**), **t**he initial cleaning did not affect the QY prior to the monitoring, as no differences were found in terms of QY between the ashlars (QY = 0.48 ± 0.01 for all three ashlars). The QY remain constant throughout the monitoring for NL and MH (QY non-effect test *p*-value = 0.10 for NL and 0.10 for MH) but changed for AG (QY non-effect test *p*-value = 0.03) in a non-linear way (QY linear test *p*-value = 0.03).

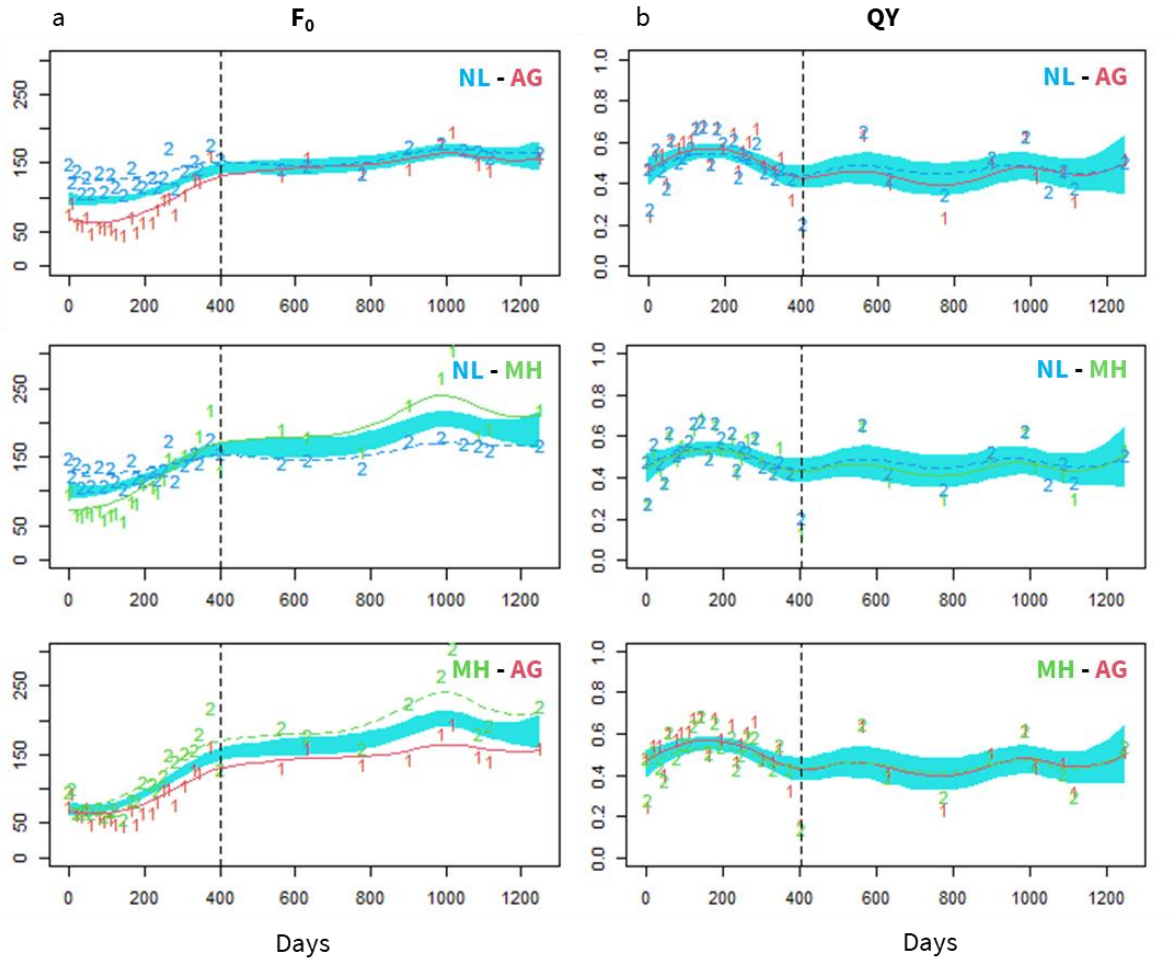

Figure 28. Equality test (non-parametric ANCOVA) test of the a) minimum fluorescence (F_0) and b) quantum yield (QY) in the three ashlars under the studied ornamental lighting conditions during the monitoring. Dashed lines (---) mark the division between the first and second part of the monitoring at 404 days.

Non-parametric ANCOVA confirmed that F_0 evolution (**Fig. 28a**) differed significantly among lighting conditions (F_0 equality test *p*-values: <0.01 for NL-AG; <0.01 for NL-MH and 0.12 for MH-AG) and that neither of the F_0 curves were parallel among lighting conditions (F_0 parallel test *p*-values = <0.01 for NL-AG; <0.01 for NL-MH and

0.12 for MH-AG). However, during the second part of the monitoring (days 404–1251), F_0 trends in NL and AG appear equal, while MH continued to increase distinctly. For QY (**Fig. 28b**), the non-parametric ANCOVA showed no differences for the QY curves for the three ashlars (QY equality test *p*-values = 0.99 for NL-AG; 1 for NL-MH and 0.99 for MH-AG).

Despite the initial differences in F_0 after the mechanical cleaning, the SABs in the ashlars increased during the monitoring. The SAB under NL maintained a constant increase of F_0 while the ones under ornamental lighting increased faster and non-linearly. However, the SABs under AG light stabilized around levels like NL while the SAB under MH continued to increase. In the work of Eyssautier-Chuine et al. (2015), the application of surface treatments against the development of algal biofouling also caused the stabilization of some of the treatments to the level of colonisation of the untreated control. For example, the application of tetraethoxysilane with only hydrophobic silica or with a low concentration of $AgNO_3$ and chitosan was not effective over limestone slabs colonized by *Chlorella vulgaris* and cause that the activity of the PSII (measured as photochemical quenching trough PAM fluorometry) reach the same values as the untreated control. Meanwhile, the combination of their proposed treatments altogether did decrease the development of the *Chlorella vulgaris* biofilm being reflected as a lower activity of the PSII. In the present work, the use of amber+green (AG) light successfully controlled the development of the SAB to levels similar to the unilluminated (NL) control, showing their long-term validity in outdoor previously shown in laboratory conditions (Méndez et al., 2025). The amber+green light has a restricted spectra only emitting in a narrow width band centred around 528 nm (green) and 593 nm (amber), while the metal halide lamp comprises the full visible light spectra, resulting in a white light with important peaks at 435 nm, 508 nm, 546 nm, 578 nm, and 589 nm (**Fig. 27b**) (Méndez et al., 2022). Ra et al. (2016) showed that liquid cultures of the several species of the green alga *Nannochloropsis* (*N. oculata, N. oceanica,* and *N. salina*) had a higher growth after 21 days under white, fluorescent light than under green LED light (at 520 nm), and that the use of yellow LED light (at 640 nm) yielded the same results as the white fluorescence. However, they found that the illumination with blue LED light (at 465 nm) yielded the highest biomass followed by red LED light (660 nm), both wavelengths being emitted by the metal halide lamp but absent in the amber+green LED. In bioreactors with the green alga *Chlorella vulgaris* and the cyanobacteria *Gloeothece membranacea* the dry biomass production was higher under white LED light than under orange LED light (peaking around 590 nm) for *C. vulgaris,* but the orange light increased the biomass for *G. membranacea* (Mohsenpour and Willoughby, 2013). Similar results with cyanobacteria were found by Chini Zittelli et al. (2022) were the cyanobacteria *Arthrospira platensis*, were the use of orange LED light (at 615 nm) produced a higher biomass than under white LED light after 5 days in a liquid culture.

The QY did not changed with the application of ornamental light at night (either MH or AG) and the unilluminated control. Zhang et al. (2019) applied different photoperiods of white LED light over algal biofilms of *Nannochloris oculata, Chlorella* sp. and *Chlorella*

pyrenoidosa, either in intermittent pulses ranging from 3 seconds to 30 minutes, or with photoperiods of 12 hours light follow by 12 hours of darkness or continuous illumination. Except from the 3 seconds pulses, none of the photoperiods affected the maximum quantum yield of the biofilms of neither of the species, despite causing changes in the final biomass after 6-day cultivation. As the QY remained unchanged in all lighting conditions, it solidifies that the changes observed in F_0 were due to changes in biomass and no other factor causing stress that would affect the QY in green algae like nutrient stress (Parkhill et al., 2001), stress due to high irradiance (Smith et al., 1990) or hydric stress (Gray et al., 2007).

However, the QY in this study did change throughout the monitoring in all lighting conditions (**Fig. 28b**) as reflected by the non-effect test. The QY values were lower around the summer months (ranging around 0.2 to 0.4 in July depending on the measurement) and increasing towards the normal values of quantum yield of green algae (0.6 to 0.7, see Schuurmans et al., 2015), which are the main component of the SABs under study, around November to January (depending on the measurement). As shown in **Table 5**, the months were the QY increase during the months with the lower temperatures and high relative humidities, being subjected to the low solar irradiation and lower sunlight hours from those months. The same pattern was found in populations of the red alga *Cystoseira tamariscifolia* were maximum quantum yield (measured though PAM fluorometry) decreased to lower levels in the summer months (around 0.4 of QY) than in the fall–winter months (around 0.6 of QY) (Abdala-Díaz et al., 2006). Contrary to those findings, algal biofilms (mainly composed by the red microalga *Cyanidium* sp.) colonizing the interior of the Nerja Cave in Málaga (Spain) and illuminated for its visit with low-pressure fluorescent lamps (with a CCT of 4845 K and 1030 lumens) displayed higher light-adapted quantum yields during the summer (Del Rosal et al., 2021). However, this might be related to the lower illuminance that the artificial lighting (its only light source) is providing compared to natural sunlight. Indeed, Wang et al. (2021) showed that cultured biofilms of *Chlorella* sp. (grown at 25 ºC and continuous irradiance from white LEDs) under light intensities below 100 μmol m^{-2} s^{-1} had a quantum yield value above 0.65, but started to decrease under 200 μmol m^{-2} s^{-1} bellow 0.60 and until reaching 0.43 μmol m^{-2} s^{-1} at 400 μmol m^{-2} s^{-1}, indicating signs of light-related stress.

3.3. Colour measurements

Figure 29 shows the evolution of the colour parameters during the monitoring. Lightness (L*, **Fig. 29a**) values were similar between the three ashlars after the mechanical cleaning (L* = 46.89 ± 1.70 CIELAB units) and decreased under the all-lighting conditions during the first stage of monitoring (days 0 – 404. L* non-effect test *p*-values = 0.02 for NL; 0.02 for MH and 0.02 for AG), to then remain constant until the end of the monitoring (days 405 – 1251. L* non-effect test *p*-values = 0.30 for NL; 0.17 for MH and 0.25 for AG). During the first stage of the monitoring NL behaved non-linearly (days 0 – 404. Non-effect test *p*-values = 0.04) while MH and AG decreased linearly (days 0 – 404. L* non-

effect test *p*-values = 0.15 for MH and 0.06 for AG) at a rate of -0.03 in both lighting conditions.

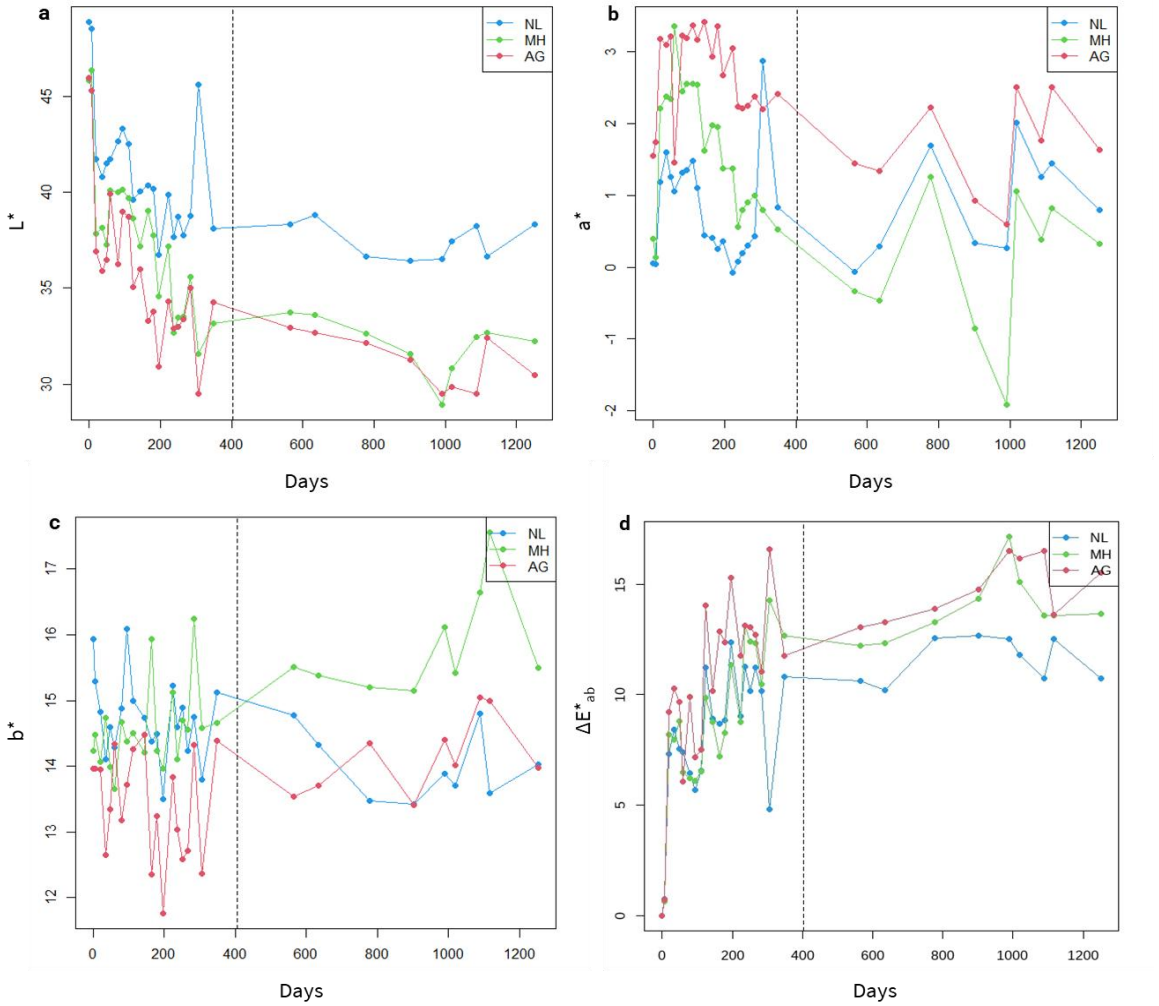

Figure 29. Representation of the CIELAB parameters a) L*, b) a*, c) b* and d) ΔE^*_{ab} in the three ashlars under the studied ornamental lighting conditions during the monitoring. Dashed lines (---) mark the division between the first and second part of the monitoring at 404 days.

For the red-green axis (a*, **Fig. 29b**), the starting values after the mechanical cleaning were equal between the three ashlars (a* = 0.66 ± 0.79 CIELAB units). NL remained constant (a* non-effect test *p*-values = 0.53 for NL) and linear (linearity test *p*-values = 0.46 for NL) throughout the entire monitoring, whereas MH and AG decreased their a* values (a* non-effect test *p*-values = 0.01 for MH and 0.01 for AG) in a non-linear way (a* linearity test *p*-values = 0.03 for MH and 0.08 for AG). However, when focusing on the second part of the monitoring, all lighting conditions remain unchanged until the end of the monitoring (days 405 – 1251. a* non-effect test *p*-values = 0.51 for NL; 0.77 for MH and 0.80 for AG). The yellow-blue axis (b*, **Fig. 29c**) remains constant under the three lighting conditions under study for the entire duration of the monitoring (b* non-

effect test *p*-values = 0.75 for NL; 0.12 for MH and 0.65 for AG). Finally, ΔE^*_{ab} changed under all lighting conditions through the entire monitoring (non-effect *p*-values = 0.01 for NL; <0.01 for MH and <0.01 for AG) in a non-linear way (ΔE^*_{ab} linearity test *p*-values = 0.02 for NL; 0.01 for MH and 0.02 for AG) (**Fig. 29d**), but remain constant when focusing on the second part of the monitoring (days 404 – 1251. ΔE^*_{ab} linearity test *p*-values = 0.29 for NL; 0.19 for MH and 0.24 for AG).

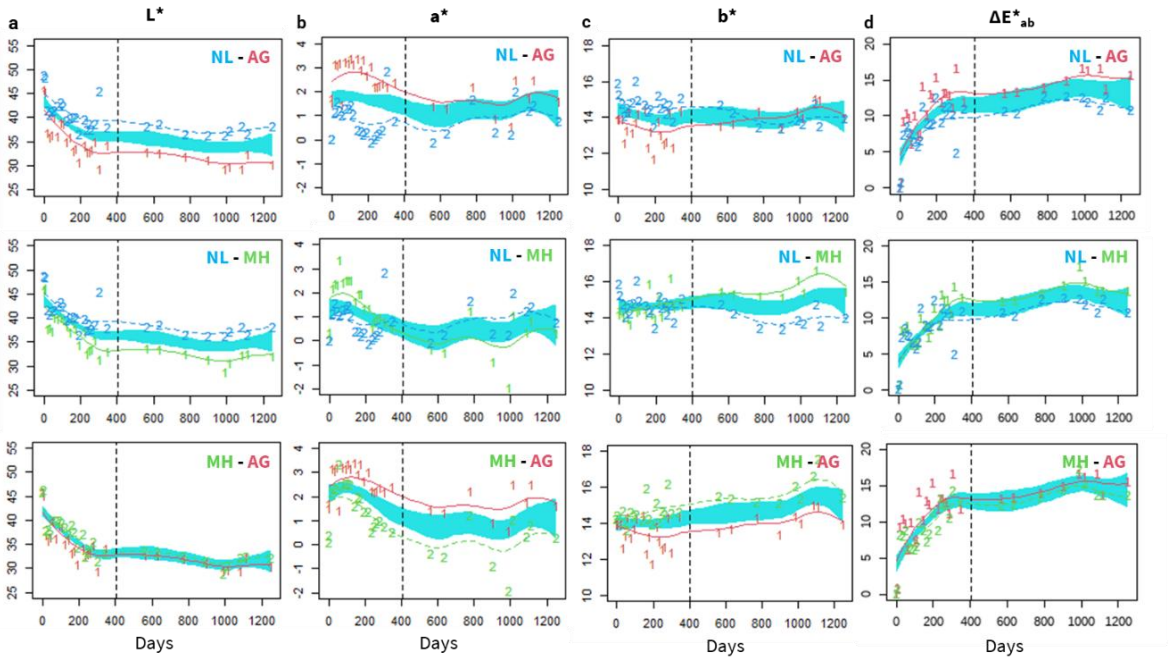

Figure 30. Equality test (non-parametric ANCOVA) test of the CIELAB parameters a) L*, b) a*, c) b* and d) ΔE^*_{ab} in the three ashlars under the studied ornamental lighting conditions during the monitoring. Dashed lines (---) mark the division between the first and second part of the monitoring at 404 days.

The non-parametric ANCOVA (**Fig. 30**) revealed that the evolution of the CIELAB parameters L* (L* equality test *p*-values: <0.01 for NL-AG; <0.01 for NL-MH and 0.12 for MH-AG), a* (a* equality test *p*-values: <0.01 for NL-AG; <0.01 for NL-MH and <0.01 for MH-AG) and ΔE^*_{ab} (ΔE^*_{ab} equality test *p*-values: <0.01 for NL-AG; 0.01 for NL-MH and 0.15 for MH-AG) was different for the entire monitoring period under the different light conditions, except for the L* and ΔE^*_{ab} between MH and AG. The values of b* remained equal between the three lighting conditions (b* equality test *p*-values: 0.15 for NL-AG; 0.05 for NL-MH and 0.11 for MH-AG) except between NL and MH.

The parallelism test showed that for L* (L* parallelism test *p*-values: 0.28 for NL-AG; 0.09 for NL-MH and 0.90 for MH-AG) and ΔE^*_{ab} (ΔE^*_{ab} parallelism test *p*-values = 0.37 for NL-AG; 0.13 for NL-MH and 0.90 for MH-AG) all curves are parallel. However, the parallelism test shows that only the MH and AG a* curves only are parallel between each other (parallelism test *p*-values = 0.03 for NL-AG; <0.01 for NL-MH and 0.25 for

MH-AG). It also shows that the b* curves between NL and MH are not parallel (parallelism test *p*-values = 0.50 for NL-AG; 0.04 for NL-MH and 0.95 for MH-AG).

The development of the SABs during the monitoring caused a change in the surface colour of the ashlars. The lightness (L*) decreased during the first 404 days and the remained constant under the three lighting conditions. However, under the two ornamental lightings the surface became darker, with L* values reaching 32.22 ± 5.87 CIELAB units for MH and 30.47 ± 4.60 CIELAB units for AG, compared to the 38.30 ± 5.50 CIELAB units of NL. A similar pattern was found with the a* parameter for MH and AG, which reflects the red-green colour, as a* changed during the first part of the monitoring and then remained constant. The surface became greener under the metal halide (MH) lamp achieving values of 0.33 ± 1.32 CIELAB units, whereas under the amber+green light the surface became redder with values of 1.63 ± 1.17 CIELAB units. Despite the changes in L* and a* there were no effects to the yellow-blue colours as the b* remained unchanged throughout the monitoring with a value around 14.50 ± 3.23 CIELAB units.

Lightness (L*) and greenness (< a*) is often used as an indicative of algal development over rock as both L* and tend to decrease (thus making the surface appear darker and greener) in recolonisation processes (see Prieto et al. 2005; Bartoli et al., 2023. However, in the work of Sanmartín et al. (2012) L* failed to be as useful as a* or b* in determine the recolonisation, as the variations of L* of an algal SAB recolonizing a granite wall mechanically cleaned were erratic. Thus, enough organisms in a darker surface are needed to properly assess colonisation through L* (see Prieto et al., 2005).

Despite MH and AG having the same L* throughout the monitoring, they both differ in the a* parameter as the SAB under AG appear redder (higher a*) than NL, while MH appear greener (lower a*). The light spectra of nocturnal illumination can change the colour of phototrophic organisms. In the work of Sanmartín et al. (2017), a multi-specifical algal culture (derived from SAB growing on a granite wall) under red light during nighttime (peaking at 612 nm) became greener (decreasing their a* value), but those illuminated by green light (peaking at 547 nm) became redder (increased their a* value).

3.4. Taxonomic composition

Table 6. Evolution of the specifical composition (Green: Chlorophyta species; Blue: Cyanophyta species and Orange: Bacillariophyta species) of the SABs in the three ashlars during the monitoring time.

Filum	Specie	Lighting condition	Date			
			APR 2020	MAY 2021	FEB 2022	FEB 2024
Chlorophyta	*Trentepohlia cf. annulata*	NL	2	400	0	0
		MH	350	250	0	0
		AG	400	150	0	0
	Myrmecia irregularis	NL	286000	245000	357000	235000
		MH	326000	365000	532000	512000
		AG	175000	210000	234000	131000
	Apatococcus lobatus	NL	0	0	0	0
		MH	0	0	0	1020
		AG	0	0	0	3280
	Desmococcus olivaceus	NL	0	0	0	0
		MH	0	0	0	4070
		AG	0	0	0	9560
	Geminella minor	NL	23100	11200	13400	7300
		MH	50000	3400	3400	3400
		AG	42000	5300	6100	6100
		Scale	532000			0
Cyanophyta	*Calothrix* sp.	NL	4200	900	2400	1000
		MH	1200	1000	2200	1500
		AG	1500	1100	1800	800
		Scale	4200			0
Bacillariophyta	*Hantzschia amphioxus*	NL	0	200	500	500
		MH	0	150	0	100
		AG	0	850	200	250
	Frustulia vulgaris	NL	0	0	0	0
		MH	0	0	0	0
		AG	0	0	300	0
	Humidophila contenta	NL	100	200	100	0
		MH	200	100	300	0
		AG	100	400	600	0
	Achnanthes coarctata	NL	0	300	800	0
		MH	0	200	400	0
		AG	0	500	100	0
		Scale	850			0

SABs on the granite ashlars were predominantly composed of Chlorophyta, with *Myrmecia irregularis* (**Table 6**) representing the dominant specie, accounting for 79.90% to 98.83% of the total algal community. The abundance of *M. irregularis* increased from April 2020 to February 2022, followed by a decline observed in February 2024. Under NL

and AG ornamental lighting conditions, *M. irregularis* cell counts decreased to below the initial levels after monitoring. In contrast, under metal halide (MH) lighting, the final cell counts of *M. irregularis* exceeded the initial value. *Apatococus lobatus* (0.27% to 1.50% of the total SAB community) and *Desmococcus olivaceus* (1.07% to 4.36% of the total SAB community) were not detected in the SABs until the final monitoring in February 2024, only appearing under the MH and AG ornamental lighting conditions. Both *Trentepohlia* cf. *annulata* (0.06% to 0.18% of the total SAB community) and *Geminella minor* (0.63% to 19.18% of the total SAB community) decreased its presence in the SABs during the monitoring, with *Trentepohlia* cf. *annulata* not being undetected since February 2022.

Cyanophyta is only represented in the SABs by *Calothrix* sp., accounting for 0.27% to 1.34% of the total SAB community. Its abundance was maintained relatively constant throughout the monitoring.

Figure 31. Specifical composition of the SABs colonizing the granite ashlars in the inner courtyard of the Raxoi Palace (Santiago de Compostela. (A) *Myrmecia irregularis* (J.B.Petersen) Ettl and Gärtner; (B) *Geminella minor* (Nägeli) Heering; (C) *Calothrix* sp.; (D) *Frustulia vulgaris* (Thwaites) De Toni; (E) *Humidophila contenta* (Grunow) Lowe; (F) *Achnanthes coarctata* (Brébisson ex W. Smith) Grunow: oblique view (a), valvar view (b) and girdle view (c). Scale = 10 µm (a-d, f); 5 µm (e). Image by R. Carballeira.

The presence of diatoms (Bacillariophyta) indicates the periodic availability of water as they prefer very humid and stable habitats Falasco et al., 2014, although they only represent around 0.03% to 0.78% of the total SAB community and being undetected on some of the samplings. Both *Humidophila contenta* and *Achnanthes coarctata* appear during the monitoring but were absent in the last monitoring of February 2024. The only

Bacillariophyta detected at the end of the monitoring was *Hantzeschia amphioxus*, that was undetected in April 2020 and remain relatively constant throughout the monitoring. *Frustulia vulgaris* appear only under AG in February 2022 with an abundance of 0.40% of the total SAB community. Images of some of the species found can be found in **Figure 31**.

The only Chlorophyta species consistently present in the SABs through the entire monitoring time were *M. irregularis* and *G. minor*. Both species were previously described growing on granite monuments in Galicia (NW Spain), as well as *A. lobatus* and *D. olivaceus* (Rifón-Lastra and Noguerol-Seoane, 2001). Species from the *Trentepohlia* genus are also frequent colonizers of granite monuments, forming also symbiotic relations in lichens (see Prieto et al., 1994, Rifón-Lastra and Noguerol-Seoane, 2001). The genus *Myrmecia* appears to be frequently the photobionts of lichens. For example, Pino-Bodas et al. (2023) found that individuals from the genus *Myrmecia* are the main photobionts of the lichen *Cladonia subturgida* from lichen samples from all the mediterranean basin. Despite variations through the monitoring, the abundance of *M. irregulris* maintained constant under NL and AG, even ending decreasing 0.82 and 0.75 times less respectively, compared to the initial April 2022 sampling. However, under MH the abundance of *M. irregularis* increased 1.57 times. No specific literature was found on the responses of species from the genus *Myrmecia* to changes in light intensity or photoperiod, neither by themselves nor in symbiosis forming a lichen. Nonetheless, being the dominant species in the SAB by several orders of magnitude, the increase in F_0 and the greening found in the ashlars under the metal halide lamp may be related to the development of *M. irregulris*.

The rest of the Chlorophyta diversity appeared with low abundances, and no specific effects of the lighting conditions were detected. Interestingly, both *A. lobatus* and *D. olivaceus* appeared only in the ashlars under ornamental illumination and not in the no light control. The lower abundance of cyanobacteria is common in European countries (Gaylarde and Gaylarde, 2005) and the presence of *Calothrix* sp. was already detected on granite walls in Galicia (Pavlović et al., 2022; Genova et al., 2023). There was a small decrease from the first to the last sampling under AG and especially under NL, while the *Calothrix* sp. slightly increased under MH. However, those changes are too subtle to see a pattern in the influence of the lighting conditions.

Finally, diatoms are occasionally found or very close to the ground surface (Gorbushina, 2007). Diatoms from the genus *Achnanthes* were also found over walls from stone monuments in Spain (Samad and Adhikary, 2008). *Humidophila contenta* was first reported in a stone monument by Gaylarde et al. 2025 in two limestone churches in Salvador (Brazil). Thus, this is the first time that *Humidophila contenta* is reported on a historic building in the northern hemisphere. Moreover, and to the best of the authors knowledge, no instances of the diatom *Frustulia vulgaris* appearing over stone monuments were found. This genus has widespread distribution and is primarily found in benthic freshwater environments, with *Frustulia vulgaris* being more resistant to disturbed habitats than other *Frustulia* species (Bouchard et al., 2019). No specific patterns were detected under the lighting conditions for the Bacillariophyta community, which can be attributed to

its very low abundance compared to the other groups. Previous work from Diamantopoulou et al. 2021 on the effect of nocturnal illumination on marine diatom communities show that the use of green (525 nm) and red (624 nm) light at 0.02 W m^{-2} promotes the growth rate and chlorophyll content in comparison to white light (peak at 470 nm and lower peaks between 550 and 600 nm) and no artificial lighting at night. Thus, diatom communities must be considered when employing the amber+green light to halt the development of SABs as specific wavelengths can promote their growth.

4. Conclusions

Long-term monitoring studies in Cultural Heritage are fundamental but scarce. For the first time, the effect of ornamental lighting over algal colonisation (in the form of SABs) growing on a granite wall was measured over a period of 1251 days (≈ 3.4 years). Previous research had validated the biostatic capacity of the use of amber+green light as nocturnal ornamental illumination against other light sources, but the capacity was not tested in a long-term study in real outdoor conditions. After the 3.4-year monitoring, the results seem to validate the biostatic capacity, through the use of PAM fluorometry, colour measurements and taxonomic analysis of the species comprising the colonizing SABs of granite ashlars in the Raxoi Palace in Santiago de Compostela.

Despite both the amber+green light and the metal halide lamp causing an initial increase in the F_0 after (used as a proxy variable for phototrophic development), the SABs growing over the granite ashlars reached F_0 levels equal to the ones from SABs under no ornamental illumination, while the ones subjected to the metal halide lamp continue to increase its F_0 until the end of the monitoring. The lighting conditions under studied did not affected the quantum yield (QY) of the SABs and followed the normal annual variations for algal species.

The biostatic effect was also validated through colourimetry. The SAB under the metal halide lamp became greener (decrease in a*), which is related to algal development, while the one under the amber+green light increased its a* becoming more red. However, the results with the lightness (L*) did not show a lower development under the amber+green light as the L* evolution throughout the monitoring was the same as under the metal halide lamp. Finally, the specific composition in the SAB was dominated by the green alga *Myrmecia irregularis*, which increased its abundance in the SAB under the metal halide lamp. However, its abundance was maintained under the amber+green light similarly to the control with no ornamental lighting.

Authors' contribution

Conceptualization, A.M., R.M.C., J.A. and P.S.; methodology, A.M., R.M.C., J.A. and P.S.; formal analysis, R.M.C.; investigation, A.M., R.M.C. and J.A.; writing—original draft preparation, A.M.; writing—review and editing, R.M.C, J.A. and P.S.; supervision, R.M.C., J.A. and P.S.; project administration, P.S.; funding acquisition, P.S.

4.3 PART 3: BIODIVERSITY IMPACT

4.3.1 CHAPTER 7

MICROBIOME SHIFTS ELICITED BY ORNAMENTAL LIGHTING OF GRANITE FACADES IDENTIFIED BY MINION SEQUENCING

Anxo Méndez, Francesca Maisto, Jelena Pavlović, Magdaléna Rusková, Domenico Pangallo, Patricia Sanmartín

Journal of Photochemistry and Photobiology B - Biology 261, 113065 (2024). doi: 10.1016/j.jphotobiol.2024.113065

JCR index (IF) 2024 = 3.7 (16/79, 80.4 percentile in Biophysics)

Open access. Citations (to September 2025): 6

The work from this chapter is result of the scientific visit of A. Méndez in the Slovak Academy of Sciences, Institute of Molecular Biology, Bratislava (Slovakia), under supervision D. Pangallo, from September to November 2022. As a result of that short-stay, the following paper was also made, related but not covered in this thesis:

Maisto, F.; **Méndez, A.**; Pavlović, J.; Kraková, L.; Sanmartín, P.; Pangallo, D. (2025) Microbiome and response to cleaning and biocidal treatments on granite historical buildings using MinION sequencing. Constr Build Mater 490, 142589. doi: 10.1016/j.conbuildmat.2025.142589

Journal of Photochemistry & Photobiology, B: Biology 261 (2024) 113065

Contents lists available at ScienceDirect

Journal of Photochemistry & Photobiology, B: Biology

journal homepage: www.elsevier.com/locate/jphotobiol

Microbiome shifts elicited by ornamental lighting of granite facades identified by MinION sequencing

Anxo Méndez [a], Francesca Maisto [b], Jelena Pavlović [b], Magdaléna Rusková [b], Domenico Pangallo [b,c,*,1], Patricia Sanmartín [a,1]

[a] CRETUS, Gemap (GI-1243), Departamento de Edafoloxía e Química Agrícola, Facultade de Farmacia, Universidade de Santiago de Compostela, 15782 Santiago de Compostela, Spain
[b] Institute of Molecular Biology, Slovak Academy of Sciences, Dúbravská cesta 21, 845 51 Bratislava, Slovakia
[c] Caravella, s.r.o., Tupolevova 2, 851 01 Bratislava, Slovakia

ARTICLE INFO

Keywords:
Microbiota
Culture-dependent analysis
Granite monuments
Nanopore sequencing technology
Monumental illumination

ABSTRACT

Night-time outdoor illumination in combination with natural sunlight can influence the visible phototrophic colonizers (mainly algae) growing on stone facades; however, the effects on the microbiome (invisible to the naked eye) are not clear. The presence of stone-dwelling microbes, such as bacteria, diatoms, fungi, viruses and archaea, drives further biological colonization, which may exacerbate the biodeterioration of substrates. Considering the microbiome is therefore important for conservation of the built heritage. The impact of the following types of lighting on the relative abundance and diversity of the microbiome on granite ashlars was evaluated in a year-long outdoor pilot study: no lighting; lighting with a metal halide lamp (a traditional lighting system currently used to illuminate monuments); and lighting with a novel LED lamp (an environmentally sound prototype lamp with a biostatic effect, halting biological colonization by phototrophs, currently under trial). Culturable fractions of microbiome and whole-genome sequencing by metabarcoding with Oxford Nanopore Sequencing (MinION) was conducted for bacteria and fungi in order to complement both community characterization strategies. In addition, the possible biodeteriorative profiles of the isolated strains, relative to calcium carbonate precipitation/solubilisation and iron oxidation/reduction, were investigated by plate assays. Alpha and beta diversity indexes were also determined, along with the abundance of biocide and antibiotic resistance genes. Culture-dependent microbiological analysis failed to properly show changes in community composition, for which metagenomic approaches like MinION are better suited. Thus, MinION analysis identified shifts in the granite microbiome elicited by ornamental lighting. The novel LED lamp with the biostatic effect on phototrophs caused an increase in the diversity of bacteria and fungi. In this case, the microbiome was more similar to that in the unlit samples. In the samples illuminated by the metal halide lamp, dominance of bacteria was favoured and the presence of fungi was negligible.

1. Introduction

The presence of living organisms on monuments and built heritage results in damage that leads to biodeterioration of the building material. Physical damage can be caused, for example, by the growth of fungal hyphae or plant roots, but chemical damage also occurs due to the metabolic activity of organisms. In this sense, chemolithotrophic bacteria can use the substrate for energy. Their metabolism, like that of fungi, can produce biocorrosive organic acids or weaken the mineral network by oxidation of metal cations [1], resulting in a significant damage to the integrity of the material of stone heritage buildings.

Granite is a common material in heritage buildings, most commonly in the northwest of the Iberian Peninsula (see e.g., [2]). On this substrate, biological activity generally produces visible effects of chemical weathering, such as staining and coating due to the oxidation of, among others, the iron present in the biotite minerals [3]. Joint mortars

* Corresponding author at: Institute of Molecular Biology, Slovak Academy of Sciences, Dúbravská cesta 21, 845 51 Bratislava, Slovakia.
E-mail addresses: anxo.mendez.villar@usc.es (A. Méndez), francesca.maisto@savba.sk (F. Maisto), jelena.pavlovic@savba.sk (J. Pavlović), magdalena.kapustova@savba.sk (M. Rusková), domenico.pangallo@savba.sk (D. Pangallo), patricia.sanmartin@usc.es (P. Sanmartín).
[1] These authors share last (co-senior) authorship: D. Pangallo and P. Sanmartín.

https://doi.org/10.1016/j.jphotobiol.2024.113065
Received 22 May 2024; Received in revised form 7 September 2024; Accepted 7 November 2024
Available online 12 November 2024

(containing calcium) are also susceptible of alteration by the presence of microorganisms (see e.g., [4,5]). Because of the damage that microorganisms can cause, cleaning and maintenance operations are often carried out to remove them, usually by the use of biocides or other chemical compounds (see e.g., [6]).

The dissemination and growth of colonizing microorganisms is supported by the environmental conditions. However, the impact of artificial light is relevant due to ornamental illumination at night of monuments but is often overlooked [7]. Light affects all living organisms and can be used as a tool for inhibition in the case of colonizing microbial communities. Photodynamic inactivation (PDI) of microbes (generally bacteria and fungi) mainly involves the violet-blue (380–495 nm) and red (620–740 nm) regions at either end of the visible spectrum [8,9,10,11]. The PDI is caused by reactive oxygen species (ROS), which are activated in these wavelength ranges and which have the potential to deconstruct proteins, lipids and nucleic acids inside microbial cells and thus cause death of the cells (see e.g. [12,11,13]). Gram-positive bacteria are highly susceptible to PDI, especially in the blue region (at 405 nm) [11]. In a study conducted in the Roman Catacombs (Italy), the presence of Gram-negative bacteria also decreased after exposure of target areas to blue light (at 490 nm) [14]. Most fungal species have photoreceptors that are sensitive to blue light and that regulate several physiological responses, such as regulation of gene expression and circadian rhythms [15]. Use of wavelengths in the centre of the visible spectrum (i.e. the green-yellow/amber spectral region, at wavelengths between 495 nm and 625 nm) to inactivate bacteria and fungi is not common. In some fungal species, such as *Phycomyces blakesleeanus* and *Mucor circinelloides*, phototropism is driven by green light. In their review paper, Hessling et al. [10] point out that wavelengths within this range may have photoinhibitory effects on bacteria, depending on which endogenous photosensitizers the bacteria normally produce, e.g. different porphyrins. Many species of bacteria appear to be sensitive to wavelengths around 520 nm (green) and 620–660 nm (amber-red). Green light (521 nm) was found to induce sublethal damage in *Staphylococcus aureus* or even to exert antibacterial activity against this species [16]. *Escherichia coli* and *Porphyromonas gingivalis* can also be inactivated by exposure to several regions of the visible spectrum, including amber and green light, but the median dose necessary to achieve the photoinactivation increases as the wavelength increases [17,18]. This was shown by [19], and the efficacy of inactivation of different bacteria species with light at 405 nm was much higher than when the same dose of light at 520 nm was used.

Since the invention of the first practical incandescent light bulb in the late 1870s, urban monuments have been ornamentally illuminated by artificial lights at night (ALAN) to highlight their character, age and historical significance, with the current global trend being to install LEDs [20]. At present, colored LEDs (purple, red, green, yellow, blue, etc.) are used to create different effects and to launch messages of support on monuments and buildings (e.g. green is used to promote climate change action, blue indicates support for refugees, and purple is used to mark women's day and holocaust memorial day, etc.). The emission bands of these luminaires are included in the visible spectrum of light (350–750 nm), within which the photosynthetically active radiation (PAR) (400–700 nm) occurs. PAR is a particularly important factor in the growth of the phototrophic organisms that cause green staining ('greening'). In subterranean monuments, the selection of artificial lights with certain bands with low photosynthetic quantum efficiency for the target phototrophs have been shown to have a biostatic (halting) effect (see e.g. [21,22,23]). In a more complicated scenario, such as outdoor monuments, where the artificial light is applied together with natural sunlight, the same is being demonstrated in an ongoing research project (the CromaLux project). However, the impact that artificial lighting has on the microbiome (mainly consisting of bacteria and fungi) of outdoor monuments is not known. It is possible that the light elicits a shift in the bacterial and fungal diversity. This is the main question considered in the present study, in which the combined use of culture-dependent and culture-independent (MinION third-generation sequencing platform from Oxford Nanopore Technologies) approaches were applied to samples (excluding green algae from analysis) obtained after exposure of granite ashlars for one year (in a pilot study) to different lighting conditions. The target granite ashlars were either unlit, lit by a metal halide lamp (a traditional lighting system currently used to illuminate monuments) or lit by a novel LED lamp (currently under trial; an environmentally sound prototype lamp with a biostatic effect, halting biological colonization by phototrophs). In addition, the potential biodeterioration capacity of culturable bacterial and fungal isolates was determined, relative to calcium carbonate precipitation/solubilisation and iron oxidation/reduction, and analysis of biocide- and antibiotic-resistance genes (ARGs) was conducted.

2. Materials and methods

2.1. Site description and sampling

A year-long outdoor pilot study, from May 2021 to May 2022, was conducted in the inner courtyard (245 m^2) of the old prison yard of the local police building, located behind the city council building, and belonging to Pazo de Raxoi buildings, a neoclassical palace completed in 1766 and located in front of the cathedral of Santiago de Compostela, a UNESCO World Heritage city since 1985 in northwestern Spain (UTM 537047 X,4747615 Y, Datum ETRS89; elevation, 250 m a.s.l.). There was evaluated the impact of the following types of lighting on the relative abundance and diversity of the microbiome on granite ashlars under lighting with a traditional lighting system currently used to illuminate monuments (a metal halide lamp onto target area A); lighting with an environmentally sound prototype lamp with a biostatic effect, halting biological colonization by phototrophs, currently under trial (a novel LED lamp onto target area B) and no lighting (unlit or unilluminated target area C) (Fig. 1).

Moreover, in the summer of 2018, Atila®, a non-selective systemic herbicide based on glyphosate 36 % (isopropylamine salt), was applied to the granite and schist masonry walls with joint mortar of the courtyard.

Rock samples (per triplicate) of about 30 mm of diameter were obtained from the three ashlars, within which the target areas A, B and C found. The samples were examined by microphotography under a stereomicroscope (Nikon, SMZ-2 T) and light microscope (Nikon Eclipse 50i). Then of each ashlar, one sample was chosen for further analysis under scanning electron microscopy (SEM) coupled with electron dispersive spectroscopy (EDS) as in Sanmartín and Prieto [24], and the other two samples per ashlar were ground and analyzed by X-ray diffraction (XRD) to identify the mineral composition as in Sanmartín et al. [25].

To ensure a common starting point, the three ashlars were cleaned mechanically with distilled water and a brush at the beginning of the experiment. Both types of lamps were switched on every night for five hours or five hours and half depending on the time of year. The lighting conditions onto the three granite ashlars were measured with a radiometrically calibrated spectroradiometer (SilverNova, Stellarnet, Inc.) and they were: 2.5 cd in A, 1.8 cd in B, and 0.3 cd in C (for more data about both lighting systems, see [26]). To ensure that there is no light interference on the target areas (A, B and C) rigid sheets were placed on both sides of both lighting systems (Fig. 1), and measurements over the entire surface on A, B and C, mapping the illumination received were carried out.

In May 2022, each biological sample was collected from an area of 10 cm^2 of the granite ashlars (A, B and C target areas) by using sterile cotton swabs moistened with sterile PBS buffer solution (10 mL).

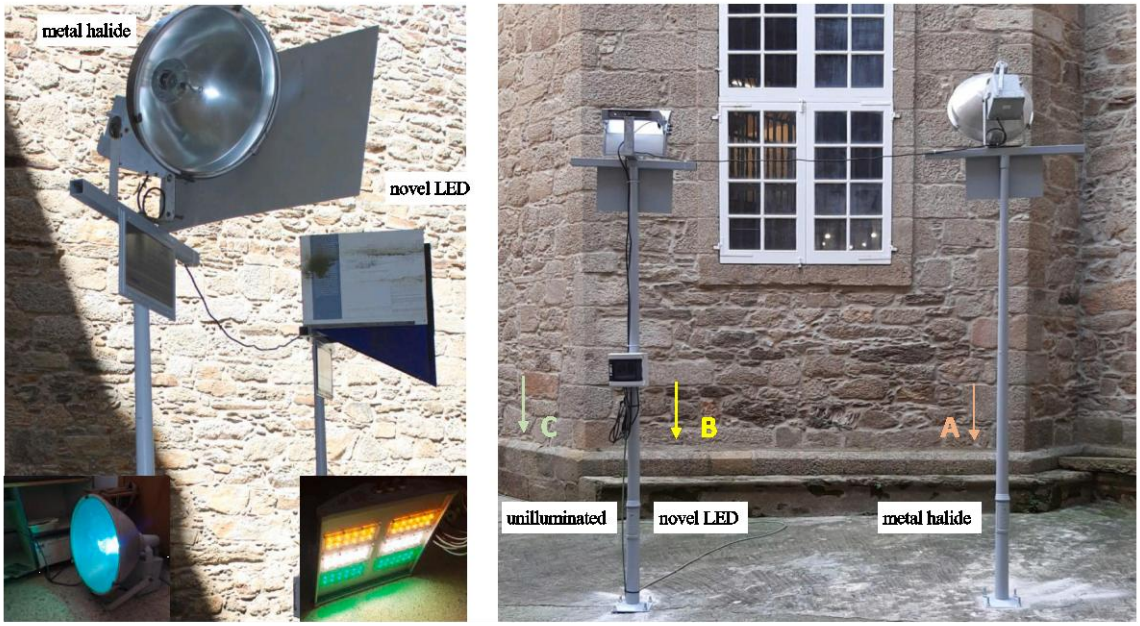

Fig. 1. Study site, inner courtyard in Pazo de Raxoi (city council buildings). Left: Both lighting systems (below in the image, photographs taken in the lab while the lights were on). Rigid sheets were used to prevent interference between them. Right: Target areas (North-East facing granite ashlars) lit by a metal halide lamp (A), lit by a novel LED lamp (B) and unilluminated (C).

2.2. Culture-dependent analysis

2.2.1. Isolation of microorganisms

Aliquots from the collected samples were plated in Tryptone Soy Agar (TSA) to cultivate bacteria and Potato Dextrose Agar (PDA) to cultivate fungi. Each plate was divided into four quadrants, on which five 10 μL drops of a serial dilution (10^{-1}, 10^{-2}, 10^{-3}, 10^{-4}) of each sample were inoculated using the drop-plating technique. Over the following days, those colonies (both of bacteria and fungi) that were morphologically different from the quadrant from which the colonies appeared properly separated were isolated onto new TSA or PDA plates. For bacteria, samples from A and B areas were isolated from the quadrant with 10^{-4} dilution and sample from C area from the quadrant with 10^{-3} dilution. For fungi, all colonies were isolated from the quadrant with 10^{-4} dilution. In case of contamination of the isolated strains plates, successive isolations were carried out until separate strains were obtained. Prior to identification, the strain colonies were morphologically characterized by their size, color, texture and particular characteristics.

2.2.2. Identification of the microorganisms isolated

The DNA of bacterial isolates were extracted with the DNasy Blood & Tissue Kit (Qiagen, Hilden, Germany) according to the manufacturer's protocol. The fungal isolates were inoculated in Potato Dextrose Broth (PDB, Sigma Chemical Co., St. Louis, Mo) at 25 °C until growth. The fungal pellets were separated from the broth by filtration through sterile filter paper. The DNA of the fungal pellets was extracted with the DNeasy Plant Mini Kit (Qiagen) according to the manufacturer's protocol. The bacterial isolates were identified by DNA sequencing, the 16S rRNA gene was amplified using the primers 27F (5′–AGA GTT TGA TCC TGG CTC AG-3′) and 685R (5′-TCT ACG CAT TTC ACC GCT AC-3′) according to Lane [27]. The fungal isolates were identified by the sequencing of their ITS fragment which was amplified using the primers ITS1 (5′-TCC GTA GGT GAA CCT GCG G-3′) and ITS4 (5′-TCC TCC GCT TAT TGA TAT GC-3′) according to White et al. [28]. Twenty-five microliters of PCR mixture contained 50 pmol of each primer, 200 μmol/L of dNTP (Life Technologies, Gaithersburg, MD, USA), 1.5 U HotStar Taq plus DNA polymerase (Qiagen), 1 × PCR buffer and 3 μL of the extracted bacterial or fungal DNA. The PCR program consisted of initial denaturation at 94 °C for 5 min, followed by 30 cycles (denaturation at 94 °C for 30 s, annealing at 54 °C for 45 s, extension at 72 °C for 1 min) and a final polymerization step at 72 °C for 8 min. PCR products from bacterial and fungal isolates were purified using ExoSAP-IT (Affymetrix, Cleveland, OH, USA) and sequenced at a commercial facility (Eurofins Genomics, Ebersberg, Germany). The sequences obtained were directly compared with sequences in GenBank by using the BLAST program (http://blast.ncbi.nlm.nih.gov/Blast.cgi) and were subsequently deposited in GenBank under the accession numbers PP326030-PP326049 (bacterial isolates) and PP325889-PP325899 (fungal isolates). Sequences of bacterial isolates were also identified using the EzBioCloud database, obtaining results consistent with GenBank.

2.2.3. Specific plate assays

The possible biodeteriorative profiles of the bacterial and fungal isolates, relative to calcium carbonate precipitation/solubilisation and iron oxidation/reduction, were investigated by specific agar plate assays.

The capacities/activities of isolates to precipitate and solubilise calcium carbonate were screened using B4 medium (calcium acetate 2.5 g; yeast extract 4 g; glucose 10 g; agar 15 g; distilled water 1 L, the final pH of the medium was adjusted to 8.0; [29]) and $CaCO_3$ glucose agar (glucose 10 g; calcium carbonate 5 g; agar 15 g, distilled water 1 L; [30]) respectively. All plates were incubated at room temperature (24–26 °C) and monitored over a period of 3 weeks. On B4, the positive strains produced crystals, whereas on $CaCO_3$ glucose agar, a clear zone was observed around positive strains. All assays were performed in triplicate on 90-mm Petri plates.

Iron reducing bacteria (IRB) were detected according to Ottow and

Glathe [31] protocol. The isolates were inoculated into tube with 7 mL of 2 % glucose-asparagine broth (glucose 20.0 g; asparagine 5.0 g; K_2HPO_4 3.0 g; KH_2PO_4 0.8 g; KCl 0.2 g; $MgSO_4.7H_2O$ 0.2 g; yeast extract 0.5 g; Fe_2O_3 - reagent grade powdered 1.0 g; distilled water 1 L; pH adjusted to 7.0). After 5 days cultivation at room temperature (24–26 °C) each tube received 1 mL of 2,2′- dipyridin solution (0.2 %) in 10 % of acetic acid. The color change from pink to red indicated the positivity of the test. Detection of iron oxidizing bacteria (IOB) were performed by using Winogradsky broth medium (WBM) according to Sachan et al. [32] protocol. WBM consists of $NaNO_3$ 0.5 g; $MgSO_4.7H_2O$ 0.5 g; $CaCl_2.2H_2O$ 0.2 g; K_2HPO_4 0.5 g; NH_4NO_3 0.5 g; Ammonium iron citrate 6.0 g; distilled water 1 L; pH adjusted to 6.5. Bacteria were incubated at 25 °C for 48 h. The change in color of WBM from light green to rusty brown indicates the presence of IOB. The culture was serially diluted in WBM and inoculated on Winogradsky agar medium (WAM). After 24 h of cultivation, rusty brown colonies related to IOB appeared.

2.3. MinION sequencing analysis

2.3.1. Extraction of the DNA and sequencing

Genomic DNA extraction was performed using the DNeasy PowerSoil kit (Qiagen, Hilden, Germany) following the manufacturer's instructions. Quantification of the extracted DNA was conducted using the DeNovix dsDNA Broad Range Kit on the DeNovix QFX Fluorometer (DeNovix Inc., Wilmington, DE, USA). Sequencing libraries were prepared according to the Ligation sequencing gDNA - PCR barcoding kit protocol with Expansion kit PBC001 (SQK-LSK109 with EXP-PBC001, Oxford Nanopore Technologies, ONT, Oxford, UK, version: PBGE96_9068_v109_revT_14Aug2019) downloaded from the ONT website. Sixteen barcoded libraries were pooled in desired ratios to a total concentration of 1 μg in 49 μL and ligated with the AMX adapter included in the SQK-LSK109 kit (ONT). The final sequencing library was adjusted to the recommended molar concentration of 50 fmol and loaded onto a primed FLO-MIN106D R9.4.1 flow cell on a MinION Mk1B device for a 48 h run. Device control and data acquisition were performed using the MinKNOW software. The sequences obtained by the metagenomic analysis are registered and publicly available as BioProject PRJNA1084728.

2.3.2. Metagenomic data analysis

Raw ONT signal data were base-called using the high accuracy model by Guppy Basecalling Software Version 6.5.0. Resulting FASTQ files were then de-multiplexed by barcode, followed by adapter and quality trimming using Porechop (https://github.com/bonsai-team/Porechop_ABI). Metagenomic fastq reads underwent ARG annotation against the Comprehensive Antibiotic Resistance Database v 3.0.4 (CARD) (https://card.mcmaster.ca/download) [33] and biocide genes annotation against the biocide database BacMet2 – experimentally confirmed [34] using Diamond Blastx [35]. Filtering criteria included an 80 % similarity and an *E*-value of 1e-5. ARG abundance was normalized to the copy number of 16S rRNA genes identified using Metaxa2 [36]. Microbiome profiling employed Kraken2 (v2.1.1) [37] with the PlusPF database. Alpha diversity was estimated by richness (observed Operational Taxonomic Units - OTUs), together with Shannon and Chao1 diversity indexes, using the phyloseq package in R v. 4.0.2. statistical software [38]. Distance between microbial community groups was calculated in R statistical software using the Bray-Curtis method for subsequent Principal Coordinates analysis (PCoA). STAMP software (v.2.1.3) was used to generate the heat map for ARGs abundance.

3. Results

3.1. Granite ashlars

The granite facades of the courtyard have a heterogeneous masonry (Fig. 1). The choice of the three ashlars for the study was made on the basis of their same orientation (North-East facing) and their similar macroscopic appearance: coarse-medium grained with some ochre spots surrounding biotite and reddish-brown coloration on feldspars and quartz in certain areas, formed by the oxidation of the biotite mica (the main iron-containing silicate in the granite). The mineralogical semi-quantitative results obtained by DRX (Table S1) plotted on a Streckeisen [39] ternary diagram classified the three target ashlars as the same rock type: granite (sensu stricto). The presence of iron oxides and hydroxides (such as goethite, hematite, maghemite, lepidocrocite, and ferric hydroxide) on the three ashlars was confirmed by SEM-EDS analysis (Fig. S1).

A previous taxonomic identification by morphological characters of the phototrophic colonization of the courtyard granite facades showed mainly the presence of chlorophyta, such as the coccoid green alga associated with lichens *Myrmecia irregularis* (J.B.Petersen) Ettl & Gärtner which was the main taxon. Also, a notable presence of diatoms which indicates the periodic availability of water in the walls.

3.2. Culture-dependent analysis

Bacterial and fungal strains isolated from samples of the three target areas A, B and C are shown in Table 1. The number of isolates in A, B and C was very similar, with 6–7 bacteria and 5–6 fungi in each of the samples. Bacteria of the genera *Microbacterium* and *Arthrobacter* were spread in all three samples. Fugi were represented mainly by species belonged to the genera *Alternaria* (in A and C) and *Penicillium* (in A and B). Other fungal isolates included the species *Stagonosporopsis cucurbitacearum* and *Pestalotiopsis maculiformans* (in A and B), *Letendraea helminthicola* and *Boeremia exigua* (in B and C).

The possible biodeteriorative profiles of the isolates were tested by agar plate assays and showed the growth of almost all the isolates on $CaCO_3$ glucose (relative to $CaCO_3$ solubilisation) and B4 agar (relative to $CaCO_3$ precipitation) (Table 1). On B4 agar the fungal isolates grew very well and very fast. However, few isolates, only *Pantoea* sp. (probably *deleyi*) from A and *Penicillium spathulatum* from B produced halos indicating $CaCO_3$ solubilisation, and *Arthrobacter* sp. (probably *parietis*) and *Glutamicibacter creatinolyticus* from B, together with *Bacillus aryabhattai* or *megaterium* (syn. *Priestia megaterium*) from C formed crystals indicating $CaCO_3$ precipitation. Two of these strains, *Pantoea* sp. (probably *deleyi*) from A and *Bacillus aryabhattai* or *megaterium* (syn. *Priestia megaterium*) from C, together with *Pseudomonas quebecensis* from C displayed a positive reaction to iron oxidation. Iron reduction assays did not show positive results.

3.3. MinION sequencing analysis

The Nanopore sequencing run produced a total of 1.02 million reads with an average read length of 2 kb. Among the polished fastq reads marked as classified, there were 469,971 for sample A, 165,309 for sample B, and 51,961 for sample C. Stone microbiome analysis by whole-genome sequencing (WGS) identified the most abundant kingdoms, as illustrated in Fig. 2, consisted of bacteria: 99.44 % in A, 78.58 % in B, and 57.71 % in C and eukaryote: 0.52 % in A, 21.02 % in B, and 41.89 % in C, while archaea only accounted for 0.02 % in A, 0.30 % in B, and 0.31 % in C, and viruses for 0.004 % in A, 0.092 % in B, and 0.084 % in C.

The number of bacterial counts identified in samples A, B and C were 469,971, 115,309, and 25,961, respectively. Among the 39 detected bacterial phyla, 12 phyla exhibited a minimum abundance of 0.1 %. The predominant phylum across all samples was firmicutes, constituting 96.00 % in A (practically all phylum-level diversity), 71.97 % in B, and 70.00 % in C. Followed by proteobacteria with 2.28 % in A, 11.77 % in B, and 13.98 % in C. Other abundant phyla included bacteroidota (5.07 % in B and 7.02 % in C), cyanobacteria (4.81 % in B), and actinobacteria (4.62 % in B and 5.30 % in C). At the genus-level of bacteria (Fig. 3), *Peribacillus* was the most abundant genus in A (89.96 %) and B (33.93

Table 1
Identification and capacities/activities relative to possible biodeteriorative profiles of the bacteria and fungi isolated from the three target areas A, B and C.

Sample	Isolate*	Morphology	Identification**	Growth on $CaCO_3$ glucose agar	Growth on B4 agar	Iron oxidation activity
A	1	Small colonies, with irregular edges, transparent halo and orange color	MK414932 *Pantoea* sp. 100 % [EF688011 *Pantoea deleyi* 99.83 % (42 %)]	+++ (S)	+	O
	2	Semitransparent colonies, mucous texture and yellowish color	MK713695 *Sanguibacter inulinus* 100 % [X79451 *Sanguibacter inulinus* 100 % (42.5 %)]	+	+	–
	3	Small, pale yellow, shiny, small colonies, diffused by the edges	MW546189 *Microbacterium* sp. 99.37 % [AB004718 *Microbacterium luteolum* 98.56 % (44.2 %)]	+	+	–
	4	Small colonies, irregular edges and orange color	ON715339 *Microbacterium* sp. 99.84 % [AB286030 *Microbacterium lacus* 99.04 % (43.3 %)]	++	–	–
	5	Small pink colonies	MT397140 *Arthrobacter agilis* 100 % [MT397140 *Arthrobacter bussei* 100 % (43 %)]	+	+	–
	6	Small, pale yellow, shiny, small colonies, diffused by the edges	MG547956 *Microbacterium* sp. 100 % [JYIU01000006 *Microbacterium foliorum* 99.19 % (42.8 %)]	+	+	–
	7	Small, yellow colonies with reticulated texture	MN227659 *Dermacoccus nishinomiyaensis* 99.84 % [X87757 *Dermacoccus nishinomiyaensis* 99.52 % (43.5 %)]	+	+	–
	8	Gray color, fluffy texture, forming a whitish halo or lighter on the edges	*Stagonosporopsis cucurbitacearum*	+	+++	–
	9	White color, cottony texture, forming concentric circles	KX067822 *Penicillium brevicompactum* 100 %	–	+++	–
	10	White color with grayish rim and presence of blackish fruiting bodies	*Pestalotiopsis maculiformans*	–	+++	–
	11	Brownish green color with white edges	*Alternaria obovoidea*	+	++	–
	12	Brownish green color	ON207646 *Cladosporium pseudocladosporioides* 99.79 %	+	++	–
	13	White color	MT444991 *Alternaria solani* 100 %	–	+++	–
B	1	Large, bright orange/yellow colored colonies	OR632271 *Arthrobacter flavus* 100 % [AB537168 *Arthrobacter flavus* 99.84 % (42.5 %)]	+	–	–
	2	Large white colonies	LN774285 *Staphylococcus equorum* 100 % [AF527483 *Staphylococcus equorum* 99.69 % (44.3 %)]	–	+++	–
	3	Orange and semitransparent colonies, with low color and medium size	MK424288 *Microbacterium hydrocarbonoxydans* 99.37 % [BCRF01000095 *Microbacterium hydrocarbonoxydans* 99.06 % (44.2 %)]	+	+++	–
	4	Off-orange, semitransparent colonies	JX177706 *Acinetobacter* sp. 100 % [JN175353 *Prolinoborus fasciculus* 99.02 % (43.5 %)] ***	+	+	–
	5	Large orange colonies	FR693344 *Arthrobacter* sp. 100 % [AJ639830 *Arthrobacter parietis* 99.84 % (42.6 %)]	+	++ (P)	–
	6	Large, orange, regular-shaped colonies	MT313111 *Glutamicibacter creatinolyticus* 100 % [BAXF01000117 *Glutamicibacter creatinolyticus* 99.84 % (42.7 %)]	+	+++ (P)	–
	7	White color with grayish rim and presence of blackish fruiting bodies	KR909209 *Pestalotiopsis maculiformans* 99.82 %	–	++	–
	8	Gray color, fluffy texture, forming a whitish halo or lighter on the edges	MW798760 *Stagonosporopsis cucurbitacearum* 99.80 %	+	+++	–
	9	Grayish brown with dark center	MN759659 *Penicillium spathulatum* 100 %	+ (S)	+++	–
	10	White color, cottony texture, beige edges	MH398546 *Letendraea helminthicola* 100 %	+	+++	–
	11	Gray color, fluffy texture, forming a whitish halo or lighter on the edges	OQ606977 *Boeremia exigua* 99.80 %	+	+++	–
C	1	Yellow colonies with mucous and granular texture	CP031423 *Microbacterium lemovicicum* 100 % [CP031423 *Microbacterium lemovicicum* 100 % (43.3 %)]	–	+	–
	2	Large, dull yellow colonies	LC529488 *Rhodococcus* sp. 100 % [FNTL01000001 *Rhodococcus jostii* 99.83 % (41.9 %)]	+	–	–
	3	Very transparent whitish colonies	MH463717 *Pseudomonas quebecensis* 100 % [MH463717 *Pseudomonas quebecensis* 100 % (43.5 %)]	–	–	O
	4	Intense pink colored colonies	MH061260 *Arthrobacter* sp. 99.69 [OL471353 *Arthrobacter antioxidans* 99.84 % (43.5 %)]	+	+	–

(continued on next page)

Table 1 (*continued*)

Sample	Isolate*	Morphology	Identification**	Growth on $CaCO_3$ glucose agar	Growth on B4 agar	Iron oxidation activity
	5	Small orange colonies	FJ999590 *Rhodococcus fascians* 99.68 % [JMEN01000010 *Rhodococcus fascians* 99.35 % (43.1 %)]	−	++	−
	6	Whitish, transparent colonies with irregular edges	MN515130 *Bacillus aryabhattai* 100 % [JJMH01000057 *Priestia megaterium* 99.85 % (44.5 %)] ***	−	+++ (P)	O
	7	Orange colonies	NR_025732 *Brevibacterium permense* 99.52 % [AY243343 *Brevibacterium permense* 100 % (42.8 %)]	+	+++	−
	8	Brownish green color with white edges	MN481951 *Alternaria obovoidea* 99.47 %	+	+++	−
	9	White color, cottony texture, beige edges	*Letendraea helminthicola*	+	+++	−
	10	White color, cottony texture, staining the agar base a slightly orange	MT860222 *Epicoccum nigrum* 99.61 %	+	+++	−
	11	Brownish green color with white edges	ON074973 *Aureobasidium* sp. 100.00 %	+	+++	−
	12	Gray color, fluffy texture, forming a whitish halo or lighter on the edges	*Boeremia exigua*	+	+++	−

-: no reaction displayed; +: positive reaction; ++: extensive positive reaction; +++: extensive and rapid positive reaction.
(S): $CaCO_3$ solubilisation activity; (P): $CaCO_3$ precipitation activity; (O): iron oxidation activity.
*: Normal number indicates bacterium and italic number indicates fungus.
**: EzBioCloud database identification in square brackets.
***: *Prolinoborus fasciculus* CIP 103579 T shares 99.8 % 16S rRNA gene sequence similarity with *Actinetobacter lwoffii* DSM 2403 T [40]. *Bacillus aryabhattai* is a later heterotypic synonym of *Bacillus megaterium* (syn. *Priestia megaterium*) [41].

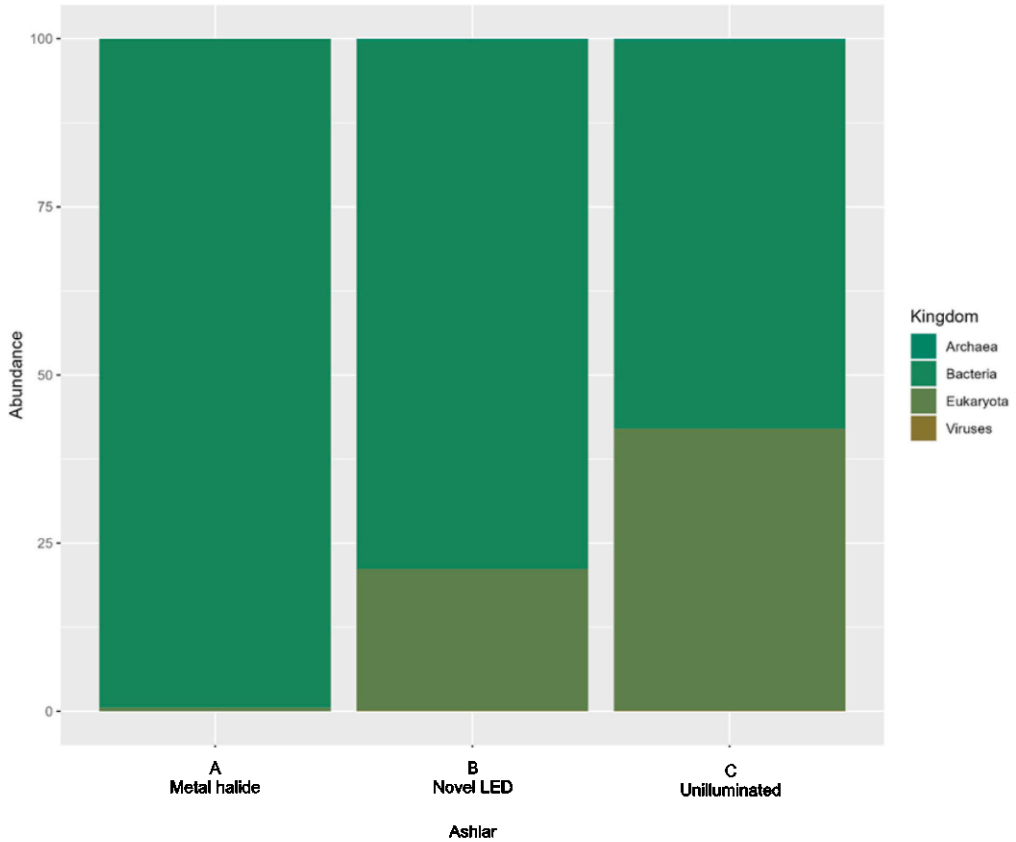

Fig. 2. Relative abundance and distribution of the microbial kingdom detected in the samples.

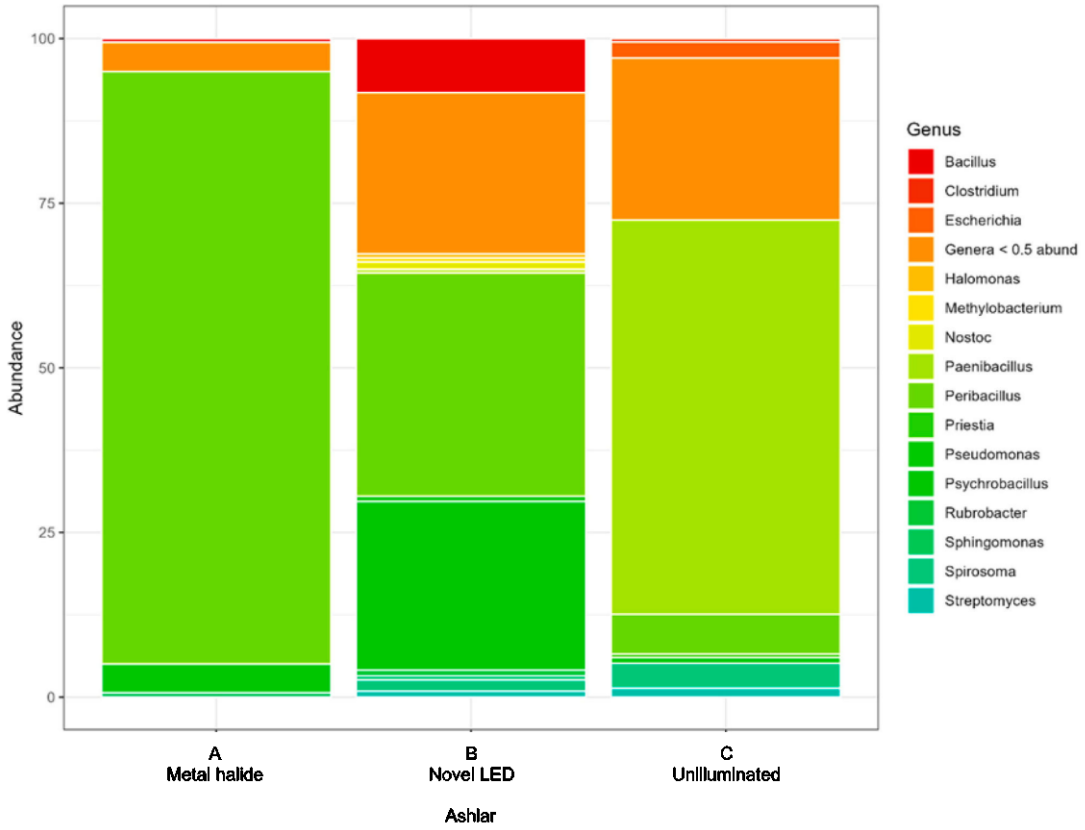

Fig. 3. Relative abundance and distribution of the bacterial genera detected in the samples.

%). In addition, in sample A, appeared *Psychrobacillus* (4.38 %), *Sphingomonas* (0.67 %), and *Bacillus* (0.57 %), and in sample B, *Psychrobacillus* (25.64 %), *Bacillus* (8.18 %), and *Spirosoma* (1.73 %). In sample C, *Paenibacillus* was the dominant genus at 59.89 %, followed by *Peribacillus* (6.04 %), *Spirosoma* (3.78 %), *Escherichia* (2.44 %), and *Streptomyces* (1.37 %). Additional genera with lower abundances (< 0.5 %) constituted 4.42 %, 24.46 % and 24.58 % in samples A, B and C respectively.

For fungi a total of 341, 15,866, and 13,845 reads were obtained in samples A, B and C, respectively. The most abundant phylum in all three samples was Ascomycota, with relative abundances of 82.99 % in sample A, 53.11 % in sample B, and 96.57 % in sample C, followed by Basidiomycota. The most abundant fungal genera (Fig. 4) were *Aspergillus* (12.02 %), followed by *Fusarium* (10.26 %), *Pyricularia* (5.87 %), and *Psilocybe* (5.57 %) in sample A; *Psilocybe* (26.97 %), followed by *Thermothelomyces* (15.71 %), *Thermothielavioides* (8.72 %), and *Marasmius* (8.15 %) in sample B; and *Neurospora* (28.54 %), followed by *Thermothelomyces* (15.31 %), *Colletotrichum* (10.57 %), and *Fusarium* (8.31 %) in sample C. In addition, genera with abundances less than 0.5 %, contributed to 1.47 % of the total abundance in A, 6.28 % in B, and 3.24 % in C. Of the algal community (excluding green algae not considered in this study), a total of 145 diatoms reads, of two genera *Thalassiosira* (mainly) and *Phaeodactylum*, were identified (Fig. S2). Of archaea 120, 443 and 141 reads were obtained for samples A, B and C, respectively. *Halorubrum* and *Halobaculum*, with abundances around 6 %, and *Halobacterium*, *Halovivax*, and *Methanobacterium*, with abundances around 4 %, were the most abundant genera in sample A. *Methanosarcina* (5.47 %) followed by *Thermococcus* and *Candidatus Nitrosocosmicus*, with abundances around 4 %, were the most abundant genera in sample B. Similarly in sample C, *Thermococcus* and *Methanosarcina*, with relative abundances around 5 % and 4 % were the most abundant genera. Genera with less than 1 % abundance collectively made up approximately 22.41 % of the sample A, 32.57 % of the sample B, and 1.43 % of the sample C (Fig. S3).

Alpha diversity indexes (Observed, Chao1 and Shannon) were determined (Fig. 5) and evidenced the highest bacterial (Fig. 5A) and fungal (Fig. 5B) species richness and evenness (only for bacteria) in sample B. As shown in Fig. 5A, the observed species count of bacteria, ranged from 6441 in sample B to 3385 in sample C, with 4596 in sample A. Similarly, the Chao1 index showed the highest estimate at 7717.71 in sample B, followed by sample A at 6294.92, and sample C at 5905.54. The Shannon index, related to both species richness and evenness, showed the highest value at 4.08 from sample B, followed by sample C with a value of 3.95, and sample A with a value of 0.94, which suggests that the bacterial species in C, while fewer in number than in sample A, are more evenly distributed than in the latter. As shown in Fig. 5B, the observed species count of fungi was 100 in sample B, 92 in sample C, and 75 in sample A. The Chao1 index mirrored this trend, with sample B showing the highest estimate at 101, followed by sample C at 95.6, and sample A at 80.2. However, the Shannon index in fungi, showed the highest value at 4.01 from sample A, followed by sample B with a value of 3.10, and sample C with a value of 2.92. Sample A despite has the lowest fungal species number (reads by MinION, observed and Chao 1 indexes), they are more evenly distributed.

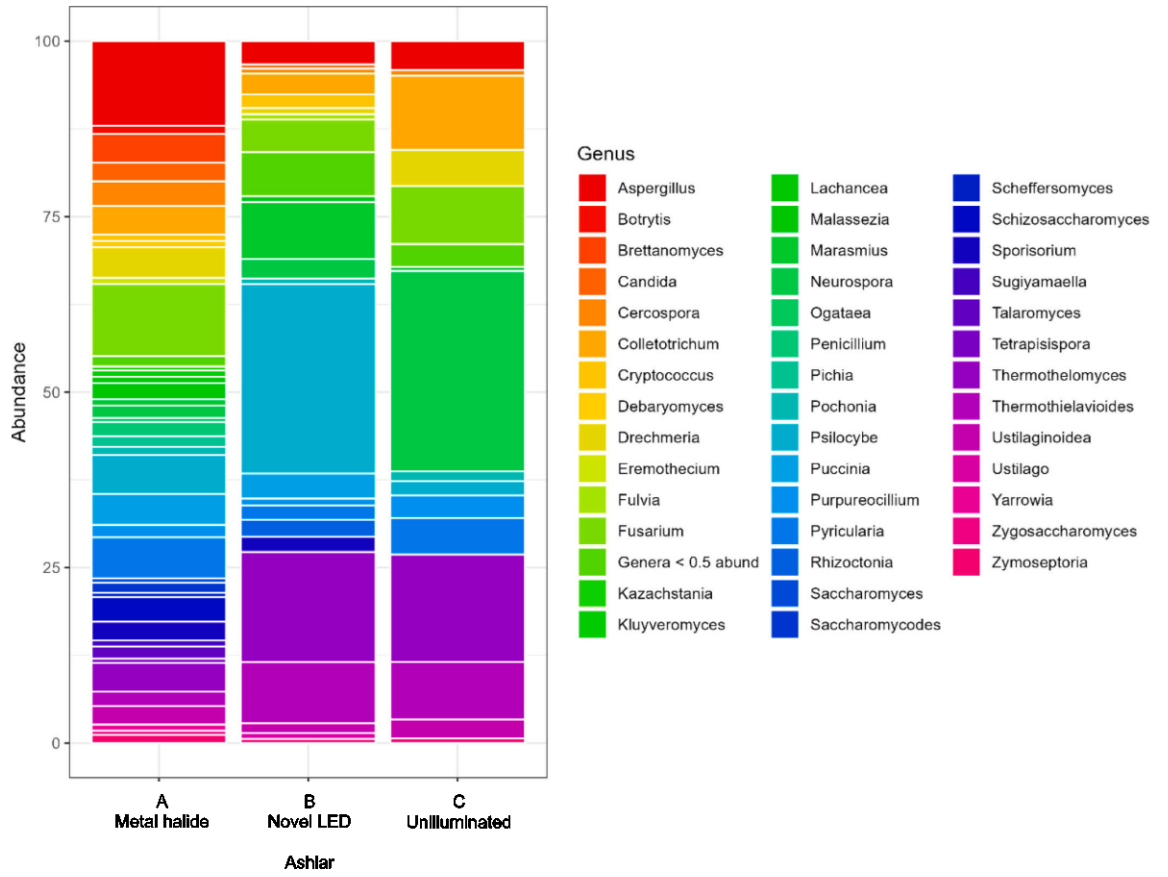

Fig. 4. Relative abundance and distribution of the fungal genera detected in the samples.

Principal coordinate analysis (PCoA) based on Bray Curtis dissimilarity metrics, showing the distance in the bacterial (Fig. 6A) and fungal (Fig. 6B) communities between samples A, B and C, clearly clustered into different groups samples A, B and C, which indicates that the three samples had discernible distinct bacterial and fungal communities.

3.4. Abundance of biocide and antibiotic resistance genes

In the analysis of Antibiotic Resistance Genes (ARGs), a total of 43 genes were identified across three samples A, B and C. The abundance of ARGs ranged from 4.84e^{-4} to 8.4 e^{-2} copies of ARGs per copy of 16S rRNA genes.

The proportions of ARGs for each sample are shown in Fig. 7. In sample A, the most abundant ARG was *vanR_in_vanF_cl* with a relative abundance of 27.26 %, followed by *vanS_in_vanF_cl* at 21.26 %, *FosM1* at 4.60 %, *FosM2* at 2.32 %, *FosM3* at 4.54 %, *blt* at 2.83 %, *vatH* at 3.74 %, and *vmlR* at 2.96 %. In sample B, the most abundant ARG was *vanS_in_vanF_cl* with a relative abundance of 17.97 %, followed by *vanR_in_vanF_cl* at 14.17 %, *BcIII* at 6.91 %, *ErmC* at 4.47 %, *efrB* at 3.03 %, and *tet(45)* at 2.39 %. In sample C, the most abundant ARG was *DfrA38* with a relative abundance of 25.91 %, followed by *vanXY_in_vanC_cl* at 22.7 %, *vanR_in_vanF_cl* at 18.57 %, and *FIA-1* at 17.31 %.

The most abundant biocide-resistance genes in sample A was blt and *fabL/ygaA*, each with a relative abundance of 18.40 %. The next most abundant gene was *sodA* with a relative abundance of 10.80 %. Other genes with notable relative abundances include *ruvB* at 4.80 %, *actP* at 4.00 %, and *perR* at 5.60 %. The most abundant gene in B_PdlC_NE was *fabL/ygaA* with a relative abundance of 18.06 %. *SodA* also showed a significant presence with 12.51 % relative abundance, *arsH* was notably abundant at 13.89 % and *smrA* had a relative abundance of 8.33 %. The most abundant gene in Sample C_PdlC_NE was *sodA* with a relative abundance of 58.31 %, higher than in the other samples. This was followed by *ykkC* which had a relative abundance of 16.68 %, *fabK* and *ykkD* each showed a relative abundance of 8.34 %, and *smdA* also had a relative abundance of 8.34 % (Fig. 8).

4. Discussion

In recent years, metagenomics tools, like high-throughput sequencing techniques, have made it easier to know in a deeper detail the communities that inhabit the surfaces of the built cultural heritage [42,43], without resorting to the culturable fraction that end up biasing the microbial communities. Oxford Nanopore Technologies sequencing through the MinION device has increased its popularity in cultural heritage. In addition to the affordable price of the device, the system is capable of producing long read lengths, which provide more comprehensive genomic information and consequently a reliable identification of the microbial species present in a sample [44]. However, the cultivation method also has its positive side since it discriminates between live and dead microorganisms, evidencing those metabolically active, and on stone buildings, dead biomass, dust particles and/or bird droppings may blur, bury or override the actual microbial community in situ

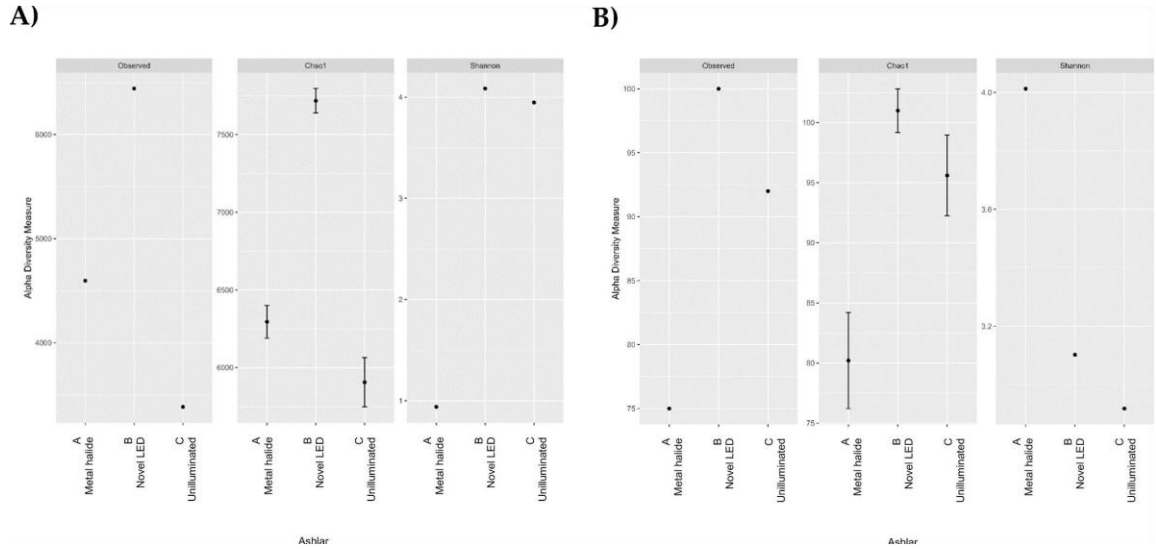

Fig. 5. Alpha diversity analysis of the microbial community in the samples including Observed, Chao1, and Shannon indexes. **A)** Alpha diversity values for the bacterial community. **B)** Alpha diversity values for the fungal community.

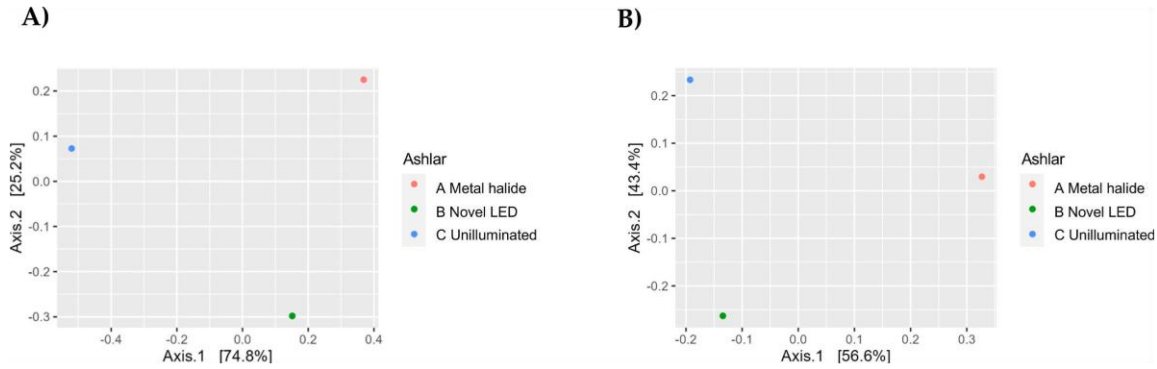

Fig. 6. Beta diversity analysis of the microbial community (A: Bacteria, B: Fungi) in the samples. Principal coordinate analysis (PCoA) of Bray-Curtis distances is shown.

[45]. Therefore, a combination of both methods is, in the opinion of the authors of the paper, the best choice. Here, samples from target areas (North-East facing granite ashlars) lit by a metal halide lamp (A), lit by a novel LED lamp (B) and unilluminated (C) showed similar number (five to seven) of bacterial and fungal isolates by culture-dependent analysis (section 3.2), while MinION sequencing (section 3.3) displayed different microbiome ratios in the three analyzed samples, especially in fungi, with a negligible presence in sample A.

Bacteria of the genera *Arthrobacter* and *Microbacterium* were isolated from all three samples. The former had already been isolated from colonized heritage assets in Portugal [46,47] and related to mineral weathering of granite by production of gluconic acid and biotite dissolution [48], as well as production of oxalate for the release of Fe, Ca, K, Mg, and Mn [49]. The latter was isolated from another granite building in Santiago de Compostela [50], testing positive for $CaCO_3$ precipitation. Fuentes et al. [51] detected the presence of *Alternaria* and *Penicillium*, the most representative fungi genera isolated from the samples, in churches of rural areas in Lugo (northwestern Spain). The rest of the fungal species isolated have been found in granite or other kinds of lithic substrates [52,53]. From sample A, *Pantoea* sp. (probably *deleyi*), which tested positive for $CaCO_3$ solubilisation and iron oxidation, and from sample C, *Bacillus aryabhattai* or *megaterium* (syn. *Priestia megaterium*), which tested positive for $CaCO_3$ precipitation and iron oxidation, and *Pseudomonas quebecensis*, which tested positive for iron oxidation, are the isolates with highest-risk potential biodeterioration capacity in the granite monument because oxidation of biotite plays the main role in granite weathering.

MinION analysis identified shifts in the granite microbiome elicited by ornamental lighting. In the ashlar lit by a metal halide lamp (A) showed a hegemony of bacteria and a negligible presence of fungi, while in the unilluminated ashlar (C) a similar relative abundance of bacteria and fungi. It also evidenced the notable presence of *Nostoc* cyanobacteria (with 4.80 % of reads) in the ashlar lit by a novel LED lamp (B), which were present in half abundance in C (with 2.10 % of reads), and almost nonexistent in A (with 0.27 % of reads). This can be explained because there is a competition between green algae and cyanobacteria in the ashlars, and that the greater presence of green algae in A and reduced in B and C (unpublished data), has slowed the presence of

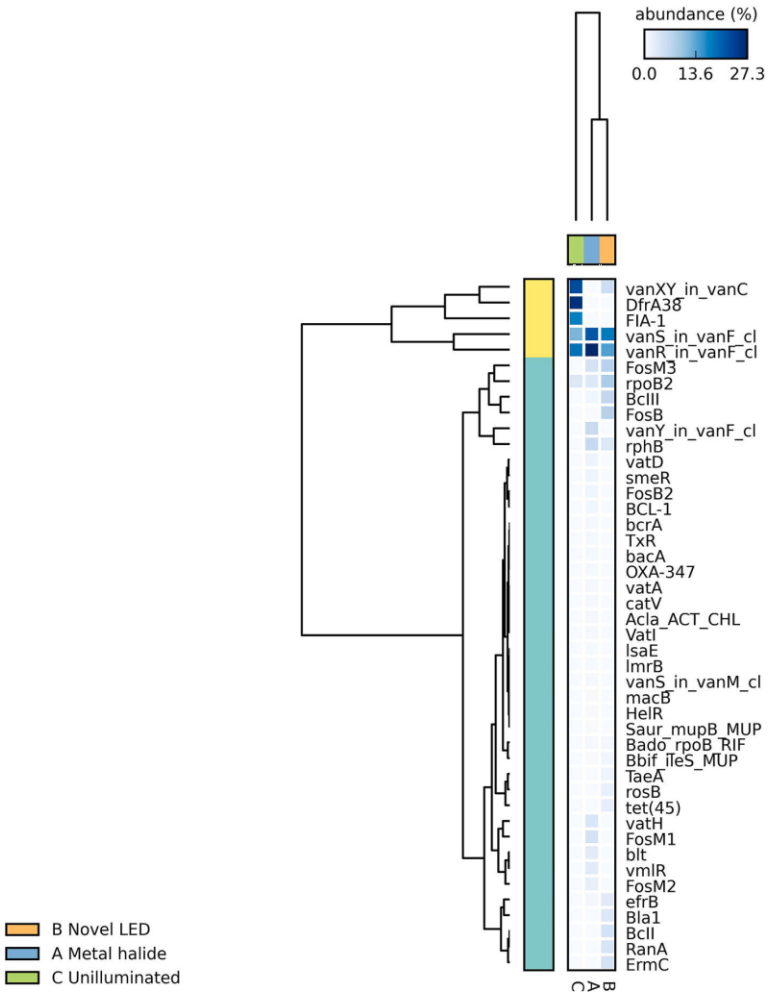

Fig. 7. Relative abundance of ARGs in the samples.

cyanobacteria in the former. Also, because they are *Nostoc* strains found in granite walls, which are rich in phycocyanin blue pigments (see e.g. [54]), so that their growth can be slowed down under blue wavelengths such as those contained in the metal halide lamp (A) and not contained in the novel LED lamp (B). In this line, warm white light (focused on the yellow part of the spectrum) in the Resavska Cave (Serbia) promoted cyanobacterial growth versus green algae growth, which grew more in areas illuminated by cold white light, with a high percentage of blue color [55].

The high-throughput sequencing showed that in all the samples, and mainly in sample A, members of the phylum firmicutes (Bacillota) and the genus *Peribacillus* (a new taxonomic genus composed by several species formerly *Bacillus*, [56]) were the most abundant. They are known as colonizers of stone materials and calcium carbonate biomineralizing microorganisms [57]. Other stone colonizers are the second most abundant species in sample B, *Psychrobacillus* [58] and the dominant species in sample C, *Paenibacillus* [59]. Fessia et al. [60] demonstrated that the growth of some *Bacillus* species is light-dependent, identifying the white (432–658 nm) and red (610–643 nm) lights, related to the metal halide lamp (A), as the most effective in promoting their growth.

Regarding fungi, members of the genus *Psilocybe*, mainly known as hallucinogenic basidiomycota [61] and their deterioration abilities oriented primarily to wood and various organic substrates [62] were the most abundant in sample B and were also present in sample A. *Thermothelomyces* species, which can produce several kinds of thermophilic enzymes, especially those able to hydrolyze lignocellulosic materials [63], occur with a high percentage in the samples B and C. Also, notably present in sample B, appeared members of the genus *Thermothielavioides*, which play a significant role in the global carbon cycle due to its ability to degrade polysaccharides from biomass [64], and those included in the genus *Marasmius*, mushroom-forming fungi that act as saprotrophs and are frequently encountered on leaves and wood debris within forest litter across the globe [65]. According to our knowledge, there are no reports in the literature that have investigated the impact of different wavelengths of the visible spectrum on these fungal species. However, there are studies that indicate how different wavelengths of visible light can influence the growth, production of pigments and diverse, secondary metabolites of different kinds of phytopathogenic species, including *Colletotrichum*, *Fusarium*, *Aspergillus* and *Neurospora* genera, mainly

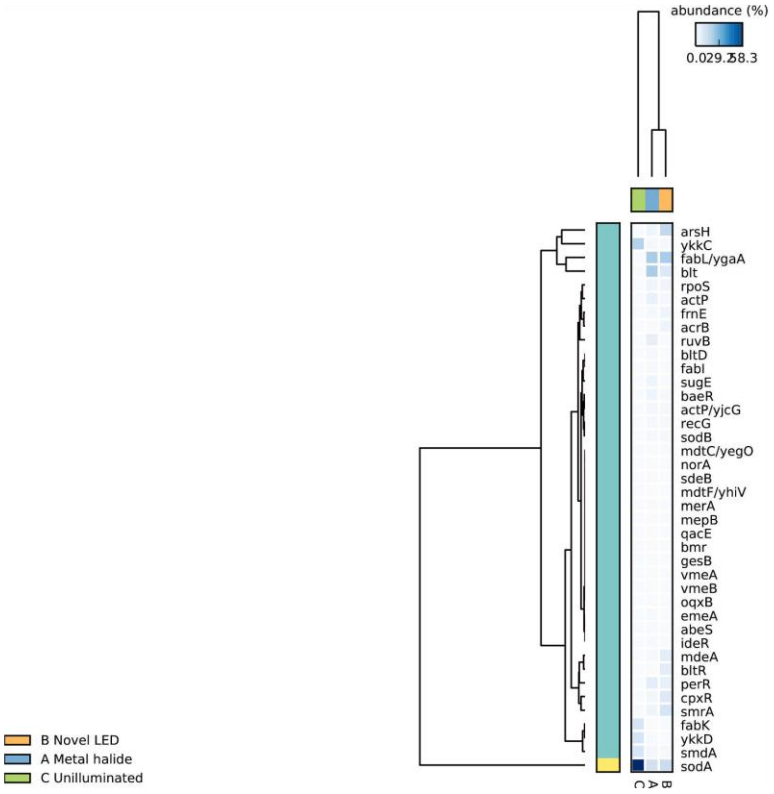

Fig. 8. Relative abundance of biocide resistance genes in the samples.

concerned by the studies [66,67,68] and barely detected in the present study.

The alpha diversity indexes of bacteria evidenced a highest richness and evenness in the sample B respect to sample A, both of the illuminated ashlars. The broad light spectrum of metal halide light (A) can decrease de diversity of detected microorganisms by promoting the dominance of a specific group of species-specific sensitivities to artificial light (probably within the *Peribacillus* spp.) within microbial communities [69]. In addition, the relevant presence of *Peribacillus* may be promoted by the higher presence of green algae in the ashlar A compared to ashlars B and C (unpublished data), as previous studies in epiphytic lacustrine biofilm communities [70] have found that the presence of microalgae in biofilms was positively correlated with the presence of Firmicutes (group in which *Peribacillus* is included). The highest richness in fungi was also in sample B while the highest evenness in sample A with a negligible fungal presence. The latter may be due to the photoinhibitiory effect of visible spectrum light with blue wavelengths (like the metal halide lamp) over fungal production [71,72]. Beta diversity analysis revealed distinct microbial communities across the three samples for both bacteria and fungi. However, despite the overall differences, certain microbial taxa were more similar between the LED-lit and unlit samples.

The distribution of antibiotic resistance genes (ARGs) in microbial communities colonizing stone monuments is highly influenced by human activities [73], and it can be considered as a threat to the conservation of the monument since it undermines the resistance of microorganisms to biocides [74]. The most detected antibiotic resistance genes (ARGs) belonged to the family which confers the resistance to glycopeptides, for example to the antibiotic vancomycin. Indeed, the *vanR* and *vanS* genes in *vanF* cluster occurred in all three samples; these genes are possessed by different species of the Bacilli class [75]. Therefore, the taxonomically results which displayed the high presence of genera of this class (*Paenibacillus*, *Bacillus*, *Peribacillus* and *Psychrobacillus*) are in concordance with the distribution of these ARGs. In sample C was revealed also the *vanXY* gene in *vanC* cluster, this gene originally was detected in *Enterococcus gallinarum* [76]. Since the taxonomic analysis failed to reveal any member of the *Enterococcus* genus, it could be hypothesized that the detected *vanXY* gene is a homologous to the original registered or that the results of present study have revealed the presence of this gene in other members of the Bacillota phylum (Firmicutes) widely present in sample C. The gene *dfrA38*, which is responsible for resistance to diaminopyrimidine antibiotics, was also detected in sample C. This gene was recently discovered in *Acinetobacter baumannii* (Gammaproteobacteria class; [77]). Considering the complicate nomenclature of the genes belonged to the *dfrA* group [78] and also their presence in several members of the phylum Proteobacteria (Pseudomonadota; [79,80]) it can be indicated that the presence of the *dfrA38* gene is in concordance with the taxonomy results which attested the presence of Proteobacteria (13.98 %) in the sample C. Moreover, from sample B an *Acinetobacter* was isolated, but its isolation was not successful for sample C.

The microbiota of samples B and C harbored several genes conferring the resistance to beta-lactam antibiotics. The gene *bla1* and the genes encoding BCII, BCIII (almost only in sample B) with the FIA-1 replicon (exclusively in sample C) were the most detected. The FIA-1 is more characteristic for species belonged to the family Enterobacteriaceae (Proteobacteria / Pseudomonadota; [81]), while the other genetic elements (BCII, BCIII and *bla1*) are more associated to the family

Bacillaceae (Firmicutes / Bacillota; [82]). It is necessary also to say that the studied wall in the past was treated with the herbicide Atila containing the 36 % of Glyphosate which was showed to promote the antibiotic resistance in bacteria inducing the production of Extended Spectrum Beta Lactamases in particular in various species of Enterobacteriaceae [83].

ARGs common, exclusively, to samples A and B encode enzymes (FosM1, FosM2, FosM3 and FosB2 in sample A; FosB and FosM3 in sample B) lead to the resistance of Fosfomycin. Although, the *fosM1*, *fosM2* and *fosM3* genes were recently discovered, it is necessary to note that together with the *fosB* and *fosB2* genes are mainly present in members of the Bacillaceae [84]. Therefore, also this group of genes matches with the most identified bacterial assemblages of samples A and B.

Other common genes of samples A and B were rphB (detected especially in A) and *rpoB2* (present more in B). The *rphB* and *rpoB2* genes confer the resistance to rifamycin antibiotics, they are almost typical for Bacillota (Firmicutes; [85]) and Actinomycetota (Actinobacteria; [86]), respectively.

In Sample A, the most abundant biocide resistance genes were blt, multidrug efflux transporters found in *Bacillus subtilis* [87] and fabL/ygaA, encoding a new family of the proteins involved in the enoyl-ACP reductase step in type II fatty-acid synthases [88]. The upregulation of the fabL and ygaA genes has been linked to triclosan resistance, as this compound is recognized for its efficacy as a biocide against *E. coli* and other bacteria due to the incapacity of the proteins encoded by these genes to establish a stable ternary complex with triclosan [88]. These genes were also found to be the most abundant in sample B. Since these genes are commonly associated with Bacillus, which was abundant in our samples, this might be the reason why these genes were detected. Gene arsH highly abundant in Sample B, encodes organoarsenical oxidase. This enzyme facilitates the detoxification of trivalent methylated and aromatic arsenicals through an oxidation reaction, converting them into their pentavalent forms [89]. The gene is clustered with other ars genes and was identified in Phytobacter [90]. Additionally, transposase genes were found near the ars gene cluster, suggesting horizontal gene transfer (HGT) [90]. This could explain the presence of the arsH gene in sample B, considering that Phytobacter was not detected in our samples. Arsenic, along with antimony, are chemical elements widely distributed in rocks. Therefore, it is unsurprising to find this gene in our samples, as it confers resistance to both elements. Arsenic, along with antimony, are chemical elements widely distributed in rocks. Therefore, it is unsurprising to find this gene in our samples, as it confers resistance to both elements. In sample C, the prevailing gene was sodA, known for conferring resistance to peroxide [91]. This gene encodes superoxide dismutase (SOD), a crucial agent in combating oxidative stress [92]. Notably, sodA was also dominant in the other two samples. All three samples were subjected to glyphosate treatment, a herbicide commonly used to control weeds in agriculture [93,94]. It has been suggested that contaminants like herbicides can cause oxidative stress in bacteria by generating reactive oxygen species [95]. Thus, the presence of the sodA gene may signify a response of the existing bacterial community to the oxidative stress induced by glyphosate exposure.

Regarding the influence of the light to promote the bacterial antibiotic resistance some studies showed that the UVC and the sunlight accelerate and spread the ARGs in the environment through conjugative transfer [96,97]. Therefore, artificial white light can contribute to shaping the resistome of an environment, this is a detail that deserves attention and targeted studies in order to choose the right and safety lighting in the future.

5. Conclusions

Culture-dependent microbiological analysis failed to properly show changes in community composition, for which metagenomic approaches like MinION are better suited. Thus, MinION analysis identified shifts in the granite microbiome elicited by ornamental lighting. The novel LED lamp with the biostatic effect on phototrophs caused an increase in the diversity of bacteria and fungi. In this case, the microbiome was more similar to that in the unlit samples. In the samples illuminated by the metal halide lamp, dominance of bacteria was favoured and the presence of fungi was negligible.

CRediT authorship contribution statement

Anxo Méndez: Writing – review & editing, Writing – original draft, Investigation, Formal analysis, Conceptualization. **Francesca Maisto:** Writing – original draft, Methodology, Investigation, Formal analysis, Conceptualization. **Jelena Pavlović:** Writing – original draft, Methodology, Investigation, Formal analysis, Conceptualization. **Magdaléna Rusková:** Methodology, Investigation, Formal analysis, Conceptualization. **Domenico Pangallo:** Writing – review & editing, Writing – original draft, Supervision, Resources, Methodology, Investigation, Conceptualization. **Patricia Sanmartín:** Writing – review & editing, Writing – original draft, Supervision, Conceptualization.

Declaration of competing interest

The authors declare that they have no known competing financial interests or personal relationships that could have appeared to influence the work reported in this paper.

Data availability

No data was used for the research described in the article.

Acknowledgements

This study was developed within the framework of the CROMALUX project: Third SMARTIAGO Challenge – Smart lighting system for Heritage Conservation. A. Méndez acknowledges receipt of a grant in the Programa de Doutoramento Industrial (04_IN606D_2021_2598528) financed by the Xunta de Galicia. P. Sanmartín acknowledges receipt of a Ramón y Cajal contract (RYC2020-029987-I) financed by the Spanish State Research Agency (AEI) of the Ministry of Science and Innovation (MCIN). Méndez and Sanmartín are also grateful to the Xunta de Galicia for concession of the FONTES project (ED431F 2022/14) and the Competitive Reference Group (GRC) grant ED431C 2022/09. This study has been also supported by the grants VEGA 2/099/2021, APVV-23-0235 and the European Regional Development Fund project 313011 V578.

Appendix A. Supplementary data

Supplementary data to this article can be found online at https://doi.org/10.1016/j.jphotobiol.2024.113065.

References

[1] T. Warscheid, J. Braams, Biodeterioration of stone: a review, International Biodeterioration and Biodegradation 46 (4) (2000) 343–368.
[2] J.S. Pozo-Antonio, T. Rivas, A.J. López, M.P. Fiorucci, A. Ramil, Effectiveness of granite cleaning procedures in cultural heritage: a review, Sci. Total Environ. 571 (2016) 1017–1028.
[3] A.C. Hernandez, J. Sanjurjo-Sánchez, C. Alves, C.A. Figueiredo, Study of the geochemical decay and environmental causes of granite stone surfaces in the built heritage of Barbanza peninsula (Galicia, NW Spain), Coatings 14 (2) (2024) 169.
[4] A.J. Fonseca, F. Pina, M.F. Macedo, N. Leal, A. Romanowska-Deskins, L. Laiz, A. Gómez-Bolea, C. Saiz-Jimenez, Anatase as an alternative application for preventing biodeterioration of mortars: evaluation and comparison with other biocides, Int. Biodeterior. Biodegrad. 64 (5) (2010) 388–396.
[5] F.L. Guerra, W. Lopes, J.C. Cazarolli, M. Lobato, A.B. Masuero, D.C. Dal Molin, F. M. Bento, A. Schrank, M.H. Vainstein, Biodeterioration of mortar coating in historical buildings: microclimatic characterization, material, and fungal community, Build. Environ. 155 (2019) 195–209.

[6] D. Pinna, Can we do without biocides to cope with biofilms and lichens on stone heritage? International Biodeterioration and Biodegradation 172 (2022) 105437.
[7] A. Méndez, B. Prieto, Aguirre i Font, J.M, P. Sanmartín, Better, not more, lighting: policies in urban areas towards environmentally-sound illumination of historical stone buildings that also halts biological colonization, Sci. Total Environ. 906 (2024) 167560.
[8] P.P. Akhila, K.V. Sunooj, B. Aaliya, M. Navaf, C. Sudheesh, S. Sabu, A. Sasidharan, S.A. Mir, J. George, A.M. Khaneghah, Application of electromagnetic radiations for decontamination of fungi and mycotoxins in food products: a comprehensive review, Trends Food Sci. Technol. 114 (2021) 399–409.
[9] A.J. De Lucca, C. Carter-Wientjes, K.A. Williams, D. Bhatnagar, Blue light (470 nm) effectively inhibits bacterial and fungal growth, Lett. Appl. Microbiol. 55 (6) (2012) 460–466.
[10] M. Hessling, B. Spellerberg, K. Hoenes, Photoinactivation of bacteria by endogenous photosensitizers and exposure to visible light of different wavelengths–a review on existing data, Microbiology Letters 364 (2) (2017) fnw270.
[11] R.M. Tomb, T.A. White, J.E. Coia, J.G. Anderson, S.J. MacGregor, M. Maclean, Review of the comparative susceptibility of microbial species to photoinactivation using 380–480 nm violet-blue light, Photochem. Photobiol. 94 (3) (2018) 445–458.
[12] M. Hasenleitner, K. Plaetzer, In the right light: photodynamic inactivation of microorganisms using a LED-based illumination device tailored for the antimicrobial application, Antibiotics 1 (2019) 13.
[13] D. Wang, H. Pan, Y. Yan, F. Zhang, Rose bengal-mediated photodynamic inactivation against periodontopathogens in vitro, Photodiagnosis Photodyn. Ther. 34 (2021) 102250.
[14] L. Bruno, S. Bellezza, F. De Leo, C. Urzì, A study for monitoring and conservation in the Roman catacombs of St. Callistus and Domitilla, Rome (Italy), in: C. Saiz-Jimenez (Ed.), The Conservation of Subterranean Cultural Heritage, CRC Press/Balkema, Leiden, The Netherlands, 2014, pp. 37–44.
[15] Z. Yu, R. Fischer, Light sensing and responses in fungi, Nat. Rev. Microbiol. 17 (1) (2019) 25–36.
[16] V.S. Ghate, K.S. Ng, W. Zhou, H. Yang, G.H. Khoo, W.B. Yoon, H.G. Yuk, Antibacterial effect of light emitting diodes of visible wavelengths on selected foodborne pathogens at different illumination temperatures, Int. J. Food Microbiol. 166 (3) (2013) 399–406.
[17] S. Kim, J. Kim, W. Lim, S. Jeon, O. Kim, J.T. Koh, C.S. Kim, H.R. Choi, O. Kim, In vitro bactericidal effects of 625, 525, and 425 nm wavelength (red, green, and blue) light-emitting diode irradiation, Photomed. Laser Surg. 31 (11) (2013) 554–562.
[18] G.Y. Lui, D. Roser, R. Corkish, N.J. Ashbolt, R. Stuetz, Point-of-use water disinfection using ultraviolet and visible light-emitting diodes, Sci. Total Environ. 553 (2016) 626–635.
[19] A. Kumar, V. Ghate, M.J. Kim, W. Zhou, G.H. Khoo, H.G. Yuk, Inactivation and changes in metabolic profile of selected foodborne bacteria by 460 nm LED illumination, Food Microbiol. 63 (2017) 12–21.
[20] J.C. Oliva, E.R. Vela, J.Z. Salido, Control systems and ornamental lighting. A case study: Illumination of the facade of Santiago Hospital in Úbeda (Jaén), in: M. J. Hermoso-Orzáez, A. Gago-Calderón (Eds.), Energy Efficiency and Sustainable Lighting - a Bet for the Future, United Kingdom, IntechOpen, London, 2020, pp. 247–262.
[21] P. Albertano, L. Bruno, The importance of light in the conservation of hypogean monuments, in: C. Saiz-Jiménez (Ed.), Molecular Biology and Cultural Heritage, CRC Press/Bakelma, Rotterdam, The Netherlands, 2003, pp. 171–177.
[22] Y. Bao, Y. Ma, W. Liu, X. Li, Y. Li, P. Zhou, Y. Feng, M. Delgado-Baquerizo, Innovative strategy for the conservation of a millennialmausoleum from biodeterioration through artificial light management, npj Biofilms and Microbiomes 9 (69) (2023).
[23] J. Muñoz-Fernández, Y. Del Rosal, F. Álvarez-Gómez, M. Hernández-Mariné, R. Guzmán-Sepúlveda, N. Korbee, F.L. Figueroa, Selection of LED lighting systems for the reduction of the biodeterioration of speleothems induced by photosynthetic biofilms in the Nerja cave (Malaga, Spain), J. Photochem. Photobiol. B Biol. 217 (2021) 112155.
[24] P. Sanmartín, B. Prieto, Identifying the original colour of the paintwork on the artistic and industrial recreation pavilion designed by Antonio Palacios for the Galician regional exhibition held in 1909, Heritage 3 (2) (2020) 331–341.
[25] P. Sanmartín, F. Villa, F. Cappitelli, S. Balboa, R. Carballeira, Characterization of a biofilm and the pattern outlined by its growth on a granite built cloister in the monastery of san Martiño Pinario (Santiago de Compostela, NW Spain), International Biodeterioration and Biodegradation 147 (2020) 104871.
[26] A. Méndez, L. Martín, J. Arines, R. Carballeira, P. Sanmartín, Attraction of insects to ornamental lighting used on cultural heritage buildings: a case study in an urban area, Insects 13 (12) (2022) 1153.
[27] D.J. Lane, 16S/23S rRNA sequencing, in: E. Stackebrandt, Goodfellow (Eds.), Nucleic Acid Techniques in Bacterial Systematics, Wiley, New York, USA, 1991, pp. 115–175.
[28] T.J. White, T. Bruns, S. Lee, J. Taylor, Amplification and direct sequencing of fungi ribosomal RNA genes for phylogenetics, in: M.A. Innis, D.H. Gelfand, J.J. Sninsky, T.J. White (Eds.), PCR protocols. A guide to methods and applications, Academic Press, San Diego, USA, 1990, pp. 315–322.
[29] E. Boquet, A. Boronat, A. Ramos-Cormenzana, Production of calcite (calcium carbonate) crystals by soil bacteria is a general phenomenon, Nature 246 (5434) (1973) 527–529.
[30] P. Albertano, C. Urzì, Structural interactions among epilithic cyanobacteria and heterotrophic microorganisms in Roman hypogea, Microb. Ecol. 38 (1999) 244–252.
[31] J.C.G. Ottow, H. Glathe, Isolation and identification of iron-reducing bacteria from gley soils, Soil Biol. Biochem. 3 (1) (1971) 43–55.
[32] R. Sachan, A.K. Singh, Y.S. Negi, Study of microbially influenced corrosion in the presence of iron-oxidizing bacteria (strain DASEWM2), Journal of Bio-and Tribo-Corrosion 6 (2020) 1–14.
[33] A.G. McArthur, N. Waglechner, F. Nizam, A. Yan, M.A. Azad, A.J. Baylay, K. Bhullar, M.J. Canova, G. De Pascale, L. Ejim, L. Kalan, A.M. King, K. Koteva, M. Morar, M.R. Mulvey, J.S. O'Brien, A.C. Pawlowski, L.J.V. Piddock, P. Spanogiannopoulos, A.D. Sutherland, I. Tang, P.L. Taylor, M. Thaker, W. Wang, M. Yan, T. Yu, G.D. Wright, The comprehensive antibiotic resistance database, Antimicrob. Agents Chemother. 57 (7) (2013) 3348–3357.
[34] C. Pal, J. Bengtsson-Palme, C. Rensing, E. Kristiansson, D.J. Larsson, BacMet: antibacterial biocide and metal resistance genes database, Nucleic Acids Res. 42 (D1) (2014) D737–D743.
[35] B. Buchfink, C. Xie, D.H. Huson, Fast and sensitive protein alignment using DIAMOND, Nat. Methods 12 (1) (2015) 59–60.
[36] J. Bengtsson-Palme, M. Hartmann, K.M. Eriksson, C. Pal, K. Thorell, D.G.J. Larsson, R.H. Nilsson, METAXA2: improved identification and taxonomic classification of small and large subunit rRNA in metagenomic data, Mol. Ecol. Resour. 15 (6) (2015) 1403–1414.
[37] D.E. Wood, J. Lu, B. Langmead, Improved metagenomic analysis with kraken 2, Genome Biol. 20 (2019) 1–13.
[38] R Core Team, R: A Language and Environment for Statistical Computing; R Foundation for Statistical Computing: Vienna, Austria, 2020.
[39] A. Streckeisen, To each plutonic rocks its proper name, Earth Sci. Rev. 12 (1976) 73–85.
[40] Glaeser, S.P., Pulami, D., Blom, J., Eisenberg, T., Goesmann, A., Bender, J., Wilharm, G., Kämpfer, P., 2020. The status of the genus *Prolinoborus* (Pot et al. 1992) and the species *Prolinoborus fasciculus* (pot et al. 1992). Int. J. Syst. Evol. Microbiol., 70(9), 5165–5171.
[41] M.P. Narsing Rao, Z.Y. Dong, G.H. Liu, L. Li, M. Xiao, W.J. Li, Reclassification of *Bacillus aryabhattai* Shivaji et al. 2009 as a later heterotypic synonym of *Bacillus megaterium* de Bary 1884 (approved lists 1980), FEMS Microbiol. Lett. 366 (22) (2019) fnz258.
[42] B. Gutarowska, The use of-omics tools for assessing biodeterioration of cultural heritage: a review, J. Cult. Herit. 45 (2020) 351–361.
[43] X. Liu, Y. Qian, Y. Wang, F. Wu, W. Wang, J.D. Gu, Innovative approaches for the processes involved in microbial biodeterioration of cultural heritage materials, Curr. Opin. Biotechnol. 75 (2022) 102716.
[44] J. Pavlovic, D. Cavalieri, G. Mastromei, D. Pangallo, B. Perito, M. Marvasi, MinION technology for microbiome sequencing applications for the conservation of cultural heritage, Microbiol. Res. 247 (2021) 126727.
[45] M. Marvasi, D. Cavalieri, G. Mastromei, A. Casaccia, B. Perito, Omics technologies for an in-depth investigation of biodeterioration of cultural heritage, International Biodeterioration and Biodegradation 144 (2019) 104736.
[46] S. Macedo-Arantes, A. Piçarra, A.T. Caldeira, A.E. Candeias, M.R. Martins, Essential oils of Portuguese flavouring plants: potential as green biocides in cultural heritage, The European Physical Journal Plus 136 (2021) 1–15.
[47] J. Trovão, A. Portugal, The impact of stone position and location on the microbiome of a marble statue, The Microbe 2 (2024) 100040.
[48] Y. Sun, Y. Wang, L. Li, L. Sun, L. He, X. Sheng, Distinct biotite-weathering activities of *Arthrobacter pascens* F74 under different contact conditions, J. Basic Microbiol. 60 (4) (2020) 362–371.
[49] B. Frey, S.R. Rieder, I. Brunner, M. Plötze, S. Koetzsch, A. Lapanje, H. Brandl, G. Furrer, Weathering-associated bacteria from the Damma glacier forefield: physiological capabilities and impact on granite dissolution, Appl. Environ. Microbiol. 76 (14) (2010) 4788–4796.
[50] J. Pavlović, P. Bosch-Roig, M. Rusková, M. Planý, D. Pangallo, P. Sanmartín, Long-amplicon MinION-based sequencing study in a salt-contaminated twelfth century granite-built chapel, Appl. Microbiol. Biotechnol. 106 (11) (2022) 4297–4314.
[51] E. Fuentes, R. Carballeira, B. Prieto, Role of exposure on the microbial consortiums on historical rural granite buildings, Appl. Sci. 11 (9) (2021) 3786.
[52] G.M. Gadd, M. Fomina, F. Pinzari, Fungal biodeterioration and preservation of cultural heritage, artwork, and historical artifacts: extremophily and adaptation, Microbiol. Mol. Biol. Rev. 88 (2024) e00200–e00222.
[53] E. Stanaszek-Tomal, Environmental factors causing the development of microorganisms on the surfaces of national cultural monuments made of mineral building materials, Coatings 10 (12) (2020) 1203.
[54] P. Sanmartín, N. Aira, R. Devesa-Rey, B. Silva, B. Prieto, Relationship between color and pigment production in two stone biofilm-forming cyanobacteria (*Nostoc* sp. PCC 9104 and *Nostoc* sp. PCC 9025), Biofouling 26 (5) (2010) 499–509.
[55] S. Popović, N. Nikolić, M. Pećić, A. Anđelković, G.S. Simić, Comparative analysis of lampenflora in two show caves in Serbia, ARPHA Conference Abstracts 5 (2022) e87188.
[56] S. Patel, R.S. Gupta, A phylogenomic and comparative genomic framework for resolving the polyphyly of the genus *Bacillus*: proposal for six new genera of *Bacillus* species, *Peribacillus* gen. Nov., *Cytobacillus* gen. Nov., *Mesobacillus* gen. Nov., *Neobacillus* gen. Nov., *Metabacillus* gen. Nov. and *Alkalihalobacillus* gen. Nov, Int. J. Syst. Evol. Microbiol. 70 (1) (2020) 406–438.
[57] C. Lors, C. Gassie, R. Guyoneaud, D. Damidot, Impact of a biorepair treatment on the diversity of calcifying bacterial communities at the surface of cracked concrete walls, Appl. Microbiol. Biotechnol. 107 (1) (2023) 187–200.
[58] F. Benedetti, M. Kratter, P. Atanasio, F. Mura, M. Beccaccioli, J. Scifo, I. di Sarcina, M.C. Tomassetti, K. Schneider, M. Rossi, A. Cemmi, Isolation of carbonatogenic bacteria for biorestoration, Journal of Cultural Heritage 64 (2023) 282–289.

[59] L. Schröer, T. De Kock, V. Cnudde, N. Boon, Differential colonization of microbial communities inhabiting Lede stone in the urban and rural environment, Sci. Total Environ. 733 (2020) 139339.

[60] A. Fessia, R. Ponzio, L. Arcibia, G. Barros, A. Nesci, Effects of different light wavelengths on Bacillus subtilis and Bacillus velezensis, two biocontrol agents isolated from the maize phyllosphere, Arch. Microbiol. 206 (3) (2024) 104.

[61] H. Lowe, N. Toyang, B. Steele, H. Valentine, J. Grant, A. Ali, W. Ngwa, L. Gordon, The therapeutic potential of psilocybin, Molecules 26 (10) (2021) 2948.

[62] M. Meyer, J. Slot, The evolution and ecology of psilocybin in nature, Fungal Genet. Biol. 167 (2023) 103812.

[63] M.F. Viegas, R.P. Neves, M.J. Ramos, P.A. Fernandes, QM/MM study of the reaction mechanism of thermophilic glucuronoyl esterase for biomass treatment, ChemPhysChem 23 (20) (2022) e202200269.

[64] M. Tõlgo, O.A. Hegnar, H. Østby, A. Várnai, F. Vilaplana, V.G. Eijsink, L. Olsson, Comparison of six lytic polysaccharide monooxygenases from *Thermothielavioides terrestris* shows that functional variation underlies the multiplicity of LPMO genes in filamentous fungi, Appl. Environ. Microbiol. 88 (6) (2022) e00096–22.

[65] J.J.S. Oliveira, J.M. Moncalvo, S. Margaritescu, M. Capelari, A morphological and phylogenetic evaluation of Marasmius sect. Globulares (Globulares-Sicci complex) with nine new taxa from the Neotropical Atlantic Forest, Persoonia-Molecular Phylogeny and Evolution of Fungi 44 (1) (2020) 240–277.

[66] M. Cerón-Bustamante, E. Balducci, G. Beccari, P. Nicholson, L. Covarelli, P. Benincasa, Effect of light spectra on cereal fungal pathogens, a review, Fungal Biol. Rev. 43 (2023) 100291.

[67] L.M. Corrochano, Light in the fungal world: from photoreception to gene transcription and beyond, Annu. Rev. Genet. 53 (2019) 149–170.

[68] A.S.Y. Ting, P.T. Gan, Influence of coloured lights on growth and enzyme production of beneficial endophytic fungi, Int. Microbiol. 27 (1) (2024) 1–12.

[69] E. Maggi, I. Bertocci, L. Benedetti-Cecchi, Light pollution enhances temporal variability of photosynthetic activity in mature and developing biofilm, Hydrobiologia 847 (7) (2020) 1793–1802.

[70] P. Xia, D. Yan, R. Sun, X. Song, T. Lin, Y. Yi, Community composition and correlations between bacteria and algae within epiphytic biofilms on submerged macrophytes in a plateau lake, Southwest China, Sci. Total Environ. 727 (2020) 138398.

[71] J. Du, Y. Zhang, L. Liu, M. Qv, Y. Lv, Y. Yin, Y. Zhou, M. Cui, Y. Zhu, H. Zhang, Can visible light impact litter decomposition under pollution of ZnO nanoparticles? Chemosphere 187 (2017) 368–375.

[72] G. Pu, D. Zeng, L. Mo, J. Liao, X. Chen, S. Qiu, Y. Lv, Artificial light at night alter the impact of arsenic on microbial decomposers and leaf litter decomposition in streams, Ecotoxicol. Environ. Saf. 191 (2020) 110014.

[73] J. He, N. Zhang, X. Shen, A. Muhammad, Y. Shao, Deciphering environmental resistome and mobilome risks on the stone monument: a reservoir of antimicrobial resistance genes, Sci. Total Environ. 838 (2022) 156443.

[74] Q. Li, C. Wu, J. He, B. Zhang, Unraveling the microbiotas and key genetic contexts identified on stone heritage using illumina and nanopore sequencing platforms, Int. Biodeter. Biodegr. 185 (2023) 105688.

[75] P.J. Stogios, A. Savchenko, Molecular mechanisms of vancomycin resistance, Protein Sci. 29 (3) (2020) 654–669.

[76] P.E. Reynolds, C.A. Arias, P. Courvalin, Gene vanXYC encodes D, D-dipeptidase (VanX) and D, D-carboxypeptidase (VanY) activities in vancomycin-resistant Enterococcus gallinarum BM4174, Mol. Microbiol. 34 (2) (1999) 341–349.

[77] S.J. Ambrose, R.M. Hall, A novel trimethoprim resistance gene, dfrA38, found in a sporadic Acinetobacter baumannii isolate, J. Antimicrob. Chemother. 75 (12) (2020) 3694–3695.

[78] S.J. Ambrose, R.M. Hall, dfrA trimethoprim resistance genes found in gram-negative bacteria: compilation and unambiguous numbering, Journal of Antimicrobial Chemotherapy 76 (11) (2021) 2748–2756.

[79] A. Brolund, M. Sundqvist, G. Kahlmeter, M. Grape, Molecular characterisation of trimethoprim resistance in *Escherichia coli* and *Klebsiella pneumoniae* during a two year intervention on trimethoprim use, PloS One 5 (2) (2010) 9233.

[80] H.N.K. Nguyen, T.T.H. Van, H.T. Nguyen, P.M. Smooker, J. Shimeta, P.J. Coloe, Molecular characterization of antibiotic resistance in Pseudomonas and Aeromonas isolates from catfish of the Mekong Delta, Vietnam, Veterinary Microbiology 171 (3–4) (2014) 397–405.

[81] H.Y. Kang, K.Y. Kim, J. Kim, J.C. Lee, Y.C. Lee, D.T. Cho, S.Y. Seol, Distribution of conjugative-plasmid-mediated 16S rRNA methylase genes among amikacin-resistant Enterobacteriaceae isolates collected in 1995 to 1998 and 2001 to 2006 at a university hospital in South Korea and identification of conjugative plasmids mediating dissemination of 16S rRNA methylase, J. Clin. Microbiol. 46 (2) (2008) 700–706.

[82] D. Girlich, R. Leclercq, T. Naas, P. Nordmann, Molecular and biochemical characterization of the chromosome-encoded class a β-lactamase BCL-1 from Bacillus clausii, Antimicrob. Agents Chemother. 51 (11) (2007) 4009–4014.

[83] A.H. Van Bruggen, M.M. He, K. Shin, V. Mai, K.C. Jeong, M.R. Finckh, J. G. Morris Jr., Environmental and health effects of the herbicide glyphosate, Sci. Total Environ. 616 (2018) 255–268.

[84] S. Khabthani, M. Hamel, S.A. Baron, S.M. Diene, J.M. Rolain, V. Merhej, fosM, a new family of fosfomycin resistance genes identified in bacterial species isolated from human microbiota, Antimicrob. Agents Chemother. 65 (2) (2021) 10–1128.

[85] Y. Wu, C. Liu, W.G. Li, J.L. Xu, W.Z. Zhang, Y.F. Dai, J.X. Lu, Independent microevolution mediated by mobile genetic elements of individual Clostridium difficile isolates from clade 4 revealed by whole-genome sequencing, Msystems 4 (2) (2019) e00252–18.

[86] J. Ishikawa, K. Chiba, H. Kurita, H. Satoh, Contribution of rpoB2 RNA polymerase β subunit gene to rifampin resistance in *Nocardia* species, Antimicrob. Agents Chemother. 50 (4) (2006) 1342–1346.

[87] M. Ahmed, L. Lyass, P.N. Markham, S.S. Taylor, N. Vázquez-Laslop, A.A. Neyfakh, Two highly similar multidrug transporters of Bacillus subtilis whose expression is differentially regulated, J. Bacteriol. 177 (1995) 3904–3910.

[88] R.J. Heath, N. Su, C.K. Murphy, C.O. Rock, The Enoyl-[acyl-carrier-protein] reductases FabI and FabL from *Bacillus subtilis*, J. Biol. Chem. 275 (51) (2000) 40128–40133.

[89] J. Chen, H. Bhattacharjee, B.P. Rosen, ArsH is an organoarsenical oxidase that confers resistance to trivalent forms of the herbicide monosodium methylarsenate and the poultry growth promoter roxarsone, Mol. Microbiol. 96 (2015) 1042–1052.

[90] S. Xiao, W. Wang, C. Amanze, R. Anaman, B.A. Fosua, W. Zeng, Antimony oxidation and whole genome sequencing of *Phytobacter* sp. X4 isolated from contaminated soil near a flotation site, J. Hazard. Mater. 445 (2023) 130462.

[91] N.R. Amarasekara, A.I. Mafiz, X. Qian, J.M. Tiedje, W. Hao, Y. Zhang, Exploring the co-occurrence of antibiotic, metal, and biocide resistance genes in the urban agricultural environment, Journal of Agriculture and Food Research 11 (2023) 100474.

[92] M.D. Scott, S.R. Meshnick, J.W. Eaton, Superoxide dismutase-rich bacteria. Paradoxical increase in oxidant toxicity, J. Biol. Chem. 262 (8) (1987) 3640–3645.

[93] S.O. Duke, S.B. Powles, Glyphosate: a once-in-a-century herbicide, Pest Manag. Sci. 64 (4) (2008) 319–325.

[94] J.E. Fitzgibbon, H.D. Braymer, Cloning of a gene from *Pseudomonas* sp. strain PG2982 conferring increased glyphosate resistance, Appl. Environ. Microbiol. 56 (11) (1990) 3382–3388.

[95] M.N. Dourado, M.R. Franco, L.P. Peters, P.F. Martins, L.A. Souza, F.A. Piotto, R. A. Azevedo, Antioxidant enzymes activities of *Burkholderia* spp. strains—oxidative responses to Ni toxicity, Environ. Sci. Pollut. Res. 22 (24) (2015) 19922–19932.

[96] Y. Cai, T. Sun, G. Li, T. An, Traditional and emerging water disinfection technologies challenging the control of antibiotic-resistant bacteria and antibiotic resistance genes, Acs Es&T Engineering 1 (7) (2021) 1046–1064.

[97] X. Chen, H. Yin, G. Li, W. Wang, P.K. Wong, H. Zhao, T. An, Antibiotic-resistance gene transfer in antibiotic-resistance bacteria under different light irradiation: implications from oxidative stress and gene expression, Water Res. 149 (2019) 282–291.

4.3 PART 3: BIODIVERSITY IMPACT

4.3.2 CHAPTER 8

ATTRACTION OF INSECTS TO ORNAMENTAL LIGHTING USED ON CULTURAL HERITAGE BUILDINGS: A CASE STUDY IN AN URBAN AREA

Anxo Méndez, Luis Martín, Justo Arines, Rafael Carballeira, Patricia Sanmartín

Insects 13(12), 1153 (2022). doi: 10.3390/insects13121153

JCR index (IF) 2022 = 3.0 (15/100, 85.5 percentile in Entomology)

Open access. Citations (to September 2025): 13

---

insects

MDPI

Article

Attraction of Insects to Ornamental Lighting Used on Cultural Heritage Buildings: A Case Study in an Urban Area

Anxo Méndez [1,†], Luis Martín [1,†], Justo Arines [2,3], Rafael Carballeira [4] and Patricia Sanmartín [1,5,*]

1 GEMAP (GI-1243), Departamento de Edafoloxía e Química Agrícola, Facultade de Farmacia, Universidade de Santiago de Compostela, 15782 Santiago de Compostela, Spain
2 Departamento de Física Aplicada, Facultade de Óptica e Optometría, Universidade de Santiago de Compostela, 15782 Santiago de Compostela, Spain
3 iMATUS (Instituto de Materiais), Universidade de Santiago de Compostela, 15782 Santiago de Compostela, Spain
4 Centro de Investigacións Científicas Avanzadas (CICA), Facultade de Ciencias, Universidade da Coruña, 15008 A Coruña, Spain
5 CRETUS, Universidade de Santiago de Compostela, 15782 Santiago de Compostela, Spain
* Correspondence: patricia.sanmartin@usc.es; Tel.: +34-881814984
† These authors contributed equally to this work.

Simple Summary: The increasing use of ornamental illumination has an impact on nocturnal insect communities in urban areas. The objective of this study is to verify if the selection of specific wavelengths reduces the attraction of insects towards ornamental lighting. We compared the number and diversity of insects captured onto grey sticky traps of an unilluminated area with two light sources: a metal halide lamp and a more efficient, environmentally sound prototype lamp (CromaLux) comprising a combination of green and amber LEDs. By limiting the light emitted to amber and green, the CromaLux lamps considerably reduced the attraction to the light, with similar numbers captured as in the unilluminated area, while the metal halide lamp attracted a greater number and diversity of insects.

Abstract: Artificial light at night (ALAN) reduces insect populations by altering their movements, foraging, reproduction, and predation. Although ALAN is mainly associated with streetlights and road networks, the ornamental illumination of monuments is making an increasing (but not well-studied) contribution. We compared insect attraction to two different types of light sources: a metal halide lamp (a type currently used to illuminate monuments) and an environmentally sound prototype lamp (CromaLux) comprising a combination of green and amber LEDs. The experiment was performed within the pilot CromaLux project in Santiago de Compostela (NW Spain). The abundance and diversity of the insects captured between June and October 2021 in the areas surrounding both light sources and in an unlit area were compared. By limiting the light emitted to amber and green, the CromaLux lamps reduced the number and diversity of insects, morphospecies, and orders attracted to the light, with similar numbers captured as in the unilluminated area, while a greater diversity of insects was captured beside the metal halide lamp. This effect has been demonstrated for almost all insect orders trapped, especially in Diptera, Lepidoptera, Coleoptera, Hemiptera, and Hymenoptera. On the contrary, Psocoptera showed a similar attraction to the CromaLux and metal halide lamps, a phenomenon whose causes deserve further investigation. As expected, Diptera were the most diverse and abundant insects in all samples, but the abundance of Lepidoptera was unexpectedly low (4%), which is in line with the worldwide evidence of the progressive decline of populations of this group. The study findings provide evidence that selecting specific wavelengths for ornamental lighting reduces the attraction of insects while maintaining adequate illumination of monuments for aesthetic purposes, resulting in a lower environmental impact on nocturnal insects. This study provides reference data for developing principles of good practices leading to possible regulatory and legal solutions and the incorporation of specific measures for artificial lighting of monuments and urban structures.

check for updates

Citation: Méndez, A.; Martín, L.; Arines, J.; Carballeira, R.; Sanmartín, P. Attraction of Insects to Ornamental Lighting Used on Cultural Heritage Buildings: A Case Study in an Urban Area. *Insects* **2022**, *13*, 1153. https://doi.org/10.3390/insects13121153

Academic Editors: Francesco Parisi, Klaus H. Hoffmann, Enrico Ruzzier and Simone Sabatelli

Received: 8 November 2022
Accepted: 12 December 2022
Published: 14 December 2022

Publisher's Note: MDPI stays neutral with regard to jurisdictional claims in published maps and institutional affiliations.

Keywords: artificial light at night (ALAN); biodiversity; flight-to-light behaviour; insect decline; light-emitting diode (LED); pilot study; public lighting; Santiago de Compostela

1. Introduction

Night-time illumination of architectural objects has been common practice for centuries [1], enhancing historical or important constructions and distinguishing them from other buildings while also strengthening the significance of the cultural identity of cities [2]. The shift towards more sustainable lighting technologies with the development of light-emitting diodes (LEDs) has reduced the energy consumption and economic cost of urban illumination. However, LEDs are still problematical, as the light emitted glows in the night sky, reducing the level of darkness. In fact, 88% of the land surface in Europe experiences nightglow [3], disrupting the natural day–night cycles of many organisms [4–6] and luring insects and birds to their deaths [7]. Nightglow is increasing globally at a rate of 2% per year [8]; in 2014, the contribution made by the ornamental lighting of cultural heritage objects to the nightglow was between 5% and 20% [9], rising to 21% in Spain in 2018 [10].

Artificial light at night (ALAN) has a serious impact on diverse organisms, many of which (around 30% of all vertebrates and more than 60% of all invertebrates) display nocturnal behaviour, with, e.g., reproduction and feeding taking place during night hours [3]. Insects are declining rapidly around the world [11], and the widespread adoption of ALAN presents a growing threat to the biodiversity of insects in general and of nocturnal insects in particular. Thus, ALAN causes (i) the mortality of nocturnal insects due to direct collisions with the lamps, (ii) exhaustion from continuous circling around the light, (iii) temporal disorientation, desynchronization of natural biorhythms, and (iv) spatial disorientation, which interferes with navigation in nocturnal landscapes [12–15], along with indirect effects such as enhancement of predation by bats or other predators [16] and parasitism of moth larvae [17,18].

Furthermore, the frequent replacement of ornamental public lighting sources modifies the flight-to-light behaviour of insects [15], accustomed since the first half of the last century to mercury vapour lamps and fluorescent lights [19], which emit UV radiation that is extremely attractive to many nocturnal insects [13,14,20]. Still used today, these light sources coexist with the high- and low-pressure sodium lamps that became popular in the 1950s [21] and with the more economical metal halide lamps [22]. These types of lights, which are increasingly being replaced with LED lamps, enable greater control over the dominant wavelength and correlated colour temperature (CCT), i.e., whether a white light is relatively more blue or yellow–amber in terms of shades of white; in other words, its colour appearance expressed in Kelvin (K).

Although extensive research has addressed the effects of night-time illumination on insects, the specific effects and contributions of ornamental illumination of monuments are little known, with only a few studies focusing on wooded areas [23] and, to the best of our knowledge, no studies in urban areas.

The present study formed part of a larger research project entitled "CromaLux: Development of a lighting system with artificial intelligence support for the control of biological colonization in elements of high heritage value (2020–2022)" (The CromaLux project. Available online: http://cromalux.santiagodecompostela.gal/en, accessed on 13 December 2022, Figure 1), conducted in the city of Santiago de Compostela (NW Spain). The aim of the present study was to compare the numbers and diversity of insects attracted to an innovative LED lamp (CromaLux, currently under trial) emitting amber and green light, those attracted to a metal halide lamp (positive control), and those attracted to an unilluminated area (negative control). We tested two main hypotheses: (i) the novel LED lamps will attract significantly fewer insects than the metal halide lamps, with numbers similar to those in the unilluminated area, and (ii) the composition of the insect community will be significantly less affected by the LED lamps than by the metal halide lamps.

Figure 1. The baroque facade of the Casa do Cabildo house, built in 1758, illuminated by the CromaLux lighting.

2. Materials and Methods

2.1. Study Location and Sampling Set-Up

The study was conducted in the historical centre of Santiago de Compostela (Figure 2a), a UNESCO World Heritage city in northwestern Spain. The experiments were conducted in an inner courtyard of an area of approximately 245 m^2 (the old prison yard of the local police building, located behind the city council building, Pazo de Raxoi: UTM 537047 X, 4747615 Y, Datum ETRS89; elevation, 250 m a.s.l.) (Figure 2b). Sticky coloured boards were used to trap the insects, as in previous studies [9,24,25]. The boards, of a length of 24.5 cm and a width of 42.7 cm, and each marked with 100 rectangles of a length of 4.0 cm and a width of 2.3 cm, were obtained from PestWest (Sarasota, FL, USA). Preliminary tests were carried out with sticky boards of different colours (black, yellow, and grey) to check the light reflectance (with a spectroradiometer SilverNova, StellarNet, Inc., Tampa, FL, USA) and suitability for the identification of insects. The black board was rejected because it was very difficult to identify the insects due to the low contrast. The yellow board was rejected due to the yellowish colour of the reflected spectrum. Finally, the grey board was selected for the experiments, as it provided a good contrast, enabling the insects to be observed against the background. Furthermore, we confirmed with a spectroradiometer (SilverNova, Stellarnet,

Inc.) that the grey board did not change significantly the reflected spectra. The sticky board traps (PestWest, Sarasota, FL, USA) were placed under the CromaLux lamp (under trial) and the metal halide lamp (positive control) at a height of three metres (Figure 2c). The sticky board trap used in the unlit area (negative control) was placed on a wall without any artificial illumination at the same height and orientation as the other two traps (Figure 2d). The sticky traps were removed and replaced after 5–16 days, depending on the number of insects trapped on the board, under the metal halide lamp (helping insect identification by avoiding saturation) and also on the probability of rain, which could damage the boards. A total of fifteen replacements were made (forty-five sticky traps in total), and these were grouped into five similar time periods for data analysis (Table 1).

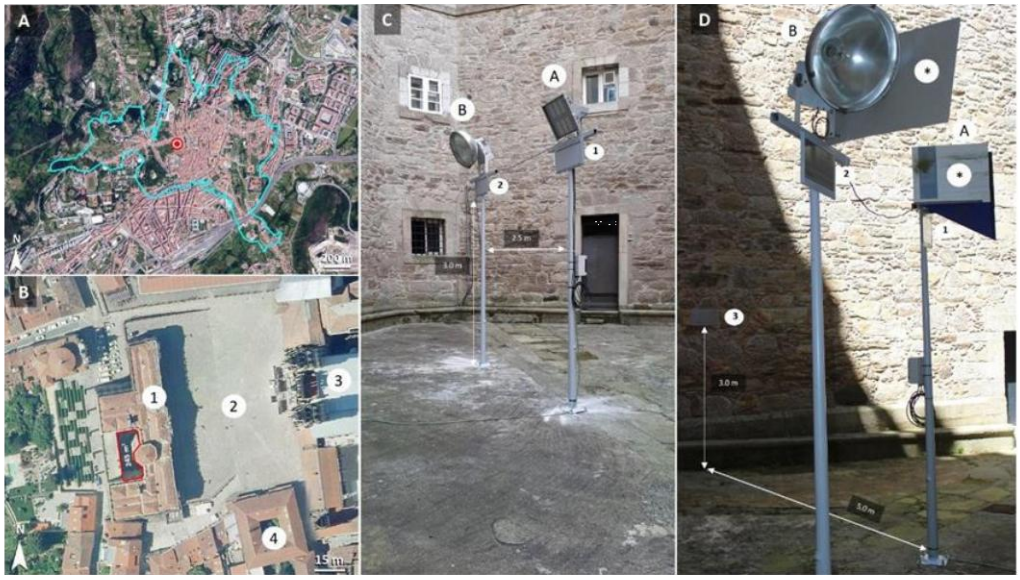

Figure 2. Experimental layout. (**A**) Overview of the historical centre of Santiago de Compostela (outlined in blue) and the location of the study site (red point). (**B**) Study site, inner courtyard (outlined in red), 1: Pazo de Raxoi (city council buildings), 2: Praza do Obradoiro (Obradoiro Square), 3: Cathedral of Santiago de Compostela, 4: Colexio de San Xerome (a university building). (**C**,**D**) Experimental set-up details in the inner courtyard. A: CromaLux light, B: Metal halide lamp (positive control). 1: location of the insect trap beside the CromaLux lamp, 2: location of the insect trap beside the metal halide lamp, 3: location of the insect trap in the unilluminated area. *: sheets used to prevent interference between both light systems. Aerial photographs from PNOA 2020 © CNIG.

Table 1. Sampling (clustered in five similar time periods) carried out between 1 June and 20 October 2021 and corresponding meteorological data, extracted from METEOGALICIA. Available online: www.meteogalicia.gal, accessed on 13 December 2022.

Period	N° of Replacements	Rain (L m^{-2})	Sunshine Duration (h)	Mean Relative Humidity (%)	Average Air Temperature (°C)
[1] 1–21 June	3	3.18 ± 6.98	8.10 ± 4.93	78.95 ± 7.91	16.25 ± 3.32
[2] 21–30 June	3	0.58 ± 1.38	7.16 ± 4.38	80.56 ± 7.62	16.93 ± 2.23
[3] 30–28 July	4	0.44 ± 1.30	8.15 ± 3.41	81.25 ± 5.13	18.30 ± 1.54
[4] 28–26 August	3	2.76 ± 5.01	6.10 ± 3.33	83.03 ± 6.96	17.32 ± 2.08
[5] 26 September–20 October	2	4.27 ± 8.58	5.12 ± 3.69	87.88 ± 6.31	14.72 ± 1.26

2.2. Artificial Lighting and Environmental Conditions

Both types of lamps were switched on for five hours (between 22:00 h and 03:00 h) every night during the study period. The spectra of the lamps were measured with a radiometrically calibrated spectroradiometer (SilverNova, Stellarnet, Inc.) with a spectral resolution of 5 nm. The temperature of the sticky board traps while the lamps were switched on was monitored with HOBO MX2202 data logger (Onset, Bourne, OR, USA). The humidity in the inner courtyard was monitored with a HOBO MX2302A data logger (Onset, Bourne, OR, USA). These data were completed with data on precipitation, daylight hours, and average temperature and relative humidity throughout the study period from the web-based repository www.meteogalicia.gal (the Galician meteorological service) (Table 1).

2.3. Insect Collection and Identification

Insects were collected during the warmest time of year in the study location, between 1 June and 20 October 2021 (Table 1), covering the main activity period (caused by the mild temperatures and no high rainfall) of flying insects in the region [26–28]. After collection, (see the Section 2.1), the sticky boards were transported to the laboratory in a box that kept them cool and dry (conditions that were maintained for storage throughout the study). In the laboratory, each sticky board was photographed (with a Canon EOS 100D camera), and the number of insects on each board was counted. The insects were examined under a stereomicroscope (Olympus SZX7, Olympus, Hamburg, Germany) and photographed in greater detail (with an Olympus C180 digital camera, Olympus, Hamburg, Germany). All specimens or individuals were sorted, identified, and classified by a trained entomologist to recognizable taxonomic units (or morphospecies) and order level, and, when possible, to suborder, family, and genera/species levels. Taxonomic keys and manuals used included [29] for the general study of Iberian arthropods, [30] for Trichoptera, [31] for Diptera, [32], for other taxa, and the web-based repository Fauna Ibérica project (Available online: www.faunaiberica.es/, accessed on 13 December 2022) for verification of the nomenclature.

2.4. Biodiversity and Statistical Analysis

The diversity of morphospecies for each lighting condition was evaluated using the Shannon–Wiener index, a popular metric used in ecology, that summarise the diversity of a community quantifying the number of individuals and their relative abundance [33]. Differences between lighting conditions were determined using Hutcheson's *t*-test [34] and were considered statistically significant at $p > 0.05$.

The data on the insects captured on the sticky board traps were analysed using the nonparametric Kruskal–Wallis test (K), as the assumptions of normal distribution were not fulfilled (Shapiro–Wilk test; $p > 0.05$). A post hoc Conover–Iman test © was used for multiple pairwise comparisons ($p < 0.05$) [35,36]. The temperature data from the loggers fitted to the sticky boards were also analysed in the same way. The data on the morpho-species, with specimens in the three lighting conditions, or with more than 10 specimens in one of the conditions, were previously selected for the statistical analysis, and a logarithmic transformation was applied. The data analysis was conducted using R statistical software (v. 4.0.2., R Core Team 2020, Vienna, Austria) [37].

3. Results

The optical spectra of both illumination systems under study are shown in Figure 3. The prototype LED lamp (CromaLux) yields a bimodal spectrum with two peaks, one at 528 nm, with full width at half maximum (FWHM) of 14 nm, and a main peak at 593 nm, with FWHM of 7 nm, producing a correlated colour temperature (CCT) of 3000 K. The spectrum of the metal halide lamp (positive control) falls in the visible range, with five main peaks centred at 435 nm, 508 nm, 546 nm, 578 nm, and 589 nm, with other important peaks at 473 nm, 569 nm, and 624 nm. The spectrum includes large amount of ultraviolet-A

(UVA) light in the range 350–400 nm, with a peak at 365 nm. The lamp provided a CCT of 4668 K.

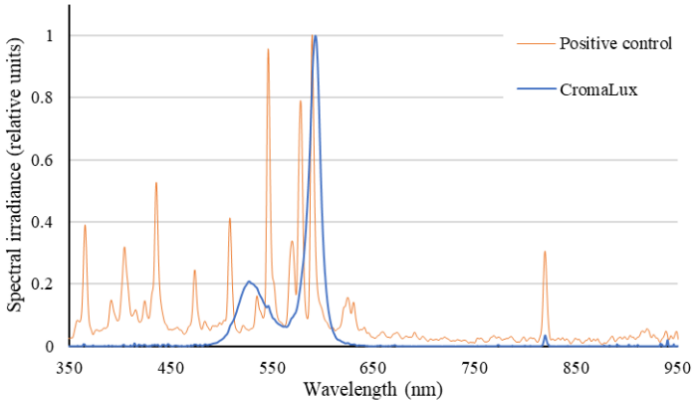

Figure 3. Normalised spectra of the CromaLux lamp with a CCT of 3000 K (blue line) and the metal halide lamp with a CCT of 4668 K (orange line). No significant differences were found between the mean values of light intensity in luxes of both lamps in the surrounding areas where the insects were trapped. The spectral sensitivity range of insects is 330–640 nm [38].

The temperature did not differ significantly between the sticky board traps beside the metal halide (12.25 ± 2.42 °C) and CromaLux (12.13 ± 2.53 °C) lamps, while the temperature of the traps in the unilluminated area was significantly higher (16.97 ± 1.75 °C). These results may lead to think that the negative control should have been placed at a height of three metres in the centre of the inner courtyard, as with its two counterparts, instead of on the wall (Figure 2). However, there was no unlit areas except for on the walls and it was considered that placing the trap on the wall would overestimate the impact results, never otherwise, because the temperature there is higher. The relative humidity at the study site was 80.92 ± 0.43%, which is consistent with the data extracted from the web-based repository, ranging sequentially from 78.95 ± 7.91% at the beginning to 87.88 ± 6.31% at the end of the experiment (Table 1). The average air temperature peaked in August, at 18.30 ± 1.54 °C, and was minimal in October, at 14.72 ± 1.26 °C. Rainfall levels were only 0.58 ± 1.38 L m^{-2} in July and 0.44 ± 1.30 L m^{-2} in August, but were higher in October, at 4.27 ± 8.58 L m^{-2}. Finally, sunshine duration decreased, as expected, from summer to autumn.

A total of 1804 specimens or individuals and 160 insect morphospecies were captured on the sticky boards during the study period (Table 2, Figure 4). Nine insect orders were identified across all samples: Diptera represented 47% of the insects trapped (842 specimens and 65 morphospecies); Hemiptera represented 25% (457 specimens and 28 morphospecies); Psocoptera represented 15% (268 specimens and 8 morphospecies); Coleoptera represented 5.5% (100 specimens and 14 morphospecies); Lepidoptera represented 4% (74 specimens and 24 morphospecies); Hymenoptera represented 2.6% (47 specimens and 14 morphospecies); Neuroptera represented 0.3% (6 specimens and 1 morphospecies); and Trichoptera and Thysanoptera represented, respectively, 0.3% and 0.2% (6 and 4 specimens and 3 morphospecies in each order). It is summarized in Table 2. The order level, and when it was possible, the suborder, family, and genera/species levels of the insects trapped are also summarized in Table S1. The most abundant suborders of Diptera were Nematocera (24 morphospecies) and Schizophora (7 morphospecies), including the taxa Chironomidae, Psychodidae, Tipuloidea, and Muscidae. Hemiptera specimens comprised the suborders Cicadomorpha (18 morphospecies, mainly belonging to the family Cicadellidae, e.g., *Cicadella viridis* (Linnaeus, 1758) at the species level), Heteroptera (5 morphospecies), Sternorrhyncha (4 morphospecies), and Aphidodea (1 morphospecies). All Psocoptera specimens caught belonged

to the suborder Psocomorpha. Polyphaga (12 morphospecies) was the most abundant suborder of Coleoptera, including species of Bostrichidae, Chrysomelidae, Cryptophagidae, Latridiidae, Nitidulidae, Ptiliidae, Silvanidae, Staphylinidae, and Tenebrionidae families, and genera such as *Cybocephalus* and *Schistocerus*. Within the order Coleoptera, specimens of the family Carabidae (suborder Adephaga) were also found. Lepidoptera species with nocturnal or crepuscular habits, mainly belonging to the family Noctuidae, such as *Lacanobia oleracea* (Linnaeus, 1758) and *Noctua pronuba* (Linnaeus, 1758), were captured. Trapped Hymenoptera specimens mainly included the suborders Apocrita (Chrysididae, Formicidae, and Ichneumonidae families) and *Symphyta* (Cephidae family). The order Neuroptera included a single species, i.e., *Chrysoperla carnea* (Stephens, 1836), which belongs to the family Chrysopidae, suborder Hemerobiiformia. Species of *Trichoptera*, i.e., *Lepidostoma basale* (Kolenati, 1848), which belong to the family Lepidostomatidae, suborder Integripalpia, and *Wormaldia* (McLachlan, 1865), which belongs to the family Philopotamidae, were also found.

Table 2. Number of specimens and morphospecies of the orders trapped throughout the experiment.

Order	% of Insects Trapped	N° Specimens	N° of Morphospecies
Diptera	47.1	842	65
Hemiptera	25.0	457	28
Psocoptera	15.0	268	8
Coleoptera	5.5	100	14
Lepidoptera	4.0	74	24
Hymenoptera	2.6	47	14
Neuroptera	0.3	6	1
Trichoptera	0.3	6	3
Thysanoptera	0.2	4	3
Total	100	1804	160

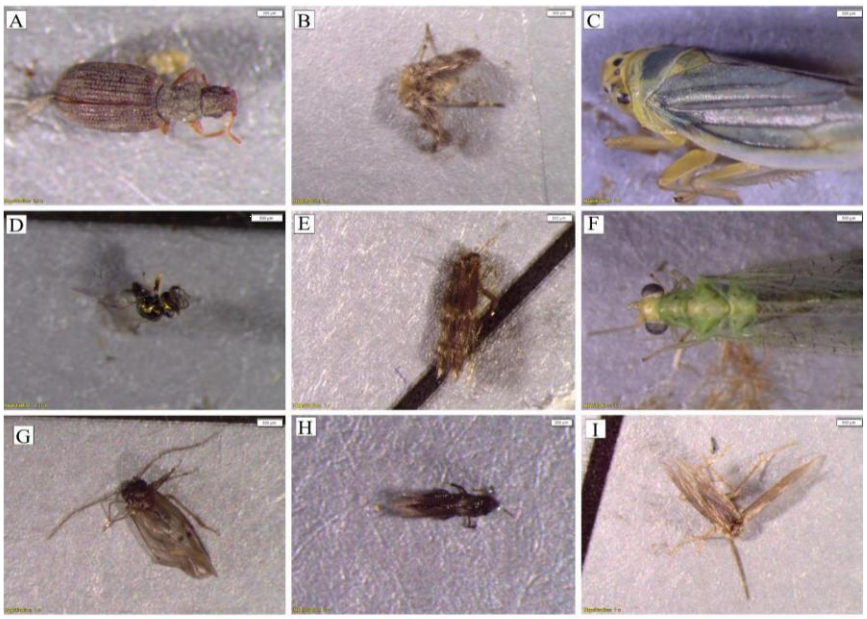

Figure 4. Photographs of some of the insects captured. **(A)** Coleoptera (Latridiidae), **(B)** Diptera (*Psychodidae*), **(C)** Hemiptera (*Cicadella viridis*), **(D)** Hymenoptera (Chrysididae), **(E)** Lepidoptera, **(F)** Neuroptera (*Chrysoperla carnea*), **(G)** Psocoptera (Psocomorpha), **(H)** Thysanoptera, and **(I)** *Trichoptera* (Hydroptilidae).

The number of insects trapped differed significantly between the three lighting conditions (CromaLux lamp, metal halide lamp, and no illumination), according to the results of the Kruskal–Wallis test (K = 66.5; p-value < 0.0001) and the post hoc Conover–Iman test for pairwise comparisons (no illumination vs. metal halide lamp, C = 58.050, p-value < 0.0001; no illumination vs. CromaLux lamp, C = 12.263, p-value = 0.016; metal halide lamp vs. CromaLux lamp, C = 45.788, p-value < 0.0001), with higher values for the metal halide lamp (1421 insects) than for the CromaLux lamp (260 insects) and no illumination (114 insects) (Figure 5). Relative to the number of insects captured in the unilluminated control area, roughly twelve times more were attracted to the metal halide lamp and roughly two times more to the CromaLux lamp.

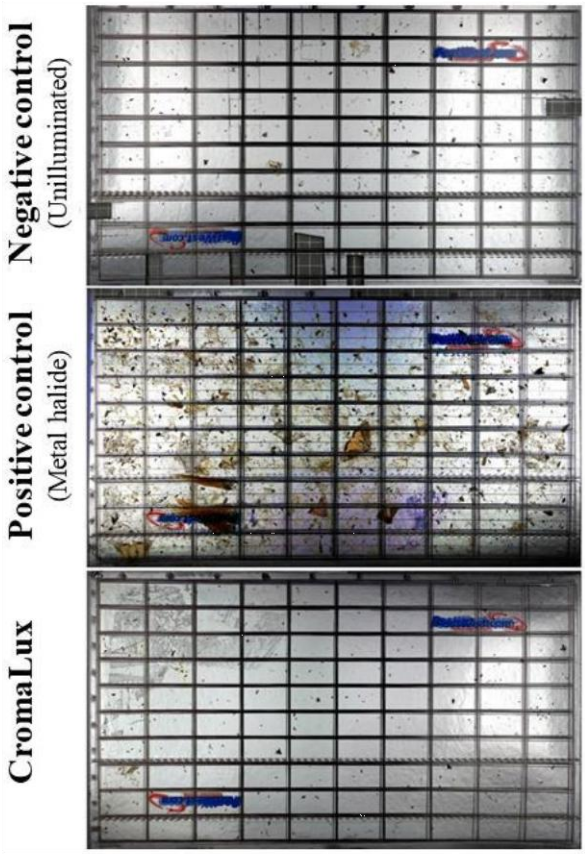

Figure 5. Overlapped photographs of all sticky board traps for the three lighting systems.

Figure 6 shows the distribution of the number of individuals and the number of morphospecies per insect order under the three lighting conditions. A total of 1421 individuals and 145 morphospecies were trapped beside the metal halide lamp. Values were significantly higher than those obtained for the CromaLux lamp and the unilluminated area, where respectively 260 and 114 individuals, and 62 and 40 morphospecies were caught. The number of individuals and morphospecies captured beside the CromaLux lamp was lower than in the positive control for all nine orders, except Psocoptera and Thysanoptera. Members of the orders Neuroptera and *Trichoptera* were absent from the traps beside the CromaLux lamps and in the unilluminated area, while Thysanoptera was absent from the traps beside the metal halide lamp. Although more morphospecies were captured beside the CromaLux lamp than beside the metal halide lamp, Lepidoptera morphospecies were

only found on the latter. Members of the order Psocoptera were caught in equal numbers on the sticky traps beside the metal halide lamp (133) and the CromaLux lamp (128), while for the other orders greater numbers of insects were captured beside the metal halide lamp.

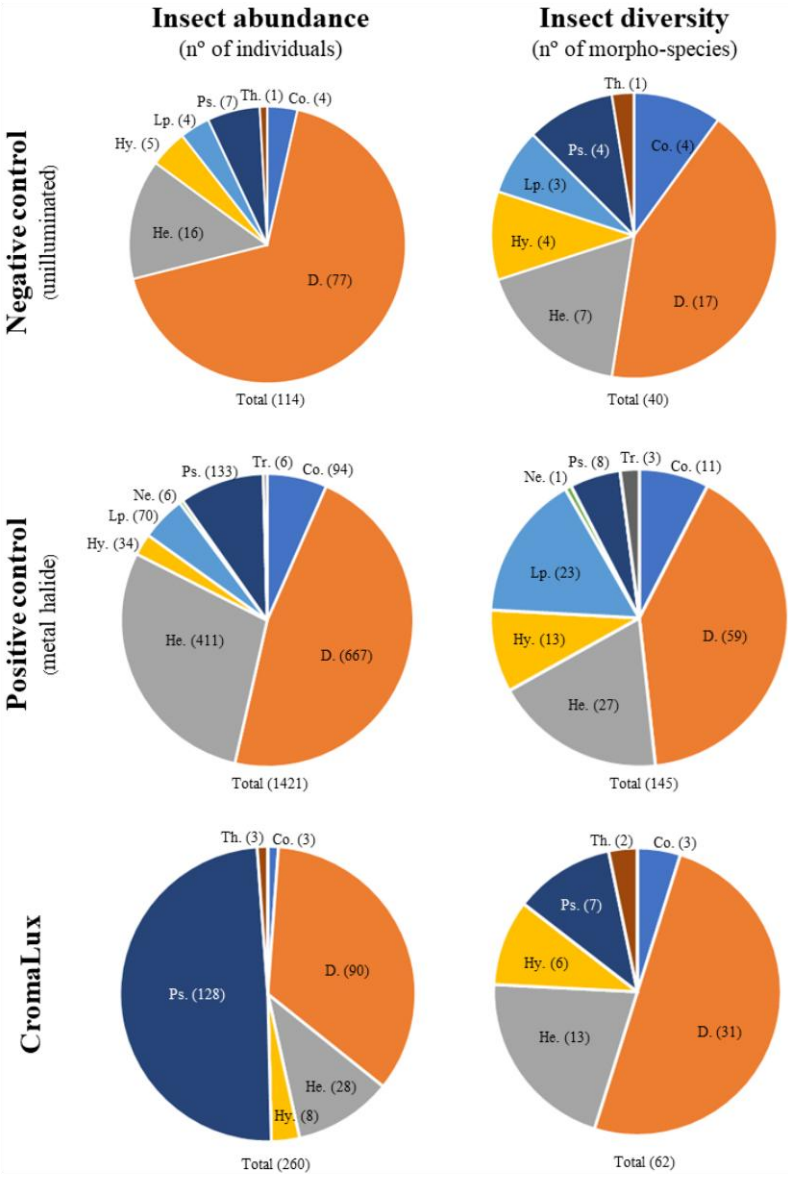

Figure 6. Insect abundance and insect biodiversity captured beside the three lighting systems. Co: Coleoptera, D.: Diptera, He.: Hemiptera, Hy.: Hymenoptera, Lp.: Lepidoptera, Ne.: Neuroptera, Ps.: Psocoptera, Th.: Thysanoptera, Tr.: *Trichoptera*.

The changes in the number of individuals and morphospecies of each insect order throughout the experiment (Table 1) are shown in Figure 7. Except for some individuals of the order Psocoptera on the CromaLux, the orders Diptera and Hemiptera were the most abundant (by more than 60%) in all samples. Members of the order Hymenoptera were only present during the summer months. Insect abundance (Figure 7A) in the unilluminated

area and beside the CromaLux lamp increased until August and then decreased sharply, the former in September and the latter in October. The number of members of Psocoptera captured on the traps beside the CromaLux lamp increased in the last three sample collections, representing just over half of the individuals captured in August, September, and October.

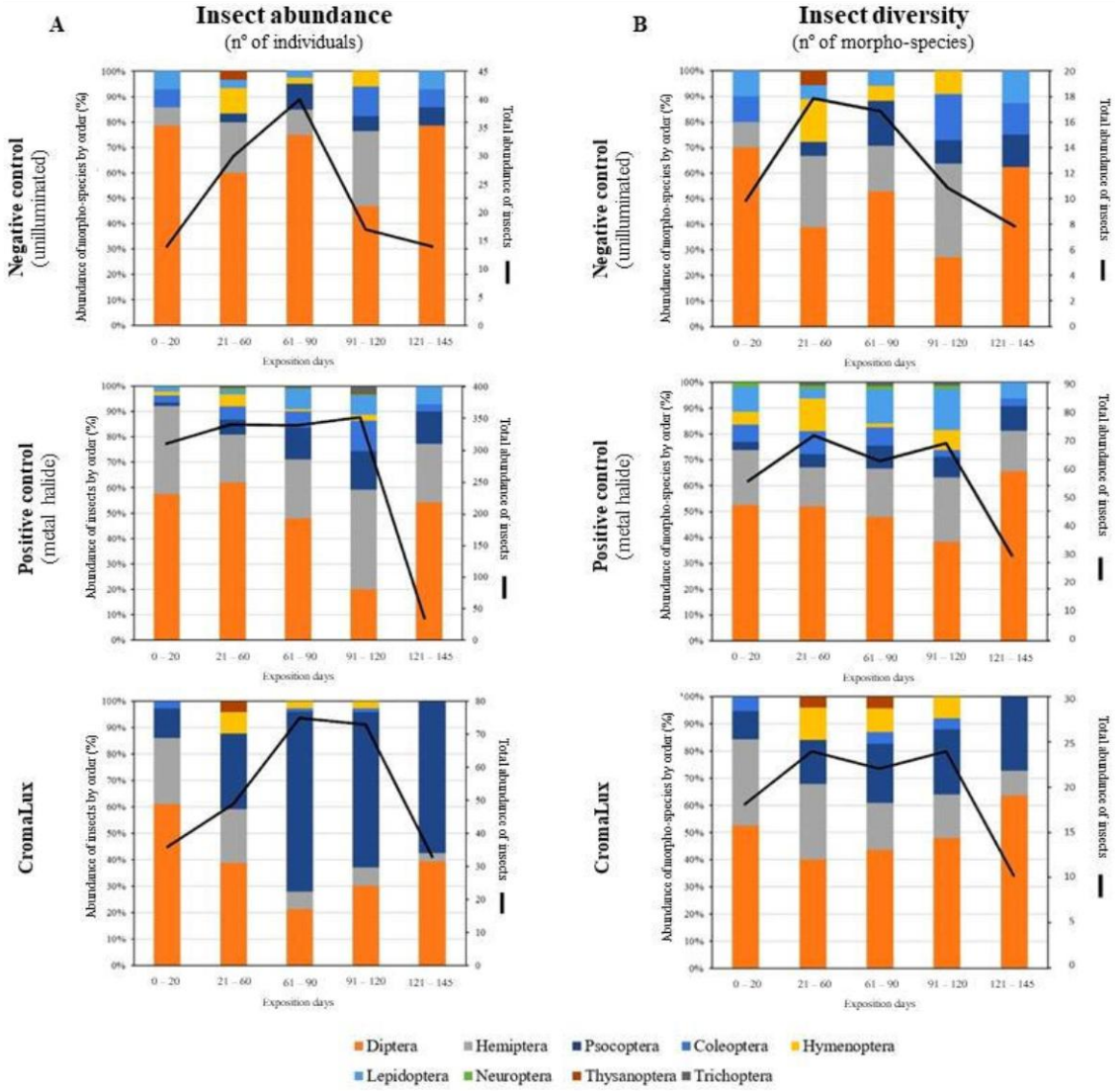

Figure 7. Temporal succession of insect abundance (**A**) and insect diversity (**B**) corresponding to the three lighting conditions during the five study periods (see Table 1). The black line represents the total abundance of insects (**A**) and of insect morphospecies (**B**). The numbers in (**B**) indicate the Shannon–Wiener index for each time period.

The number of specimens captured beside the metal halide lamp remained high and constant until September and then decreased sharply in October. Figure 7B shows the changes in morphospecies over time. The total number of morphospecies followed a similar pattern for the metal halide and CromaLux lamps (though not the same scale, ranging

between 70 and 50 and 30 morphospecies number in the former and between 23 and 17 and 10 morphospecies number in the latter) with peaks in July and September, somewhat lower values in June, and to a lesser extent in August, and significant lower numbers in October. However, the number of morphospecies captured in the unilluminated area increased significantly between June and July, and then decreased gradually until October. The global variation (all data) in morphospecies diversity (Shannon–Wiener index; data used for the calculation appear in Table S2) was 2.80 for the unilluminated area, 4.07 for the metal halide lamp, and 2.95 for the CromaLux lamp. The monthly variation in the index (Figure 7B) ranged from 1.54 (October) to 2.59 (July) for the negative control, from 2.93 (October) to 3.86 (August) for the metal halide lamp, and from 1.74 (October) to 2.63 (June) for the CromaLux lamp. The Hutcheson t-test did not reveal any differences in the lighting conditions between the unilluminated area and the area lit by the CromaLux lamp (p-value = 0.401) but did reveal significant differences between the area lit by the metal halide lamp and the unilluminated area (p-value < 0.001) and the metal halide and CromaLux lamps ($p < 0.001$).

4. Discussion

The general use of artificial light at night (ALAN) may affect human perception [2], human health [39], and biodiversity [11]. It will also impact nocturnal insects, most of which display positive phototaxis at night and a large proportion of which have trichromatic vision, with receptor sensitivities in the ultraviolet, blue, and green spectral range [40]. Spectral composition is thus a key factor in insect attraction [18], and lights with peak wavelengths in blue and ultraviolet regions have been widely used to trap nocturnal insects in taxonomic and ecological research [41,42] and in pest control [24]. However, regarding ALAN, the focus is centred on streetlights and road networks, and scant attention has been given to ornamental or artistic illumination despite the increasing trend for cities to install external lighting systems on historical buildings and monuments [43,44].

In this study, we tested how CromaLux (Figure 1, designed for illuminating monuments because its biostatic activity against phototrophic organisms) a warm LED light of 3000 K and absence of UV-blue light (Figure 3) impacts nocturnal biodiversity (considering the insect community as the reference group). For comparative purposes, we also tested a metal halide lamp of the type currently in use to illuminate monuments (4668 K, Figure 2) and no artificial lighting. There were no significant differences in abundance or composition of the insects captured in the traps beside the CromaLux LED light and the in the unilluminated area, but the impact was significantly lower than that caused by the metal halide lamps (Figures 5–7). Although the heat emitted by metal halide lamp may be expected to contribute to attracting insects, the temperatures of the sticky board traps beside the metal halide and CromaLux lamps were almost identical (12.25 ± 2.42 °C vs. 12.13 ± 2.53 °C, respectively). Differences in CCT is another possible factor; however, previous studies have shown that colour temperature and insect attraction are not necessarily related, because the spectral composition also influences phototaxis for nocturnal insects [45]. Thus, CCT per se is not the reason for the attraction, and it is the differences in lighting spectra that cause the difference as confirmed by the statistical analysis.

It is surprising the small number of captured Lepidoptera (4% of the total), particularly when considering that baiting the light is the best way to catch many kinds of butterflies and moths. In our opinion, the three main reasons for this to happen are: (i) the location of the experiment in an inner courtyard inside an urban area (instead of a wooded area), (ii) the decline of Lepidoptera in recent decades, especially in urban environments and caused in large part by the anthropogenic light, which has been shown to lead, for example, to negative population trends of some European moths [17], and (iii) the insufficient strength of the sticky board traps used to trap the insects for those larger and heavier. Indeed, we have observed throughout the experiment in the traps signs of impact (remains of scales, tarsal segments, etc.) associated with larger and heavier insects, such as moths of a certain size and larger genera of Coleoptera, which have managed to escape after being partially adhered.

Regarding the insects captured and their relationship with the three lighting conditions, nine insect orders expected to be found in an urban environment [46] were identified, although they were less abundant in June and October (Figure 7) when mean precipitation was higher and average temperature was lower (Table 1). The insect capture followed a trend that can be explained in terms of the spectral sensitivity of the visual systems.

There is some variation in dipteran spectral sensitivity, ranging from UV and green photoreceptors (e.g., *Aedes*) to UV, blue, blue–green, and green photoreceptors (e.g., *Musca*) [47]. In the present study, members of the order Diptera (the most abundant order here) were particularly attracted to the light emitted by the metal halide lamp. This concurs with the findings of previous studies. For example, *Tanytarsus barbitarses* (Diptera: Chironomidae) was more strongly attracted to white light than to green light, with peak attraction near the ultraviolet region at 370–400 nm [48] and *Lutzomyia longipalpis* (Diptera: Psychodidae) was mainly attracted to the UV wavelengths (<400 nm) rather than to the blue–green wavelengths [49].

Hemiptera typically responds to the ultraviolet (330–350 nm), blue (405–490 nm), and green (520–560 nm) wavelengths [38], emitted in the present study by the metal halide lamp to which they were most attracted, but some species also exhibit a unimodal response centred in the green wavelengths (emitted by both lamps), such as the aphid *Acyrthosiphon pisum* [50] and the bedbug *Cimex lectularius* [51].

Psocids (Psocoptera) have shown spectral sensitivity to UV and green wavelengths. *Liposcelis paeta* (Psocoptera: Liposcelididae) females responded positively to two UV wavelengths (351 and 400 nm) and to green light (527 nm) [52], and 351 nm UV light triggers a very strong phototaxis response from *Liposcelis bostrychophila* (Psocoptera: Liposcelididae) adults [53]. Sensitivity to those parts of the spectrum is common in most arthropods [37]. In the present study, the number captured of members of the order Psocoptera was similar beside the CromaLux and metal halide lamps (Figure 6). This could suggest that there was no great impact on the presence or absence of UV-blue wavelengths (or other spectral/intensity differences between the lamps) on phototaxis in the specimens of this group trapped here. In this regard, although the peaks are different, the total photon count may be similar in the green-wavelength portion of both lamps (Figure 3), and this could generate the same attraction in the Psocoptera group of the present study. In addition, the similar responses could also be explained by a lack of input from any UV or blue photoreceptors (if present) to the phototaxis system of the Psocoptera members trapped.

Some members of Carabidae family (Coleoptera) have two peaks (UV and green) and others have been shown to have four peaks of spectral sensitivity (UV, blue, green, and red) [38]. The pollen beetle *Meligethes aeneus* (Coleoptera: Nitidulidae) displays a peak in spectral sensitivity at around 550 nm (green region) and a secondary sensitivity peak is observed in the UV range (370 nm), but not in the blue region [50]. In the present study, Coleoptera individuals were particularly attracted to the light emitted by the metal halide lamp, suggesting an influence, at least of the UV light difference between both lamps, on these individuals.

Lepidoptera are strongly attracted to the UV and blue part of the spectrum [54]. Some noctuid moths, such as *N. pronuba*, appear to have additional sensitivity to red light [40] and thus may be affected by traditional warm LED illumination (~3000 K), which often emits in the red part of the spectrum. The reproductive cycle of nocturnal Lepidoptera (or moths) is particularly sensitive to light pollution [17], which can have important consequences for the conservation of populations. The lack of attraction of the CromaLux to Lepidoptera specimens due to the spectral composition of the light emitted makes this an ideal system to prevent the negative effects of monumental lighting on these populations.

The Shannon–Wiener index values showed that the CromaLux lamps did not increase the diversity of morphospecies attracted to the light, resulting in a lower effect on the nocturnal biodiversity of this type of lamp relative to metal halide lamps. The findings are consistent with previous studies with streetlights, such as [14,55], who reported the transition to LED from traditional light technologies reduces the impact on aerial nocturnal

insects, and also with those of [18,45], who reported that specific selection of the spectra of the LED changes the overall attraction to the light. The present study went a step further by specifically selecting an adequate spectrum for monumental illumination.

5. Conclusions

In summary, the study findings show that an LED lamp emitting a combination of amber and green light (as shown in Figure 3) effectively reduced both the abundance and diversity of insects attracted to the light source compared to traditional light sources such as metal halide lamps. This effect has been demonstrated for almost all insect orders trapped, especially in Diptera, Lepidoptera, Coleoptera, Hemiptera, and Hymenoptera. On the contrary, Psocoptera showed a similar attraction to the CromaLux and metal halide lamps, a phenomenon whose causes deserve further investigation. As expected, Diptera were the most diverse and abundant insects in all samples, but the abundance of Lepidoptera was unexpectedly low (4%), which, regardless of certain methodological limitations or site-dependent effects, is in line with the worldwide evidence of the progressive decline of populations of this group.

Conscious selection of the light spectra used for ornamental illumination will reduce the impact on insect biodiversity, relative to more traditional lighting systems, while still showcasing the artistic and aesthetic features of heritage buildings (Figure 1). Illumination of monuments is also part of night-time street lighting and thus contributes to public safety. The study provides reference findings regarding the application of principles of good practices leading to possible regulatory and legal solutions and the incorporation of specific measures for artificial lighting of monuments or urban structures.

Supplementary Materials: The following supporting information can be downloaded at: https://www.mdpi.com/article/10.3390/insects13121153/s1, Table S1: Taxonomic identification of the insects trapped throughout the experiment; Table S2: Data used for the calculation of the Shannon-Wiener index.

Author Contributions: Conceptualization, A.M., J.A., R.C. and P.S.; data curation, L.M.; formal analysis, A.M., L.M. and R.C.; funding acquisition, P.S.; investigation, A.M., L.M. and J.A.; methodology, A.M., J.A., R.C. and P.S.; project administration, P.S.; supervision, P.S.; writing—original draft, A.M., L.M., J.A., R.C. and P.S.; writing—review and editing, P.S. All authors have read and agreed to the published version of the manuscript.

Funding: A. Méndez acknowledges receipt of a grant from the Programa de Doutoramento Industrial (04_IN606D_2021_2598528) financed by the Xunta de Galicia. P. Sanmartín acknowledges receipt of a Ramón y Cajal contract (RYC2020-029987-I) financed by the Spanish Ministry of Science and Innovation (MICINN). The authors also would like to express their gratitude to the Xunta de Galicia for concession of the FONTES project (ED431F 2022/14) and the Competitive Reference Group (GRC) grant ED431C 2022/09.

Data Availability Statement: During the present research entities, the datasets and results gathered and generated from the analysis after the identification of the specimens recollected are available from the corresponding author upon reasonable request.

Acknowledgments: This pilot study was developed within the framework of the CromaLux project: Third SMARTIAGO Challenge—Smart lighting system for Heritage Conservation. The authors are very grateful to Marcos González for his careful reviews of the manuscript. Additionally, thanks to J.C. Otero for his help in the coleoptera identification.

Conflicts of Interest: The authors declare no conflict of interest.

References

1. Mazur, D.; Wachta, H.; Leśko, K. Research of cohesion principle in illuminations of monumental Objects. In *Analysis and Simulation of Electrical and Computer Systems*, 1st ed.; Mazur, D., Golebiowski, M., Korkosz, M., Eds.; Springer: Cham, Switzerland, 2018; pp. 395–406.

2. Zielinska-Dabkowska, K.M.; Xavia, K. Historic Urban Settings, LED Illumination and its Impact on Nighttime Perception, Visual Appearance, and Cultural Heritage Identity. In Proceedings of the 5th International Multidisciplinary Scientific Conference on Social Sciences and Arts, Florence, Italy, 23–26 October 2018; SGEM: Sofia, Bulgaria, 2018.
3. Falchi, F.; Cinzano, P.; Duriscoe, D.; Kyba, C.C.; Elvidge, C.D.; Baugh, K.; Portnov, B.; Rybnikova, N.; Furgoni, R. The new world atlas of artificial night sky brightness. *Sci. Adv.* **2016**, *2*, e1600377. [CrossRef] [PubMed]
4. Hölker, F.; Wolter, C.; Perkin, E.K.; Tockner, K. Light pollution as a biodiversity threat. *Trends Ecol. Evol.* **2010**, *25*, 681–682. [CrossRef]
5. Sanders, D.; Gaston, K.J. How ecological communities respond to artificial light at night. *J. Exp. Zool.* **2018**, *329*, 394–400. [CrossRef]
6. Touzot, M.; Lengagne, T.; Secondi, J.; Desouhant, E.; Thery, M.; Dumet, A.; Duchamp, C.; Mondy, N. Artificial light at night alters the sexual behaviour and fertilisation success of the common toad. *Environ. Pollut.* **2020**, *259*, 113883. [CrossRef]
7. Kyba CC, M.; Mohar, A.; Pintar, G.; Stare, J. Reducing the environmental footprint of church lighting: Matching facade shape and lowering luminance with the EcoSky LED. *Int. J. Sustain. Light.* **2018**, *20*, 1–10. [CrossRef]
8. Kyba, C.C.M.; Kuester, T.; de Miguel, A.S.; Baugh, K.; Jechow, A.; Hölker, F.; Bennie, J.; Elvidge, C.D.; Gaston, K.J.; Guanter, L. Artificially lit surface of Earth at night increasing in radiance and extent. *Sci. Adv.* **2017**, *3*, e1701528. [CrossRef]
9. Mohar, A.; Zagmajster, M.; Verovnik, R.; Skaberne, B. Nature-Friendlier Lighting of Objects of Cultural Heritage (Churches). Dark-Sky Slovenia, Liubliana. 2014. Available online: https://www.anl.bayern.de/publikationen/anliegen/additional_data/an37200notizen_2015_kulturdenkmaeler_life_bericht_engl.pdf (accessed on 8 November 2022).
10. Jechow, A.; Ribas, S.J.; Domingo, R.C.; Hölker, F.; Kolláth, Z.; Kyba, C. Tracking the dynamics of skyglow with differential photometry using a digital camera with fisheye lens. *J. Quant. Spectrosc. Radiat. Transf.* **2018**, *209*, 212–223. [CrossRef]
11. Owens, A.C.; Cochard, P.; Durrant, J.; Farnworth, B.; Perkin, E.K.; Seymoure, B. Light pollution is a driver of insect declines. *Biol. Conserv.* **2020**, *241*, 108259. [CrossRef]
12. Gaston, K.J.; Visser, M.E.; Hölker, F. The biological impacts of artificial light at night: The research challenge. *Philos. Trans. R. Soc.* **2015**, *370*, 20140133. [CrossRef] [PubMed]
13. Owens, A.C.; Lewis, S.M. The impact of artificial light at night on nocturnal insects: A review and synthesis. *Ecol. Evol.* **2018**, *8*, 11337–11358. [CrossRef] [PubMed]
14. van Grunsven, R.H.; Becker, J.; Peter, S.; Heller, S.; Hölker, F. Long-term comparison of attraction of flying insects to streetlights after the transition from traditional light sources to light-emitting diodes in urban and peri-urban settings. *Sustainability* **2019**, *11*, 6198. [CrossRef]
15. Boyes, D.H.; Evans, D.M.; Fox, R.; Parsons, M.S.; Pocock, M.J. Street lighting has detrimental impacts on local insect populations. *Sci. Adv.* **2021**, *7*, eabi8322. [CrossRef] [PubMed]
16. Acharya, L.; Fenton, M.B. Bat attacks and moth defensive behavior around street lights. *Can. J. Zool.* **1999**, *77*, 27–33. [CrossRef]
17. Boyes, D.H.; Evans, D.M.; Fox, R.; Parsons, M.S.; Pocock, M.J. Is light pollution driving moth population declines? A review of causal mechanisms across the life cycle. *Insect Conserv. Divers.* **2021**, *14*, 167–187. [CrossRef]
18. Deichmann, J.L.; Ampudia Gatty, C.; Andía Navarro, J.M.; Alonso, A.; Linares-Palomino, R.; Longcore, T. Reducing the blue spectrum of artificial light at night minimises insect attraction in a tropical lowland forest. *Insect Conserv. Divers.* **2021**, *14*, 247–259. [CrossRef]
19. Harris, J.B. Electric lamps, past and present. *J. Eng. Educ.* **1993**, *2*, 161–170. [CrossRef]
20. Davies, T.W.; Bennie, J.; Inger, R.; De Ibarra, N.H.; Gaston, K.J. Artificial light pollution: Are shifting spectral signatures changing the balance of species interactions? *Glob. Chang. Biol.* **2013**, *19*, 1417–1423. [CrossRef]
21. Gendre, M. Two Centuries of Electric Light Source Innovations. 2003. Available online: https://www.einlightred.tue.nl/lightsources/history/light_history.pdf (accessed on 8 November 2022).
22. Rea, M.S.; Bullough, J.D.; Akashi, Y. Several views of metal halide and high-pressure sodium lighting for outdoor applications. *Light. Res. Technol.* **2009**, *41*, 297–320. [CrossRef]
23. Verovnik, R.; Fišer, Ž.; Zakšek, V. How to reduce the impact of artificial lighting on moths: A case study on cultural heritage sites in Slovenia. *J. Nat. Conserv.* **2015**, *28*, 105–111. [CrossRef]
24. Otieno, J.A.; Weller, J.; Poehling, H.M. Efficacy of LED-enhanced blue sticky traps combined with the synthetic lure Lurem-TR for trapping of western fower thrips (*Frankliniella occidentalis*). *J. Pest. Sci.* **2018**, *91*, 1301–1314. [CrossRef]
25. Shi, L.; He, H.; Yang, G.; Huang, H.; Vasseur, L.; You, M. Are yellow sticky cards and light traps effective on tea green leafhoppers and their predators in Chinese Tea plantations? *Insects* **2021**, *12*, 14. [CrossRef] [PubMed]
26. Shreeve, T. The effect of weather on the life cycle of the speckled wood butterfly *Pararge aegeria*. *Ecol. Entomol.* **1986**, *11*, 325–332. [CrossRef]
27. Scott JEpstein, M. Factors affecting phenology in a temperate insect community. *Am. Midl. Nat.* **1987**, 103–118. [CrossRef]
28. Gutiérrez, D.; Wilson, R. Intra-and interspecific variation in the responses of insect phenology to climate. *J. Anim. Ecol.* **2021**, *90*, 248–259. [CrossRef]
29. Barrientos, J.A. (Ed.) *Curso Práctico de Entomología*; Univ. Autònoma de Barcelona: Barcelona, Spain, 2004; Volume 41.
30. Malicky, H. *Atlas of European Trichoptera*, 2nd ed.; Springer: Dordrecht, The Netherlands, 2004; p. 385.
31. Oosterbroek, P. *The European Families of the Diptera: Identification-Diagnosis-Biology*; KNNV Publishing: Utrecht, The Netherlands, 2006; p. 205.

32. Leraut, P. *Insectos de España y Europa*; Lynx Edicions: Barcelona, Spain, 2007; p. 527.
33. Shannon, C.E.; Weaver, W. *The Mathematical Theory of Communication*; University of Illinois Press: Urbana, IL, USA, 1949; p. 144.
34. Hutcheson, K. A test for comparing diversities based on the Shannon formula. *J. Theor. Biol.* **1970**, *29*, 151–154. [CrossRef] [PubMed]
35. Conover, W.J.; Iman, R.L. On some alternative procedures using ranks for the analysis of experimental designs. *Commun. Stat.-Theory Methods* **1976**, *5*, 1349–1368. [CrossRef]
36. Conover, W. *Practical Nonparametric Statistics*; John Wiley & Sons: New York, NY, USA, 1980; p. 493.
37. R Core Team. *R: A Language and Environment for Statistical Computing*; R Foundation for Statistical Computing: Vienna, Austria, 2020.
38. van der Kooi, C.J.; Stavenga, D.G.; Arikawa, K.; Belušič, G.; Kelber, A. Evolution of insect color vision: From spectral sensitivity to visual ecology. *Annu. Rev. Entomol.* **2021**, *66*, 435–461. [CrossRef]
39. Schlangen, L.; Lang, D.; Novotny, P.; Plischke, H.; Smolders, K.; Beersma, D.; Wulff, K.; Foster, R.; Cajochen, C.; Nikunen, H.; et al. Lighting for Health and Well-Being in Education, Work Places, Nursing Homes, Domestic Applications, and Smart Cities. 2014. Available online: https://lightingforpeople.eu/2016/wp-content/uploads/2016/03/SSLerate-3.2-3.4-v4.pdf (accessed on 1 December 2022).
40. Briscoe, D.B.; Chittka, L. The evolution of color vision in insects. *Annu. Rev. Entomol.* **2001**, *46*, 471–510. [CrossRef]
41. Brehm, G. A new LED lamp for the collection of nocturnal Lepidoptera and a spectral comparison of light-trapping lamps. *Nota Lepidopterol.* **2017**, *40*, 87–108. [CrossRef]
42. Brehm, G.; Niermann, J.; Nino LM, J.; Enseling, D.; Jüstel, T.; Axmacher, J.C.; Warrant, E.; Fiedler, K. Moths are strongly attracted to ultraviolet and blue radiation. *Insect Conserv. Divers.* **2021**, *14*, 188–198. [CrossRef]
43. Sanmartín, P.; Vázquez-Nion, D.; Arines, J.; Cabo-Domínguez, L.; Prieto, B. Controlling growth and colour of phototrophs by using simple and inexpensive coloured lighting: A preliminary study in the Light4Heritage project towards future strategies for outdoor illumination. *Int. Biodeterior. Biodegrad.* **2017**, *122*, 107–115. [CrossRef]
44. Sanmartín, P. New perspectives against biodeterioration through public lighting. In *Microorganisms in the Deterioration and Preservation of Cultural Heritage*; Joseph, E., Ed.; Springer: Cham, Switzerland, 2021; pp. 155–171.
45. Longcore, T.; Aldern, H.L.; Eggers, J.F.; Flores, S.; Franco, L.; Hirshfield-Yamanishi, E.; Laina Petrinec, L.N.; Yan, W.A.; Barroso, A.M. Tuning the white light spectrum of light emitting diode lamps to reduce attraction of nocturnal arthropods. *Philos. Trans. R. Soc.* **2015**, *370*, 20140125.
46. Hakami, A.R.; Khan, K.A.; Ghramh, H.A.; Ahmad, Z.; Al-Zayd, A. Impact of artificial light intensity on nocturnal insect diversity in urban and rural areas of the Asir province, Saudi Arabia. *PLoS ONE* **2020**, *15*, e0242315. [CrossRef] [PubMed]
47. Stavenga, D.G.; Wehling, M.F.; Belušič, G. Functional interplay of visual, sensitizing and screening pigments in the eyes of *Drosophila* and other red-eyed dipteran flies. *J. Physiol.* **2017**, *595*, 5481–5494. [CrossRef]
48. Kokkinn, M.J.; Williams, W.D. An experimental study of phototactic responses of *Tanytarsus barbitarsis* Freeman (Diptera: Chironomidae). *Mar. Freshw. Res.* **1989**, *40*, 693–702. [CrossRef]
49. Mellor, H.E.; Hamilton, J. Navigation of *Lutzomyia longipalpis* (Diptera: Psychodidae) under dusk or starlight conditions. *Bull. Entomol. Res.* **2003**, *93*, 315–322. [CrossRef]
50. Döring, T.F.; Kirchner, S.M.; Skorupski, P.; Hardie, J. Spectral sensitivity of the green photoreceptor of winged pea aphids. *Physiol. Entomol.* **2011**, *36*, 392–396. [CrossRef]
51. McNeill, C.A.; Allan, S.A.; Koehler, P.G.; Pereira, R.M.; Weeks, E. Vision in the common bed bug *Cimex lectularius* L. (Hemiptera: Cimicidae): Eye morphology and spectral sensitivity. *Med. Vet. Entomol.* **2016**, *30*, 426–434.
52. Diaz-Montano, J.; Campbell, J.F.; Phillips, T.W.; Throne, J.E. Evaluation of light attraction for the stored-product psocids, *Liposcelis entomophila*, *Liposcelis paeta*, and *Liposcelis brunnea*. *J. Econ. Entomol.* **2018**, *111*, 1476–1480. [CrossRef]
53. Diaz-Montano, J.; Campbell, J.F.; Phillips, T.W.; Cohnstaedt, L.W.; Throne, J.E. Evaluation of light attraction for the stored-product psocid, *Liposcelis bostrychophila*. *J. Pest. Sci.* **2016**, *89*, 923–933. [CrossRef]
54. van Langevelde, F.; Ettema, J.A.; Donners, M.; WallisDeVries, M.F.; Groenendijk, D. Effect of spectral composition of artificial light on the attraction of moths. *Biol. Conserv.* **2011**, *144*, 2274–2281. [CrossRef]
55. Wakefield, A.; Broyles, M.; Stone, E.L.; Harris, S.; Jones, G. Quantifying the attractiveness of broad-spectrum street lights to aerial nocturnal insects. *J. Appl. Ecol.* **2018**, *55*, 714–722. [CrossRef]

4.4 PART 4: SOCIO-ECONOMIC IMPACT

4.4.1 CHAPTER 9

CARBON FOOTPRINT OF BIOSTATIC, TARGETED ORNAMENTAL LIGHTING AND RELATED CLEANING SERVICE FOR SUSTAINABLE CONSERVATION OF ARCHITECTURAL HERITAGE

Anxo Méndez, Patricia Sanmartín, Almudena Hospido

Submitted to Journal of Cultural Heritage (under review)

JCR index (IF) 2024 = 3.3 (8/44, 83.0 percentile in Spectroscopy)

Currently available as pre-print at SSRN: http://dx.doi.org/10.2139/ssrn.5208653

Carbon footprint of biostatic, targeted ornamental lighting and related cleaning service for sustainable conservation of architectural heritage

Anxo Méndez[1], Patricia Sanmartín[1], Almudena Hospido[2]

1. CRETUS, Departamento de Edafoloxía e Química Agrícola, Universidade de Santiago de Compostela, 15782 Santiago de Compostela, Spain

2. CRETUS, Chemical Engineering Department, Universidade de Santiago de Compostela, 15782 Santiago de Compostela, Spain

Abstract

Studies evaluating the sustainability of architectural heritage conservation are scarce. Given the impact of nocturnal ornamental lighting on biofouling, in this case study, the carbon footprint and economic cost of the lighting and associated biofouling control were evaluated in a historic building in the heritage city of Santiago de Compostela (NW Spain). The novel CromaLux LED lighting system was first used in this UNESCO World Heritage city in 2021, and its impact on both services (lighting and cleaning) has already been reported. The expected improved environmental performance and the associated costs can therefore now be quantified. To this end, three ornamental lighting systems (metal halide, white LED, CromaLux LED) and five cleaning methods (laser, water vapour, Biotin T®, Biotin R® and reinforced ethanol) were compared. CromaLux LED outperformed both the traditional metal halide and white LEDs systems (reducing the lighting service carbon footprint by 80% and 20%, respectively). The best-performing cleaning methods were those based on laser (0.49 kg $CO_{2\text{-eq}}$) and reinforced ethanol (2.76 kg $CO_{2\text{-eq}}$), although the ethanol-based method is more costly than the others (up to 21.41% more). The reduction in biofouling yielded by CromaLux reduced energy consumption by up to 16.83 kg $CO_{2\text{-eq}}$. If implemented at city level, the CromaLux LED system could potentially yield annual savings of up to 3.64 tonnes of $CO_{2\text{-eq}}$ and €1,269.91. The findings thus confirm the advantages of CromaLux for improving the environmental and economic sustainability of lighting and cleaning architectural heritage.

Keywords: Biocides; cultural heritage; public lighting; smart cities; buildings and monuments; sustainable development goals.

Highlights:

- CromaLux lighting and cleaning systems were evaluated in a case study
- The carbon footprint is 24% lower for CromaLux LEDs than for conventional white LEDs
- Reinforced-ethanol cleaning uses ~ 20% less CO2-eq but is 22% more costly than Biotin
- CromaLux could halt biofouling and reduce carbon emissions by up to 16.83 kg CO2-eq
- CromaLux could yield annual savings of up to 3.64 tCO2-eq and €1,269.91 at city level

1. Introduction

The promotion of sustainable heritage management is often overlooked in urban planning, which may lack targeted perspectives and tools adapted to the specific characteristics of heritage sites (Elnaggar, 2024). Sustainable Development Goal (SDG) 11 "Sustainable cities and communities" United Nations, 2024 states the need to "strengthen efforts to protect and safeguard the world's cultural and natural heritage". In addition, it defines sustainability in the context of urban heritage as "how we can optimize the appreciation of our heritage in such a way that it will still be relevant in the future".

Outdoor artificial lighting at night (ALAN), particularly when used for ornamental purposes, is one way of enabling urban heritage to be appreciated. The use of ALAN has been described as concerning the conservation of architectural works and the creation of nocturnal cultural landscapes (Zielinska-Dabkowska and Xavia, 2018. However, ALAN is frequently overlooked in discussions on the sustainability of urban heritage conservation Kyba et al., 2018. Although nocturnal lighting has strong environmental and economic impacts (see e.g. Falchi et al., 2011; Anderson et al., 2024), it is increasingly used worldwide (Mohar et al., 2014; Kyba et al., 2017), partly because of an increase in nocturnal tourism (Eldridge and Smith, 2019). Light used as an ornamental feature plays an economic role in nocturnal tourism activities, as it can enhance the attractiveness of sites for tourists (Valetti et al., 2020; Zhang and Zhang, 2023). This is particularly relevant in world heritage cities, such as Santiago de Compostela (NW Spain). Tourism has increased by 420% in this city in the last two decades, with record numbers of visitors in 2024 (Sequeiro, 2024; Rodriguez, 2024). The local government spends €3.5 million per year on powering and maintaining luminaires (Innovation Procurement Compass, 2024). In 2023, an additional €923,000 was allocated to rehabilitation and urban recovery interventions in the historic city, including heritage structures and service infrastructure (Consorcio de Santiago, 2022).

In this context, the CromaLux project (https://cromalux.santiagodecompostela.gal/en, 2020-2024) was developed as an innovative public procurement project within the SMARTiAGO project (https://smartiago.santiagodecompostela.gal) to transform Santiago de Compostela into a smart city. The overall aim of the CromaLux project is to improve the energy efficiency of ornamental lighting systems, thus enhancing the value of architectural heritage through ornamental lighting while reducing maintenance costs. This lighting system has been developed to target and reduce the development of phototrophic biofouling by a biostatic effect. It is therefore proposed as a preventive conservation tool that utilises the existing ornamental lighting infrastructure. The CromaLux luminaires, designed ad-hoc for the project and currently under trial, can provide adequate lighting, according to the Spanish legislation for heritage (Méndez, Prieto, et al., 2024), with effects similar to those in unlit areas, with little or no impact on the insects in the surrounding aerial area (Méndez et al., 2022) and slight enhancement of the microbiome on the monument facades that is not visible to the naked eye (Méndez, Maisto, et al., 2024).

Phototrophic biofouling is directly affected by changes in ornamental lighting properties, especially light spectra (see e.g. Popović et al., 2022; Bao et al., 2023). In phototrophic biofilms, highly structured communities of microbial cells are embedded in an extracellular polymeric (EPS) matrix that enables the cells to adhere to surfaces and protects them from the environment (Pinna, 2021). The phototrophs that predominate in these biofilms depend on light as a source of energy for metabolism (i.e. photosynthesis). Thus, algae (the main phototrophs present in biofilms in Europe (Gaylarde and Gaylarde, 2005) and cyanobacteria use sunlight to produce glucose and regulate other physiological processes (Caneva et al., 2008). Light at night disrupts the normal circadian rhythms of these organisms and allows them to continue the photosynthetic process (Roux et al., 2024) and potentially undergo an increase in biomass (see e.g. Jacob-Lopes et al., 2009; González-Camejo et al., 2019). These organisms use different pigments to harness light between 400 nm and 700 nm (photosynthetic active radiation, PAR), including chlorophylls and carotenoids, which mainly absorb blue (430-488 nm) and red (612-662 nm) wavelengths and scarcely absorb light in the centre of PAR (Aguirre-Gomez et al., 2001).

The presence of visible biofouling (sometimes considered unsightly and to be caused by lack of maintenance) forces public authorities to plan cleaning operation to prevent further biodeterioration of monuments, whether the stone material is being weathered or simply has an aesthetic impact (see e.g. Villa et al., 2020; Nowicka-Krawczyk et al., 2022). Life-cycle assessment, specifically carbon footprint quantification, is useful for guiding cleaning operations and for evaluating ornamental lighting services (and how both interact), towards environmental sustainability. This tool appears appropriate for supporting decision-making processes in the management of urban heritage sites, and when coupled with cost analysis tools they help anticipate the economic performance of the services at said sites (see e.g. Dwaikat and Ali, 2018; Stubbs, 2004). It is possible that recent life-cycle assessments of cleaning techniques and application of consolidants and biocides to historic buildings (Franzoni et al., 2020; Dal Pozzo et al., 2024) have overlooked how other systems used in the urban fabric may interact and thus affect the associated carbon footprint.

This study evaluated the expected environmental and economic benefits of the CromaLux lighting system for architectural heritage, considering its impact on two functions (lighting and cleaning). To this end, the associated carbon footprints were quantified and compared with those associated with other widely used lighting and cleaning systems. The study thus aimed to guide public and private heritage owners regarding use of the most appropriate ornamental lighting for their properties, as well as providing data about the impacts and cost of cleaning building facades. Following the UNE-EN ISO 14067:2019 (ISO, 2019) standard for carbon footprint quantification (**Fig. 32**), Section 2 describes the CromaLux lighting system in further detail. The findings regarding the selected case study, the functional unit (FU) defined, and the evaluation

methods used for both services (lighting and cleaning) are reported. Section 3 describes and lists the required life cycle inventory in terms of the carbon footprint of the service and the economic performance. Section 4 assesses the main results regarding the carbon footprint and economic performance. Section 5 discusses and evaluates the interactions between the functions and proposes extrapolations at city level. Finally, Section 6 summarises the main conclusions derived from this study.

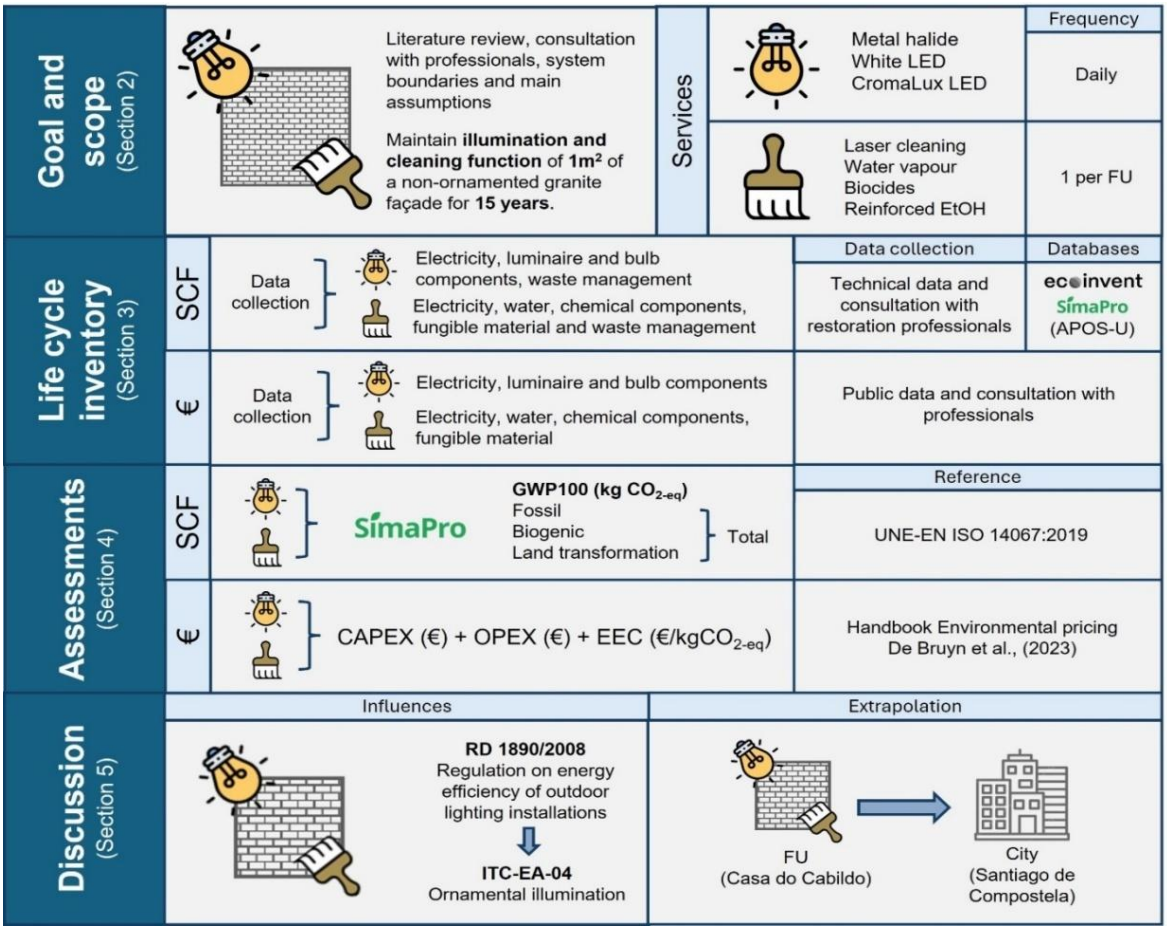

Figure 32. Summary of the approach used for carbon footprint quantification based on the UNE-EN ISO 14067:2019 standard (ISO, 2019).

2. Materials and methods

2.1. The CromaLux project: a novel ornamental lighting system

The CromaLux luminaire uses two different lights for ornamental lighting at night: a highly efficient warm white LED with very low blue light emissions and 2580K of correlated colour temperature (CCT), used during the first hours of the night; and an amber plus green LED combination with a biostatic effect on phototrophic biofouling, used during the remaining hours of the night. The first light is used to reduce the energy consumption, and thus the economic cost of the lighting during the first hours of use, as the monochromatic amber plus green LED would not fulfil the energy saving objectives. The

second light is based on a bimodal spectrum with a narrow width band emitting in the amber (593nm) and green (528nm) regions of the visible spectrum, producing a warm white-like light with 3000K of CCT. Both lights follow international outdoor lighting recommendations (International Dark-Sky Association, 2010; American Medical Association, 2016) based on reducing blue light wavelengths (emission below 500 nm) to minimize potential harmful human and environmental effects (see e.g. Svechkina et al., 2020). Thus, blue light emissions are reduced in the highly efficient warm white light and completely removed in the biostatic amber plus green light. Research has been conducted on the use of monochromatic light (e.g. red and green) to control phototrophic colonisation of outdoor monuments (Sanmartín, 2021), but monochromatic light cannot be used for long-term lighting of monuments (Méndez, Prieto, et al., 2024).

Therefore, it is hypothesised (currently being tested) that exposure to the bimodal spectrum centred on amber and green colours will decrease the photosynthetic efficiency of phototrophs, expose them to oxidative stress (see e.g. Chen et al., 2023; Méndez, Sanmartín, et al., 2024) and have an overall biostatic effect. This is expected to have a positive impact by reducing the need to clean stone facades and structures. It should be noted that the light has a biostatic not biocidal effect, and its role is not therefore to replace the use of chemicals to remove any existing biofouling, but to delay the need for cleaning treatments. Parallel work conducted in the framework of the project has included almost 4 years of field monitoring. This research has shown that the formation of phototrophic biofilms on granite ashlars exposed to a combination of amber plus green LED light is similar to or even less than that on unilluminated ashlars and significantly lower than on ashlars exposed to the light from metal halide luminaires, which have been found to significantly increase the development of photosynthetic organisms (Méndez et al., 2025). Laboratory tests have also been conducted to evaluate the impact on phototrophic biofilms of both the warm white LED and amber plus green LED lights in the CromaLux luminaire under low and high levels of daylight illuminance. The test findings have shown that although the biostatic capacity of amber plus green light is superior in both low and high daylight illuminance, the warm white output also inhibits phototrophic growth and reduces production of the EPS matrix under high illuminance (Méndez et al., 2025).

2.2. The Casa do Cabildo historic building: a case study

Santiago de Compostela was designated a World Heritage city by UNESCO in 1985. Its unique heritage includes 110,000 m^2 of built surface monuments and 30,000 m^2 of buildings of exceptional architectural merit (https://xeoportal.santiagodecompostela.gal/xeoportal/#/). The urban lighting infrastructure in Santiago de Compostela comprises 30,936 luminaires, of which 216 currently function as ornamental night-time lights (data provided by Ferrovial Construcción S.A.). Within the CromaLux project, the main pilot project was conducted in the historic *Casa do Cabildo* building (coordinates WGS84: 42.879845679897585, -8.544406413861658), where the CromaLux lighting system was installed in November 2021 (**Fig. 33**).

This granite building is one of most important examples of Galician baroque scenography. It was built between 1754 and 1758 to embellish the *Praza de Praterías* and has a depth of only 4 to 6 meters (Taín Guzmán, 2012). Between 1999 and 2019, the building was illuminated with a metal halide lighting system, like other historic buildings and monuments in the city. The building was not illuminated between 2019 and 2021, when the CromaLux system was installed on a balcony of the adjacent Pilgrimage Museum, 14 metres from the centre of the main facade of the *Casa do Cabildo*. The main facade was cleaned in 2010 to remove the existing biofouling (much of it algal), mainly by applying the biocidal agent Biotin R®; the next cleaning operation is scheduled for 2025.

Figure 33. Frontal facade of the *Casa do Cabildo* building in Santiago de Compostela, illuminated by the CromaLux lighting system (image provided by A. Méndez, June 2023).

2.3.Environmental cost analysis

The carbon footprint of the products/services was quantified in order to evaluate the environmental performance of the lighting and cleaning services. The carbon footprint was calculated according to the UNE-EN ISO 14067:2019 standard (ISO, 2019), which measures the direct and indirect greenhouse gas (GHG) emissions resulting from the activities required to provide a given service.

Functional units (FU) are used to describe the quantity of a product or service on the basis of the performance delivered in the end-use application. Using functional units enables objective comparisons of different products or systems with the same final function, as the units serve as the reference quantity for data analysis. Defining the functional unit FU, i.e. quantifying the system function, is essential for analysing processes related to cultural heritage conservation (Franzoni et al., 2020) as is is strongly dependent

on the skills, experience and practices of the restorer and on the particular characteristics of the building been treated.

In this study, the FU was defined as the maintenance of 1 m^2 of surface of a non-ornamented granite facade in a period of 15 years[1], considering the following characteristics of both the primary lighting function and the concomitant cleaning function:

- **lighting** for 6 hours per day (from 21:00 to 03:00, i.e. a total of 2,190 hours per year), with an illuminance of 75 lux according to the average values for architectural heritage in the historic centre of Santiago de Compostela and meeting the requirements established in Royal Decree 1890/2008 and its complementary technical instructions EA-01 to EA-07 (MINCOTUR, 2008). Note that urban lighting in Santiago de Compostela is programmed to switch on at sunset, which varies between around 18:10 and 22:20 throughout the year, with the median being around 20:30 (Ministry of Transport and Sustainable Mobility, 2022). For the sake of simplicity, a switch-on time of 21:00 was assumed (the switch-off time was 03:00).
- **cleaning** treatments required, based on expert opinions of professional restorers and architects, for correct cleaning as defined in the 'Green Paper on the Sustainable Management of Cultural Heritage' (Ministry of Culture, 2024), i.e. the effective removal of phototrophic biofouling without affecting the underlying material.

2.3.1. Lighting function

The CromaLux lighting system (**Fig. 34c**) was compared with two baseline systems (metal halide (**Fig. 34a**) and white LED (**Fig. 34b**), the ornamental lighting systems most commonly used in Santiago de Compostela.

Metal halide system: The light spectrum of this system falls in the photosynthetic active radiation (PAR) range, between 350–400 nm and 700–750 nm, with five main peaks centred at 435 nm, 508 nm, 546 nm, 578 nm and 589 nm, other important peaks at 473 nm, 569 nm and 624 nm, and a significant peak at 365 nm at the UV-A region. The lamp provides a CCT of 4668 K.

White LED system: The energy efficiency of this system is higher than that of a metal halide lamp Sankhwar, 2024. The light spectrum also falls in the PAR range, with a main peak at 450 nm and a second peak at around 600 nm, resulting in a CCT of 4000K. For the sake of simplicity, as both lamps emit in the entire PAR range, both metal halide and white LED systems were considered equal regarding the cleaning function.

CromaLux LED system: Both types of LED lights in the CromaLux lighting system (see section 2.1) are programmed to switch on at different times of the night to improve the

[1] The average frequency of cleaning treatments in monuments and historical buildings of the historical centre of Santiago de Compostela according to the expert architects consulted from the Consorcio of Santiago (http://www.consorciodesantiago.org) who supervise architectural heritage conservation works.

energy efficiency. The highly efficient warm white LED light is switched for the first 2 hours (21:00-23:00), and the amber plus green LEDs are then switched on for the remaining 4 hours (23:00-03:00). Details of the LED light configurations and technical specifications are confidential.

Figure 34. Photographs of the three ornamental lighting systems considered in the current study. A) Metal halide system (image provided by P. Sanmartín), B) white LED system (image provided by Televés S.A.U.) and C) CromaLux system (image provided by A. Méndez).

2.3.2. Cleaning function

In humid temperate climates, architectural heritage is affected by biofouling caused by (micro)organisms and generating unsightly staining ('greening') due to the presence of phototrophs. Such visible biofouling must be removed frequently by restoration teams due to its aesthetic impact and weathering potential (Smith et al., 2011; Cutler et al., 2013). Three cleaning methods that are widely used by professional restorers were evaluated in the present study: laser cleaning (**Fig. 35a**), steam (water vapour) (**Fig. 35b**) and three different chemical biocides (**Fig. 35c**).

Figure 35. Photographs showing examples of the three cleaning methods evaluated in the current study. a) Application of laser cleaning, with inset showing detail of the device (image provided by Parteluz Estudio S.L.). b) steam application (image provided by Parteluz Estudio S.L.). c) application of chemical biocides (image provided by María Gómez García, restorer).

Laser cleaning: based on ablation by a thermal mechanism to remove undesired layers from the surface (Zanini et al., 2018). Use of this method on outdoor stone surfaces has been studied extensively in the last decade because of the advantages it has over traditional mechanical cleaning methods, as it is highly controllable and does not require direct contact with the material (Cappitelli et al., 2020).

Steam (water vapour): works via the combined pressure and temperature of a water vapour jet, usually applied together with biocidal agents (Bouichou et al., 2010) but also alone (Hallmann et al., 2013). In the present study, it was applied alone.

Chemical biocides: commonly used to prevent biological colonisation (Zhu et al., 2023) although the use of some of these biocides is now being legally restricted due to their associated toxicity (Lo Schiavo et al., 2020; Pinna, 2022).

Biotin T®: one of the biocides currently most commonly used in Spain to treat stone-built heritage. It is an aqueous solution of a quaternary ammonium salt (typically didecyldimethylammonium chloride) and 2-octyl-2H-isothiazole (OIT) (see e.g. Dresler et al., 2017; Becerra et al., 2019). In the present study, a concentration of 2.5% of Biotin T® in distilled water was used. After completion of the treatment, the surface must be rinsed with water.

Biotin R®: used in 2010 to clean the *Casa do Cabildo* building, but scarcely available nowadays. It is composed of OIT with Iodopropynylbutylcarbamate (IPBC) diluted in isopropyl alcohol (see e.g. Gomoiu et al., 2022). In the present study, a concentration of 2.5% of Biotin R® in isopropyl alcohol was used. After completion of the treatment, the surface must be rinsed with water.

Reinforced ethanol: the use of ethanol (both at 96% and 70%) reinforced with benzalkonium chloride at 0.1% to 0.3% is becoming a popular treatment for cleaning stone surfaces (e.g. Pozo-Antonio et al., 2016b), and it is deemed the preferred method according to the 'Green Paper on the Sustainable Management of Cultural Heritage' (Ministry of Culture, 2024) due to its safety, low environmental impact and cost-effectiveness. The solution used in the present study was 70% ethanol reinforced with 0.1% benzalkonium chloride. No final rinse with water is needed in this case.

2.3.2. Interactions between lighting and cleaning functions

The effect of the CromaLux system on the formation of phototrophic biofilms (see section 2.1) was taken into account for estimating the improvement in cleaning requirements for the building. Thus, it was assumed that the time between cleaning treatments (defined as 15 years in the FU) will increase as CromaLux will reduce the formation of biofilm relative to the other two lighting systems. Two extreme scenarios were defined to cover the entire range of effectiveness of the CromaLux lighting system on biofouling: an improvement of 10% (worst case scenario for CromaLux, hereinafter WCS_C), thus increasing the time between cleaning operations to 16.5 years; and an improvement of 40% (best case scenario for CromaLux, hereinafter BCS_C), thus increasing the time between cleaning operations to 21 years.

In addition to the possible impacts of biofouling on the conservation of architectural heritage, i.e. biofilm formation and biodeterioration, the presence of biofouling also affects the lighting of facades. The Spanish legislation recommends (in technical instruction ITC-EA-02 of the Royal Decree 1890/2008 (MINCOTUR, 2008) incrementing the illuminance of ornamental lighting to compensate for the loss of reflected light by fouling (whether biotic or abiotic) on the construction material, as the fouling decreases its natural reflection factor and thus increasing the energy consumption (Méndez, Prieto, et al., 2024). The construction material of the architectural heritage in the historic centre of Santiago de Compostela (including the *Casa do Cabildo*) is included in the grey granite category according to the above-mentioned instruction. The instruction states the need to multiply the illuminance by 2 when the facade is 'dirty' and by 3 when the facade is 'very dirty'. However, the terms 'dirty' and 'very dirty' are not clearly defined in the instruction and are left to free interpretation. Experts in stone heritage (bio)fouling, several of whom have published articles on the subject (see e.g. Piazza et al., 1998; Morando et al., 2019; Pinna et al., 2018; Favero-Longo, Matteucci, Voyron, et al., 2023, Favero-Longo, Matteucci, Castelli, et al., 2023) were consulted in order to establish the time frame within which the facade would become 'dirty' and 'very dirty' in the case under study, based on their knowledge and expert opinion. Two corner scenarios were considered to cover a longer time for development of biofouling, as indicated in **Table 7**. Thus, the worst-case scenario for biofouling (WCS_B) and the best-case scenario for biofouling (BCS_B) were used to determine the number of years used as correction factors to comply with the instruction, applied to the 15 years established in the FU.

Table 7. Number of years used as the correction factor for fouling on the ITC-EA-02 applied to the 15 years established in the functional unit (FU).

	Correction factor (number of years)		
Scenario	Clean	Dirty	Very dirty
WCS_B	7	5	3
BCS_B	10	4	1

2.4.Economic evaluation

Life Cycle Costing (LCC) assesses the costs associated with the life cycle of a product, process or service and that are directly covered by one or more actors during the lifetime of the product, process or service, including the cost of externalities (Swarr et al., 2011). Building design and civil construction are the areas in which the most advanced integration of environmental and economic assessment has been achieved, e.g. in a recent study that applied the UNE-EN ISO 15686-5:2017 standard (ISO, 2017) for LCC analysis of lighting systems for roads Picardo et al., 2023. The calculation tools developed by the European Commission European Commission, 2024 with the aim of promoting green public procurement were also used here with the same functional unit (FU) as in the carbon footprint analysis.

Both capital expenditure (CAPEX; i.e. cost of acquiring, building or installing physical assets) and operational expenditure (OPEX; i.e. cost of running and maintaining said physical assets) were considered in the present study (in €); more detailed information is provided in Supplementary Material (Table SM11).

The prices of the electricity and luminaires were verified by one the companies responsible for managing urban lighting in Santiago de Compostela (Ferrovial Construcción S.A.). Given that the metal halide lighting system currently in use is outdated, its cost was estimated on the basis of that of other metal halide luminaires with similar characteristics. In addition, as the CromaLux lighting system is not yet on the market, it was assumed to cost the same as the white LED luminaire.

The prices of the cleaning system components were ascertained through consultation with several retailers specialising in restoration and preservation products. The water cost is based on the average prices quoted by the municipal water services.

The cost of waste management was not included, for several reasons. On the one hand, there is a flat rate charge for municipal solid waste management, and the price is only increased for operations that generate large amounts of waste, which was not the case for the FU in the current study. On the other hand, the Spanish legislation on waste electrical and electronic equipment (Ministry of Agriculture, 2015) follows the producer responsibility principle, and management and disposal of luminaires are thus considered beyond the scope of the present study. Moreover, the waste management cost is commonly assumed to be included in the price of the luminaire.

Finally, GHG emissions (computed as kg $CO_{2\text{-eq}}$) cause a loss of economic welfare that can be included in the economic cost of the service. To this end, the environmental economic cost (EEC) (€/$kg_{CO2\text{-eq}}$) reported by De Bruyn et al., (2023) was applied in the present study.

3. Life cycle inventory

Primary data on the lighting function (**Table 8**) were obtained from the technical data sheets of the lighting systems evaluated. These data included information on the cost of materials and electricity consumption. When no such data were not available, data on alternative outdoor luminaires with similar characteristics were used. Further information regarding the datasets used to model each component of the luminaries and the bulbs, as well as electricity consumption and waste management, is provided in the Supplementary Material (SM12).

Table 8. Inventory data for the three lighting systems evaluated per FU.

Element	Metal halide		White LED		CromaLux LED*	
Luminaire (g)	Aluminium	14620	Aluminium	3540	Aluminium	3540
	Porcelain	2000	Polycarbonate (PC)	3310	Polycarbonate (PC)	3310
	Tempered glass	1330	Printed circuit board	460	Printed circuit board	460
	Stainless steel	1000	Stainless steel	430	Stainless steel	430
	Silicone	50	Electric ballast	410	Electric ballast	410
			Electric connectors	400	Electric connectors	400
			Acrylonitrile butadiene styrene (ABS)	240	Acrylonitrile butadiene styrene (ABS)	240
			Silicone	200	Silicone	200
			Vinyl polychloride (PVC)	80	Vinyl polychloride (PVC)	80
			Copper	20	Copper	20
			Polybutylene terephthalate (PBT)	20	Polybutylene terephthalate (PBT)	20
Bulb (g)	Steatite	31.90	Printed circuit board	85.40	Printed circuit board	85.40
	Silicone	30.00	Diodes	16.80	Diodes	23.10
	Quartz	14.60				
	Copper	3.10				
	Cement	1.80				
	Ferrous metals	1.60				
	Mercury	0.08				
Electricity consumption (kWh)		9424.52		1443.35		1090.59

* Structural materials identical to those in the white LED luminaire

LED luminaires have not yet been installed as ornamental lighting systems in Santiago de Compostela; however, renovation of the existing metal halide luminaires has been approved and is expected to be completed in the next few years. The company managing the ornamental lighting of Santiago de Compostela, Ferrovial Construcción S.A., was consulted regarding the characteristics and models of luminaires to be installed and the data were scaled to the proportions of CromaLux.

Primary data on the cleaning function were gathered by consultation with professional restorers (Parteluz Estudio S.L. and the biodeterioration division of the Spanish Cultural Heritage Institute), who provided average data for cleaning an area of 1 m^2 non-ornamented granite facade to fully remove phototrophic biofouling. The composition and quantity of materials used, the electrical power consumption of machinery for laser and vapour cleaning, and the duration of the operations are summarised in **Table 9**. Machinery production was disregarded as its contribution within the established FU was deemed negligible owing to the long lifespan of the equipment (e.g. more than 100,000 hours for laser cleaning according to manufacturers) and can be used for multiple interventions, as well as other infrastructure/items needed for the cleaning such as scaffolding and reusable personal protective equipment. Similarly, wastewater treatment

was omitted as the impact of the cleaning activities on the volume daily treated by the municipal facility was considered negligible.

Additional data were obtained from the Ecoinvent 3 database (Wernet et al., 2016), constructed following the 'Allocation at the point of Substitution – Unit' (APOS U) approach. In accordance with the UNE-EN ISO 14067:2019 standard (ISO, 2019), only materials comprising a minimum of 1% of the total mass of the element (i.e. luminaries) were subjected to analysis. In the absence of data on the specific materials listed, the most similar elements in the Ecoinvent 3 database were selected. As information about the exact proportions of the chemical components in the biocides is not publicly available, the proportion with the highest emissions was used in the calculations. Further information on the Ecoinvent processes is provided in Supplementary Material (SM13 and SM14).

Table 9. Characteristics of the cleaning systems.

Cleaning system	Element		Material/ Compound	Amount per m^2 (g)	Lifespan
Laser	Laser cleaning equipment		Electricity consumption (kWh)	0.05	
Water vapour	Steam cleaner equipment		Water	200	
			Electricity consumption (kWh)	0.40	
Chemical biocides	Biotin T®		N-octyl isothiazolinone (OIT)	18.57	
			Quaternary ammonium salt	0.31	
			Water	173	
	Biotin R®		Isopropyl alcohol	19.80	
			N-octyl isothiazolinone (OIT)	18.57	
			Iodopropynylbutylcarbamate (IPBC)	0.32	
			Water	100	
	Reinforced ethanol		Ethanol	110.46	
			Benzalkonium chloride	0.19	
			Water	57.83	
Consumables*	Brushes		Wood	108.50	1.2 per day
			Coconut fibre	40.00	
	Personal protective equipment (PPE)	Masks	Polypropylene (masks)	25	1 per day
		Gloves	Latex	30	6 per day

*Consumables were used in equal amounts in the chemical cleaning method with all three biocides.

4. Environmental and economic assessments

4.1. Carbon footprint

Lighting and cleaning functions were each evaluated in terms of Global Warming Potential for 100 years (GWP100) according to the UNE-EN ISO 14067:2019 standard

(ISO, 2019). The three lighting systems were evaluated in relation to the 15-year period considered in the (**Fig. 36**). In all cases, 99% of the carbon footprint was associated with fossil $CO_{2\text{-eq}}$ emissions (see Supplementary Material SM15).

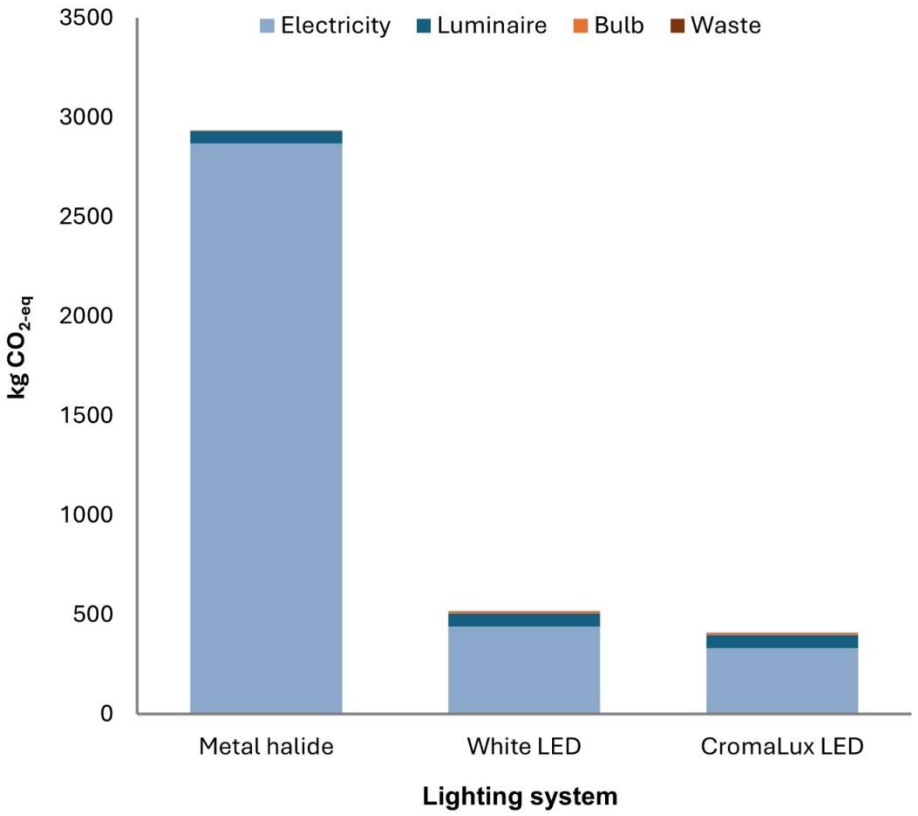

Figure 36. Carbon Footprint (GWP100) of the different lighting systems, calculated on the basis of the defined FU.

The transition from traditional metal halide to white LED technology reduced the associated carbon footprint by 82.46%, from 2,932.46 kg $CO_{2\text{-eq}}$ during the FU to 514.31 kg $CO_{2\text{-eq}}$; this could be further reduced to 106.87 kg $CO_{2\text{-eq}}$ with the CromaLux lighting system. The lifespan of LED systems is twice that of metal halide systems, with the latter requiring 2.74 bulb replacements over the 15 years considered in the FU. Despite the higher emissions during manufacture of the LED systems (74.81 kg $CO_{2\text{-eq}}$ relative to 63.11 kg $CO_{2\text{-eq}}$ for the metal halide lighting system), the metal halide systems consume much more electricity, accounting for 97.83% of emissions and resulting in a larger carbon footprint. As the structural materials for both LED systems were deemed equal, the reduction in emissions is due to lower power consumption, with CromaLux consuming 24.44% less electricity than the conventional white LED evaluated. These results are consistent with those of previous studies regarding the reduction of GWP in the transition to LED lighting. In the case of road lighting, substituting high-pressure sodium lamps with LED lighting was reported to lead to a reduction in emissions of 1,300 kg $CO_{2\text{-eq}}$ per

gigalumen/hour (Tähkämö and Halonen, 2015) and a GHG mitigation potential of up to 11.9 Mt $CO_{2\text{-eq}}$/year in cities in China (Chang et al., 2021).

Regarding the cleaning function, comparison of the five cleaning systems, based on the FU, is shown in **Figure 37**.

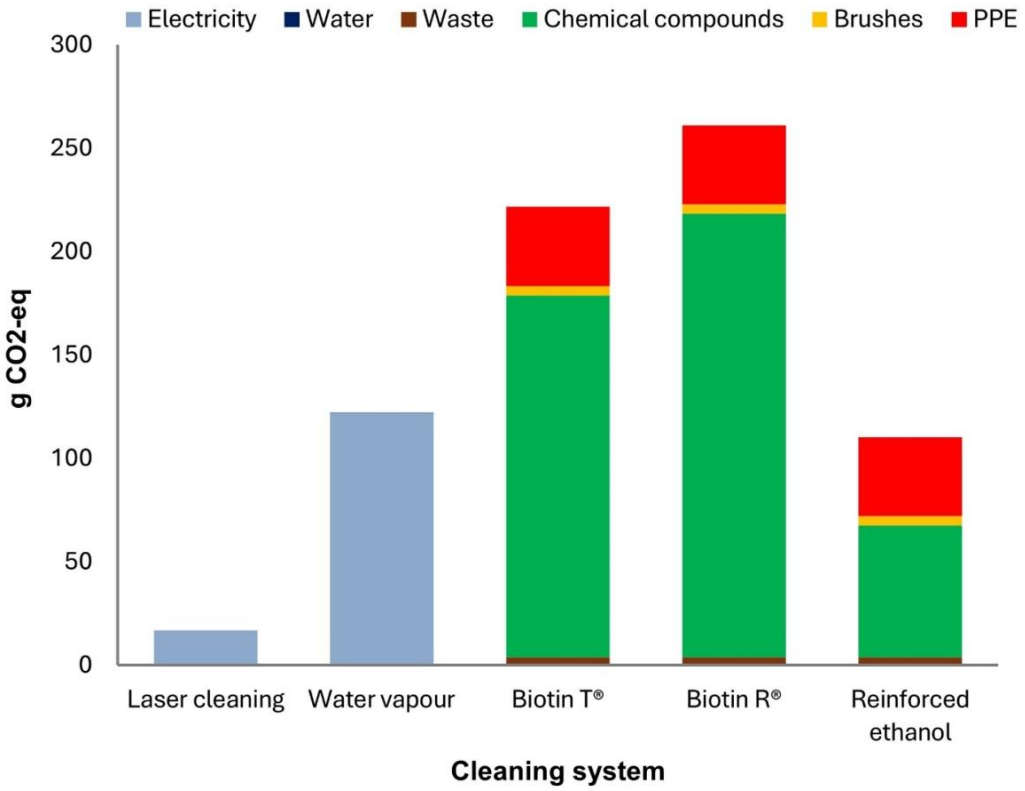

Figure 37. Carbon Footprint (GWP100) of the different cleaning methods, calculated on the basis of the defined FU.

Of the methods analysed, laser cleaning has the lowest carbon footprint (16.74 g $CO_{2\text{-eq}}$ per m^2). This method does not involve contact with the target surface and does not introduce foreign chemical compounds, yielding precise, efficient removal of layers covering the surface being cleaned. Nevertheless, some technical considerations must be taken into account to ensure correct cleaning of the surface and prevent any possible damage (see e.g. Pozo-Antonio et al., 2016; Tserevelakis et al., 2019), particularly to prevent side effects when removing biofouling (Cappitelli et al., 2020). The higher power output of the steam machine 1600W vs 220W for laser) and the water requirement (200 g per m^2) make the steam cleaning system less favourable in terms of the carbon footprint, although the carbon footprint associated with water use was almost negligible (less than 0.01%), relative to that associated with the electricity consumed by the steam machine. The high carbon footprint of the steam method, together with recommendations not to clean cultural heritage surfaces using water-based methods, which can mobilize soluble salts

towards unaffected structures or endanger sensitive material like paintings (Pozo-Antonio et al., 2016), further invalidates this option. Regarding the contributions to the GWP100 categories, 99% of the emissions from both laser and steam cleaning methods were related to fossil $CO_{2\text{-eq}}$ (see Supplementaty Material SM16).

Regarding the chemical biocides, the manufacturing processes used to produce Biotin T® and R® explain the high carbon footprint of these cleaning methods (**Fig. 37**). Among all of the cleaning methods evaluated, that using reinforced ethanol yielded the second lowest carbon footprint. In all chemical treatments, the chemical itself is the main contributor to the carbon footprint (between 57.76% and 82.15%), followed by the personal protective equipment (PPE) required for the activity (i.e. masks and gloves), which accounts for 14.66 - 17.26 % in the method using biocides and 34.68% in that using reinforced ethanol. The remaining elements make minor contributions to the carbon footprint (2.64% for brushes on average, 2.19% for waste management on average and less than 0.01% for water). Thus, the method using reinforced ethanol was found to be the best alternative among the chemical cleaning systems evaluated owing to the lower carbon footprint and the fact that it is less hazardous to human health and the environment than other biocides (see e.g. Fidanza and Caneva, 2019; Caldeira, 2021).

The carbon footprints determined in the present study are lower than those reported by Franzoni et al., (2020), in a study in which the carbon footprint of several chemical and physical cleaning methods used to remove a black crust amounted to around 5 to 18 kg $CO_{2\text{-eq}}$ per m^2 (according to GWP 100a). This discrepancy is possibly due to the difference in the system boundaries, the characteristics of the equipment and the size of the case study, all of which affect the amount of material needed. For example, the "Solvent-B" chemical cleaning method requires the use of ethanol as a solvent, similarly to the Biotin R® evaluated in the present study, which must be dissolved in isopropyl alcohol. Nonetheless, the authors of the earlier study report using 1 kg of ethanol as solvent and then 25 kg of deionized water to rinse the product after cleaning a building in Bologna. By contrast, in the present study only 0.5 kg of the isopropyl alcohol (0.02 kg per m^2) solvent was required, and only 0.25 kg of water was needed to remove the excess Biotin R® (0.1 per m^2). Regarding consolidants (materials used to increase cohesion and mechanical properties in deteriorated building materials), some of those recommended for carbonate substrates yielded around 0.75 kg (diammonium hydrogen phosphate) to 3.06 kg (ethyl silicate) of $CO_{2\text{-eq}}$ per kilogram of consolidant (Dal Pozzo et al., 2024). In a life cycle assessment of the restoration of a sandstone fortress in the Uncastillo village in Zaragoza (Spain), Mohaddes Khorassani et al., (2019) reported a low impact, with carbon emissions mainly being derived from transportation of the materials rather than from the materials themselves. Materials account for a small fraction of the environmental impact in conservation practices and treatments, which often seek to minimise intervention to ensure the least possible disruption to historically valuable structures (Zhang and Dong, 2021).

4.2.Economic performance

Lighting and cleaning functions were also each evaluated in terms of their economic performance. The economic costs associated with the three lighting systems evaluated for the FU, in terms of CAPEX, OPEX and EEC, are compared in **Figure 38**.

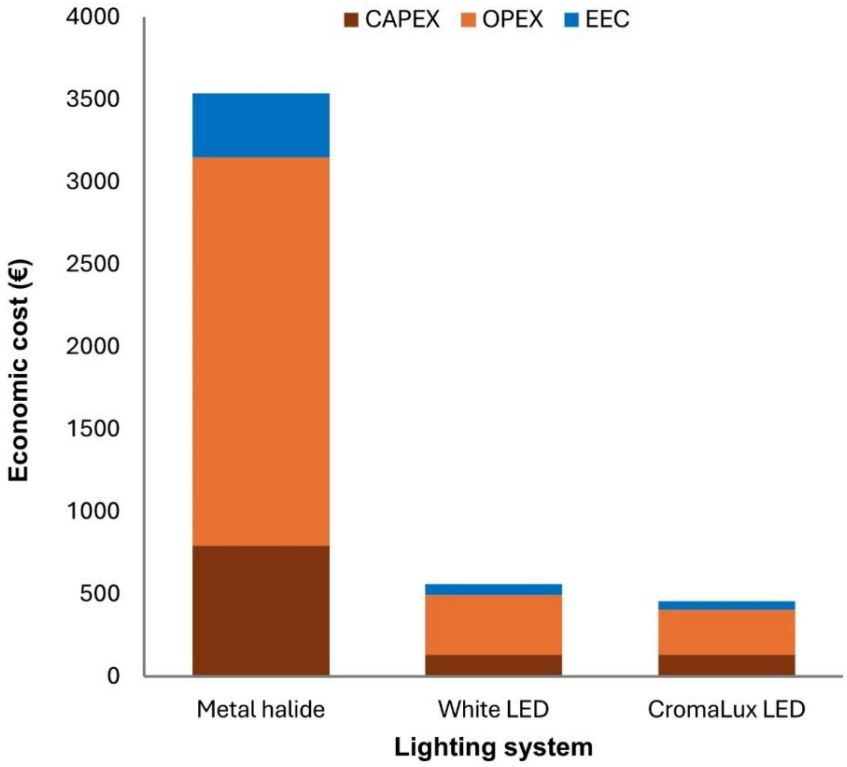

Figure 38. Economic cost (in €) in terms of CAPEX, OPEX and EEC of the lighting systems evaluated.

Not surprisingly, the prices of both LED systems are much lower than that of the metal halide lighting due to the cost of the bulbs (€244.06/each) and their short lifespan (2.74 units are required for the FU defined). The OPEX of the metal halide (€157.07/year) greatly exceeds the cost of the two LED systems. The ECC for metal halide (€24.86/year) is also higher, with the costs of material (€8.20) and waste management (€0.07) being negligible compared to operational expenses during the 15 years considered in the FU (€372.94). Urban LED luminaires can drastically lower emissions and expenses (see e.g. Hendrickson et al., 2016). Indeed, both LED options are economically preferable to metal halide, but CromaLux outperforms the white LED in both sustainability and cost. Given that the CAPEX was same (€132.00), the advantage of Cromalux stems from the lower OPEX (€18.18/year vs €24.05/year for white LED) and reduced EEC (€2.89/year vs €3.08/year for white LED).

The economic costs of the five cleaning systems evaluated for the cleaning of the frontal facade of the *Casa do Cabildo* building are compared in **Figure 39**, both in terms of the OPEX (divided in the figure between their different constituent elements) and the EEC.

The CAPEX was not considered here as the equipment used has long life and the value corresponding to one cleaning event is considered negligible (see section 3).

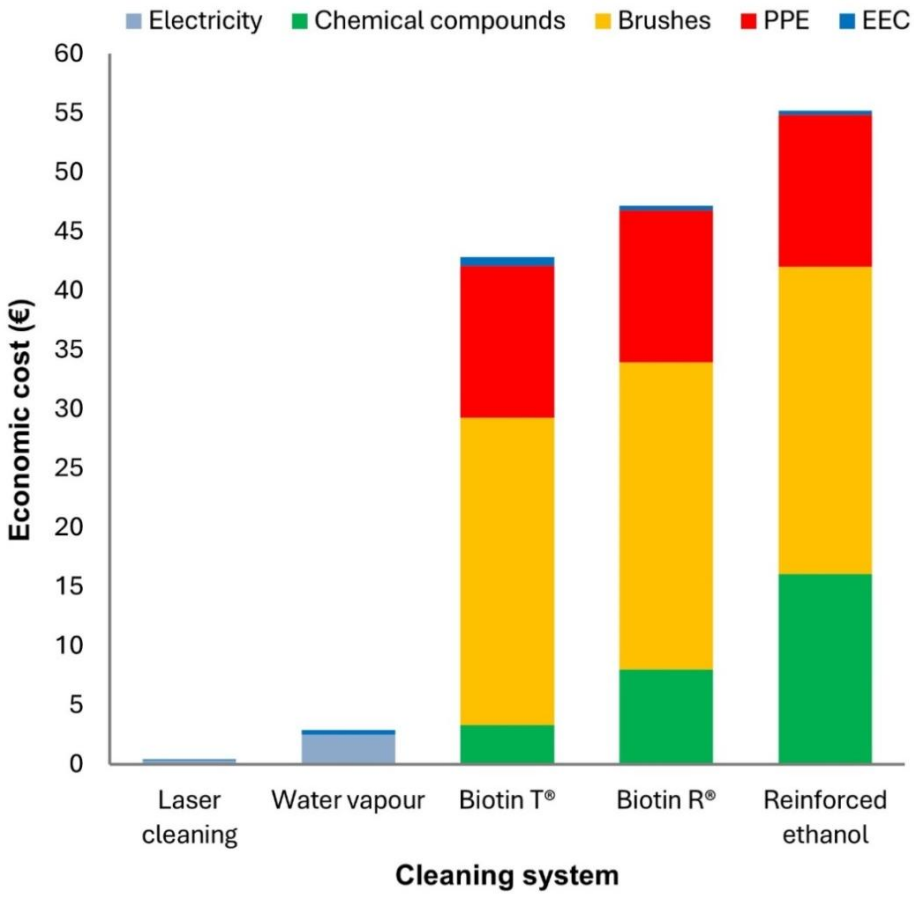

Figure 39. Economic cost (in €) in terms of OPEX (divided into the constituent elements) and EEC of the cleaning systems calculated on the basis of the FU. Water use was omitted from the figure as its contribution was negligible.

The laser cleaning and the steam cleaning methods yielded the lowest OPEX (€0.34 and €2.50 respectively), but the cost of the machinery (CAPEX) was not included in the analysis as the proportion for cleaning a single facade would be negligible. Although the laser cleaning method was the least expensive to operate, the cost of acquiring laser equipment is highly variable and may represent a significant financial barrier for its use by professionals (see e.g. Pouli et al., 2012). According to Rodriguez-Navarro et al., (2003), lightweight portable laser systems for stone conservation can cost approximately €20,000, but high-end models may cost up to €140,000. In such cases, assuming a negligible amount in cost allocation may not be valid and the cost may actually be higher than for the other methods evaluated.

Although reinforced ethanol is the preferred biocide with the lowest environmental impact, it was the most expensive (€54.83). While the prices of Biotin R® and Biotin T® are higher per L (€40–50/L vs. €4/L for reinforced ethanol), the reinforced ethanol method requires a greater volume and two applications, leading to a higher cost (€16.06), which is twice that of Biotin R® (€8.02) and nearly five times that of Biotin T® (€3.32). However, the EEC of all three chemical systems was found to be negligible (<1% of total cost), and the main expense was derived from consumables (brushes and PPE), which represent 90.53% of the cost for Biotin T®, 82.22% for Biotin R®, and 70.24% for reinforced ethanol. Given the toxicity of Biotin T® and Biotin R® (see e.g. Caldeira, 2021) it is important to recognise that their lower cost (between 14.56 % to 22.41% respectively against the reinforced ethanol) may not offset the associated health risks.

5. Discussion

5.1. Interactions between lighting and cleaning functions

Given that the three lighting systems evaluated are already (or are scheduled to be) installed as ornamental lighting systems and that the cleaning methods are standardly used by professional restorers, the potential interactions between both functions must be considered. The $CO_{2\text{-eq}}$ emissions from the ornamental lighting of the *Casa do Cabildo* building ranged from 407.44 to 2932.46 kg, whereas cleaning the 25 m^2 main facade generated a maximum of 6.53 kg $CO_{2\text{-eq}}$ with the least sustainable system (Biotin R®). This stark contrast arises because the lighting is operated nightly, whereas cleaning is performed only once (within the FU). The environmental impact of cleaning is thus negligible (<0.1%) within the FU, revealing that efforts to reduce the environmental footprint should primarily focus on lighting. The CromaLux system yielded the most significant reduction in the carbon footprint, outperforming metal halide, with a lower carbon footprint and economically more efficient than white LED (see Sections 4.1 and 4.2). Additionally, the spectral composition of the light used is expected to control phototrophic colonisation, thus affecting the lighting and cleaning function in another two ways (see section 2.3.3). Thus, the time between cleaning operations could be extended from 15 years to 16.5 or 21 years, depending on WCS_C and BSC_C, reducing both the carbon footprint and the cost of cleaning by reducing the amount in the FU. Applying the ITC-EA-02 correction factors from the Spanish legislation shows that biostatic effect on phototrophic biofouling could reduce the need to compensate for surface reflectance, ultimately reducing electricity consumption, the primary driver of carbon emissions.

The $CO_{2\text{-eq}}$ emissions (in g) associated with the cleaning systems evaluated in relation to the influence of the three lighting systems, calculated for the frontal facade of the *Casa do Cabildo* building are shown in **Table 10**.

Table 10. $CO_{2\text{-eq}}$ emissions (in g) from the cleaning systems evaluated in relation to the influence of the three lighting systems for the facade of the *Casa do Cabildo* building.

Cleaning system	**GWP100 - Total (g $CO_{2\text{-eq}}$)** for the facade of the *Casa do Cabildo* building			
	Metal halide	White LED	CromaLux LED (WCS_C)	CromaLux LED (BCS_C)
Laser cleaning	418.54	418.54	376.69	226.01
Water vapour	3,045.01	3,045.01	2,740.51	1,644.30
Biotin T®	5,540.03	5,540.03	4,986.03	2,991.62
Biotin R®	6,526.56	6,526.56	5,873.91	3,524.34
Reinforced ethanol	2,757.875	2,757.87	2,482.09	1,489.25

In 2010, in the cleaning treatment applied to the *Casa do Cabildo* building, Biotin R® was used to remove biofouling. If the CromaLux ornamental lighting system had been operating at that time, $CO_{2\text{-eq}}$ emissions would have been reduced by 656.66 g –3,002.22 g under the WCS_C and BCS_C scenarios. In comparison, reductions for lower-impact methods range from 41.85 g –192.53 g $CO_{2\text{-eq}}$ for laser cleaning and 275.79 g –1,268.62 g $CO_{2\text{-eq}}$ for reinforced ethanol. Considering reinforced ethanol to be the preferred biocide in chemical cleaning systems, the OPEX is projected to decrease by €5.48–€21.93.

The estimated total $CO_{2\text{-eq}}$ emissions associated with electrical consumption in the FU, after applying the 'dirty' and 'very dirty' correction factors, are shown in **Table 11**.

Table 11. Estimated total $CO_{2\text{-eq}}$ emissions (in kg) and electrical consumption of the lighting systems within the 15-year period considered FU after application of the correction factors for fouling level in the ITC-EA-02.

Lighting system	**Total kg $CO_{2\text{-eq}}$**		
	Without correction factor	**WCS_B**	**BCS_B**
Metal halide	2,932.46	4,972.57	4,016.31
White LED	514.31	761.54	615.09
CromaLux LED (WCS_C)	407.44	575.42	442.63
CromaLux LED (BCS_C)	407.44	509.02	407.44

Application of the correction factors increased the estimated energy consumption in the *Casa do Cabildo* building because of how ornamental lighting influences phototrophic biofouling (based on the WCS_B and BCS_B proposed). This increase was most pronounced for the metal halide system, leading to an additional 1,083.84 –2,040.11 kg $CO_{2\text{-eq}}$ emissions and an increase in the OPEX from €72.26 to €136.01 for the 15 years considered in the FU. For the LED technology, application of the correction factor would not cause such a large increase as with the metal halide system, thus allowing adequate illuminance to be maintained for ornamental illumination without compromising the environmental and economic performance of the method. However, the CromaLux lighting system is more

efficient than the white LED, although the energy consumption, and thus the carbon footprint, is the same (**Table 11**) when applying the correction factors as without applying them if both the BCS_C and BCS_B scenarios are considered. In 2005, lighting accounted for 19% of the worldwide global energy consumption, with street and road lighting accounting for 53% of the global amount (Bará, 2013). Indeed, Bará, (2013) stated that the improvements in existing luminaires and the design of new ones (optimizing their spectral composition) is possibly one of the most important contributions regarding the environmental effect of ALAN. Thus, by influencing both lighting and cleaning functions, the CromaLux lighting system provides a multifunctional solution, aligning with the growing demand for integrated urban services in smart cities (see e.g. Beccali et al., 2019; Belany et al., 2021). In addition, the importance of nocturnal lighting in a country such as Spain is heightened by the time lag existing due to its location within the Central European Time (CET) zone (Roenneberg et al., 2019). This results in a discrepancy of more than two and a half hours between standard time and true solar time (Stick, 2007), which influences how people use public spaces at night, with Spaniards frequently staying out later at night than in other European countries. There is therefore a greater political imperative for policymakers to regulate electricity demand (López, 2020).

5.2.Extrapolation to city level

In Santiago de Compostela, the $CO_{2\text{-eq}}$ emissions of the ornamental lighting amount to 42.23 tonnes of $CO_{2\text{-eq}}$ per year, considering that the ornamental lighting infrastructure currently consists of metal halide (216 luminaires). However, if the entire ornamental lighting infrastructure were to be replaced by the CromaLux lighting system rather than white LED lighting system, an additional reduction of 1.54 tonnes of $CO_{2\text{-eq}}$ per year would be achieved, without accounting for the savings generated by the cleaning function. However, the initial investment required to fully update the existing infrastructure of metal halide lamps to LED, either CromaLux or white LEDs, may represent a significant financial challenge. This was observed by Lindawati et al., (2019) in the context of replacing street lighting in the city of Bandung (Indonesia) and also that the cost of the replacement can be offset by long-term savings due to the lower energy consumption. Similar conclusions were drawn by Campisi et al., (2018) in a study conducted in Rome (Italy), as the savings achieved by the replacement with LED luminaries at city level were expected to outperform the impact and cost of other traditional systems, with a reduction of 44,461.10 $tCO_{2\text{-eq}}$ per year and an annual saving of €29,073,538 (the cost of energy from a metal halide luminaire varies by around €100 – €730 per year, depending on the power, compared to the €157.07 in OPEX of metal halide lighting system evaluated in the current study), thus compensating for the cost of the replacement (Campisi et al., 2018).

In the present study, the annual cost at city level (Santiago de Compostela) of the OPEX for the metal halide lighting system for the 216 ornamental luminaires was estimated to be €33,928.28, whereas it would be reduced to €5,196.04 with the white LED system and to €3,926.13 with the CromaLux system. Considering that the CAPEX of both LED lighting

systems at city level was €28,512.00, the cost would be covered within a year with the savings of the OPEX after substituting the metal halide luminaires, either with the white LED or the CromaLux lighting systems. It was also estimated that the city would save €19,048.65 over the duration of the FU (15 years) by using the CromaLux lighting system (€1,269,91 per year) rather than the white LED lighting system.

Assuming that the same level of biofouling would develop on the other historic buildings as in the *Casa do Cabildo* (considering the WCS_B and BCS_B scenarios for biofouling development and the WCS_C and BCS_C scenarios for the effectiveness of CromaLux lighting system), application of the correction factor used in the ITC-EA-02 could result in a reduction of 51.46 – 64.28 tonnes of $CO_{2\text{-eq}}$/year relative to the metal halide lighting system and 2.48 – 3.64 tonnes of $CO_{2\text{-eq}}$/year relative to the white LED lighting system after installation of the CromaLux lighting system for ornamental illumination. Moreover, the reduction in carbon footprint would also be accompanied by an improvement in the economic performance. The cost (accounting for both the OPEX and EEC) of the CromaLux lighting system is expected to be reduced by between €883.45/year – €1543.25/year relative to the metal halide lighting system and by €58.03/year – €702.34/year relative to the white LED lighting system.

Although solutions like the CromaLux system are meant to be used as ornamental lighting for architectural heritage, which accounts for only 0.70% of urban lighting in Santiago de Compostela, small improvements in the efficiency of nocturnal lighting practices would have a large impact. Considering that the other 99.30% (30,720 luminaires) of the nocturnal lighting infrastructure already consists of white LEDs (for the sake of this extrapolation, with the same environmental impact and cost of the presented white LED lighting system), installation of a lighting system similar to the CromaLux system could yield savings of €180,146.42 per year for the city of Santiago de Compostela, with a reduction of 1.54 $tCO_{2\text{-eq}}$ of carbon emissions per year. In 2005, lighting consumed 19% of the global energy consumption, with street and road lighting accounting for 53% of energy demand for lighting (Bará, 2013). Further studies are required to determine the feasibility of installing technological infrastructure (like lighting) in historic heritage cities. For example, installation of a fibre optic network in the historic centre of Santiago de Compostela took more than four years in order to overcome the technical difficulties associated with protection of the architectural heritage (for further information see Consorcio de Santiago, 2024). In this context, Cucchiella et al., (2017) established a framework for the transition to efficient lighting in historic centres to safeguard cultural heritage and assessed the benefits (both in terms of economic savings and $CO_{2\text{-eq}}$) of the adoption of LED luminaires to enhance productivity of the cultural-urban resources according to SDG 11.

Regarding the cleaning function, estimated $CO_{2\text{-eq}}$ emissions associated with cleaning the facade of the 54 main historic buildings in the historic centre of Santiago de Compostela Concello de Santiago, 2024, following the same assumptions made in this section about the development of biofouling, are shown in **Table 12**. For this extrapolation,

it was also assumed that the surface area of the main facades of those buildings was the same as that of the *Casa do Cabildo* building.

Table 12. Estimation of the total $CO_{2\text{-eq}}$ emissions (in kg) associated with cleaning the main frontal facades of the 54 main historic buildings in Santiago de Compostela.

Cleaning system	Lighting system			
	Metal halide*	White LED*	CromaLux LED (WCS_C)	CromaLux LED (BCS_C)
Laser cleaning	22.18	22.18	19.96	11.98
Water vapour	161.39	161.39	145.25	87.15
Biotin T®	293.62	293.62	264.26	158.56
Biotin R®	345.91	345.91	311.32	186.79
Reinforced ethanol	146.17	146.17	131.55	78.93

*The impact of both the metal halide and white LED lighting systems was considered equal (see section 2.3.1)

Considering the recommended cleaning system, i.e. used of reinforced ethanol, the CromaLux lighting system could yield a reduction of between 14.62 and 67.24 kg $CO_{2\text{-eq}}$ emissions, relative to a facade illuminated by the other two lighting systems. Regarding the economic performance, the cost (in terms of OPEX and EEC) of cleaning of the 54 main historic buildings in Santiago de Compostela (illuminated by either the metal halide or the white LED lighting system) with reinforced ethanol amounts to €2980.31, which is estimated to be reduced with the CromaLux lighting system to €2682.28 in WCS_C and to €1788.19 in BCS_C.

The results of the current study show that the cost of the materials used to clean one facade of a historic building such as the *Casa do Cabildo* is very low, especially compared to the lighting function. A single worker could clean the surface of a non-ornamented granite facade in one day with a chemical cleaning system, and the labour cost clearly exceeds the cost of the materials. According to information provided by the company[2] consulted (from which the operational time for cleaning in the FU was derived), removing biofouling from a smooth, non-ornamented granite facade could be accomplished at a rate of 4 m^2 per day with a chemical cleaning system. Thus, the frontal facade of the *Casa do Cabildo* building could treated in approximately 6 to 7 days. For the professional category of construction workers in Galicia (which conservators and restorers often use as a basis for calculating their salaries) the daily pay could range from €49.16 to €70.87, depending on the position and experience (Consellería de Promoción do Emprego e Igualdade, 2023). Thus, the labour cost for removing biofouling from the main facade of the *Casa do Cabildo* would be around €295.14 to €425.22 (for one worker), which is 5.38 to 7.55 times higher than the €54.83 derived from the OPEX of the cleaning system based on reinforced ethanol.

However, human labour is essential in cleaning buildings, as automatic methods are difficult to implement Martínez-Rocamora et al., 2016. Although innovations like guided robotic cleaners claim to cut the cost of facade cleaning by 49.21% (Yeom et al., 2022),

these are unsuitable for cultural heritage conservation due to the intricacy and value of heritage structures. An alternative framework that prioritizes sustainability by minimizing LCC and carbon emissions while ensuring labour requirements remain viable for long-term building maintenance has been proposed (Ilies et al., 2023).

As recently pointed out Elnaggar, (2024), studies in which life-cycle costing and carbon footprint analysis are applied to the heritage sector are scarce. This line of research is in its infancy and faces many challenges, mainly due to a lack of consistency in the methods used, as cultural heritage is strongly object-dependent and comparison with other systems is therefore difficult. Much research is now focused on the search for eco-friendly solutions for the conservation and cleaning of cultural heritage. For example, coatings like titanium oxide have been proposed to prevent microbial colonisation and limit the need for cleaning and maintenance and thereby reduce the cost of conserving stone architectural heritage (see e.g. Quagliarini et al., 2013; Ilies et al., 2023). Systems such as the CromaLux lighting system applied to architectural heritage as preventative solutions appear to be an efficient way of managing urban heritage while maintaining the ornamental lighting function. The end goal is to minimize the need for removal of phototrophic biofouling, considering the lower impact of the cleaning strategies than that of other urban services (like lighting) and the disparity between the cost of materials and of labour. Further research should focus on the interactions between sustainable conservation practices (in terms of materials and human labour) that focus on the points of maximum emissions or costs, for example by carbon footprint analysis and life-cycle costing already carried out on historic constructions to improve subsequent operations. Additionally, the relationship between cities and biofouling must be reframed, by recognising the presence of these organisms as an inherent aspect of the built environment, provided there is no evidence of damage and rigorous monitoring is conducted, to minimise the impact of management and cleaning.

6. Conclusions

In the present study, carbon footprint analysis and life-cycle costing were used to evaluate the environmental and economic impacts of a novel lighting system (CromaLux) for architectural heritage, in comparison with current lighting systems (metal halide and white LED). The effects of the lighting systems on the carbon footprint and on the costs associated with different biofouling removal systems (laser cleaning, water vapour, chemical biocides and reinforced ethanol) were also evaluated. The findings provide further information regarding correct definition of the functional unit and parameters measured and life-cycle inventory of conservation techniques, as emphasized in the relevant literature.

Use of the novel CromaLux lighting system is expected to reduce the contribution of ornamental lighting both in terms of carbon emissions and economic costs, with consumption of 24.44% less electricity than a white LED lighting system. Thus, a significant greater reduction of the carbon footprint would be expected if the metal halide lighting system is replaced with the CromaLux lighting system rather than with white

LEDs (reductions of 82.46% and 86.11% in kg $CO_{2\text{-eq}}$ respectively). The calculations were based on a specific case study (the *Casa do Cabildo* historic building), and overall estimates were also made for the city of Santiago de Compostela (UNESCO World Heritage city, NW Spain). Thus, use of the CromaLux lighting system at municipal level could yield a reduction of up to 3.64 tonnes of $CO_{2\text{-eq}}$ annually. Substituting metal halide luminaires with white LEDs and the novel CromaLux lighting system would yield reductions in economic costs of respectively 17.89% and 20.70%, and the cost of the CAPEX would be covered in 3.98 years with the electrical savings yielded by CromaLux relative to the white LEDs.

Regarding the cleaning function, the steam-based method had the third highest carbon footprint (121.80 g $CO_{2\text{-eq}}$ per m^2) and is not recommended for use on surfaces of architectural heritage. Laser thus proved the most sustainable cleaning system with the lowest carbon emissions (16.74 g $CO_{2\text{-eq}}$ per m^2). The reinforced ethanol produced lower $CO_{2\text{-eq}}$ emissions (2.76 kg $CO_{2\text{-eq}}$) than the other biocides (221.60 g $CO_{2\text{-eq}}$ for Biotin T® and 261.06 g $CO_{2\text{-eq}}$ for Biotin R® per m^2) but the cost per m^2 is up to 21.54% higher (€2.55 per m^2). However, considering that the largest part of the cost of the cleaning methods using chemical biocides is derived from consumables such as brushes and PPE (contributing between 70.24% to 90.53 % to the total cost), the difference in the cost of the chemicals themselves does not compensate for the health risks associated with Biotin T® and R®. The system using reinforced ethanol is therefore the best chemical-based cleaning method.

Considering the cleaning treatment applied to the *Casa do Cabildo* building in 2010 (which used Biotin R®), the CromaLux lighting system could have reduced the carbon footprint of removing the phototrophic biofouling by up to 3kg $CO_{2\text{-eq}}$. The impact of the cleaning function (both in terms of the carbon footprint and the life-cycle cost) is much lower than that of the lighting function. However, considering biostatic capacity enabling control of phototrophic biofouling, a delay of between 1.5 and 6 years between cleaning treatments is expected. In the case of the *Casa do Cabildo* building, a further decrease in the emissions associated with electrical consumption of up to 38.83% (16.83 kg $CO_{2\text{-eq}}$ per year) for the CromaLux lighting system, accompanied by a reduction in biofouling on the facade (according to the adjustments proposed in the technical instruction ITC-02-EA in the Spanish regulation) and a reduction up to €13.82 in the OPEX. However, the benefits of the CromaLux lighting system are relevant at the city level, with extrapolations showing a reduction of 1.54 tonnes of $CO_{2\text{-eq}}$ emissions (up to 3.64 tonnes of $CO_{2\text{-eq}}$ with the application of the ITC-EA-02 because of the effect of the CromaLux light onphototrophic biofouling) and savings of €19,048.71 for the 15-year period considered in the FU.

Authors' contribution

Conceptualization: A.M., P.S., A.H.; Data curation: A.M., A.H.; Formal analysis: A.M., A.H.; Investigation: A.M., P.S., A.H.; Writing – original draft: A.M.; Writing – review and editing: P.S., A.H.; Funding acquisition: P.S.; Project administration: P.S.; Supervision: P.S., A.H.

4.4 PART 4: SOCIO-ECONOMIC IMPACT

4.4.2 CHAPTER 10

SOCIAL ACCEPTANCE OF ORNAMENTAL LIGHTING FOR THE CONSERVATION OF ARCHITECTURAL HERITAGE: USE OF THE CROMALUX TECHNOLOGY IN THE HERITAGE CITY OF SANTIAGO DE COMPOSTELA

Anxo Méndez, Sergio Vila-Tojo, Cristina Gómez-Román, Andrea Correa-Chica, José-Manuel Sabucedo, Patricia Sanmartín

Submission to the journal at the end of 2025 – beginning 2026

Social acceptance of an ornamental lighting technology for the conservation of architectural heritage: the CromaLux example in the heritage city of Santiago de Compostela (NW Spain)

Anxo Méndez[1], Sergio Vila-Tojo[2], Cristina Gómez-Román[2], Andrea Correa-Chica[2], José-Manuel Sabucedo[2], Patricia Sanmartín[1]

1. CRETUS, Departamento de Edafoloxía e Química Agrícola, Universidade de Santiago de Compostela, 15782 Santiago de Compostela, Spain
2. CRETUS, Department of Social Psychology, Basic Psychology and Methodology, Faculty of Psychology, University of Santiago de Compostela, Santiago de Compostela, Spain

Abstract

The use of ornamental illumination for outdoor architectural heritage was recently studied for its role in biodeterioration, with the use of amber+green light spectra to halt the development of phototrophic biofouling as a strategy of preventive conservation. However, overcoming the citizen reluctance to accept this technology is still a challenge, thus two studies were conducted in the search of strategies towards public acceptance. Graphic material of the amber+green LED light is compared with two suitable and widely accepted lightings: warm white (yellower hue) and cool white (bluer hue), over images of a building of in the UNESCO World Heritage city of Santiago de Compostela (NW Spain), digitally altered to present a facade either clean or affected with biofouling. First, a qualitative exploration was conducted through discussion sessions among experts in fields pertaining to ornamental illuminations and representatives from neighborhood associations. The information obtained was then used for the development of a quantitative exploration on a field survey framed with a message condition (preventive, urgent and no message) and an affectation condition (clean and affected). Both studies show an initial dislike of the amber+green light. However, participants from the qualitative study expressed interest in heritage conservation and that habituation, information and trust in science can lead towards acceptance of the amber+green light. The quantitative study reveals neutral attitudes and shows that place identification increases acceptance of the amber+green light. These results can guide strategies towards the implementation of CromaLux in heritage cities without the rejection of the public.

Keywords: heritage city; lighting; smart city; sustainable conservation; environmental technology; acceptance; social perception

Highlights:

- Public response assessment to CromaLux (novel amber+green light, biostatic) on monuments
- Participants show distrust in the institutions that manage heritage conservations
- Participants highlighted the importance of information to accept CromaLux
- Higher place identification led to higher acceptance of CromaLux

1. Introduction

Anthropogenic or artificial light at night (ALAN) pollution derived from monument illumination can be defined as "the ornamental lighting on monuments that is not being efficiently or completely utilized and exceeds the limits of the object and scatters to the atmosphere (often because is pointed outwards or upwards), causing artificial ambient brightness that has an overall negative effect on the environment" according to (Méndez, Prieto, et al. 2024).

Many attempts to reduce ALAN run up against positive connotations of lighting (e.g., aesthetics, modernity, and security), which are deeply ingrained in modern societies (Jakle and Thompson, 2001; Hölker, Moss, et al., 2010). Indeed, there is a general perception that urban lighting improves safety and security regarding traffic accidents and crime, despite the empirical evidence not being very solid (e.g., Marchant and Norman, 2023)). Should monuments be lit at night? Cities now dedicate a significant amount of money to the beautification of the city through nocturnal lighting zieli (see Giordano, 2018); Eldridge and Smith, 2019). Cities like New York, Hong Kong or Tokyo use lighting strategies to attract tourism (Eldridge and Smith, 2019), creating iconic nocturnal landscapes that live in the collective imagination. In contrast, a growing movement advocates for minimizing nighttime illumination to fulfil the safety necessities. Some researchers emphasise the role of ALAN as a pollutant (more information Bará et al., 2022b) and highlight the negative impacts that ALAN has over the environment, biodiversity, human health and the starry sky as a scientific and cultural global commons (see Longcore and Rich, 2004; Hölker, Wolter, et al., 2010; Bará et al., 2021).

When dealing with cultural heritages sites, ornamental illumination should be planned considering their conservation and protection of their cultural attributes (see Valetti et al., 2020). About 20 years ago, Albertano et al. 2004 performed the only study published in English and in an easily accessible journal to date, to our knowledge, on the public response to an innovative biodeterioration control strategy (also based on illumination) in the frame of the European Cyanobacteria attack rocks (CATS) project for Roman hypogean monuments conservation. In one cubiculum of the Catacomb of Saint Callistus (Rome, Italy) a blue light with a main peak around 490 nm was installed from February to September 2003, which resulted in loss of full colour vision of the frescoes there. From 24th April to 31st August during that period, 1,500 visitors were exposed to informational posters about the project and then filled in a simple and short questionnaire. The study revealed that the majority of visitors expressed support for the newly implemented blue lighting system (50.8% strongly in favor and 32.7% generally in favor) despite the loss in colour vision, recognizing it as a crucial measure for the preservation of a monument of significant historical value and revealing the importance of scientific communication in the acceptance of new technologies in heritage sites.

Now, the CromaLux project (http://cromalux.santiagodecompostela.gal/en) tries to apply the use of ornamental illumination towards the preventive conservation of outdoor

architectural heritage, adhering to principles of sustainability and energy efficiency. (Méndez, Prieto, et al., 2024, see **Chapter 9**). The combinatory use of amber+green light, with a bimodal spectrum with two peaks at 528 nm (green) and a main peak at 593 nm (amber), was tested in laboratory settings (Méndez, Sanmartín, et al., 2024; Méndez et al., 2025) and in an outdoor pilot study (see **Chapter 6**). The results point towards a biostatic capacity of this light over phototrophic biofouling (that caused by the colonisation of green algae and cyanobacteria), halting its development in comparison to commonly used white LED lights.

To assess public perceptions of ornamental lighting and its role in the conservation of architectural heritage, two complementary studies were conducted towards designing strategies aimed at increasing social acceptance of the amber+green light of CromaLux. The first study was a qualitative exploration through discussion sessions with professionals and representatives of neighbourhood associations, which provided insights into public concerns and interests (see Phase 1). These findings were used in design of a subsequent quantitative field study (see Phase 2) in which participants were exposed to different framings with the aim of observing whether acceptance of CromaLux light was susceptible to variation depending on the deterioration of the building (affected vs. unaffected) and the type of message (preventive or urgent).

2. Phase 1. Initial exploration of public acceptance to CromaLux: Qualitative approach

2.1.Method

2.1.1. Participants and procedure

Phase 1 was conducted through three discussion sessions. The first brought together five experts in ornamental lighting, with professional backgrounds in urban planning, heritage architecture, lighting engineering, and ecological research. The other two sessions engaged four representatives from neighbourhood associations in Santiago de Compostela, one session with representatives of associations from outside the historic centre and another with those based within it. These sessions were held between September and October 2024.

All sessions took place in lecture halls at the University of Santiago de Compostela. Prior to each session, participants were briefed on the study's objectives and informed about confidentiality procedures in accordance with data protection legislation and the ethical guidelines of the university's bioethics committee (see Supplementary Material MS17). Written informed consent, including permission for audio recording, was obtained from all participants (see Supplementary Material MS18).

Two expert moderators conducted the sessions following a standardized protocol designed to ensure consistency in data collection across sessions. Each session lasted approximately one hour. The sessions begun with questions about the current state of conservation historic buildings, conservation efforts, and the role of public and private

institutions. Then, participants were reintroduced to the CromaLux project and were shown six images without any text or labels (**Fig. 40**) using the classroom projectors and were encouraged to express their opinions about the topic and images freely in response to the moderators' guiding questions.

2.1.2. Photographic material

An image of a baroque-style granite building located in the historic centre of Santiago de Compostela, known as *Casa do Cabildo* or *Casa da Estrela* (House of the Chapter or House of the Star), was selected as is the main pilot study from the CromaLux project. The image was captured using a Canon EOS R7 (Canon, Japan) in July 2024. The image underwent two types of digital modifications. First, three types of light were applied to the building: (i) cool white light (~4000K), (ii) warm white (~3000K), and (ii) the novel amber+green combination (3000K). The latter was installed in the building and was therefore not digitally altered. All light modifications maintained an appearance of 20 lx of illuminance. Second, each of the lights was presented through two building affectation conditions: (i) clean building and (ii) affected building. As the frontal facade has remained un(bio)fouled since a 2010 cleaning intervention, a simulated layer of biological fouling was added to represent pre-cleaning colonisation patterns for the affected condition Image modifications were undertaken by a company specialized in energy efficiency and energy management, with expertise in rendering images for artificial illumination.

Figure 40. Study images representing three types of light (left to right: cool white, warm white and amber+green) on the two deterioration conditions (top row: clean; bottom row: affected) affecting the *Casa do Cabildo* frontal facade.

2.1.3. Data analysis

Audio recordings were automatically transcribed using TurboScribe software (https://turboscribe.ai/) and then verified through manual review to correct punctuation, syntax, and speaker identification. A qualitative thematic analysis was conducted to explore perceptions, attitudes and factors related to the acceptance of the amber+green

light (V. Braun and Clarke, 2006). The analysis consisted of 4 phases: (i) development of a coding system based on transcript review and literature, comprising 5 categories, 10 subcategories, and 30 codes; (ii) definition of units of analysis by expert reviewers, identifying key insights from the transcripts; (iii) independent coding of all units to assess intercoder consistency, with agreement evaluated using simple percentage agreement, Holsti's index, binary α, cu-α, and Cu-α, confirming coding system stability after three iterative rounds (Krippendorff and Bock, 2008; Díaz et al., 2021) and (iv) synthesis of results to evaluate participants' perceptions of conservation challenges, attitudes toward heritage management, and perspectives on the amber+green light.

2.2.Results of Phase 1

After analyzing the discussion sessions, five thematic categories emerged: (1) perceptions of building deterioration, (2) perceptions of previous solutions implemented, (3) perception of institutions, (4) attitudes toward CromaLux, and (5) associated contextual factors. Below is provided detailed descriptions of each thematic category in both groups, the neighborhood associations representatives (NA) and experts (E). **Table 13** shows a summary of the results.

Table 13. Summary of the categories and subcategories analysed, with quote examples of participants and the frequency of codes appearing during the discussion sessions.

Category	Subcategory	Code	Frequency of code	
			NA	E
Perception of building deterioration	Perception of the problem	Perception of need for restoration	16	10
		Perception of seriousness	13	1
		Absence of perception of the problem	8	0
	Aesthetic perception	Habituation over time	5	7
		Preference for the aesthetics of the unrestored building	5	6
		Preference for the aesthetics of the restored building	2	3
Perception of solutions	Perception of the actions taken	Negative attitudes towards actions taken	17	2
		Knowledge of actions taken	3	7
		Positive attitudes towards actions taken	2	5
	Proposal of solutions	Obstacles to proposals from owners or neighbours	15	8
		Recommendations possible actions	9	4
Perception of institutions	Attitudes towards management	Dissatisfaction with current management	30	1
	Assignment of responsibility	Assignment of responsibility to government	12	6
		Assignment of responsibility to owners or civil society	4	5
		Assignment of responsibility to other public institutions	8	1
Attitudes towards amber+green light	Disadvantages, doubts or perceived costs	Lack of visual appeal	10	19
		Importance of hours of operation	8	16
		Perception of safety	10	9
		Perceived effectiveness	2	6
		Associated effects	2	5
	Perceived advantages	Conservation benefits	7	3
		Visual attractiveness	6	0
		Economic benefits	0	5
	Acceptance of amber+green light	Citizen rejection	7	12
		Citizen acceptance	11	6
	Strategies to address resistance	Information	7	10
		Other strategies	3	1
Associated factors		Beliefs in science	7	7
		Traditionalism	8	8
		Identity factors	3	3

30

0

NA = Neighbourhood Associations representatives; E = Experts

2.2.1. Pre-existing Social Perception of the Conservation of Historic Buildings

Regarding *perceptions of building deterioration*, both groups acknowledged significant deterioration and conservation challenges affecting Santiago de Compostela's historic buildings (*"They have to get their act together and restore more"*, NA; *"[...] if we don't want it [a historic building] to fall down, we have to maintain it*", E). Participants

from NA expressed concerns about the urgent need for restoration, perceiving the situation as severe. However, within this same group, a contrasting perspective was mentioned: some participants downplayed the need for intervention, considering the aging of historic structures to be positive (*"...I like it when... stone weathers, right? Well... it's what I know"* NA).

In reference to *aesthetic perception*, some participants expressed founding an aesthetic value in the current state of deterioration (*"On a personal level, so clean the stone didn't appeal to me"*, NA), with both groups attributing positive aesthetic qualities more frequently to unrestored buildings than to restored ones. Nonetheless, participants acknowledged that any initial discomfort with the visual changes in restored buildings tends to diminish over time through habituation (*[...] It seems that maybe it's a matter of habit"*, E).

A significant polarization emerged between the two groups regarding *perceptions of solutions* previously implemented for heritage conservation. Participants from NA tended to express negative attitudes toward the current interventions (*"It's all kind of nonsensical at times, the conservation of this area"*, NA) and perceive certain measures as inconvenient or even unfair like the use of certain materials, such as metal, between private residences and singular buildings or urban infrastructure ("*Aluminum is not allowed in the historic area*, […]. *I cannot use it in my windows [...] and nonetheless they use it*.". NA). In contrast, E participants highlighted that positive and technically proficient restoration efforts are taking place in the city. Drawing on their technical expertise and knowledge with the municipal regulations, they exhibited more familiarity with the measures being implemented ("*Now there are interventions with detail and made by professionals*", E).

Furthermore, participants frequently reported numerous obstacles and constraints faced by property owners and citizens in the conservation of historic heritage buildings. Participants of NA reported issues such as excessive bureaucracy, lack of financial support, high maintenance costs and perceived inconsistencies within the regulatory framework. Associated with these issues, participants expressed frustration over stringent requirements and feelings of neglect or unfair treatment by institutional authorities. Consequently, they suggested implementing measures emphasizing the need for enhanced institutional support for heritage conservation, including subsidies, financial assistance, and improved administrative processes. Participants also highlighted the importance of continuous, incremental maintenance rather than infrequent, costly interventions *("more targeted, continuous actions instead of a major investment made every many years"* E). This view aligns with the principles of preventative conservation, focused on avoid, monitor and control the apparition and spread of unwanted damage Vandesande and Van Balen, 2018 rather than undertaking more severe restorations or reconstructions.

Regarding *perceptions of institutions*, NA participants expressed significant dissatisfaction with current heritage management, with no positive comments made by any participant across both groups. The responsibility for conservation was primarily attributed

to government entities at local, regional or national levels, followed by civil society. However, in Spain the responsibility for the maintenance and restoration of real estate assets lies with the property owner according to the law (Ministerio de Fomento, 2015), either an individual in the case of private residences (even the ones located in the historic center) or the relevant public administration in the case of publicly owned heritage buildings. Participants, particularly from NA, also mentioned other public institutions, such as the Catholic Church. They consider that is an institution that is difficult to engage with and suggested strengthening the relations between the Catholic Church and the rest of the public institutions to enhance heritage conservation efforts.

2.2.2. Attitudes towards the amber+green ornamental light

When the graphical material was presented showcasing the lighting of a monument with amber+green light compared to the two commonly accepted lighting options participants expressed their *attitudes* towards it. Dissatisfaction with the amber+green light visual appeal was common, with a clear preference for warm white lighting, particularly among E participants. However, some experts also indicated that pedestrians did not complain about the colour of the light at the the pilot study installed in *Casa do Cabildo* ("*People are barely conscious of the change*", E).

Some concerns were raised regarding the amber+green light: (i) the perceived insecurity due to reduced brightness, despite all lights having the same illuminance (i.e. amount of light incident on the surface); (ii) the lighting schedule and operation hours; (iii) some participants from NA voiced concerns about the practical implications (of installing the amber+green light) for them (*"I don't know how that would... they put that kind of lighting on the facade of my house. Then what happens with my shutters, with my windows? I mean, how does it affect me?" NA*), even though direct illumination of facades is not allowed for commercial and private buildings Concello de Santiago, 1997; and (iv) E participants questioned the suitability of CromaLux from an urban image perspective and expressed skepticism about its overall effectiveness, doubting the positive impact of the amber+green light over biofouling against their knowledge in heritage conservation. In contrast, participants from NA tended to place greater trust in the scientific foundations of the CromaLux project.

Participants also acknowledged CromaLux's project *perceived advantages*: (i) architectural heritage conservation benefits; (ii) possible economic advantages (only expressed by E participants) (*"[...] we save money and at the same time…, I don't know, I think that people in general are in favor of innovation [...]"*, E), that for the CromaLux lighting system are both related to the savings in electrical consumption and the decrease in the cost associated to biofouling cleaning (see **Chapter 9**); and (iii) positive visual attractiveness of the amber+green light (only expressed by NA participants).

Thus, participants from NA believe that citizens would be more receptive to the amber+green light than those from group E, who tend to anticipate greater public rejection. Both groups mentioned the importance of providing clear information (through detailed

communication about its implementation and evidence of its effectiveness) to overcome resistances for its implementation, among other strategies voiced.

Three associated factors emerged as relevant to the implementation of CromaLux, primarily raised by participants from NA. First, beliefs about science played a dual role. While some participants expressed trust in scientific research and expert-led interventions *("We trust what you, as researchers, are saying"* NA), others voiced skepticism about costs and priorities for cost allocation *("Spending that kind of budget to bring in experts from who-knows-where... it kind of annoys me"* NA). Second, traditionalism appeared as a barrier to acceptance, as participants prefer the white light as they have been accustomed to it *("I don't really like that green light… I prefer the warm light we've always had"* NA). Finally, a strong sense of place and identity with Santiago's historic center emerged as a key consideration, as participants expressed pride in their heritage and concerns for its preservation (*"I used to feel proud of being from Santiago"; "This is part of our DNA"* NA).

3. Phase 2. Quantitative exploration of vote intention and general attitudes to CromaLux in response to framing

3.1.Method

3.1.1. Participants and design

A total of 172 participants residing in the city of Santiago de Compostela were surveyed in person (55.2% women; $M_{age} = 55.35$, $SD = 16.86$) and from different neighbourhoods in Santiago de Compostela (48.8% from the historic centre and 51.2% from other neighbourhoods). The experimental design consisting of 2 (deterioration conditions: clean and affected) x 3 (message conditions: preventive, urgent, and no message, see Supplementary Material MS19) conditions, resulting in 6 possible conditions (**Table 14**).

Table 14. Experimental conditions used in the Phase 2.

Experimental conditions	*N*	%
C1 (clean, preventive)	29	16.9
C2 (affected, urgent)	29	16.9
C3 (clean, urgent)	28	16.3
C4 (affected, preventive)	28	16.3
C5 (clean, no message)	29	16.9
C6 (affected, no message)	29	16.9

3.1.2. Procedure

Participants were randomly assigned one of the 6 possible conditions (**Table 13**). After asking about the sociodemographic information, each participant was presented with three high quality sheets with the three different lights (same graphical material as Phase 1, see **Fig. 40**) of the clean or affected building depending on the deterioration condition assigned. While viewing the graphic material the interviewer provided the message (preventive, urgent or no message) depending on the message condition assigned. Participants were asked about the light colour preference, their attitudes about the amber+green light and their identification with their neighbourhood.

The surveys were conducted by interviewers from a market and opinion research company. The interviewers approached participants at various locations throughout the historic centre of Santiago de Compostela. Participants were informed of their rights to confidentiality and anonymity in accordance with data protection laws. Participants were also required to give informed consent to participate in the study.

3.1.3. Measurements

Preference for the light quality of the ornamental lighting (cool white, warm white or amber+green light) was measured with the following statement: "*Based on the information available to you. If there were a referendum in the city council of Santiago de Compostela to decide on the lighting of the historic buildings in the historic centre, between the three lights, which would you vote for?*".

Attitudes to the amber+green light were measured using a 7-point semantic differential scale consisting of 9 items in which participants had to rate the amber+green light according to a) 1 = *unpleasant* – 7 = *pleasant*, b) 1 = *bad* – 7 = *good*, c) 1 = *useless* – 7 = *useful*, d) 1 = *unnecessary* – 7 = *necessary,* e) 1 = *costly* – 7 = *cheap,* f) 1 = *harmful* – 7 = *beneficial,* g) 1 = *ugly* – 7 = *attractive,* h) 1 = *ineffective* – 7 = *effective* and i) 1 = *traditional* – 7 = *innovative* ($\alpha = 0.86$).

Attachment to the neighbourhood was measured using a 7-point Likert scale (1 = *strongly disagree* to 7 = *strongly agree)* based on the Boley et al. 2021 scale of place attachment, according to: (i) *place identity* ("I feel attached to my neighbourhood", " My neighbourhood is special for me" and "I feel identified with my neighbourhood"; $\alpha = 0.92$) and (ii) *place dependence* ("My neighbourhood is the best place to my lifestyle", "No other neighbourhood can be compared to mine", "I would not change my neighbourhood for the life quality it offers me"; $\alpha = 0.81$).

S*ocial identification* was also measured using a 7-point Likert scale (1 = *strongly disagree* to 7 = *strongly agree)* based on. Postmes et al. (2013) and Gómez-Román et al. (2024) ("I identify with the people in my neighbourhood", "I feel a compromise with the people in my neighbourhood", "I am happy being a neighbour", "Being a neighbour is an important part of my self-image"; $\alpha = 0.87$).

3.1.4. Data analysis

Percentages, means, and standard deviations were calculated for the study variables. To test differences in proportions across conditions, chi-square tests of independence were conducted, as the dependent variable was dichotomous. In addition, simple moderation analyses were performed using Model 1 with 10,000 bootstrap samples (Hayes, 2018), All analyses were conducted with SPSS (version 28) and the PROCESS macro (version 4.2).

3.2.Results of Phase 2

3.2.1. General Social Perception to Ornamental Lighting and effect of the priming

First, the results showcase in **Table 15** that the warm white light was the most preferable ornamental light between the participants (n = 77), in comparison to the cool white (n = 47) and placing the novel amber+green LED light that received the least number of votes (n = 45).

Table 15. Votes allocated to each ornamental light by the participants.

Light quality	*N*	%
Cool white	47	27.8%
Warm white	77	45.6%
Amber+green	45	26.6%
Total	169	100%

Table 16 presents the results of comparing voting preferences for the amber+green light versus the two white light options (cool and warm) across the six experimental conditions. When analysing how the impact and message conditions, as well as the six possible experimental conditions (C1 to C6), affect the selection of the amber+green light against the two possible white lights, the results show that there are no significant differences **(**all *p-values* > 0.05) between the neither of the conditions (**Table 13**), meaning that the selection of the light colour for ornamental illumination attending to their impact in the biofouling of the architectural heritage has no relation to the priming employed.

Table 16. Contingency table for the voting preferences in the six study conditions.

Impact condition	Message condition	Vote		Total	x^2	*p-value*	φ/*V**
		Cool/warm white	Amber+green				
Clean	No message condition	65	19	84	1.37	0.24	0.09
Affected		59	26	85			
No impact condition	Preventive	39	17	56	0.67	0.72	0.06
	Urgent	42	13	55			
	No message	43	15	58			
Clean	Preventive (C1)	21	7	28	0.74	0.69	0.09
	Urgent (C3)	20	7	27			
	No message (C5)	24	5	29			
Affected	Preventive (C2)	18	10	28	1.66	0.44	0.14
	Urgent (C4)	22	6	28			
	No message (C6)	19	10	29			

Table 17 shows the voting preferences for the amber+green light versus the two white light options (cool and warm) between the participants residing in the historic centre or in other neighbourhoods. No statistically significant differences were observed among neighbourhoods (all *p-values* > 0.05).

Table 17. Contingency table for the voting preferences in the six study conditions.

Neighborhood	Vote		Total	x^2	*p-value*	φ
	Cool/warm white	Amber+green				
Historic centre	58	24	82	0.6	0.45	-0.06
Other neighborhood	66	21	87			

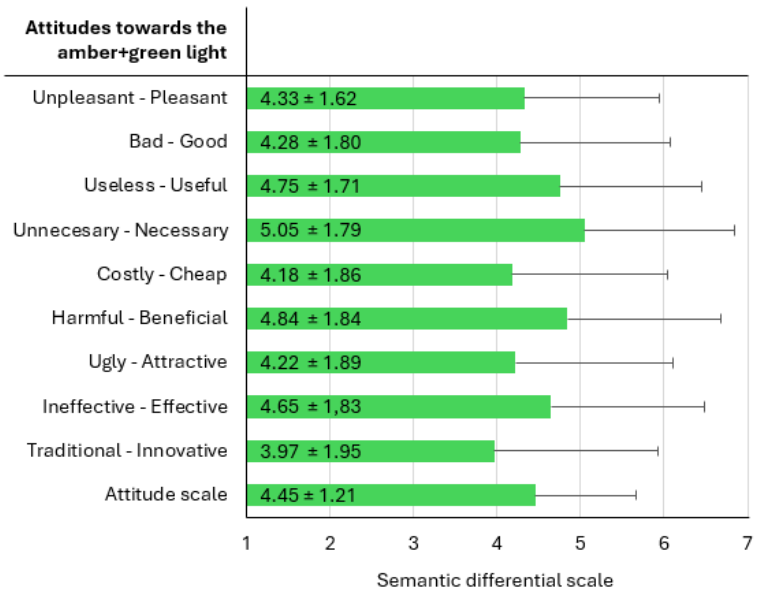

Figure 41. Attitudes towards the amber+green light. Whiskers indicate standard deviation (*SD*).

After reviewing the graphic material and selecting their preferred lighting option, participants evaluated their *attitudes toward the novel amber+green light* (**Fig. 41**). The responses centred around the mean value of the scale (M = 4.45; SD = 1.21), indicating neutral to slightly positive attitudes. The most positively rated item was the perceived *necessity* of the amber+green lighting (M = 5.05; SD = 1.79), while the perceived *cost* was the least rated (M = 4.18; SD = 1.86). Similarly, no significant differences were observed in the participants attitudes (measured as attitude scale) across the six experimental conditions (message, deterioration, or their combination) (**Table 18**). Focusing on specific attitudes under the message condition, the use of an urgent message (M = 4.45; SD = 1.90) did significantly increase the perception of the amber+green light as *innovative* (F = 4.71; *p-value* = 0.01; η^2 = 0.05) against the no message (M = 3.38; SD = 1.86).

When combining both message and impact conditions, the use of a preventive message (M = 4.44; SD = 1.87) did significantly decreased the perception of the amber+green light as *necessary* (F = 4.45; *p-value* = 0.01; η^2 = 0.05) against the urgent (M = 5.67; SD = 1.31) and no message (M = 5.61; SD = 1.50) when the facade was unbiofouled (clean condition). Nonetheless, when the facade was biofouled (affected condition) the use of a message, either preventive (M = 5.19; SD = 1.78) or urgent (M = 5.07; SD = 1.69), did increase the perception of the *necessity* (F = 4.45; *p-value* = 0.01; η^2 = 0.05) against the no message (M = 4.38; SD = 1.86). Thus, the preventive message does not seem useful to highlight this technology as innovative for the conservation of the architectural heritage if the buildings already appear cleaned, whereas if the building appear affected by biofouling, the use of a message appear to rase awareness on the necessity of this technology.

Table 18. Univariate analysis between the experimental conditions and the attitudes scale towards the amber+green light.

Attitude scale		N	*M*	*SD*	*F*	*p-value*	η^2
Clean		86	4.51	1.26	0.34	0.56	0.00
Affected		86	4.40	1.16			
Preventive		57	4.50	1.25			
Urgent		57	4.57	1.17	0.87	0.42	0.01
No message		58	4.29	1.22			
Clean	Preventive	29	4.36	1.36	1.18	0.31	0.014
	Urgent	28	4.73	1.27			
	No message	29	4.44	1.18			
Affected	Preventive	28	4.65	1.13			
	Urgent	29	4.42	1.08			
	No message	29	4.13	1.26			

3.2.2. Moderating effect of attachment to neighbourhood and social identification

Participants show a neutral *identification to the neighbourhood* in the *place identity* scale (M = 4.67; SD = 1.65) and the *place dependence* scale (M = 4.09, SD = 1.58). The *social identification* scale also shows moderate levels of identification (M = 4.39, SD = 1.52) of the participants with the people of their neighbourhood. There were no significant differences in the *identification to the neighbourhood* (both in the *place identity* scale and the *place dependence* scale) or in the *social identification* scale when considering the neighbourhood of residency of the participants (**Fig. 42**, all p-values > 0.05).

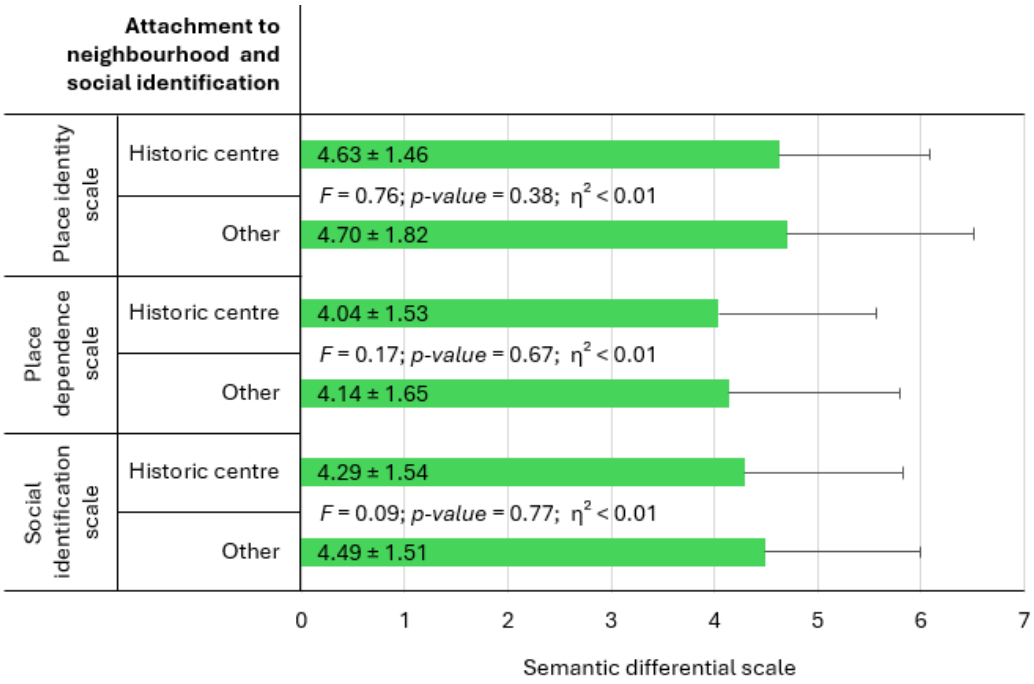

Figure 42. Average value for the attachment to neighbourhood and social identification of the participants. Whiskers indicate standard deviation (*SD*).

To examine whether attachment or social identification modulated the effects of the experimental conditions, moderation analyses were conducted for both voting behaviour (logistic regression) and attitudes (linear regression). The principal effect on the voting preference of the experimental manipulation was no significant (B = -1.91; 95% CI [-4.17, 0.336], p = 0.09). The effect of *place identity* was no significant (B = -0.21, 95% CI [-0.57, 0.15], p-value = 0.25). However, the interaction between the deterioration condition and the *place identity* was statistically significant (B = 0.50, 95% CI [0.04, 0.95], *p-value* = 0.03; J-N [5.47]; **Fig. 43**). The moderator effect of place dependence was no significant (B = 0.35, 95% CI [-0.10, 0.79], p = 0.12) and marginally significant for social identification (B = 0.43, 95% CI [-0.04, 0.89], *p-value* = 0.07). The results show that a higher level of place identity increases the effect of the affectation on the probability of voting for the amber+green light against the two white lights proposed in this study.

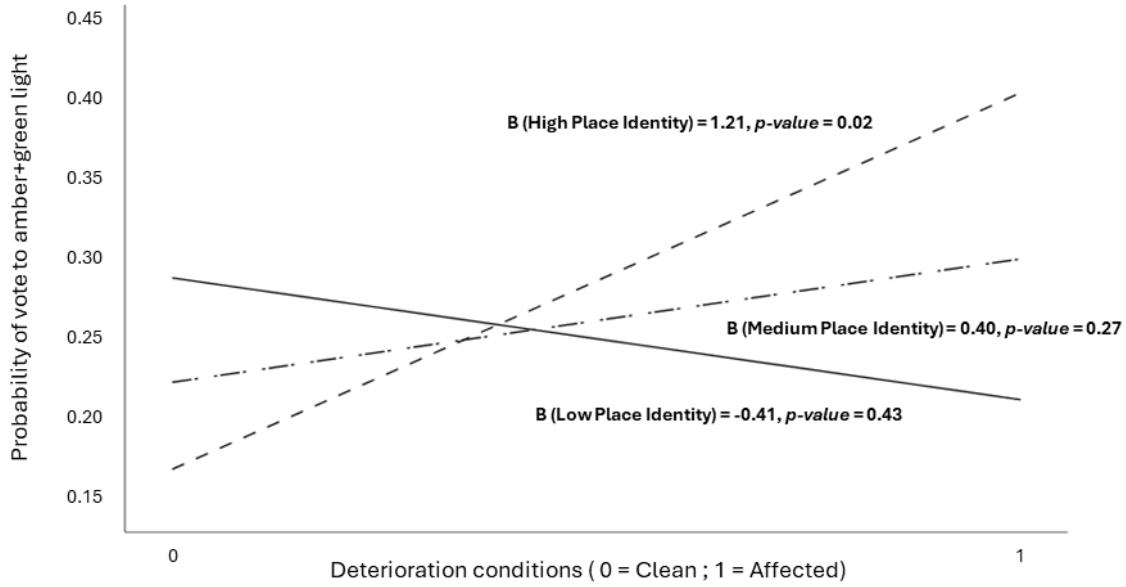

Figure 43. Moderating effect of place identity on the impact of the deterioration condition on the likelihood of voting for the amber+green light.

Regarding the *attitudes towards the amber+green light*, the principal effect of the experimental manipulation was statistically significant (*B* = -1.48, 95% *CI* [-2.57, -0.39], *p-value* = 0.01). The effect of *social identification* was non-significant (*B* = -0.03, 95% *CI* [-0.20, 0.14], *p* = 0.70), but the interaction between the deterioration condition and the *social identification* was statistically significant (*B* = 0.32, 95% *CI* [0.08, 0.55], *p-value* = 0.01; J-N [3.21,6.56]; **Fig. 44**). Thus, *attitudes towards the amber+green* light increased in the 'affected' condition when the degree of 'social identification' is high.

The moderating effect of *place identity* (*B* = 0.21, 95% *CI* [-0.02, 0.43], *p-value* = 0.07) and *place dependence* (*B* = 0.22, 95% *CI* [-0.10, 0.79], *p-value* = 0.01) were marginally significant. Finally, there are no moderating effect of none of the three variables (*place identity*, *place dependence* and *social identification*) between the effect of the message condition over the attitudes towards the amber+green light.

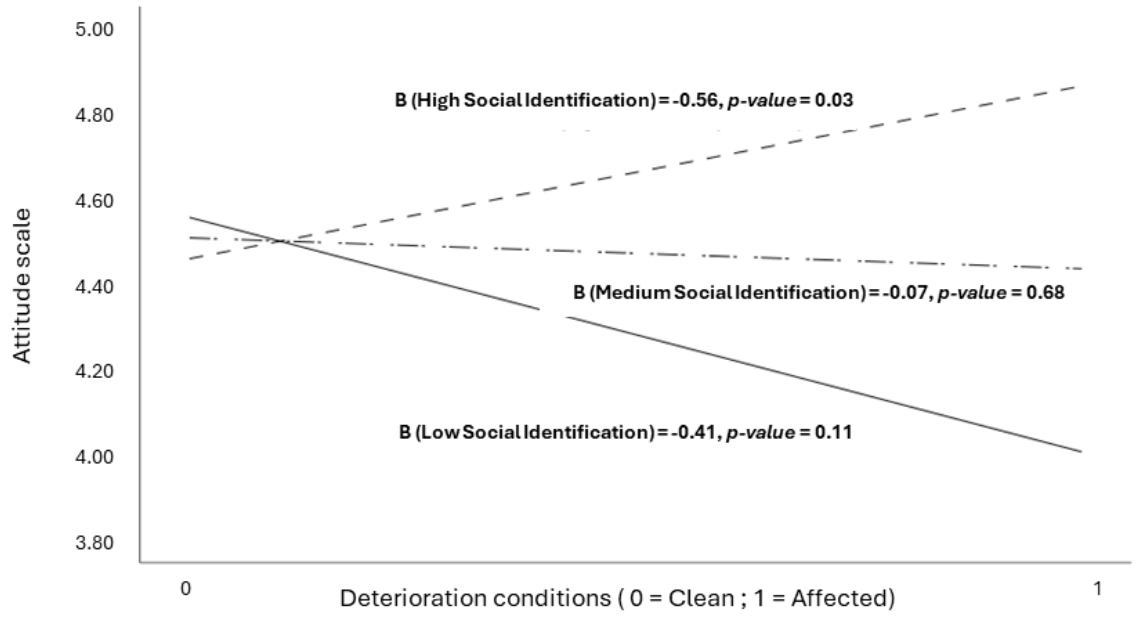

Figure 44. Moderating effect of social identification on the impact of the deterioration condition on attitudes toward the amber+green light.

4. Discussion

Since the research carried out by Albertano et al. (2004) is (to the best of the authors knowledge) the only one before the present one dealing with the public perception of ornamental illumination used as an environmental technology for the conservation of cultural heritage, a preliminary qualitative study was conducted through different discussion sessions. An unpleasant appearance at night of a monument illuminated the amber+green light spectra may impair the acceptance of the CromaLux technology. To overcome possible reluctance of the public, considering the use of an affected (by biofouling) state of a heritage building against a clean one may increase the perception of the necessity to protect the architectural heritage as awareness is linked to support for sustainable technologies (see Tuazon et al., 2024). Finally, the involvement of representatives from neighborhood associations in the city, together with experts in various fields related to lighting, is key, as participation in heritage preservation is important for various stakeholders, not just experts (see Foroughi et al., 2023). The end goal of Phase 1 is to gain insights on the problematic of conservation of architectural heritage and the perceptions of the CromaLux project to develop a systematic qualitative approach aimed to the general public (see Phase 2).

Based on the two studies, a clear preference for the warm white light was found in both studies, with the cool white light being least preferred in the discussion sessions (Phase 1) and the amber+green light the least preferred in the field survey (Phase 2). According to Zielinska-Dabkowska and Xavia (2018), warm white light (bellow 3000K) is preferred for the illumination of heritage buildings as has more similarities with candle or

fire light, creating a more “historic” atmosphere, which go in line with the familiarity attitude that the participants from the discussion session display towards the warm white light. However, the results of Phase 1 seem to indicate that people habituate over time to changes in the aesthetic perception of architectural heritage. In the study of Braun et al. (2016), negative emotions against technologies for solar radiation management cool off over time and acceptance increase. This also applies to lighting. When Italian cities like Milan and Rome change the warm light from sodium-vapour lamps white 4000K cool white LEDs (that in the present studies were the least or second to last favourite), people complain with the retrofit of the Italian government in 2017 due to an increase in light pollution (Zielinska-Dabkowska, 2018).

Participants from Phase 1 perceived the restoration of architectural heritage as something necessary and serious, as according to Greffe (2004) most contemporary societies are very keen on the preservation of their heritage, and express knowledge of the actions taken by the administrations in matter of heritage conservation. Nonetheless, participants from NA have negative opinions towards the actions taken, whereas E participants consider in their expertise that all actions undertaken over architectural heritage are performed conscientiously and professionally. This could reflect that in-depth knowledge of the actions is behind satisfaction with the measures taken. This goes in line with Khatibi et al. (2021) which stated that 77% of the research that deals with public adaptation to climate change policies highlights the importance of understanding, awareness and individual knowledge. Moreover, most participants from the NA expressed a degree of dissatisfaction towards the institutions in which they deposit the responsibility of heritage conservation. Indeed, trust in public institutions and politics is generally in decline in Spain, mainly due to the 2008 recession, the shortcomings of politicians and corruption, according to Torcal and Christmann (2021).

Despite the distrust in public institutions, participants from Phase 1 expressed trust in scientists and some of them (mostly from neighbourhood associations) to the particularly technical knowledge behind the CromaLux project, which is key towards a well-functioning public participation in governance, certainty and ultimately implementation of science-based polices (see Johnson and Scicchitano, 2000; Gundersen et al., 2022). The trust in science and the technical basis of the CromaLux project seem to lead NA participants to believe that citizens will end up accepting the amber+green light. This clashes with the E participants which mostly believe in public rejection due to their reticence in believing its conservation benefits and their rejection from an aesthetic and urban image standpoint.

Finally, when asked for strategies to address resistance, participants from Phase 1 expressed that information is the main strategy for the public to accept the CromaLux technology. Greffe (2004) stated that information campaigns increase interest in heritage conservation, regardless of the stage in which actions towards conservations are in a particular monument. Moreover, according Chan et al. (2023) knowledge transfer is

positively related to heritage building revitalization, because of the public understanding about the monument and the actions taken over it.

The outputs gained from Phase 1 was used to further analyse public response towards the CromaLux project through a quantitative Phase 2. As stated previously, the amber+green light was the least preferred among the participants (45 votes), followed by the cool white (47 votes) and the warm white being the most voted (77 votes). The application of both the message condition and affected condition failed to improve the votes of the amber+green light or against the other two options (either cool or warm white light). After analysing the results and examining the experimental design (face to face interviews), the authors consider that the message was too subtle to have an effect in a noisy urban environment where participants stopped in their transit to participate in the study. A low priorization of this issue may also be hindering voting of the amber+green light, as traditional values of the aesthetic of the warm white light may be more influential in the voting behaviour of the participants (see Steg and de Groot, 2018).

When asked about the *attitudes toward the novel amber+green light,* participants expressed neutral attitudes centred around the average value. A study by Azhari and Mohamed (2012) in Kuala Lumpur found that public awareness on the current condition of heritage buildings conservation was also neutral. Although that study finds that the public has a high level of interest in heritage protection, they may not have a clear idea of the actions being taken. According to Johnson and Scicchitano (2000), certainty in the actions undertaken affect the extent to which the public will support public policies designed to improve, in the case of their study, the environmental quality. Attitudes give stimulus for behaviour to emerge (Niaura, 2013), this is that an attitude is a precedent and thus will predict a subsequent behaviour (Bonnes et al., 2017). Despite being the least voted ornamental light, it is not perceived as unpleasant, useless or unnecessary, and the neutrality of the attitudes may be result of the novelty and unfamiliarity of the new amber+green light. Thus, there is not a formed public opinion affected by biases or ideologic discourses, which gives room for stablishing strategies to influence public reactions (see Semadeni et al., 2004).

The *attachment to neighbourhood* and *social identification* also scored around the average value among the participants. Interestingly, there was no difference in the attachment to neighbourhood between people residing in the historic centre and other neighbourhoods. Considering that Santiago de Compostela a relatively small city (with 99,491 residents in 2024 census, INE, 2025), the results may indicate that all residents tend to perceive the historic center as part of their collective urban identity, regardless of their specific neighborhood. People are no confined to their neighbourhoods and can easily move (see Connor et al., 2025), and indeed place attachment relates to walkability in cities according to González et al. (2024). A similar case may be the study of Sari et al. (2018) in Yogyakarta (Indonesia) where both long-term residents and newcomers shared similar perceptions of urban heritage.

Contrary to Greffe (2004) assertion that poor conservation of heritage structures tends to lead to public neglect, the findings from Phase 2 suggest that affection may instead increase voting to the amber+green light when place attachment is strong. This could mean that when confronted with the issue (i.e. affected condition) the higher identification with the neighbourhood will make the conservation of their heritage a higher priority. In the context of energy projects, Devine-Wright (2011) highlights that place attachment as a key factor in fostering positive public responses. Moreover, Chan et al. (2023) found that emotional ties to neighborhood cultural heritage enhance acceptance and promote positive word-of-mouth in rehabilitation initiatives.

Finally, *social identification* in Phase 2 modulated the attitudes towards the amber+green light also in the affected condition. Similarly, Bartels and Reinders (2010) found that *social identification* plays an important role in the acceptance of new food products, or the results of Lee et al. (2001) where social identity factors significantly influence the acceptance behavior towards information technologies.

Thus, it seems clear that the intervention strategies needed towards increasing the acceptance of the CromaLux project are those that appeal to citizens' identity and with the heritage of Santiago de Compostela and their social identity towards its community, expressed by participants from Phase 1 and the results from the moderation effect found in Phase 2. Specifically, emphasizing the affectation of architectural heritage may increase awareness of the need for action. This aligns with McLachlan (2009), who argues that developers of renewable energy projects should consider place-related symbolic meanings when implementing land-use changes and engaging with affected communities. These strategies should inform people about the benefits of CromaLux technology as a tool for preventive conservation, as recommended by participants from Phase 1. Overcoming the traditional views (preference towards warm white light due familiarity) is also fundamental, although participants from Phase 1 confess to habituate over time to the aesthetic changes that the deterioration of architectural heritage causes.

5. Conclusions

This research presents two studies pertaining to the implementation of an ornamental lighting technology (using an amber+green light spectra) for the preventive conservation of architectural heritage against biofouling and its social acceptance. Qualitative and a subsequent quantitative study were performed in order to stablish strategies to overcome initial reluctance in the implementation of this technology. From Phase 1 it is derived that people perceived the restoration of architectural heritage as a serious issue, although representatives from neighborhood associations, unlike experts, display negative attitudes towards the actions currently undertaken in Santiago de Compostela, primarily assigning responsibility to public institutions to which management they feel dissatisfied. When asked about the amber+green light of CromaLux, participants expressed lack of visual appeal and preference to the warm white light due to familiarity, although they express

conservation and economic benefits for the implementation of the technology. Participants from the expert group are more prone to think that citizens will reject the use of the amber+green light as an ornamental light, whereas representatives of the neighborhood associations believe that people will accept this technology. All participants believe that information is the way to promote acceptance of the CromaLux project. The results of Phase 2 show that a higher place identification to the neighborhood increases the probability of voting for the amber+green light in comparison to the cool and warm white lights. Thus, appealing to cultural connections to the city is the strategy to follow to increase acceptance of the CromaLux project, as the results show neutral attitudes towards this technology.

Authors' contribution

Conceptualization, A.M., S.V.T., J.-M. S. and P.S.; methodology, A.M., S.V.T. and J.-M. S.; formal analysis, A.M., S.V.T., C.G.R. and A.C.C.; investigation, A.M., S.V.T., C.G.R. and A.C.C.; writing—original draft preparation, A.M.; writing—review and editing, S.V.T., C.G.R., A.C.C., J.-M. S. and P.S.; supervision, J.-M. S. and P.S.; project administration, P.S.; funding acquisition, P.S

5 DISCUSSION

Innovative environmental technologies can help make cities more sustainable (see e.g. Hernandez-Moreno, 2009) and have been proposed as solutions to reduce the environmental impact of building management systems, which include artificial illumination. Ornamental illumination of historical buildings and monuments is increasingly used in public spaces, and it is important to optimize the practice and consider the impact on architectural heritage. Cultural heritage conservation is an increasingly multidisciplinary science (Talamo et al., 2020). Current research focuses on the development of innovative, ecologically sustainable strategies for documentation, diagnostics, treatment and prevention of biodeterioration, addressing physical, mechanical, chemical and aesthetic damage, of stone architectural heritage (see e.g. Okpalanozie et al., 2021; Cirone et al., 2023). The research reported in this thesis was conducted from four complementary perspectives, each explored in a different part of the document. Each part of the research was designed to address critical aspects to ensure the global sustainability of the CromaLux lighting system, based on the use of amber+green light as a preventive strategy to protect architectural heritage from biodeterioration. ***Part 1*** presents a literature review on light pollution policies, together with an analysis of European, Spanish national and regional regulations governing the illumination of monuments. ***Part 2***, which forms the backbone of the thesis, focuses on validating the biostatic capacity of the amber+green light to halt the growth of phototrophic subaerial biofilms (SABs). ***Part 3*** assesses the ecological impact of the amber+green light, focusing on the microbiota inhabiting stone monuments and the insect communities in the surrounding area. ***Part 4*** evaluates the environmental, economic and social sustainability of the CromaLux lighting system.

5.1 PART 1: LEGISLATIVE FRAMEWORK

The establishment of relevant environmental regulations can promote innovation in sustainable technologies (Li et al., 2021), although new technologies are often developed outside the existing regulations (Kemp, 2000). According to Cetindamar 2001, governments must take a leading role in creating a policy framework to increase the demand for cleaner technologies, in combination with effective measures to assist compliance and to increase awareness of environmental issues. **Chapter 1** discusses how the conflicting definitions of light pollution used by scientists and professionals have led to different approaches to the regulation of artificial illumination technologies, within a

barely regulated framework for ornamental illumination. Research in policies regulating light pollution has been much less well studied than other related areas of research. The review paper by Rodrigo-Comino et al. (2021) addressed the general effects of light pollution on the environment and health and the economic implications but did not consider the policies regulating light pollution. Of the 821 research papers about light pollution examined in the literature review reported in **Chapter 1,** only 2.56% deal with policies. This clearly highlights a gap in current knowledge regarding the extent to which light pollution mitigation policies are being implemented and are effective.

Spain introduced pioneering legislation within Europe, addressing astronomical light pollution, with Law 31/1988, of 31 October, on the Protection of the Astronomical Quality of the Observatories of the Instituto de Astrofísica de Canarias (Head of Spanish state, 1988), This law addresses light pollution through two different types of jurisdiction and paved the way to the approach used in subsequent legislation. Regulations concerning environmental protection (article 149.1.23 EC) were then expanded with regulations at different administration levels in the state. In addition, energy regulations (articles 149.1.13 EC and 149.1.25 EC) later became the focus of the current legislation on ornamental illumination in Spain, in the form of the Royal Decree 1890/2008, of 14 November, approving the Regulation on energy efficiency in outdoor lighting installations and its Complementary Technical Instructions EA-01 to EA-07 (MINCOTUR, 2008).

Ornamental illumination is regulated in said Complementary Technical Instructions (ITC for the acronym in Spanish), specifically in ITC-EA-02, considered in **Chapter 1.** Nonetheless, this regulation has rapidly become outdated due to the proliferation of LED technology and the subsequent increase in light pollution (García Gil et al., 2022). This regulation was advanced through Royal Decree-Law 18/2022, of 18 October (Head of the Spanish State, 2022), implemented in response to the energy crisis triggered by Russia's invasion of Ukraine. The regulation included lighting technologies not covered in 2008 and raised energy efficiency requirements for outdoor lighting installations.

The regulatory framework regarding light pollution is outlined in Spanish Law 34/2007, of 15 November, on air quality and atmospheric protection (Head of the Spanish State, 2007). However, specific provisions for the lighting of monuments and urban structures have only been made in the autonomous regions of Catalonia and Cantabria, in their regulations concerning light pollution. Moreover, in these cases, the law only regulates operational lighting schedules. The Catalonian Law 6/2001, of 31 May, on the Environmental Regulation of Lighting for the Protection of the Nocturnal Environment (Autonomous Community of Catalonia, 2001) prohibits outdoor lighting at night-time (defined as the *"time interval from the time established by the regulations until dawn"*) but stipulates that exceptions must be made in the specific cases of monuments or other elements of cultural, historical or touristic interest. The law was then altered thorough Decree 190/2015, of 25 of August (Autonomous Community of Catalonia, 2015) by stating that "luminaires for the illumination of vertical surfaces shall be installed above the object

to be illuminated" (although allowing upward illumination for monuments after obtaining prior authorisation from the local council) and allowing maximum illumination levels to be used to showcase individual elements. Law 6/2006, of 9 June, on the Prevention of Light Pollution in the Autonomous Community of Cantabria (Autonomous Community of Cantabria, 2006) adopts a similar approach, although it delegates to local councils the authority to determine night-time lighting schedules. There are no specific regulations governing light pollution or outdoor lighting in Galicia, and higher-level regulations (national and European) or specific municipal ordinances regulating outdoor lighting, in terms of schedules, zoning or particular exceptions, thus apply.

The lack of uniformity in the definition and measurement of light pollution is also reflected in the regulations adopted across Europe, within diverse legal frameworks and strategies (Morgan-Taylor, 2014). This has resulted in regulatory solutions, in some cases in the form of legislation, but in others merely as non-binding guidelines or instructions issued by governments, industry or interested parties concerned with protecting the night sky for environmental or scientific reasons. The issue has only been addressed in a partial, highly tangential manner, such as in the eco-design requirements for the marketing of lamps under the now repealed Commission Regulation (EC) No 245/2009 of 18 March 2009, or in the current EU Green Public Procurement criteria for street lighting and traffic signals (Donatello et al., 2019). In the new Commission Regulation (EU) 2019/2020 of 1 October 2019, laying down eco-design requirements for light sources and separate control gears (European Parliament, 2020), which derogates the European Regulation No 245/2009, the topic of light pollution has still not been addressed, and only ecological light design is regulated. However, this regulation includes exceptions to the criteria for specific purposes. For example, light sources for horticultural applications are exempted from the reduction in Correlated Colour Temperature (CCT) (aimed at reducing the contribution of blue wavelengths) to maintain photosynthetic efficiency but can still be labelled as of ecological design.

The current regulations do not specifically consider a legal framework for ornamental lighting of elements of high heritage value. As such, future regulations on the ecological design of ornamental illumination should consider the impact of light on phototrophic colonization, to minimize growth of these microorganisms, in the same way that the regulations are adapted to horticultural lighting to promote photosynthetic efficiency. This gap in legislation is also covered in the information generated in lighting research (as reported in **Chapters 2** to **6**), which if included in the current regulatory framework could lead to the development of good practice principles (see Rodriguez Lorite, 2016) and the later development of regulatory solutions and measures (see Morgan-Taylor, 2023).

Local governments also play an important role in advancing these types of new regulations as they have a relatively high degree of autonomy regarding urban infrastructure such as lighting. According to Martinsons et al. (2025), municipalities can be

at the forefront in implementing innovative technologies and adapting the legislation through evidence-based solutions. For example, some cities in the United States use narrow-spectrum amber LED technologies to reduce the impact of lighting systems on organisms and the environment (Pothukuchi, 2025), in the same way as the amber+green LED light included in the CromaLux system tends to have a lower impact on biodiversity (**Chapters 7** and **8**).

5.2 PART 2: ASSESSMENT OF BIOSTATIC CAPACITY

In humid and temperate climates, such as the oceanic or Atlantic climate, the development of algal biofilms on architectural heritage is a common pathology that conservators must address to prevent biological weathering of stone substrates ICOMOS-ISCS, 2008. According to Wilimzig (1996) biological activity may cause 20% to 30% of stone deterioration. The use of biocides (i.e. chemicals that kill any biodeteriogenic microorganisms) is the method usually used to remove microbial biomass from cultural heritage artefacts (Lo Schiavo et al., 2020). For long-lasting interventions, the application of water repellents, antimicrobial coatings or antifouling products is often recommended in order to slow down or delay the biological growth (see Caneva and Tescari, 2017; Cappitelli et al., 2020; Lo Schiavo et al., 2020).

Caneva and Tescari (2017) also mention the use of indirect methods to prevent biodeterioration of stone. Indirect methods are designed to slow down or inhibit biological growth by acting on the factors affect the growth. In addition to water, light was also found to be a critical factor explaining the distribution of microorganisms. For example, cyanobacteria and lichens in the Khmer temples in Angkor (Cambodia) grew preferably under the high humidity and low light conditions caused by forest canopy coverage at the site (Caneva et al., 2016). According to these researchers, knowing the ecological limits of these communities will help fine-tune interventions that create sub-optimal conditions for the development of microorganisms.

Modulation of artificial lighting has previously been used to control the development of subaerial biofilms (SABs) in artificially illuminated underground heritage sites open to the public. Research has shown that by adjusting the emission spectra of lighting sources, it is possible to create conditions that are sub-optimal for growth of microalgae and cyanobacteria, by avoiding wavelengths with high photosynthetic efficiency for the species comprising the SABs (see Albertano et al., 1991; Muñoz-Fernández et al., 2021). The research reported in this thesis proposed the use of amber+green light to control phototrophic biofouling on outdoor monuments, while also considering sunlight exposure as an unavoidable source of light for phototrophic SABs. Thus, the research presented in ***Part 2*** sought to validate the proposed biostatic (halting growth) capacity of amber+green light, in laboratory-based experiments using membranes (**Chapters 2** to **4**) and mineral specimens (**Chapter 5**), and also in a long-term (3.4 years) outdoor monitoring study (**Chapter 6**).

5.2.1 Formation of phototrophic SABs

(Micro)algae use light to produce biomass through photosynthesis. When photosynthesis processes are not active, e.g. after sunset, respiratory pathways are the only sources of ATP available to maintain cell metabolism. Light can provide the NAD(P)H and ATP required for the biosynthesis of lipids, proteins and nucleic acids. However, in dark conditions the only source of these compounds is the carbon synthesized during the Calvin-Benson cycle and other metabolic pathways (Raven and Beardall, 2016). According to Ogbonna and Tanaka (1996), up to 35% of daily photosynthetic productivity may be lost through respiration processes at night, depending on the species and the environmental conditions (see Edmundson and Huesemann, 2015). In industrial microalgal production, the loss is often compensated for by extending the artificial photoperiod or by adding supplementary night-time light in outdoor bioreactors (see Parveen et al., 2023). A parallel can be drawn with (micro)algae growing on illuminated built structures. Ornamental illumination of monuments extends the natural photoperiod to which phototrophic SABs are subjected, and changes in the biomass, biochemical composition and diversity are thus expected.

The main objective of the research reported in **Chapter 2** was to determine the optimal length of time that ornamental illumination with coloured LED lighting should be switched on to achieve a biostatic effect. The effects of red-green-blue narrow-spectrum LED lights were compared with those of warm white LED and unilluminated controls. The ornamental lighting conditions were operated for photoperiods of 2, 4, 6 and 8 hours after 16 hours of simulated daylight. The daily 24 hours were completed with a dark period of variable duration depending on the ornamental lighting photoperiod.

The results showed that exposure to 4 hours of green LED light decreases biomass production relative to that produced by the other lighting conditions. Moreover, exposure to between 4 and 6 hours of green light decreased the numbers of green algae cells and also the chlorophyll-a and -b and total carotenoid contents.

Different algal species respond differently to photoperiod. For example, species such as *Botryococcus braunii* and *Scenedesmus obliquus* have a higher growth rate under continuous illumination than species of the genus *Neochloris*, which thrive better with a 12:12h light:dark photoperiod (growing under fluorescent light at 60 μmol m^{-2} s^{-1}) (Krzemińska et al., 2014). Although *Botryococcus braunii* does not appear to be a common coloniser of stone heritage, *Scenedesmus obliquus* frequently colonises granite heritage in Galicia (Rifón-Lastra and Noguerol-Seoane, 2001). Research by Gao et al. 2024 shows that growth of biofilms formed by the green alga *Chlorella vulgaris* benefits from dark periods without light. Moreover, biofilms formed without continuous lighting appear to cope better with high light intensity (above 270 μmol m^2 s^{-1}) than biofilms growing under continuous lighting. Thus, growth of green (micro)algae appears to be improved by extending the natural photoperiod and including a dark period (reflecting the situation of SABs subjected to ornamental illumination).

The results reported in **Chapter 2** were used to determine the timing (periodicity) of the ornamental illumination system in subsequent research while complying with the legislative framework (**Chapter 1**) and sustainable energy use (**Chapter 9**). In Santiago de Compostela, the artificial lighting is switched on at sunset and switched off at 03:00, and it thus operates for a median time of around 6 hours, depending on the time of the year. Therefore, in the studies reported in ***Part 2***, photoperiods of 5 or 6 hours were tested. In the studies reported from **Chapter 2** onwards, in addition to green LED light (peak wavelength, 530 nm), amber+green light (peak wavelength, 593 and 528 nm) was used with the aim of achieving a biostatic effect. This decision was taken in accordance with municipal guidelines that advise against the use of coloured light for heritage lighting (Méndez, Prieto, et al., 2024).

In the studies reported in **Chapters 3** to **5**, the amber+green LED light was compared with two different types of white LED lights: a cool white light (CCT of 4300 K, peak wavelengths, 530 and 457 nm) and a warm white light (CCT of 2580 K, peak wavelengths, 530 and 604 nm). In the research presented in **Chapter 6**, the amber+green LED light was compared with a metal halide lamp, rather than with other white LEDs, in an outdoor environment (the inner courtyard of Pazo de Raxoi). Metal halide lamps are currently (at the time of writing) used in the ornamental lighting system operated in Santiago de Compostela. All lighting conditions considered in **Chapters 2** to **6** included a control without ornamental illumination.

The growth of SABs was quantified directly, by measuring biomass gravimetrically (**Chapters 2** and **3**), and indirectly, by determining parameter F_0 by PAM chlorophyll fluorescence (**Chapters 2, 3** and **6**). The photosynthetically inefficient light qualities or wavelengths, i.e. green light at 530 nm (**Chapter 2)** and amber+green light at 593 nm and 528 nm (**Chapter 3**), yielded lower biomass (as wet weight) than either the coloured or white light sources. Moreover, both low (50.07 µmol s^{-1} m^{-2}) and high (252.59 µmol s^{-1} m^{-2}) daylight illuminance yielded the least biomass **(Chapter 3)**. F_0 followed the same pattern as the wet biomass (**Chapter 3**) thus supporting use of this parameter as a proxy for SAB development.

Green light is weakly absorbed by chlorophylls and other pigments (Terashima et al., 2009). In a review paper, Folta and Maruhnich (2007) concluded that the green and yellow wavelengths between 500 nm and 600 nm generally have a negative effect on photosynthetic growth. Note here that most studies tend to refer to the green to yellow wavelengths as green. Despite being photosynthetically inefficient, these wavelengths may have some functions. Green light (500 – 600 nm) induces plant responses such as phototropism and gene expression and can signal photosynthetically unfavourable conditions mediated by phytochromes and cryptochromes. At high light intensity, green light (500 – 600 nm) can also penetrate further in leaves or thick cell aggregations than red wavelengths (600 – 700 nm), which are more strongly absorbed by chlorophylls. Green light also causes less photoinhibition than blue wavelengths (400 –500 nm) (see Terashima et al., 2009).

Nonetheless, green light (500 nm - 600 nm) is not as efficient for growth of green (micro)algae and cyanobacteria as white light (400 – 700 nm) at light intensity ranging from 100 – 1150 μmol m^{-2} s^{-1} (see Kaushik and Kumar, 1970; Jung et al., 2019; Helamieh et al., 2024; Sumanasekara et al., 2025). There is clearly a dichotomy in the effects of green light at high and low light intensity, as shown by Le Noac'h et al. (2025) in research in which outdoor cultures of the green alga *Dunaliella salina* were covered with coloured plastic to modify the quality of light reaching them. The covering that reduced the blue (400 – 500 nm) and red (600 – 700 nm) components, and thus increased the green wavelengths (500 – 600 nm), decreased biomass production in winter (maximum of 700 μmol m^{-2} s^{-1}) but increased the biomass yield during summer (maximum of 1600 μmol m^{-2} s^{-1}).

The lights used in urban artificial lighting are much less intense than those used in (micro)algal cultivation and of course than natural sunlight. Anthropogenic or artificial light at night (ALAN), of which illumination of monuments is an emerging contribution (Méndez, Prieto, et al., 2024), uses light intensity around 7 to 200 lx (accounting for 0.08 to 20 μmol m^{-2} s^{-1} of the illuminance depending on the light source) (see Poulin et al., 2014; Hölker et al., 2015; Grubisic et al., 2017; Diamantopoulou et al., 2021 Vrba et al., 2024). Ornamental lighting is often more intense than other types of urban illumination, in order to highlight the monument against other elements; however, while Spanish legislation allows up to 600 lx (for illumination of aluminium cladding where there is a high level of surrounding illumination), an intensity of only 20 to 300 lx is required for good illumination of most stone material (MINCOTUR, 2008). Thus, as a rough estimation, the maximum intensity of ornamental illumination in Spain will be around 30 μmol m^{-2} s^{-1} (although this will greatly depend on the lighting source).

Enhanced biofilm development was also reported in **Chapter 5**, in terms of biofilm thickness and hardness of the SAB-mineral interface. The use of white (either cool or warm) ornamental illumination increased the biofilm thickness and decreased the surface hardness of the samples (at 9.20 and 5.65 μmol s^{-1} m^{-2}, respectively). By contrast, under amber+green light (at 4.45 μmol s^{-1} m^{-2}), both parameters were more similar to those in the unilluminated control. The effect on the cement mortar samples was not as pronounced. The biomass of biofilms is usually directly related to the thickness (see e.g. Sandeep et al., 2023). The same applies to hardness, and an increase in biofilm biomass tended to decrease the surface hardness of the biofilm-material interphase (see e.g. Oliveira et al., 2017).

The biostatic effect of the amber+green light was also tested in an outdoor monument, to validate its long-term capacity to control phototrophic SABs. The results of the 3.4 years of the monitoring performed in the inner courtyard of Pazo de Raxoi (**Chapter 6**) showed that F_0 values (measured using PAM chlorophyll fluorometry) are not significantly different in SAB subjected to amber+green light than SAB in non-illuminated areas. By contrast, the SABs under metal halide lighting continued to grow until the end of the monitoring period. A higher fluorescence signal represents a higher quantity of photosynthetic biomass on the surface of the stone (Miller et al., 2011), as indicated by the

significant correlation between the minimum fluorescence (F_0) and the wet biomass of the SABs reported in **Chapter 2**. PAM chlorophyll fluorometry was successfully used as a non-destructive technique to monitor SAB development and thus validate the aforementioned effects of ornamental amber+green LED light, both in a real outdoor scenario and sustained over time.

5.2.2 Photosynthetic responses of SABs

Photosynthesis requires an enormous amount of energy to split water molecules (photolysis) and to reduce the primary electron donors in the PSII and PSI. The photosynthetic pigments involved in oxygenic photosynthesis have adapted to absorb photons in the 400 – 700 nm region. According to Planck's law, photons have a higher energy at 400 nm than at longer wavelengths. However, the photon flux of sunlight peaks at 700 nm. Thus, the absorption peaks of chlorophyll-a coincide to take advantage of the high energy blue photon flux (see Chen and Blankenship, 2011). The quantum yield (photosynthetic efficiency) thus has a wavelength dependency (Evans, 1987), which is highest for red light (600 – 640 nm) and lowest for green light (400 – 570 nm) (Hogewoning et al., 2012). The photosynthetic efficiency of blue light (400 – 500 nm) is lower than that of red light, as a significant fraction is absorbed by carotenoids and other pigments. Energy is lost (in the form of heat) as the energy transfer between carotenoids and chlorophylls is significantly less efficient than energy transfer between chlorophylls (Terashima et al., 2009; Hogewoning et al., 2012).

Although the photosynthetic efficiency of green light is relatively low, there are some instances in which green light is efficiently used by green microalgae to grow, both under exposure to ALAN in natural environments (Diamantopoulou et al., 2021), and in microalgal bioreactors (Paper et al., 2022). In addition, some marine species seem to utilise green light more efficiently to outcompete other species with specific pigments, making use of the greater penetration of green light in the water column (see Luimstra et al., 2020; Seki et al., 2025). For example, Paper et al. (2022) reported that the marine microalga *Picochlorum* sp. produces chlorophyll derivates after cultivation with green LED light (peaking at 510 nm) that appear to have beneficial effects on growth. The structural analysis reveal that those pigments are chlorophylls with up to three additional C=C double bond insertions in the phytol side chain.

The pigment composition of the SABs varies owing to the influence of ALAN, and a general decrease in chlorophyll concentration (mg L^{-1}) was observed in the study reported in **Chapter 2**. Red (631 nm), green (530 nm) and white (448.5 nm and 611 nm) LED light lowered the concentrations of both chlorophyll-a and -b in most of the photoperiods tested. The total carotenoid concentration remained unaltered, except under exposure to green and white lights for 6 hours. A general decrease in the amount of chlorophyll-a in the cells (mg Chl-a g^{-1} SAB), measured both by direct quantification (only being significant under cool white light) and by confocal microscopy, was observed in the study reported in **Chapter 3**.

Neither the cool white, warm white or amber+green lights caused changes in the chlorophyll-b content. However, growth of SABs under high daylight irradiance (252.59 µmol s^{-1} m^{-2}) decreased the chlorophyll-a content relative to that under low daylight irradiance (50.07 µmol s^{-1} m^{-2}). Microalgae tend to accumulate chlorophyll-a under low light conditions but reduce the content when irradiance increases, to enable the microalgae to cope with light stress (Gao et al., 2024). Indeed, the biochemical profile of the SABs (pigments and EPS) was not affected by ornamental illumination as a response to the higher daylight irradiance (**Chapter 3**).

The proteomic analysis reported in **Chapter 4** revealed specific responses to amber+green ornamental lighting. In particular, there was an increase in peptides involved in protein metabolism (synthesis, assembly and degradation), oxidative stress management and LHCs (mainly the antenna protein-like and proteins of both PSII and PSI). Interestingly, among the LHC proteins, production of the PS II extrinsic protein O (PsbO) was not enhanced. This protein catalyses the splitting of water to O_2 and $4H^+$, thus producing the electrons for the z-scheme process that ends in the synthesis of NAD(P)H and ATP. The LHCs in photosynthetic organisms are affected by the quality of light received. *Lemna minor* plants grown under blue (peaking around 450 nm) and green (peaking around 500 nm) lights synthesized fewer proteins that bind ß-carotene to the chlorophyll-a in P700 and increased the synthesis of LHC proteins (Mäenpää and Aro, 1986). The opposite response occurred under orange light (peaking around 550 nm). Green light also promoted synthesis of the antenna complex and P680 of PSII (Mäenpää and Aro, 1986).

Microalgae can also modify and acclimate their pigment antenna and LHC in response to changes in lighting and thus adapt the photosynthetic processes in accordance with the light conditions (see e.g. Bautista and Necchi Jr., 2007; Schnurr and Allen, 2015). As red light is the most photosynthetically efficient, exposure to red wavelengths will promote fluorescence quenching to dissipate the excess absorbed light energy as heat. Ueno et al. (2019) showed reduced energy transfer to PSII and induced quenching of the LHC in *Chlorella vulgaris* grown under continuous illumination (at 50 µmol m^{-2} s^{-1}) with red light (peaking at 666 nm). However, these researchers also found that green light (peaking at 514 nm) caused the LHC proteins of *Chlorella vulgaris* to shift from "quenching mode" to "light-harvesting mode" to increase light-harvesting ability, thus accounting for the lower photosynthetic efficiency. Nonetheless, in the study reported in **Chapter 3**, the NPQ (which reflects the energy dissipation in the PSs) changed in accordance with the changes in SAB biomass and did not show any particular response to the ornamental lighting conditions. Protein metabolism was also higher in the SABs exposed to amber+green light, accompanied by an increase in ATP content (**Chapter 3**). Proteins related to carbon metabolism generally decrease under ornamental lighting conditions. An environmental proteomics approach was used to study the broad proteome of the SAB samples. This hinders biological conclusions being reached as only the most abundant proteins are detected and important changes in less abundant proteins are overlooked (Dowd, 2012).

ALAN can also affect the quantum yield of microalgae. Ayalon et al. 2021 reported that ALAN (at 0.15 µmol s^{-1} m^{-2}) decreased the QY_{max} of the green microalga *Symbiodinium.* Similar results were found with the cyanobacteria *Microcystis aeruginosa*, with the QY_{max} impaired by ALAN (high pressure sodium lamp at 0.08 µmol s^{-1} m^{-2}).

In the study reported in **Chapter 2**, the QY_{max} was measured with a phytoplankton analyzer (Phyto-PAM, model EDF version, Walz, Effeltrich, Germany) equipped with a fibre optic emitter-detector unit (PHYTO-EDF) that measured chlorophyll-a fluorescence at specific wavelengths (470, 520, 645 and 665 nm). All of the ornamental lighting conditions (red, green blue and warm white LED) affected the QY_{max} of the SABs, at one of the specific wavelengths of the PAM device and/or in the photoperiods studied (2, 4, 6 and 8 h). By contrast, the quantum yield of the SABs was not dampened by the ornamental lighting conditions considered in **Chapter 3** (cool white, warm white and amber+green LED lights) and in **Chapter 6** (metal halide light and amber+green LED light). The cool white light exhibited a lower QY (in the light adapted state) than the other ornamental lights (**Chapter 3**). This finding can be tentatively explained by the higher blue component of the cool white light, which has a lower photosynthetic efficiency (although with subtle differences). In the research presented in **Chapters 2** and **3**, PAM imaging was conducted with a Handy FluorCam FC 1000-H (Photon Systems Instruments, Czech Republic), which uses white LED to excite chlorophyll-a. There are several possible reasons for the different responses of the quantum yield of the SABs: (i) the different ornamental light intensities considered in **Chapter 2** (≈ 6 µmol s^{-1} m^{-2}) and **Chapter 3** (≈ 1 µmol s^{-1} m^{-2}); (ii) differences in the measurement devices used (one using specific wavelengths for induce fluorescence signal and the other white light); and/or (iii) different responses of the species comprising the SAB.

The biostatic effect of amber+green light is thought to work in the following way. During night-time, ATP and NAD(P)H are required for maintenance of protein turnover (synthesis, repair and degradation) (see Raven and Beardall, 2016). When photosynthetic microorganisms are exposed to ornamental light, at least part of the energy required for cell maintenance will be provided by photosynthesis and the microbes will thus be less dependent on the breakdown of carbohydrate molecules. However, amber+green light is less efficient in driving photosynthesis than white light (which includes emissions in both the blue and red fractions of the spectrum). Thus, increased synthesis of LHC and PSs proteins in the microorganisms enhances light harvesting; however, the absence of the PsbO indicates that e.g. the electron transport chain is hindered relative to that under the white lights. Consequently, SAB growth becomes reduced as (i) amber+green light is less efficient for synthesis of ATP and NAD(P)H and (ii) protein turnover and cell maintenance at night consumes some of the biomass produced during the day for production of ATP and NAD(P)H. The fact that SABs can acclimate and adapt their LHC to light quality may explain why the PAM parameters did not reflect any changes in response to the ornamental lighting.

5.2.3 Changes in SABs structure

The amber+green light also caused a reduction in exopolysaccharide production (exopolysaccharides are the main component of the EPS matrix), as reported in **Chapter 2**. The amount of exopolysaccharides (mg g^{-1} SAB) was only affected when the SABs were cultivated under low daylight irradiance (50.07 µmol s^{-1} m^{-2}). As observed with high daylight irradiance (252.59 µmol s^{-1} m^{-2}), the daylight had a greater effect than ornamental illumination, despite the higher biomass of SAB recorded. Loustau et al. (2021) showed that biomass and EPS production are negatively correlated in biofilms formed by the green filamentous microalga *Uronema confervicolum*. These researchers also reported that changes in the lighting conditions change the quantity and composition of the EPS matrix. In particular, they showed that biofilms exposed to light at 30 µmol s^{-1} m^{-2} produced more exopolysaccharides and exoproteins than at 70 µmol s^{-1} m^{-2} (16:8 h photoperiod of unspecified white light). Production of EPS in microalgae depends on the organic carbon produced by photosynthesis (see Staats et al., 2000). Underwood and Paterson (2003) proposed that part of EPS synthesis responds to allocation of overflow organic carbon to maintain the electron flow through the photosystems. Moreover, in mature algal biofilms, EPS production seems to increase, possibly due to reallocation of organic carbon from growth and reproduction to stabilization (Schnurr and Allen, 2015). This is consistent with the proposed mechanism for the biostatic capacity, as amber+green light is less photosynthetically effective in terms of producing organic carbon. The finding is also consistent with those of You and Barnett 2004, who reported by cultures of red microalga *Porphyridium cruentum* increased the production of exopolysaccharides under blue (440–550 nm) and red (550–770 nm) light due to higher photosynthetic efficiency (continuous illumination at 40 µmol s^{-1} m^{-2}).

The complex, three-dimensional structure of the biofilm is influenced by the EPS matrix, which maintains the microbial community structure. Thus, the reduction in exopolysaccharides caused by the amber+green light is expected to alter the architecture and properties of the SABs. Biofilms display viscoelastic properties which protect the biofilm by absorbing stress energy through deformation (see Flemming and Wingender, 2010; Peterson et al., 2015; Schnurr and Allen, 2015). Thus, the decrease in exopolysaccharides under amber+green light reported in **Chapter 2** could explain the reduction in surface hardness (as HLC) of the granite sample blocks, discussed in **Chapter 5**, and in the increased the contact angle (in º) and the water absorption time (WAT, in s) of the surface in both the granite and cement mortar samples.

The surface roughness measurements (as R_a, in mm) in both the granite and cement mortar samples followed similar patterns as the surface hardness. The presence of the SAB increased the R_a and decreased the HLC relative to the blank sample blocks, with the amber+green light being more similar to the unilluminated control and both white lights (cool and warm) further increasing the R_a or decreasing the HLC. These results are also consistent with the wet biomass values reported in **Chapter 3**, as the amber+green light

yielded similar biomass as the unilluminated control whereas the white lights promoted development of the SABs. The behaviour of the SAB-mineral interphase studied in **Chapter 5** thus appears consistent with the proposed biostatic capacity of the amber+green light included in the CromaLux lighting system. The effect of the presence of algae on a stone surface causes both a reduction in surface hardness (at least in carbonate rocks, see Zhao et al., 2024) and a decrease in the variability of the hardness relative to uncolonized stone (in the case of sandstone as reported by Cutler et al., 2013), as clearly observed in the surface hardness data reported in **Chapter 5** and that has been related to a bioprotective role of SABs in open-air lithic cultural heritage (see e.g. Zhu et al., 2025).

The surface roughness of a material is a key factor determining microbial adhesion and growth on natural stone and cement-like materials (see e.g. Li et al., 2025), with greater surface roughness often associated with greater attachment and biofilm formation on the surface. Although the findings appear consistent with the biomass growth under the different ornamental lighting conditions tested in the present research, other researchers report different correlations between biofilm formation and surface roughness. For example, Sanmartín et al. (2020) reported that formation of an algal biofilm (mainly composed by *Apatococcus lobatus*) led to a decrease in the surface roughness (measured as R_a, in mm) on granite sample blocks (Grissal and Rosa Porriño varieties). The surface roughness of biofilms of *Chlorella vulgaris* grown on polystyrene surfaces in the laboratory also decreased as the biofilms matured, thus reflecting an inverse relation between biovolume and roughness (Fanesi et al., 2019). Mueller et al. (2006) observed a positive correlation between biovolume, thickness and roughness in marine phototrophic biofilms formed on glass slides, in a flow chamber with fresh unfiltered natural seawater that induced development of a biofilm mainly composed by diatoms (undetermined species).

Regarding the petrographic analysis made in **Chapter 5**, it was stated that the SAB barely covered any of the biotite minerals that appear in the surfaces of the granite thin sections, despite the muscovite minerals being almost always covered by the SAB. Algal species were found to attach to mineral surfaces with Fe content (see Phillips-Lander et al., 2020). Moreover, there is evidence that suggests that biofilms of the green alga *Palmellococcus* sp. and several filamentous cyanobacteria can dissolve biotite from sandstone as a source of nutrient Fe (Mustoe, 2018). Although it seems that the bioweathering of the biotite minerals are more caused by the cyanobacterial filaments growing inside the sandstone and their production of citric acid which chelates the Fe, of which the green alga produces much less than the cyanobacterial species. The main plane of exfoliation of biotite in granite specimens is basal ({001} in crystallographic notation). Exfoliation in this plane is perfect, meaning that biotite breaks easily into thin sheets or flakes parallel to that plane, while in a perpendicular plane the surface can become rougher. Therefore, the lack of colonisation on biotite may be due to foliation preventing SAB attachment.

The presence of small rhomboidal gypsum crystals embedded in the SAB could be the results of calcium leakage from the cement mortar specimens. Guillitte and Dreesen 1995 indicate that water-logged cement-based materials often suffer from remotion and a subsequent recrystallization of soluble salts.

5.2.4 Changes in the diversity of phototrophs in SABs

Recent research shows that ALAN affects the community composition in phototrophic microorganisms. Hölker et al. (2015) showed that exposure to ALAN from light pressure sodium lamps (with a CCT of 2000 K and intensity levels around 0.09 mmol m^{-2} s^{-1}) increased the abundance of phototrophs living in freshwater sediment (microalgae, diatoms and cyanobacteria) relative to those living in sediments not exposed to ALAN. The community responses to ALAN are, however, dependent on the response of each photosynthetic microorganism to light quality (colour or wavelength). Thus, changes in light quality from different lighting sources can influence the competitive outcome in communities (Marzetz et al., 2025).

The use of ornamental red (631 nm) and green (530 nm) LED lights, discussed in **Chapter 2**, strongly altered the community in the SABs independently of the photoperiod. In addition to a general decrease in total cell count (showing the lowest values at 4 and 6 hours of green light), the number of cyanobacterial cells increased under the red and green LED ornamental lighting. The diversity analysis conducted by morphological taxonomic determination of phototrophs reported in the following chapters did not reveal an increase in cyanobacterial species in relation to the use of amber+green light. Only the outdoor study conducted in the inner courtyard of the Pazo de Raxoi (**Chapter 8**) revealed a greater abundance of DNA reads from the cyanobacteria *Nostoc* sp. under the amber+green light than under the metal halide lamp and the unilluminated control. **Chapter 4** reports that the use of the warm white LED light (2580 K) for ornamental illumination affected the cyanobacterial proteome in the SABs, as *Synechocystis* sp. had almost double the amount of peptides as measured under the other lighting conditions.

In artificially lit phototrophic communities, cyanobacteria tend to become more dominant under warmer lights. Stockenreiter et al. (2021) found that reducing the blue component of white light (under continuous illumination at 65 µmol photons $m^{-2}s^{-1}$) increased the proportion of cyanobacterial species (*Microcystis* sp., *Lyngbya* sp. and *Pseudoanabaena* sp.) in a phytoplankton community. Blue light also seems to reduce the photosynthetic efficiency of *Synechococcus* sp. as the growth rate was lower in cultures exposed to blue light (450 nm) than in those exposed to orange (625 nm) or red (660 nm) lights Luimstra et al., 2018. Indeed, the results reported in **Chapter 3** show that the abundance of *Synechocystis* sp. decreased under cool white light (peaking at 604 nm and an intensity of 1.13 µmol s^{-1} cm^{-2}) at low daylight intensity of 50.07 µmol s^{-1} m^{-2} (as there was no change under high daylight intensity of 252.59 µmol s^{-1} m^{-2}). According to Luimstra et al. (2018), the lower efficiency in use of the blue wavelengths may stem from

an imbalance between PSI and PSII. Cyanobacterial PSI contains much more chlorophyll-a than PSII, and the imbalance is compensated for by a LHC with phycobilisomes that associate with the PSII to transmit photons. The phycobilisomes contain pigments such as phycocyanin or phycoerythrin, which respectively transmit orange (peaking at 620 nm) and green (peaking at 565 nm) photons to the PSII (Luimstra et al., 2018). Phycobilisomes absorb blue photons ineffectively and thus hinder the production of both ATP and NADPH required for growth. In the research reported in **Chapter 4**, the environmental proteomic analysis of the SABs indeed showed an increase in peptides from the phycocyanin beta subunit and from phycobilisomes by the use of warm white light (with the maximum peak at 604 nm).

The cyanobacterial sensitivity towards warmer lights has also been observed in underground heritage sites. SABs growing on artificially illuminated caves in Serbia suffered different changes in response to the light quality used (Popović et al., 2022). Thus, the presence of cyanobacteria increased under illumination with warm white lights (no technical information reported) but decreased under the cool white light (no technical information) in favour of green microalgae (mainly *Mesotaenium* sp.). Orange light (560 – 620 nm at around 1.4 μmol s^{-1} m^{-2}) also increased growth of cyanobacterial species in a biofilm (*Oculatella subterranea*, *Leptolyngbya* sp. and *Fischerella* sp.) collected from the Roman Catacombs of Domitilla (Italy) (Bruno and Valle, 2017). Interestingly, use of green light (peak wavelength, 530 nm) in the Shunling imperial mausoleum in China decreased the cyanobacterial abundance when applied within a 12:12 light:dark photoperiod, and in contrast to previous findings the cyanobacterial community was barely affected by illumination with red (peak wavelength, 640 nm), blue (peak wavelength, 455 nm) or white (400–700 nm) (Bao et al., 2023).

The diversity of green microalgae varied with the use of coloured ornamental lighting (**Chapter 2**) but was barely affected by the ornamental lighting conditions (cool white, warm white and amber+green LED lights) (**Chapters 3**, **4** and **6**).

The photoperiods of ornamental lighting (2, 4, 6 and 8 hours) used in the study reported in **Chapter 2** did not alter the relative abundance of species in the SABs, and only light quality (red, green, blue and white LED lights) promoted changes. The presence of *Bracteacoccus minor* decreased under red (631 nm) and green (530 nm) lighting and increased under blue light (450 nm). By contrast, the abundance of *Stichococcus bacillaris* decreased under illumination with blue light but increased under red light. Although no changes in the abundance of the species were reported in **Chapter 3** (with SABs mainly composed by *Chlorella vulgaris*), the ornamental lighting affected the proteome of the microalgal species comprising the SAB **(Chapter 4)**. Finally, the only important change in the relative abundance found in the long-term monitoring reported in **Chapter 6** was an increase in the abundance of *Myrmecia irregularis* under metal halide lighting (and that remained stable under amber+green light similarly to the unilluminated control).

When SABs were cultivated under low daylight intensity (50.07 µmol s^{-1} m^{-2}) (**Chapter 3)**, both ornamental warm white light and amber+green light caused a decrease in the abundance of *Klebsormidium flaccidum* of 58.32% and 39.63% respectively. An increase in peptides related to the genus *Klebsormidium* under warm white light and amber+green light was subsequently observed (**Chapter 4**). These lighting conditions (252.59 µmol s^{-1} m^{-2} of daylight and around 1 µmol s^{-1} m^{-2} of ornamental lighting) did not cause any changes in the abundance of *Klebsormidium flaccidum*, as determined by morphological taxonomic determination (**Chapter 3**). However, the increase in peptides was related to the photosynthetic process. The increase could be attributed to *Klebsormidium* adapting to light that is inefficient for its growth through metabolism related to the LHCs. *Klebsormidium flaccidum* appears forming green and black sulphated crusts and biofilms in several cathedrals (Pinheiro et al., 2019). The findings of Komar et al. (2023) showed that the filaments from *Klebsormidium flaccidum* filled deeper layers and cavities from red brick and polysilicate plaster samples, thus facilitating attachment by other microalgal species and increasing the bioweathering potential to fracture the stone material.

5.3 PART 3: BIODIVERSITY IMPACT

Biodiversity conservation ensures the maintenance of multiple ecological services provided by healthy ecosystems. In urban settings, biodiversity is critically important to support human quality of life (Rastandeh et al., 2017). The use of LED lighting for outdoor lighting has increased the extent to which ALAN affects nocturnal biodiversity (Evans, 2023), and new illumination projects must therefore mitigate negative impacts. For example, LED lighting spectra can be modified to avoid high emission of blue wavelengths (≈ 400 to 500 nm), which are a strong component of other technologies like metal halide lamps, and which negatively impact the health of humans and ecosystems (Falchi et al., 2011).

In **Chapter 1**, the pollution caused by ALAN was defined in the context of ornamental illumination of monuments as *"the ornamental lighting on monuments that is not being efficiently or completely utilized and exceeds the limits of the object and scatters to the atmosphere (often because is pointed outwards or upwards), causing artificial ambient brightness that has an overall negative effect on the environment"* (Méndez, Prieto, et al., 2024).

The negative impacts on biodiversity of ALAN derived from ornamental lighting can be reduced by following different strategies: reducing the intensity of ALAN (Charvalakis et al., 2025), removing unnecessary lighting (see e.g. Van Doren et al., 2017), shielding luminaires to avoid light spilling outside the monument limits (see e.g. Kobav et al., 2021) and spectral tuning (see e.g. Deichmann et al., 2021; Robert et al., 2025). Spectral tuning (as in the use of the amber+green light in the CromaLux system) consists

of removing sensitive wavelengths (like blue or UV wavelengths) that are particularly detrimental to nocturnal animal communities (Longcore et al., 2015) while maintaining a white-like appearance to the human eye. Assessment of the impact of ornamental lighting to biodiversity was conducted using the lighting set-up installed in the inner courtyard of Pazo de Raxoi as reported in **Chapter 7** (microbial communities) and **Chapter 8** (insect communities).

ALAN is known to cause changes in the microbial community structure (see e.g. Hölker et al., 2015) and even to destabilize bacterial communities by, for example, replacing taxa with light-tolerant species (see e.g. Li et al., 2024). The microbial communities inhabiting the granite walls in the inner courtyard in the Pazo de Raxoi shifted under ornamental lighting (**Chapter 7**). The microbial communities were mainly composed of the genera *Peribacillus* and *Paenibacillus* (bacteria) and *Aspergillus* and *Fusarium* (fungi), according to the MinION sequencing. The amber+green light (peak wavelengths, 593 nm and 528 nm) induced fewer changes in the community than the metal halide light (peak wavelengths, 435 nm, 508 nm, 546 nm, 578 nm and 589 nm), making the community exposed to the amber+green light more similar to the unilluminated control, as measured by the Shannon index. The highest bacterial DNA counts were reported under the metal halide light, with the bacterial microbiome being strongly dominated by *Peribacillus*. However, fungal DNA counts were more abundant under the amber+green light and the unilluminated control.

Maisto et al., (2025) found that bacterial communities were more diverse in parts of a granite wall colonised by a phototrophic SAB than in areas with no SAB. Maggi et al., (2019) reported a significant increase in the diversity of the photoautotrophic component and a decrease in that of the heterotrophic component of microbial biofilms in a rocky shore in La Spezia (Italy) exposed to ALAN (white LED lamp at ≈27 lux). According to Wang et al. (2024), fungal communities growing on plant surfaces are more sensitive to ALAN than bacteria, even though the diversity of both decreases when exposed to ALAN (white LED light at ≈ 21 lx).

Here, the metal halide lamp enhanced development of the phototrophic SAB growing on the granite ashlars of Pazo de Raxoi relative to the amber+green light and the unilluminated control, measured as an increase in F_0 (biomass proxy variable) and a higher abundance of the green alga *Myrmecia irregularis* (**Chapter 6**). Following the results of Maggi et al. (2019), growth of the SAB was accompanied by a decrease in bacterial diversity. Indeed, the presence of light is known to benefit microalgae in competition with heterotrophic bacteria (see e.g. González-Camejo et al., 2019). Although non-phototrophic microorganisms do not depend on light for growth, light still plays an important role in their metabolism. For example, the genus *Actinobacteria* is able to sense light and upregulate carbohydrate transport and thus increase its growth rate, through a specific cryptochrome photosensor (Maresca et al., 2019), and this genus is therefore more competitive under light. The genus of bacteria most frequently identified in green SABs

growing on the artificially illuminated walls (unspecified white light) of the underground Roman Houses of Caelian Hill (Italy) was *Peribacillus* (Isola et al., 2023). These researchers also reported that *Peribacillus* was very actively involved in carbonate precipitation, and this genus thus appears to be associated with microalgal SABs under white ornamental illumination.

Regarding the effects of lighting on insect communities (**Chapter 8**), spectral tuning (use of amber+green light instead of the broad white light of the metal halide lamp) reduced the number and diversity of insects attracted to ornamental lighting relative to those captured on the unilluminated sticky traps. The species most abundantly trapped belonged to the orders Diptera (flies and other two-winged insects), Hemiptera (aphids, bedbugs and other insects with sucking mouthparts) and Psocoptera (booklice, barklice and other lice). Interestingly, members of the order Lepidoptera (butterflies and moths) were not trapped under the amber+green light, as this group is strongly affected by shortwave radiation (blue and UV wavelengths) (see e.g. Mikkola, 1972; Brehm et al., 2021).

Although spectral tuning is commonly practiced to reduce the impact of ALAN on animal communities, authors such Owens et al. (2024) doubt its usefulness and conclude that the benefits are ambiguous and frequently negligible. They point out that most studies (like that reported in **Chapter 8**) only account for flight-to-light behaviour and ignore other impacts that ALAN have on insect communities, such as alterations in the food web (see e.g. Sanders et al., 2021). Thus, even though fewer insects will be attracted to a light source that emits fewer wavelengths (especially short wavelengths), restructuration of the community will still take place.

Shielding appears to be one of the most efficient ways to decrease the impact of ALAN (apart from the obvious elimination of unnecessary lighting) (Owens et al., 2024) proposed the design of shutters made ad-hoc with the silhouette of specific monuments to block any stray light that may pass the outside the limits of the monument and thus effectively reducing the contribution to ornamental ALAN according to the definition provided in **Chapter 1**. The direction of light is also important for insects, which orient themselves using the direction of light, tilting their body towards the brightest visual hemisphere to maintain proper flight. The direction of natural sunlight is usually from above (with the position changing between sunrise and sunset). Thus, ALAN directed upwards will create erratic flight patterns as the brightest visual hemisphere will be opposite to that of the sun (Fabian et al., 2024). As discussed in **Chapter 1** and **section 5.1**, upward illumination of cultural objects its prohibited or at least not recommended. Future recommendations or legislation regarding monumental illumination should also include shielding and spectral tuning, as combining all these strategies is the most effective way to create environmentally sound ornamental lighting systems.

5.4 PART 4: SOCIO-ECONOMIC IMPACT

The CromaLux lighting system can be considered an environmental technology for the preventive conservation of architectural heritage. Several definitions of environmental technologies have been proposed. For example, the United Nations Conference on Environment and Development (UNCED) concluded that *"environmentally sound technologies that protect the environment, are less polluting, use all resources in a more sustainable manner, recycle more of their wastes and products, and handle residual wastes in a more acceptable manner than the technologies for which they were substitutes"* and that they *"include know-how, procedures, goods and services, and equipment as well as organizational and managerial procedures"* (World Health Organization, 1992). Kuehr (2007) expanded on this definition, indicating that environmental technologies must reduce emissions and improve the quality of products and services. This researcher notes that there is currently greater investment in environmental technologies that focus on preventing undesired impacts rather than dealing with the impacts.

Life cycle assessment (LCA) and Life Cycle Costing (LCC) tools are useful for evaluating the sustainability of preventive strategies in the conservation of cultural heritage (see e.g. Menegaldo et al., 2023). The study reported in **Chapter 9** assessed the expected environmental and economic benefits of the CromaLux lighting system (highly efficient warm white LED followed by the novel amber+green LED light with biostatic effect) relative to a metal halide lighting system (used to date for ornamental illumination in Santiago de Compostela) and a conventional white LED system. The results validate the CromaLux lighting system as a more environmentally sound and sustainable lighting technology for the preventive conservation of stone-built heritage. Studying the sustainability of cultural heritage conservation has gained increasing attention in recent years. According to the ISI Web of Science (WOS), 64 publications addressing LCA in the context of cultural heritage were published between 2003 and 2025, with 61.56% of these appearing in the last three years. In relation to carbon footprint, only 45 articles were published between 2013 and 2025, with 55.55% of these being published in the last three years. Akşar et al. (2025) also reported that the number of LCA studies applied to historic buildings rose rapidly between 2019 and 2025, with energy efficiency being one of the key themes appearing regarding evaluating sustainability in heritage buildings.

The biostatic capacity of the CromaLux lighting system (produced by the amber+green light) was estimated to reduce both the CF (Carbon Footprint, in kg $CO_{2\text{-eq}}$) and the operational expenditure costs (OPEX, in €) of ornamental lighting. The study presented in **Chapter 9** also examined how ornamental lighting may influence the CF (in g $CO_{2\text{-eq}}$) and economic performance of methods commonly used to remove phototrophic SABs (laser cleaning, water vapour and the biocides Biotin T®, Biotin R® and reinforced ethanol), based on the findings reported in **Chapters 2** to **6**.

In addition to consuming less energy, the CromaLux lighting system could also reduce the CF and OPEX, in two ways. First, the halting of growth caused by amber+green light could delay the need to apply correction factors recommended by Spanish legislation (see **Chapter 1**; MINCOTUR, 2008), thus minimizing the associated increase in CF and OPEX linked to increased illuminance required to compensate for surface reflectance loss due to biofouling. Ornamental illumination of built heritage accounts for a much higher CF than cleaning. Operational energy accounts for a large part of the $CO_{2\text{-eq}}$ emissions in historic buildings, and improving the sustainability of the built heritage will thus improve the energy use efficiency (Berthold et al., 2025). Second, the reduced growth of SABs delays the need for cleaning interventions, in turn decreasing $CO_{2\text{-eq}}$ emissions associated with the cleaning methods evaluated. Paolino et al. (2025) used LCA tools to evaluate the environmental impacts of the various stages of painting restoration (disinfection, consolidation, cleaning and aesthetic presentation) on the conservation of a canvas painting. The authors reported that the use of chemical products for cleaning (e.g. to remove varnish) and disinfection (e.g. using thio-carbamate-based biocides) contributes significantly to climate change. The findings presented in **Chapter 9,** rating reinforced ethanol as the most environmentally friendly evaluated chemical cleaning method, are consistent with those of the aforementioned researchers, who showed that replacing conventional solvents with ethanol led to a substantial reduction in $CO_{2\text{-eq}}$ emissions.

The success of the introduction of new sustainable technologies is not only dependent on the economic profitability, but also on public opinion (Scovell, 2022). The social context and public attitudes are key components of the social context influencing technological development and adoption (Frewer et al., 1998). In this context, two different types of study were used in the research reported in **Chapter 10**: the first was a qualitative study involving discussions with experts and representatives from neighbourhood associations, while the second consisted of a quantitative field survey. The first study also served to identify key topics for the design of the survey used in the second. The objective of both studies was to identify perceived strengths and weaknesses of amber+green lighting, in order to provide information fostering social acceptance of the lighting system. The results of the first study highlighted concerns about the visual appeal of amber+green light, with a general preference for traditional warm white lighting. However, the participants acknowledged that most individuals would either not notice or would eventually adapt to the change. Experts expressed greater reluctance to accept the benefits of amber+green lighting and voiced more concerns than neighbourhood representatives, who placed greater trust in the scientific foundation of the CromaLux system and were more receptive to the new technology. The key findings of the second study were consistent with those of the first, confirming the lower visual attractiveness of amber+green light, which was ranked after cool and warm white lights in order of preference. The study revealed overall neutral attitudes toward amber+green lighting. It also showed that participants with a strong sense of identification with their neighbourhood were more likely to choose amber+green light over white lights (either cool or warm), and

that stronger social identification with the community was associated with more positive attitudes toward the amber+green light.

The aim of assessing participants' attitudes was to evaluate the positive or negative aspects of their judgments (e.g. whether they considered the amber+green light to be pleasant, useful or necessary, etc.), which is thought to guide individual behaviour (Fazio, 1986). Individuals who have strong favourable attitudes towards a given technology may be more likely to continue using it (Kim et al., 2009), whereas weakly held attitudes are more susceptible to change and may shift toward negative attitudes and opposition (see e.g. Sánchez-Tabernero et al., 2025). Although attitudes toward the amber+green light were not negative, fostering a stronger positive view of the technology could ensure the successful implementation of the CromaLux system.

In the study by Maketo and Ashworth (2025), public perceptions of green hydrogen energy sources in the UK were found to be neutral, with no clear trend toward acceptance or rejection. The authors suggest that the neutral attitude may reflect either indifference or insufficient knowledge for informed opinion, and that attitudes may evolve as awareness increases. Educating people about a new technology is typically the first step towards either acceptance or rejection and may precede eventual adoption of the technology (Upham et al., 2015). Therefore, strategies aimed at increasing public understanding of the benefits of amber+green lighting could contribute to more favourable attitudes. Thus, raising awareness was the main approach used to address reluctance to the amber+green light voiced by both experts and representatives of neighbourhood associations in **Chapter 10** (Phase 1). In a similar way, Albertano et al. 2004 found that educating visitors about the conservation benefits of blue light (around 490 nm) to protect the St. Callistus Catacomb (Rome, Italy) from biodeterioration led to the visitors approving use of the light, despite the loss of colour of the frescoes.

Chapter 10 reports that strong place identity (understood here as the attachment to the physical environment that define an individual's personal identity) increased the probability of participants voting in favour of the amber+green light. Attachment to the neighbourhood did not differ significantly between residents of the historic centre and those of other neighbourhoods in Santiago de Compostela, and these groups had similar opinions about the new lighting system. The physical appearance of urban spaces is constantly changing and influences the attachment of people towards places (von Wirth et al., 2016). According to Fresque-Baxter and Armitage 2012, when a place is threatened by a change (either real or perceived), place identity is also threatened as it breaks the continuity between the self-concept of the place and the reality (see e.g. Twigger-Ross and Uzzell, 1996). Both Devine-Wright 2011 and von Wirth et al. 2016 state that perceiving changes in the urban environment as an attractive upgrade is positively related to place attachment and support. Stronger place attachment is also correlated with a greater willingness to engage in place-protective action (see e.g. Mesch and Manor, 1998;

Stedman, 2002). Chan et al. (2023) reported that informing people about the actions taken towards protecting architectural heritage strengthened place attachment.

The results reported in **Chapter 10** also indicated that stronger social identification with the community created clear-cut attitudes towards the amber+green light. Similar results were reported by Gómez-Román et al. (2024) in a study in which pro-environmental social identity resulted in greater acceptance of decentralized wastewater treatment systems. Ashforth and Mael (1989) defines social identification as *"the perception of oneness with or belongingness to some human aggregate"*, which accounts for the values, norms, behaviours and attitudes that regulate a group of people and that motivate individuals (see e.g. Tajfel and Turner, 2004). Social identification can impose social pressure towards favouring an action (such as the acceptance of an environmental technology), so that individuals will shift their actions and thoughts towards those valued by the community as positive or negative (see e.g. Ajzen, 1991; Tirotto, 2022).

Thus, it can be concluded that the strategies aimed at increasing the acceptance of the amber+green light (both by increasing the probability of its selection and by enhancing positive attitudes towards it) should appeal to the residents' place attachment (to Santiago de Compostela) and to their social identification with the community.

6 CONCLUSIONS

The use of amber+green light as ornamental illumination has been proposed as a sustainable strategy for preventive conservation, aimed at halting the growth of phototrophic microorganisms colonising architectural stone heritage. The research conducted in this thesis has validated the biostatic capacity of amber+green light in short-term laboratory-based experiments and in long-term field monitoring. It has also provided deeper insights into the impact of ornamental lighting on biological colonisation of architectural heritage. A comprehensive, multidisciplinary approach was used to evaluate the environmental impact, energy efficiency and social perception of the novel lighting the system. The research was divided into four specific parts with a total of 10 chapters, from which the following conclusions have been drawn:

The literature review reported in **Chapter 1** highlighted the lack of research on light pollution policies. Spain has detailed legislation regarding monumental illumination. However, this is included in broader legislation concerning energetic efficiency and in regional environmental policies addressing light pollution, and the impact on heritage conservation is generally overlooked. It was concluded that local based illumination projects such as CromaLux can provide recommendations for future legislation.

Exposure to between 4 and 6 hours of green ornamental illumination inhibited SAB growth (assessed by wet biomass yield and cell count) (**Chapter 2**), and this was thus established as the optimal timing for induction of a biostatic effect. A lower biomass yield was also reported (**Chapter 3**) with the use of amber+green light in conditions of both low and high daylight irradiance.

The amber+green light also reduced production of exopolysaccharides in the EPS matrix of the SABs with low daylight conditions (**Chapter 3**). However, the use of a high daylight irradiance masked the impact of nocturnal ornamental lighting on the biochemical profile of the SABs.

The possible mechanisms of action underlying the biostatic effect were elucidated by proteomic analysis (**Chapter 4**). The findings revealed a negative impact on photosystems I and II in the SABs under amber+green light, especially the absence of peptides related to the PsbO subunit of the PSII, which catalyses the splitting of water to O_2 and $4H^+$. The amber+green light also triggered an increase in protein turnover.

The biostatic effect of amber+green light is probably derived from the lower photosynthetic efficiency than that of the white light tested. ATP and NAD(P)H production

will thus be reduced, limiting the energy available for night-time protein turnover and forcing organisms to consume more biomass for maintenance rather than relying on the photosynthesis driven by ornamental illumination.

In the study reported in **Chapter 5**, the presence of SAB on the granite and cement mortar sample blocks caused an increase in surface roughness, contact angle and water absorption time, while decreasing the surface hardness. However, the SAB-mineral interphase behaved similarly under the amber+green light and in the absence of ornamental illumination, thus reinforcing the biostatic effect even on lithic materials. The petrographic analysis also revealed that the biotite minerals in the granite were not colonised by the SABs, probably due to foliation.

The research reported in **Chapter 6** validated the biostatic effect of amber+green light in an outdoor setting for a period of 3.4 years. At the end of the monitoring period, the SABs under amber+green lighting yielded values of F_0 (used as proxy for biomass), equal to those in the absence of ornamental illumination, while those under metal halide light increased further. The quantum yield was not affected by ornamental lighting but underwent changes throughout the monitoring period, with higher values in winter months and lower values in summer.

The amber+green light slightly increased the bacterial and fungal diversity (**Chapter 7)**. The ornamental lighting caused shifts in the microbial community, but the bacterial and fungal communities were more similar in the unilluminated control and the amber+green light than under the metal halide lamp, as shown by the Shannon index. The amber+green light attracted fewer insects (both in terms of number and diversity, especially of members of the orders Diptera, Lepidoptera, Coleoptera, Hemiptera and Hymenoptera) (**Chapter 8**).

The carbon footprint quantification, reported in **Chapter 9**, estimated that CromaLux lighting system can reduce the $CO_{2\text{-eq}}$ emissions from ornamental lighting by 80%, relative to the metal halide system, and by 20%, relative to a traditional white LED system. If implemented at city level, the CromaLux lighting system could potentially yield annual savings of up to 3.64 tonnes of $CO_{2\text{-eq}}$ and €1,269.91.

The research reported in **Chapter 10** identified a clear preference of residents for the warm white light, with both the qualitative and quantitative phases showing concerns about the visual appeal of the amber+green light. However, representatives of neighbourhood associations perceive conservation benefits and believe that the amber+green light will be publicly accepted, which experts are more reticent to believe. A high level of place identification increases the preference towards the amber+green light, while a high level of social identification increases the initially neutral attitudes towards the light.

Overall, the findings reported in this thesis validate the biostatic effect of the amber+green light and confirm the advantages of the CromaLux lighting system for improving the environmental and economic sustainability of ornamental lighting. The biostatic capacity was validated under a wide array of experimental and lighting

conditions, and the system was compared with several white light sources (cool and warm white LEDs and metal halide lamps) in both laboratory and outdoor experiments. The findings also confirmed that the amber+green light minimises the impact of ornamental lighting on the microbial and insect biodiversity, relative to that of traditional metal halide lamps. In addition, the CromaLux lighting system can reduce the $CO_{2\text{-eq}}$ emissions from ornamental lighting by 80%, relative to metal halide lamps, and by 20%, relative to a traditional white LEDs; the amber+green light may become accepted, and even preferred, by the inhabitants of Santiago de Compostela.

7 BIBLIOGRAPHY

Abdala-Díaz, R. T., Cabello-Pasini, A., Pérez-Rodríguez, E., Conde Álvarez, R. M., and Figueroa, F. L. (2006). Daily and seasonal variations of optimum quantum yield and phenolic compounds in Cystoseira tamariscifolia (Phaeophyta). Marine Biology, 148(3), 459–465. https://doi.org/10.1007/S00227-005-0102-6/FIGURES/6

Abomohra, A. E. F., Shang, H., El-Sheekh, M., Eladel, H., Ebaid, R., Wang, S., and Wang, Q. (2019). Night illumination using monochromatic light-emitting diodes for enhanced microalgal growth and biodiesel production. Bioresource Technology, 288. https://doi.org/10.1016/j.biortech.2019.121514

Acuña, A. M., Snellenburg, J. J., Gwizdala, M., Kirilovsky, D., Van Grondelle, R., and Van Stokkum, I. H. M. (2015). Resolving the contribution of the uncoupled phycobilisomes to cyanobacterial pulse-amplitude modulated (PAM) fluorometry signals. Photosynthesis Research 2015 127:1, 127(1), 91–102. https://doi.org/10.1007/S11120-015-0141-X

Aguirre-Gomez, R., Weeks, A. R., and Boxall, S. R. (2001). The identification of phytoplankton pigments from absorption spectra. International Journal of Remote Sensing, 22(2–3), 315–338. https://doi.org/10.1080/014311601449952

Ahmad, I., Abdullah, N., Koji, I., Mohamad, S. E., Al-Dailami, A., Malaysia, T., Sultan, J., Petra, Y., Lumpur, K., and Yuzir, M. A. (2022). Role of Algae in Built Environment and Green Cities: A Holistic approach towards Sustainability. International Journal of Built Environment and Sustainability, 9(2–3), 69–80. https://doi.org/10.11113/IJBES.V9.N2-3.1039

Akşar, S., Beceren Öztürk, R., and Cahantimur, A. (2025). Life Cycle Assessment in Historic Buildings: A Bibliometric Exploration of Global Research Trends. Bilge International Journal of Science and Technology Research, 9(2), 118–130. https://doi.org/10.30516/bilgesci.1763443

Albertano, P., and Bruno, L. (2017). The importance of light in the conservation of hypogean monuments. In Molecular Biology and Cultural Heritage (pp. 171–178). Routledge. https://doi.org/10.1201/9780203746578-22

Albertano, P., Luongo, L., and Grilli Caiola, M. (1991). Influence of different lights of mixed cultures of microalgae from ancient frescoes. International Biodeterioration, 27(1), 27–38. https://doi.org/10.1016/0265-3036(91)90021-I

Albertano, P., Moscone, D., Palleschi, G., Hermosin, B., Saiz-Jimenez, C., Sanchez-Moral, S., Hernandez-Marine, M., Urzì, C., Groth, I., Schroeckh, V., Saarela, M., Mattila-Sandholm, T., Gallon, J. R., Graziottin, F., Bisconti, F., and Giuliani, R. (2003). Cyanobacteria attack rocks (CATS): Control and preventive strategies to avoid damage caused by cyanobacteria and associated microorganisms in Roman hypogean monuments. Molecular Biology and Cultural Heritage, 151–162. https://doi.org/10.1201/9780203746578-20

Albertano, P., Pacchiani, D., and Capucci, E. (2004). The public response to innovative strategies for the control of biodeterioration in archaeological hypogea. Journal of Cultural Heritage, 5(4), 399–407. https://doi.org/10.1016/J.CULHER.2004.06.003

Allsopp, D., Seal, K. J., and Gaylarde, C. C. (2004). Introduction to Biodeterioration. Cambridge University Press. https://doi.org/10.1017/CBO9780511617065

American Medical Association. (2016). Human and Environmental Effects of Light Emitting Diode (LED) Community Lighting . Https://Darksky.Org/App/Uploads/Bsk-Pdf-Manager/AMA_Report_2016_60.Pdf.

Amini Khoeyi, Z., Seyfabadi, J., and Ramezanpour, Z. (2012). Effect of light intensity and photoperiod on biomass and fatty acid composition of the microalgae, Chlorella vulgaris. Aquaculture International, 20(1), 41–49. https://doi.org/10.1007/s10499-011-9440-1

Anderl, J. N., Franklin, M. J., and Stewart, P. S. (2000). Role of Antibiotic Penetration Limitation in Klebsiella pneumoniae Biofilm Resistance to Ampicillin and Ciprofloxacin. Antimicrobial Agents and Chemotherapy, 44(7), 1818–1824. https://doi.org/10.1128/AAC.44.7.1818-1824.2000

Anderson, N. L., and Anderson, N. G. (1998). Proteome and proteomics: New technologies, new concepts, and new words. Electrophoresis, 19(11), 1853–1861.

Anderson, S. J., Kubiszewski, I., and Sutton, P. C. (2024). The Ecological Economics of Light Pollution: Impacts on Ecosystem Service Value. Remote Sensing, 16(14), 2591. https://doi.org/10.3390/rs16142591

Aubé, M., Roby, J., and Kocifaj, M. (2013). Evaluating Potential Spectral Impacts of Various Artificial Lights on Melatonin Suppression, Photosynthesis, and Star Visibility. PLoS ONE, 8(7). https://doi.org/10.1371/journal.pone.0067798

Autonomous Community of Cantabria. (2006). Ley 6/2006, de 9 de junio, de prevención de la Contaminación Lumínica. «BOE» núm. 184, de 03/08/2006.

Autonomous Community of Catalonia. (2001). Ley 6/2001, de 31 de mayo, de Ordenación Ambiental del Alumbrado para la Protección del Medio Nocturno. In «BOE» núm. 149, de 22/06/2001. Agencia Estatal Boletín Oficial del Estado.

Ayalon, I., Benichou, J. I. C., Avisar, D., and Levy, O. (2021). The Endosymbiotic Coral Algae Symbiodiniaceae Are Sensitive to a Sensory Pollutant: Artificial Light at Night, ALAN. Frontiers in Physiology, 12, 695083. https://doi.org/10.3389/FPHYS.2021.695083/BIBTEX

Azhari, N. F. N., and Mohamed, E. (2012). Public Perception: Heritage Building Conservation in Kuala Lumpur. Procedia - Social and Behavioral Sciences, 50, 271–279. https://doi.org/10.1016/J.SBSPRO.2012.08.033

Azman, M. I., Dalimin, M. N., Mohamed, M., and Abu Bakar, M. F. (2019). A Brief Overview on Light Pollution. IOP Conference Series: Earth and Environmental Science, 269(1), 012014. https://doi.org/10.1088/1755-1315/269/1/012014

Baker, N. R., and Oxborough, K. (2004). Chlorophyll Fluorescence as a Probe of Photosynthetic Productivity. Chlorophyll a Fluorescence, 65–82. https://doi.org/10.1007/978-1-4020-3218-9_3

Bao, Y., Ma, Y., Liu, W., Li, X., Li, Y., Zhou, P., Feng, Y., and Delgado-Baquerizo, M. (2023). Innovative strategy for the conservation of a millennial mausoleum from biodeterioration through artificial light management. Npj Biofilms and Microbiomes, 9(1), 69. https://doi.org/10.1038/s41522-023-00438-9

Bará, S. (2013). Light pollution and solid-state lighting: reducing the carbon dioxide footprint is not enough (M. F. P. C. Martins Costa, Ed.; p. 87852G). https://doi.org/10.1117/12.2025344

Bará, S., Bao-Varela, C., and Falchi, F. (2022). Light pollution and the concentration of anthropogenic photons in the terrestrial atmosphere. Atmospheric Pollution Research, 13(9), 101541. https://doi.org/10.1016/J.APR.2022.101541

Bará, S., Falchi, F., Lima, R. C., and Pawley, M. (2021). Keeping light pollution at bay: A red-lines, target values, top-down approach. Environmental Challenges, 5, 100212. https://doi.org/10.1016/J.ENVC.2021.100212

Barbosa, R. P. D. S., Pereira-Cenci, T., Silva, W. M. Da, Coelho-De-Souza, F. H., Demarco, F. F., and Cenci, M. S. (2012). Effect of cariogenic biofilm challenge on the surface hardness of direct restorative materials in situ. Journal of Dentistry, 40(5), 359–363. https://doi.org/10.1016/J.JDENT.2012.01.012

Barrientos, J. A. (2005). Curso Practico de Entomología (1st ed.). Universitat Autonoma de Barcelona - Servei de Publicacione.

Bartels, J., and Reinders, M. J. (2010). Social identification, social representations, and consumer innovativeness in an organic food context: A cross-national comparison. Food Quality and Preference, 21(4), 347–352. https://doi.org/10.1016/J.FOODQUAL.2009.08.016

Bartoli, F., Isola, D., Casanova Municchia, A., Kumbaric, A., and Caneva, G. (2023). Science for art: multi-years' evaluations of biocidal efficacy in support of artwork conservation. Frontiers in Microbiology, 14, 1178900. https://doi.org/10.3389/FMICB.2023.1178900/BIBTEX

Bartolomé Rodriguez, I. (2007). LA INDUSTRIA ELÉCTRICA EN ESPAÑA (1890-1936) (1st ed.). Imprenta del Banco de España.

Bashiri, F. (2014). Light Pollution and Its Effect on the Environment. International Journal of Fundamental Physical Sciences, 4(1), 8–12. https://doi.org/10.14331/ijfps.2013.330061

Bautista, A. I. N., and Necchi Jr., O. (2007). Photoacclimation in three species of freshwater red algae. Brazilian Journal of Plant Physiology, 19(1), 23–34. https://doi.org/10.1590/S1677-04202007000100003

Beccali, M., Bonomolo, M., Lo Brano, V., Ciulla, G., Di Dio, V., Massaro, F., and Favuzza, S. (2019). Energy saving and user satisfaction for a new advanced public lighting system. Energy Conversion and Management, 195, 943–957. https://doi.org/10.1016/j.enconman.2019.05.070

Becerra, J., Mateo, M., Ortiz, P., Nicolás, G., and Zaderenko, A. P. (2019). Evaluation of the applicability of nano-biocide treatments on limestones used in cultural heritage. Journal of Cultural Heritage, 38, 126–135. https://doi.org/10.1016/j.culher.2019.02.010

Begonha, A. (2009). Mineralogical study of the deterioration of granite stones of two Portuguese churches and characterization of the salt solutions in the porous network by the presence of diatoms. Materials Characterization, 60(7), 621–635. https://doi.org/10.1016/J.MATCHAR.2008.12.019

Belany, P., Hrabovsky, P., and Kolkova, Z. (2021). Combination of lighting retrofit and life cycle cost analysis for energy efficiency improvement in buildings. Energy Reports, 7, 2470–2483. https://doi.org/10.1016/j.egyr.2021.04.044

Bell, R. A., and Sommerfeld, M. R. (1987). Algal biomass and primary production within a temperate zone sandstone. American Journal of Botany, 74(2), 294–297. https://doi.org/10.1002/j.1537-2197.1987.tb08608.x

Bellia, L., Birolo, L., Casillo, A., Corsaro, M. M., De Natale, A., Fragliasso, F., Genovese, A., Palella, B. I., Petraretti, M., Pollio, A., Riccio, G., and Stanzione, I. (2025). Analyzing the Effects of Monochromatic Lights on the Fungal Growth to Control the Progression of Microbial Deterioration on Animal Collections Preserved in the Zoological Museum of Naples, Italy. LEUKOS, 21(4), 404–422. https://doi.org/10.1080/15502724.2024.2387575

Bennie, J., Davies, T. W., Cruse, D., and Gaston, K. J. (2016). Ecological effects of artificial light at night on wild plants. Journal of Ecology, 104(3), 611–620. https://doi.org/10.1111/1365-2745.12551

Bergey, E. A. (2006). Measuring the surface roughness of stream stones. Hydrobiologia, 563(1), 247–252. https://doi.org/10.1007/S10750-006-0016-4/METRICS

Berthold, É., Pawliw, K., and Righi, S. (2025). Built Religious Heritage, Circular Economy, and Life-Cycle Assessment: A Case Study of a Convent Property in the Province of Quebec, Canada. Energies 2025, Vol. 18, Page 2512, 18(10), 2512. https://doi.org/10.3390/EN18102512

Berti, L., Villa, F., Toniolo, L., Cappitelli, F., and Goidanich, S. (2024). Methodological challenges for the investigation of the dual role of biofilms on outdoor heritage. Science of The Total Environment, 954, 176450. https://doi.org/10.1016/j.scitotenv.2024.176450

Bischoff, H. W., and Bold, H. C. (1963). Phycological Studies IV. Some Soil Algae from Enchanted Rock and Related Algal Species. University of Texas Publication, 6318, 95–95.

Bista, D., Bista, A., Shrestha, A., Doulos, L. T., Bhusal, P., Zissis, G., Topalis, F., and Chhetri, B. B. (2021). Lighting for Cultural and Heritage Site: An Innovative Approach for Lighting in the Distinct Pagoda-Style Architecture of Nepal. Sustainability, 13(5), 2720. https://doi.org/10.3390/su13052720

Boichou, M., Marie-Victoire, E., Congar, T., and Blanchard, R. (2015). Concrete cultural heritage in France—inventory and state of conservation. In Concrete Repair, Rehabilitation and Retrofitting IV. CRC Press.

Boley, B. B., Strzelecka, M., Yeager, E. P., Ribeiro, M. A., Aleshinloye, K. D., Woosnam, K. M., and Mimbs, B. P. (2021). Measuring place attachment with the Abbreviated Place Attachment Scale (APAS). Journal of Environmental Psychology, 74, 101577. https://doi.org/10.1016/J.JENVP.2021.101577

Bonnes, M., Lee, T., and Bonaiuto, M. (2017). Psychological Theories for Environmental Issues (M. Bonnes, T. Lee, and M. Bonaiuto, Eds.). Routledge. https://doi.org/10.4324/9781315245720

Borderie, F., Alaoui-Sossé, B., and Aleya, L. (2015). Heritage materials and biofouling mitigation through UV-C irradiation in show caves: state-of-the-art practices and future challenges. Environmental Science and Pollution Research, 22(6), 4144–4172. https://doi.org/10.1007/s11356-014-4001-6

Bouchard, A. J., Hamilton, P. B., Savoie, A. M., and Starr, J. R. (2019). Molecular and morphological data reveal hidden diversity in common North American Frustulia species (Amphipleuraceae). Diatom Research, 34(4), 205–223. https://doi.org/10.1080/0269249X.2019.1704889

Bouichou, M., Marie-Victoire, E., Bousta, F., and Orial, G. (2010). Elimination of biological covering on concrete: Tests in situ of different techniques. In P. Castro-Borges, E. I. Moreno, K. Sakai, O. E. Gjorv, and N. Banthia (Eds.), Concrete under Severe Conditions (1st ed., Vol. 2, pp. 1181–1188). CRC Press.

Bowman, A., and Azzalini, A. (1997). Applied Smoothing Techniques for Data Analysis: The Kernel Approach with S-Plus Illustrations (1st ed., Vol. 18). Oxford University Press.

Bowman, A., and Azzalini, A. (2021). R package “sm”: nonparametric smoothing methods (version 2.2-6.0) (pp. 1–75).

Bradford, M. M. (1976). A rapid and sensitive method for the quantitation of microgram quantities of protein utilizing the principle of protein-dye binding. Analytical Biochemistry, 72(1–2), 248–254. https://doi.org/10.1016/0003-2697(76)90527-3

Braun, C., Rehdanz, K., and Schmidt, U. (2016). Exploring public perception of environmental technology over time . Kiel Working Paper, 2027.

Braun, V., and Clarke, V. (2006). Using thematic analysis in psychology. Qualitative Research in Psychology, 3(2), 77–101. https://doi.org/10.1191/1478088706QP063OA

Brehm, G., Niermann, J., Jaimes Nino, L. M., Enseling, D., Jüstel, T., Axmacher, J. C., Warrant, E., and Fiedler, K. (2021). Moths are strongly attracted to ultraviolet and blue radiation. Insect Conservation and Diversity, 14(2), 188–198. https://doi.org/10.1111/ICAD.12476

Bremer, P., Flint, S., Brooks, J., and Palmer, J. (2015). Introduction to biofilms: Definition and basic concepts. Biofilms in the Dairy Industry, 1–16. https://doi.org/10.1002/9781118876282.CH1;PAGEGROUP:STRING:PUBLICATION

Bruno, L., Belleza, S., Urzì, C., and De Leo, F. (2014). A study for monitoring and conservation in the Roman Catacombs of St. Callistus and Domitilla, Rome (Italy). In The Conservation of Subterranean Cultural Heritage (pp. 37–44). CRC Press. https://doi.org/10.1201/b17570-6

Bruno, L., and Valle, V. (2017). Effect of white and monochromatic lights on cyanobacteria and biofilms from Roman Catacombs. International Biodeterioration and Biodegradation, 123, 286–295. https://doi.org/10.1016/j.ibiod.2017.07.013

Caldeira, A. T. (2021). Green Mitigation Strategy for Cultural Heritage Using Bacterial Biocides. In Microorganisms in the Deterioration and Preservation of Cultural Heritage (pp. 137–154). Springer International Publishing. https://doi.org/10.1007/978-3-030-69411-1_6

Calleja, L., Ruiz de Argandoña, V. G., Sánchez-Delgado, N., and Setién, A. (2020). Interpretation of petrographic anisotropy in ornamental granites based on P wave velocity measurements. Materiales de Construcción, 70(339), e227. https://doi.org/10.3989/mc.2020.15419

Calvo, M. (2024, March 21). Nuevas luces. Diario de Burgos. https://www.diariodeburgos.es/noticia/zc39be845-a714-80e7-e5cb4e54b6e8a358/202403/nuevas-luces

Campisi, D., Gitto, S., and Morea, D. (2018). Economic feasibility of energy efficiency improvements in street lighting systems in Rome. Journal of Cleaner Production, 175, 190–198. https://doi.org/10.1016/j.jclepro.2017.12.063

Caneva, G., Bartoli, F., Fontani, M., Mazzeschi, D., and Visca, P. (2019). Changes in biodeterioration patterns of mural paintings: Multi-temporal mapping for a preventive conservation strategy in the Crypt of the Original Sin (Matera, Italy). Journal of Cultural Heritage, 40, 59–68. https://doi.org/10.1016/J.CULHER.2019.05.011

Caneva, G., Bartoli, F., Savo, V., Futagami, Y., and Strona, G. (2016). Combining Statistical Tools and Ecological Assessments in the Study of Biodeterioration Patterns of Stone Temples in Angkor (Cambodia). Scientific Reports, 6(1), 1–8. https://doi.org/10.1038/SREP32601;TECHMETA

Caneva, G., Nugari, M. P., and Salvadori, O. (Eds.). (2008). Plant Biology for Cultural Heritage: Biodeterioration and Conservation. The Getty Conservation Institute.

Caneva, G., and Tescari, M. (2017). Stone biodeterioration: treatments and preventive conservation. International Symposium of Stone Conservation, 95–114.

Caneve, L., Guarneri, M., Lai, A., Spizzichino, V., Ceccarelli, S., and Mazzei, B. (2019). Non-destructive laser based techniques for biodegradation analysis in cultural heritage. NDT and E International, 104, 108–113. https://doi.org/10.1016/J.NDTEINT.2019.03.007

Cao, Y., Bowker, M. A., Delgado-Baquerizo, M., and Xiao, B. (2023). Biocrusts protect the Great Wall of China from erosion. Science Advances, 9(49). https://doi.org/10.1126/SCIADV.ADK5892

Cappitelli, F., Cattò, C., and Villa, F. (2020). The Control of Cultural Heritage Microbial Deterioration. Microorganisms, 8(10), 1542. https://doi.org/10.3390/microorganisms8101542

Cetindamar, D. (2001). The role of regulations in the diffusion of environment technologies: micro and macro issues. European Journal of Innovation Management, 4(4), 186–193. https://doi.org/10.1108/14601060110408099

Chan, S. H. G., Lee, W. H. H., Tang, B. M., and Chen, Z. (2023). Legacy of culture heritage building revitalization: place attachment and culture identity. Frontiers in Psychology, 14, 1314223. https://doi.org/10.3389/FPSYG.2023.1314223/XML

Chang, Y., Wei, Y., Zhang, J., Xu, X., Zhang, L., and Zhao, Y. (2021). Mitigating the greenhouse gas emissions from urban roadway lighting in China via energy-efficient luminaire adoption and renewable energy utilization. Resources, Conservation and Recycling, 164, 105197. https://doi.org/10.1016/j.resconrec.2020.105197

Charvalakis, G. A., Stavenga, D. G., Visser, M. E., Spoelstra, K., and Hut, R. A. (2025). Intensity and colour of artificial light at night affect insect attraction in a taxon-dependent manner. Insect Conservation and Diversity. https://doi.org/10.1111/ICAD.12855

Chen, M., and Blankenship, R. E. (2011). Expanding the solar spectrum used by photosynthesis. Trends in Plant Science, 16(8), 427–431. https://doi.org/10.1016/j.tplants.2011.03.011

Chen, W., Liu, J., Chu, G., Wang, Q., Zhang, Y., Gao, C., and Gao, M. (2023). Comparative evaluation of four Chlorella species treating mariculture wastewater under different photoperiods: Nitrogen removal performance, enzyme activity, and antioxidant response. Bioresource Technology, 386, 129511. https://doi.org/10.1016/j.biortech.2023.129511

Chen, X., Bai, F., Huang, J., Lu, Y., Wu, Y., Yu, J., and Bai, S. (2021). The Organisms on Rock Cultural Heritages: Growth and Weathering. Geoheritage 2021 13:3, 13(3), 1–17. https://doi.org/10.1007/S12371-021-00588-2

Chen, X., He, P., and Qin, Z. (2018). Damage to the Microstructure and Strength of Altered Granite under Wet–Dry Cycles. Symmetry 2018, Vol. 10, Page 716, 10(12), 716. https://doi.org/10.3390/SYM10120716

Chevrier, M. H. (2019). Nocturnal ritual activities in tourist development of pilgrimage cities. Journal of Policy Research in Tourism, Leisure and Events, 11(3), 436–454.

Chini Zittelli, G., Mugnai, G., Milia, M., Cicchi, B., Silva Benavides, A. M., Angioni, A., Addis, P., and Torzillo, G. (2022). Effects of blue, orange and white lights on growth, chlorophyll fluorescence, and phycocyanin production of Arthrospira platensis cultures. Algal Research, 61, 102583. https://doi.org/10.1016/J.ALGAL.2021.102583

Cirone, M., Figoli, A., Galiano, F., La Russa, M. F., Macchia, A., Mancuso, R., Ricca, M., Rovella, N., Taverniti, M., and Ruffolo, S. A. (2023). Innovative Methodologies for the Conservation of Cultural Heritage against Biodeterioration: A Review. Coatings 2023, Vol. 13, Page 1986, 13(12), 1986. https://doi.org/10.3390/COATINGS13121986

Colica, G., Li, H., Rossi, F., Li, D., Liu, Y., and De Philippis, R. (2014). Microbial secreted exopolysaccharides affect the hydrological behavior of induced biological soil crusts in desert sandy soils. Soil Biology and Biochemistry, 68, 62–70. https://doi.org/10.1016/J.SOILBIO.2013.09.017

Concello de Santiago. (1997). Plan especial de protección e rehabilitación da cidade histórica.

Concello de Santiago. (2024). Monumentos. Https://Www.Santiagoturismo.Com/Monumentos.

Connor, D. S., Xie, S., Jang, J., Frazier, A. E., Kedron, P., Jain, G., Yu, Y., and Kemeny, T. (2025). Big cities fuel inequality within and across generations. PNAS Nexus, 4(2). https://doi.org/10.1093/PNASNEXUS/PGAE587

Consellería de Promoción do Emprego e Igualdade. (2023). Resolución pola que se inscribe e publica o convenio colectivo para o sector da construción da Coruña 2022-2026 (código de convenio 15000395011982). Https://Www.Empresarios-Ferrolterra.Org/Images/Convenio_Colectivo_Sector_Construcci%C3%B3n_A_Coru%C3%B1a._BOP_180723.Pdf.

Consorcio de Santiago. (2022). MEMORIA PRESUPUESTO 2023. Http://Www.Consorciodesantiago.Org/Sites/Default/Files/Consorcio_presupuestos2023.Pdf.

Consorcio de Santiago. (2024). La instalación de fibra óptica en el Casco Histórico compostelano es ya una realidad para la vecindad. Http://Www.Consorcio-Santiago.Org/Es/Noticias/La-Instalacion-de-Fibra-Optica-En-El-Casco-Historico-Compostelano-Es-Ya-Una-Realidad-Para .

Council of Europe. (1985). Convention for the Protection of the Architectural Heritage of Europe (pp. 1–8).

Courard, L., Zhao, Z., and Michel, F. (2021). Influence of hydrophobic product nature and concentration on carbonation resistance of cultural heritage concrete buildings. Cement and Concrete Composites, 115, 103860. https://doi.org/10.1016/J.CEMCONCOMP.2020.103860

Cucchiella, F., De Berardinis, P., Lenny Koh, S. C., and Rotilio, M. (2017). Planning restoration of a historical landscape: A case study for integrating a sustainable street lighting system with conservation of historical values. Journal of Cleaner Production, 165, 579–588. https://doi.org/10.1016/j.jclepro.2017.07.089

Cutler, N. A., Viles, H. A., Ahmad, S., McCabe, S., and Smith, B. J. (2013). Algal “greening” and the conservation of stone heritage structures. Science of the Total Environment, 442(November), 152–164. https://doi.org/10.1016/j.scitotenv.2012.10.050

Cutler, N., and Viles, H. (2010). Eukaryotic Microorganisms and Stone Biodeterioration. Geomicrobiology Journal, 27(6–7), 630–646. https://doi.org/10.1080/01490451003702933

Dahech, P., Schlömann, M., and Ortiz, C. (2021). Light intensity stimulates the production of extracellular polymeric substances (EPS) in a culture of the desert cyanobacterium Trichormus sp. Journal of Applied Phycology, 33(5), 2795–2804. https://doi.org/10.1007/s10811-021-02516-x

Dakal, T. C., and Arora, P. K. (2012). Evaluation of potential of molecular and physical techniques in studying biodeterioration. Reviews in Environmental Science and Bio/Technology, 11(1), 71–104. https://doi.org/10.1007/s11157-012-9264-0

Dakal, T. C., and Cameotra, S. S. (2012). Microbially induced deterioration of architectural heritages: Routes and mechanisms involved. Environmental Sciences Europe, 24(1), 1–13. https://doi.org/10.1186/2190-4715-24-36/FIGURES/1

Dal Pozzo, A., Masi, G., Sassoni, E., and Tugnoli, A. (2024). Life cycle assessment of stone consolidants for conservation of cultural heritage. Building and Environment, 249, 111153. https://doi.org/10.1016/j.buildenv.2023.111153

de Beer, D., Stoodley, P., Roe, F., and Lewandowski, Z. (1994). Effects of biofilm structures on oxygen distribution and mass transport. Biotechnology and Bioengineering, 43(11), 1131–1138. https://doi.org/10.1002/BIT.260431118,

De Bruyn, S., de Vries, J., Bijleveld, M., van der Giesen, Korteland, M., van Santen, W., and Pápai, S. (2023). Handboek Milieuprijzen. Https://Cedelft.Eu/Wp-Content/Uploads/Sites/2/2023/03/CE_Delft_220175_Handboek_Milieuprijzen_2023_DEF.Pdf .

De Muynck, W., Ramirez, A. M., De Belie, N., and Verstraete, W. (2009). Evaluation of strategies to prevent algal fouling on white architectural and cellular concrete. International Biodeterioration and Biodegradation, 63(6), 679–689. https://doi.org/10.1016/J.IBIOD.2009.04.007

Autonomous Community of Catalonia. (2015). DECRET 190/2015, de 25 d'agost, de desplegament de la Llei 6/2001, de 31 de maig, d'ordenació ambiental de l'enllumenament per a la protecció del medi nocturn. In DOGC. DOGC núm. 6944 de 27 de Agosto de 2015.

Deichmann, J. L., Gatty, C. A., Manuel, J., Navarro, A., Alonso, A., Linares-Palomino, R., Longcore, T., Bautista, J., De Entomología, M., Büller, K. R., Agraria, N., and Molina, L. (2021). Reducing the blue spectrum of artificial light at night minimises insect attraction in a tropical lowland forest. Insect Conservation and Diversity, 14(2), 247–259. https://doi.org/10.1111/ICAD.12479

Del Rosal, Y., Muñoz-Fernández, J., Celis-Plá, P., Hernández-Mariné, M., Álvarez-Gómez, F., Merino, S., and Figueroa, F. (2021). Monitoring photosynthetic activity using in vivo chlorophyll a fluorescence in microalgae and cyanobacteria biofilms in the Nerja Cave (Malaga, Spain). International Journal of Speleology, 51(1), 29–42. https://doi.org/10.5038/1827-806X.51.1.2404

Desarnaud, J., Kiriyama, K., Bicer Simsir, B., Wilhelm, K., and Viles, H. (2019). A laboratory study of Equotip surface hardness measurements on a range of sandstones: What influences the values and what do they mean? Earth Surface Processes and Landforms, 44(7), 1419–1429. https://doi.org/10.1002/esp.4584

Devine-Wright, P. (2011). Place attachment and public acceptance of renewable energy: A tidal energy case study. Journal of Environmental Psychology, 31(4), 336–343. https://doi.org/10.1016/J.JENVP.2011.07.001

Diamantopoulou, C., Christoforou, E., Dominoni, D. M., Kaiserli, E., Czyzewski, J., Mirzai, N., and Spatharis, S. (2021). Wavelength-dependent effects of artificial light at night on phytoplankton growth and community structure. Proceedings of the Royal Society B, 288(1953). https://doi.org/10.1098/RSPB.2021.0525

Díaz, J., López-Fernández, D., Pérez, J., and González-Prieto, Á. (2021). Why are many businesses instilling a DevOps culture into their organization? Empirical Software Engineering, 26(2), 1–50. https://doi.org/10.1007/S10664-020-09919-3/TABLES/17

Donatello, S., Rodriguez, R., De Oliveira, M. N., Wolf, O., Van Tichelen, P., Van Hoof, V., and Geerken, T. (2019). Revision of the EU Green Public Procurement Criteria for Road Lighting and traffic signals. In Publications Office of the European Union (1st ed.). Publications Office of the European Union. https://doi.org/10.2760/372897

Dowd, W. W. (2012). Challenges for Biological Interpretation of Environmental Proteomics Data in Non-model Organisms. Integrative and Comparative Biology, 52(5), 705–720. https://doi.org/10.1093/icb/ics093

Drelich, J. (2013). Guidelines to measurements of reproducible contact angles using a sessile-drop technique. Surface Innovations, 1(4), 248–254. https://doi.org/10.1680/SI.13.00010

Dresler, C., Saladino, M. L., Demirbag, C., Caponetti, E., Chillura Martino, D. F., and Alduina, R. (2017). Development of controlled release systems of biocides for the conservation of cultural heritage. International Biodeterioration and Biodegradation, 125, 150–156. https://doi.org/10.1016/j.ibiod.2017.09.007

DuBois, Michel., Gilles, K. A., Hamilton, J. K., Rebers, P. A., and Smith, Fred. (1956). Colorimetric Method for Determination of Sugars and Related Substances. Analytical Chemistry, 28(3), 350–356. https://doi.org/10.1021/ac60111a017

Dwaikat, L. N., and Ali, K. N. (2018). Green buildings life cycle cost analysis and life cycle budget development: Practical applications. Journal of Building Engineering, 18, 303–311. https://doi.org/10.1016/j.jobe.2018.03.015

Eagly, A. H., and Chaiken, S. (1993). The Psicology of Attitudes. In The psychology of attitudes (1st ed.). Harcourt Brace College Publishers.

Edmundson, S. J., and Huesemann, M. H. (2015). The dark side of algae cultivation: Characterizing night biomass loss in three photosynthetic algae, Chlorella sorokiniana, Nannochloropsis salina and Picochlorum sp. Algal Research, 12, 470–476. https://doi.org/10.1016/J.ALGAL.2015.10.012

Eggert, A., Häubner, N., Klausch, S., Karsten, U., and Schumann, R. (2006). Quantification of algal biofilms colonising building materials: Chlorophyll α measured by PAM-fluorometry as a biomass parameter. Biofouling, 22(2), 79–90. https://doi.org/10.1080/08927010600579090

Eldridge, A., and Smith, A. (2019). Tourism and the night: towards a broader understanding of nocturnal city destinations. Journal of Policy Research in Tourism, Leisure and Events, 11(3), 371–379. https://doi.org/10.1080/19407963.2019.1631519

Elnaggar, A. (2024). Nine principles of green heritage science: life cycle assessment as a tool enabling green transformation. Heritage Science, 12(1), 7. https://doi.org/10.1186/s40494-023-01114-z

Elrayies, G. M. (2018). Microalgae: Prospects for greener future buildings. Renewable and Sustainable Energy Reviews, 81, 1175–1191. https://doi.org/10.1016/J.RSER.2017.08.032

Espejo Gutierrez, F. J., and González Gasca, M. del C. (2008). La iluminación de edificios religiosos en España (1959-1985). Oppidium, 4, 213–236.

Estévez, C. B., Merino, L. M., Román, A. de la L., and Valsero, J. J. D. (2019). The lampenflora in show caves and its treatment: An emerging ecological problem. International Journal of Speleology, 48(3), 249–277. https://doi.org/10.5038/1827-806X.48.3.2263

Ettl, H., and Gärtner, G. (1995). Syllabus der Boden-, Luft- und Flechtenalgen. Springer Berlin Heidelberg. https://doi.org/10.1007/978-3-642-39462-1

European Commission. (2024). Life-cycle costing. Https://Green-Business.Ec.Europa.Eu/Green-Public-Procurement/Life-Cycle-Costing_en.

European Parliament. (2020). Commission Regulation (EU) 2019/2020 of 1 October 2019 laying down ecodesign requirements for light sources and separate control gears pursuant to Directive 2009/125/EC of the European Parliament and of the Council and repealing Commission Regulations (EC) No 244/2009, (EC) No 245/2009 and (EU) No 1194/2012 . Official Journal of the European Union.

European Standard. (2009). EN 15802:2009. Conservation of cultural property — Test methods — Determination of static contact angle. European Committee for Standarization.

European Standard. (2010). EN 15886:2010 Conservation of cultural property - Test methods - Colour measurement of surfaces. European Committee for Standarization. https://www.en-standard.eu/bs-en-15886-2010-conservation-of-cultural-property-test-methods-colour-measurement-of-surfaces/?srsltid=AfmBOoqW24dZyJdHUSQSdgWoDFUsoW6a3i84EI3klaSsavNPaqAY8JdG

European Standard. (2012). UNE-EN 197-1:2011 - Cement - Part 1: Composition, specifications and conformity criteria for common cements. Asociación Española de Normalización.

European Standard. (2020). UNE-EN 12407:2020 Métodos de ensayo para piedra natural - Estudio petrográfico. Asociación Española de Normalización. https://www.une.org/encuentra-tu-norma/busca-tu-norma/norma?c=N0063142

Evans, D. M. (2023). Mitigating the impacts of street lighting on biodiversity and ecosystem functioning. Philosophical Transactions of the Royal Society B, 378(1892). https://doi.org/10.1098/RSTB.2022.0355

Evans, J. (1987). The Dependence of Quantum Yield on Wavelength and Growth Irradiance. Functional Plant Biology, 14(1), 69. https://doi.org/10.1071/PP9870069

Eyssautier-Chuine, S., Vaillant-Gaveau, N., Gommeaux, M., Thomachot-Schneider, C., Pleck, J., and Fronteau, G. (2015). Efficacy of different chemical mixtures against green algal growth on limestone: A case study with Chlorella vulgaris. International Biodeterioration and Biodegradation, 103, 59–68. https://doi.org/10.1016/J.IBIOD.2015.02.021

Fabian, S. T., Sondhi, Y., Allen, P. E., Theobald, J. C., and Lin, H.-T. (2024). Why flying insects gather at artificial light. Nature Communications, 15(1), 689. https://doi.org/10.1038/s41467-024-44785-3

Falasco, E., Ector, L., Isaia, M., Wetzel, C., Hoffmann, L., and Bona, F. (2014). Diatom flora in subterranean ecosystems: a review. International Journal of Speleology, 43(3), 231–251. https://doi.org/10.5038/1827-806X.43.3.1

Falchi, F., Cinzano, P., Elvidge, C. D., Keith, D. M., and Haim, A. (2011). Limiting the impact of light pollution on human health, environment and stellar visibility. Journal of Environmental Management, 92(10), 2714–2722. https://doi.org/10.1016/j.jenvman.2011.06.029

Falcón, J., Torriglia, A., Attia, D., Viénot, F., Gronfier, C., Behar-Cohen, F., Martinsons, C., and Hicks, D. (2020). Exposure to Artificial Light at Night and the Consequences for Flora, Fauna, and Ecosystems. Frontiers in Neuroscience, 14, 602796. https://doi.org/10.3389/FNINS.2020.602796/XML

Fan, J., and Gijbels, I. (2018). Local Polynomial Modelling and Its Applications. Routledge. https://doi.org/10.1201/9780203748725

Fanesi, A., Paule, A., Bernard, O., Briandet, R., and Lopes, F. (2019). The Architecture of Monospecific Microalgae Biofilms. Microorganisms 2019, Vol. 7, Page 352, 7(9), 352. https://doi.org/10.3390/MICROORGANISMS7090352

Favero-Longo, S. E., Matteucci, E., Castelli, D., Iacomussi, P., Martire, L., Ruggiero, M. G., and Segimiro, A. (2023). An ecological investigation on lichens and other lithobionts colonizing rock art in Valle Camonica (UNESCO WHS n. 94) addresses preventive conservation strategies. The Lichenologist, 55(5), 409–422. https://doi.org/10.1017/S0024282923000452

Favero-Longo, S. E., Matteucci, E., Voyron, S., Iacomussi, P., and Ruggiero, M. G. (2023). Lithobiontic recolonization following cleaning and preservative treatments on the rock engravings of Valle Camonica, Italy: A 54-months monitoring. Science of The Total Environment, 901, 165885. https://doi.org/10.1016/j.scitotenv.2023.165885

Favero-Longo, S. E., and Viles, H. A. (2020). A review of the nature, role and control of lithobionts on stone cultural heritage: weighing-up and managing biodeterioration and bioprotection. World Journal of Microbiology and Biotechnology, 36(7), 1–18. https://doi.org/10.1007/s11274-020-02878-3

Fazio, R. H. (1986). How do attitudes guide behavior? In R. M. Sorrentino and E. T. Higgins (Eds.), Handbook of motivation and cognition: Foundations of social behavior (pp. 204–243). Guilford Press.

Fernández Paradas, M. (2008). La industria eléctrica y su actividad en el negocio del alumbrado en España (1901-1935). Ayer, 71, 245–265. https://www.jstor.org/stable/41325984?seq=15

Ferrari, C., Santunione, G., Libbra, A., Muscio, A., Sgarbi, E., Siligardi, C., and Barozzi, G. S. (2015). Review on the influence of biological deterioration on the surface properties of building materials: organisms, materials, and methods. International Journal of Design and Nature and Ecodynamics, 10(1), 21–39. https://doi.org/10.2495/DNE-V10-N1-21-39

Ferrero, A., Gómez Moreno, G., Lombardero, M., and Roel, J. (1992). The granites of Galicia used as industrial rock. Laboratorio Xeolóxico de Laxe, 17, 363–382.

Fidanza, M. R., and Caneva, G. (2019). Natural biocides for the conservation of stone cultural heritage: A review. Journal of Cultural Heritage, 38, 271–286. https://doi.org/10.1016/j.culher.2019.01.005

Fischer, T., Veste, M., Wiehe, W., and Lange, P. (2010). Water repellency and pore clogging at early successional stages of microbiotic crusts on inland dunes, Brandenburg, NE Germany. CATENA, 80(1), 47–52. https://doi.org/10.1016/J.CATENA.2009.08.009

Flemming, H. C., Neu, T. R., and Wozniak, D. J. (2007). The EPS Matrix: The "House of Biofilm Cells." Journal of Bacteriology, 189(22), 7945–7947. https://doi.org/10.1128/JB.00858-07

Flemming, H. C., and Wingender, J. (2010). The biofilm matrix. Nature Reviews Microbiology, 8(9), 623–633. https://doi.org/10.1038/NRMICRO2415;SUBJMETA

Folta, K. M., and Maruhnich, S. A. (2007). Green light: A signal to slow down or stop. Journal of Experimental Botany, 58(12), 3099–3111. https://doi.org/10.1093/jxb/erm130

Foroughi, M., de Andrade, B., Roders, A. P., and Wang, T. (2023). Public participation and consensus-building in urban planning from the lens of heritage planning: A systematic literature review. Cities, 135, 104235. https://doi.org/10.1016/j.cities.2023.104235

Franzoni, E., Volpi, L., and Bonoli, A. (2020). Applicability of life cycle assessment methodology to conservation works in historical building: The case of cleaning. Energy and Buildings, 214, 109844. https://doi.org/10.1016/j.enbuild.2020.109844

Freire-Lista, D. M. (2016). Deterioro de granito utilizado en construcción tradicional. Naturaleza Aragonesa, 33, 27–31. https://digital.csic.es/handle/10261/184702

Freire-Lista, D. M., and Fort, R. (2016). Causes of scaling on bush-hammered heritage ashlars: a case study—Plaza Mayor of Madrid (Spain). Environmental Earth Sciences, 75(10). https://doi.org/10.1007/S12665-016-5688-0

Freire-Lista, D. M., Fort, R., and Varas-Muriel, M. J. (2015). Freeze–thaw fracturing in building granites. Cold Regions Science and Technology, 113, 40–51. https://doi.org/10.1016/J.COLDREGIONS.2015.01.008

Fresque-Baxter, J. A., and Armitage, D. (2012). Place identity and climate change adaptation: a synthesis and framework for understanding. Wiley Interdisciplinary Reviews: Climate Change, 3(3), 251–266. https://doi.org/10.1002/WCC.164

Frewer, L. J., Howard, C., and Shepherd, R. (1998). Understanding public attitudes to technology. Journal of Risk Research, 1(3), 221–235. https://doi.org/10.1080/136698798377141

Friulla, L., and Varone, L. (2025). Artificial Light at Night (ALAN) as an Emerging Urban Stressor for Tree Phenology and Physiology: A Review. Urban Science, 9(1), 14. https://doi.org/10.3390/urbansci9010014

Fuentes, E., Carballeira, R., and Prieto, B. (2021). Role of Exposure on the Microbial Consortiums on Historical Rural Granite Buildings. Applied Sciences, 11(9), 3786. https://doi.org/10.3390/app11093786

Fuentes, E., and Prieto, B. (2021). Recovery Capacity of Subaerial Biofilms Grown on Granite Buildings Subjected to Simulated Drought in a Climate Change Context. Microbial Ecology, 82(3), 761–769. https://doi.org/10.1007/S00248-021-01692-0/FIGURES/4

Fuíková, K., Flechtner, V. R., and Lewis, L. A. (2012). Revision of the genus Bracteacoccus Tereg (Chlorophyceae, Chlorophyta) based on a phylogenetic approach. Nova Hedwigia, 96(1–2), 15–59. https://doi.org/10.1127/0029-5035/2012/0067

Galve, E. (1935, November 24). Mañana se inaugura la iluminación de la Catedral de Burgos. El Debate, 1.

Gantt, E., and Cunningham Jr., F. X. (2001). Algal Pigments. ENCYCLOPEDIA OF LIFE SCIENCES, 1–5.

Gao, Y., Bernard, O., Fanesi, A., Perré, P., and Lopes, F. (2024). The effect of light intensity on microalgae biofilm structures and physiology under continuous illumination. Scientific Reports, 14(1), 1–11. https://doi.org/10.1038/S41598-023-50432-6;SUBJMETA

García Gil, M., Parcío Ferreró, S., and Masana Fresno, E. (2022). Limitaciones en la normativa y oportunidades para la reducción de la contaminación lumínica. Luces CEI, 75, 10–18.

Gaylarde, C. C., and Baptista-Neto, J. A. (2021). Microbiologically induced aesthetic and structural changes to dimension stone. Npj Materials Degradation, 5(1), 1–8. https://doi.org/10.1038/S41529-021-00180-7;SUBJMETA=169,171,172,209,326,631,704;KWRD=ENVIRONMENTAL+MICROBIOLOGY,GEOCHEMISTRY

Gaylarde, C. C., and Gaylarde, P. M. (2005). A comparative study of the major microbial biomass of biofilms on exteriors of buildings in Europe and Latin America. International Biodeterioration and Biodegradation, 55(2), 131–139. https://doi.org/10.1016/j.ibiod.2004.10.001

Gaylarde, C. C., Gaylarde, P. M., and Neilan, B. A. (2012). Endolithic phototrophs in built and natural stone. Current Microbiology, 65(2), 183–188. https://doi.org/10.1007/S00284-012-0123-6/FIGURES/2

Gaylarde, C. C., Gutarowska, B., Beech, I. B., Szulc, J., Acharjee, A., Grzyb, T., da Silva de Freitas, A., and Baptista Neto, J. A. (2025). Metagenomic and morphological analysis of biodeteriogenic biofilms on historic stone buildings in the tropical north-east of Brazil. International Biodeterioration and Biodegradation, 204, 106143. https://doi.org/10.1016/J.IBIOD.2025.106143

Gaylarde, C., Ribas Silva, M., and Warscheid, T. (2003). Microbial impact on building materials: An overview. Materials and Structures/Materiaux et Constructions, 36(259), 342–352. https://doi.org/10.1617/13867

Ge, H., Zhang, J., Zhou, X., Xia, L., and Hu, C. (2014). Effects of light intensity on components and topographical structures of extracellular polymeric substances from Microcoleus vaginatus (Cyanophyceae). Phycologia, 53(2), 167–173. https://doi.org/10.2216/13-163.1

Genova, C., Fuentes, E., Favero, G., and Prieto, B. (2023). Evaluation of the Cleaning Effect of Natural-Based Biocides: Application on Different Phototropic Biofilms Colonizing the Same Granite Wall. Coatings 2023, Vol. 13, Page 520, 13(3), 520. https://doi.org/10.3390/COATINGS13030520

Genty, B., Briantais, J. M., and Baker, N. R. (1989). The relationship between the quantum yield of photosynthetic electron transport and quenching of chlorophyll fluorescence. Biochimica et Biophysica Acta - General Subjects, 990(1), 87–92. https://doi.org/10.1016/S0304-4165(89)80016-9

Giordano, E. (2018). Outdoor lighting design as a tool for tourist development: the case of Valladolid. European Planning Studies, 26(1), 55–74. https://doi.org/10.1080/09654313.2017.1368457

Glazer, A. N., and Hixson, C. S. (1977). Subunit structure and chromophore composition of rhodophytan phycoerythrins. Porphyridium cruentum B phycoerythrin and b phycoerythrin. Journal of Biological Chemistry, 252(1), 32–42. https://doi.org/10.1016/s0021-9258(17)32794-1

Goeres, D. M., Hamilton, M. A., Beck, N. A., Buckingham-Meyer, K., Hilyard, J. D., Loetterle, L. R., Lorenz, L. A., Walker, D. K., and Stewart, P. S. (2009). A method for growing a biofilm under low shear at the air–liquid interface using the drip flow biofilm reactor. Nature Protocols, 4(5), 783–788. https://doi.org/10.1038/nprot.2009.59

Gómez-Román, C., Jans, L., Steg, L., Vila-Tojo, S., and Sabucedo, J. M. (2024). 'Yes, we care': pro-environmental social identity framing to promote acceptance of decentralized wastewater treatment systems. Water Reuse, 14(4), 510–526. https://doi.org/10.2166/WRD.2024.015/1506739/JWRD2024015.PDF

Gomoiu, I., Cojoc, R., Ruginescu, R., Neagu, S., Enache, M., Dumbrăvician, M., Olteanu, I., Rădvan, R., and Ghervase, L. (2022). The Susceptibility to Biodegradation of Some Consolidants Used in the Restoration of Mural Paintings. Applied Sciences, 12(14), 7229. https://doi.org/10.3390/app12147229

González, L., Alfonso Escudero Gómez, L., Barreiro Quintáns, D., Kamani Fard, A., and Paydar, M. (2024). Place Attachment and Related Aspects in the Urban Setting. Urban Science 2024, Vol. 8, Page 135, 8(3), 135. https://doi.org/10.3390/URBANSCI8030135

González-Camejo, J., Viruela, A., Ruano, M. V., Barat, R., Seco, A., and Ferrer, J. (2019). Effect of light intensity, light duration and photoperiods in the performance of an outdoor photobioreactor for urban wastewater treatment. Algal Research, 40, 101511. https://doi.org/10.1016/j.algal.2019.101511

Gorbushina, A. A. (2007). Life on the rocks. Environmental Microbiology, 9(7), 1613–1631. https://doi.org/10.1111/J.1462-2920.2007.01301.X

Govindjee. (2004). Chlorophyll a Fluorescence: A Bit of Basics and History. In G. C. Papageorgiou and Govindjee (Eds.), Chlorophyll a Fluorescence (1st ed., pp. 1–41). Springer Netherlands. https://doi.org/10.1007/978-1-4020-3218-9_1

Gray, D. W., Lewis, L. A., and Cardon, Z. G. (2007). Photosynthetic recovery following desiccation of desert green algae (Chlorophyta) and their aquatic relatives. Plant, Cell and Environment, 30(10), 1240–1255. https://doi.org/10.1111/J.1365-3040.2007.01704.X

Greffe, X. (2004). Is heritage an asset or a liability? Journal of Cultural Heritage, 5(3), 301–309. https://doi.org/10.1016/J.CULHER.2004.05.001

Grigoryeva, N. Yu., and Grigoryeva, N. Yu. (2020). Studying Cyanobacteria by Means of Fluorescence Methods: A Review. Fluorescence Methods for Investigation of Living Cells and Microorganisms. https://doi.org/10.5772/INTECHOPEN.93543

Grubisic, M., Singer, G., Bruno, M. C., van Grunsven, R. H. A., Manfrin, A., Monaghan, M. T., and Hölker, F. (2017). Artificial light at night decreases biomass and alters community composition of benthic primary producers in a sub-alpine stream. Limnology and Oceanography, 62(6), 2799–2810. https://doi.org/10.1002/lno.10607

Guglielmin, M., Favero-Longo, S. E., Cannone, N., Piervittori, R., and Strini, A. (2011). Role of lichens in granite weathering in cold and arid environments of continental Antarctica. Geological Society, London, Special Publications, 354(1), 195–204. https://doi.org/10.1144/SP354.12

Guillitte, O., and Dreesen, R. (1995). Laboratory chamber studies and petrographical analysis as bioreceptivity assessment tools of building materials. Science of the Total Environment, 167(1–3), 365–374. https://doi.org/10.1016/0048-9697(95)04596-S

Guisande, C., Heine, J., González-DaCosta, J., and García-Roselló, E. (2014). RWizard Software. University of Vigo. Vigo, Spain.

Gundersen, T., Alinejad, D., Branch, T. Y., Duffy, B., Hewlett, K., Holst, C., Owens, S., Panizza, F., Tellmann, S. M., Van Dijck, J., and Baghramian, M. (2022). A New Dark Age? Truth, Trust, and Environmental Science. Annual Review of Environment and Resources, 47(Volume 47, 2022), 5–29. https://doi.org/10.1146/ANNUREV-ENVIRON-120920-015909/CITE/REFWORKS

Gutleben, J., Chaib De Mares, M., van Elsas, J. D., Smidt, H., Overmann, J., and Sipkema, D. (2018). The multi-omics promise in context: from sequence to microbial isolate. Critical Reviews in Microbiology, 44(2), 212–229. https://doi.org/10.1080/1040841X.2017.1332003;PAGE:STRING:ARTICLE/CHAPTER

Hallmann, C., Wedekind, W., Hause-Reitner, D., and Hoppert, M. (2013). Cryptogam covers on sepulchral monuments and re-colonization of a marble surface after cleaning. Environmental Earth Sciences, 69(4), 1149–1160. https://doi.org/10.1007/s12665-012-2213-y

Hamacher, D. W., de Napoli, K., and Mott, B. (2020). Whitening the Sky: light pollution as a form of cultural genocide. https://arxiv.org/pdf/2001.11527

Han, B. P., Virtanen, M., Koponen, J., and Straškraba, M. (2000). Effect of photoinhibition on algal photosynthesis: a dynamic model. Journal of Plankton Research, 22(5), 865–885. https://doi.org/10.1093/PLANKT/22.5.865

Hannibal, J. T., Kramar, S., and Cooper, B. J. (2020). Worldwide examples of global heritage stones: an introduction. Geological Society Special Publication, 486(1), 1–6. https://doi.org/10.1144/SP486-2020-84

Hans Wedepohl, K. (1995). The composition of the continental crust. Geochimica et Cosmochimica Acta, 59(7), 1217–1232. https://doi.org/10.1016/0016-7037(95)00038-2

Hauer, T., Mühlsteinová, R., Bohunická, M., Kaštovský, J., and Mareš, J. (2015). Diversity of cyanobacteria on rock surfaces. Biodiversity and Conservation, 24(4), 759–779. https://doi.org/10.1007/S10531-015-0890-Z/TABLES/1

Hayes, A. F. (2018). Partial, conditional, and moderated moderated mediation: Quantification, inference, and interpretation. Communication Monographs, 85(1), 4–40. https://doi.org/10.1080/03637751.2017.1352100

He, J., Zhang, N., Shen, X., Muhammad, A., and Shao, Y. (2022). Deciphering environmental resistome and mobilome risks on the stone monument: A reservoir of antimicrobial resistance genes. Science of The Total Environment, 838, 156443. https://doi.org/10.1016/J.SCITOTENV.2022.156443

Head of the Spanish State. (2022). Real Decreto-ley 18/2022, de 18 de octubre, por el que se aprueban medidas de refuerzo de la protección de los consumidores de energía y de contribución a la reducción del consumo de gas natural en aplicación del "Plan + seguridad para tu energía (+SE)", así como medidas en materia de retribuciones del personal al servicio del sector público y de protección de las personas trabajadoras agrarias eventuales afectadas por la sequía. In «BOE» núm. 251, de 19/10/2022. Agencia Estatal Boletín Oficial del Estado.

Helamieh, M., Reich, M., Rohne, P., Riebesell, U., Kerner, M., and Kümmerer, K. (2024). Impact of green and blue-green light on the growth, pigment concentration, and fatty acid unsaturation in the microalga Monoraphidium braunii. Photochemistry and Photobiology, 100(3), 587–595. https://doi.org/10.1111/PHP.13873

Hendrickson, T. P., Nikolic, M., and Rakas, J. (2016). Selecting climate change mitigation strategies in urban areas through life cycle perspectives. Journal of Cleaner Production, 135, 1129–1137. https://doi.org/10.1016/j.jclepro.2016.06.075

Hernández, A. C., Sanjurjo-Sánchez, J., Alves, C., and Figueiredo, C. A. M. (2023). Comparative Study of Deterioration in Built Heritage in a Coastal Area: Barbanza Peninsula (Galicia, NW Spain). Geosciences 2023, Vol. 13, Page 375, 13(12), 375. https://doi.org/10.3390/GEOSCIENCES13120375

Hernandez, A. C., Sanjurjo-Sánchez, J., Alves, C., and Figueiredo, C. A. M. (2024). Study of the Geochemical Decay and Environmental Causes of Granite Stone Surfaces in the Built Heritage of Barbanza Peninsula (Galicia, NW Spain). Coatings 2024, Vol. 14, Page 169, 14(2), 169. https://doi.org/10.3390/COATINGS14020169

Hernández-Andrés, J., Lee, R. L., and Romero, J. (1999). Calculating correlated color temperatures across the entire gamut of daylight and skylight chromaticities. Applied Optics, 38(27), 5703–5709.

Hernandez-Moreno, S. (2009). CURRENT TECHNOLOGIES APPLIED TO URBAN SUSTAINABLE DEVELOPMENT. Theoretical and Empirical Researches in Urban Management, 4(13), 125–140.

Herrera, L. K., Le Borgne, S., and Videla, H. A. (2008). Modern Methods for Materials Characterization and Surface Analysis to Study the Effects of Biodeterioration and Weathering on Buildings of Cultural Heritage. International Journal of Architectural Heritage, 3(1), 74–91. https://doi.org/10.1080/15583050802149995

Hill, R., and Bendall, F. (1960). Function of the Two Cytochrome Components in Chloroplasts: A Working Hypothesis. Nature, 186(4719), 136–137. https://doi.org/10.1038/186136a0

Hogewoning, S. W., Wientjes, E., Douwstra, P., Trouwborst, G., van Ieperen, W., Croce, R., and Harbinson, J. (2012). Photosynthetic Quantum Yield Dynamics: From Photosystems to Leaves. The Plant Cell, 24(5), 1921–1935. https://doi.org/10.1105/TPC.112.097972

Hölker, F., Moss, T., Griefahn, B., Kloas, W., Voigt, C. C., Henckel, D., Hänel, A., Kappeler, P. M., Völker, S., Schwope, A., Franke, S., Uhrlandt, D., Fischer, J., Klenke, R., Wolter, C., and Tockner, K. (2010). The Dark Side of Light: A Transdisciplinary Research Agenda for Light Pollution Policy. Proceedings of the National Academy of Sciences of the United States of America, 15(4). https://doi.org/10.1073/PNAS.0808772106

Hölker, F., Wolter, C., Perkin, E. K., and Tockner, K. (2010). Light pollution as a biodiversity threat. In Trends in Ecology and Evolution (Vol. 25, Issue 12, pp. 681–682). https://doi.org/10.1016/j.tree.2010.09.007

Hölker, F., Wurzbacher, C., Weißenborn, C., Monaghan, M. T., Holzhauer, S. I. J., and Premke, K. (2015). Microbial diversity and community respiration in freshwater sediments influenced by artificial light at night. Philosophical Transactions of the Royal Society B: Biological Sciences, 370(1667). https://doi.org/10.1098/RSTB.2014.0130

Honeywill, C., Paterson, D., and Hagerthey, S. (2002). Determination of microphytobenthic biomass using pulse-amplitude modulated minimum fluorescence. European Journal of Phycology, 37(4), 485–492. https://doi.org/10.1017/S0967026202003888

Hopkins, G. R., Gaston, K. J., Visser, M. E., Elgar, M. A., and Jones, T. M. (2018). Artificial light at night as a driver of evolution across urban–rural landscapes. Frontiers in Ecology and the Environment, 16(8), 472–479. https://doi.org/10.1002/fee.1828

Hsieh, P., Pedersen, J. Z., and Albertano, P. (2013). Generation of reactive oxygen species upon red light exposure of cyanobacteria from Roman hypogea. International Biodeterioration and Biodegradation, 84, 258–265. https://doi.org/10.1016/j.ibiod.2012.11.007

Hu, F., Cang, S., Zhu, Q., Li, Y., Sun, D., and Tan, H. (2024). Extended photoperiods enhance the production and water treatment performance of algal-bacterial bioflocs from aquaculture wastewater. Journal of Water Process Engineering, 67, 106258. https://doi.org/10.1016/J.JWPE.2024.106258

Hueck, E. H. (1968). The microbiological deterioration of porous building materials. International Biodeterioration Bulletin, 4(1), 11-28.

Huguet, M. A. (2013). El alumbrado eléctrico en Barcelona, 1881-1935. Infraestructuras urbanas, iniciativas privadas y limitaciones públicas. Barcelona Quaderns d'història, 19, 157–157. https://raco.cat/index.php/BCNQuadernsHistoria/article/view/271951

Hyun, H. K., Salehi, S., and Ferracane, J. L. (2015). Biofilm formation affects surface properties of novel bioactive glass-containing composites. Dental Materials, 31(12), 1599–1608. https://doi.org/10.1016/J.DENTAL.2015.10.011

ICOMOS. (2003). Principios para el análisis, conservación y restauración de las estructuras del Patrimonio Arquitectónico. https://icomos.es/wp-content/uploads/2020/01/10.PRINCIPIOS-PARA-EL-AN%C3%81LISIS-CONSERVACI%C3%93N-Y.pdf

ICOMOS-ISCS. (2008). Illustrated glossary on stone deterioration patterns (V. Vergès-Belmin, Ed.; 1st ed.). ICOMOS-International Documentation Centre.

IDAE. (2003). Estrategia de Ahorro y Eficiencia Energética en España 2004-2012 (E4).

IGME. (2008). Mapa de rocas y minerales industriales de Galicia.

Ilies, D. C., Blaga, L., Ilies, A., Pereș, A. C., Caciora, T., Hassan, T. H., Hodor, N., Turza, A., Taghiyari, H. R., Barbu-Tudoran, L., Dahal, R. K., Dejeu, P., Safarov, B., and Hossain, M. A. (2023). Green Biocidal Nanotechnology Use for Urban Stone-Built Heritage—Case Study from Oradea, Romania. Minerals, 13(9), 1170. https://doi.org/10.3390/min13091170

INE. (2025). Población por unidad poblacional. Instituto Nacional de Estadística. https://ine.es/nomen2/index.do?accion=busquedaAvanzadaandentidad_amb=noandcodProv=15andcodMuni=78andcodEC=0andcodES=0andcodNUC=0anddenominacion_op=likeanddenominacion_txt=andL=0

Innovation Procurement Compass. (2024). SMARTIAGO-Cromalux. Sistema de alumbrado ornamental para la conservación del patrimonio. Https://Innovationprocurementcompass.Com/Wp-Content/Uploads/2024/04/Caso-4-SMARTIAGO-Cromalux-Sistema-de-Alumbrado.Pdf .

Instituto de Estudos do Territorio. (2025). Serie Galicia 250K | Información Xeográfica de Galicia. https://mapas.xunta.gal/es/serie-250

International Dark-Sky Association. (2010). Visibility, Environmental, and Astronomical Issues Associated with Blue-Rich White Outdoor Lighting. Https://Darksky.Org/App/Uploads/2016/12/IDA-Blue-Rich-Light-White-Paper.Pdf.

ISO. (2017). Buildings and constructed assets — Service life planning — Part 5: Life-cycle costing.

ISO. (2019). Greenhouse gases - Carbon footprint of products - Requirements and guidelines for quantification (ISO 14067:2018).

Isola, D., Bartoli, F., Morretta, S., and Caneva, G. (2023). The Roman Houses of the Caelian Hill (Rome, Italy): Multitemporal Evaluation of Biodeterioration Patterns. Microorganisms, 11(7), 1770. https://doi.org/10.3390/microorganisms11071770

Jacob-Lopes, E., Scoparo, C. H. G., Lacerda, L. M. C. F., and Franco, T. T. (2009). Effect of light cycles (night/day) on CO2 fixation and biomass production by microalgae in photobioreactors. Chemical Engineering and Processing: Process Intensification, 48(1), 306–310. https://doi.org/10.1016/j.cep.2008.04.007

Jakle, J. A., and Thompson, G. F. (2001). CITY LIGHTS: Illuminating the American Night by John A. Jakle Review by: Mika Roinila. In Material Culture (1st ed., Issue 1). Baltimore : Johns Hopkins University Press.

Jechow, A., Ribas, S. J., Domingo, R. C., Hölker, F., Kolláth, Z., and Kyba, C. C. M. (2018). Tracking the dynamics of skyglow with differential photometry using a digital camera with fisheye lens. Journal of Quantitative Spectroscopy and Radiative Transfer, 209, 212–223. https://doi.org/10.1016/j.jqsrt.2018.01.032

Johnson, R. J., and Scicchitano, M. J. (2000). Uncertainty risk trust and information: Public perception of environmental issues and willingness to take action. Policy Studies Journal, 28(3), 633–647. https://doi.org/10.1111/J.1541-0072.2000.TB02052.X

Jung, J. H., Sirisuk, P., Ra, C. H., Kim, J. M., Jeong, G. T., and Kim, S. K. (2019). Effects of green LED light and three stresses on biomass and lipid accumulation with two-phase culture of microalgae. Process Biochemistry, 77, 93–99. https://doi.org/10.1016/J.PROCBIO.2018.11.014

Kala, R., and Pandey, V. D. (2023). Cyanobacterial Extracellular Polymeric Substances and their role in Biodeterioration of Temples and Monuments. Journal of Mountain Research, 18(2). https://doi.org/10.51220/jmr.v18i2.19

Katz, Y., and Levin, N. (2016). Quantifying urban light pollution — A comparison between field measurements and EROS-B imagery. Remote Sensing of Environment, 177, 65–77. https://doi.org/10.1016/J.RSE.2016.02.017

Kaushik, M., and Kumar, H. D. (1970). The effect of light on growth and development of two nitrogen fixing blue-green algae. Archiv Für Mikrobiologie, 74(1), 52–57. https://doi.org/10.1007/BF00408687/METRICS

Kautsky, H., and Hirsch, A. (1931). Neue Versuche zur Kohlensureassimilation. Die Naturwissenschaften, 19(48), 964–964. https://doi.org/10.1007/BF01516164

Ke, B. (2001). Photosynthesis: Photobiochemistry and Photobiophysics (Vol. 10). Springer Netherlands. https://doi.org/10.1007/0-306-48136-7

Kemp, R. (2000). Technology and Environmental Policy—Innovation effects of past policies and suggestions for improvement. In OECD (Ed.), Innovation and the Environment (1st ed., pp. 35–62). Organisation for Economic Co-operation and Development (OECD).

Khatibi, F. S., Dedekorkut-Howes, A., Howes, M., and Torabi, E. (2021). Can public awareness, knowledge and engagement improve climate change adaptation policies? Discover Sustainability, 2(1), 1–24. https://doi.org/10.1007/S43621-021-00024-Z/FIGURES/5

Khaybullina, L. S., Gaysina, L. A., Johansen, J. R., and Krautová, M. (2010). Examination of the terrestrial algae of the Great Smoky Mountains National Park, USA. Fottea, 10(2), 201–215. https://doi.org/10.5507/fot.2010.011

Kidron, G. J. (2007). Millimeter-scale microrelief affecting runoff yield over microbiotic crust in the Negev Desert. CATENA, 70(2), 266–273. https://doi.org/10.1016/J.CATENA.2006.08.010

Kidron, G. J., Wang, Y., and Herzberg, M. (2020). Exopolysaccharides may increase biocrust rigidity and induce runoff generation. Journal of Hydrology, 588, 125081. https://doi.org/10.1016/J.JHYDROL.2020.125081

Kim, Y. J., Chun, J. U., and Song, J. (2009). Investigating the role of attitude in technology acceptance from an attitude strength perspective. International Journal of Information Management, 29(1), 67–77. https://doi.org/10.1016/J.IJINFOMGT.2008.01.011

Kisser, J., Wirth, M., De Gusseme, B., Van Eekert, M., Zeeman, G., Schoenborn, A., Vinnerås, B., Finger, D. C., Repinc, S. K., Bulc, T. G., Bani, A., Pavlova, D., Staicu, L. C., Atasoy, M., Cetecioglu, Z., Kokko, M., Haznedaroglu, B. Z., Hansen, J., Istenič, D., … Beesley, L. (2020). A review of nature-based solutions for resource recovery in cities. Blue-Green Systems, 2(1), 138–172. https://doi.org/10.2166/BGS.2020.930

Kobav, M. B., Eržen, M., and Bizjak, G. (2021). Sustainable Exterior Lighting for Cultural Heritage Buildings and Monuments. Sustainability, 13(18), 10159. https://doi.org/10.3390/su131810159

Komar, M., Nowicka-Krawczyk, P., Ruman, T., Nizioł, J., Dudek, M., and Gutarowska, B. (2023). Biodeterioration potential of algae on building materials - Model study. International Biodeterioration and Biodegradation, 180, 105593. https://doi.org/10.1016/J.IBIOD.2023.105593

Komárek, J. (2013). Süßwasserflora von Mitteleuropa, Bd. 19/3: Cyanoprokaryota (1st ed.).

Korkanç, M., and Savran, A. (2015). Impact of the surface roughness of stones used in historical buildings on biodeterioration. Construction and Building Materials, 80, 279–294. https://doi.org/10.1016/J.CONBUILDMAT.2015.01.073

Krippendorff, Klaus., and Bock, M. Angela. (2008). The content analysis reader (1st ed.). Sage Publications.

Krzemińska, I., Pawlik-Skowrońska, B., Trzcińska, M., and Tys, J. (2014). Influence of photoperiods on the growth rate and biomass productivity of green microalgae. Bioprocess and Biosystems Engineering, 37(4), 735–741. https://doi.org/10.1007/s00449-013-1044-x

Kuehr, R. (2007). Environmental technologies – from misleading interpretations to an operational categorisation and definition. Journal of Cleaner Production, 15(13–14), 1316–1320. https://doi.org/10.1016/J.JCLEPRO.2006.07.015

Kumar, D., Kvíderová, J., Kaštánek, P., and Lukavský, J. (2017). The green alga Dictyosphaerium chlorelloides biomass and polysaccharides production determined using cultivation in crossed gradients of temperature and light. Engineering in Life Sciences, 17(9), 1030–1038. https://doi.org/10.1002/elsc.201700014

Kyba, C. C. M. (2018). Is light pollution getting better or worse? Nature Astronomy, 2(4), 267–269. https://doi.org/10.1038/s41550-018-0402-7

Kyba, C. C. M., Kuester, T., De Miguel, A. S., Baugh, K., Jechow, A., Hölker, F., Bennie, J., Elvidge, C. D., Gaston, K. J., and Guanter, L. (2017). Artificially lit surface of Earth at night increasing in radiance and extent. Science Advances, 3(11), 1–9. https://doi.org/10.1126/sciadv.1701528

Kyba, C. C. M., Mohar, A., Pintar, G., and Stare, J. (2018). Reducing the environmental footprint of church lighting: matching facade shape and lowering luminance with the EcoSky LED. In International Journal of Sustainable Lighting IJSL. www.lightpollutionmap.info

Lacour, T., Babin, M., and Lavaud, J. (2020). Diversity in Xanthophyll Cycle Pigments Content and Related Nonphotochemical Quenching (NPQ) Among Microalgae: Implications for Growth Strategy and Ecology. Journal of Phycology, 56(2), 245–263. https://doi.org/10.1111/JPY.12944

Laver, T., Harrison, J., O'Neill, P. A., Moore, K., Farbos, A., Paszkiewicz, K., and Studholme, D. J. (2015). Assessing the performance of the Oxford Nanopore Technologies MinION. Biomolecular Detection and Quantification, 3, 1–8. https://doi.org/10.1016/J.BDQ.2015.02.001

Le Noac'h, P., Ayata, S.-D., Pruvost, E., Marty, S., Bernard, O., and Laviale, M. (2025). Ecophysiological modeling of the impact of light intensity and quality on microalgal growth in outdoor high-density open ponds. Algal Research, 91, 104248. https://doi.org/10.1016/J.ALGAL.2025.104248

Lee, Y., Lee, J., and Lee, Z. (2001). The effect of self identity and social identity on technology acceptance. ICIS 2001 Proceedings, 481–490.

Leite Magalhães, S., and Sequeira Braga, M. A. (2000). Biological colonization features on a granite monument from Braga (NW, Portugal. In V. Fassina (Ed.), Proceedings of the 9th International Congress on Deterioration and Conservation of Stone (pp. 521–529). Elsevier.

Leraut, Patrice. (2007). Insectos de España y Europa (1st ed.). Lynx Edicions. https://lynxnaturebooks.com/es/producto/insectos-de-espana-y-europa/

Head of Spanish state. (1988). Ley 31/1988, de 31 de octubre, sobre Protección de la Calidad Astronómica de los Observatorios del Instituto de Astrofísica de Canarias. In BOE núm. 264, de 3 de noviembre de 1988 (pp. 31451–31451). Agencia Estatal Boletín Oficial del Estado.

Li, X., Hu, Z., and Zhang, Q. (2021). Environmental regulation, economic policy uncertainty, and green technology innovation. Clean Technologies and Environmental Policy, 23(10), 2975–2988. https://doi.org/10.1007/S10098-021-02219-4/TABLES/8

Li, X. M., Hu, H. F., and Chen, S. C. (2024). Artificial light at night causes community instability of bacterial community in urban soils. Science of The Total Environment, 921, 171129. https://doi.org/10.1016/J.SCITOTENV.2024.171129

Li, Z., Ye, P., and Li, Y. (2025). Environmental Factors Influence Lichen Colonization and the Biodeterioration of Brick Carvings on Roof Ridges of Historic Buildings in Luoyang, China. Sustainability 2025, Vol. 17, Page 3721, 17(8), 3721. https://doi.org/10.3390/SU17083721

Lichtenthaler, H. K., Ač, A., Marek, M. V., Kalina, J., and Urban, O. (2007). Differences in pigment composition, photosynthetic rates and chlorophyll fluorescence images of sun and shade leaves of four tree species. Plant Physiology and Biochemistry, 45(8), 577–588. https://doi.org/10.1016/J.PLAPHY.2007.04.006

Lichtenthaler, H. K., Buschmann, C., and Knapp, M. (2005). How to correctly determine the different chlorophyll fluorescence parameters and the chlorophyll fluorescence decrease ratio R Fd of leaves with the PAM fluorometer. In PHOTOSYNTHETICA (Vol. 43, Issue 3).

Lindawati, L., Nugraha, N., Mayasari, M., and Supriatna, N. (2019). Financial estimation on street lighting using LED technology . Journal of Engineering Science and Technology, Special Issue on AASEC2018, 68–81.

Lister, G. G., Lawler, J. E., Lapatovich, W. P., and Godyak, V. A. (2004). The physics of discharge lamps. Reviews of Modern Physics, 76(2), 541. https://doi.org/10.1103/RevModPhys.76.541

Liu, X., Qian, Y., Wu, F., Wang, Y., Wang, W., and Gu, J. D. (2022). Biofilms on stone monuments: biodeterioration or bioprotection? Trends in Microbiology, 30(9), 816–819. https://doi.org/10.1016/j.tim.2022.05.012

Liu, X. Y., Jiao, X. L., Chang, T. T., Guo, S. R., and Xu, Z. G. (2018). Photosynthesis and leaf development of cherry tomato seedlings under different LED-based blue and red photon flux ratios. Photosynthetica, 56(4), 1212–1217. https://doi.org/10.1007/s11099-018-0814-8

Lo Schiavo, S., De Leo, F., and Urzì, C. (2020). Present and Future Perspectives for Biocides and Antifouling Products for Stone-Built Cultural Heritage: Ionic Liquids as a Challenging Alternative. Applied Sciences, 10(18), 6568. https://doi.org/10.3390/app10186568

Longcore, T., Aldern, H. L., Eggers, J. F., Flores, S., Franco, L., Hirshfield-Yamanishi, E., Petrinec, L. N., Yan, W. A., and Barroso, A. M. (2015). Tuning the white light spectrum of light emitting diode lamps to reduce attraction of nocturnal arthropods. Philosophical Transactions of the Royal Society B: Biological Sciences, 370(1667). https://doi.org/10.1098/RSTB.2014.0125

Longcore, T., and Rich, C. (2004). Ecological light pollution. Frontiers in Ecology and the Environment, 2(4), 191–198. https://doi.org/10.1890/1540-9295(2004)002[0191:ELP]2.0.CO;2

López, M. (2020). Daylight effect on the electricity demand in Spain and assessment of Daylight Saving Time policies. Energy Policy, 140, 111419. https://doi.org/10.1016/j.enpol.2020.111419

Loustau, E., Leflaive, J., Boscus, C., Amalric, Q., Ferriol, J., Oleinikova, O., Pokrovsky, O. S., Girbal-Neuhauser, E., and Rols, J. L. (2021). The Response of Extracellular Polymeric Substances Production by Phototrophic Biofilms to a Sequential Disturbance Strongly Depends on Environmental Conditions. Frontiers in Microbiology, 12, 742027. https://doi.org/10.3389/FMICB.2021.742027/BIBTEX

Luimstra, V. M., Schuurmans, J. M., Verschoor, A. M., Hellingwerf, K. J., Huisman, J., and Matthijs, H. C. P. (2018). Blue light reduces photosynthetic efficiency of cyanobacteria through an imbalance between photosystems I and II. Photosynthesis Research, 138(2), 177–189. https://doi.org/10.1007/S11120-018-0561-5/FIGURES/8

Luimstra, V. M., Verspagen, J. M. H., Xu, T., Schuurmans, J. M., and Huisman, J. (2020). Changes in water color shift competition between phytoplankton species with contrasting light-harvesting strategies. Ecology, 101(3), e02951. https://doi.org/10.1002/ECY.2951

Macário, I. P. E., Veloso, T., Fernandes, A. P. M., Martins, M., Frankenbach, S., Serôdio, J., Gonçalves, F. J. M., Ventura, S. P. M., and Pereira, J. L. (2023). Are cyanobacteria a nearly immortal source of high market value compounds? Journal of Chemical Technology and Biotechnology, 98(3), 734–743. https://doi.org/10.1002/JCTB.7278

Mäenpää, P., and Aro, E.-M. (1986). Chlorophyll-protein Complexes, Chlorophyll a/b Ratio and Chloroplast Ultrastructure in Lemna minor L. Grown under Different Light Conditions. Journal of Plant Physiology, 123(2), 161–168. https://doi.org/10.1016/S0176-1617(86)80137-7

Magdy, M. (2024). A Concise Look into Contact Angle Measurements in Heritage Characterization. Advanced Research in Conservation Science, 5(2), 54–69. https://doi.org/10.21608/ARCS.2024.336172.1054

Maggi, E., Bertocci, I., and Benedetti-Cecchi, L. (2019). Light pollution enhances temporal variability of photosynthetic activity in mature and developing biofilm. Hydrobiologia, 847(7), 1793–1802. https://doi.org/10.1007/s10750-019-04102-2

Mahmoud, M. M. (2021). Economic applications for LED lights in industrial sectors. In M. Casalino and J. Thirumalai (Eds.), Light-emitting diodes and photodetectors: advances and future directions (1st ed., p. 21). IntechOpen.

Maisto, F., Méndez, A., Pavlović, J., Kraková, L., Sanmartín, P., and Pangallo, D. (2025). Microbiome and response to cleaning and biocidal treatments on granite historical buildings using MinION sequencing. Construction and Building Materials, 490, 142589. https://doi.org/10.1016/j.conbuildmat.2025.142589

Maketo, L., and Ashworth, P. (2025). Social acceptance of green hydrogen in European Union and the United Kingdom: A systematic review. Renewable and Sustainable Energy Reviews, 218, 115827. https://doi.org/10.1016/J.RSER.2025.115827

Malicky, H. (2004). Atlas of European Trichoptera / Atlas der Europäischen Köcherfliegen / Atlas des Trichoptères d'Europe. In Atlas of European Trichoptera / Atlas der Europäischen Köcherfliegen / Atlas des Trichoptères d'Europe (2nd ed.). Springer Netherlands. https://doi.org/10.1007/978-1-4020-3026-0

Maluquer de Motes, J. (1992). Los pioneros de la segunda revolución industrial en España: la Sociedad Española de Electricidad (1881-1894). Revista de Historia Industrial, 2, 121–142. https://revistes.ub.edu/index.php/HistoriaIndustrial/article/view/18171/20766

Marchant, P., and Norman, P. (2023). In the best light? Road safety and public spending. Significance, 20(3), 30–31. https://doi.org/10.1093/JRSSIG/QMAD046

Maresca, J. A., Keffer, J. L., Hempel, P. P., Polson, S. W., Shevchenko, O., Bhavsar, J., Powell, D., Miller, K. J., Singh, A., and Hahn, M. W. (2019). Light Modulates the Physiology of Nonphototrophic Actinobacteria. Journal of Bacteriology, 201(10). https://doi.org/10.1128/JB.00740-18

Martínez-Rocamora, A., Solís-Guzmán, J., and Marrero, M. (2016). Toward the Ecological Footprint of the use and maintenance phase of buildings: Utility consumption and cleaning tasks. Ecological Indicators, 69, 66–77. https://doi.org/10.1016/j.ecolind.2016.04.007

Martinsons, C., Gerasimidis, T., Rayburg, S., and Rodwell, J. (2025). A Pragmatic Approach to Lighting Policy Incorporating Behaviour: The Example of Light Pollution. Sustainability 2025, Vol. 17, Page 8543, 17(19), 8543. https://doi.org/10.3390/SU17198543

Marvasi, M., Cavalieri, D., Mastromei, G., Casaccia, A., and Perito, B. (2019). Omics technologies for an in-depth investigation of biodeterioration of cultural heritage. International Biodeterioration and Biodegradation, 144, 104736. https://doi.org/10.1016/J.IBIOD.2019.104736

Marzetz, V., Katz, A., Wuthe, J., Striebel, M., and Wacker, A. (2025). The role of light quality and species richness in shaping phytoplankton communities. Limnology and Oceanography, 70(8), 2097–2108. https://doi.org/10.1002/LNO.70086

Masojídek, J., Torzillo, G., Kopecký, J., Koblížek, M., Nidiaci, L., Komenda, J., Lukavská, A., and Sacchi, A. (2000). Changes in chlorophyll fluorescence quenching and pigment composition in the green alga Chlorococcum sp. grown under nitrogen deficiency and salinity stress. Journal of Applied Phycology, 12(3–5), 417–426. https://doi.org/10.1023/A:1008165900780/METRICS

Mata, T. M., Oliveira, G. M., Monteiro, H., Silva, G. V., Caetano, N. S., and Martins, A. A. (2021). Indoor Air Quality Improvement Using Nature-Based Solutions: Design Proposals to Greener Cities. International Journal of Environmental Research and Public Health 2021, Vol. 18, Page 8472, 18(16), 8472. https://doi.org/10.3390/IJERPH18168472

McLachlan, C. (2009). Technologies in place: Symbolic interpretations of renewable energy. Sociological Review, 57(SUPPL. 2), 181–199. https://doi.org/10.1111/J.1467-954X.2010.01892.X/ASSET/A810D9D6-24D3-4834-BA05-11331AFE47A2/ASSETS/J.1467-954X.2010.01892.X.FP.PNG

Méndez, A., Carballeira, R., Balboa, S., and Sanmartín, P. (2025). Novel ornamental lighting used to halt phototrophic colonization on architectural heritage is effective under low and high daylight illuminance conditions. Journal of Building Engineering, 112, 113798. https://doi.org/10.1016/j.jobe.2025.113798

Méndez, A., Maisto, F., Pavlović, J., Rusková, M., Pangallo, D., and Sanmartín, P. (2024). Microbiome shifts elicited by ornamental lighting of granite facades identified by MinION sequencing. Journal of Photochemistry and Photobiology B: Biology, 261, 113065. https://doi.org/10.1016/j.jphotobiol.2024.113065

Méndez, A., Martín, L., Arines, J., Carballeira, R., and Sanmartín, P. (2022). Attraction of Insects to Ornamental Lighting Used on Cultural Heritage Buildings: A Case Study in an Urban Area. Insects, 13(12), 1153. https://doi.org/10.3390/insects13121153

Méndez, A., Prieto, B., Aguirre i Font, J. M., and Sanmartín, P. (2024). Better, not more, lighting: Policies in urban areas towards environmentally-sound illumination of historical stone buildings that also halts biological colonization. Science of The Total Environment, 906, 167560. https://doi.org/10.1016/j.scitotenv.2023.167560

Méndez, A., Sanmartín, P., Balboa, S., and Trueba-Santiso, A. (2024). Environmental Proteomics Elucidates Phototrophic Biofilm Responses to Ornamental Lighting on Stone-built Heritage. Microbial Ecology, 87(1), 147. https://doi.org/10.1007/s00248-024-02465-1

Menegaldo, M., Livieri, A., Isigonis, P., Pizzol, L., Tyrolt, A., Zabeo, A., Semenzin, E., and Marcomini, A. (2023). Environmental and economic sustainability in cultural heritage preventive conservation: LCA and LCC of innovative nanotechnology-based products. Cleaner Environmental Systems, 9, 100124. https://doi.org/10.1016/j.cesys.2023.100124

Mesch, G. S., and Manor, O. (1998). Social Ties, Environmental Perception, And Local Attachment. Environment and Behavior, 30(4), 504–519. https://doi.org/10.1177/001391659803000405

MIBACT. (1972). Carta del Restauro. https://sabap-pr.cultura.gov.it/wp-content/uploads/2019/01/Carta_Restauro_1972_122.pdf

Mikkola, K. (1972). Behavioural and electrophysiological responses of night-flying insects, especially Lepidoptera, to near-ultraviolet and visible light. Annales Zoologici Fennici, 9(4), 225–254.

Miller, A. Z., Rogerio-Candelera, M. A., Dionisio, A., and Macedo, M. F. (2011). Microalgae as biodeteriogens of stone cultural heritage: Qualitative and quantitative research by non-contact techniques. In M. N. Johansen (Ed.), Microalgae: Biotechnology, Microbiology and Energy (1st ed., pp. 345–358). Nova Science Publishers Pub Inc.

Miller, A. Z., Sanmartín, P., Pereira-Pardo, L., Dionísio, A., Saiz-Jimenez, C., Macedo, M. F., and Prieto, B. (2012). Bioreceptivity of building stones: A review. Science of The Total Environment, 426, 1–12. https://doi.org/10.1016/J.SCITOTENV.2012.03.026

MINCOTUR. (2008). Real Decreto 1890/2008, de 14 de noviembre, por el que se aprueba el Reglamento de eficiencia energética en instalaciones de alumbrado exterior y sus Instrucciones técnicas complementarias EA-01 a EA-07. Https://Www.Boe.Es/Buscar/Doc.Php?Id=BOE-A-2008-18634.

Mineeva, N. M. (2011). Plant Pigments as Indicators of Phytoplankton Biomass (Review). International Journal on Algae, 13(4), 330–340. https://doi.org/10.1615/INTERJALGAE.V13.I4.20

Ministerio de Fomento. (2015, October 31). Real Decreto Legislativo 7/2015, de 30 de octubre, por el que se aprueba el texto refundido de la Ley de Suelo y Rehabilitación Urbana. https://www.boe.es/buscar/act.php?id=BOE-A-2015-11723

Ministry of Agriculture, F. and the E. (2015). Real Decreto 110/2015, de 20 de febrero, sobre residuos de aparatos eléctricos y electrónicos. Https://Www.Boe.Es/Buscar/Doc.Php?Id=BOE-A-2015-1762.

Ministry of Culture. (2024). Green paper on the Sustainable Management of Cultural Heritage. Https://Libreria.Cultura.Gob.Es/Libro/Green-Paper-on-the-Sustainable-Management-of-Cultural-Heritage_10467/.

Ministry of Transport and Sustainable Mobility. (2022). Salida y puesta del sol para 2022 - Provincia de A Coruña. Https://Cdn.Mitma.Gob.Es/Portal-Web-Drupal/Salidapuestasol/2022/Coruna-2022.Txt.

Misumi, M., Katoh, H., Tomo, T., and Sonoike, K. (2016). Relationship Between Photochemical Quenching and Non-Photochemical Quenching in Six Species of Cyanobacteria Reveals Species Difference in Redox State and Species Commonality in Energy Dissipation. Plant and Cell Physiology, 57(7), 1510–1517. https://doi.org/10.1093/PCP/PCV185

Mohaddes Khorassani, S., Ferrari, A. M., Pini, M., Settembre Blundo, D., García Muiña, F. E., and García, J. F. (2019). Environmental and social impact assessment of cultural heritage restoration and its application to the Uncastillo Fortress. The International Journal of Life Cycle Assessment, 24(7), 1297–1318. https://doi.org/10.1007/s11367-018-1493-1

Mohar, A., Zagmajster, M., Verovnik, R., and Ska, B. B. (2014). Nature-friendlier lighting of objects of cultural heritage (churches) - Recommendations. 32. http://ec.europa.eu/environment/life/project/Projects/index.cfm?fuseaction=home.showFileandrep=fileandfil=LifeatNight_Recommendations_EN.pdf

Mohsenpour, S. F., and Willoughby, N. (2013). Luminescent photobioreactor design for improved algal growth and photosynthetic pigment production through spectral conversion of light. Bioresource Technology, 142, 147–153. https://doi.org/10.1016/j.biortech.2013.05.024

Mokrzycki, W., and Maciej, T. (2011). Colour difference σE — a survey. Machine Graphics and Vision, 20(4), 383–411.

Morando, M., Matteucci, E., Nascimbene, J., Borghi, A., Piervittori, R., and Favero-Longo, S. E. (2019). Effectiveness of aerobiological dispersal and microenvironmental requirements together influence spatial colonization patterns of lichen species on the stone cultural heritage. Science of The Total Environment, 685, 1066–1074. https://doi.org/10.1016/j.scitotenv.2019.06.238

Moreno Osorio, J. H., De Natale, A., Del Mondo, A., Frunzo, L., Lens, P. N. L., Esposito, G., and Pollio, A. (2020). Early colonization stages of fabric carriers by two Chlorella strains. Journal of Applied Phycology, 32(6), 3631–3644. https://doi.org/10.1007/S10811-020-02244-8/TABLES/4

Morgan-Taylor, M. (2014). Regulating Light Pollution in Europe: Legal Challenges and Ways Forward. In J. Meier, U. Hasenöhrl, K. Krause, and M. Pottharst (Eds.), Urban Lighting, Light Pollution and Society (1st ed.). Routledge.

Morgan-Taylor, M. (2023). Regulating light pollution: More than just the night sky. Science, 380(6650), 1118–1120. https://doi.org/10.1126/SCIENCE.ADH7723

Mottershead, D., and Lucas, G. (2000). The Role of Lichens in Inhibiting Erosion of a Soluble Rock. The Lichenologist, 32(6), 601–609. https://doi.org/10.1006/lich.2000.0300

Mueller, L. N., de Brouwer, J. F., Almeida, J. S., Stal, L. J., and Xavier, J. B. (2006). Analysis of a marine phototrophic biofilm by confocal laser scanning microscopy using the new image quantification software PHLIP. BMC Ecology, 6(1), 1. https://doi.org/10.1186/1472-6785-6-1

Mulec, J. (2019). Lampenflora. Encyclopedia of Caves, Third Edition, 635–641. https://doi.org/10.1016/B978-0-12-814124-3.00075-3

Muñoz-Fernández, J., Del Rosal, Y., Álvarez-Gómez, F., Hernández-Mariné, M., Guzmán-Sepúlveda, R., Korbee, N., and Figueroa, F. L. (2021). Selection of LED lighting systems for the reduction of the biodeterioration of speleothems induced by photosynthetic biofilms in the Nerja Cave (Malaga, Spain). Journal of Photochemistry and Photobiology B: Biology, 217(January). https://doi.org/10.1016/j.jphotobiol.2021.112155

Murdock, J. N., and Dodds, W. K. (2007). LINKING BENTHIC ALGAL BIOMASS TO STREAM SUBSTRATUM TOPOGRAPHY1. Journal of Phycology, 43(3), 449–460. https://doi.org/10.1111/J.1529-8817.2007.00357.X

Mustoe, G. E. (2018). Biogenic Weathering: Solubilization of Iron from Minerals by Epilithic Freshwater Algae and Cyanobacteria. Microorganisms 2018, Vol. 6, Page 8, 6(1), 8. https://doi.org/10.3390/MICROORGANISMS6010008

Mutaf, T., Oz, Y., Kose, A., Elibol, M., and Oncel, S. S. (2019). The effect of medium and light wavelength towards Stichococcus bacillaris fatty acid production and composition. Bioresource Technology, 289. https://doi.org/10.1016/j.biortech.2019.121732

Myckatyn, T. M., Cohen, J., and Chole, R. A. (2016). Clarification of the definition of a "Biofilm." Plastic and Reconstructive Surgery, 137(1), 237e–238e. https://doi.org/10.1097/PRS.0000000000001911

Nanishi, Y. (2014). Nobel Prize in Physics: The birth of the blue LED. Nature Photonics, 8(12), 884–886. https://doi.org/10.1038/NPHOTON.2014.291;SUBJMETA=1020,1089,624,639,706;KWRD=INORGANIC+LEDS,SCIENTIFIC+COMMUNITY+AND+SOCIETY

Narayan, A., Misra, M., and Singh, R. (2012). Chlorophyll Fluorescence in Plant Biology. In Biophysics. InTech. https://doi.org/10.5772/35111

National Research Council. (2007). The new science of metagenomics: Revealing the secrets of our microbial planet. The national academies press.

Negi, A., and Sarethy, I. P. (2019). Microbial Biodeterioration of Cultural Heritage: Events, Colonization, and Analyses. In Microbial Ecology (Vol. 78, Issue 4, pp. 1014–1029). Springer New York LLC. https://doi.org/10.1007/s00248-019-01366-y

Nelson, N., and Yocum, C. F. (2006). Structure and function of photosystems I and II. Annual Review of Plant Biology, 57(Volume 57, 2006), 521–565. https://doi.org/10.1146/ANNUREV.ARPLANT.57.032905.105350/CITE/REFWORKS

Niaura, A. (2013). Using the Theory of Planned Behavior to Investigate the Determinants of Environmental Behavior among Youth. Environmental Research, Engineering and Management, 63(1). https://doi.org/10.5755/j01.erem.63.1.2901

Nickerson, D. (1960). Light Sources and Color Rendering. JOSA, Vol. 50, Issue 1, Pp. 57-69, 50(1), 57–69. https://doi.org/10.1364/JOSA.50.000057

Nicol, L., and Croce, R. (2018). Light harvesting in higher plants and green algae. In R. Grondelle, H. van Amerongen, and I. van Stokkum (Eds.), Light Harvesting in Photosynthesis (1st ed., pp. 59–76). CRC Press. https://doi.org/10.1201/9781351242899-4/LIGHT-HARVESTING-HIGHER-PLANTS-GREEN-ALGAE-LAUREN-NICOL-ROBERTA-CROCE-RIENK-VAN-GRONDELLE-HERBERT-VAN-AMERONGEN-IVO-VAN-STOKKUM

NIH. (2025). Definition of next-generation sequencing. National Cancer Institute. https://www.cancer.gov/publications/dictionaries/genetics-dictionary/def/next-generation-sequencing

Nowicka-Krawczyk, P., Komar, M., and Gutarowska, B. (2022). Towards understanding the link between the deterioration of building materials and the nature of aerophytic green algae. In Science of the Total Environment (Vol. 802). Elsevier B.V. https://doi.org/10.1016/j.scitotenv.2021.149856

Ogbonna, J. C., and Tanaka, H. (1996). Night biomass loss and changes in biochemical composition of cells during light/dark cyclic culture of Chlorella pyrenoidosa. Journal of Fermentation and Bioengineering, 82(6), 558–564. https://doi.org/10.1016/S0922-338X(97)81252-4

Okpalanozie, O. E., Samson Adetunji, O., Soldovieri, F., and Masini, N. (2021). Architectural Heritage Conservation in Nigeria: The Need for Innovative Techniques. Heritage 2021, Vol. 4, Pages 2124-2139, 4(3), 2124–2139. https://doi.org/10.3390/HERITAGE4030120

Oliveira, B. E. C., Cury, J. A., and Filho, A. P. R. (2017). Biofilm extracellular polysaccharides degradation during starvation and enamel demineralization. PLOS ONE, 12(7), e0181168. https://doi.org/10.1371/JOURNAL.PONE.0181168

Oncel, S. S., and Şenyay Öncel, D. (2020). Bioactive Facade System Symbiosis as a Key for Eco-Beneficial Building Element. Green Energy and Technology, 97–122. https://doi.org/10.1007/978-3-030-20637-6_5

Oosterbroek, P. (2015). The European Families of the Diptera: Identification - Diagnosis - Biology. In The European Families of the Diptera. KNNV Publishing. https://doi.org/10.1163/9789004278066

Ortega-Calvo, J. J., Ariño, X., Hernandez-Marine, M., and Saiz-Jimenez, C. (1995). Factors affecting the weathering and colonization of monuments by phototrophic microorganisms. Science of The Total Environment, 167(1–3), 329–341. https://doi.org/10.1016/0048-9697(95)04593-P

Ortega-Morales, O., Guezennec, J., Hernández-Duque, G., Gaylarde, C. C., and Gaylarde, P. M. (2000). Phototrophic Biofilms on Ancient Mayan Buildings in Yucatan, Mexico. Current Microbiology, 40(2), 81–85. https://doi.org/10.1007/s002849910015

Osticioli, I., Mascalchi, M., Pinna, D., and Siano, S. (2013). Potential of chlorophyll fluorescence imaging for assessing bio-viability changes of biodeteriogen growths on stone monuments. Https://Doi.Org/10.1117/12.2020563, 8790, 12–18. https://doi.org/10.1117/12.2020563

O'Toole, G. A. (2003). To build a biofilm. Journal of Bacteriology, 185(9), 2687–2689. https://doi.org/10.1128/JB.185.9.2687-2689.2003/ASSET/05178B79-EB37-4A98-8686-ABAD91684AC6/ASSETS/GRAPHIC/JB0930073001.JPEG

Owens, A. C., Pocock, M. J., and Seymoure, B. M. (2024). Current evidence in support of insect-friendly lighting practices. Current Opinion in Insect Science, 66, 101276. https://doi.org/10.1016/J.COIS.2024.101276

Paolino, B., Prestileo, F., Carnazza, P., Sacco, F., Strozzi, A., Congeduti, A., and Macchia, A. (2025). Life Cycle Impact Assessment (LCIA) of Materials in Painting Conservation: A Pilot Protocol for Evaluating Environmental Impact in Cultural Heritage. Heritage 2025, Vol. 8, Page 212, 8(6), 212. https://doi.org/10.3390/HERITAGE8060212

Papageorgiou, G. C., Tsimilli-Michael, M., and Stamatakis, K. (2007). The fast and slow kinetics of chlorophyll a fluorescence induction in plants, algae and cyanobacteria: A viewpoint. Photosynthesis Research, 94(2–3), 275–290. https://doi.org/10.1007/s11120-007-9193-x

Paper, M., Glemser, M., Haack, M., Lorenzen, J., Mehlmer, N., Fuchs, T., Schenk, G., Garbe, D., Weuster-Botz, D., Eisenreich, W., Lakatos, M., and Brück, T. B. (2022). Efficient Green Light Acclimation of the Green Algae Picochlorum sp. Triggering Geranylgeranylated Chlorophylls. Frontiers in Bioengineering and Biotechnology, 10, 885977. https://doi.org/10.3389/FBIOE.2022.885977/BIBTEX

Papida, S., Murphy, W., and May, E. (2000). Enhancement of physical weathering of building stones by microbial populations. International Biodeterioration and Biodegradation, 46(4), 305–317. https://doi.org/10.1016/S0964-8305(00)00102-5

Parkhill, J. P., Maillet, G., and Cullen, J. J. (2001). Fluorescence-based maximal quantum yield for psii as a diagnostic of nutrient stress. Journal of Phycology, 37(4), 517–529. https://doi.org/10.1046/J.1529-8817.2001.037004517.X

Parveen, A., Bhatnagar, P., Gautam, P., Bisht, B., Nanda, M., Kumar, S., Vlaskin, M. S., and Kumar, V. (2023). Enhancing the bio-prospective of microalgae by different light systems and photoperiods. Photochemical and Photobiological Sciences, 22(11), 2687–2698. https://doi.org/10.1007/S43630-023-00471-9/TABLES/2

Pavissich, J. P., Li, M., and Nerenberg, R. (2021). Spatial distribution of mechanical properties in Pseudomonas aeruginosa biofilms, and their potential impacts on biofilm deformation. Biotechnology and Bioengineering, 118(4), 1545–1556. https://doi.org/10.1002/bit.27671

Pavlović, J., Bosch-Roig, P., Rusková, M., Planý, M., Pangallo, D., and Sanmartín, P. (2022). Long-amplicon MinION-based sequencing study in a salt-contaminated twelfth century granite-built

chapel. Applied Microbiology and Biotechnology, 106(11), 4297–4314. https://doi.org/10.1007/s00253-022-11961-8

Peers, G., Truong, T. B., Ostendorf, E., Busch, A., Elrad, D., Grossman, A. R., Hippler, M., and Niyogi, K. K. (2009). An ancient light-harvesting protein is critical for the regulation of algal photosynthesis. Nature, 462(7272), 518–521. https://doi.org/10.1038/NATURE08587;KWRD=SCIENCE

Peraza Zurita, Y., Cultrone, G., Sánchez Castillo, P., Sebastián, E., and Bolívar, F. C. (2005). Microalgae associated with deteriorated stonework of the fountain of Bibatauín in Granada, Spain. International Biodeterioration and Biodegradation, 55(1), 55–61. https://doi.org/10.1016/J.IBIOD.2004.05.006

Petersen, L. M., Martin, I. W., Moschetti, W. E., Kershaw, C. M., and Tsongalis, G. J. (2020). Third-generation sequencing in the clinical laboratory: Exploring the advantages and challenges of nanopore sequencing. Journal of Clinical Microbiology, 58(1). https://doi.org/10.1128/JCM.01315-19;SUBPAGE:STRING:FULL

Peterson, B. W., He, Y., Ren, Y., Zerdoum, A., Libera, M. R., Sharma, P. K., van Winkelhoff, A. J., Neut, D., Stoodley, P., van der Mei, H. C., and Busscher, H. J. (2015). Viscoelasticity of biofilms and their recalcitrance to mechanical and chemical challenges. FEMS Microbiology Reviews, 39(2), 234–245. https://doi.org/10.1093/FEMSRE/FUU008

Phillips-Lander, C. M., Harrold, Z., Hausrath, E. M., Lanzirotti, A., Newville, M., Adcock, C. T., Raymond, J. A., Huang, S., Tschauner, O., and Sanchez, A. (2020). Snow Algae Preferentially Grow on Fe-containing Minerals and Contribute to the Formation of Fe Phases. Geomicrobiology Journal, 37(6), 572–581. https://doi.org/10.1080/01490451.2020.1739176

Piazza, V., Bevilacqua, F., Grillini, G. C., and Pinna, D. (1998). Ravenna - Mausoleo di Teodorico. Esiti delle ultime indagini e progetto. In G. Bisconti and G. Driussi (Eds.), Progettare i Restauri. Orientamenti e Metodi –Indagini e Materiali, Atti Convegno di Studi (pp. 251–260). Arcadia Ricerche.

Picardo, A., Galván, M. J., Soltero, V. M., and Peralta, E. (2023). A Comparative Life Cycle Assessment and Costing of Lighting Systems for Environmental Design and Construction of Sustainable Roads. Buildings, 13(4), 983. https://doi.org/10.3390/buildings13040983

Pinheiro, A. C., Mesquita, N., Trovão, J., Soares, F., Tiago, I., Coelho, C., de Carvalho, H. P., Gil, F., Catarino, L., Piñar, G., and Portugal, A. (2019). Limestone biodeterioration: A review on the Portuguese cultural heritage scenario. Journal of Cultural Heritage, 36, 275–285. https://doi.org/10.1016/J.CULHER.2018.07.008

Pinna, D. (2017). Coping with Biological Growth on Stone Heritage Objects. Apple Academic Press. https://doi.org/10.1201/9781315365510

Pinna, D. (2021). Microbial Growth and its Effects on Inorganic Heritage Materials. In Microorganisms in the Deterioration and Preservation of Cultural Heritage (pp. 3–35). Springer International Publishing. https://doi.org/10.1007/978-3-030-69411-1_1

Pinna, D. (2022). Can we do without biocides to cope with biofilms and lichens on stone heritage? International Biodeterioration and Biodegradation, 172, 105437. https://doi.org/10.1016/j.ibiod.2022.105437

Pinna, D., Galeotti, M., Perito, B., Daly, G., and Salvadori, B. (2018). In situ long-term monitoring of recolonization by fungi and lichens after innovative and traditional conservative treatments of archaeological stones in Fiesole (Italy). International Biodeterioration and Biodegradation, 132, 49–58. https://doi.org/10.1016/j.ibiod.2018.05.003

Pino-Bodas, R., Blázquez, M., de los Ríos, A., and Pérez-Ortega, S. (2023). Myrmecia, Not Asterochloris, Is the Main Photobiont of Cladonia subturgida (Cladoniaceae, Lecanoromycetes). Journal of Fungi, 9(12), 1160. https://doi.org/10.3390/JOF9121160/S1

Popović, S., Pećić, M., and Subakov Simić, G. (2022). Exploring Lampenflora of Resavska Cave, Serbia. The 2nd International Electronic Conference on Diversity (IECD 2022)andmdash;New Insights into the Biodiversity of Plants, Animals and Microbes, 33. https://doi.org/10.3390/IECD2022-12425

Postmes, T., Rabinovich, A., Morton, T., and van Zomeren, M. (2013). Toward Sustainable Social Identities : Including Our Collective Future Into the Self-Concept. In H. C. M. van Trijp (Ed.), Encouraging Sustainable Behavior (1st ed., pp. 185–201). Psychology Press. https://doi.org/10.4324/9780203141182-19

Pothukuchi, K. (2025). Mitigating urban light pollution: A review of municipal regulations and implications for planners. Journal of Urban Affairs, 47(5), 1663–1690. https://doi.org/10.1080/07352166.2023.2247506

Pouli, P., Oujja, M., and Castillejo, M. (2012). Practical issues in laser cleaning of stone and painted artefacts: Optimisation procedures and side effects. Applied Physics A: Materials Science and Processing, 106(2), 447–464. https://doi.org/10.1007/S00339-011-6696-2/FIGURES/15

Poulin, C., Bruyant, F., Laprise, M. H., Cockshutt, A. M., Marie-Rose Vandenhecke, J., and Huot, Y. (2014). The impact of light pollution on diel changes in the photophysiology of Microcystis aeruginosa. Journal of Plankton Research, 36(1), 286–291. https://doi.org/10.1093/PLANKT/FBT088

Pozo-Antonio, J. S., Rivas, T., López, A. J., Fiorucci, M. P., and Ramil, A. (2016). Effectiveness of granite cleaning procedures in cultural heritage: A review. Science of The Total Environment, 571, 1017–1028. https://doi.org/10.1016/J.SCITOTENV.2016.07.090

Prieto, B., and Sanmartín, P. (2016). Air Pollution and Changes to the Biology of Urban Fabric (P. Brimblecombe, Ed.; 1st ed., pp. 193–224). Imperial College Press. https://doi.org/10.1142/9781783268863_0008

Prieto, B., Sanmartín, P., Aira, N., and Silva, B. (2010). Color of cyanobacteria: some methodological aspects. Applied Optics, Vol. 49, Issue 11, Pp. 2022-2029, 49(11), 2022–2029. https://doi.org/10.1364/AO.49.002022

Prieto, B., Sanmartín, P., Silva, B., and Martínez-Verdú, F. (2010). Measuring the color of granite rocks: A proposed procedure. Color Research and Application, 35(5), 368–375. https://doi.org/10.1002/COL.20579;PAGEGROUP:STRING:PUBLICATION

Prieto, B., Silva, B., Aira, N., and Laiz, L. (2005). Induction of biofilms on quartz surfaces as a means of reducingthe visual impact of quartz quarries. Biofouling, 21(5–6), 237–246. https://doi.org/10.1080/08927010500421294

Prieto, B., Silva, B., Carballal, R., and de Silanes, M. E. L. (1994). Colonization by lichens of granite dolmens in Galicia (NW Spain). International Biodeterioration and Biodegradation, 34(1), 47–60. https://doi.org/10.1016/0964-8305(94)90019-1

Prieto, B., Silva, B., and Lantes, O. (2004). Biofilm quantification on stone surfaces: comparison of various methods. Science of The Total Environment, 333(1–3), 1–7. https://doi.org/10.1016/J.SCITOTENV.2004.05.003

Proshansky, H. M., Fabian, A. K., and Kaminoff, R. (1983). Place-identity: Physical world socialization of the self. Journal of Environmental Psychology, 3(1), 57–83. https://doi.org/10.1016/S0272-4944(83)80021-8

Psachoulia, P., and Chatzidoukas, C. (2021). Illumination Policies for Stichococcus sp. Cultures in an Optimally Operating Lab-Scale PBR toward the Directed Photosynthetic Production of Desired Products. Sustainability 2021, Vol. 13, Page 2489, 13(5), 2489. https://doi.org/10.3390/SU13052489

Quagliarini, E., Bondioli, F., Goffredo, G. B., Licciulli, A., and Munafò, P. (2013). Self-cleaning materials on Architectural Heritage: Compatibility of photo-induced hydrophilicity of TiO2 coatings on stone surfaces. Journal of Cultural Heritage, 14(1), 1–7. https://doi.org/10.1016/j.culher.2012.02.006

R Core Team. (2024). R: A Language and Environment for Statistical Computing. R Foundation for Statistical Computing.

Ra, C. H., Kang, C. H., Jung, J. H., Jeong, G. T., and Kim, S. K. (2016). Effects of light-emitting diodes (LEDs) on the accumulation of lipid content using a two-phase culture process with three microalgae. Bioresource Technology, 212, 254–261. https://doi.org/10.1016/J.BIORTECH.2016.04.059

Ramil, A., Vázquez-Nion, D., Pozo-Antonio, J. S., Sanmartín, P., and Prieto, B. (2020). Using hyperspectral imaging to quantify phototrophic biofilms on granite. Journal of Environmental Informatics, 35(1), 34. https://doi.org/10.3808/JEI.201800401

Rappé, M. S., and Giovannoni, S. J. (2003). The Uncultured Microbial Majority. Annual Review of Microbiology, 57(Volume 57, 2003), 369–394. https://doi.org/10.1146/ANNUREV.MICRO.57.030502.090759/1

Rastandeh, A., Brown, D., and Pedersen Zari, M. (2017). Biodiversity conservation in urban environments: a review on the importance of spatial patterning of landscape. Ecocity World Summit.

Raven, J. A., and Beardall, J. (2016). Dark Respiration and Organic Carbon Loss. In The Physiology of Microalgae (pp. 129–140). Springer International Publishing. https://doi.org/10.1007/978-3-319-24945-2_6

Redacción del periódico Diario de Burgos. (1935, November 25). España monumental y artística. Diario de Burgos.

Redacción del periódico El Castellano. (1934, January 18). La sesión municipal de ayer. El Castellano.

Rifón-Lastra, A., and Noguerol-Seoane, Á. (2001a). Algunas Chlorellaceae nuevas o poco citadas para la Península Ibérica. Botanica Complutensis, 25, 165–177. https://revistas.ucm.es/index.php/BOCM/article/view/BOCM0101110165A/6385

Rifón-Lastra, A., and Noguerol-Seoane, Á. (2001b). Green algae associated with the granite walls of monuments in Galicia (NW Spain). Cryptogamie Algologie, 22(3), 305–326. https://doi.org/10.1016/S0181-1568(01)01069-8

Rippka, R., Deruelles, J., and Waterbury, J. B. (1979). Generic assignments, strain histories and properties of pure cultures of cyanobacteria. Journal of General Microbiology, 111(1), 1–61. https://doi.org/10.1099/00221287-111-1-1/CITE/REFWORKS

Robert, K. A., Dimovski, A. M., Contos, P., Khwaja, N., and Griffiths, S. R. (2025). Divergent responses of insectivorous bats and flying insects to experimental LED illumination of different spectra. Ecosphere, 16(5), e70291. https://doi.org/10.1002/ECS2.70291

Rodrigo-Comino, J., Seeling, S., Seeger, M. K., and Ries, J. B. (2021). Light pollution: A review of the scientific literature. The Anthropocene Review, 10(2), 367–392. https://doi.org/10.1177/20530196211051209

Rodriguez, J. (2024). Santiago experimenta un auge turístico este agosto. Https://Www.Diariodesantiago.Es/Santiago/Santiago-Experimenta-Un-Auge-Turistico-Este-Agosto/#:~:Text=En%20total%2C%20108.348%20personas%20visitaron,Establece%20un%20nuevo%20r%C3%A9cord%20hist%C3%B3rico.

Rodriguez Lorite, M. A. (2016). Guía de iluminación eficiente de monumentos. 209.

Rodriguez-Navarro, C., Elert, K., Sebastian, E., Esbert, R. M., Grossi, C. M., Rojo, A., Alonso, F. J., Montoto, M., and Ordaz, J. (2003). Laser cleaning of stone materials: an overview of current research. Studies in Conservation, 48(sup1), 65–82. https://doi.org/10.1179/SIC.2003.48.SUPPLEMENT-1.65

Roenneberg, T., Winnebeck, E. C., and Klerman, E. B. (2019). Daylight Saving Time and Artificial Time Zones – A Battle Between Biological and Social Times. Frontiers in Physiology, 10. https://doi.org/10.3389/fphys.2019.00944

Rojo, A., Alonso, F. J., and Esbert, R. M. (2003). Propiedades hídricas de algunos granitos ornamentales de la península ibérica con distintos acabados superficiales: interpretación petrofísica. Materiales de Construcción, 53(269), 61–72.

Romaní, J. R. V. (2023). Introduction to the Geology of Galicia. In The Environment in Galicia: A Book of Images (pp. 21–35). Springer International Publishing. https://doi.org/10.1007/978-3-031-33114-5_3

Rosentritt, M., Schneider-Feyrer, S., and Kurzendorfer, L. (2024). Comparison of surface roughness parameters Ra/Sa and Rz/Sz with different measuring devices. Journal of the Mechanical Behavior of Biomedical Materials, 150, 106349. https://doi.org/10.1016/J.JMBBM.2023.106349

Rossi, F., Micheletti, E., Bruno, L., Adhikary, S. P., Albertano, P., and De Philippis, R. (2012). Characteristics and role of the exocellular polysaccharides produced by five cyanobacteria isolated from phototrophic biofilms growing on stone monuments. Biofouling, 28(2), 215–224. https://doi.org/10.1080/08927014.2012.663751

Roux, C., Madru, C., Millan Navarro, D., Jan, G., Mazzella, N., Moreira, A., Vedrenne, J., Carassou, L., and Morin, S. (2024). Impact of urban pollution on freshwater biofilms: Oxidative stress, photosynthesis and lipid responses. Journal of Hazardous Materials, 472, 134523. https://doi.org/10.1016/j.jhazmat.2024.134523

Saiz-Jimenez, C. (1995). Deposition of anthropogenic compounds on monuments and their effect on airborne microorganisms. Aerobiologia, 11(3), 161–175. https://doi.org/10.1007/BF02450035/METRICS

Salata, F., Golasi, I., Falanga, G., Allegri, M., De Lieto Vollaro, E., Nardecchia, F., Pagliaro, F., Gugliermetti, F., and De Lieto Vollaro, A. (2015). Maintenance and energy optimization of lighting systems for the improvement of historic buildings: A case study. Sustainability (Switzerland), 7(8), 10770–10788. https://doi.org/10.3390/su70810770

Samad, L. K., and Adhikary, S. P. (2008). Diversity of Micro-algae and Cyanobacteria on Building Facades and Monuments in Ind. Algae, 23(2), 91–114.

Sánchez-Tabernero, G., Muñoz-Sosa, C., Hidalgo-Muñoz, A. R., Galán, J. I., and Tabernero, C. (2025). Understanding the Causes of Social Acceptance and Rejection of a Uranium Mine Development Project in Northwestern Spain. Sustainability (Switzerland), 17(2), 429. https://doi.org/10.3390/SU17020429/S1

Sandeep, R., Muscolino, J. F., Macêdo, W. V., Piculell, M., Christensson, M., Poulsen, J. S., Nielsen, J. L., and Vergeynst, L. (2023). Effect of biofilm thickness on the activity and community composition of phosphorus accumulating bacteria in a moving bed biofilm reactor. Water Research, 245, 120599. https://doi.org/10.1016/J.WATRES.2023.120599

Sanders, D., Frago, E., Kehoe, R., Patterson, C., and Gaston, K. J. (2021). A meta-analysis of biological impacts of artificial light at night. Nature Ecology and Evolution, 5(1), 74–81. https://doi.org/10.1038/s41559-020-01322-x

Sanjurjo-Sánchez, J., Alves, C., and Freire-Lista, D. M. (2024). Biomineral deposits and coatings on stone monuments as biodeterioration fingerprints. Science of The Total Environment, 912, 168846. https://doi.org/10.1016/J.SCITOTENV.2023.168846

Sankhwar, P. (2024). Conversion of Streetlights to Light-emitting Diode (LED) Type. https://doi.org/10.21203/rs.3.rs-5085635/v1

Sanmartín, P. (2021). New Perspectives Against Biodeterioration Through Public Lighting. In Microorganisms in the Deterioration and Preservation of Cultural Heritage (pp. 155–171). Springer International Publishing. https://doi.org/10.1007/978-3-030-69411-1_7

Sanmartín, P., Méndez, A., Carballeira, R., and López, E. (2021). New insights into the growth and diversity of subaerial biofilms colonizing granite-built heritage exposed to UV-A or UV-B radiation plus red LED light. International Biodeterioration and Biodegradation, 161(April). https://doi.org/10.1016/j.ibiod.2021.105225

Sanmartín, P., Vázquez-Nion, D., Arines, J., Cabo-Domínguez, L., and Prieto, B. (2017). Controlling growth and colour of phototrophs by using simple and inexpensive coloured lighting: A preliminary study in the Light4Heritage project towards future strategies for outdoor illumination. International Biodeterioration and Biodegradation, 122, 107–115. https://doi.org/10.1016/j.ibiod.2017.05.003

Sanmartín, P., Vázquez-Nion, D., Silva, B., and Prieto, B. (2012). Spectrophotometric color measurement for early detection and monitoring of greening on granite buildings. Biofouling, 28(3), 329–338. https://doi.org/10.1080/08927014.2012.673220

Sanmartín, P., Villa, F., Cappitelli, F., Balboa, S., and Carballeira, R. (2020). Characterization of a biofilm and the pattern outlined by its growth on a granite-built cloister in the Monastery of San Martiño Pinario (Santiago de Compostela, NW Spain). International Biodeterioration and Biodegradation, 147. https://doi.org/10.1016/j.ibiod.2019.104871

Sanmartín, P., Villa, F., Silva, B., Cappitelli, F., and Prieto, B. (2011). Color measurements as a reliable method for estimating chlorophyll degradation to phaeopigments. Biodegradation, 22(4), 763–771. https://doi.org/10.1007/s10532-010-9402-8

Santabarbara, S., Villafiorita Monteleone, F., Remelli, W., Rizzo, F., Menin, B., and Casazza, A. P. (2019). Comparative excitation-emission dependence of the F V /F M ratio in model green algae and cyanobacterial strains. Physiologia Plantarum, 166(1), 351–364. https://doi.org/10.1111/PPL.12931;ISSUE:ISSUE:DOI

Santi, P., and Pereira, D. (2023). The Value of Natural Stones to Gain in the Cultural and Geological Diversity of Our Global Heritage. Heritage 2023, Vol. 6, Pages 4542-4556, 6(6), 4542–4556. https://doi.org/10.3390/HERITAGE6060241

Sari, P., Munandar, A., and Fatimah, I. S. (2018). Perception of place attachment between cultural heritage in Yogyakarta City. IOP Conference Series: Earth and Environmental Science, 179, 012012. https://doi.org/10.1088/1755-1315/179/1/012012

Schanda, J. (2007). Colorimetry: Understanding the CIE System. In Colorimetry: Understanding the CIE System (1st ed.). John Wiley and Sons. https://doi.org/10.1002/9780470175637

Schneider, T., and Riedel, K. (2010). Environmental proteomics: Analysis of structure and function of microbial communities. PROTEOMICS, 10(4), 785–798. https://doi.org/10.1002/pmic.200900450

Schnurr, P. J., and Allen, D. G. (2015). Factors affecting algae biofilm growth and lipid production: A review. Renewable and Sustainable Energy Reviews, 52, 418–429. https://doi.org/10.1016/J.RSER.2015.07.090

Schreiber, U. (2004). Pulse-Amplitude-Modulation (PAM) Fluorometry and Saturation Pulse Method: An Overview. In G. C. Papageorgiou and Govindjee (Eds.), Chlorophyll a Fluorescence. Advances in Photosynthesis and Respiration (Vol. 19, pp. 279–319). Springer,. https://doi.org/10.1007/978-1-4020-3218-9_11

Schröer, L., De Kock, T., Godts, S., Boon, N., and Cnudde, V. (2022). The effects of cyanobacterial biofilms on water transport and retention of natural building stones. Earth Surface Processes and Landforms, 47(8), 1921–1936. https://doi.org/10.1002/ESP.5355

Schultz, P. W., Shriver, C., Tabanico, J. J., and Khazian, A. M. (2004). Implicit connections with nature. Journal of Environmental Psychology, 24(1), 31–42. https://doi.org/10.1016/S0272-4944(03)00022-7

Schuurmans, R. M., Van Alphen, P., Schuurmans, J. M., Matthijs, H. C. P., and Hellingwerf, K. J. (2015). Comparison of the Photosynthetic Yield of Cyanobacteria and Green Algae: Different Methods Give Different Answers. PLOS ONE, 10(9), e0139061. https://doi.org/10.1371/JOURNAL.PONE.0139061

Scovell, M. D. (2022). Explaining hydrogen energy technology acceptance: A critical review. International Journal of Hydrogen Energy, 47(19), 10441–10459. https://doi.org/10.1016/J.IJHYDENE.2022.01.099

Seamon, D., and Gill, H. K. (2015). Qualitative Approaches to Environment–Behavior Research. Research Methods for Environmental Psychology, 115–135. https://doi.org/10.1002/9781119162124.CH7

Sekar, R., Venugopalan, V. P., Satpathy, K. K., Nair, K. V. K., and Rao, V. N. R. (2004). Laboratory studies on adhesion of microalgae to hard substrates. Asian Pacific Phycology in the 21st Century: Prospects and Challenges, 109–116. https://doi.org/10.1007/978-94-007-0944-7_14

Seki, S., Kobayashi, K., and Fujii, R. (2025). Photosynthetic capacity and pigment distribution of a siphonous green alga, Dichotomosiphon tuberosus. Photosynthesis Research, 163(3), 1–12. https://doi.org/10.1007/S11120-025-01148-3/TABLES/1

Semadeni, M., Hansmann, R., and Flüeler, T. (2004). Public Attitudes in Relation to Risk and Novelty of Future Energy Options. Energy and Environment, 15(5), 755–777. https://doi.org/10.1260/0958305042886787

Sequeiro, N. (2024). La transformación turística de Santiago: un 420% más de viajeros que hace dos décadas. Https://Www.Elcorreogallego.Es/Santiago/2024/10/06/Transformacion-Turistica-Santiago-Viajeros-Dos-Decadas-108958376.Html.

Serôdio, J., Da Silva, J. M., and Catarino, F. (2001). Use of in vivo chlorophyll a fluorescence to quantify short-term variations in the productive biomass of intertidal microphytobenthos. Marine Ecology Progress Series, 218, 45–61. https://doi.org/10.3354/MEPS218045

Seviour, T., Derlon, N., Dueholm, M. S., Flemming, H. C., Girbal-Neuhauser, E., Horn, H., Kjelleberg, S., van Loosdrecht, M. C. M., Lotti, T., Malpei, M. F., Nerenberg, R., Neu, T. R., Paul, E., Yu, H., and Lin, Y. (2019). Extracellular polymeric substances of biofilms: Suffering from an identity crisis. Water Research, 151, 1–7. https://doi.org/10.1016/J.WATRES.2018.11.020

Shirobokova, T. A., Shuvalova, L. A., Novoselov, I. M., and Pokoev, P. N. (2022). Prospects for the Use of LED Lighting Devices in Poultry Farming. AIP Conference Proceedings, 2661(1). https://doi.org/10.1063/5.0107533/2832186

Siegesmund, S., and Dürrast, H. (2011). Physical and Mechanical Properties of Rocks. In R. Snethlage (Ed.), Stone in Architecture: Properties, Durability (pp. 97–225). Springer. https://doi.org/10.1007/978-3-642-14475-2_3

Siegesmund, S., and Török, Á. (2011). Building Stones. Stone in Architecture: Properties, Durability, 11–95. https://doi.org/10.1007/978-3-642-14475-2_2

Silva, B. (2024). La piedra de los monumentos gallegos, formas de alteración y procesos de deterio (B. Prieto Lamas and T. Rivas Brea, Eds.). Universidade de Vigo. https://libreriaabrente.es/products/la-piedra-de-los-monumentos-gallegos

Singh, D., Basu, C., Meinhardt-Wollweber, M., and Roth, B. (2015). LEDs for energy efficient greenhouse lighting. Renewable and Sustainable Energy Reviews, 49, 139–147. https://doi.org/10.1016/J.RSER.2015.04.117

Singh, S. K., Reddy, V. R., Fleisher, D. H., and Timlin, D. J. (2016). Relationship between photosynthetic pigments and chlorophyll fluorescence in soybean under varying phosphorus nutrition at ambient and elevated CO2. Photosynthetica 2017 55:3, 55(3), 421–433. https://doi.org/10.1007/S11099-016-0657-0

Škaloud, P., Rindi, F., Boedeker, C., and Leliaert, F. (2018). Freshwater Flora of Central Europe, Vol 13: Chlorophyta: Ulvophyceae . In Freshwater Flora of Central Europe, Vol 13: Chlorophyta: Ulvophyceae (Süßwasserflora von Mitteleuropa, Bd. 13: Chlorophyta: Ulvophyceae) (1st ed.). Springer Spektrum Berlin. https://doi.org/10.1007/978-3-662-55495-1

Skandali, C., and Whitlock Blundell, E. (2022). Conceiving monument networks through lighting design. Academia Letters. https://doi.org/10.20935/AL4496

Sliney, D. H. (2016). What is light? the visible spectrum and beyond. Eye (Basingstoke), 30(2), 222–229. https://doi.org/10.1038/EYE.2015.252;SUBJMETA=160,499,648,692,706;KWRD=EDUCATION,RISK+FACTORS

Smith, B. J., McCabe, S., McAllister, D., Adamson, C., Viles, H. A., and Curran, J. M. (2011). A commentary on climate change, stone decay dynamics and the 'greening' of natural stone buildings: new perspectives on 'deep wetting.' Environmental Earth Sciences, 63(7–8), 1691–1700. https://doi.org/10.1007/s12665-010-0766-1

Smith, B. M., Morrissey, P. J., Guenther, J. E., Nemson, J. A., Harrison, M. A., Allen, J. F., and Melis, A. (1990). Response of the Photosynthetic Apparatus in Dunaliella salina (Green Algae) to Irradiance Stress. Plant Physiology, 93(4), 1433–1440. https://doi.org/10.1104/PP.93.4.1433

Staats, N., Stal, L., de Winder, B., and Mur, L. (2000). Oxygenic photosynthesis as driving process in exopolysaccharide production of benthic diatoms. Marine Ecology Progress Series, 193, 261–269. https://doi.org/10.3354/meps193261

Stedman, R. C. (2002). Toward a Social Psychology of Place. Environment and Behavior, 34(5), 561–581. https://doi.org/10.1177/0013916502034005001

Steg, L., and de Groot, J. I. M. (2018). Environmental Psychology (L. Steg and J. I. M. Groot, Eds.). Wiley. https://doi.org/10.1002/9781119241072

Steiger, M. (2016). Air Pollution Damage to Stone. In P. Brimblecore (Ed.), Urban Pollution and Changes to Materials and Building Surfaces (Vol. 5, pp. 65–102). Imperial College Press. https://doi.org/10.1142/9781783268863_0003

Steiger, M., Charola, A. E., and Sterflinger, K. (2011). Weathering and Deterioration. In S. Siegesmund and R. Snethlage (Eds.), Stone in Architecture: Properties, Durability (4th ed., pp. 227–316). Springer-Verlag Berlin Heidelberg. https://doi.org/10.1007/978-3-642-14475-2_4

Stick, C. (2007). Sonnenzeit - die Bedeutung der gesetzlichen Zonenzeit für die UV-Exposition der Haut. JDDG: Journal Der Deutschen Dermatologischen Gesellschaft, 5(9), 788–792. https://doi.org/10.1111/j.1610-0387.2007.06421.x

Stockenreiter, M., Isanta Navarro, J., Buchberger, F., and Stibor, H. (2021). Community shifts from eukaryote to cyanobacteria dominated phytoplankton: The role of mixing depth and light quality. Freshwater Biology, 66(11), 2145–2157. https://doi.org/10.1111/FWB.13822

Streckeisen, A. (1976). To each plutonic rock its proper name. Earth-Science Reviews, 12(1), 1–33. https://doi.org/10.1016/0012-8252(76)90052-0

Stubbs, M. (2004). Heritage-sustainability: developing a methodology for the sustainable appraisal of the historic environment. Planning Practice and Research, 19(3), 285–305. https://doi.org/10.1080/0269745042000323229

Sumanasekara, H., Jayasingha, H., Amarasooriya, G., Dayarathne, N., Mainali, B., Senevirathna, L., Gamage, A., and Merah, O. (2025). Hybrid Machine Learning Models for Predicting the Impact of Light Wavelengths on Algal Growth in Freshwater Ecosystems. Phycology 2025, Vol. 5, Page 23, 5(2), 23. https://doi.org/10.3390/PHYCOLOGY5020023

Sun, Y. Y., Gossling, S., and Zhou, W. (2022). Does tourism increase or decrease carbon emissions? A systematic review. Annals of Tourism Research, 97, 103502. https://doi.org/10.1016/J.ANNALS.2022.103502

Svechkina, A., Portnov, B. A., and Trop, T. (2020). The impact of artificial light at night on human and ecosystem health: a systematic literature review. Landscape Ecology, 35(8), 1725–1742. https://doi.org/10.1007/s10980-020-01053-1

Swarr, T. E., Hunkeler, D., Klöpffer, W., Pesonen, H.-L., Ciroth, A., Brent, A. C., and Pagan, R. (2011). Environmental life-cycle costing: a code of practice. The International Journal of Life Cycle Assessment, 16(5), 389–391. https://doi.org/10.1007/s11367-011-0287-5

Taboada, J., Alejano, L. R., Bastante, F. G., and Ordoñez, C. (2005). APROVECHAMIENTO INTEGRAL DE UNA CANTERA DE GRANITO ORNAMENTAL. Materiales de Construcción, 5, 279–298.

Tähkämö, L., and Halonen, L. (2015). Life cycle assessment of road lighting luminaires – Comparison of light-emitting diode and high-pressure sodium technologies. Journal of Cleaner Production, 93, 234–242. https://doi.org/10.1016/j.jclepro.2015.01.025

Taín Guzmán, M. (2012). La Casa del Cabildo: inmueble y solar en el paisaje urbano del barroco compostelano. Quintana: Revista Do Departamento de Historia Da Arte, 11. https://doi.org/10.15304/qui.11.1615

Tajfel, H. (1981). Human groups and social categories : studies in social psychology. Cambridge University Press.

Talamo, M., Valentini, F., Dimitri, A., and Allegrini, I. (2020). Innovative Technologies for Cultural Heritage. Tattoo Sensors and AI: The New Life of Cultural Assets. Sensors 2020, Vol. 20, Page 1909, 20(7), 1909. https://doi.org/10.3390/S20071909

Ter Braak, C. J. F. (1983). Principal Components Biplots and Alpha and Beta Diversity. Ecology, 64(3), 454–462. https://doi.org/10.2307/1939964

Terashima, I., Fujita, T., Inoue, T., Chow, W. S., and Oguchi, R. (2009). Green Light Drives Leaf Photosynthesis More Efficiently than Red Light in Strong White Light: Revisiting the Enigmatic Question of Why Leaves are Green. Plant and Cell Physiology, 50(4), 684–697. https://doi.org/10.1093/pcp/pcp034

Toli, A. M., and Murtagh, N. (2020). The Concept of Sustainability in Smart City Definitions. Frontiers in Built Environment, 6, 496662. https://doi.org/10.3389/FBUIL.2020.00077/BIBTEX

Torcal, M., and Christmann, P. (2021). Responsiveness, Performance and Corruption: Reasons for the Decline of Political Trust. Frontiers in Political Science, 3, 676672. https://doi.org/10.3389/FPOS.2021.676672/BIBTEX

Tretiach, M., Bertuzzi, S., and Salvadori, O. (2010). Chlorophyll a fluorescence as a practical tool for checking the effects of biocide treatments on endolithic lichens. International Biodeterioration and Biodegradation, 64(6), 452–460. https://doi.org/10.1016/J.IBIOD.2010.05.004

Tribaudino, M., Angel, R. J., Cámara, F., Nestola, F., Pasqual, D., and Margiolaki, I. (2010). Thermal expansion of plagioclase feldspars. Contributions to Mineralogy and Petrology, 160(6), 899–908. https://doi.org/10.1007/s00410-010-0513-3

Tserevelakis, G. J., Pozo-Antonio, J. S., Siozos, P., Rivas, T., Pouli, P., and Zacharakis, G. (2019). On-line photoacoustic monitoring of laser cleaning on stone: Evaluation of cleaning effectiveness and detection of potential damage to the substrate. Journal of Cultural Heritage, 35, 108–115. https://doi.org/10.1016/j.culher.2018.05.014

Tuazon, K. J. L., Moñedera, S. P., Corpuz, J. T., Mijares, A. M. I., Singh, R. C., Guillo, A. J., and De Guzmán, S. D. (2024). Assessing the Impact of Environmental Education on Sustainable Practices: A Semi-Systematic Literature Review. International Journal of Arts and Social Science, 7(11), 127–156.

Tural, M., and Yener, C. (2006). Lighting monuments: Reflections on outdoor lighting and environmental appraisal. Building and Environment, 41(6), 775–782. https://doi.org/10.1016/j.buildenv.2005.03.014

Twigger-Ross, C. L., and Uzzell, D. L. (1996). PLACE AND IDENTITY PROCESSES. Journal of Environmental Psychology, 16(3), 205–220. https://doi.org/10.1006/JEVP.1996.0017

Tyystjärvi, E., Koski, A., Keränen, M., and Nevalainen, O. (1999). The Kautsky curve is a built-in barcode. Biophysical Journal, 77(2), 1159–1167. https://doi.org/10.1016/S0006-3495(99)76967-5

Ueno, Y., Aikawa, S., Kondo, A., and Akimoto, S. (2019). Adaptation of light-harvesting functions of unicellular green algae to different light qualities. Photosynthesis Research, 139(1–3), 145–154. https://doi.org/10.1007/S11120-018-0523-Y/FIGURES/4

Underwood, G. J. C., and Paterson, D. M. (2003). The importance of extracellular carbohydrate productionby marine epipelic diatoms. Advances in Botanical Research, 40, 183–240. https://doi.org/10.1016/S0065-2296(05)40005-1

UNESCO. (2023). UNESCO Urban Heritage Atlas: Cultural mapping for historic cities and settlements. World Heritage Convention. https://whc.unesco.org/en/urban-heritage-atlas/

United Nations. (2023). Objetivo 11: Lograr que las ciudades sean más inclusivas, seguras, resilientes y sostenibles. Sustainable Development Goals . https://www.un.org/sustainabledevelopment/es/cities/

United Nations. (2024). The 17 Goals. Https://Sdgs.Un.Org/Goals.

United Nations. (2025). Goal 13: Climate Change . Sustainable Development Goals. https://www.un.org/sustainabledevelopment/climate-change/

Upham, P., Oltra, C., and Boso, À. (2015). Towards a cross-paradigmatic framework of the social acceptance of energy systems. Energy Research and Social Science, 8, 100–112. https://doi.org/10.1016/J.ERSS.2015.05.003

Urzì, C., De Leo, F., Bruno, L., Pangallo, D., and Krakova, L. (2014). New species description, biomineralization processes and biocleaning applications of Roman catacombs-living bacteria. In The Conservation of Subterranean Cultural Heritage (pp. 65–72). CRC Press. https://doi.org/10.1201/b17570-10

Urzì, C., De Leo, F., Krakova, L., Pangallo, D., and Bruno, L. (2016). Effects of biocide treatments on the biofilm community in Domitilla's catacombs in Rome. Science of The Total Environment, 572, 252–262. https://doi.org/10.1016/J.SCITOTENV.2016.07.195

Utermohl, H. (1958). Zur Ver vollkommung der quantitativen phytoplankton-methodik. Mitteilung Internationale Vereinigung Fuer Theoretische Unde Amgewandte Limnologie, 9, 39.

Valdez, M. T., Machado Ferreira, C., and Maciel Barbosa, F. P. (2017). Study and Lighting Design in an Electrical Engineering Programme. 2017 27th EAEEIE Annual Conference (EAEEIE), 1–5. https://doi.org/10.1109/EAEEIE.2017.8768724

Valetti, L., Pellegrino, A., and Aghemo, C. (2020). Cultural landscape: Towards the design of a nocturnal lightscape. Journal of Cultural Heritage, 42, 181–190. https://doi.org/10.1016/j.culher.2019.07.023

Van Doren, B. M., Horton, K. G., Dokter, A. M., Klinck, H., Elbin, S. B., and Farnsworth, A. (2017). High-intensity urban light installation dramatically alters nocturnal bird migration. Proceedings of the National Academy of Sciences of the United States of America, 114(42), 11175–11180. https://doi.org/10.1073/PNAS.1708574114/SUPPL_FILE/PNAS.1708574114.SM08.AVI

Vandesande, A., and Van Balen, K. (2018). Preventive conservation applied to built heritage: A working definition and influencing factors. Innovative Built Heritage Models - Edited Contributions to the International Conference on Innovative Built Heritage Models and Preventive Systems, CHANGES 2017, 63–72. https://doi.org/10.1201/9781351014793-8/PREVENTIVE-CONSERVATION-APPLIED-BUILT-HERITAGE-WORKING-DEFINITION-INFLUENCING-FACTORS-VANDESANDE-VAN-BALEN

Varela Perez, A. M. (2023). The increasing effects of light pollution on professional and amateur astronomy. Science, 380(6650), 1136–1140. https://doi.org/10.1126/SCIENCE.ADG0269/ASSET/A94F4339-E65A-4718-B353-AB0BE036D585/ASSETS/IMAGES/LARGE/SCIENCE.ADG0269-F4.JPG

Vázquez-Nion, D., Rodríguez-Castro, J., López-Rodríguez, M. C., Fernández-Silva, I., and Prieto, B. (2016). Subaerial biofilms on granitic historic buildings: microbial diversity and development of phototrophic multi-species cultures. Biofouling, 32(6), 657–669. https://doi.org/10.1080/08927014.2016.1183121

Verrecchia, E., Yair, A., Kidron, G. J., and Verrecchia, K. (1995). Physical properties of the psammophile cryptogamic crust and their consequences to the water regime of sandy soils, north-western Negev Desert, Israel. Journal of Arid Environments, 29(4), 427–437. https://doi.org/10.1016/S0140-1963(95)80015-8

Viles, H. A., and Goudie, A. S. (2004). Biofilms and case hardening on sandstones from Al-Quwayra, Jordan. Earth Surface Processes and Landforms, 29(12), 1473–1485. https://doi.org/10.1002/esp.1134

Villa, F., and Cappitelli, F. (2019). The ecology of subaerial biofilms in dry and inhospitable terrestrial environments. Microorganisms, 7(10). https://doi.org/10.3390/microorganisms7100380

Villa, F., Gulotta, D., Toniolo, L., Borruso, L., Cattò, C., and Cappitelli, F. (2020). Aesthetic Alteration of Marble Surfaces Caused by Biofilm Formation: Effects of Chemical Cleaning. Coatings, 10(2), 122. https://doi.org/10.3390/coatings10020122

Villa, F., Ludwig, N., Mazzini, S., Scaglioni, L., Fuchs, A. L., Tripet, B., Copié, V., Stewart, P. S., and Cappitelli, F. (2023). A desiccated dual-species subaerial biofilm reprograms its metabolism and affects water dynamics in limestone. Science of The Total Environment, 868, 161666. https://doi.org/10.1016/J.SCITOTENV.2023.161666

Villa, F., Pitts, B., Lauchnor, E., Cappitelli, F., and Stewart, P. S. (2015). Development of a Laboratory Model of a Phototroph-Heterotroph Mixed-Species Biofilm at the Stone/Air Interface. Frontiers in Microbiology, 6. https://doi.org/10.3389/fmicb.2015.01251

Villa, F., Wu, Y.-L., Zerboni, A., and Cappitelli, F. (2022). In Living Color: Pigment-Based Microbial Ecology At the Mineral–Air Interface. BioScience, 72(12), 1156–1175. https://doi.org/10.1093/biosci/biac091

Vitaterna, M. H., Takahashi, J. S., and Turek, F. W. (2001). Overview of Circadian Rhythms. Alcohol Research and Health, 25(2), 85. https://pmc.ncbi.nlm.nih.gov/articles/PMC6707128/

Volpe, C. Della, and Siboni, S. (2017). Use, Abuse, Misuse and Proper use of Contact Angles: A Critical Review. REVIEWS OF ADHESION AND ADHESIVES, 3(4), 365–385. https://doi.org/10.7569/RAA.2015.097310

von Moos, A., and de Quervain, F. (1948). Das Verhalten der Gesteine als Baugrund. In F. Quervain (Ed.), Technische Gesteinskunde (Vol. 15, pp. 145–167). Birkhäuser. https://doi.org/10.1007/978-3-0348-6799-3_4

von Wirth, T., Grêt-Regamey, A., Moser, C., and Stauffacher, M. (2016). Exploring the influence of perceived urban change on residents' place attachment. Journal of Environmental Psychology, 46, 67–82. https://doi.org/10.1016/J.JENVP.2016.03.001

Vrba, R., Lavoie, I., Creusot, N., Eon, M., Millan-Navarro, D., Feurtet-Mazel, A., Mazzella, N., Moreira, A., Planas, D., and Morin, S. (2024). Experimental testing of two urban stressors on freshwater biofilms. Aquatic Toxicology, 272, 106972. https://doi.org/10.1016/J.AQUATOX.2024.106972

Wakefield, R. D., and Jones, M. S. (1998). An introduction to stone colonizing micro-organisms and biodeterioration of building stone . Quarterly Journal of Engineering Geology, 301–313.

Walter, A., and Schöbel, H. (2023). Shed light on photosynthetic organisms: a physical perspective to correct light measurements. Photosynthesis Research, 156(3), 325–336. https://doi.org/10.1007/s11120-023-01001-5

Wand, M. P., and Jones, M. C. (1994). Kernel Smoothing. Chapman and Hall/CRC. https://doi.org/10.1201/b14876

Wang, P., You, G., Hou, J., Wang, C., Xu, Y., Miao, L., Feng, T., and Zhang, F. (2018). Responses of wastewater biofilms to chronic CeO2 nanoparticles exposure: Structural, physicochemical and microbial properties and potential mechanism. Water Research, 133, 208–217. https://doi.org/10.1016/j.watres.2018.01.031

Wang, Y., Jiang, Z., Lai, Z., Yuan, H., Zhang, X., Jia, Y., and Zhang, X. (2021). The self-adaption capability of microalgal biofilm under different light intensities: Photosynthetic parameters and biofilm microstructures. Algal Research, 58, 102383. https://doi.org/10.1016/J.ALGAL.2021.102383

Wang, Z., Peng, W., Li, X., Zhao, D., Chen, L., Yang, Y., Chen, J., and Wang, H. (2024). Artificial light at night decreases phyllosphere microbial diversity and functionality in grassland plants. Global Ecology and Conservation, 53, e03027. https://doi.org/10.1016/J.GECCO.2024.E03027

Warburg, O. (1920). Über die Geschwindigkeit der photochemischen kohlensäurezersetzung in lebenden zellen. Biochemische Zeitschrift, 103, 188–217.

Wellburn, A. R. (1994). The Spectral Determination of Chlorophylls a and b, as well as Total Carotenoids, Using Various Solvents with Spectrophotometers of Different Resolution. Journal of Plant Physiology, 144(3), 307–313. https://doi.org/10.1016/S0176-1617(11)81192-2

Wernet, G., Bauer, C., Steubing, B., Reinhard, J., Moreno-Ruiz, E., and Weidema, B. (2016). The ecoinvent database version 3 (part I): overview and methodology. The International Journal of Life Cycle Assessment, 21(9), 1218–1230. https://doi.org/10.1007/s11367-016-1087-8

White, T. J., Bruns, T. D., Lee, S. B., and Taylor, J. W. (1990). Amplification and Direct Sequencing of Fungal Ribosomal RNA Genes for Phylogenetics. In M. A. Innis, D. H. Gelfand, J. J. Sninsky, and White T. J. (Eds.), PCR Protocols (1st ed., pp. 315–322). Aacademic Press, Inc.

Whitney, D. L., and Evans, B. W. (2010). Abbreviations for names of rock-forming minerals. American Mineralogist, 95(1), 185–187. https://doi.org/10.2138/AM.2010.3371

Wilhelm, K., Viles, H., and Burke, Ó. (2016). Low impact surface hardness testing (Equotip) on porous surfaces – advances in methodology with implications for rock weathering and stone deterioration research. Earth Surface Processes and Landforms, 41(8), 1027–1038. https://doi.org/10.1002/esp.3882

Wilhelm, K., Viles, H., Burke, O., and Mayaud, J. (2016). Surface hardness as a proxy for weathering behaviour of limestone heritage: a case study on dated headstones on the Isle of Portland, UK. Environmental Earth Sciences, 75(10), 1–16. https://doi.org/10.1007/S12665-016-5661-Y/TABLES/8

Wilimzig, M. (1996). Biodeterioration of building materials. In J. Riederer (Ed.), Proceedings of the 8th International Congress on Deterioration and Conservation of Stone (pp. 579–584).

Williams, D. R., and Vaske, J. J. (2003). The Measurement of Place Attachment: Validity and Generalizability of a Psychometric Approach. Forest Science, 49(6), 830–840. https://doi.org/10.1093/forestscience/49.6.830

Wirilander, H. (2012). Preventive Conservation: a Key Method to Ensure Cultural Heritage's Authenticity and Integrity in Preservation Process. E-Conservation Magazine, 24. https://jyx.jyu.fi/handle/123456789/39406

Wood, M. (2009). How do LEDs work? ETC Connect, 18–22.

World Health Organization. (1992). United Nations Conference on Environment and Development (UNCED).

Yadav, S., and Purchase, D. (2025). Biodeterioration of cultural heritage monuments: A review of their deterioration mechanisms and conservation. International Biodeterioration and Biodegradation, 201, 106066. https://doi.org/10.1016/J.IBIOD.2025.106066

Yan, Y., and Wang, Y. (2024). A Review of Atmospheric Deterioration and Sustainable Conservation of Calcareous Stone in Historical Buildings and Monuments. Sustainability 2024, Vol. 16, Page 10751, 16(23), 10751. https://doi.org/10.3390/SU162310751

Yeom, D.-J., Kim, J.-H., Kim, J.-S., and Kim, Y. S. (2022). Life cycle cost analysis of a built-in guide-type robot for cleaning the facade of high-rise buildings. Journal of Asian Architecture and Building Engineering, 21(5), 1736–1753. https://doi.org/10.1080/13467581.2022.2060984

You, T., and Barnett, S. M. (2004). Effect of light quality on production of extracellular polysaccharides and growth rate of Porphyridium cruentum. Biochemical Engineering Journal, 19(3), 251–258. https://doi.org/10.1016/J.BEJ.2004.02.004

Young, G. S., and Wainwright, I. N. M. (1995). The control of algal biodeterioration of a marble petroglyph site. Studies in Conservation, 40(2), 82–92. https://doi.org/10.1179/sic.1995.40.2.82

Yuan, H., Wang, Y., Xi, Y., Jiang, Z., Zhang, X., Wang, X., and Zhang, X. (2020). Light-Emitting Diode Power Conversion Capability and CO2 Fixation Rate of Microalgae Biofilm Cultured Under Different Light Spectra. Energies 2020, Vol. 13, Page 1536, 13(7), 1536. https://doi.org/10.3390/EN13071536

Yuan, H., Zhang, X., Jiang, Z., Wang, X., Wang, Y., Cao, L., and Zhang, X. (2020). Effect of light spectra on microalgal biofilm: Cell growth, photosynthetic property, and main organic composition. Renewable Energy, 157, 83–89. https://doi.org/10.1016/J.RENENE.2020.04.109

Zanardini, E., Abbruscato, P., Ghedini, N., Realini, M., and Sorlini, C. (2000). Influence of atmospheric pollutants on the biodeterioration of stone. International Biodeterioration and Biodegradation, 45(1–2), 35–42. https://doi.org/10.1016/S0964-8305(00)00043-3

Zanini, A., Trafeli, V., and Bartoli, L. (2018). The laser as a tool for the cleaning of Cultural Heritage. IOP Conference Series: Materials Science and Engineering, 364, 012078. https://doi.org/10.1088/1757-899X/364/1/012078

Zhang, J., and Zhang, Y. (2023). Does tourism contribute to the nighttime economy? Evidence from China. Current Issues in Tourism, 26(8), 1295–1310. https://doi.org/10.1080/13683500.2022.2053073

Zhang, X., Yuan, H., Guan, L., Wang, X., Wang, Y., Jiang, Z., Cao, L., and Zhang, X. (2019). Influence of Photoperiods on Microalgae Biofilm: Photosynthetic Performance, Biomass Yield, and Cellular Composition. Energies, 12(19), 3724. https://doi.org/10.3390/en12193724

Zhang, Y., and Dong, W. (2021). Determining Minimum Intervention in the Preservation of Heritage Buildings. International Journal of Architectural Heritage, 15(5), 698–712. https://doi.org/10.1080/15583058.2019.1645237

Zhang, Y., Fonslow, B. R., Shan, B., Baek, M.-C., and Yates, J. R. (2013). Protein Analysis by Shotgun/Bottom-up Proteomics. Chemical Reviews, 113(4), 2343–2394. https://doi.org/10.1021/cr3003533

Zhao, A., Sun, J., and Liu, Y. (2023). Understanding bacterial biofilms: From definition to treatment strategies. Frontiers in Cellular and Infection Microbiology, 13, 1137947. https://doi.org/10.3389/FCIMB.2023.1137947/FULL

Zhao, J., Xiong, K., and Yan, N. (2024). Research progress on algal biokarst and its implications for carbonate rock dissolution and weathering. Environment, Resource and Ecology Journal, 8(1). https://doi.org/10.23977/erej.2024.080116

Zhu, C., Wang, B., Liu, Z., Guo, Y., Zheng, L., Zhang, B., and Hu, Y. (2025). Unveiling the dual role of biocolonization: a case study on the deterioration and preservation of sandstone monuments in Leshan Giant Buddha, China. World Journal of Microbiology and Biotechnology 2024 41:2, 41(2), 25-. https://doi.org/10.1007/S11274-024-04237-Y

Zhu, C., Wang, L., Wang, B., Wang, B., Tang, M., Wang, X., Li, Q., Hu, Y., and Zhang, B. (2023). Application and evaluation of a new blend of biocides for biological control on cultural heritages. International Biodeterioration and Biodegradation, 178, 105569. https://doi.org/10.1016/j.ibiod.2023.105569

Zielinska-Dabkowska, K. M. (2018). Make lighting healthier. Nature, 553(7688), 274–276. https://doi.org/10.1038/d41586-018-00568-7

Zielinska-Dabkowska, K., and Xavia, K. (2018, October 20). Historic Urban Settings, LED Illumination and its Impact on Nighttime Perception, Visual Appearance, and Cultural Heritage Identity. 5th INTERNATIONAL Multidisciplinary Scientific Conference On Social Sciences And Arts SGEM 2018. https://doi.org/10.5593/sgemsocialF2018/6.3/S15.033

8 SUPPLEMENTARY MATERIAL

SM1. CHAPTER 2. F_0 values (Minimum fluorescence) measured at 470 nm, 520 nm 645 nm and 665 nm on resuspended samples of biofilm after the exposure to the four nocturnal LED lights (red, green, blue, and white) with the different time (2, 4, 6, 8 hours) of LED application. The histogram and the bars represent the I, II and III quartiles of five randomly selected points for four replicates. Statistically significant differences with respect to control are represented with (*) when $p < 0.05$.

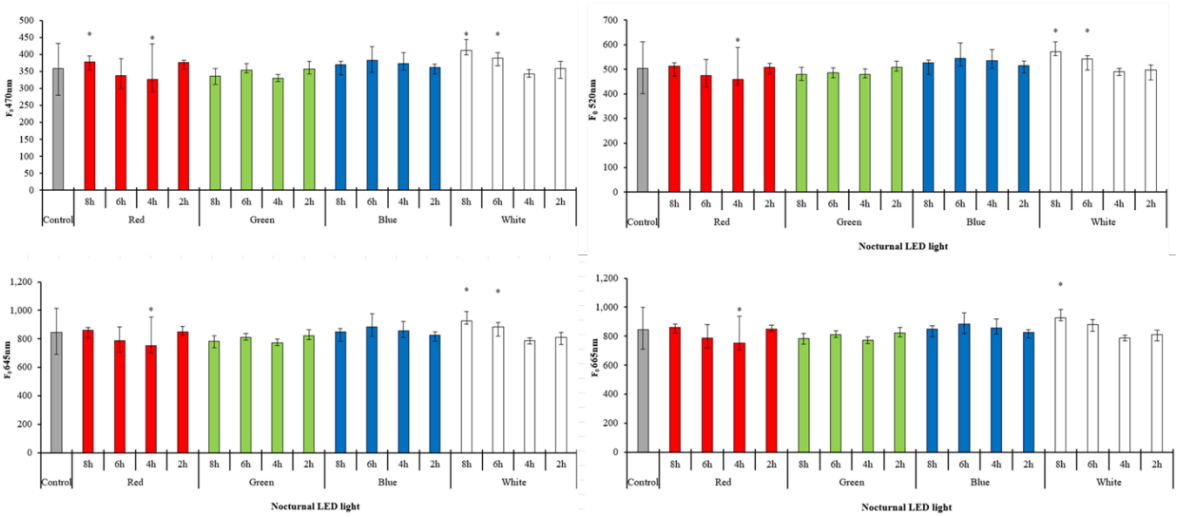

SM2. CHAPTER 2. Relative abundance of the different species found in the SABs under the four nocturnal LED lights (red, green, blue, and white) with the different time of LED application. Statistically significant differences with respect to control are represented with (*) when $p < 0.05$.

Nocturnal LED light	Exposure time	*Bracteacoccus minor*			*Stichococcus bacillaris*			Other green algae			*Isocystis* sp.			Other cyanobacteria		
		Mean	SD		Mean	SD		Mean	SD		Mean	SD		Mean	SD	
Red	Control	52.27	2.89		27.77	1.99		4.78	0.76		13.15	1.56		2.04	0.11	
	8h	22.38	1.95	*	44.01	2.13	*	1.96	0.19	*	28.61	2.74	*	3.06	1.15	
	6h	23.23	0.81	*	43.60	2.11	*	1.76	0.17	*	29.23	1.03	*	2.19	0.09	
	4h	21.28	0.82	*	43.48	0.31	*	1.43	0.28	*	31.15	0.64	*	2.67	0.77	
	2h	20.00	0.28	*	42.92	0.34	*	1.37	0.24	*	31.81	0.44	*	3.90	0.42	
Green	8h	19.35	1.20	*	31.55	1.48	*	0.68	0.11	*	42.40	1.70	*	6.02	1.10	*
	6h	18.04	2.60	*	35.18	0.88	*	0.81	0.24	*	41.30	3.11	*	4.68	0.61	*
	4h	18.21	4.40	*	34.73	5.34	*	0.56	0.19	*	41.31	1.29	*	5.20	0.54	*
	2h	17.86	1.50	*	34.40	1.56	*	0.54	0.06	*	42.19	0.73	*	5.02	0.73	*
Blue	8h	61.95	2.19	*	20.20	1.41	*	0.38	0.11	*	16.85	0.49		0.63	0.18	*
	6h	61.85	1.20	*	18.27	0.37	*	0.50	0.14	*	18.77	0.76		0.62	0.08	*
	4h	62.18	3.85	*	18.54	0.94	*	0.50	0.17	*	18.30	2.97		0.49	0.11	*
	2h	61.19	0.92	*	18.97	0.66	*	0.42	0.14	*	18.91	0.55		0.51	0.16	*
White	8h	53.74	2.14		28.46	0.88		4.13	0.75		11.98	2.04		1.71	0.23	
	6h	54.81	4.26		27.12	1.30		3.32	0.31		13.07	2.08		1.68	0.57	
	4h	56.62	3.00		27.94	1.65		2.14	0.29		11.54	1.43		1.77	0.21	
	2h	54.46	1.98		28.42	3.98		2.46	0.84		13.08	2.06		1.60	0.90	

SM3. CHAPTER 5. Images of the custom-made intermittent flow cascade, with granite specimens developing a SAB. Images taken by P. Sanmartín.

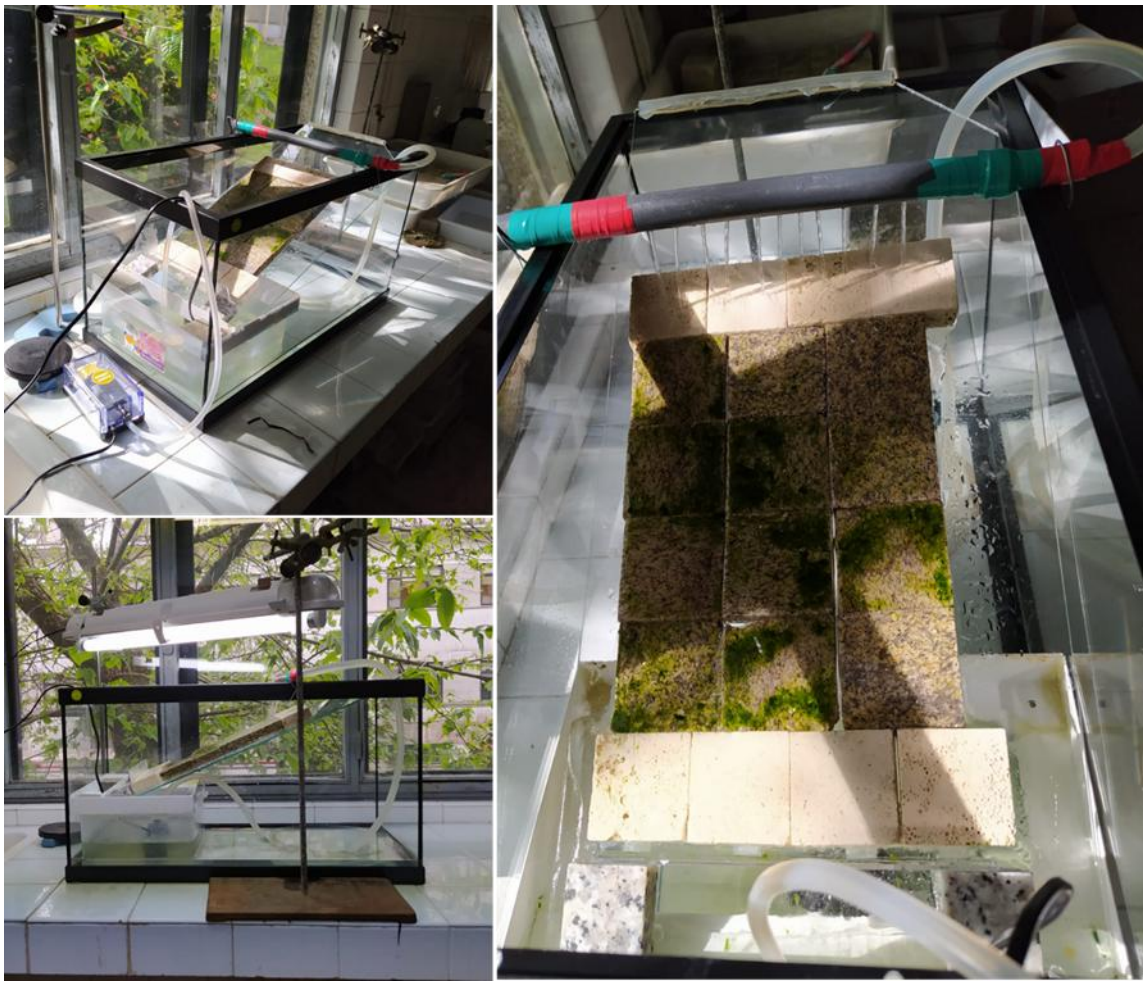

SM4. CHAPTER 5. Full photographs of the thin sections made with the petrographic microscope for the granite samples, both with parallel and cross Nicols.

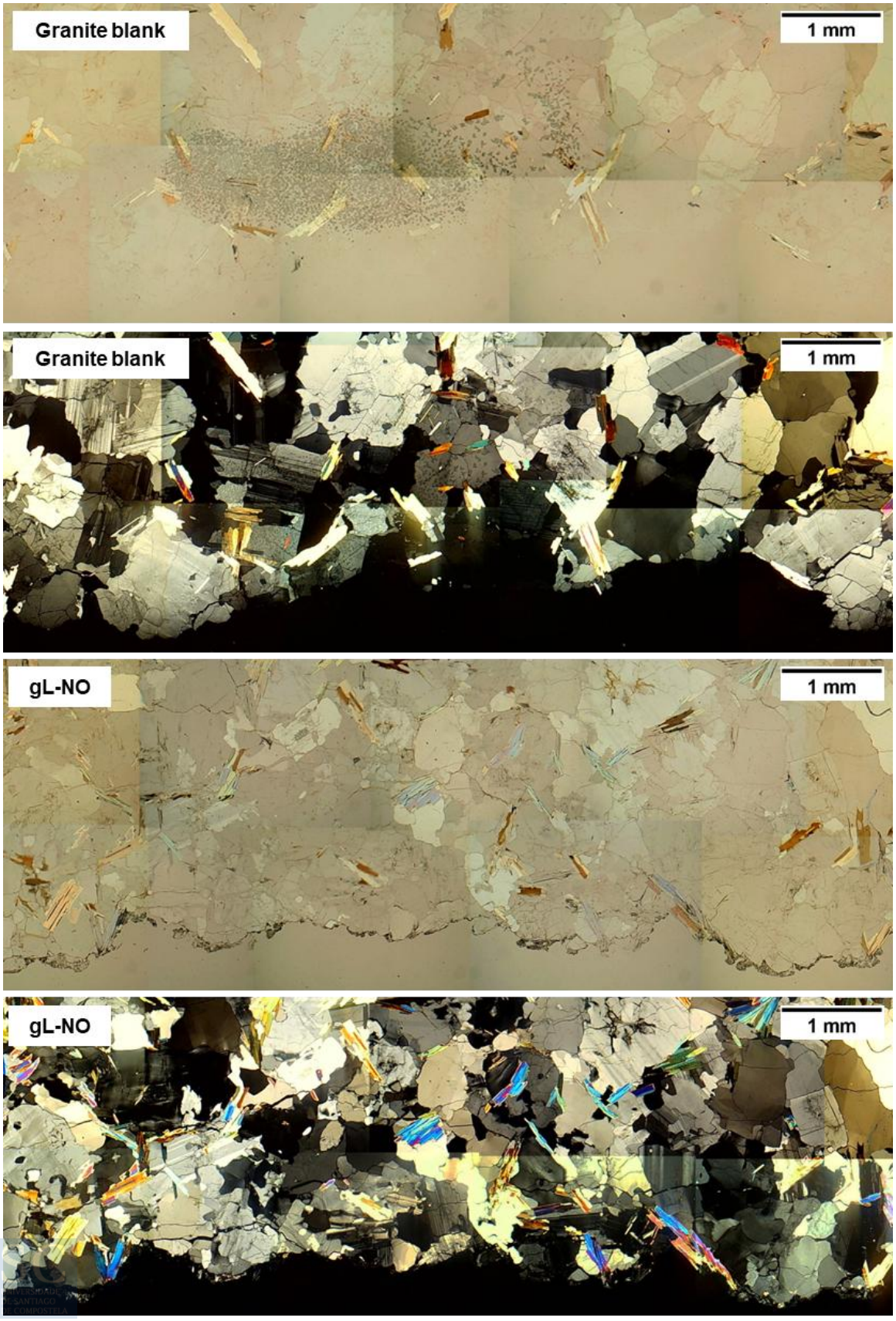

SM4. CHAPTER 5. Continuation.

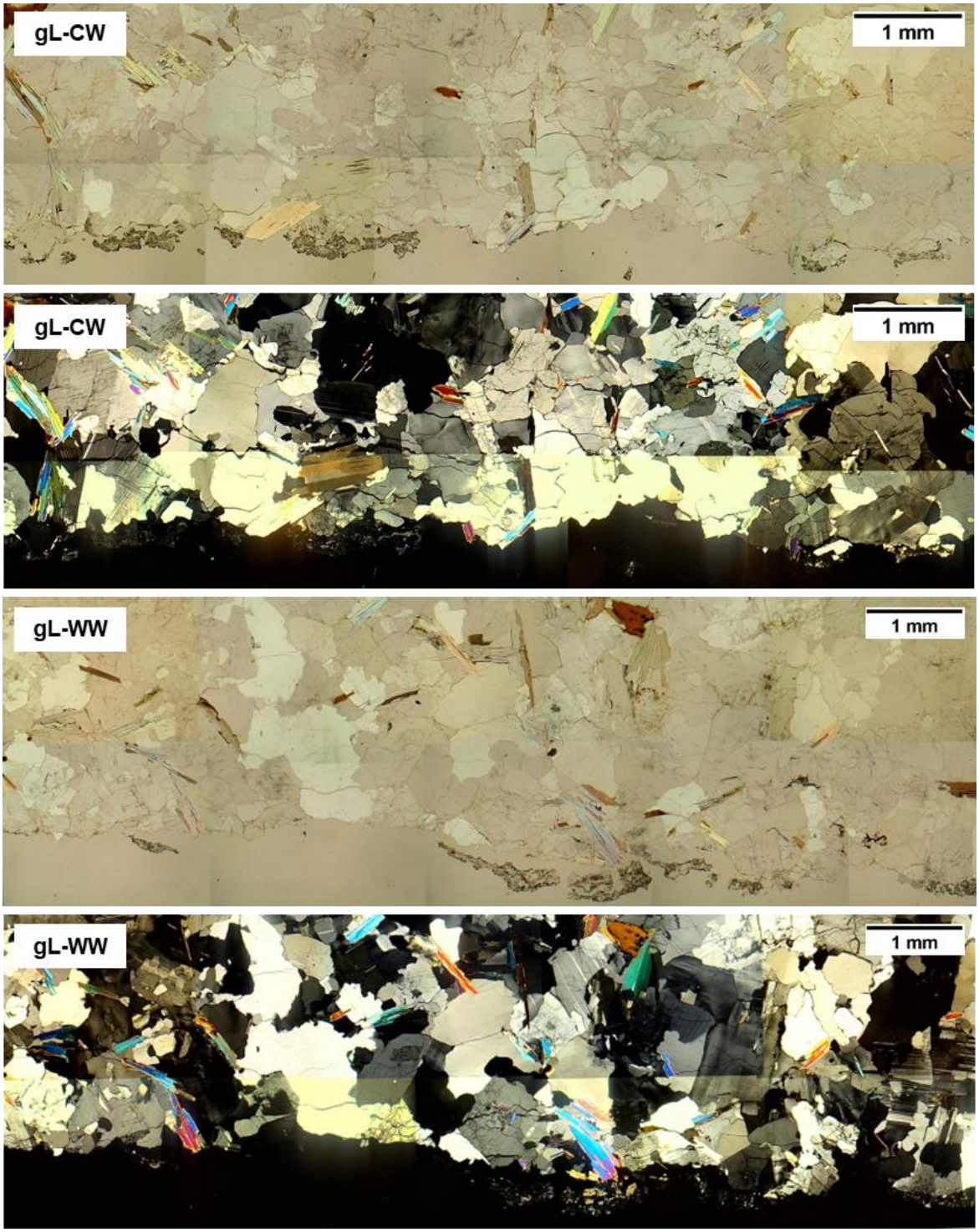

SM4. CHAPTER 5. Continuation.

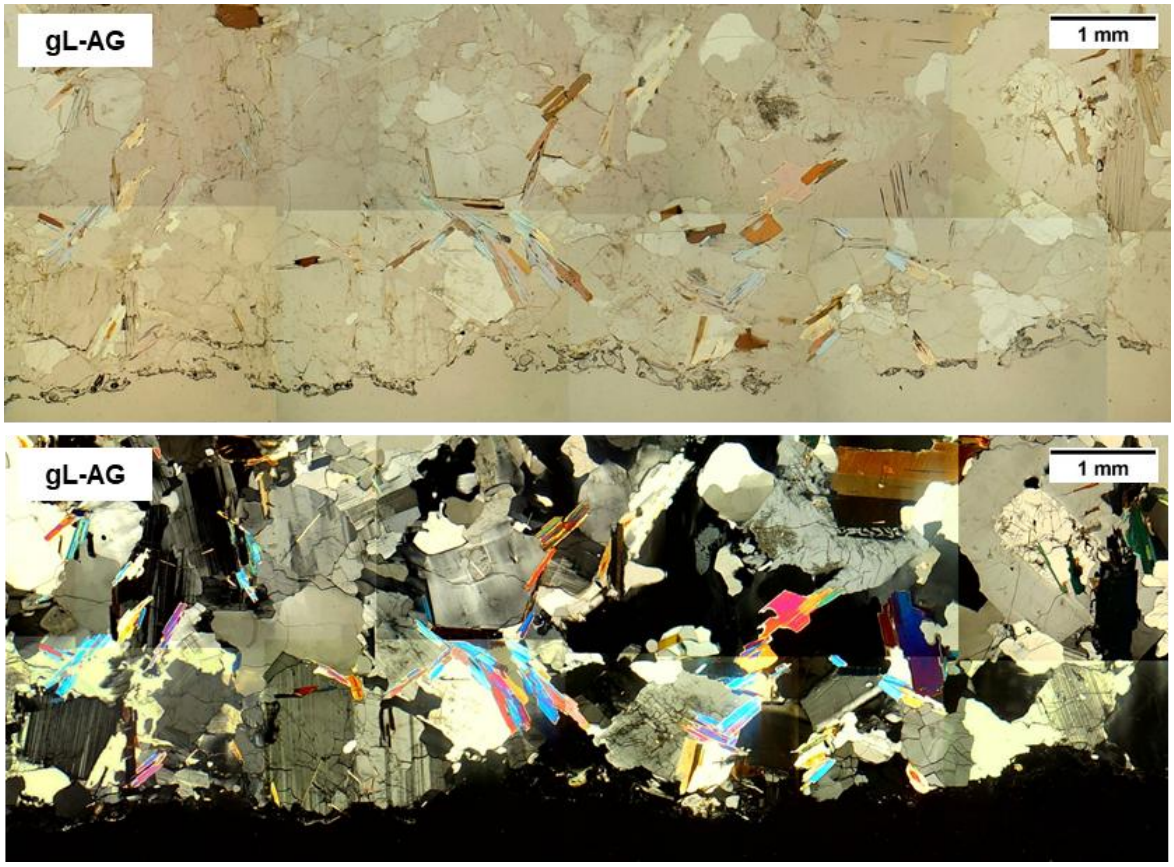

SM5. CHAPTER 5. Full photographs of the thin sections made with the petrographic microscope for the mortar samples, both with parallel and cross Nicols.

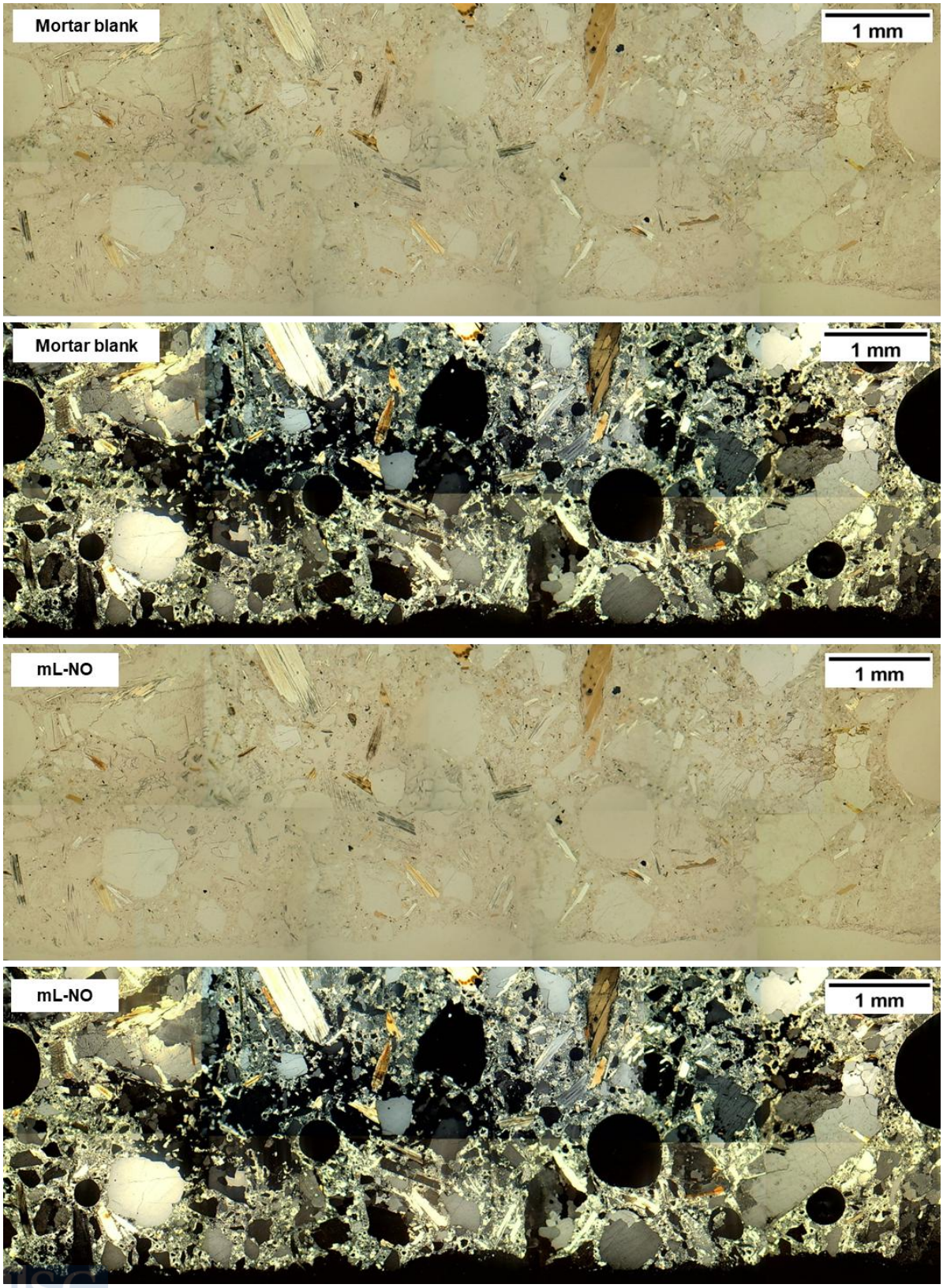

SM5. CHAPTER 5. Continuation.

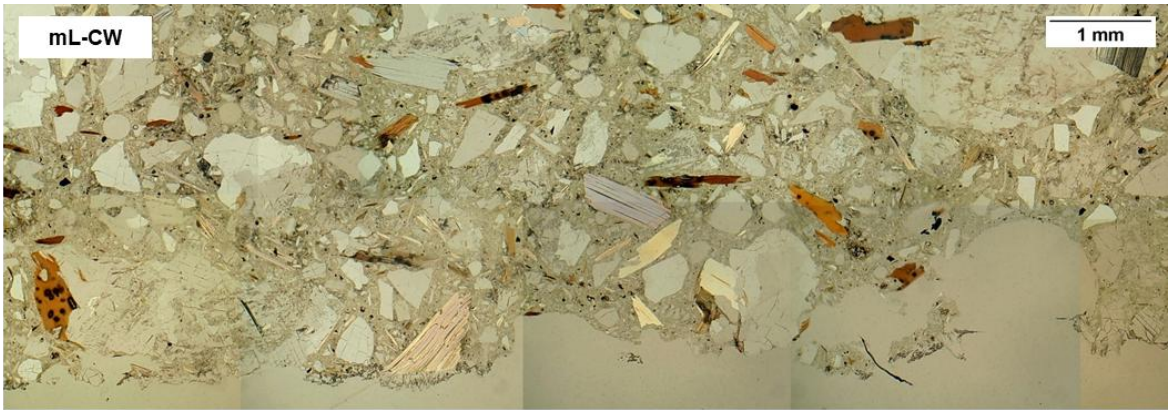

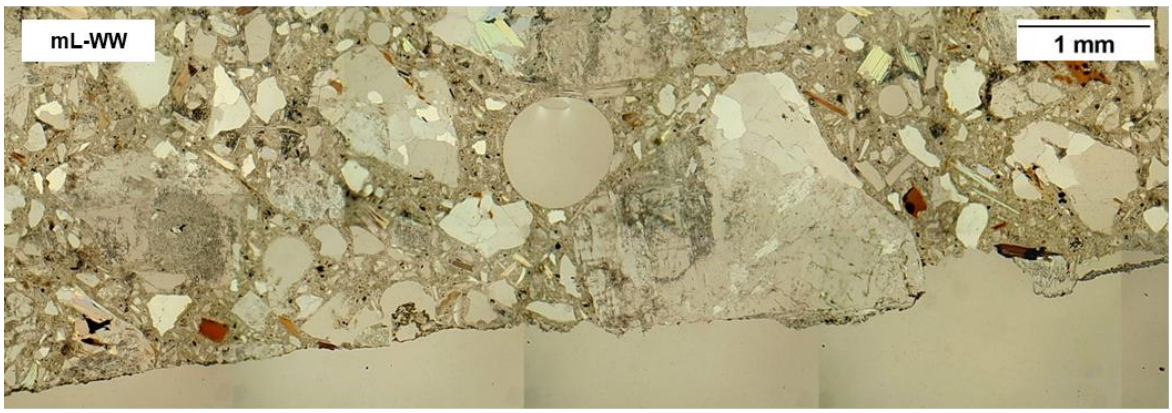

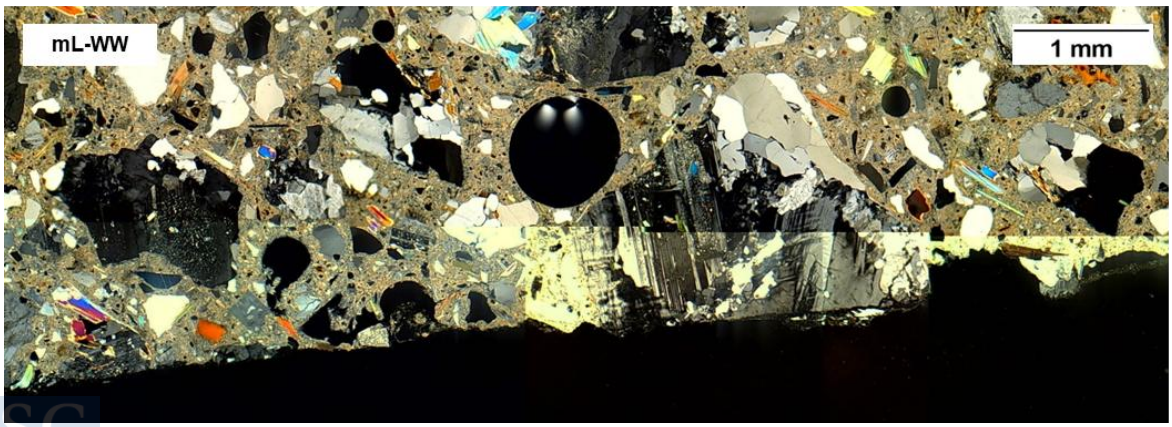

SM5. CHAPTER 5. Continuation.

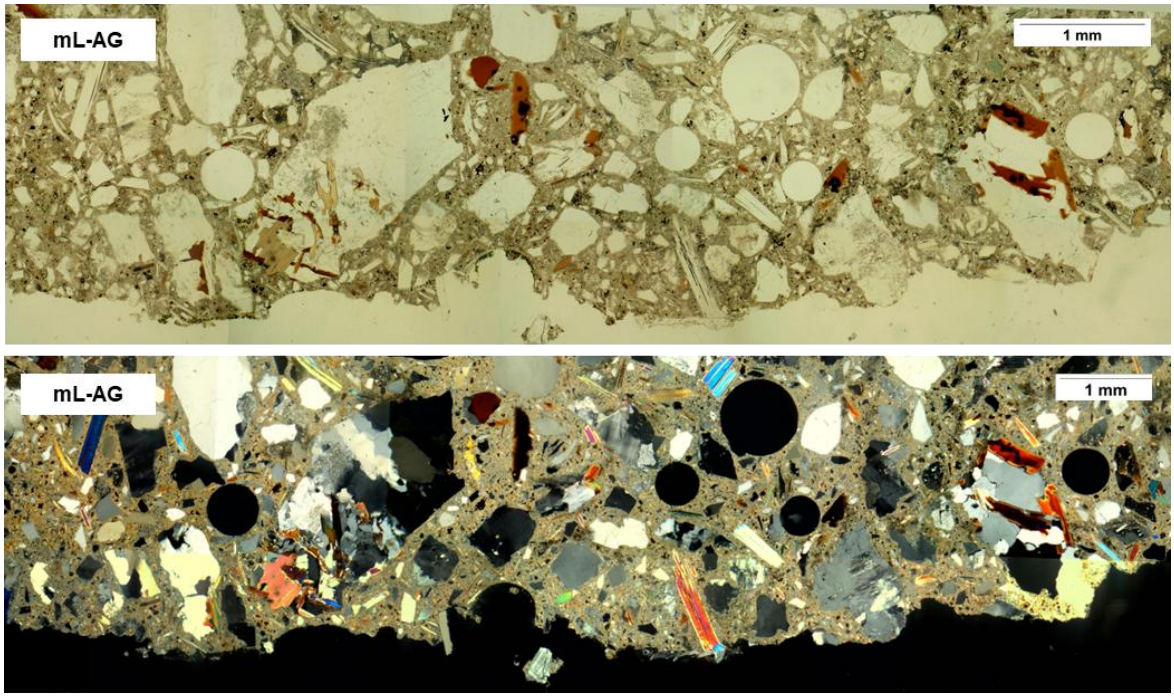

SM6. CHAPTER 5. Detailed images of the SAB growing around but not over minerals of the biotite group. Yellow arrows indicate gaps over the continuity of the SAB over the biotite minerals.

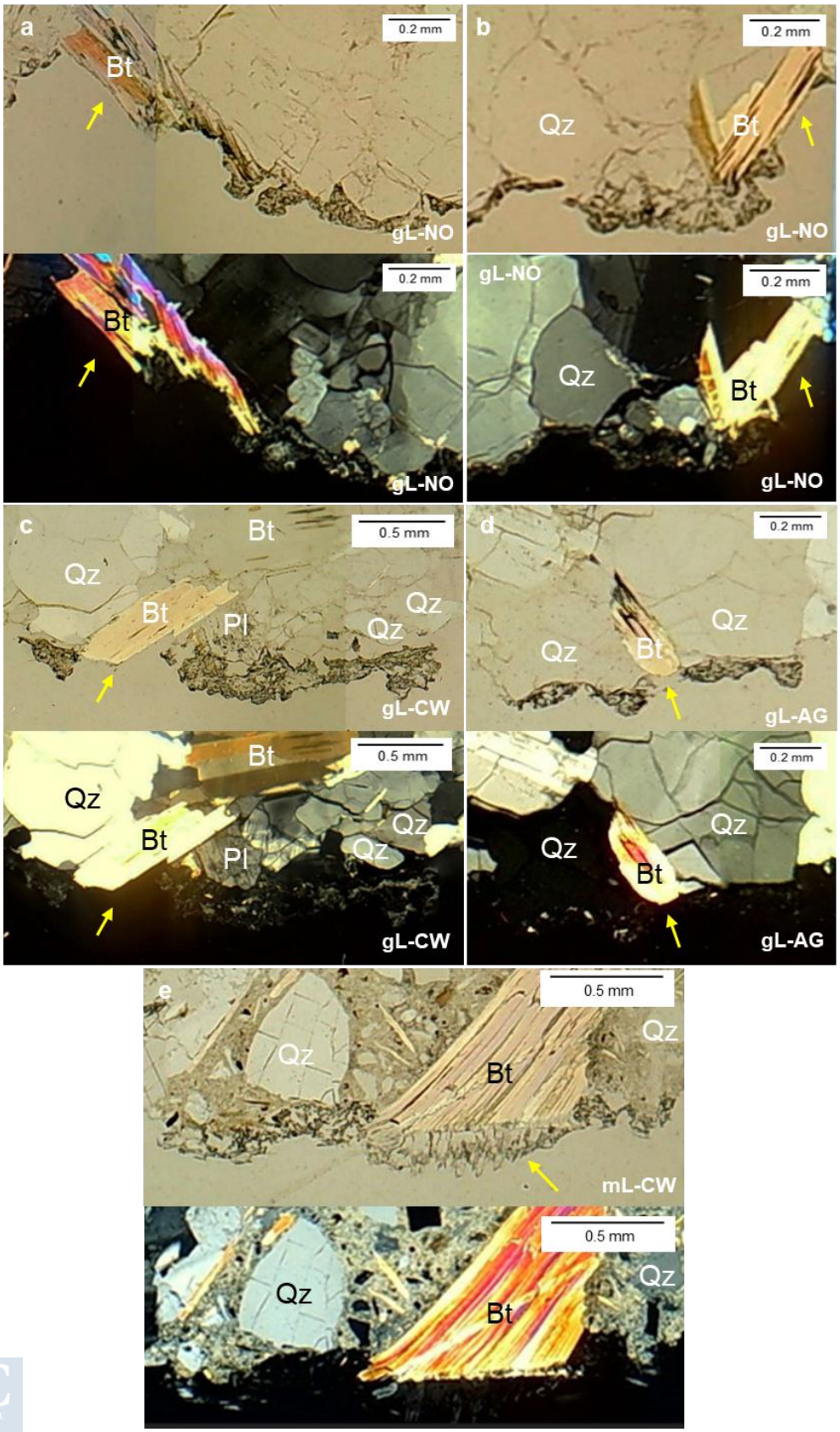

SM7. CHAPTER 5. Detailed images of the SAB growing around minerals of the moscovite group. Yellow arrows indicate SAB growth.

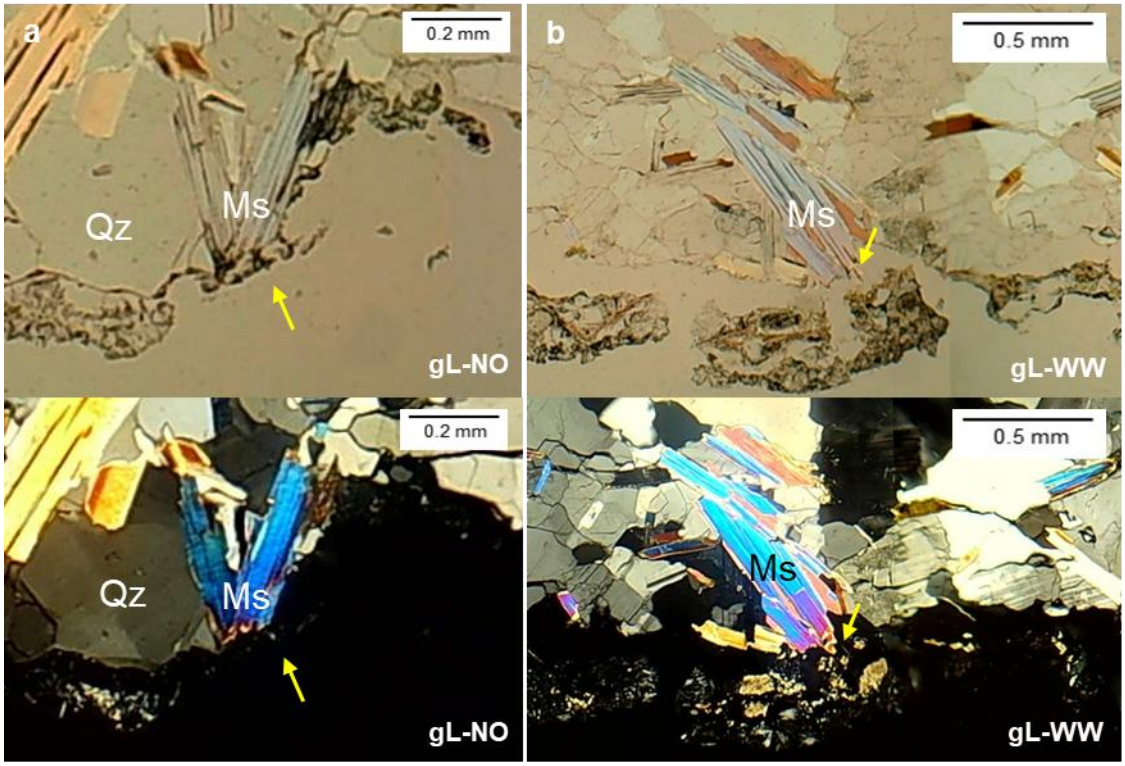

SM8. CHAPTER 5. Detailed images of the SAB growing around minerals like quartzs, potassium feldspars and plagioclases. Yellow arrows indicate SAB growth and blue arrows indicate surface fissures.

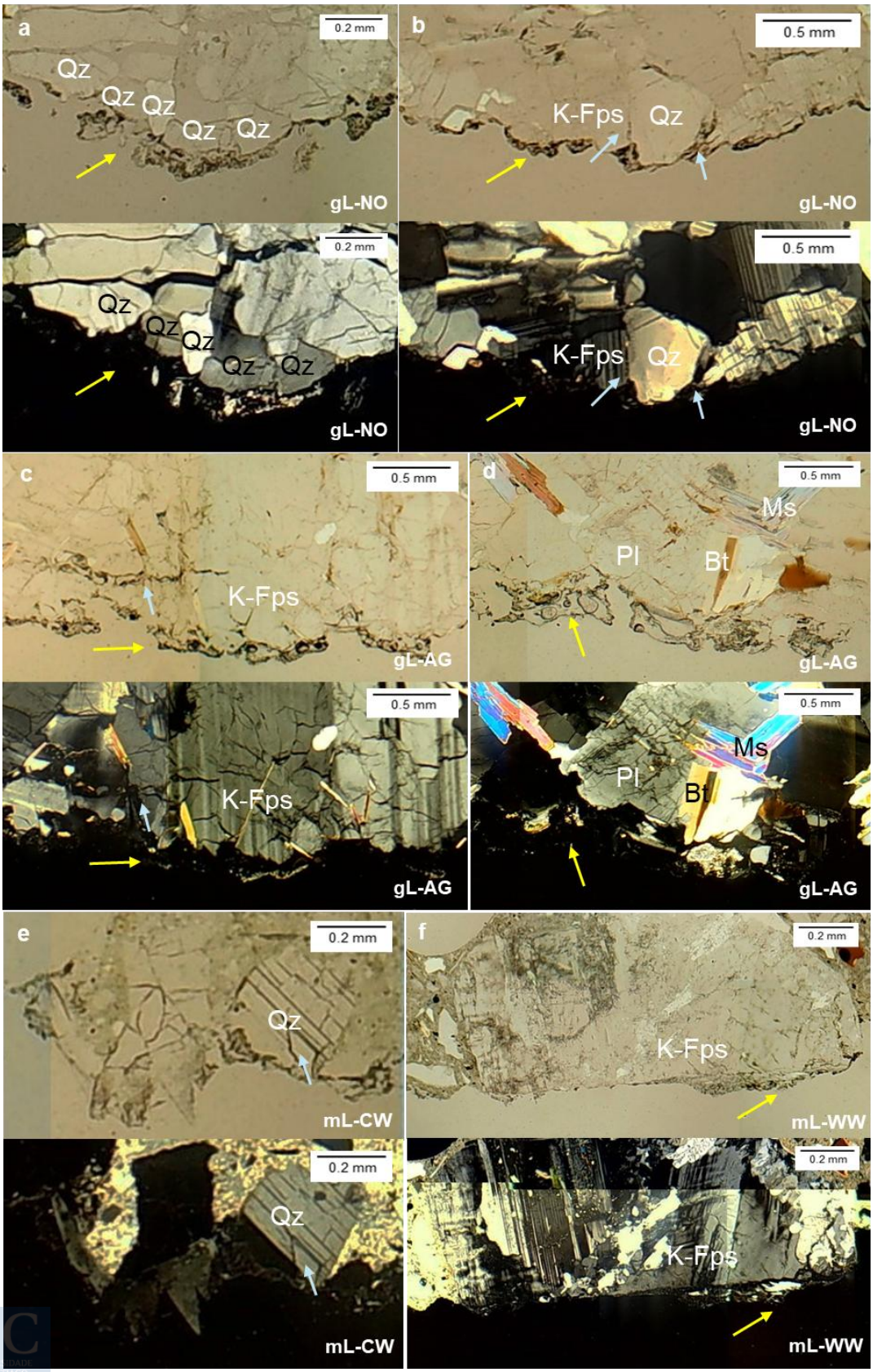

SM9. Detailed image of a superficial macropore.

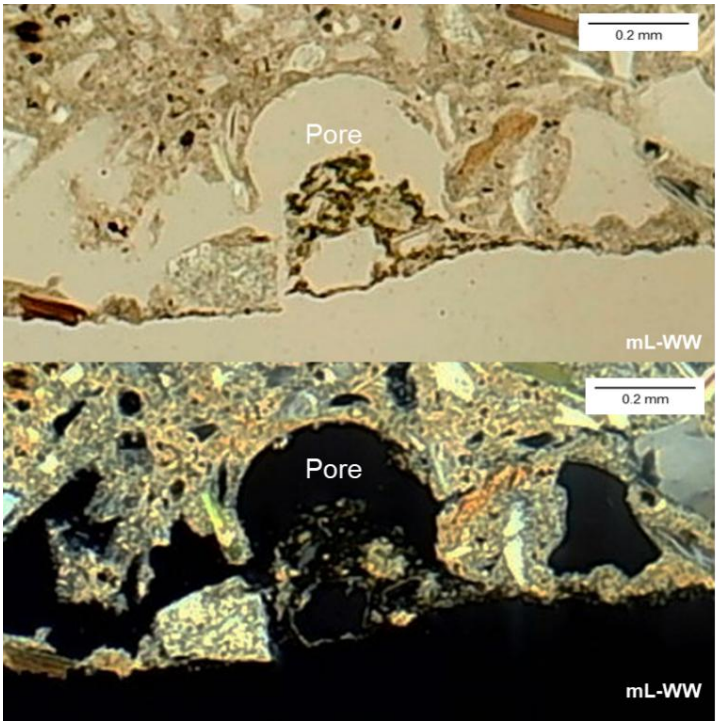

SM10. CHAPTER 5. Detailed images rhombohedral crystals growing into the SABs, indicated by yellow arrows.

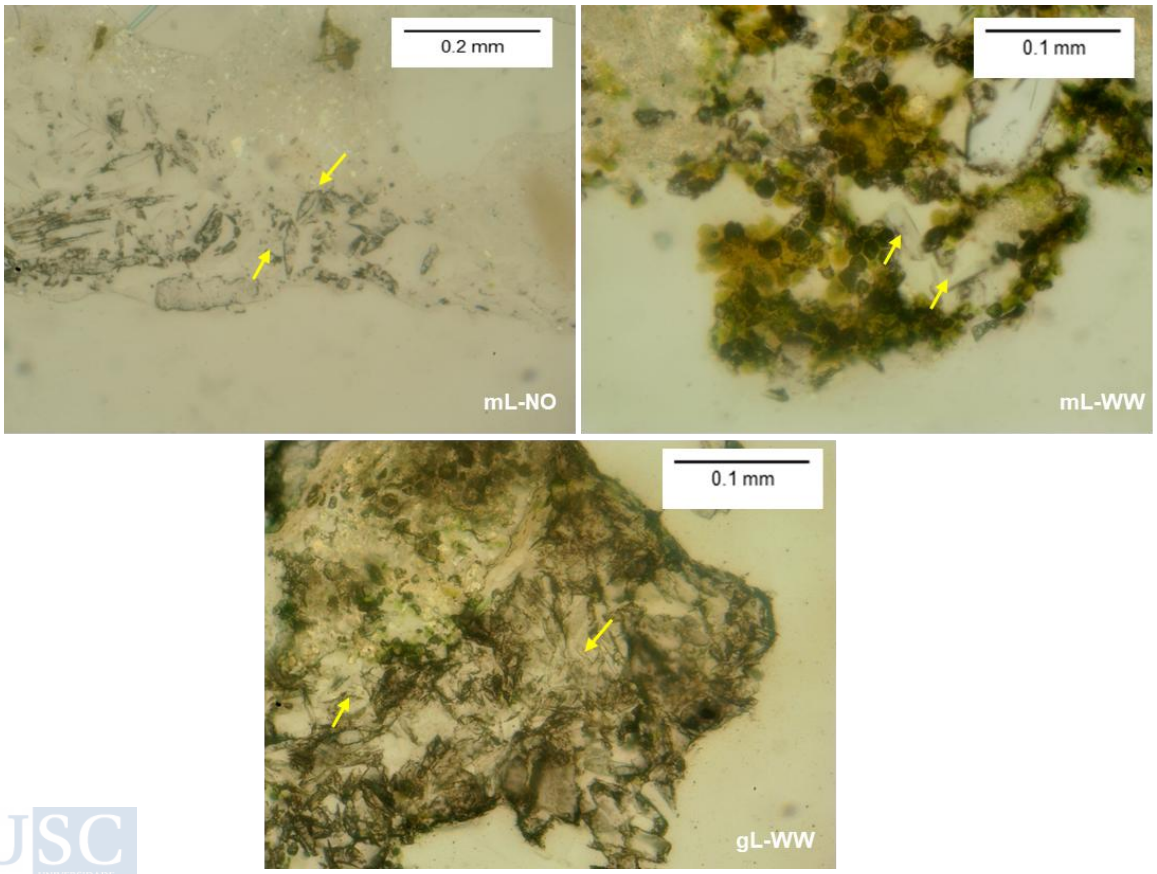

SM11. CHAPTER 8. Economic value (in €) of the elements analysed for the LCC.

Feature	Element	Price (€)	Amount	Unit	Reference
Metal halide	Luminaire	123.76	1	Units	https://www.eweal.com.sg/product/400w-matel-halide-flood-lamp/
	Bulb		1	Units	https://almacenelectricidad.es/bombillas-tubulares-de-halogenuro-metalico-osram/62379-bombilla-osram-de-halogenuros-metalicos-1000w-130v-e40-7250k-muy-blanca-powerstar-hqi-t-tecnologia-de-cuarzo.html https://almacenelectricidad.es/lampara-osram-capsula-hm-clubs-y-discotecas/50007-capsula-lok-it-hti-1000-ps-6000k-pgjx36-halogenuro-metalico.html
LEDs	Luminaire	400	1	Units	Consultation to Televés S.A.U. and Ferrovial Construcción S.A.
Consumables	Gloves	3.85	100	Units	https://www.moybe.es/p666717-guantes-de-latex-sin-polvo-100-unidades.html
	Brushes	3.46	1	Units	https://www.ferreteriacampollano.com/cepillo-buque-5x10cm-raices-1106-mexil-extra-sin-mango-barbosa.html
	Masks	1.82	50	Units	https://dispan.es/vestuario-desechable/mascarilla-polipropileno-pack-50-un
Chemical components	Biotin T®	50.00	1	Kg	Consultation to CTS España S.L.
	Biotin R®	41.50	1	Kg	Consultation to CTS España S.L.
	Reinforced ethanol	4.00	1	L	Consultation to ICIGA S.L.
	Isopropilic alcohol	3.25	1	L	Consultation to CTS España S.L.
	Destiled water	0.45	1	L	https://frank4.es/producto/agua-destilada-bosque-verde/#:~:text=El%20precio%20de%200%2C90,y%20accesible%20para%20los%20consumidores.
Electricity		0.25	1	KWh	Consultation to Ferrovial Construcción S.A.
Water		7.70E-04	1	L	https://tarifasdeagua.es/oficinas/a-coruna/santiago-de-compostela

SM12. CHAPTER 8. Technical information for the lighting systems evaluated.

Parameter	Illumination system		
	Metal halide	White LED	CromaLux LED*
Power (W)	1000	108	-
Lumens/W	115	147	-
Aperture (º)**	100	45	45
Lifespan-Spotlight (h)	219000	100000	100000
Lifespan-Bulb (h)	12000	100000	100000

* Information regarding power and Lumens/W have been omitted from the text as they are subjected to intellectual property by Televés S.A.U.

** Linearity has been assumed for the relation between power and light intensity considering light aperture for the calculations.

SM13. CHAPTER 8. Inventory for the lighting systems evaluated and their SimaPRO categories.

Lighting system	Element	Material	SimaPRO Product
Metal halide	Luminaire	Aluminum	1 kg Aluminium, cast alloy {GLO}| market for | APOS, U (of project Ecoinvent 3 - allocation at point of substitution - unit)
		Porcelain	1 kg Sanitary ceramics {GLO}| market for | APOS, U (of project Ecoinvent 3 - allocation at point of substitution - unit)
		Tempered glass	1 kg Tempering, flat glass {GLO}| market for | APOS, U (of project Ecoinvent 3 - allocation at point of substitution - unit)
		Inox Steel	1 kg Steel, chromium steel 18/8 {GLO}| market for | APOS, U (of project Ecoinvent 3 - allocation at point of substitution - unit)
		Silicone	1 kg Silicone product {RER}| market for silicone product | APOS, U (of project Ecoinvent 3 - allocation at point of substitution - unit)
	Bulb	Steatite	1 kg Sanitary ceramics {GLO}| market for | APOS, U (of project Ecoinvent 3 - allocation at point of substitution - unit)
		Quartz	1 kg Flat glass, uncoated {RER}| market for flat glass, uncoated | APOS, U (of project Ecoinvent 3 - allocation at point of substitution - unit)
		Copper	1 kg Copper, cathode {GLO}| market for | APOS, U (of project Ecoinvent 3 - allocation at point of substitution - unit)
		Silicone	1 kg Silicone product {RER}| market for silicone product | APOS, U (of project Ecoinvent 3 - allocation at point of substitution - unit)
		Cement	1 kg Cement, Portland {Europe without Switzerland}| market for | APOS, U (of project Ecoinvent 3 - allocation at point of substitution - unit)
		Ferrous metals	1 kg Cast iron {GLO}| market for | APOS, U (of project Ecoinvent 3 - allocation at point of substitution - unit)
		Mercury	1 kg Mercury {GLO}| market for | APOS, U (of project Ecoinvent 3 - allocation at point of substitution - unit)
	Electricity		1 kWh Electricity, low voltage {ES}| market for | APOS, U (of project Ecoinvent 3 - allocation at point of substitution - unit)
	Waste	Lamp	1 kg Waste electric and electronic equipment {GLO}| market for | APOS, U
		Bulb	1 kg Used fluorescent lamp {GLO}| market for | APOS, U (of project Ecoinvent 3 - allocation at point of substitution - unit)
White LED	Luminaire	Aluminium	1 kg Aluminium, cast alloy {GLO}| market for | APOS, U (of project Ecoinvent 3 - allocation at point of substitution - unit)
		Stainless steel	1 kg Steel, chromium steel 18/8 {GLO}| market for | APOS, U (of project Ecoinvent 3 - allocation at point of substitution - unit)
		Silicone	1 kg Silicone product {RER}| market for silicone product | APOS, U (of project Ecoinvent 3 - allocation at point of substitution - unit)
		Plastic PC	1 kg Polycarbonate {GLO}| market for | APOS, U (of project Ecoinvent 3 - allocation at point of substitution - unit)
		PA polyamide	1 kg Glass fibre reinforced plastic, polyamide, injection moulded {GLO}| market for | APOS, U (of project Ecoinvent 3 - allocation at point of substitution - unit)
		Polycarbonate	1 kg Polycarbonate {GLO}| market for | APOS, U (of project Ecoinvent 3 - allocation at point of substitution - unit)
		Plastic PC/ABS	1 kg Acrylonitrile-butadiene-styrene copolymer {GLO}| market for | APOS, U (of project Ecoinvent 3 - allocation at point of substitution - unit)
		Copper	1 kg Copper, cathode {GLO}| market for | APOS, U (of project Ecoinvent 3 - allocation at point of substitution - unit)
		PCBA	1 kg Printed wiring board, surface mounted, unspecified, Pb free {GLO}| market for | APOS, U (of project Ecoinvent 3 - allocation at point of substitution - unit)
		PVC	1 kg Polyvinylchloride, bulk polymerised {GLO}| market for | APOS, U (of project Ecoinvent 3 - allocation at point of substitution - unit)
		PBT	1 kg Polyethylene terephthalate, granulate, amorphous, recycled {Europe without Switzerland}| market for polyethylene terephthalate, granulate, amorphous, recycled | APOS, U (of project Ecoinvent 3 - allocation at point of substitution - unit)
		Electric comps (Connectors)	1 kg Electric connector, wire clamp {GLO}| market for | APOS, U (of project Ecoinvent 3 - allocation at point of substitution - unit)
		Electric comps (EM ballasts)	1 kg EM ballast LED ANXO (of project HC Cromalux)
	Bulb	Diodes	1 kg Light emitting diode {GLO}| market for | APOS, U (of project Ecoinvent 3 - allocation at point of substitution - unit)
		Integrated circuit	1 kg Printed wiring board, surface mounted, unspecified, Pb free {GLO}| market for | APOS, U (of project Ecoinvent 3 - allocation at point of substitution - unit)
	Electricity		1 kWh Electricity, low voltage {ES}| market for | APOS, U (of project Ecoinvent 3 - allocation at point of substitution - unit)
	Waste	Lamp + bulb	1 kg Waste electric and electronic equipment {GLO}| market for | APOS, U (of project Ecoinvent 3 - allocation at point of substitution - unit)
CromaLux LED	Luminaire	Aluminium	1 kg Aluminium, cast alloy {GLO}| market for | APOS, U (of project Ecoinvent 3 - allocation at point of substitution - unit)
		Stainless steel	1 kg Steel, chromium steel 18/8 {GLO}| market for | APOS, U (of project Ecoinvent 3 - allocation at

Lighting system	Element	Material	SimaPRO Product
			point of substitution - unit)
		Silicone	1 kg Silicone product {RER}| market for silicone product | APOS, U (of project Ecoinvent 3 - allocation at point of substitution - unit)
		Plastic PC	1 kg Polycarbonate {GLO}| market for | APOS, U (of project Ecoinvent 3 - allocation at point of substitution - unit)
		PA polyamide	1 kg Glass fibre reinforced plastic, polyamide, injection moulded {GLO}| market for | APOS, U (of project Ecoinvent 3 - allocation at point of substitution - unit)
		Polycarbonate	1 kg Polycarbonate {GLO}| market for | APOS, U (of project Ecoinvent 3 - allocation at point of substitution - unit)
		Plastic PC/ABS	1 kg Acrylonitrile-butadiene-styrene copolymer {GLO}| market for | APOS, U (of project Ecoinvent 3 - allocation at point of substitution - unit)
		Copper	1 kg Copper, cathode {GLO}| market for | APOS, U (of project Ecoinvent 3 - allocation at point of substitution - unit)
		PCBA	1 kg Printed wiring board, surface mounted, unspecified, Pb free {GLO}| market for | APOS, U (of project Ecoinvent 3 - allocation at point of substitution - unit)
		PVC	1 kg Polyvinylchloride, bulk polymerised {GLO}| market for | APOS, U (of project Ecoinvent 3 - allocation at point of substitution - unit)
		PBT	1 kg Polyethylene terephthalate, granulate, amorphous, recycled {Europe without Switzerland}| market for polyethylene terephthalate, granulate, amorphous, recycled | APOS, U (of project Ecoinvent 3 - allocation at point of substitution - unit)
		Electric comps (Connectors)	1 kg Electric connector, wire clamp {GLO}| market for | APOS, U (of project Ecoinvent 3 - allocation at point of substitution - unit)
		Electric comps (EM ballasts)	1 kg EM ballast LED (of project HC Cromalux) based on EMconverterLED BASIC 204 MH/LiFePO4 90V from TRIDONIC
	Bulb	Diodes	1 kg Light emitting diode {GLO}| market for | APOS, U (of project Ecoinvent 3 - allocation at point of substitution - unit)
		Integrated circuit	1 kg Printed wiring board, surface mounted, unspecified, Pb free {GLO}| market for | APOS, U (of project Ecoinvent 3 - allocation at point of substitution - unit)
	Electricity		1 kWh Electricity, low voltage {ES}| market for | APOS, U (of project Ecoinvent 3 - allocation at point of substitution - unit)
	Waste	Lamp + bulb	1 kg Waste electric and electronic equipment {GLO}| market for | APOS, U (of project Ecoinvent 3 - allocation at point of substitution - unit)

SM14. CHAPTER 8. Inventory for the cleaning systems evaluated and their SimaPRO categories.

Cleaning system	Element	Material	SimaPRO Product
Laser cleaning	Laser cleaning machine	Electricity	1 kWh Electricity, low voltage {ES}| market for | APOS, U (of project Ecoinvent 3 - allocation at point of substitution - unit)
Water vapour	Water vapour machine	Electricity	1 kWh Electricity, low voltage {ES}| market for | APOS, U (of project Ecoinvent 3 - allocation at point of substitution - unit)
		Water	1 kg Tap water {Europe without Switzerland}| market for | APOS, U (of project Ecoinvent 3 - allocation at point of substitution - unit)
Biotin T®	Chemical compounds	Water	1 kg Tap water {Europe without Switzerland}| market for | APOS, U (of project Ecoinvent 3 - allocation at point of substitution - unit)
		N-octyl isothiazolinone (OIT)	1 kg Benzo[thia]diazole-compound {GLO}| market for | APOS, U (of project Ecoinvent 3 - allocation at point of substitution - unit)
		Quaternary ammonium salt	1 kg Benzyl chloride {RER}| market for benzyl chloride | APOS, U (of project Ecoinvent 3 - allocation at point of substitution - unit)
	Brushes	Wood (m3)	1 m3 Hardwood forestry operation, except harvesting {GLO}| market for | APOS, U (of project Ecoinvent 3 - allocation at point of substitution - unit)
		Coconut fibre	1 kg Coconut husk {GLO}| market for coconut husk | APOS, U (of project Ecoinvent 3 - allocation at point of substitution - unit)
	Masks	Polypropylene	1 kg Textile, nonwoven polypropylene {GLO}| market for textile, nonwoven polypropylene | APOS, U (of project Ecoinvent 3 - allocation at point of substitution - unit)
	Gloves	Latex	1 kg Latex {RER}| market for latex | APOS, U (of project Ecoinvent 3 - allocation at point of substitution - unit)

Cleaning system	Element	Material	SimaPRO Product
		Waste	Based on proportions of incineration and landfill waste management in Spain
Biotin R®	Chemical compounds	Isopropyl alcohol	1 kg Isopropanol {RER}| market for isopropanol | APOS, U (of project Ecoinvent 3 - allocation at point of substitution - unit)
		N-octyl isothiazolinone (OIT)	1 kg Benzo[thia]diazole-compound {GLO}| market for | APOS, U (of project Ecoinvent 3 - allocation at point of substitution - unit)
		Iodopropynylbutylcarbamate (IPBC)	1 kg [thio]carbamate-compound {GLO}| market for | APOS, U (of project Ecoinvent 3 - allocation at point of substitution - unit)
		Water	1 kg Tap water {Europe without Switzerland}| market for | APOS, U (of project Ecoinvent 3 - allocation at point of substitution - unit)
	Brush	Wood (m3)	1 m3 Hardwood forestry operation, except harvesting {GLO}| market for | APOS, U (of project Ecoinvent 3 - allocation at point of substitution - unit)
		Coconut fibre	1 kg Coconut husk {GLO}| market for coconut husk | APOS, U (of project Ecoinvent 3 - allocation at point of substitution - unit)
	Mask		1 kg Textile, nonwoven polypropylene {GLO}| market for textile, nonwoven polypropylene | APOS, U (of project Ecoinvent 3 - allocation at point of substitution - unit)
	Gloves	Latex	1 kg Latex {RER}| market for latex | APOS, U (of project Ecoinvent 3 - allocation at point of substitution - unit)
		Waste	Based on proportions of incineration and landfill waste management in Spain
Reinforced ethanol	Chemical compounds	Ethanol	1 kg Ethanol, without water, in 95% solution state, from fermentation {GLO}| market for | APOS, U (of project Ecoinvent 3 - allocation at point of substitution - unit)
		Benzalkonium chloride	1 kg Benzyl chloride {RER}| market for benzyl chloride | APOS, U (of project Ecoinvent 3 - allocation at point of substitution - unit)
		Water	1 kg Tap water {Europe without Switzerland}| market for | APOS, U (of project Ecoinvent 3 - allocation at point of substitution - unit)
	Brushes	Wood (m3)	1 m3 Hardwood forestry operation, except harvesting {GLO}| market for | APOS, U (of project Ecoinvent 3 - allocation at point of substitution - unit)
		Coconut fibre	1 kg Coconut husk {GLO}| market for coconut husk | APOS, U (of project Ecoinvent 3 - allocation at point of substitution - unit)
	Masks		1 kg Textile, nonwoven polypropylene {GLO}| market for textile, nonwoven polypropylene | APOS, U (of project Ecoinvent 3 - allocation at point of substitution - unit)
	Gloves	Latex	1 kg Latex {RER}| market for latex | APOS, U (of project Ecoinvent 3 - allocation at point of substitution - unit)
		Waste	Based on proportions of incineration and landfill waste management in Spain

SM15. CHAPTER 8. Contribution to the different categories of the GWP100 (in kg of CO2-eq and % of the total) of the lighting systems evaluated for the FU.

Lighting system	GWP100 - fossil	GWP100 - biogenic	GWP100 - land transformation
Metal halide	9.96E+03	1.49E+01	8.53E+01
White LED	1.14E+03	1.73E+00	9.32E+00
CromaLux LED	8.83E+02	1.34E+00	7.08E+00

Lighting system	GWP100 - fossil	GWP100 - biogenic	GWP100 - land transformation
Metal halide	99.00%	0.15%	0.85%
White LED	99.04%	0.15%	0.81%
CromaLux LED	99.06%	0.15%	0.79%

SM16. CHAPTER 8. Contribution to the different categories of the GWP100 (in kg of CO2-eq and % of the total) of the cleaning systems evaluated for the FU.

Cleaning system	GWP100 - fossil	GWP100 - biogenic	GWP100 - land transformation
Laser cleaning	1.66E-02	2.45E-05	1.42E-04
Water vapour	1.21E-01	1.78E-04	1.03E-03
Biotin T®	2.19E-01	3.74E-04	2.62E-03
Biotin R®	2.58E-01	4.04E-04	2.63E-03
Reinforced ethanol	1.06E-01	1.41E-03	2.75E-03

Cleaning system	GWP100 - fossil	GWP100 - biogenic	GWP100 - land transformation
Laser cleaning	99.00%	0.15%	0.85%
Water vapour	99.00%	0.15%	0.85%
Biotin T®	98.65%	0.17%	1.18%
Biotin R®	98.84%	0.15%	1.01%
Reinforced ethanol	96.23%	1.28%	2.49%

SM17. CHAPTER 10. Written informed consent given to the participants in the study (in Galician).

Dende o Centro de Investigación Interdisciplinar en Tecnoloxías Ambientais (CRETUS) da Universidade de Santiago de Compostela en colaboración coas empresas Televés e Ferrovial Construción estamos a realizar un estudo para analizar as opinións e actitudes da cidadanía sobre a iluminación pública ornamental no patrimonio monumental de Santiago de Compostela.

Como este é un cuestionario de opinións, **non hai respostas correctas ou incorrectas**. As súas respostas son **anónimas** e serán utilizadas para fins estritamente académicos respectando a lexislación vixente[1].

Para que este traballo sexa útil para o coñecemento científico necesitamos que responda **coa máxima sinceridade**. Completar este cuestionario levaralle aproximadamente **10 minutos**.

Participar é voluntario e pode abandonar a tarefa en calquera momento, sen que iso supoña ningún prexuízo nin medida na súa contra. Enviando unha mensaxe a esta dirección de correo "patricia.sanmartin@usc.es" ten dereito a solicitar información sobre este estudo[2].

Se desexa continuar e contribuír ao noso proxecto contestando o cuestionario marca "Responder" e a continuación pulse "Seguinte". Se non desexa continuar marque "Abandonar páxina" e "Seguinte" ou simplemente pecha esta xanela.

Desexa continuar? (Ao responder e enviar o cuestionario acepta participar neste estudo).

☐ Non ☐ Si

[1]De conformidade coa Lei de Protección de Datos e Garantías dos Dereitos Dixitais Lei Orgánica 3/3018 e co Regulamento UE 2016/679, os datos recadados serán tratados pola Universidade de Santiago de Compostela (USC) coa finalidade de "Xestión dos datos de investigación", cuxa finalidade é a Xestión dos datos das investigacións en actividades científicas, históricas, culturais e lingüísticas para crear resultados de investigación con fins científicos.

[2]Pode solicitar o seguinte: consultar o proceso de conservación da súa información unha vez finalizado o estudo; solicitar a destrución da súa información; coñecer os resultados xerais da investigación. Os datos conservaranse ata a finalización do proxecto, tras o cal as copias dixitais borradas. Ata entón os datos dixitais quedarán almacenados nos servidores da USC. Os datos persoais son anónimos durante todo o proceso. Os resultados estarán dispoñibles en forma de publicación científica unha vez finalizado o proxecto.

Tratamento	Xestión dos datos de investigación.
Finalidade	Xestión dos datos das investigacións en actividades científicas, históricas, culturais e lingüísticas para crear resultados de investigacións con fins científicos.
Responsable do tratamento	Universidade de Santiago de Compostela. Praza do Obradoiro s/n, 15782 Santiago de Compostela, Correo-e protecciondedatos@usc.gal
Delegado	O contacto co Delegado de Protección de Datos é dpd@usc.gal
Dereitos	As persoas interesadas poden exercer ante o responsable os dereitos de acceso, rectificación, supresión, limitación de tratamento, oposición e portabilidade a través da Sede Electrónica da USC https://sede.usc.gal/sede/publica/catalogo/procedemento/55/ver.htm Tamén poden dirixirse á Axencia Española de Protección de Datos para realizar a reclamación que consideren oportuna. Se non se proporcionan os datos requiridos e as autorizacións para o seu tratamento, a solicitude non poderá ser tramitada.
Información adicional	A política de privacidade e protección de datos da USC pódese consultar na web *https://www.usc.gal/gl/normativa/protecciondatos/index.html*
Data de aprobación	Este estudo foi aprobado polo Comité de Bioética da Universidade de Santiago de Compostela (data: 26/09/2024)

SM18. CHAPTER 10. Favorable report from the USC Bioethics Committee for conducting the study (in Galician).

COMITÉ DE ÉTICA EN INVESTIGACIÓN DA USC

Tel. 982823558
Correo electrónico: comite.etica.investigacion@usc.es

Asistentes a reunión do CEI:

Cifuentes Martínez, Jose Manuel, Presidente
Fernández Copa, María,Secretaria
Fernandez Lorenzo, Juan Luis
Villarino del Rio, Natalia
Vázquez Rodríguez, Sonia
Magariños Ferro, Beatriz
Azevedo Gómes, Ana Manuela de
Aguiar fernández, Pablo

JOSÉ MANUEL CIFUENTES MARTÍNEZ, PRESIDENTE DO COMITÉ DE ÉTICA NA INVESTIGACIÓN DA UNIVERSIDADE DE SANTIAGO DE COMPOSTELA,

INFORMA:
Coa presenza dos membros de CEI que se citan, e unha vez analizados os informes dos grupos de traballo correspondentes, os cales teñen ponderado os aspectos metodolóxicos, éticos e legais do proxecto de investigación cuxos datos se refiren a continuación, e teñen avaliado a cualificación do investigador responsable e do equipo investigador, así como as posibilidades do proxecto conforme a lexislación vixente,

O Comité de Ética na Investigación da USC **ACORDA** a emisión de **INFORME FAVORABLE**

Título do proxecto: **Bases científicas para o deseño dunha iluminación pública eficiente e mediambientalmente responsable con capacidade biostática sobre a colonización biolóxica do patrimonio cultural**

Código: **USC 72/2024**

Investigador responsable: **Patricia Sanmartín Sánchez**

En Lugo, con data da firma electrónica.

NOTA: **O presente informe unicamente avala aquelas actuación/actividades que se desenvolvan a partir da data de sinatura do mesmo**

SM19. CHAPTER 10. Messages conditions used for the quantitative study (translated from original lenguage in Spanish and Galician).

Introductory message prior to the message conditions:

"Next, you will see three images of the *Casa do Cabildo*, a building located in the Plaza de Praterías in the historic center of Santiago de Compostela. In each image, you can observe the building under three different types of lighting. Please take a moment to carefully examine each of the images."

- **Preventive message condition:**

"This lighting is a new technology that enables scientifically proven preventive actions to be taken, which help avoid damage and degradation of the building caused by the growth of biologically originated stains. As a result, future restoration interventions can be delayed."

- **Urgent message condition:**

This lighting is a new technology that enables immediate, scientifically proven actions to urgently halt the damage and degradation of the building caused by the growth of biologicallyvoriginated stains.

- **No message condition:**

None (only the Introductory message).

TABLES AND FIGURES INDEX

TABLES

FIGURES

Ornamental lighting can promote the development of phototrophic colonisation on architectural heritage if it is emitted at wavelengths that stimulate photosynthesis. The study of the combination of narrow-band amber and green LED light with potential biostatic (halting growth) effect has been approached holistically, also considering its environmental, economic and social impact. Thus, the legislative framework governing ornamental lighting was examined (***Part 1***), the biostatic (halting growth) effect over phototrophic SABs was validated at lab and field for long-time (***Part 2***) and the biodiversity impact (***Part 3***) and the socio-economic (***Part 4***) impact were assed.